

Secondary Metabolites from the Endophytic Fungus

***Pestalotiopsis* sp. JCM2A4 and its Microbe-Host**

Relationship with the Mangrove Plant *Rhizophora*

mucronata

Inaugural-Dissertation

zur

Erlangung des Doktorgrades

der Mathematisch-Naturwissenschaftlichen Fakultät

der Heinrich-Heine-Universität Düsseldorf

vorgelegt von

Jing Xu

aus Qingdao, China

Düsseldorf, 2010

Aus dem Institut für Pharmazeutische Biologie und Biotechnologie
der Heinrich-Heine Universität Düsseldorf

Gedruckt mit der Genehmigung der
Mathematisch-Naturwissenschaftlichen Fakultät der
Heinrich-Heine-Universität Düsseldorf
Gedruckt mit der Unterstützung des
China Scholarship Council, the Ministry of Education of China
Referent: Prof. Dr. Peter Proksch, Prof. Dr. Wenhan Lin
Koreferent: Prof. Dr. Guenther Schmahl
Tag der mündlichen Prüfung: 05.18.2010

ACKNOWLEDGEMENTS

I gratefully acknowledge my wholehearted appreciation to Prof. Dr. Peter Proksch and Prof. Huashi Guan for their supervision, guidance, and giving the opportunity to pursue my doctoral research.

I am indebted to Prof. Dr. Jun Wu for his scientific advices and guidance in the interpretation of NMR spectra during my study and his kind help, continuous support and encouragement throughout this work.

Special thanks are given to Dr. Victor Wray (GBF, Braunschweig) for his instructive supervision, fruitful discussions and excellent measurements of 1D and 2D NMR spectra.

I would like to express my cordial thanks and gratitude to Prof. Dr. Dr. Gerhard Bringmann and his coworkers for their unforgettable support and the splendid CD calculation.

My deep thanks are also to Prof. Dr. Wenhan Lin for his valuable suggestions and revision of manuscripts, Dr. Amal Hassan for measured some of aliphatic values, Dr. Jandirk Sendker for LC-MS analysis, Dr. R.A. Edrada Ebel for HRMS measurements, Prof. W.E.G. Müller and Renate Steffen (Univ. Mainz) for cytotoxicity assays.

I would like to deeply thank Dr. Peters and his colleagues (HHU-Düsseldorf) for 500 MHz ¹H NMR and 125 MHz ¹³C NMR measurement as well as Dr. Keck and Dr. Tommes (HHU-Düsseldorf) for EI-mass spectra measurements.

I also appreciate Mirko Bayer's and Barbara Kalish's helps and their co-operation as a lab-mate that I finished the lab work on time. Special thanks to Claudia Eckelskemper

for her administrative help whenever needed. I am grateful to Herr Jansen, Frau Schlag, Frau Miljanovic, Frau Goldbach and Frau Müller for technical and administrative support, respectively. Many thanks to the (former) members of fungal group, Dr. Debabb, Mustapha El Amrani, Yaming Zhou, Frank Riebe, Julia Kjer, David Rönsberg and Weaam Ebrahim.

Appreciation to my past and present colleagues Ashraf Hamed, Sabri Younes, Dr. Tu N. Duong, Dr. Hefni Effendi, Annika Putz, Sherif Elsayed, Ehab Moustafa, Yao Wang, Bartosz Lipowicz. The special thanks also are given to all Chinese students as well as all other doctoral students at the Institute for their cooperation by sharing the places and works as well as the nice time during the study.

My great appreciation to China Scholarship Council, the Ministry of Education of China for the financial support during my stay in Germany.

Finally, I would like to express my thanks to my family and friends, who encouraged and supported me always in good and bad times.

ZUSAMMENFASSUNG

Endophyten aus Mangrovenpflanzen wurden bisher erst selten auf ihre Inhaltsstoffe untersucht und stellen eine wichtige Quelle für neue, bioaktive Naturstoffe dar. Das Ziel dieser Arbeit ist es, sekundäre Inhaltsstoffe aus einem Mangroven-Endophyten der Gattung *Pestalotiopsis*, der in Blättern der chinesischen Mangrove *Rhizophora mucronata* vorkommt, zu isolieren, sie strukturell zu identifizieren und ihr pharmakologisches Potential zu evaluieren. Der Endophyt wurde nach seiner Isolierung aus der Pflanze für 39 Tage auf einem Reismedium kultiviert. Anschließend wurden das Mycel und das Kulturmedium mit Ethylacetat extrahiert. Sämtliche isolierten Verbindungen wurden mittels NMR und MS strukturell aufgeklärt. Alle Verbindungen wurden sodann in verschiedenen Bioassays auf ihre zytotoxische und antibiotische Wirkung untersucht. Insgesamt wurden aus dem untersuchten Stamm des Endophyten *Pestalotiopsis* sp. 48 Naturstoffe isoliert und identifiziert, unter denen sich 40 neue Verbindungen befinden. Bei den meisten Substanzen handelt es sich um Polyketidderivate, unter denen sich z. B. neue Chromone, Cumarine, Pyrone oder Cytosporone befinden. Einige Pilzinhaltsstoffe konnten auch im Extrakt der Wirtspflanze *Rhizophora mucronata* nachgewiesen werden, was beweist, dass *in planta* die gleichen oder zumindest strukturell ähnliche Verbindungen gebildet werden wie auf dem untersuchten Reismedium.

TABLE OF CONTENTS

1 INTRODUCTION	1
1.1 Aims and Scopes of the Study	1
1.2 Mangrove plant <i>Rhizophora mucronata</i>.	1
1.2.1 Introduction of the Mangrove	1
1.2.2 <i>Rhizophora mucronata</i>.	3
1.3 Endophytic fungus <i>Pestalotiopsis</i> sp	4
1.3.1 The definition of Endophytic fungus	4
1.3.2 Biology of fungus <i>Pestalotiopsis</i> sp.	4
1.3.3 Chemistry of fungus <i>Pestalotiopsis</i> sp.	6
1.3.3.1 Alkaloids	7
1.3.3.1.1 Amines and amides	7
1.3.3.1.2 Indole derivatives	8
1.3.3.2 Terpenoids	9
1.3.3.2.1 Monoterpenes	9
1.3.3.2.2 Sesquiterpenes	10
1.3.3.2.2 Diterpenes	13
1.3.3.3 Quinones	15
1.3.3.4 Peptides	19
1.3.3.5 Xanthone derivatives	20
1.3.3.6 Phenol and phenolic acids	21
1.3.3.7 Lactones	22
1.3.3.8 Miscellaneous metabolites	25

1.3.4 Summary of the Previous Work upon <i>Pestalotiopsis</i> sp.	26
2 MATERIALS AND METHODS	28
2.1 Materials	28
2.1.1 Fungal Origin	28
2.1.2 Chemicals	28
2.1.2.1 Technical Grades Solvent for Separation	28
2.1.2.2 Solvents for HPLC and LC/MS	28
2.1.2.3 Solvents for NMR	29
2.2 Methods	29
2.2.1 Isolation and Cultivation of Fungus	29
2.2.2 Fungal Extraction	30
2.2.3 Solvent-Solvent Separation	32
2.2.4 Isolation, Purification and Identification of Secondary Metabolites	33
2.2.4.1 Chromatography	36
2.2.4.1.1 Thin Layer Chromatography	36
2.2.4.1.2 Column Chromatography	37
2.2.4.1.2.1 Silica Column	38
2.2.4.1.2.2 Reverse Phase (RP) Column	39
2.2.4.1.2.3 Sephadex Column	39
2.2.4.1.2.4 Flash Chromatography	40
2.2.4.1.2.5 Vacuum Liquid Chromatography (VLC)	40
2.2.4.1.2.6 Semi Preparative HPLC	41
2.2.4.1.2.7 Analytical HPLC	43

2.2.4.2 Determination of Maximum UV Absorption	44
2.2.4.3 Determination of Molecular Weight	45
2.2.4.3.1 Mass Spectrometry	45
2.2.4.3.1.1 Electron Impact (EI) Mass Spectrometry	46
2.2.4.3.1.2 HRMS	47
2.2.4.3.1.3 ElectroSpray Impact (ESI) Mass Spectrometry	47
2.2.4.3.2 LC/MS	48
2.2.5 Structure Elucidation of Pure Secondary Metabolites	49
2.2.5.1 NMR Measurements	51
2.2.5.1.1 One Dimensional NMR	51
2.2.5.1.1.1 Proton (¹H) NMR	51
2.2.5.1.1.2 Carbon (¹³C) NMR	52
2.2.5.1.1.3 DEPT	53
2.2.5.1.2 Two Dimensional NMR	54
2.2.5.1.2.1 COSY NMR	54
2.2.5.1.2.2 HMQC NMR	55
2.2.5.1.2.3 HMBC NMR	55
2.2.5.1.2.4 NOESY and ROESY NMR	56
2.2.5.2 Circular dichroism (CD) spectroscopy	57
2.2.6 Optical Rotation	58
2.2.7 Bioactivity	60
2.2.7.1 Cytotoxicity Assays	60
2.2.7.2 Anti-bacterial and Anti-fungal Assays	61

2.2.7.2.1 Anti-bacterial Assays	61
2.2.7.2.2 Anti-fungal Assays	61
3 RESULTS—Secondary Metabolites from <i>Pestalotiopsis</i> sp.	63
3.1 Sesquiterpene Derivatives	63
3.1.1 Pestalotiopene A (1, new compound)	63
3.1.2 Pestalotiopene B (2, new compound)	72
3.1.3 Altiloxin B (3, known compound)	76
3.2.1 Pestalotiopsone A (4, new compound)	81
3.2.2 Pestalotiopsone B (5, new compound)	86
3.2.3 Pestalotiopsone C (6, new compound)	89
3.2.4 Pestalotiopsone D (7, new compound)	92
3.2.5 Pestalotiopsone E (8, new compound)	95
3.2.6 Pestalotiopsone F (9, new compound)	98
3.2.7 2-(2'-hydroxypropyl)-5-methyl-7-hydroxy-chromone (10, known compound)	101
3.3 Cytosporone Derivatives	104
3.3.1 Cytosporone J (11, new compound)	104
3.3.2 Cytosporone K (12, new compound)	107
3.3.3 Cytosporone L (13, new compound)	110
3.3.4 Cytosporone C (14, known compound)	113
3.3.5 Cytosporone M (15, new compound)	118
3.3.6 Cytosporone N (16, new compound)	121
3.3.7 Dothiorelone A (17, known compound)	124

3.4 Coumarin Derivatives	127
3.4.1 Pestalotiopsin A (18, new compound)	127
3.4.2 Pestalotiopsin B (19, new compound)	132
3.4.3 Pestalotiopsin C (20, new compound)	135
3.4.4 Pestalotiopsin D (21, new compound)	138
3.4.5 Pestalotiopsin E (22, new compound)	140
3.4.6 3-hydroxymethyl-6,8-dimethoxycoumarin (23, known compound)	143
3.5 Pyrones	146
3.5.1 Pestalotiopyrone A (24, new compound)	146
3.5.2 Pestalotiopyrone B (25, new compound)	150
3.5.3 Pestalotiopyrone C (26, new compound)	153
3.5.4 Nigrosporapyrone D (27, known compound)	156
3.5.5 Pestalotiopyrone D (28, new compound)	159
3.5.6 Pestalotiopyrone E (29, new compound)	162
3.5.7 Pestalotiopyrone F (30, new compound)	165
3.5.8 Pestalotiopyrone G (31, new compound)	168
3.5.9 Pestalotiopyrone H (32, new compound)	171
3.6 Alkaloids	174
3.6.1 Pestalotiopyridine (33, new compound)	174
3.6.2 Pestalotiopsoid A (34, new compound)	176
3.6.3 Pestalotiopamide A (35, new compound)	179
3.6.4 Pestalotiopamide B (36, new compound)	184
3.6.5 Pestalotiopamide C (37, new compound)	191

3.6.6 Pestalotiopamide D (38, new compound)	194
3.6.7 Pestalotiopamide E (39, new compound)	198
3.7 Miscellaneous metabolites	201
3.7.1 Pestalotiopisorin A (40, new compound)	201
3.7.2 Pestalotiollide A (41, new compound)	208
3.7.3 Pestalotiollide B (42, new compound)	215
3.7.4 Pestalotiopin A (43, new compound)	219
3.7.5 2-anhydromevalonic acid (44, known compound)	222
3.7.6 <i>p</i> -hydroxy benzaldehyde (45, known compound)	224
3.7.7 Pestalotilopacid A (46, new compound)	225
3.7.8 Pestalotilopacid B (47, new compound)	229
3.7.9 Pestalotilopacid C (48, new compound)	232
3.8 Biological Activities	235
3.8.1 Cytotoxicity	235
3.9 Tracing fungal metabolites in the host plant <i>Rhizophora</i> <i>mucronata</i> extract	236
4 DISCUSSION—Secondary Metabolites from <i>Pestalotiopsis</i> sp.	240
4.1 Possible joint biosynthetic origin of new skeleton sesquiterpene derivatives (Pestalotiopenes A and B)	240
4.2 Possible biosynthetic origin of chromones (Pestalotiopsones A-F, 5-Carbomethoxymethyl-2-heptyl-7-hydroxychromone)	242
4.3 Possible biosynthetic origin of cytosporones (Cytosporone J-N, Cytosporone C, Dothiorelone B)	244

4.4 Possible biosynthetic origin of coumarins and cyclopaldic acid derivatives	
(Pestalotiopsins A-E, 3-hydroxymethyl-6,8-dimethoxycoumarin, Pestalotiopacid A-C)	247
4.5 Possible biosynthetic origin of alkaloids, pyrones and isocoumarin	
(Pestalotiopamide A-E, Pestalotiopin A, 2-anhydromevalonic acid, Pestalotiopyrones A-H and Nigrosporapyrone D)	249
4.6 Hypothesis about the relationship between the Endophytic fungus	
<i>Pestalotiopsis</i> sp. and the host plant <i>Rhizophora mucronata</i>	251
5 SUMMARY	254
6 REFERENCE	263
7 ATTACHMENTS	270
Curriculum Vitae	328

1 INTRODUCTION

1.1 Aims and Scopes of the Study

A large number of endophytic microbes are associated with plants. The types of biological associations that endophytic microbes may have developed with higher plants range from borderline pathogenic, to commensal, and to symbiotic (Strobel 2002)

In the case of our study of the relationship between endophytic microbes and their host plants, an interesting fungus *Pestalotiopsis* sp. residing within the leaves of the Chinese Mangrove plant *Rhizophora mucronata* was selected for a study of its new and unusual secondary metabolites, which may contribute to the understanding of the host–microbe relationship and at the same time provide new and interesting bioactive compounds that may find uses in medicine, industry, and agriculture.

1.2 Mangrove plant *Rhizophora mucronata*.

Why do we choose the Mangrove plant *Rhizophora mucronata* as the host plant?

1.2.1 Introduction of Mangroves

Mangroves, a kind of special host plants, is a resource which contains abundant endophytic fungi. More than 200 different species of endophytic fungi have been isolated and identified from mangroves, being the second largest community of marine fungi. (Liu

et al. 2007)

Mangroves are generally found along the coastlines of tropical and subtropical regions, between Florida, the Argentinean South coast, West- and East African coast and Indian Subcontinent up until Japan, New Zealand, Indonesia, and Malaysia.

The area of mangrove forests worldwide is estimated at around 17,000,000 hectares, which is about one percent of the entire tropical rainforest on earth.

Walsh (1874) considered the world mangroves to be broadly divided into two main areas:

- the flourishing rich mangroves of the Indo-pacific ocean “eastern mangroves”
- the poorer “western mangroves” of the Atlantic ocean.

He also suggested five basic requirements for extensive mangrove development which are: (1) tropical temperature, (2) fine grained alluvium soil, (3) low wave and tidal action, (4) salt water and (5) large tidal range.

Only very few plants can tolerate the harsh environment and flourish there - mud saturated with salt that frequently is inundated by ocean and river water.

Most land plants are killed by salt, but mangroves are able to survive under these

conditions. Most plants die if their roots are drowned in water thus leaving them without oxygen, and in the mud of mangrove swamps, the rotting leaves usually consume all available oxygen. However mangrove trees have developed special kinds of roots that stick up - out of the mud and into the air - to get oxygen.

A question then may generate, if the mangrove plant endophytic fungus enhanced their host's capabilities to endure the harsh environment?

1.2.2 *Rhizophora mucronata*.

Rhizophora mucronata occurs on the coasts of the Indian Ocean and the West-Pacific. The species is an evergreen tree of approximately 25–30 m height, with numerous branching arching stilt roots.

Extracts from *Rhizophora mucronata* are used in folklore medicine and are reported to be astringent. Asiatic mangrove is a folk remedy for angina, diabetes, diarrhea, dysentery, hematuria, and hemorrhage (Duke and Wain, 1981). Leaves are poulticed onto armored fish to cure injuries (Watt and Breyer-Brandwijk, 1962). Indochinese use the roots for the treatment of angina and hemorrhage. Malaysians use old leaves and/or roots for childbirth. Burmese use the bark for the treatment of bloody urine, Chinese and Japanese for treatment of diarrhea, and Indochinese for angina (Perry, 1980).

The next questions then may generate, if some of the secondary metabolites of the

mangrove plant endophytic fungus are the same as which generated by the host plant? Would they have the similar medicinal uses as the host plant *Rhizophora mucronata* or other kinds of bioactivities?

1.3 Endophytic fungus *Pestalotiopsis* sp.

Why do we choose the endophytic fungus *Pestalotiopsis* sp. for our research?

1.3.1 The definition of Endophytic fungus

An endophytic fungus is some kind of microorganism which spends the whole or part of its life cycle colonizing inter and /or intra-cellularly inside the healthy tissues of the host plant, typically causing no apparent symptoms of disease. (Tan *et al.* 2001)

1.3.2 Biology of fungus *Pestalotiopsis* sp.

Fungi of the genus *Pestalotiopsis*, occurring on a wide range of substrata, are broadly distributed in the world (Wang *et al.* 2005). Endophytic species of *Pestalotiopsis*, commonly isolated from tropical plants, are considered as main members of the *Pestalotiopsis* community in nature, which have been commonly isolated particularly from tropical higher plants. (Suryanarayanan *et al.* 2000; Stobel *et al.* 2004; Toofanee *et al.* 2002; Cannon *et al.* 2002; Liu *et al.* 2007)

The fungal species of the genus *Pestalotiopsis* belong to the anamorphic member of the family *Amphisphaeriaceae*, (Bayman *et al.* 1998; Zhu *et al.* 1991; Kang *et al.* 1998; Kang *et al.* 1999) whose classification was established by Steyaert, following a taxonomic amendment differentiated from the genus *Pestalotia*. (Steyaert 1949; Steyaert 1953) Molecular studies have shown a conspicuous monophyletic character that *Pestalotiopsis* possess relatively fusiform conidia formed within compact acervuli and the conidia are usually 5-celled with 3 coloured median cells and colourless end cells, and with two to more apical appendages arising from the apical cell (Jeewon *et al.* 2003). However, *Pestalotiopsis*, a complex genus, consists of members that are difficult to be classified to the species level. *Pestalotiopsis* is one of the most ubiquitously distributed genus, occurring on a wide range of substrata and 232 named species are listed in *Index Fungorum* <http://www.indexfungorum.org/Names/Names.asp>.

Many *Pestalotiopsis* species are saprobes in soil (Agarwal *et al.* 1988), degraders of plant materials (Okane and Nagagiri 1998; Osono and Takeda 1999; Tokumasu and Aoiki, 2002) or organisms growing on decaying wild fruits (Tang *et al.* 2003; Wu *et al.* 1982), while others are either plant pathogens (e.g. *Pestalotiopsis funerea*, *P. microspora*, *P. maculans*, *P. palmarum* and *P. besseyi*) (Kohlmeyer *et al.* 2001) or endophytes residing in living plant leaves and twigs (Strobel *et al.* 1996; Strobel *et al.* 1997; Strobel *et al.* 2000; Wei *et al.* 2007). Generally, this fungus causes diseases of a variety of plants, but at times it may act in a more severe manner and result in major plant loss. (Hopkins *et al.* 2000; Taylor *et al.* 2001; Keith *et al.* 2006; Li *et al.* 2001)

P. oenotherae was reported to induce leaf spot disease of evening primrose. *P. theae* and *P. longiseta* are known to be the pathogenic fungi for tea gray blight disease. During recent years, *Pestalotiopsis* species have gained much attention. Many important secondary metabolites that are potential leads for treatment of human diseases and control of plant diseases, such as acetogenins, antioxidants, immunosuppressants, and anticancer agents, *etc.*, have been identified from this genus (Li *et al.*, 2001; Strobel *et al.*, 1996). Thus, the focus of this part of introduction is to summarize the known secondary metabolites from fungi of *Pestalotiopsis* species and their bioactivities. These can be grouped into eleven types, including alkaloids, chromenones, chromones, coumarins, lactones, peptides, phenol, phenolic acids, polyketides, quinones, and terpenoids, *etc.*

1.3.3 Overview of the Chemistry of fungus *Pestalotiopsis* sp.

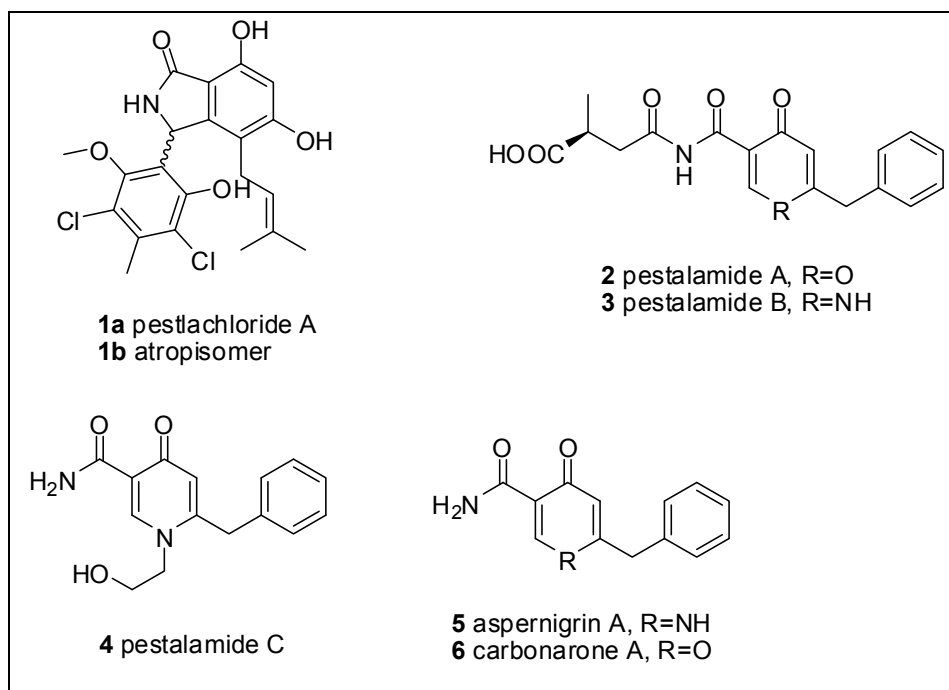
Secondary metabolites from the fungus genus *Pestalotiopsis* have a broad spectrum of biological activities. Since the discovery of the anticancer agent taxol from an endophytic fungal strain of the genus *Pestalotiopsis* (Strobel *et al.* 1996a; Li *et al.* 1996), interest to find bioactive compounds from this fungal genus has increased considerably.

Previous chemical investigations of *Pestalotiopsis* spp. led to the discovery of various bioactive natural products such as polyketides and terpenoids (Schulz *et al.* 2002). To date, secondary metabolites found from this fungal genus can be grouped into eight types, including alkaloids, terpenoids, quinones, peptides, xanthenes, phenol and phenolic acids, lactones, *etc.*

1.3.3.1 Alkaloids

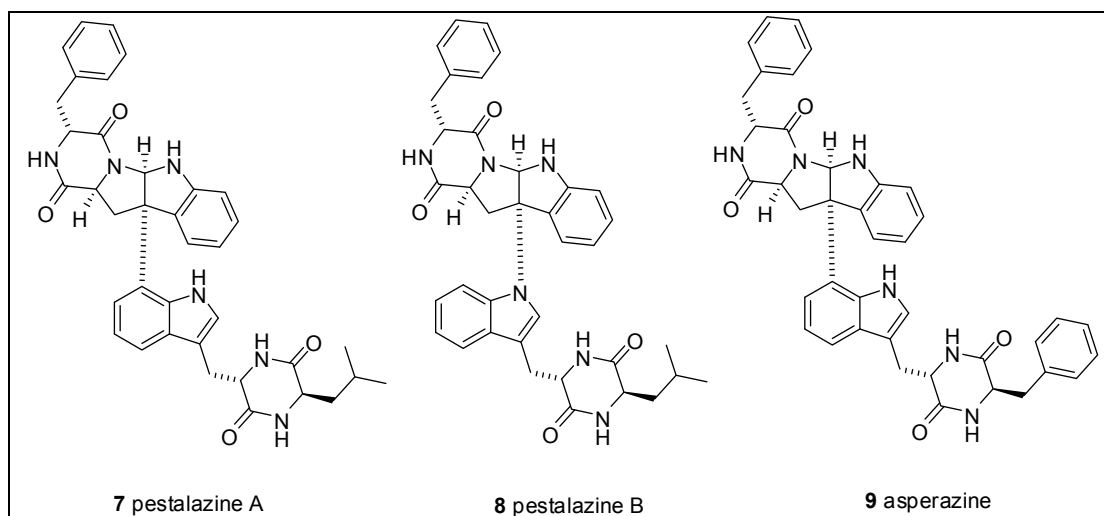
1.3.3.1.1 Amines and amides

Pestalachloride A (**1**), a new chlorinated benzophenone alkaloid, was isolated from the culture of the plant endophytic fungus *P. adusta* (Li *et al.* 2009). However, due to the hindered internal rotation around the C-8/C-9 bond in **1**, two atropisomers (**1a** and **1b**) were observed. Compound **1** differs significantly from those known alkaloids by having a relatively rare 2,4-dichloro-5-methoxy-3-methylphenol moiety connected to the isoindolin-1-one core structure. In addition, this metabolite also displayed potent antifungal activity against *Fusarium culmorum* with an IC₅₀ value of 0.89 μ M. Chemical investigation of the plant pathogenic fungus *P. theae*, obtained from branches of *Camellia sinensis*, afforded three new amides, pestalamindes A-C (**2-4**) and two known metabolites, aspernigrin A (**5**) and carbonarone A (**6**). (Ding *et al.* 2008) Bioassay tests revealed that pestalaminde B inhibited HIV-1 replication in C8166 cells with EC₅₀ of 64.2 μ M and exhibited potent antifungal activity against *A. fumigatus* with IC₅₀/MIC values of 1.50/57.8 μ M.



1.3.3.1.2 Indole derivatives

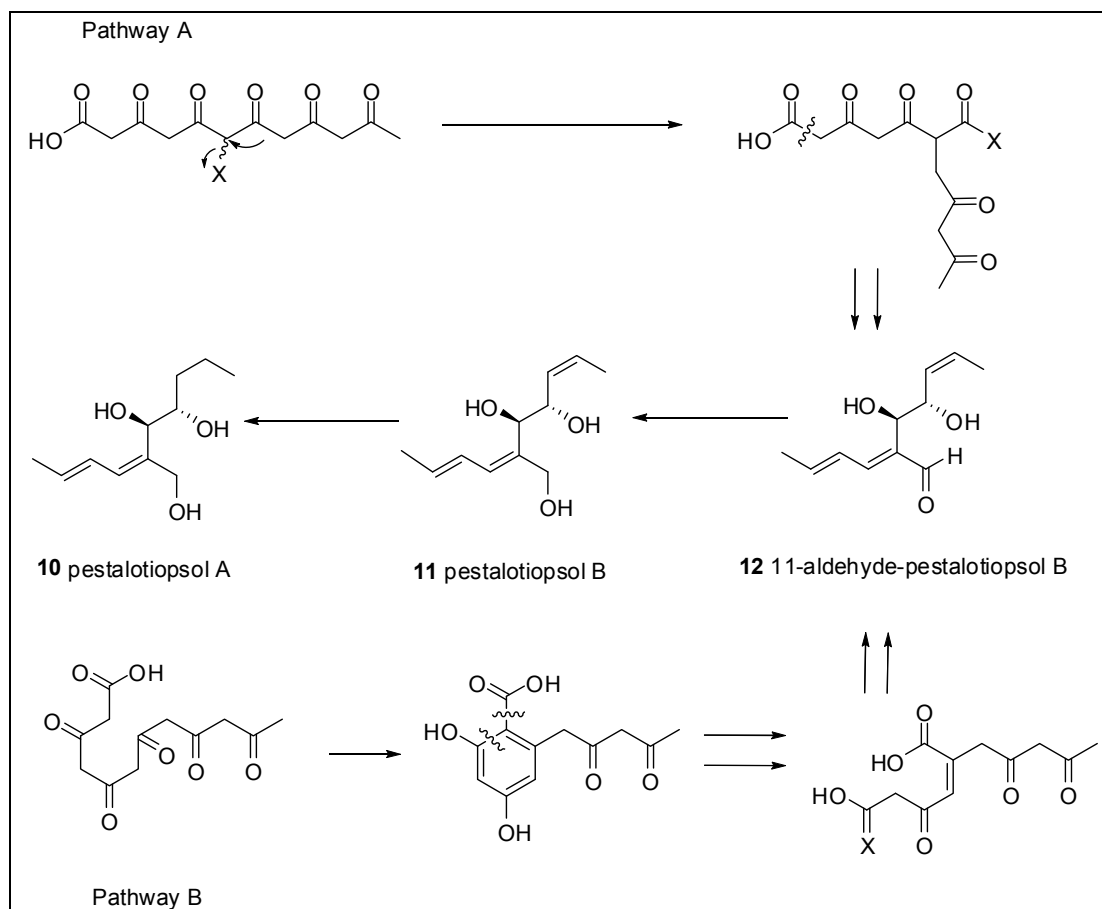
Two new diketopiperazine heterodimers, pestalazines A (**7**) and B (**8**), were isolated from the plant pathogenic fungus *P. theae* found in branches of *Camellia sinensis*, together with the known metabolite asperazine (**9**). Bioassay test *in vitro* against HIV-1 disclosed that compounds **7** and **9** showed inhibitory effects against HIV-1 replication in C8166 cells with EC₅₀ of 47.4 and 98.9 μ M, respectively. (Ding *et al.* 2008)



1.3.3.2 Terpenoids

1.3.3.2.1 Monoterpenes

Three new monoterpenes, C-methylated acetogenins **10-12**, which have been found in the endophytic fungus reside, *Pestalotiopsis* spp., in the bark and leaves of *Taxus brevifolia*, were shown to be of chemotaxonomic significance (Pulici *et al.* 1997). Two possible biosynthesis pathways related to these metabolites from polyketide precursors have been proposed as shown in [Scheme 1.3.3.2.1.1](#).



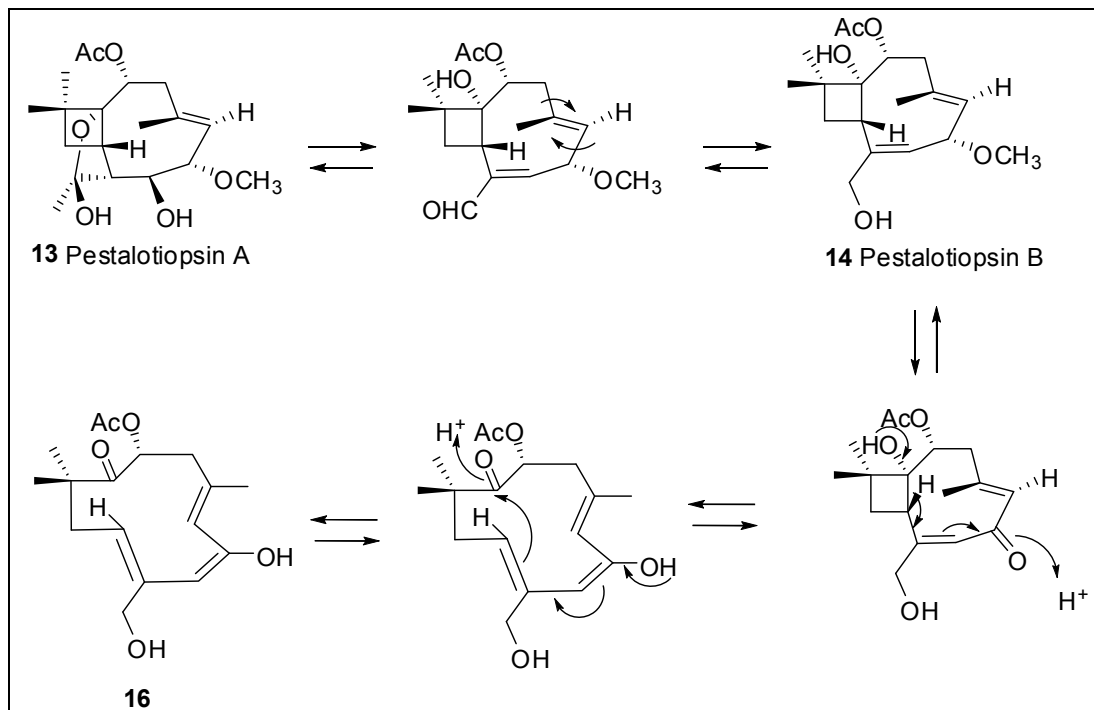
Scheme 1.3.3.2.1.1 Proposed pathways for the formation of compounds **10**, **11**, and **12**

1.3.3.2.2 Sesquiterpenes

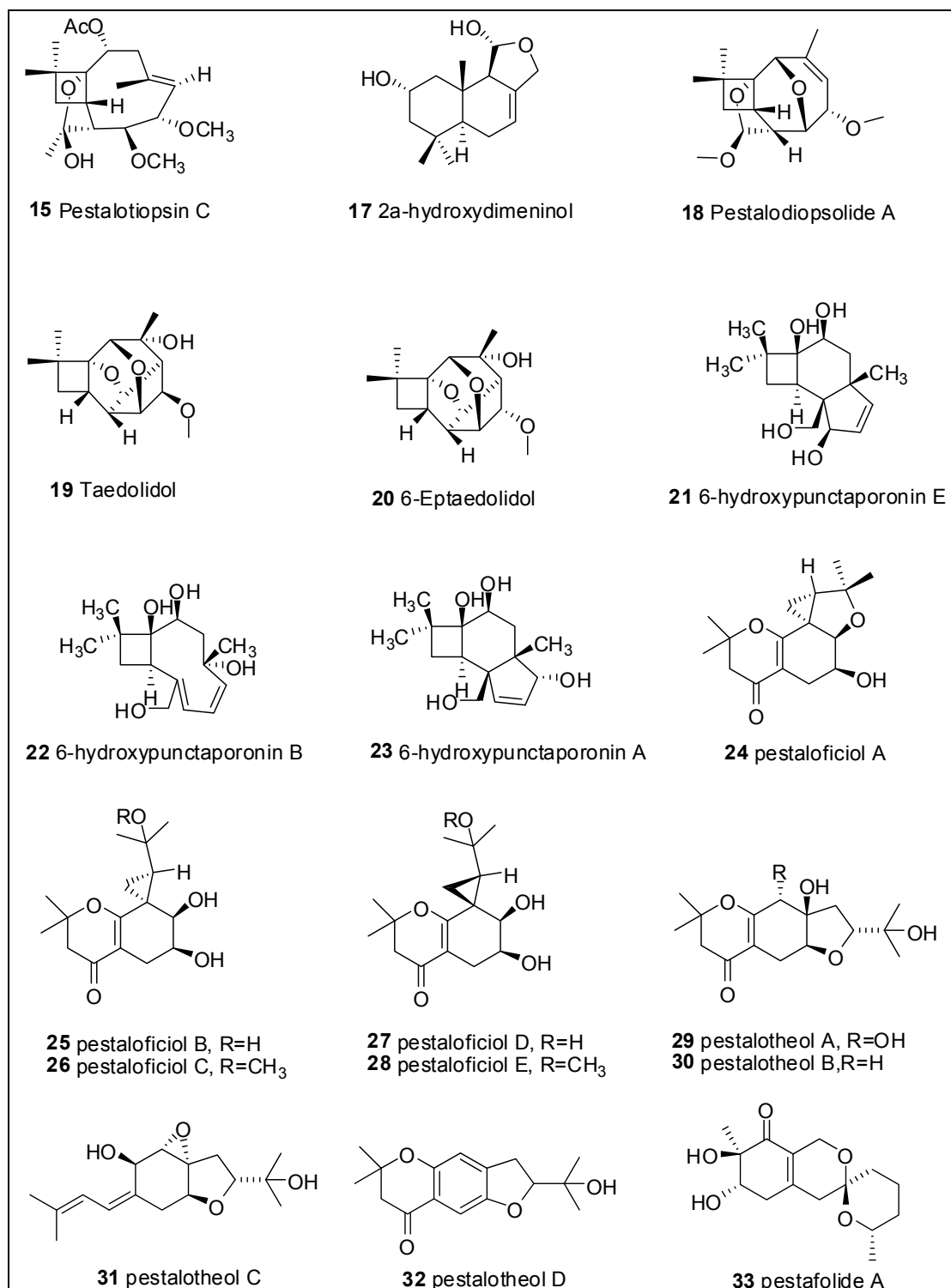
Pestalotiopsis sp. was proved to be a good source of sesquiterpenes. Detailed investigation on the first strain of endophytic fungus *Pestalotiopsis* sp. (JCM 9685 and JCM 9686) associated with the bark and leaves of *Taxus brevifolia*, revealed five sesquiterpenes, among which pestalotiopsin A-C (**13-15**) were caryophyllene type, the fourth one possessed the humulane skeleton **16** and the last one was a drimane derivative **17**. It should be noted that no sesquiterpene of highly functionalized humulane

derivatives had been reported from fungi before the isolation of compound **16**. It was suggested that a possible metabolic relationship should be among compounds **13**, **15**, and **16** in [Scheme 1.3.3.2.2.1](#) (Pulici *et al.* 1997; Pulici *et al.* 1996; Pulici *et al.* 1996). Three highly oxygenated caryophyllene sesquiterpene derivatives, named pestalotiopsolide A (**18**), taedolidol (**19**) and 6-epitaedolidol (**20**), were characterized from a liquid medium culture of a *Pestalotiopsis* sp., obtained from the trunk bark of *Pinus taeda* (Magnani *et al.* 2003). Additional, three new caryophyllene-type sesquiterpene alcohols, 6-hydroxypunctaporonin E (**21**), 6-hydroxypunctaporonin B (**22**) and 6-hydroxypunctaporonin A (**23**), were purified from the culture of the fungicolous fungus *P. disseminata*. In disk diffusion assays, metabolites **21** and **22** exhibited antibacterial activities against *Bacillus subtilis* (ATCC 6051) and *Staphylococcus aureus* (ATCC 29213) (Deyrup *et al.* 2006). A series of new chromenone type metabolites with a cyclopropane moiety, pestaloficiols A–E (**24–28**) and pestalothols A–D (**29–32**), have been reported from the cultures of the plant endophyte *P. fici* and *P. theae*, respectively (Liu *et al.* 2008; Li *et al.* 2008). Compounds **24–28** were supposed to be biogenetically derived from two units of prenoids and one polyketide, among which **24**, **25** and **27** displayed inhibitory effects against HIV-1 replication in C8166 cells (Liu *et al.* 2008). Among the products **29–32**, which could be biosynthetically derived from two units of isoprenoids and a polyketide, compound **31** was speculated to be the precursor of the other three metabolites, compound **31** displayed an inhibitory effect against HIV-1_{LAI} replication in C8166 cells with an EC₅₀ value of 16.1 μ M (Li *et al.* 2008). A new reduced spiro azaphilone derivative, pestafolide A (**33**), was purified from a culture of plant

endophytic fungus *P. foedan*, and displayed antifungal activity against *Aspergillus fumigatus* (ATCC10894) (Ding *et al.* 2008).

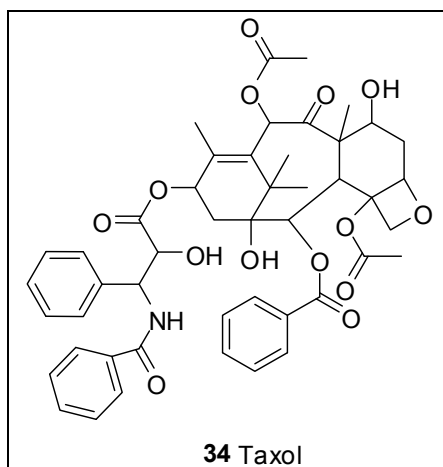


Scheme 1.3.3.2.1 Possible metabolic relationship between compounds **13**, **14** and **16**



1.3.3.2.2 Diterpenes

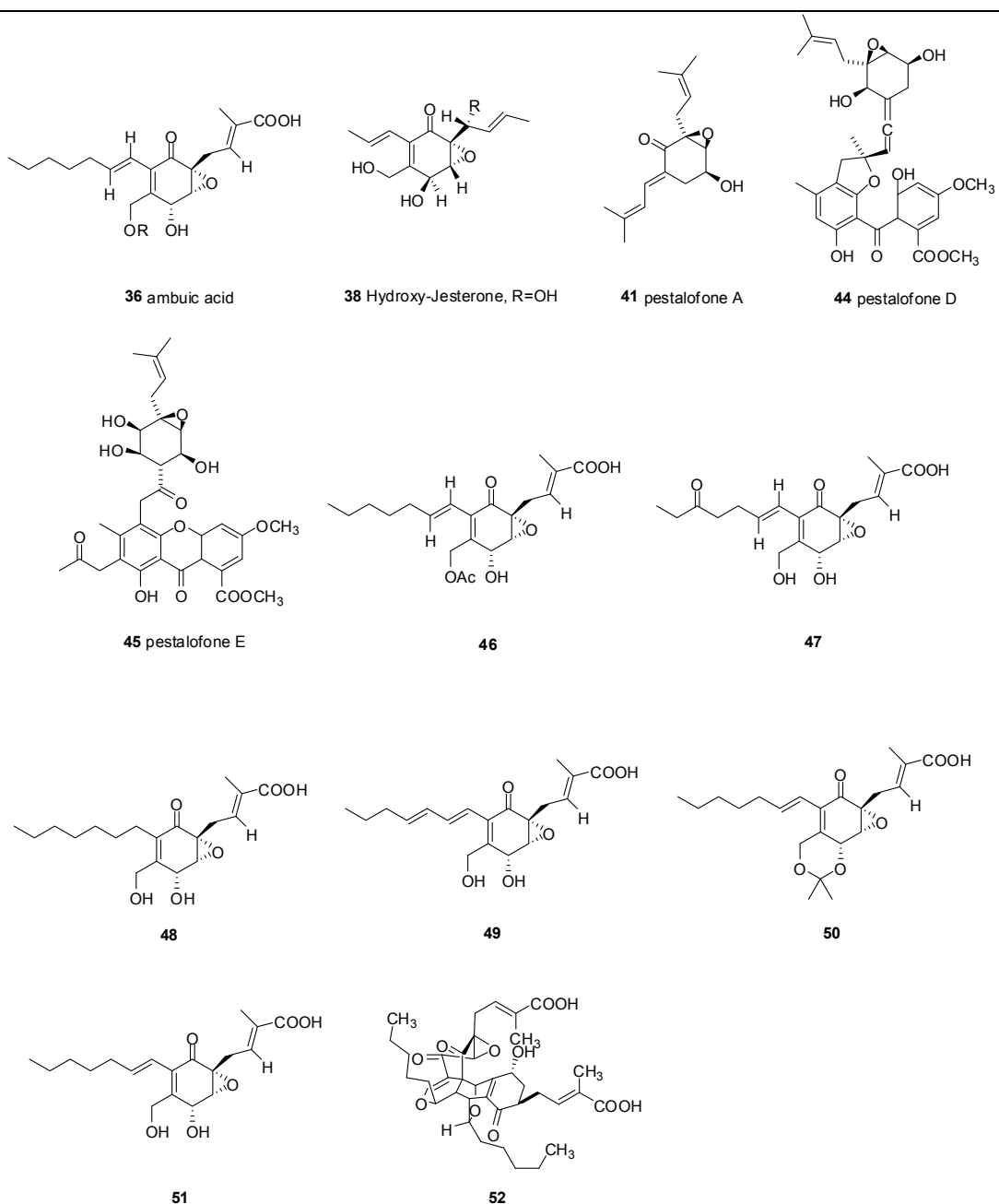
Taxol (**34**), which had been previously supposed to be occurred only in the inner bark of the Pacific yew *Taxus brevifolia* and its endophytic fungus (Stierle *et al.* 1993; Stierle *et al.* 1995; Qiu *et al.* 1994; Caruso *et al.* 2000; Wang *et al.* 2000), was surprisingly reported to be isolated from the fungi genus *Pestalotiopsis*, being even not related to *Taxus*. *P. microspora* (Strobel *et al.* 1996; Strobel *et al.* 1996a; Li *et al.* 1996), *P. guepinii* (Strobel *et al.* 1997), and *P. pauciseta* (Gangadevi *et al.* 2008) were isolated as endophytes from *Taxus wallachiana* (Strobel *et al.* 1996), *Taxus cuspidate* (Strobel *et al.* 1996a), *Taxus distichum* (Li *et al.* 1996), *Wollemia nobilis* (Strobel *et al.* 1997), and *Cardiospermum helicacabum* (Gangadevi *et al.* 2008), respectively. Compound **34**, a highly functionalized diterpene which displayed efficacious anticancer activities mainly against breast and ovarian cancer, was the world's first billion dollar anticancer drug. Its unique mode of action, preventing the depolymerization of tubulin during the processes of cell division, made it a huge success in both clinic and market (Wani *et al.* 1971; Holmes *et al.* 1995). However, the biosynthetic route to Taxol and other taxanes in endophytic fungi is still not very clear. It would be fascinating if Taxol could be supplied through a scaled-up fermentation of such *pestalotiopsis* fungi.

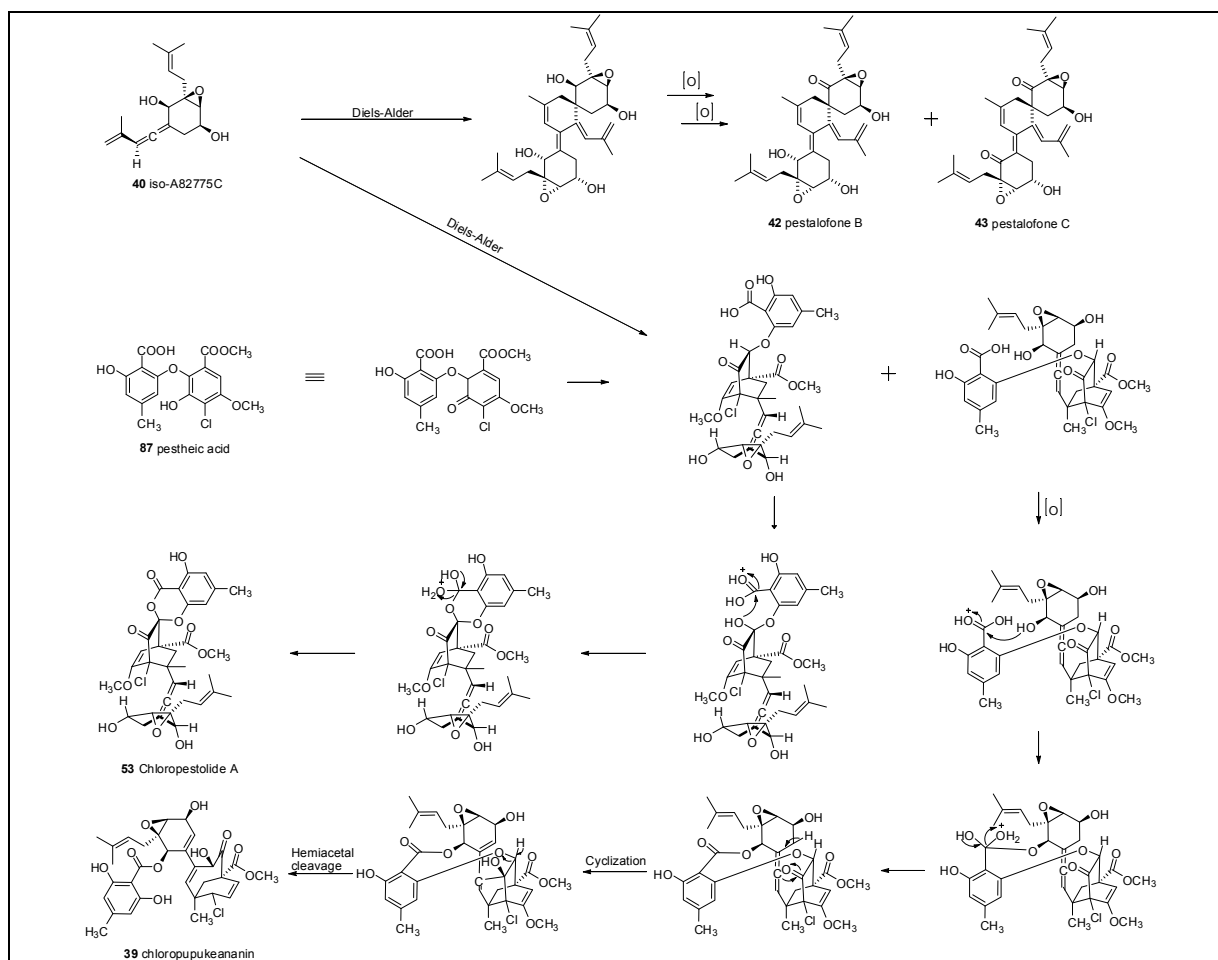


1.3.3.3 Quinones

Lee *et al.* obtained a selectively cytotoxic dimeric quinone, Torreyanic acid (**35**), from *Pestalotiopsis microspora* colonizing in the plant *Torreya taxifolia*. Compound **35** showed fifteen times more potent in cell lines that are sensitive to protein kinase C (PKC) agonists and it caused cell death by apoptosis with IC₅₀ values range from 3.5 (NEC) to 45 (A549) μM /mL, and with a mean value of 9.4 μM /mL against twenty-five different cell lines. Torreyanic acid also showed G1 arrest of G0 synchronized cells at the level of 1-5 μM /mL, depending on different cell lines. A plausible biosynthetic scheme was proposed in [Scheme 1.3.3.3.1](#) (Lee *et al.* 1996). Ambuic acid (**36**), a quinone epoxide metabolite with potent antifungal activity, was characterized from *Pestalotiopsis* spp. living in several of the major representative rainforests of the world (Li *et al.* 2001). Jesterone (**37**) and hydroxyjesterone (**38**), two novel highly functionalized cyclohexenone epoxides, were identified from the endophytic fungus species *P. jesteri* isolated from the inner bark of small limbs of *Fragraea bodenii*. Both **37** and **38** are antimycotics. Significantly, metabolite **37** displayed impressive antimycotic activity against phytopathogenic oomycetes *Pythium ultimum*, *Aphanomyces* sp., *Phytophthora citrophthora*, *P. citrophthora* and *P. cinnamomi* (Li *et al.* 2001). The total synthesis of **37** was accomplished in fourteen steps, as shown in [Scheme 1.3.3.3.2](#). The route involved a diastereoselective epoxidation of a chiral quinone monoketal derivative and regio- and stereoselective reduction of a quinone epoxide intermediate. Chloropupukeananin (**39**), the first pupukeanane chloride with highly functionalized tricyclo-[4.3.1.0^{3,7}]-decane skeleton, was currently evaluated from the plant endophyte *P. fici*, together with its

possible biosynthetic precursor iso-A82775C (**40**). The biosynthesis pathway for **39** was proposed in [Scheme 1.3.3.3.2.3](#) (Liu *et al.* 2008; Liu *et al.* 2009). Bioassay-guided separation of the culture medium of plant endophytic fungus *P. fici* resulted in the isolation of five new cyclohexanone derivatives, pestalofones A–E(**41–45**). Compounds **41**, **42** and **45** exhibited inhibitory effects against HIV-1 replication in C8166 cells with EC₅₀ values of 90.4, 64.0, and 93.7 μ M, respectively, whereas **43** and **45** showed significant antifungal activity against *Aspergillus fumigatus* with IC₅₀/MIC values of 1.10/35.3, 0.90/31.2 μ M, respectively. Compounds **42** and **43** presumed to be derived from the precursor **40** through Diels-Alder reaction were shown in [Scheme 1.3.3.3.2](#) (Liu *et al.* 2009). Six new ambuic acid derivatives **46–51** and a new torreyanic acid analogue **52** have been isolated from the crude extract of endophytic fungus *Pestalotiopsis* sp. inhabiting the lichen *Clavarioids* sp. Compounds **46** and **47** displayed antimicrobial activity against the Gram-positive bacterium *Staphylococcus aureus* (Ding *et al.* 2009). Chloropestolide A (**53**), a highly functionalized spiroketal with an unprecedented skeleton derived from a chlorinated bicyclo-[2.2.2]-oct-2-en-5-one ring and a 2,6-dihydroxy-4-methylbenzoic acid unit, has been isolated from the scale-up fermentation extract of *P. fici*. **53** could be derived from the same Diels-Alder precursors as **39** and showed significant inhibitory effects on growth of two human cancer cell lines, HeLa and HT29, with GI₅₀ values of 0.7 and 4.2 μ M, respectively. (Liu *et al.* 2009)

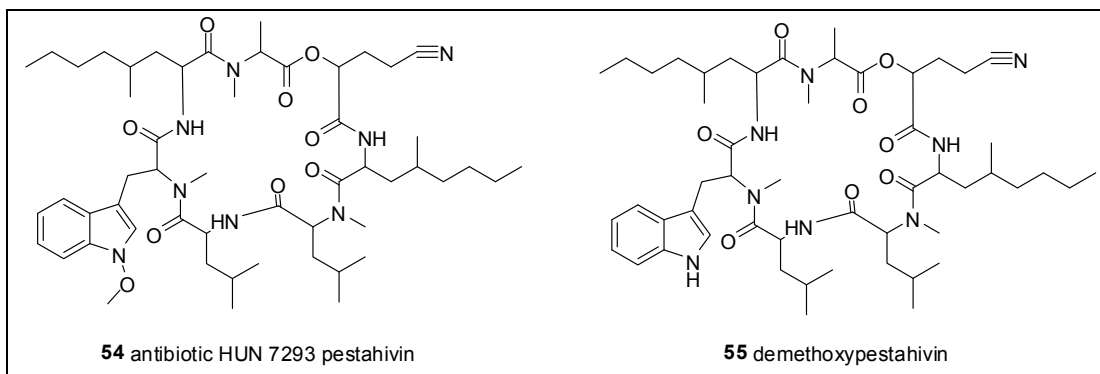




Scheme 1.3.3.3 A Proposed Biosynthetic Pathway for the Generation of **39**, **42**, **43**, **53**

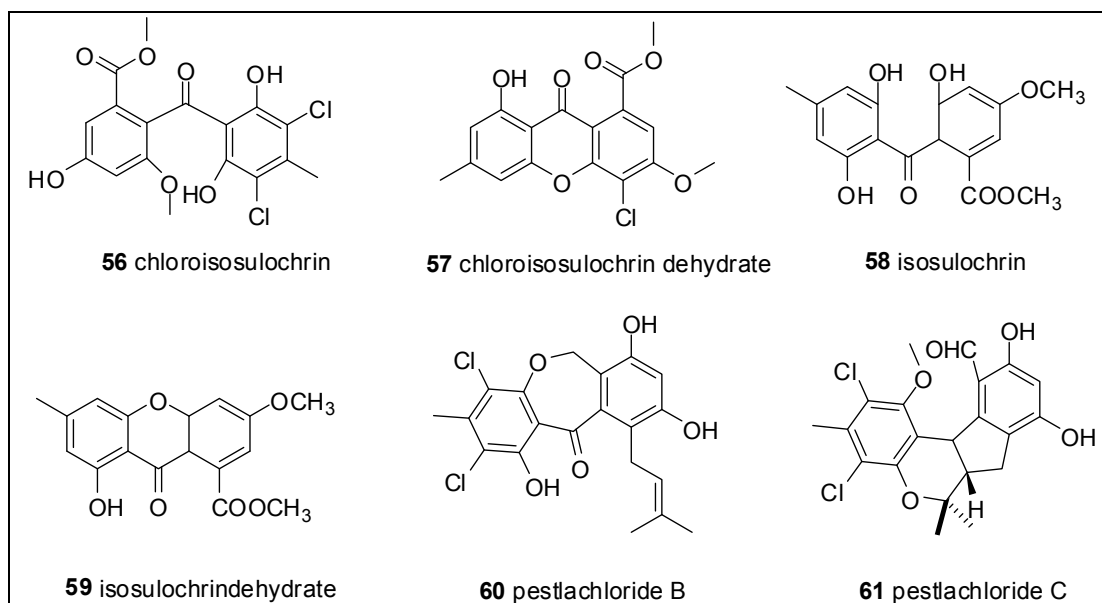
1.3.3.4 Peptides

Cyclopeptolide antibiotic HUN-7293 pestahivin (**54**) and anti-HIV agent pestahivin DM (**55**) were purified from *pestalotiopsis* sp. RF5890 (Japan Patent 1995). Compound **54**, which was reported as a naturally-occurring inhibitor of inducible cell adhesion molecule expression and the prototypical lead of a new class of potential therapeutics for the treatment of chronic inflammatory disorders or autoimmune diseases, potently suppressed cytokine-induced expression of VCAM-1 on human endothelial cells (Hommel *et al.* 1996; Foster *et al.* 1994).



1.3.3.5 Xanthone derivatives

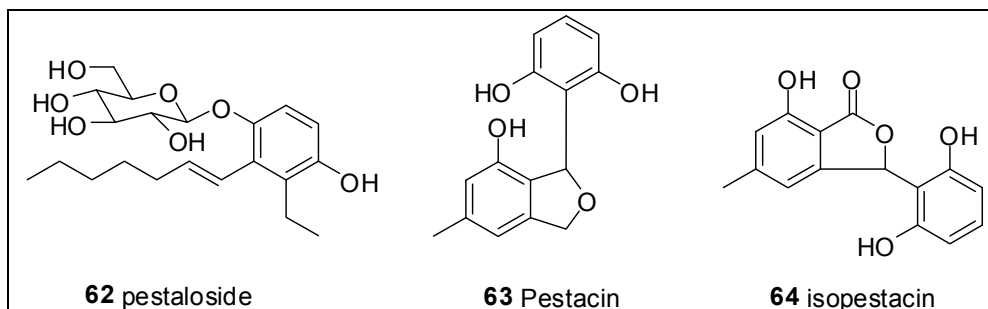
Two new plant growth regulators, named chloroisosulochrin (**56**) and chloroisosulochrin dehydrate (**57**), have been isolated from the Raulin-Thom medium cultured filtrate of *P. theae*, along with two known metabolites isosulochrin (**58**) and isosulochrindehydrate (**59**) (Shimada *et al.* 2001). Pestalachlorides B (**60**) and C (**61**) were two new chlorinated benzophenone derivatives encountered in a plant endophytic fungus *P. adusta*. Compound **60** was reported to exhibit remarkable antifungal activities against the plant pathogen *Gibberella zeae* (CGMCC 3.2873) with an IC_{50} value of 1.1 μ M (Li *et al.* 2008).



1.3.3.6 Phenol and phenolic acids

Phenol and phenolic acids are popular in cultures of fungi. Pestaloside (**62**), a phytotoxin, was characterized from the axenic fungal culture of *P. microspora*. Compound **62**, proposed to be more competitive than other fungal metabolites of *Torreya taxifolia*, showed potent antifungal activities against *Cladosporium* species, *Rhizoctonia solani*, *Geotrichum candidum*, and *Agricus campestris* (Lee et al. 1995). Two novel dihydroisobenzofuran-carrying phenols, pestacin (**63**) and isopestacin (**64**), were isolated from *P. microspora*, which was associated with the combretaceous plant *Terminalia morobensis*, being native to the rainforest of Papua New Guinea (Harper et al. 2003; Strobel et al. 2002). Compound **63** exhibited moderate antifungal activity towards the important root-invading pathogen *Pythium ultimum* and showed antioxidant activities, being eleven times greater than that of the vitamin E derivative, trolox (Harper et al. 2003). Compound **64** exhibited moderate antimycotic activities against plant pathogenic

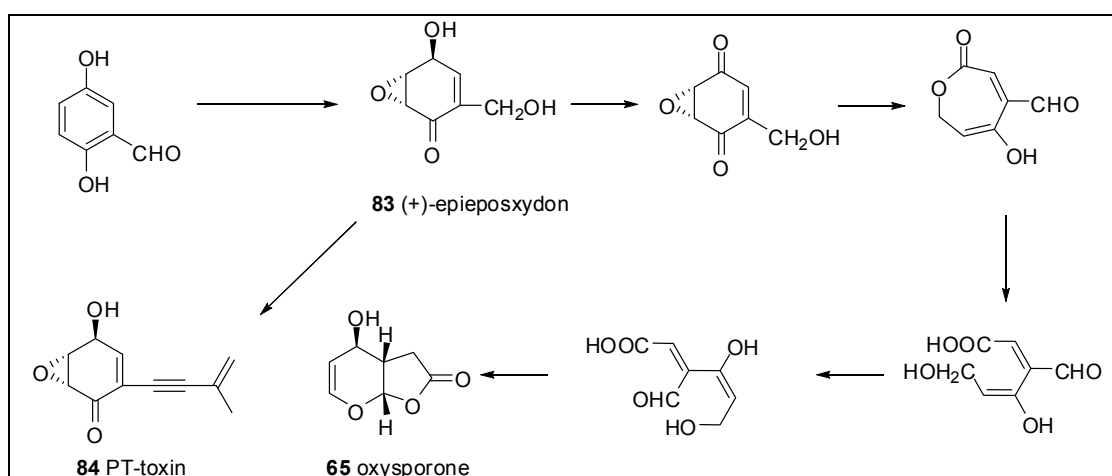
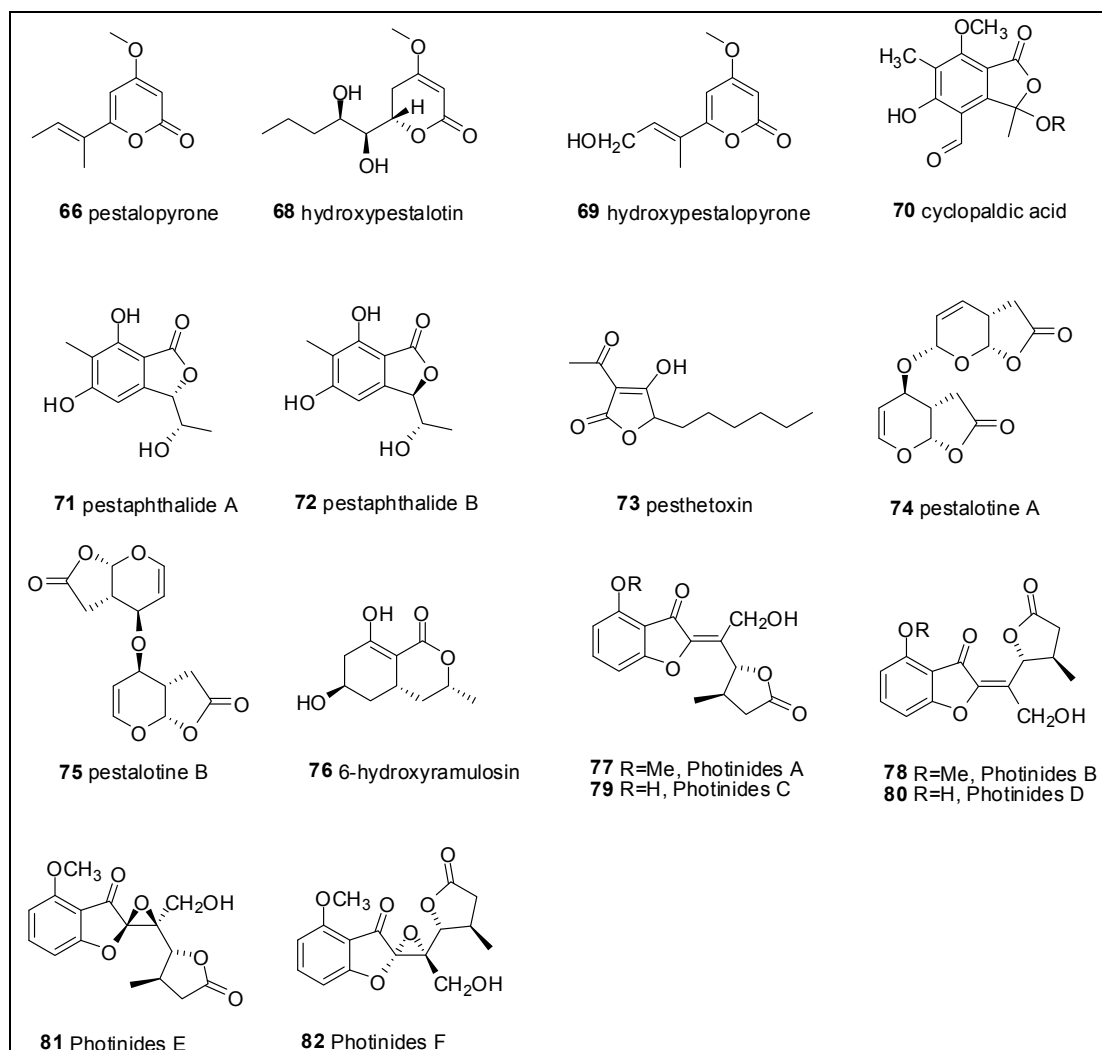
oomycete *Pythium ultimum*, ascomycete *Sclerotinia sclerotiorum* and basidiomycete *Rhizoctonia solani* (Strobel *et al.* 2002).



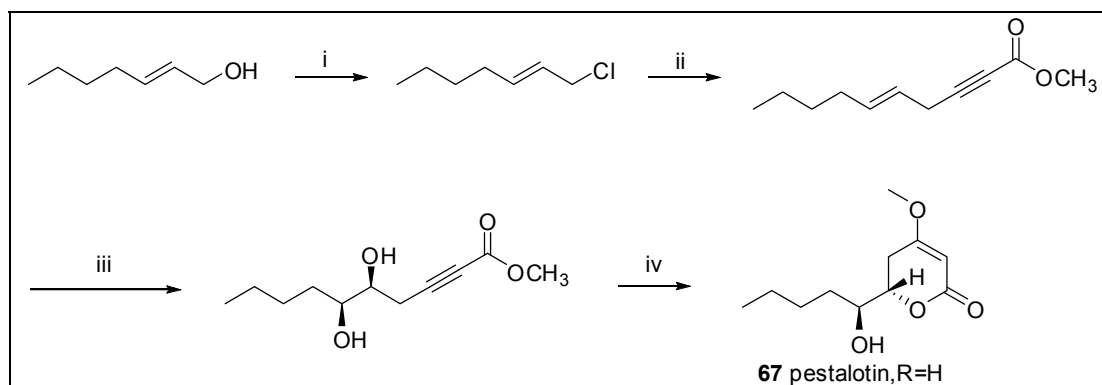
1.3.3.7 Lactones

Lactone derivative was one of the most popular type of compounds produced by the fungus genus *Pestalotiopsis*. Besides the phytotoxins, oxysporone (**65**) and pestalopyrone (**66**), two weakly toxic components and gibberellin synergists, pestalotin (**67**) and hydroxypestalotin (**68**), were isolated from a pathogen of evening primrose *P. oenotherae* (Venkatasubbaiah *et al.* 1991). A biosynthetic pathway for compound **65** was proposed in [Scheme 1.3.3.7.1](#) (Nagata *et al.* 1992). An effective synthesis route toward **67** using asymmetric dihydroxylation was achieved in four steps, as shown in [Scheme 1.3.3.7.2](#) (Wang *et al.* 1997). A similar phytotoxin, hydropestalopyrone (**69**), was characterized from *P. microspora* obtained as endophytes of plants collected from the northern American endangered trees (Lee *et al.* 1995). A previously known antibiotic, cyclopaldic acid (**70**), was elaborated by the fungal endophyte *Pestalotiopsis* and was reported to display non-selective antifungal activity towards species of *Botrytis*, *Fusarium* and *Geotrichum* (Turner *et al.* 1983; Graniti *et al.* 1992). Pestaphthalides A (**71**) and B (**72**),

having modest antifungal activity, were two new isobenzofuranones encountered in *P. foedan*, an endophyte in the branches of an unidentified tree near Dongzai, Hainan Province (Ding *et al.* 2008). The other new phytotoxin was pesthetoxin (**73**) produced by the gray blight fungus *P. theae* (Kimura *et al.* 1998). Two new phytotoxic γ -lactones, pestalotines A (**74**) and B (**75**), were isolated from the culture of *Pestalotiopsis* sp. HC02, a fungus residing in the *Chondracris roseae* gut, along with 6-hydroxyramulosin (**76**). Among the above phytotoxins, compounds **74** and **75** can notably inhibit the radical growth of *Echinochloa crusgalli* with IC_{50} values of 1.85×10^{-4} and 2.50×10^{-4} M, respectively, being comparable to that of 2-(2,4-dichlorophenoxy) acetic acid (0.94×10^{-4} M), which was used as a positive control (Zhang *et al.* 2008). Photinides A-F (**77-82**), six new unique benzofuranone-derived γ -lactones, had been isolated from the crude extract of the plant endophytic fungus *P. photiniae*. Compounds **77-82** displayed modest cytotoxic effects against the human tumor cell line MDA-MB-231 (Ding *et al.* 2009).



Scheme 1.3.3.7.1 Biosynthetic relationship between compound 65, 83 and 84



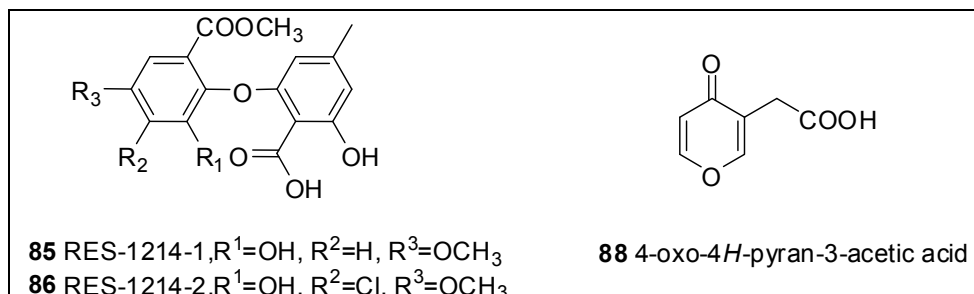
Scheme 1.3.3.7.2 stereoselective synthesis of compound **67**

i: CCl_4 , PPh_3 , r.t. (91%); ii: Methyl propiolate, DBU, CuI , phenothiazine, $\text{NH}_2\text{OH} \cdot \text{H}_2\text{O}$, HMPA/THF, 60°C (65%); iii: AD-mix- α , 0°C (94%); iv: MeONa , MeOH , 0°C (94%).

1.3.3.8 Miscellaneous metabolites

In order to find new phytotoxins, (+)-epieposxydon (**83**) and PT-toxin (**84**) were purified from the tea gray blight fungi, *P. longiseta* and *P. oenotherae*, respectively. Their biosynthetic pathway had been proposed in [Scheme 1.3.3.7.1](#) (Nagata *et al.* 1992). RES-1214-1 (**85**) and RES-1214-2 (**86**), novel and non-peptide endothelin antagonists, were isolated from the culture broth of a fungus, *Pestalotiopsis* sp. RE-1214. Compounds **85** and **86** could selectively inhibit the ET-1 binding to endothelin type A receptor (ETA receptor) with IC_{50} values of $1.5 \mu\text{M}$ and $20 \mu\text{M}$, respectively (Ogawa *et al.* 1995). Plant growth regulator, pestheic acid (**87**), has been reported from the culture of two endophytic fungal strains, *P. fici* and *P. theae*. (Liu *et al.* 2008; Shimada *et al.* 2001) Natural occurrence of **87** led to the suggestion that it might be a biosynthetic precursor of **39** (Shimada *et al.* 2001). 4-oxo-4H-pyran-3-acetic acid (**88**) was isolated by Tan and his

coworkers (Zhang *et al.* 2008) from the *Chondracris rosea* endophytic fungus *Pestalotiopsis* sp. HC02.



1.3.4 Summary of the Previous Work upon *Pestalotiopsis* sp.

In Chart 1.3.3, we have systematically summarized the chemistry and bioactivity of the secondary metabolites from the fungal genus *Pestalotiopsis*. It includes totally 88 compounds. Bioassay *in vitro* disclosed that antifungal, antimicrobial and antitumor activities are the most notable bioactivities of the secondary metabolites from the fungi of this genus. The biogenetic pathways for some monoterpenes, sesquiterpenes, quinones, and lactones are highlighted, together with their relationship.

Some secondary metabolites with novel carbon skeletons were disclosed from the fungal genus *Pestalotiopsis*. torreyanic acid (**35**) from *P. microspora* and chloropupukeananin (**53**) from *P. fici* are outstanding examples. The finding of these compounds would lead to the reinvestigation on the same endophytic fungi in the coming years in order to find more novel compounds. Some compounds are found to have significant bioactivities. Pestalachloride A (**1**), displaying potent antifungal activity against *Fusarium culmorum*, and torreyanic acid (**35**), exhibiting potent *in vitro*

anti-tumor activities against twenty-five different cell lines, would probably trigger related total synthesis works in the coming years.

The above findings demonstrate that the fungus *Pestalotiopsis* sp. is a prodigious source for new natural products but rarely studied genus. Before 2008, there are only 22 paper published about this genus and totally less than 70 compounds were discovered [Figure 1.3.4.1](#). Obviously, the research prospect for *Pestalotiopsis* sp. to uncover the structure diverse and bioactivity unique secondary metabolites is brilliant.

- Methanol LiChroSolv HPLC grade, Merck
- Nanopure water

2.1.2.3 Solvents for NMR

- DMSO- d_6 euriso-top
- CD₃OD euriso-top
- CDCl₃ euriso-top
- CD₃COCD₃ euriso-top

2.2 Methods

2.2.1 Isolation and Cultivation of Fungus

Pestalotiopsis sp. was isolated from the fresh, healthy leaf of *Rhizophora mucronata* (Rhizophoraceae) collected in October 2005 in Dong Zhai Gang-Mangrove Garden in Hainan Island, China. The fungus (strain no. JCM2A4) was isolated under sterile conditions from the inner tissue of the leaf and identified using a molecular biological protocol by DNA amplification and sequencing of the ITS region. The fungus was grown on solid rice medium at room temperature under static conditions for 39 days. The sequence data have been submitted to and deposited at GenBank (accession no. FJ465172). A voucher strain (Code No. 2) was deposited at the Institut für Pharmazeutische Biologie und Biotechnologie, Heinrich-Heine-Universität, Duesseldorf.

2.2.2 Fungal Extraction

The extraction scheme for the cultural materials of *Pestalotiopsis* sp. is described in Figure 2.2.2.1. This method was used to collect fungal extracts containing both extracellular (excreted into the medium) and intracellular metabolites. A total of 250 mL of ethylacetate was added into each cultural material of the fungus in an erlenmeyer flask and the mixture was kept overnight. The mixture was then applied to Ultrasonic for 10 minutes (for cell destruction), followed by filtration using Büchner vacuum. The extracted mycelia (cell debris) were discarded away and the filtrate containing ethyl acetate phase and medium (water phase) was collected for further work up. The ethyl acetate phase was then separated from water phase (medium) using separatory funnel. To remove the remaining salts and other polar constituents, the ethyl acetate phase was washed with water two times. Then this phase was concentrated under reduced pressure. The resulting residue was diluted in 90 % methanol and further extracted with n-hexane to remove fatty acids and other nonpolar constituents. The remaining 90% methanol phase was evaporated under reduced pressure to yield 3.0 g from the small scale and 8.0 g from the large scale residue, respectively.

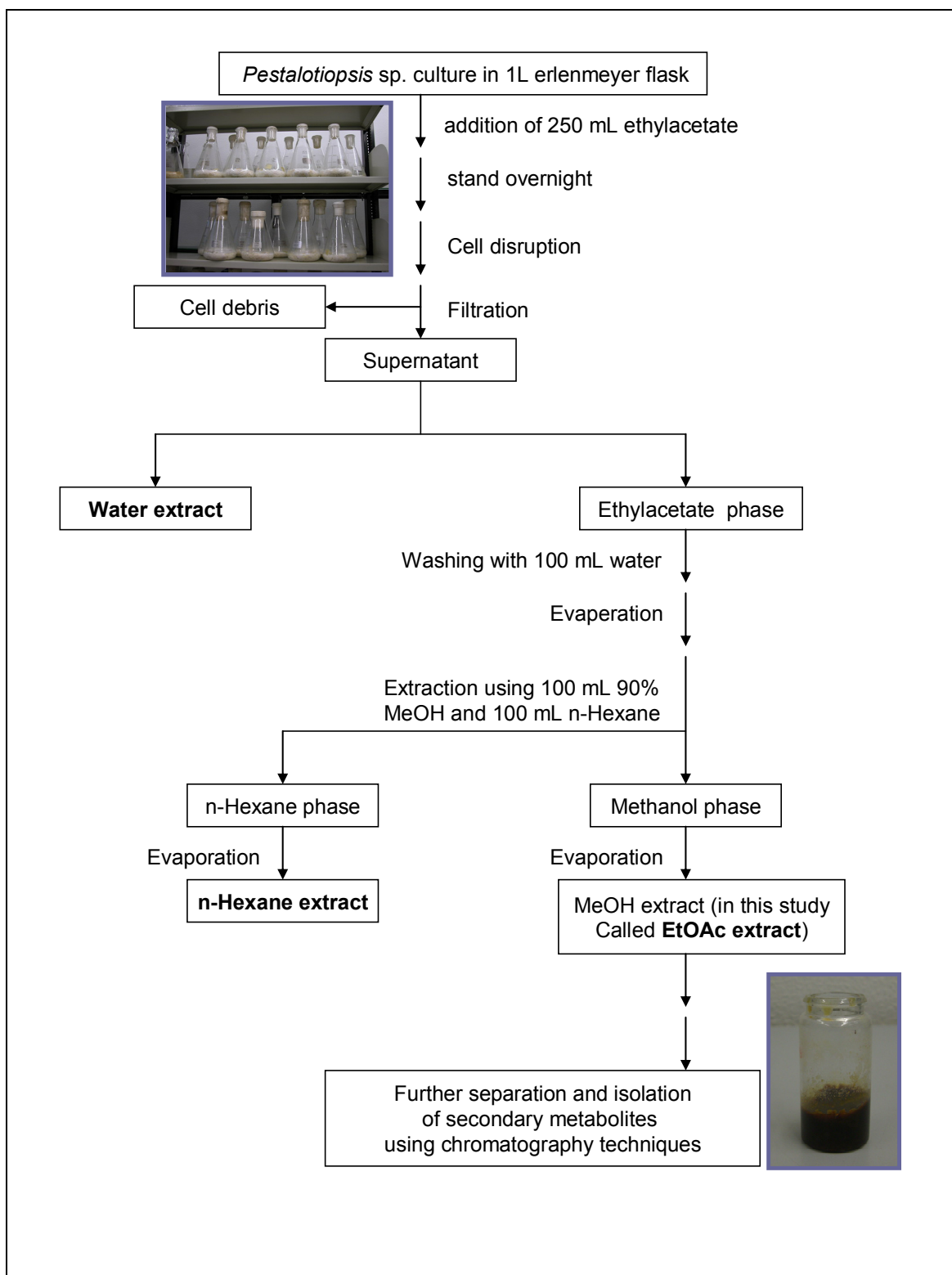


Figure 2.2.2.1 The extraction scheme of *Pestalotiopsis* sp.

2.2.3 Solvent-Solvent Separation

Solvent-solvent extraction is a widely employed technique for the separation of organic compounds from mixtures. It involves separation of compounds in two immiscible solvents. Since the technique is based upon an unequal distribution of solutes between two solvents with a different polarity, the solutes will be more soluble in one solvent compared to the other. The distribution of a component A between two phases can be expressed as distribution coefficient (K) :

$$K = \frac{H}{[A] \text{ lower phase}}$$

where, [A] is the concentration of solute A.

The following general principles should be considered in choosing a solvent for the system:

- the solvents involved in the extraction must be immiscible
- the solvents must not react with the components that will be separated
- the solvents should be easy to be removed by evaporation after the process of separation is finished

In this study, the solvent extraction was the first step in the whole separation process. It was meant to “clean” the ethyl acetate extract from salts and other undesirable polar

constituents by water-ethylacetate extraction. Subsequently, the methanol-n-hexane extraction was applied to remove fatty acids and other undesirable non polar components.

2.2.4 Isolation, Purification and Identification of Secondary Metabolites

In this study, ethyl acetate extract was selected for further isolation and purification of secondary metabolites due to the following reasons:

- It contains more secondary metabolites compared to water extract and n-hexane extract
- Secondary metabolites in ethyl acetate extract are more easily separated and isolated by using known and available chromatography techniques than those in water and *n*-hexane extracts

The isolation and purification of secondary metabolites was performed by using some chromatography techniques. The techniques used in the isolation depended on the amount and profile of secondary metabolites in the extracts. [Figure 2.2.4.1](#) and [2.2.4.2](#) showed the details of the schematic isolation of secondary metabolites from the cultural materials of the small and large scale fermentation of *Pestalotiopsis* sp..

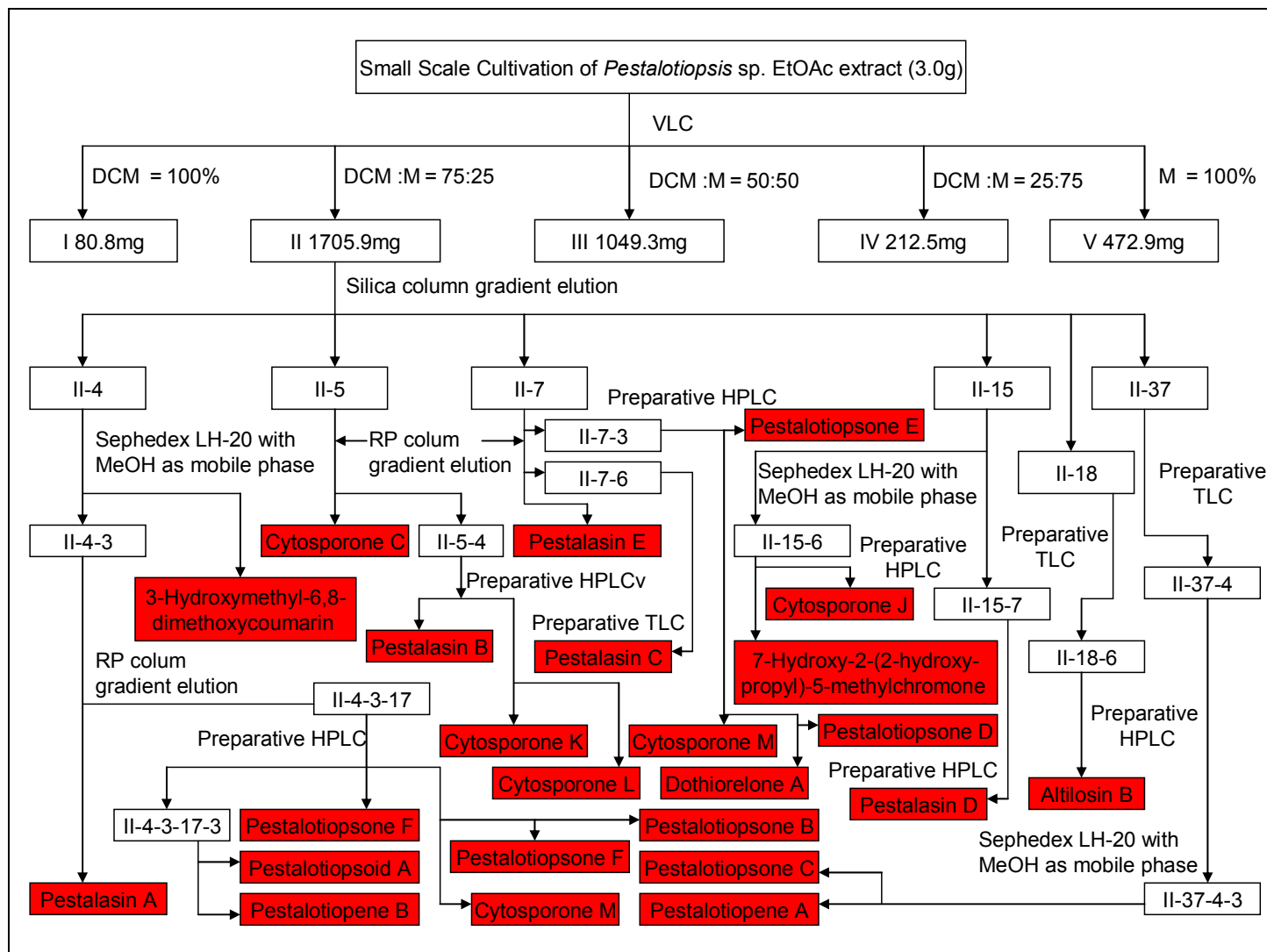


Figure 2.2.4.1 The schematic isolation of secondary metabolites from small scale fermentation of *Pestalotiopsis* sp.

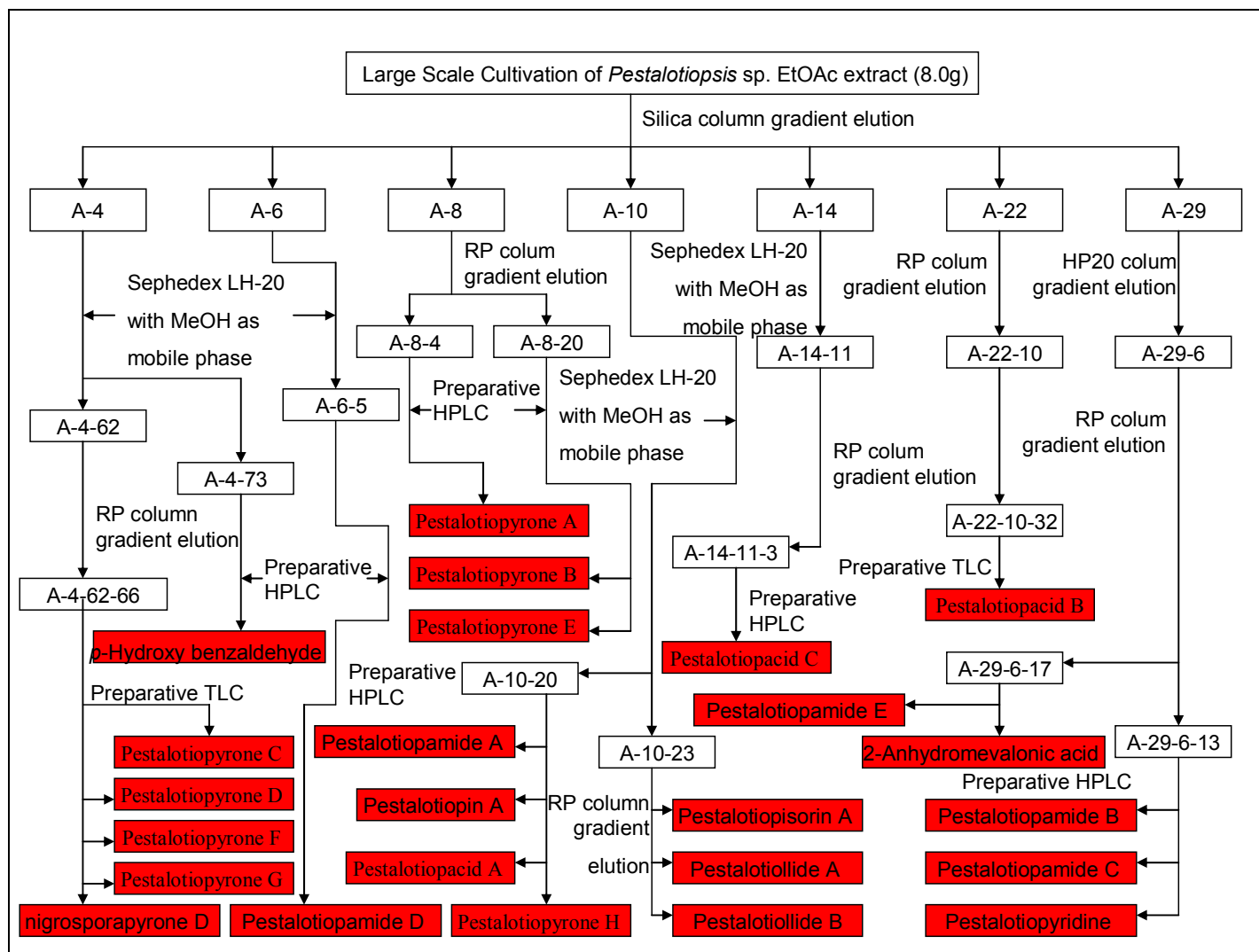


Figure 2.2.4.2 The schematic isolation of secondary metabolites from the large scale fermentation of *Pestalotiopsis* sp.

2.2.4.1 Chromatography

In chromatography, chemical components of a mixture are separated by passing a mobile phase through a stationary phase. The mixture is first placed in the stationary phase and the mobile phase is allowed to pass through the system. The chemical separation in a mixture is based on the selective interaction, such as surface absorption and relative solubility, of the components with both the stationary and mobile phase.

Three different types of chromatography, viz. a-b, based on the physical property of stationary and mobile phase, are used in this study.

- a. Thin Layer Chromatography
- b. Column Chromatography

2.2.4.1.1 Thin Layer Chromatography

Thin layer chromatography (TLC) is a simple and quick method of chromatography for analysis of the components in the mixtures and for the determination of the purity of a substance. It is also used for the choosing the best solvent system for the separation of metabolites by column chromatography. Sometimes, TLC, called as preparative TLC, is also applied for the preparative separation and purification of the components in the mixtures.

TLC plate is a sheet of glass, metal or plastic (usually polyester) coated with a

thin layer of stationary phase (usually silica, SiO_2 , and alumina, Al_2O_3 , in about 250 μm thickness). The samples are loaded close to one edge of the plate. Then the plate is “developed” by immersing the loaded edge in a mobile phase, which is usually a mixture of two or more solvents migrating through the plate (stationary phase) and causing the components of the mixture to be distributed between the stationary and the mobile phase. Then the process is terminated just before the mobile phase reaches the opposite edge of the plate. Development is performed in a solvent vapour-saturated chamber. After the separation, the separated components of the mixture appear as spots or bands on the plate (chromatogram). Sometimes strongly coloured bands are visible on the plate. The colourless bands can be visualized by spraying with some dying agents, such as anisaldehyde, on the plate to make coloured spots. Fluorescent components can be visualized under ultraviolet light. If the spots absorb UV light but do not fluoresce, the spots will appear dark on a fluorescent background due to the presence of a fluorescent dye in silica gel.

The ratio of the distance reached by a particular spot (components) to the distance reached by the front of the mobile phase is the retardation factor, R_f . It is the characteristic value of a component under the used certain solvent condition. The ideal solvent system for the column chromatography of desired components is one that gives the R_f about 0.25.

2.2.4.1.2 Column Chromatography

Column chromatography, also called liquid chromatography, is used for the preparative isolation, separation, and purification of components from a mixture. The

stationary phase is packed in an inert plastic or glass column. The ideal system of the mobile phase, usually a mixture of two or more solvents, is determined by TLC. The mobile phase is passed through the column by either external pressure or gravity. The type of interaction among the chemical components, stationary phase, and mobile phase depends on the applied stationary phase and on the nature of the mobile phase.

2.2.4.1.2.1 Silica gel Column

In column chromatography, also called liquid chromatography, a vertical glass column is packed by stationary phase, SiO₂, and the mobile phase is a mixture of organic solvents, which is added to the top of the column. The separation is based on the polar interaction of the components between the mobile and stationary phases. This technique is ideally used for the separation and purification of components in the range from semi-polar to non polar. The length of the column and interval drops (related to the rate of the eluent through the column) depend on the amount of the sample and the number of components to be separated.

The sample or the mixture to be separated is loaded on the top of the column. The mobile phase (the eluent) flows down and brings the mixture through the column by a gravity force with a fixed rate. The components are distributed along the column and the coloured components can be watched during the separation process as coloured bands on the column. The drops at the bottom of the column are collected by fraction collector and the fractions are analyzed by TLC. The process continues until all components are eluted and collected. Alternatively, the flow can be stopped during the process and the column can be packed out. Then the coloured bands are cut out

and redissolved in an ideal solvent to recover the separated components.

2.24.1.2.2 Reversed Phase (RP) Chromatography

Liquid chromatography with a stationary phase that is more polar than mobile phase is called 'normal phase'. However, 'reversed phase' refers to liquid chromatography with the mobile phase being more polar than stationary phase. The protocol of RP column is very similar to that of silica column. But the column is packed by RP-18 silica as stationary phase. The used mobile phase is usually a mixture of methanol and water. Sometimes, acetonitrile is used instead of methanol. This technique is ideally used for the separation and purification of polar components from a mixture dissolved only in water or water-methanol mixture.

2.2.4.1.2.3 Sephadex Column

The protocol of the Sephadex column chromatography is similar to that of silica and RP column. The column is packed with Sephadex LH-20 as stationary phase and the mobile phase varies from polar to non-polar organic solvents, or a mixture of them. The best system of the mobile phase is one that can dissolve all components to be separated. The mixture flows down, along with the eluent, through the column forced by gravity. The components are separated and distributed on the stationary phase according to their molecular size. Since the stationary phase consists of porous beads, the large molecules will be excluded from the beads and eluted first. The small molecules will be eluted later because they enter the porous beads and stay inside until they find the certain size of pores to exit from the beads.

2.2.4.1.2.4 Flash Chromatography

Flash chromatography is a preparative column chromatography based on an optimized prepacked column and an eluent at a high flow rate driven by air pressure . It is a simple and quick technique widely used for the separation of various organic compounds. Normally, the column, pre-packed by a dried Silica Gel G at a height of 18 cm, is filled and saturated with the desired mobile phase just prior to the sample loading on the top of the column. The mobile phase, an isocratic or gradient solvent, is then pumped through the column with the help of air pressure. This process results in the separation of samples on the column. This technique, only considered as a technique under low to medium pressure, is applied for the separation of samples of the range from a few milligram to some gram.

2.2.4.1.2.5 Vacuum Liquid Chromatography (VLC)

Vacuum liquid chromatography (VLC) column, packed with SiO₂ as a stationary phase, is similar to normal silica column. However, its mobile phase passes quickly through the column by applying vacuum condition, instead of gravity force. This technique is normally used for the separation of a large amounts of raw extract in a short time.

The lower part of the vertical column is connected to a vacuum pump to generate a vacuum condition. The sample, loaded on top of the column, passes quickly through the column by vacuum condition, together with the mobile phase, which is gradient changed from less to more polar condition by steps.

2.2.4.1.2.6 Semi Preparative High Performance Liquid Chromatography (HPLC)

Theoretically, the separation of a mixture in column chromatography is much more effective when the stationary phase is a very thin layer on the surface of very small and uniform spherical beads. However, the stationary phase in this condition is very sensitive to the flow of the mobile phase. To solve this problem, a pressure must be applied to the mobile phase in order to get a desired flow. For example, a pressure of about 2000 psi should generate a flow of 1 – 3 mL/minute. In most high performance liquid chromatography (HPLC) systems, a reciprocating piston pump is used to produce high pressure. However, a cylinder of compressed gas or diaphragm pump can be used instead.

A typical HPLC column, packed with 5 μ m silica beads bonded to octadecylsilyl (C18-Si-) groups in a stainless steel tubing, is utilized in this experiment. The column with a 8.00 mm ID flows with solvent at a rate of 5 mL/minute. However, the column with a 4.00 mm ID and a 143 mm length flows with solvent at 1 mL/minute. The mobile phase is a polar solvent or a mixture of polar solvents including, for example, methanol, acetonitrile, water (nanopure water) or their mixtures. The composition of mobile phase is continuously changed from more to less polar conditions (gradient elution). Sometimes, 0.01 % trifluoroacetic acid is added into water to get a high resolution of separated peaks.

The dissolved gas may create bubbles when the mobile phase leaves the column due to the sudden falling of the pressure. In this case, the mobile phase should be degased by the treatment of ultrasonic bath before its use. Alternatively, it can also be

applied to a vacuum to remove the gases.

A few microliters of sample solution are applied into a sample loop or an injector. When the injector is operated, the sample loop is suddenly switched into the flow of the mobile phase just before it reaches the column.

As the mobile phase leaves the column, it immediately passes into a detector which is used for the determination of the presence of the various components. The ultraviolet (UV) detector is employed in this study due to its high sensitivity. Moreover, the wavelength can be set at the UV absorption maximum of particular molecules, or at a short wavelength where most molecules have UV absorption.

An online chromato-integrator is connected to the detector in order to monitor the presence of the components when they leave the column after separation. The peaks of chromatogram account for the number of components eluted by the solvent system and their area is equal to the UV absorbance of a particular compound (component). By monitoring the chromatogram, an individual peak or a fraction can be collected in an individual sample collector.

The HPLC system used in this study is described as following:

Pump : LaChrom L-7100, Merck/Hitachi

Detector : LaChrom L-7400, Merck/Hitachi

Printer : Chromato-Integrator D-2000, Merck/Hitachi

Column : Eurospher 100-C18, Knauer ((250 × 4.6 mm, ID and 250 × 21.4 mm, ID)

Pre-column : Eurospher 100-C18, Knauer

2.2.4.1.2.7 Analytical HPLC

The principle of analytical HPLC is similar to that of semi-preparative HPLC.

Except for special statements, most gradient elutions of the mobile phase used in this study proceed as described as a standard program in [Table 2.2.4.1.2.7.1](#). The water is nanopure water, which is adjusted to pH 2 with phosphoric acid (H_3PO_4). If the components could not be properly separated by the above standard gradient elution, the program is then changed to the suitable one for the samples.

Table 2.2.4.1.2.7.1 A standard gradient elution of the mobile phase in HPLC

Time (minutes)	% Methanol	%Water
0	10	90
5	10	90
35	100	0
45	100	0
46	10	90
60	10	90

The specification of the parts in HPLC system is described as follows :

Pump : P 580, dionex

Programme : Chromeleon version 6.3

Autosampler	: ASI 100T, Dionex , with an injection volume of 20L
Column	: Eurospher 100 C-18, Knauer (bonded 5 μ m silica beads ; 4 mm ID ; 125 mm long)
Column oven	: STH 585, Dionex
Detector	: UVD 340 S - Photo Diode Array Detector, Dionex

Unfortunately, the detector of UVD 340 S can only detect the compounds with the absorption of UV light . Compounds without the absorption of UV light are analyzed by TLC, sprayed with dying agent, such as anisaldehyde, and/or these compounds are submitted to gas chromatography.

2.2.4.2 Determination of the Maximum Wavelength of UV Absorption

The absorption of UV or visible radiation corresponds to the excitation of outer electrons in the molecules. In organic molecules, most absorption is based on the transition of n electrons to the π^* excited form. Experimentally, these transitions fall in spectrum of region 200 – 700 nm. Consequently, these transitions need an unsaturated group (called as chromophores) of the molecule to provide electrons.

In this study, the determination of maximum wavelength of UV absorption is done with the help of the detector, UVD 340 S – a Photo Diode Array Detector, integrated into the analytical HPLC (see 2.2.4.1.2.7).

2.2.4.3 Determination of Molecular Weight

2.2.4.3.1 Mass Spectrometry

Mass spectrometer is an analytical instrument utilized for the determination of the molecular weight of compounds. Basically, mass spectrometer is divided into three parts, viz. ionisation source, analyser and detector, which should be maintained under a high vacuum condition in order to guarantee the travel of ions through the instrument without any hindrance derived from air molecules. Once a sample is injected into the ionisation source, the molecules are ionized to generate ions, which are then extracted by the analyser. In the analyser, the ions are separated according to the ratio (m/z) of their mass (m) to charge (z). Once the separated ions flow into the detector, the signals are then transmitted to the data system where the mass spectra are recorded.

Many different method of ionisation are used in mass spectrometry and the selection of the method depends on the type of samples to be analysed. Some known ionisation methods include:

- Electron Impact (EI)
- Electro-Spray Ionisation (ESI)
- Fast Atom Bombardment (FAB)
- Chemical Ionisation (CI)
- Atmospheric Pressure Chemical Ionisation (APCI)
- Matrix Assisted Laser Desorption Ionisation (MALDI)
- Field Desorption / Field Ionisation (FD/FI)
- Thermo-Spray Ionisation (TSI)

The mass spectrum shows the relative intensity of mass *vs* charge, viz. the ratio (m/z), which gives the information about molecular weight and relative abundance of the component in the sample. The most intense peak in the spectrum is called the base peak and others are reported relative to the intensity of the base peak (set at 100%). The fragments, which are formed from simple and predictable chemical pathways, reflect the most stable ions or radicals derived from the analyzed compound. The observed peak with the highest molecular weight represents the parent peak. Generally, small peaks are also observed close to the calculated molecular weight due to the natural isotopic abundance of ^{13}C and ^1H , etc.

In this study, only the first three ionisation methods are used for the determination of the molecular weight of the obtained pure secondary metabolites.

2.2.4.3.1.1 Electron Impact Mass Spectrometry (EI-MS)

Electron impact mass spectrometry (EI-MS) generates a molecular ion M^+ , called radical cation, by the collision of an electron with the sample in gas phase. The sample is vaporized and then directly injected into a high vacuum chamber where the sample is ionised by bombarding with neutral molecules, which have energy of 70 eV and are accelerated in a 8 kV electric field. The ionisation process is then accelerated by vacuum condition in a magnet field and ions are sorted by the ratios of mass to charge in a continued change of magnetic field.

Since the samples must be volatile and thermally stable, the measurement of EI-MS is limited to compounds with low molecular weight of 600 Da or less. Some

classes of compounds, only generating molecular ion M^+ , are not ideal for this measurement. In most cases, the information of molecular structure can be deduced from the extensive fragments occurring in the analysis.

The determination of molecular weight using this method is conducted by Dr. Keck and Dr. Tommes at the Institute of Inorganic Chemistry, University of Düsseldorf. The EI mass spectrometer type is Finnegan MAT 8200.

2.2.4.3.1.2 High Resolution Mass Spectrometry (HR-MS)

The high resolution mass spectrometry (HRMS) provides information pertaining to the molecular weight, elemental composition, and molecular structure of a compound. We perform HRMS experiments or accurate mass measurements to determine the elemental formula of new natural products.

The measurement of HRMS is conducted on a Micromass Qtof 2 mass spectrometer by Dr. RuAngelie Edrada at Institute of Pharmacy and Biomedical Science, University of Strathclyde and Dr. Wray at Helmholtz Centre for Infection Research, Braunschweig.

2.2.4.3.1.3 Electro-spray ionization Mass Spectrometry (ESI-MS)

In this method, the ionization process is carried out at atmospheric pressure (API) by spraying sample solution from a small capillary needle, to which a strong electric field is applied. This process produces highly charged droplets and the solvent is

evaporated. Only the highly charged molecules (sample ions) are left in the gas phase. Then the sample ions pass through the sampling cone to enter into an intermediate vacuum region, where they start and pass through a small aperture to reach the analyser of the mass spectrometer under high vacuum. ESI is known as a soft ionisation method. The sample is ionised by the addition or removal of a proton with a little extra energy to cause fragmentation of sample ions.

Sample (M) with the molecular weight, which is greater than ca.100 Da, give its charged molecular-related ions, such as $[M + H]^+$ in positive ionisation mode and $[M - H]^-$ in negative ionisation mode. In positive ionisation mode, a trace of formic acid is added to aid the protonation of sample molecules, while in negative ionisation mode, a trace of ammonia solution or a volatile amine is added to aid the deprotonation of the sample molecule. Besides the molecules ionised by the addition of a proton H^+ , other molecules are ionised by the addition of a sodium cation Na^+ . Thus, $[M + Na]^+$ commonly appears in the positive ionisation mode.

In this study, the determination of the molecular weight using ESI-MS is performed in LC/MS (see section 2.2.4.3.2)

2.2.4.3.2 LC–MS

Liquid chromatography–mass spectrometry (LC–MS) is widely used for the analysis of drug metabolites. Since most metabolites are either chemically or thermally labile, their isolation and purification involve some sorts of liquid chromatography. This technique allows the determination of molecular weight of a

compound not only as a pure substance but also as a mixture.

The LC–MS system used in this study was a combination of HPLC and MS. The sample is injected into the HPLC system for the fractionation and the separated fractions then flow into the ionisation chamber inside the MS system. Though APCI method can also be used in the instrument for the ionisation of the sample, ESI method is applied for the measurement of most samples in this study.

In HPLC system, nanopure water (containing 0.1 % formic acid) and methanol (and/or acetonitrile) are used as the mobile phase. It flows at a rate of 0.4 mL/minute according to one of two standard gradient elution methods as described in Table 2.4 and Table 2.5.

Table 2.2.4.3.2.1 A standard gradient elution method of the mobile phase in LC–MS

Time (minutes)	% Acetonitrile	%Water
0	10	90
5	10	90
35	100	0
45	100	0
46	10	90
60	10	90

Table 2.2.4.3.2.2 A standard gradient elution method of the mobile phase in LC–MS

Time (minutes)	% Methanol	%Water
0	10	90
5	10	90
35	100	0
45	100	0
47	10	90
60	10	90

The specification of the parts in LC–MS is described as follows :

HPLC system : HP 1100, Agilent

MS system : Finnigan LCQDeca, Thermoquest

Ion Source : ESI and APCI, Thermoquest

Pump : Edwards 30, BOC

Injector : G 1313 A ALS 1100, Agilent

Column : Knauer Eurospher 100 ; C-18A((250 × 4.6 mm, ID and 250 × 21.4 mm, ID)

Detector : G 1315 B DAD 1100, Agilent

Programme : Xcalibur, Version 1.3

2.2.5 Structure Elucidation of Pure Secondary Metabolites

After the determination of molecular weight, pure compounds are then submitted to the measurement of nuclear magnetic resonance (NMR) spectra.

2.2.5.1 NMR Measurements

NMR techniques, based on the magnetic property of atom's nucleus, are often used to obtain the structural information of a molecule. Nuclei with an odd mass (atomic number), such as ^1H and ^{13}C , have a nuclear spin, which produces a small magnetic field when the atom is introduced into an external magnetic field.

The suitable amount of the sample depends on the molecular weight of the compound and the type of NMR experiments. Before submitting to the NMR measurement, the sample should be dried in a freeze drier for at least 24 hours. The sample is then dissolved in an adequate NMR solvent and degassed by ultrasonic treatment for some minutes. The solvents used in NMR experiments are deuterated solvents, such as DMSO- d_6 , CD_3OD , and CDCl_3 .

Most NMR measurements are conducted by Dr. Peter and his colleagues at the Institute of Inorganic Chemistry, University Düsseldorf. The instrument used was NMR Bruker type DRX-500. Some measurements were performed by Dr. V. Wray at Gesellschaft Biotechnologie Forschung (GBF), Braunschweig, using NMR Bruker type AM-300, ARX-400 and DMX-600.

2.2.5.1.1 One Dimensional NMR

2.2.5.1.1.1 Proton (^1H) NMR

The measurement of ^1H NMR is a fundamental analysis for the structure elucidation. Once the sample is identified as a pure compound, it is then sent for the

measurement of ^1H NMR, which could decide if two dimensional NMR spectra are needed. Sometimes, a spectrum of ^1H NMR is enough to reveal the structure of a compound, especially for known compounds.

A spectrum of ^1H NMR gives the following information:

- the numbers of hydrogen atoms, which are indicated by the peak integration
- the type of the hydrogen atoms (related to the functional groups), which is indicated by chemical shifts.
- the type of correlation between one hydrogen atom and the other, which is indicated by coupling constant (J)
- the numbers of coupled neighbouring hydrogen atoms, which are indicated by the molecule's splitting pattern.

2.2.5.1.1.2 Carbon (^{13}C) NMR

Differing from ^1H NMR experiment, the measurement of ^{13}C NMR needs more amount of sample. This fact is attributed to the ratio of isotope abundance of ^{13}C to ^{12}C in the nature, which is less than that of ^1H to ^2H .

The spectrum of ^{13}C NMR gives the following information:

- the numbers of carbon atoms inside a molecule
- the type of carbon atoms (related to functional groups), which is indicated by the chemical shifts

In ^{13}C NMR spectrum, the peak integration does not directly represent the exact numbers of particular carbon atoms. That is to say, this experiment does not give the

information of carbon multiplicity

2.2.5.1.1.3 DEPT

Distortionless enhancement by polarisation transfer (DEPT) experiment is utilized to enhance the sensitivity of ^{13}C NMR experiment. This experiment is started by proton excitation and followed by transferring to the magnetisation of carbon atoms (called as polarisation transfer process), then the ^1H - ^{13}C polarisation transfer increases the sensitivity.

The amplitude and sign of the carbon resonance are altered by the feature editing according to the numbers of directly attached protons, resulting in CH signal multiplicity for the identification of the primary, secondary, tertiary and quaternary carbon atoms. In the experiment, different final proton pulse angles result in different signs of carbon resonance (see Table 2.2.5.1.1.3.1).

In this study, the DEPT-135 and DEPT-90 are performed to assign and elucidate the structure of the pure isolated secondary metabolites.

Table 2.2.5.1.1.3.1 The relationships of CH multiplicity and the amplitude of carbon resonance in different proton pulse angles experiment

Carbon type (C-H multiplicity)	DEPT-45	DEPT-90	DEPT-135
Quaternary, R_4C (singlet)	0	0	0
Tertiary, R_3CH (doublet)	+	+	+
Secondary, R_2CH_2 (triplet)	+	0	—
Primary, RCH_3 (quartet)	+	0	+

2.2.5.1.2 Two Dimensional NMR

Two dimensional NMR spectra provide more information about the structure of molecule than one dimensional NMR spectra. This experiment is especially applied to a molecule which is too complicated to be elucidated only by one dimensional NMR spectra.

In one dimensional NMR experiment, the signal is recorded as a function of one time variable, thus the spectrum is plotted of intensity vs frequency. While two dimensional NMR experiment is recorded as a function of two time variables, t_1 and t_2 , thus the intensity is plotted as a function of two frequencies, $F1$ and $F2$.

The $F1$ and $F2$ coordinates of the peaks correspond to those found in a normal one dimensional spectrum. In a one dimensional NMR experiment, the couplings are revealed as the multiplicity in the spectrum. In two dimensional spectrum, however, the idea of multiplicity is somewhat expanded so that the multiplicity is revealed as a correlation of the two frequency, $F1$ and $F2$.

2.2.5.1.2.1 COSY NMR

Correlation spectroscopy (COSY) NMR correlates the ^1H shifts of the coupling protons of a molecule. It means that COSY experiment, which can determine the relationship of protons by their coupling, is used for the establishment of the connectivity inside a molecule. In this two-dimensional experiment, the proton shifts are plotted on both frequency axes, resulting in a diagram with square symmetry. In

COSY spectrum, the F1 and F2 coordinates of the peaks also correspond to those found in normal one dimensional (^1H) NMR spectrum. Thus, a COSY spectrum gives information about H-H connectivities in geminal, vicinal, and w-relationships of a molecule.

If the relevant protons coupled to one another, the interpretation of its COSY spectrum is limited by the overlapping signals which are not separated by this experiment.

2.2.6.1.2.2 HMQC NMR

Heteronuclear multiple quantum correlation (HMQC) spectrum gives information about the correlation between ^1H and their directly attached heteronuclei (^{13}C). This technique provides a convenient way for the identification of two diastereotopic geminal protons, which are sometimes difficult to be distinguished by COSY. Only in this condition, two correlations to one carbon can be observed in HMQC spectrum.

2.2.5.1.2.3 HMBC NMR

Heteronuclear multiple bond correlation (HMBC) experiment correlates ^{13}C shifts in one dimension with the related ^1H shifts in the other dimension via the coupling of two or three C-H bonds. The coupling more than three bonds is usually small (exceptions include those across unsaturation bonds). This technique is valuable for the detection of quaternary carbons, which are impossible to be obtained in ^{13}C

NMR experiments due to the low amount of the available material. Sometimes, a direct CH correlation is also observed in this experiment.

2.2.5.1.2.4 NOESY and ROESY NMR

Like NOESY (Nuclear Overhauser Enhancement Spectroscopy), ROESY (Rotating Frame Overhauser Enhancement Spectroscopy) experiment is used to study the three dimensional structure and conformation of molecule by measuring its NOEs (Nuclear Overhauser Effects) in the rotating frame. NOE is a spin relaxation phenomenon which depends on molecular motion and, especially, molecular tumbling rates. Since this type of effects is a distance-depending effects, only protons which are close in space (4-5 Å) give rise to such changes.

In a solution, small molecules (<1000 Da) tumble rapidly and produce weak, positive proton NOEs that grow slowly. In contrast, large molecules (>3000 Da) tumble slowly and produce large, negative proton NOEs that grow quickly. While mid-sized molecules (1000 – 3000 Da) tumble at intermediate rate that is close to zero proton NOEs. Thus NOESY can not be applied to the mid-sized molecules. For this reason, the ROESY experiment is employed to the mid-sized molecules for mapping their NOE correlations between protons by changing the motional properties under different physical conditions.

In this study, the NOESY and ROESY experiments, conducted at GBF by Dr. V. Wray using 600 MHz NMR, are only applied to new metabolites.

2.2.5.2 Circular dichroism (CD) spectroscopy

Circular dichroism is the difference between the absorption of left-handed circularly polarised light (L-CPL) and right-handed circularly polarised light (R-CPL). It occurs when a molecule contains one or more chiral chromophores (light-absorbing groups).

$$\text{Circular dichroism} = \Delta A(\lambda) = A(\lambda)_{\text{LCPL}} - A(\lambda)_{\text{RCPL}}$$

where λ is the wavelength.

Circular dichroism (CD) spectroscopy is a spectroscopic technique. The CD of molecules is measured over a range of wavelengths. CD spectroscopy is extensively used to study chirality of molecules.

Measurements are carried out in the visible and ultra-violet region of the electro-magnetic spectrum to monitor electronic transitions. If the molecule under investigation contains chiral chromophores, one CPL state will be absorbed to a greater extent than the other and the CD signal over the corresponding wavelengths will be non-zero. A circular dichroism signal can be positive or negative, depending on whether L-CPL is absorbed to a greater extent than R-CPL (CD signal positive) or to a lesser extent (CD signal negative).

Circular dichroism spectra are measured using a circular dichroism spectrometer, which is a highly specialised derivative of an ordinary absorption spectrometer. CD

spectrometers alternately measure the absorption of L- and R-CPL, usually at a frequency of 50 KHz, and then calculate the circular dichroism signal.

During our study, the CD spectra were recorded in MeOH on a J-715 spectrometer (JASCO Deutschland, Gross-Umstadt, Germany) at room temperature by using a 0.05 cm standard cell.

2.2.6 Optical Rotation

When a polarized light is passed through a chiral molecule, the direction of polarization can be changed. This phenomenon is called optical rotation or optical activity. The measurement of this change in polarization orientation is called polarimetry and the instrument used to measure this phenomenon is called a polarimeter.

This measurement is used to study the structure of anisotropic compounds and to check the purity of chiral mixtures. If the sample contains only one enantiomer of its chiral molecule, the sample is said to be optically pure. An enantiomer is called as a levorotatory (l) or (-) enantiomer if it rotates light to the left (counterclockwise). On the contrary, if an enantiomer rotates light to the right (clockwise), it is said to be as a dextrorotary (d) or (+) enantiomer.

Since the degree of optical rotation depends on the number of optically active species (chiral) in which the light passes, the measurement of optical rotation depends on concentration (c) and light path length (l) of the sample. The specific rotation, $[\alpha]$,

expresses the optical rotation degree after correction of concentration and path length. Thus the specific rotation is a specific quantity for a chiral molecule at certain temperature T and wavelength.

$$[\alpha]_{\lambda}^T = 100 \alpha / cl$$

where :

$[\alpha]_{\lambda}^T$ is specific rotation at certain temperature T and wavelength

l is optical path length in dm

λ is wavelength

T is temperature

α is measured optical rotation degree at certain temperature T and wavelength λ

c is concentration in g/100 mL

In this study, the measurement of optical rotation was conducted on Perkin Elmer Polarimeter 341 LC using Sodium-D-lamp at wavelength of 589 nm. Unless otherwise stated, the measurement was performed at 20°C using 1 dm length of cuvette and concentration of 0.1 g/100 ml samples. Thus the result is described as:

$[\alpha]_{\text{D}}^{20}$ value (c 0.1. Solvent)

2.2.7 Bioactivity

2.2.7.1 Cytotoxicity Assays

The cytotoxicity assays is used to identify the toxicity of a compound to the cell lines by inhibiting the proliferation of the cells. The assay normally uses human or animal cancer cell lines. In this study, the cytotoxicity assays were performed using L-5178-Y (mouse lymphoma cell line), PC-12 (rat adrenal pheochromocytoma) and Hela (human cervix carcinoma) cells, and carried out by Prof. W.E.G. Müller and Renate Steffan at the Institute of Physiological Chemistry, University of Mainz, Germany.

The cell line was grown in RPMI-1640 culture medium with Na-carbonate (pH 7.2) supplemented with 10% FCS under a humidified atmosphere of 5% CO₂ and 95% air at 37 °C. An aliquot (180 μ L) of these cell suspensions at a density of 1500 cells mL⁻¹ was pipetted into 96-well microtiter plates. Subsequently, A 180 μ L solution of the test compounds (in DMSO) at different concentrations was added to each well and incubated for 72 h at the above conditions in a CO₂-incubator. The number of living cells was then identified by a method called MTT assay. MTT [3-(4,5-Dimethylthiazol-2-yl)-2,5-diphenyltertrazolium bromide] solution (20 μ L of 5 mg/mL in RPMI-1640 medium) was added to each well and further incubated for 3 h. After addition of 100 μ L DMSO and incubation for 1 h, the cells were lysed to liberate the formed formazan crystals. Absorbance was then determined on Multiscan plate reader at 595 nm, the intensity of purple formazan is directly related to the number of viable cells. Alternatively, the number of viable cells can also be determined using radioactive (methyl-3H)-thymidine. As negative controls, media with 0.1% EGMME/DMSO were included in all experiments.

2.2.7.2 Anti-bacterial and Anti-fungal Assays

The antimicrobial and antifungal assays were performed using *Escherichia coli* (gram negative bacterium) and *Bacillus subtilis* (gram positive bacterium), together with four fungal strains including *Staphylococcus aureus*, *Streptococcus pyrogenes*, *Pseudomonas aeruginosa* and *Klebsiella pneumoniae*, and carried out by Dr. A. Pretsch at Sea Life company, Wien. The method, called agar diffusion assays, was used to detect the capability of a substance to inhibit the growth of microorganisms by measuring the diameter of inhibition zone around a tested compound on agar plate.

2.2.7.2.1 Anti-bacterial Assays

The assay was performed using *E. coli* and *B. subtilis*. A 100 – 200 µL of bacterial liquid culture, in an exponential growth phase, was spread on to the surface of Luria Bertoni (LB) agar plate. Immediately, 10 – 20 µL of tested compounds (with a concentration 1 mg/ml) are loaded onto the disc paper (5 mm diameter, Oxid Ltd) and then transferred onto the surface of LB media. The culture was then incubated at 37°C for one or two days (depend on the microbial culture being used). The growth inhibition was then measured and compared to Penicillin G, streptomycin and Gentamycin as positive controls.

2.2.7.2.2 Anti-fungal Assays

Mycelia of *Staphylococcus aureus*, *Streptococcus pyrogenes*, *Pseudomonas aeruginosa* and *Klebsiella pneumoniae* (after growing the fungi for about one month) were put into a fresh fungal medium and destroyed using “ultraturax.”. The cell debris (extracted mycellium) was removed by vacuum filtration and the filtrate (medium

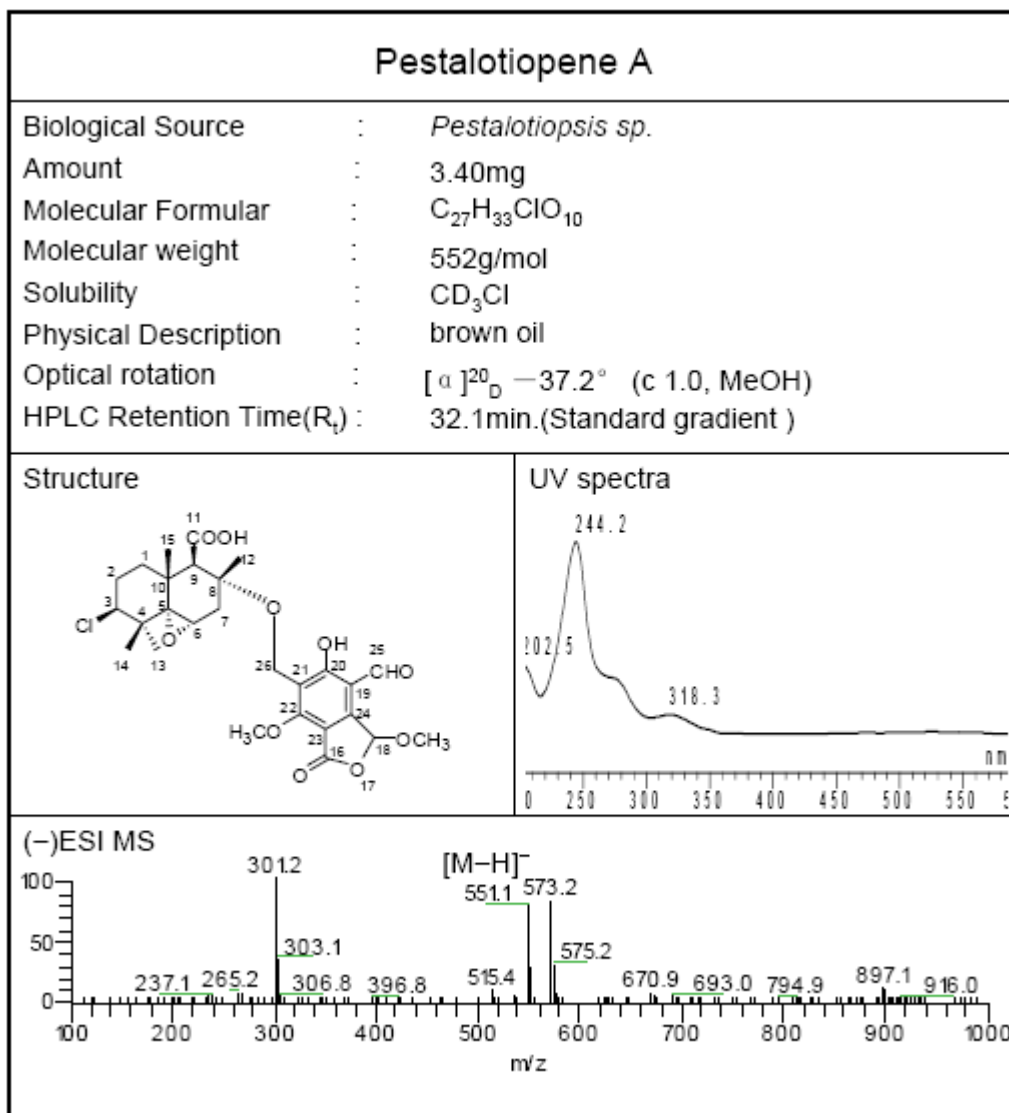
containing fungal spore) was then used for the next steps of the assay.

A 100 mL of fungal spore was spread out onto the surface of potatoes dextrose agar medium (PDA). Immediately, 10 – 20 μ L of tested compounds (with a concentration 1 mg/mL) are loaded onto the disc paper (5 mm diameter, Oxid Ltd) and then transferred onto the surface of the PDA medium. The fungal culture was then incubated at room temperature for several days and the inhibition growth was measured around the disks. The result was then compared to positive control (nystatin).

3 RESULTS—Secondary Metabolites from *Pestalotiopsis* sp.

3.1 Sesquiterpene Derivatives

3.1.1 Pestalotiopene A (1, new compound)



The first of the sesquiterpene acid derivatives, compound **1**, was isolated as an optically active ($[\alpha]_D^{20} = -37.2$) brown oil. The molecular formula $C_{27}H_{33}ClO_{10}$ as established by HR-ESIMS from the pseudo-molecular ions at m/z 551.16871 $[M-H]^-$, suggested eleven degrees of unsaturation.

The ^1H and ^{13}C NMR spectroscopy data of **1** (Table 3.1.1.1) indicated that six of the eleven elements of unsaturation came from a carboxyl group, an ester carbonyl, a ketone carbonyl, and three carbon-carbon double bonds. Therefore, the molecule was pentacyclic. DEPT experiments revealed that **1** had four tertiary methyls, two methoxys, four methylenes, four methines, and thirteen quaternary carbons. Two substructures **1a** (from C-1 to C-15) and **1b** (from C-1' to C-11') (Figure 3.1.1.1) were established by the analysis of the ^1H - ^1H COSY, HSQC, and HMBC spectral data of **1**. Thus, the ^1H - ^1H COSY and HSQC spectra suggested the presence of the fragments $-\text{CH}_2(1)-\text{CH}_2(2)-\text{CH}(3)-$ and $-\text{CH}(6)-\text{CH}_2(7)-$. In the HMBC spectrum, ^{13}C - ^1H long-range correlations were observed between C-4/H-2, C-4/H-3, C-4/H-6, C-4/H-13, C-4/H-14, C-5/H-6, C-5/H-7, C-5/H-13, C-5/H-14, C-5/H-15, C-8/H-6, C-8/H-7, C-8/H-9, C-8/H-12, C-10/H-1, C-10/H-2, C-10/H-9, C-10/H-15, and C-11/H-9. These observations led to the assignment of the substructure **1a** as a sesquiterpene acid oxygenated at C-8. Comparison of the ^1H and ^{13}C NMR spectroscopic data of **1a** with those of compound **3** revealed that the substructure **1a** was the same as the known compound, altiloxin B (Ichihara A. *et al.*, 1984). Moreover, comparison of the remaining ^1H and ^{13}C NMR resonances with those of cyclopaldic acid (Achenbach H. *et al.*, 1982; Graniti and Sparapano 1992), disclosed the analogy of the chemical shifts. However, the 3' hydroxyl group of the latter was replaced by a methoxy group (δ_{H} 3.69, s, δ_{C} 57.0, q, 3'-OCH₃) and its methyl group at C-11' was replaced by a CH₂O-group (δ_{H} 4.59, d, $J = 9.5$ Hz, δ_{H} 4.71, d, $J = 4.0$ Hz; δ_{C} 52.2, t, 11'-CH₂). The above observations demonstrated the presence of the substructure **1b**. Finally, the substructures **1a** and **1b** were linked by the analysis of the HMBC correlations. HMBC correlations between H₂-11'/C-8, H₂-11'/C-5', H₂-11'/C-6', H₂-11'/C-7', and H-11'/C-12 indicated the connection of substructures **1a** and **1b** by an oxygen bridge

between C-8 and H-11', and consequently established the planar skeleton of **1**. Moreover, the proposed structure gained further reinforcement from its ESI mass spectrum (Scheme 3.1.1.1 and 3.1.1.2), which displayed intense positive ion peaks at m/z 303, 267 and negative ion peaks at m/z 301. As shown in Scheme 3.1.1.1 and 3.1.1.2, the loss of a cyclopaldic acid radical (m/z 267) from the molecular ion generated the fragment of altiloxin B (m/z 303 in positive and m/z 301 in negative).

The relative configuration of **1** was subsequently established by a NOESY experiment. NOE crosspeaks between H₃-15/H-1 β , H₃-15/H-6, H₃-15/H-7 β , and H₃-15/H-12, indicated the β orientation of these protons. Similarly, NOE correlations between 12-Me/14-Me, 14-Me/15-Me, and 12-Me/15-Me suggested their mutual *cis* relationship and β orientation. Based on the above results, the α orientation of 13-Me and 8-*O*-substituent was thus established. Moreover, the α orientation of H-3 was deduced from the NOE crosspeak between H-3/13-Me. Therefore, the relative configuration of **1** was characterized as shown in Figure 3.1.1.1.

To establish the absolute configuration of **1**, CD spectra for both possible enantiomers, (3'R)-**1** and (3'S)-**1**, were calculated. Only the spectrum calculated for (3'S)-**1** fits with the experimental one (Figure 3.1.1.2).

All the above data confirm that the structure of **1**, named pestalotiopene A, is a unprecedented hybrid from a drimane-type sesquiterpene acid and a polyketide.

Table 3.1.1.1. ^1H , ^{13}C NMR NMR (500 MHz) data (J in Hz) for pestalotiopene A in CDCl_3

Atom no.	1 δ_{H} [ppm]	δ_{C} [ppm]	HMBC (H to C)	ROSEY
1	1.44 (dd, 13.9, 3.8) 2.41 (br d, 13.8)	35.0	2, 3, 5, 10	2, 3, 15
2	2.04 (m) 2.15 (dddd, 13.5, 13.2, 3.3, 3.1)	28.9	1, 3, 4, 10	1, 3, 14
3	3.94 (dd, 12.5, 4.2)	68.4	1, 2, 4, 5, 13, 14	1, 2, 13
4		41.2		
5		66.8		
6	3.24 (d) ^[a]	53.5	4, 5, 7, 8	7
7	2.07 (d, 17.1) 2.84 (dd, 17.1, 3.6)	32.9	5, 6, 8, 9, 12	6, 12, 11'
8		75.7		
9	3.25 (s)	55.2		11'
10		36.6		
11		171.0		
12	1.40 (s)	26.9	7, 8, 9	7, 11'
13	0.95 (s)	22.6	3, 4, 5	3
14	1.22 (s)	21.6	3, 4, 5	
15	1.47 (s)	18.3	1, 9, 10	
1'		164.5		
3'	6.44 (s)	99.9	1', 8', 3'-OCH ₃	10', 3'-OCH ₃
4'		111.6		
5'		167.0		
6'		119.6		
7'		163.9		
8'		109.5		
9'		152.4		
10'	10.08 (s)	191.8	4', 5', 9'	3', 5'-OH
11'	4.59 (d, 9.5) 4.71 (d, 9.5)	52.2	5', 6', 7'	7, 9, 12, 5'-OH, 7'-OCH ₃
5'-OH	12.42 (s)		4', 5', 6'	10', 11'
3'-OCH ₃	3.69 (s)	57.0	3'	10'
7'-OCH ₃	4.34 (s)	64.1	7'	11'

^[a]Overlapped signals without designating multiplicity

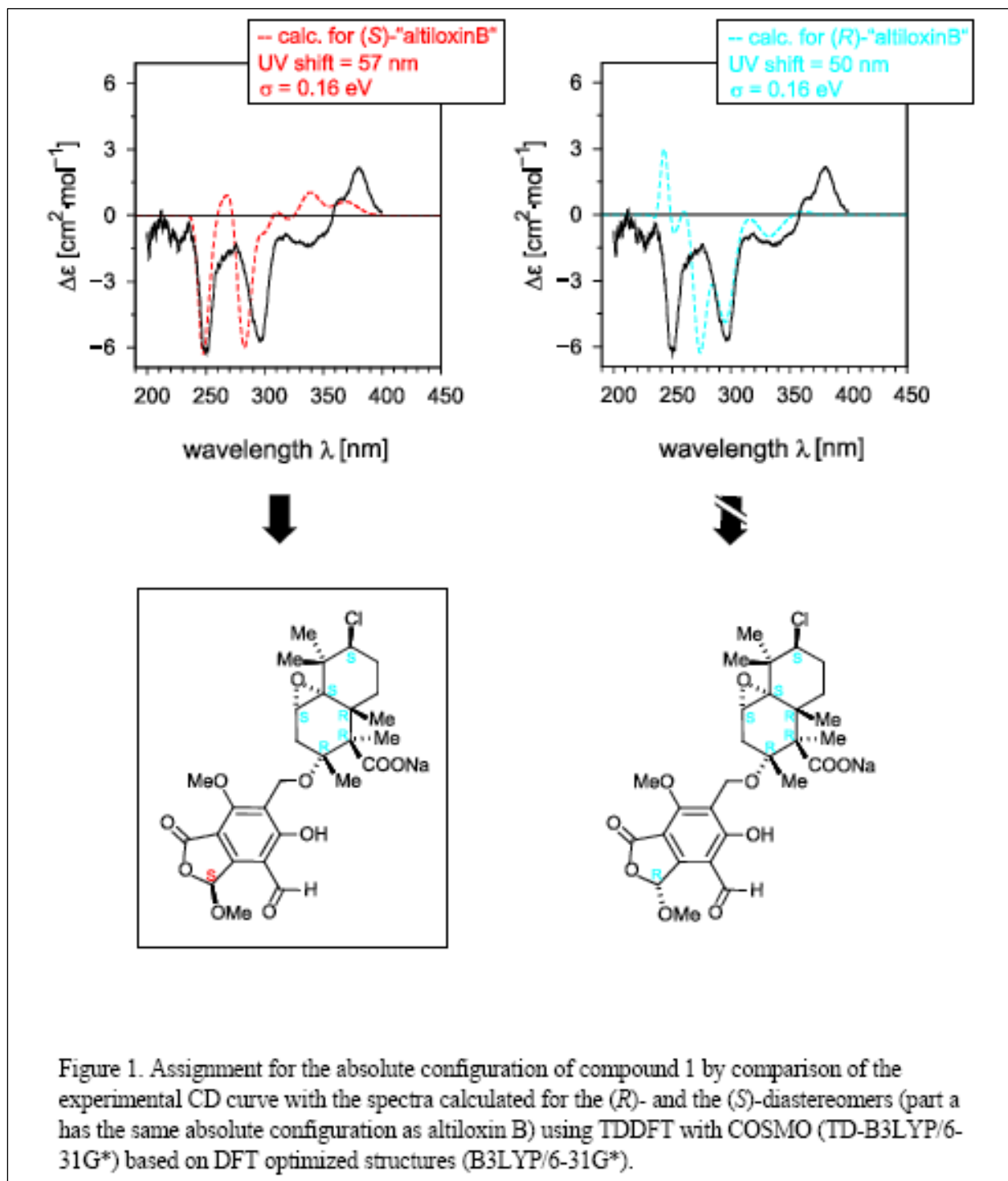


Figure 3.1.1.2a Quantum chemical CD calculation for compound 1

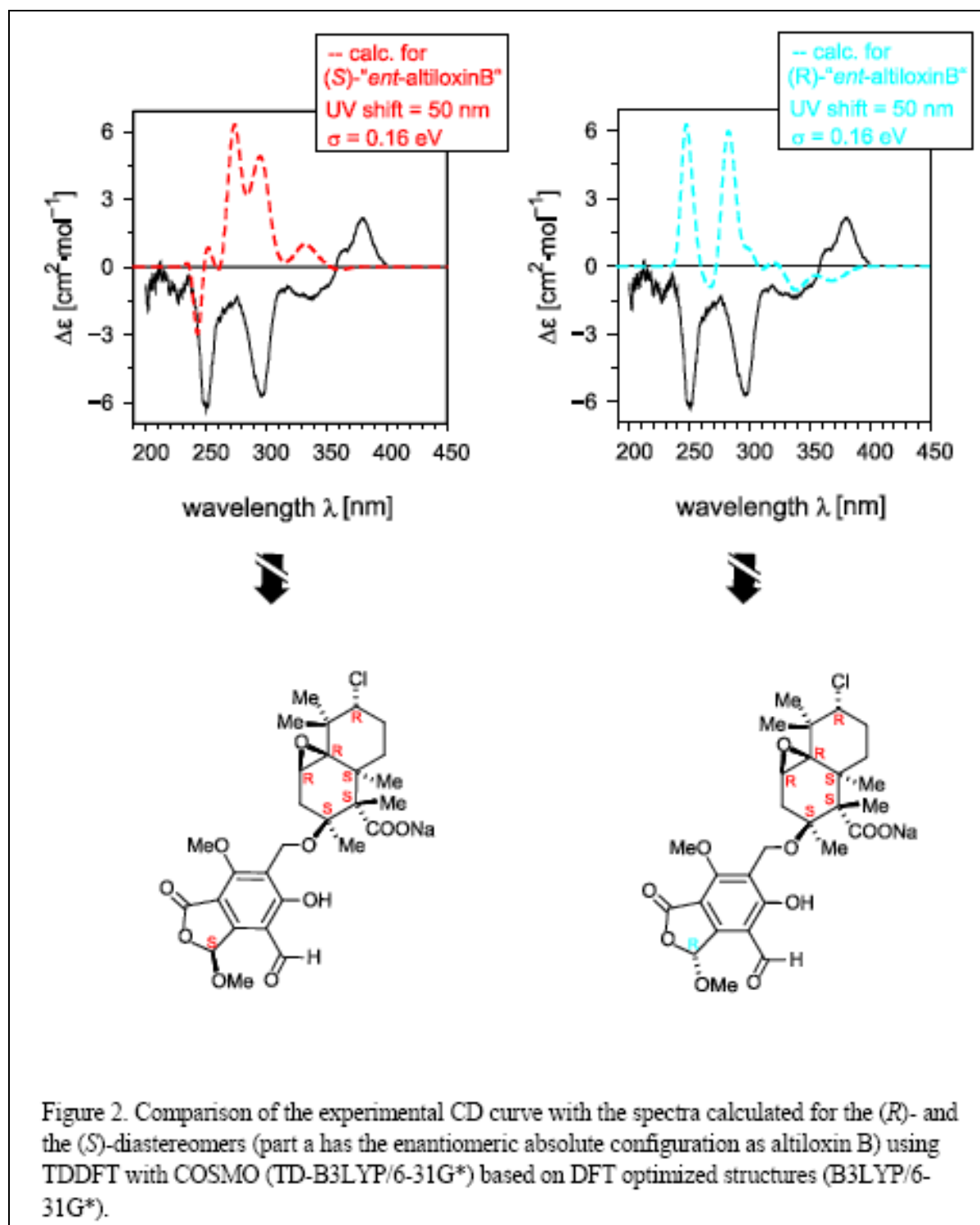
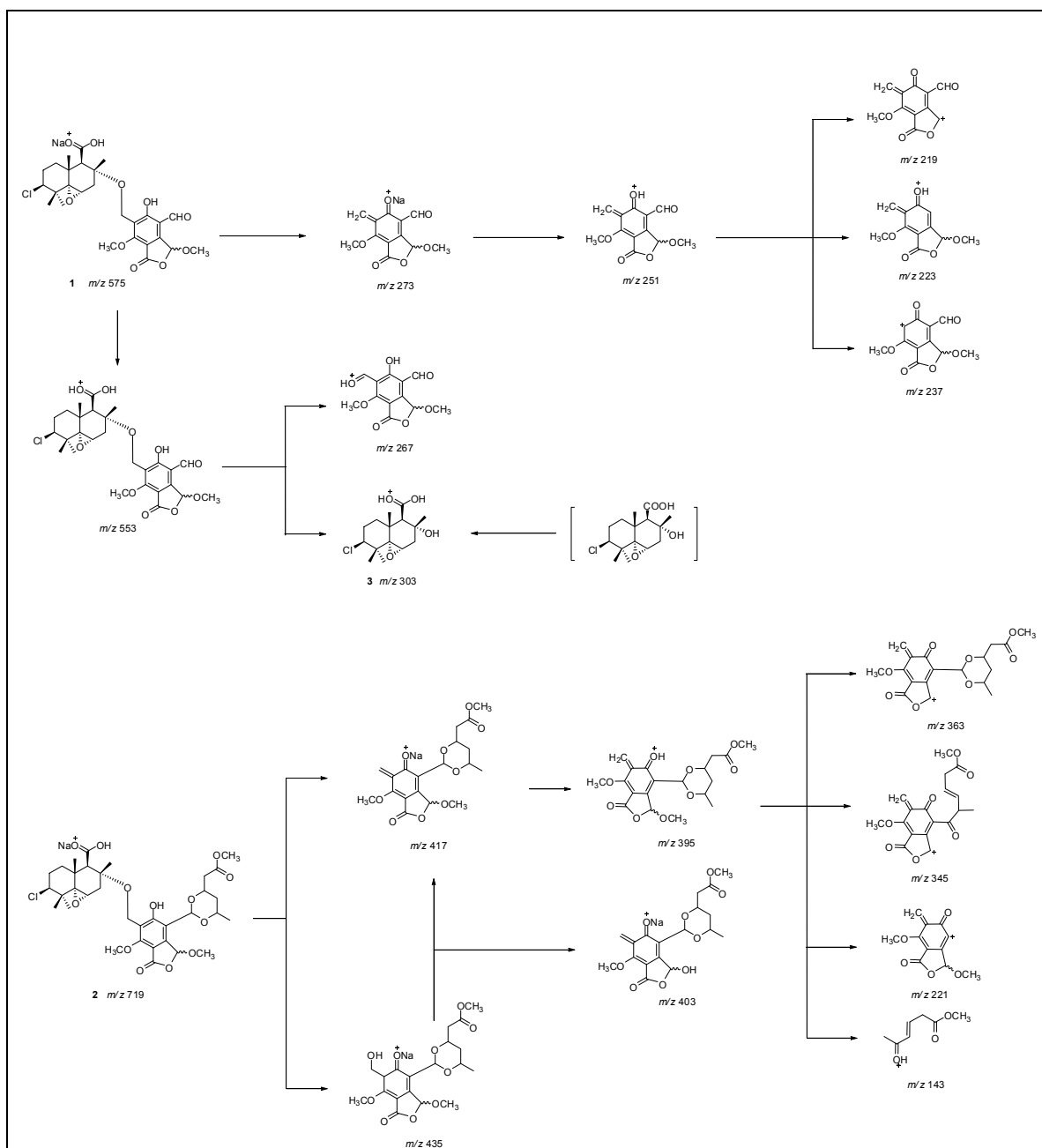
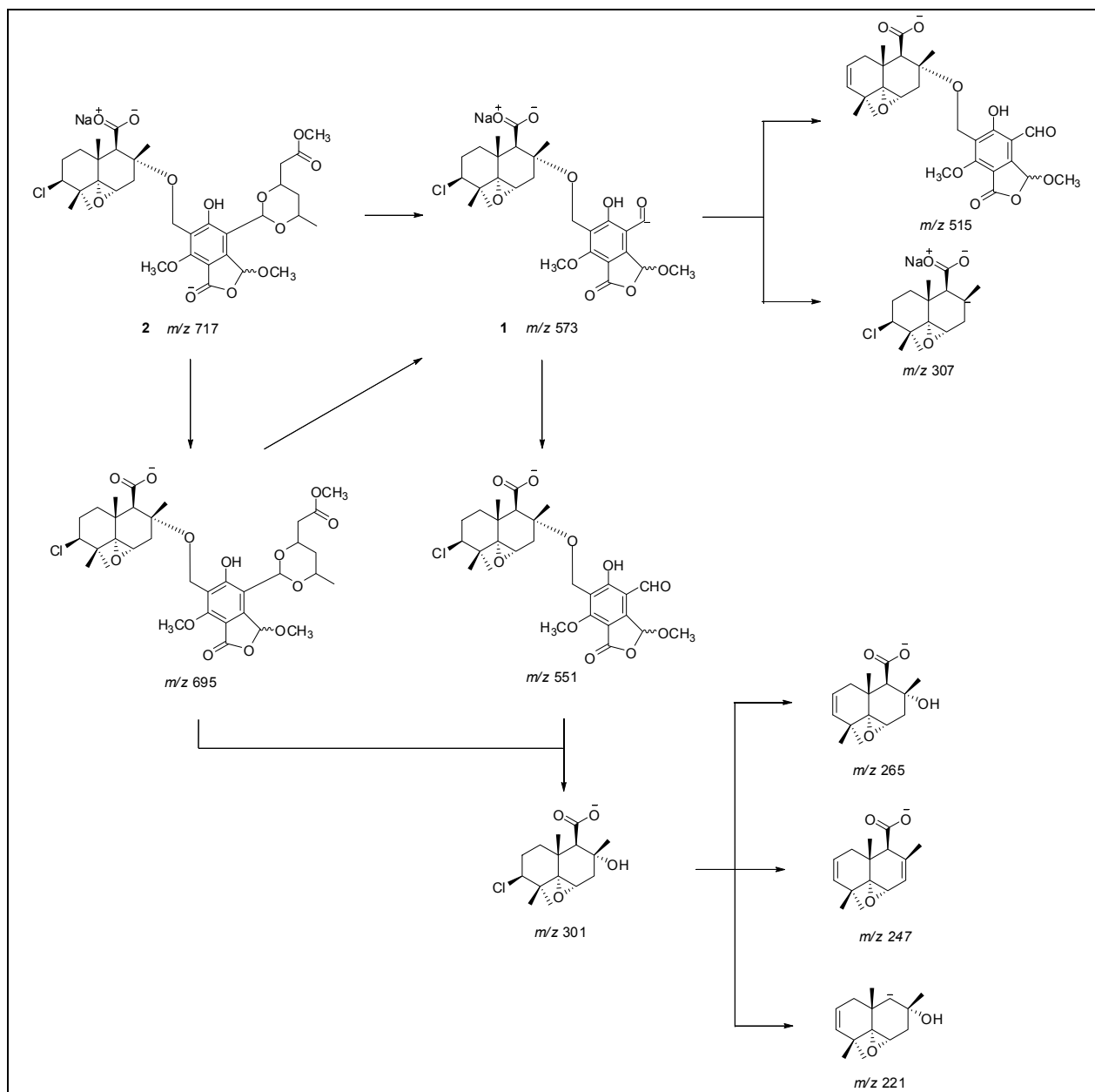


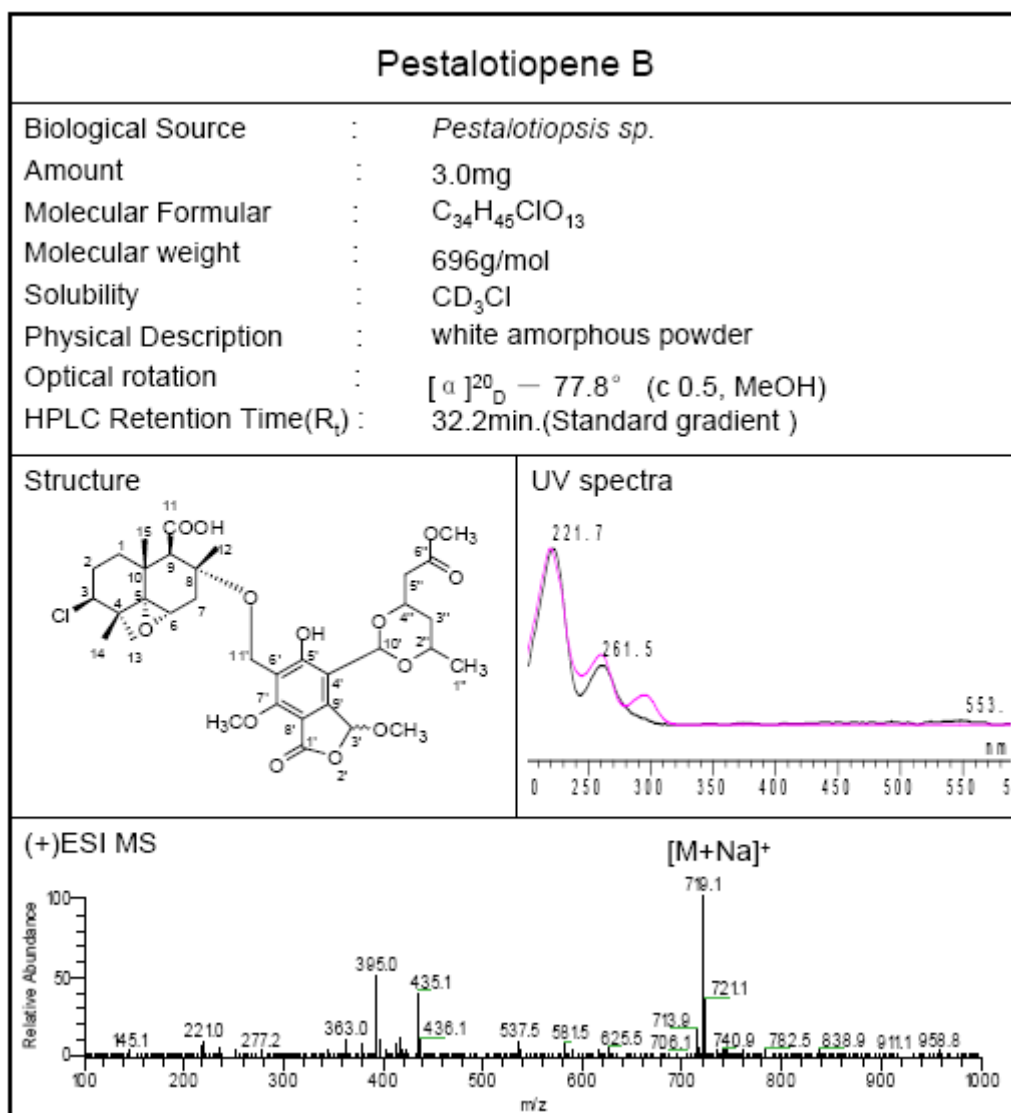
Figure 3.1.1.2b Quantum chemical CD calculation for compound 1



Scheme 3.1.1.1. Proposed (+)ESI mass fragmentation of 1 and 2

Scheme 3.1.1.2 Proposed (-)ESI mass fragmentation of **1** and **2**

3.1.2 Pestalotiopene B (2, new compound)



The second new compound with $[\alpha]_D^{20} = -77.8$, was named pestalotiopene B (**2**). Its molecular formula of $C_{34}H_{45}ClO_{13}$ was established by HR-ESIMS (m/z 695.24727, calcd for $[M-H]^-$ 695.25418).

The 1H and ^{13}C NMR spectroscopic data of **2** (Table 3.1.2.1) indicated the presence of a carboxyl group, a ketone carbonyl, two ester carbonyl, and three carbon-carbon double bonds. Therefore, the molecule was hexacyclic. By the detailed analysis of 1H - 1H COSY, HSQC, and HMBC spectra of **2**, three substructures (Figure 3.1.2.1),

namely **2a** (from C-1 to C-15), **2b** (from C-1' to C-11') and **2c** (from C-1'' to C-6'') were determined in this compound. The structural feature of substructures **2a** and **2b** was identical to that of **1a** and **1b** of compound **1**, respectively, except for the difference of chemical shifts at CH-10' (δ_{H} 5.98, s, δ_{C} 99.1, d). The third substructure **2c** could be assembled starting from the proton spin system $\text{CH}_3(1'')\text{-CH}(2'')\text{-CH}_2(3'')\text{-CH}(4'')\text{-CH}_2(5'')$ -, which was deduced from the $^1\text{H}\text{-}^1\text{H}$ COSY correlations. HMBC cross-peaks from $\text{H}_2\text{-5''}$ of **2c** to the ester carbon of a methoxycarbonyl group (δ_{H} 3.74, s, δ_{C} 52.2, d, $6''\text{-OCH}_3$; δ_{C} 170.5, s, $6''\text{-C}$) connected its C-5'' with this terminal group. The HMBC correlations between H-10'/C-2'', H-10'/C-4'', H-2''/C-10', H-4''/C-10' linked substructures **2b** and **2c** through two oxygen bridges. From all these observations, the planar structure of **2** was established as shown in [Figure 3.1.2.1](#). It was confirmed by the characteristic negative ESI-MS fragments m/z 575 and 301, which originated from sequential loss of the substructures **2c** and **2b** to form the fragments pestalotiopene A and altiloxin B, respectively ([Scheme 3.1.1.1](#) and [3.1.1.2](#)).

The relative stereostructure of **2** was established on the basis of the NOESY spectrum. The significant NOE interactions observed in **2** ([Figure 3.1.2.1](#)) between 3'-OMe/H-10', H-10'/H-2'', H-10'/H-4'' indicated their *cis* orientation.

For the flexibility of compound **2**, its absolute configuration could not be determined by quantum chemical CD calculation.

Table 3.1.2.1. ^1H , ^{13}C NMR NMR (500 MHz) data (J in Hz) for pestalotiopene B in CDCl_3

Atom no.	δ_{H} [ppm] [ppm]	δ_{C}	HMBC (H to C)	ROSEY
1	1.44 (dd, 13.9, 3.6) 2.42 (br d, 13.8)	35.0	2, 3, 5, 10	2, 3, 15
2	2.04 (m) ^[a] 2.15 (dddd, 13.5, 13.2, 3.3, 3.1)	29.0	1, 3, 4, 10	1, 3, 14
3	3.95 (dd, 12.5, 4.2)	68.5	1, 2, 4, 5, 13, 14	1, 2, 13
4		41.2		
5		66.6		
6	3.23 (d, 3.35)	53.4	4, 5, 7, 8	7
7	2.06 (d, 17.2) 2.84 (dd, 17.2, 3.7)	32.8	5, 6, 8, 9, 12	6, 12, 11'
8		75.3		
9	3.26 (s)	55.2		11'
10		36.6		
11		171.1		
12	1.39 (s)	26.9	7, 8, 9	7, 11'
13	0.95 (s)	22.6	3, 4, 5	3
14	1.22 (s)	21.6	3, 4, 5	
15	1.47 (s)	18.3	1, 9, 10	
1'		165.7		
3'	6.27 (s)	101.1	1', 8', 3'-OCH ₃	10', 3'-OCH ₃ , 1''
4'		113.3		
5'		161.2		
6'		120.3		
7'		159.1		
8'		109.9		
9'		146.4		
10'	5.98 (s)	99.1	4', 5', 9', 2'', 4''	3', 5'-OH, 3'-OCH ₃ , 2'', 4''
11'	4.59 (d, 9.3) 4.70 (d, 9.3)	53.1	5', 6', 7'	7, 9, 12, 5'-OH, 7'-OCH ₃
1''	1.35 (d, 6.2)	21.4	2'', 3''	2'', 3''
2''	4.03 (m)	73.4	10', 1'', 3'', 4''	10', 1'', 3''
3''	1.57 (m) ^[a] 1.79 (d, 13.4)	37.8	1'', 2'', 4'', 5''	2'', 4''
4''	4.34 (m)	74.1	10', 2'', 3'', 5'', 6''	10', 3'', 5''
5''	2.63 (dd, 15.8, 4.7) 2.71 (dd, 15.8, 7.5)	40.1	3'', 4'', 6''	4'', 6''
6''		170.5		
5'-OH	9.49 (s)		4', 5', 6'	10', 11'
3'-OCH ₃	3.54 (s)	56.0	3'	10'
7'-OCH ₃	4.14 (s)	63.4	7'	11'
6''-OCH ₃	3.74 (s)	52.2	6'	4'', 5''

^[a]Overlapped signals without designating multiplicity

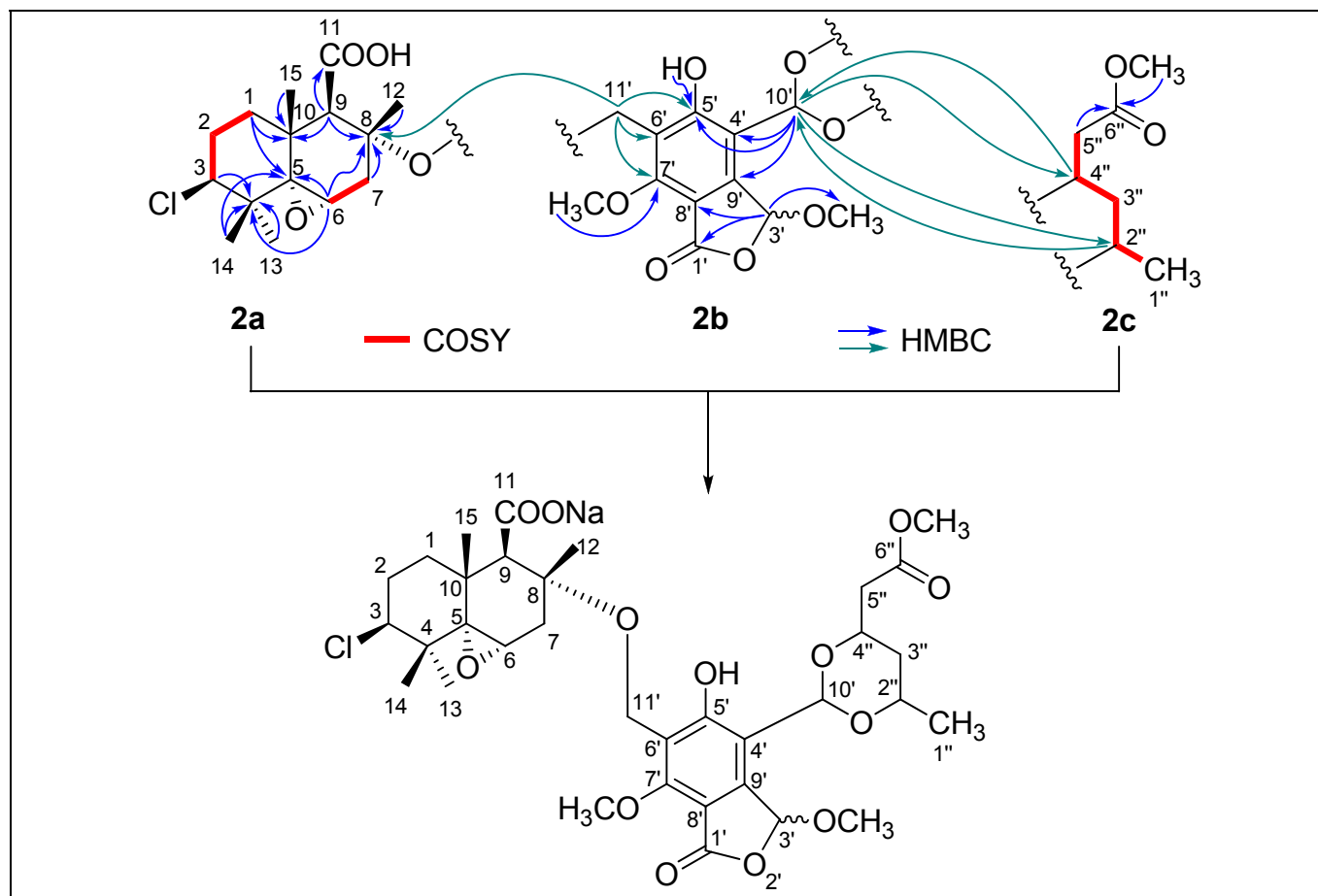
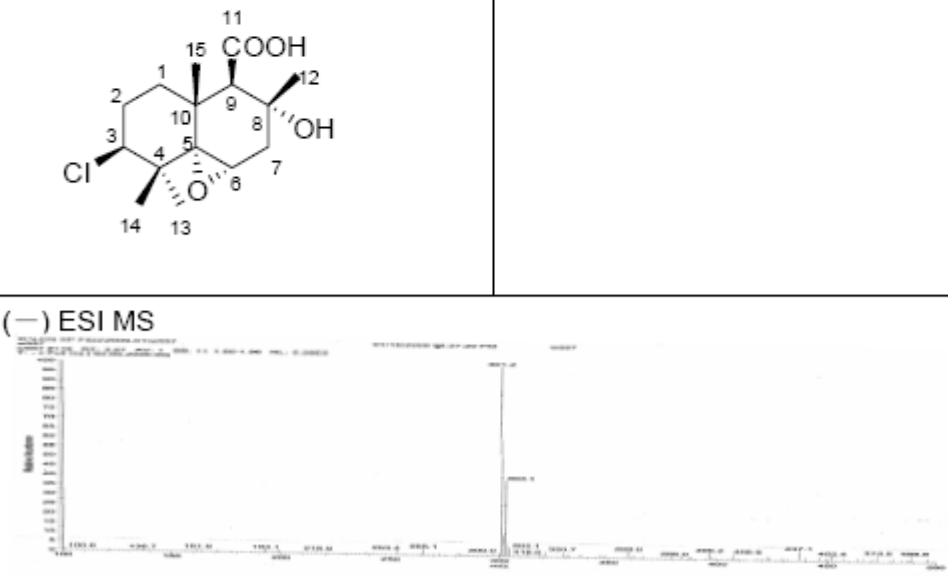


Figure 3.1.2.1 Key HMBC and ^1H - ^1H COSY correlations for **2**

3.1.3 Altloxin B (**3**, known compound)

Altloxin B	
Biological Source	: <i>Pestalotiopsis</i> sp.
Amount	: 4.94mg
Molecular Formular	: $C_{27}H_{33}ClO_{10}$
Molecular weight	: 302g/mol
Solubility	: CD_3Cl
Physical Description	: Light yellow oil
Optical rotation	: $[\alpha]_D^{20} -22.9^\circ$ (c 1.0, MeOH)
HPLC Retention Time(R_t)	: no UV absorption
Structure	UV spectra
 <p>The figure displays the chemical structure of Altloxin B (3) and its corresponding ESI-MS spectrum. The chemical structure is a complex polycyclic molecule with a carboxylic acid group (COOH) at position 11, a hydroxyl group (OH) at position 12, and a chlorine atom (Cl) at position 3. The numbering of the carbons is shown from 1 to 15. The ESI-MS spectrum shows a single prominent peak at m/z 301.2, labeled as $[M-H]^+$, with a relative intensity of approximately 100%.</p>	

Altloxin B (**3**) was isolated as a light yellow oil (MeOH). Its molecular formula was established as $C_{15}H_{23}ClO_4$ by the pseudomolecular ion in ESI-MS at m/z 301.2 $[M-H]^+$, suggested four degrees of unsaturation.

The 1H and ^{13}C NMR data of **3** (Table 3.1.3.1) indicated the presence of a carboxyl group. Therefore, the molecule was tricyclic. DEPT experiments revealed that **3** had four tertiary methyls [δ_H 1.43 (s, H-15), δ_C 17.9 (C-15); δ_H 1.30 (s, H-12), δ_C 28.9 (C-12); δ_H 1.21 (s, H-14), δ_C 21.7 (C-14); δ_H 0.95 (s, H-13), δ_C 22.6 (C-13)],

three methylenes [δ_{H} 2.43 (1H, dd, $J = 16.5\text{ Hz}$, $J = 3.8\text{ Hz}$, H-7), 2.19 (δ_{H} 1H, d, $J = 16.5\text{ Hz}$, H-7), δ_{C} 38.7 (C-7); 2.13 (m, H-2), δ_{H} 2.04 (m, H-2), δ_{C} 28.9 (C-2); δ_{H} 2.02 (m, H-1), 1.48 (ddd, $J = 14.7\text{ Hz}$, $J = 13.7\text{ Hz}$, $J = 3.9\text{ Hz}$, H-1), δ_{C} 35.5 (C-1)], three methines [δ_{H} 3.97 (1H, dd, $J = 12.2\text{ Hz}$, $J = 3.9\text{ Hz}$, H-3), δ_{C} 68.3 (C-3); δ_{H} 3.19 (1H, d, $J = 3.9\text{ Hz}$, H-6), δ_{C} 53.5 (C-6); δ_{H} 3.13 (s, H-9), δ_{C} 60.3 (C-9)], and five quaternary carbons [δ_{C} 41.2 (C-4), 67.2 (C-5), 69.6 (C-8), 36.6 (C-10), 174.7 (C-11)].

Comparison of the ^1H NMR data and optical rotation value of **3** with those of Altioxin B (Table 3.1.3.1) and its ^{13}C NMR data with those of Altioxin B methyl ester (Table 3.1.3.2) (Ichihara A. *et al.*, 1984) revealed that compound **3** is the same as Altioxin B (Figure 3.1.3.1), of which the absolute configuration (3-S, 5-S, 6-S, 8-R, 9-R, 10-R) was established by comparison of its NMR data with those of Altioxin A obtained from stereoselective synthesis (Ichihara A. *et al.*, 1986) (Scheme 3.1.3.2). The absolute configuration of **3** was further confirmed by quantum chemical CD calculation (Figure 3.1.3.3).

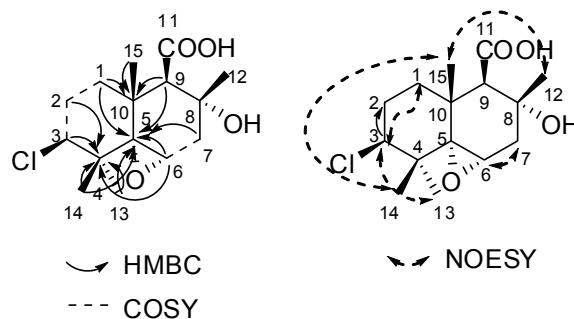


Figure 3.1.3.1 Key HMBC, ^1H - ^1H COSY and NOESY correlations for **3**

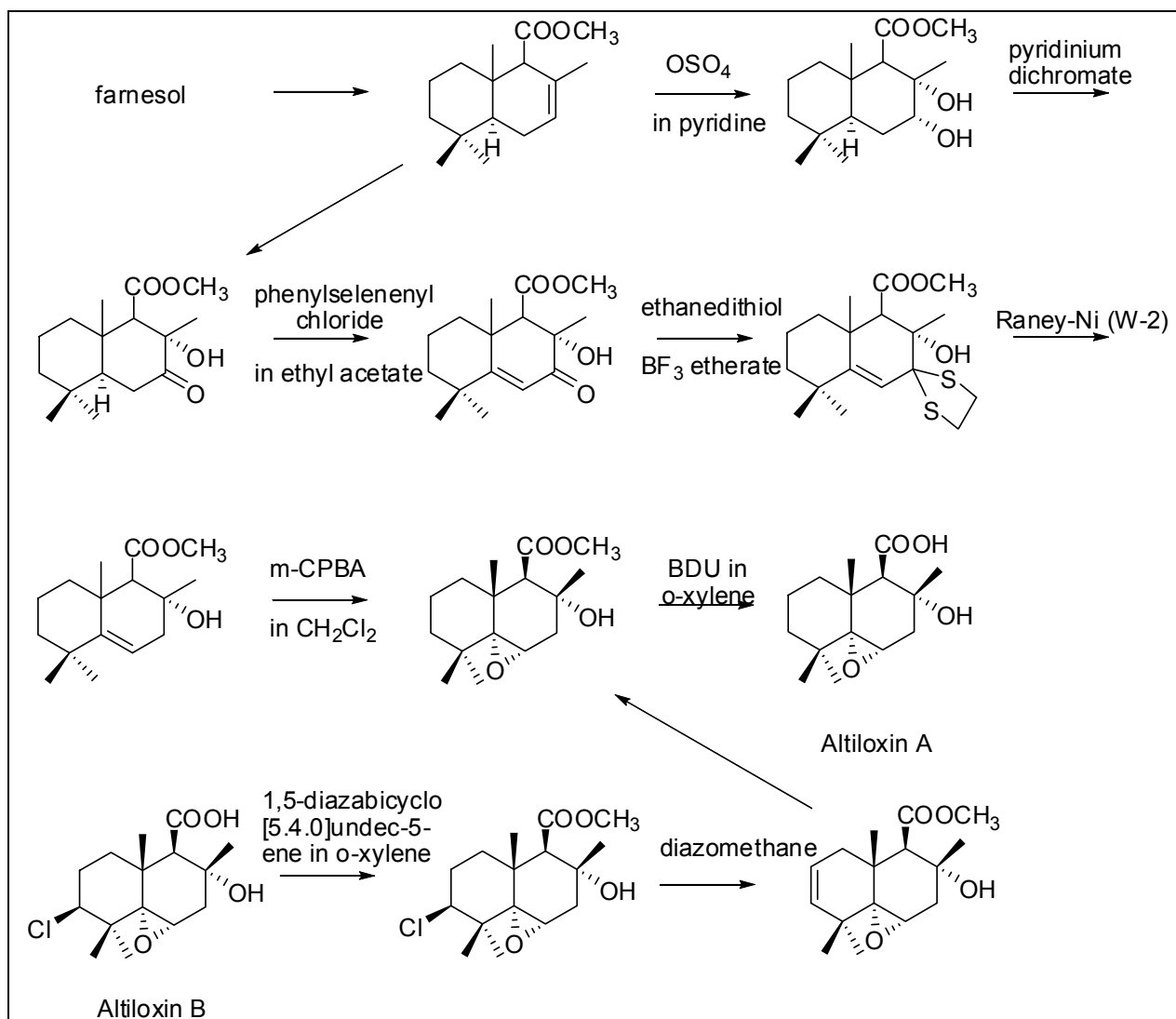
Table 3.1.3.1 ^1H , ^{13}C NMR NMR (500 MHz) data (J in Hz) for **3** and altiloxin B in CDCl_3

Atom no.	3	δ_{C} [ppm]	Altiloxin B from Reference*	
	δ_{H} [ppm]		δ_{H} [ppm]	δ_{C} [ppm]
1	1.44 (dd, 13.9, 4.0) 2.02 (m)	35.5	1.48 (ddd, 14.7, 13.7, 3.6) 2.00-2.20 ^[a]	
2	2.04 (m) 2.13 (m)	28.9	2.00-2.20 (m) ^[a]	
3	3.97 (dd, 12.5, 4.1)	68.3	3.97 (dd, 12.5, 3.9)	
4		41.2		
5		67.2		
6	3.19 (d, 3.9)	53.5	3.20 (d, 3.9)	
7	2.19 (d, 16.5) 2.84 (dd, 16.5, 3.8)	32.7	2.18 (d, 16.1) 2.43 (dd, 16.1, 3.9)	
8		69.6		
9	3.13 (s)	60.3	3.14 (s)	
10		36.6		
11		174.6		
12	1.30 (s)	28.9	1.30 (s)	
13	0.95 (s)	22.6	0.95 (s)	
14	1.21 (s)	21.7	1.21 (s)	
15	1.43 (s)	17.9	1.45 (s)	

* (Ichihara A. *et al.*, 1984)^[a] Overlapped signals without designating multiplicity**Table 3.1.3.2** ^1H , ^{13}C NMR NMR (500 MHz) data (J in Hz) for **3** and altiloxin B methyl ester in CDCl_3

Atom no.	3	δ_{C} [ppm]	Altiloxin B methyl ester from Reference*	
	δ_{H} [ppm]		δ_{H} [ppm]	δ_{C} [ppm]
1	1.44 (dd, 13.9, 4.0) 2.02 (m)	35.5	1.46 (ddd, 14.6, 13.7, 3.9) 1.79 (ddd, 14.6, 13.7, 3.9)	28.83
2	2.04 (m) 2.13 (m)	28.9	2.02 (dddd, 13.7, 3.9, 3.9, 3.4) 2.14 (13.7, 13.7, 12.5, 3.4)	35.57
3	3.97 (dd, 12.5, 4.1)	68.3	3.97 (dd, 12.5, 3.9)	68.20
4		41.2		36.74
5		67.2		66.91
6	3.19 (d, 3.9)	53.5	3.18 (d, 3.9)	60.64
7	2.19 (d, 16.5) 2.84 (dd, 16.5, 3.8)	32.7	2.15 (d, 16.1) 2.39 (dd, 16.1, 3.9)	38.67
8		69.6		69.20
9	3.13 (s)	60.3	3.08 (s)	53.44
10		36.6		41.02
11		174.6		172.03
11-OCH ₃			3.68 (s)	51.04
12	1.30 (s)	28.9	1.20 (s)	22.50
13	0.95 (s)	22.6	0.94 (s)	17.93
14	1.21 (s)	21.7	1.22 (s)	21.62
15	1.43 (s)	17.9	1.45 (s)	29.00

^[a] Overlapped signals without designating multiplicity



Scheme 3.1.3.2 The chemical stereoselective synthesis of **3** (Ichihara A. *et al.*, 1986)

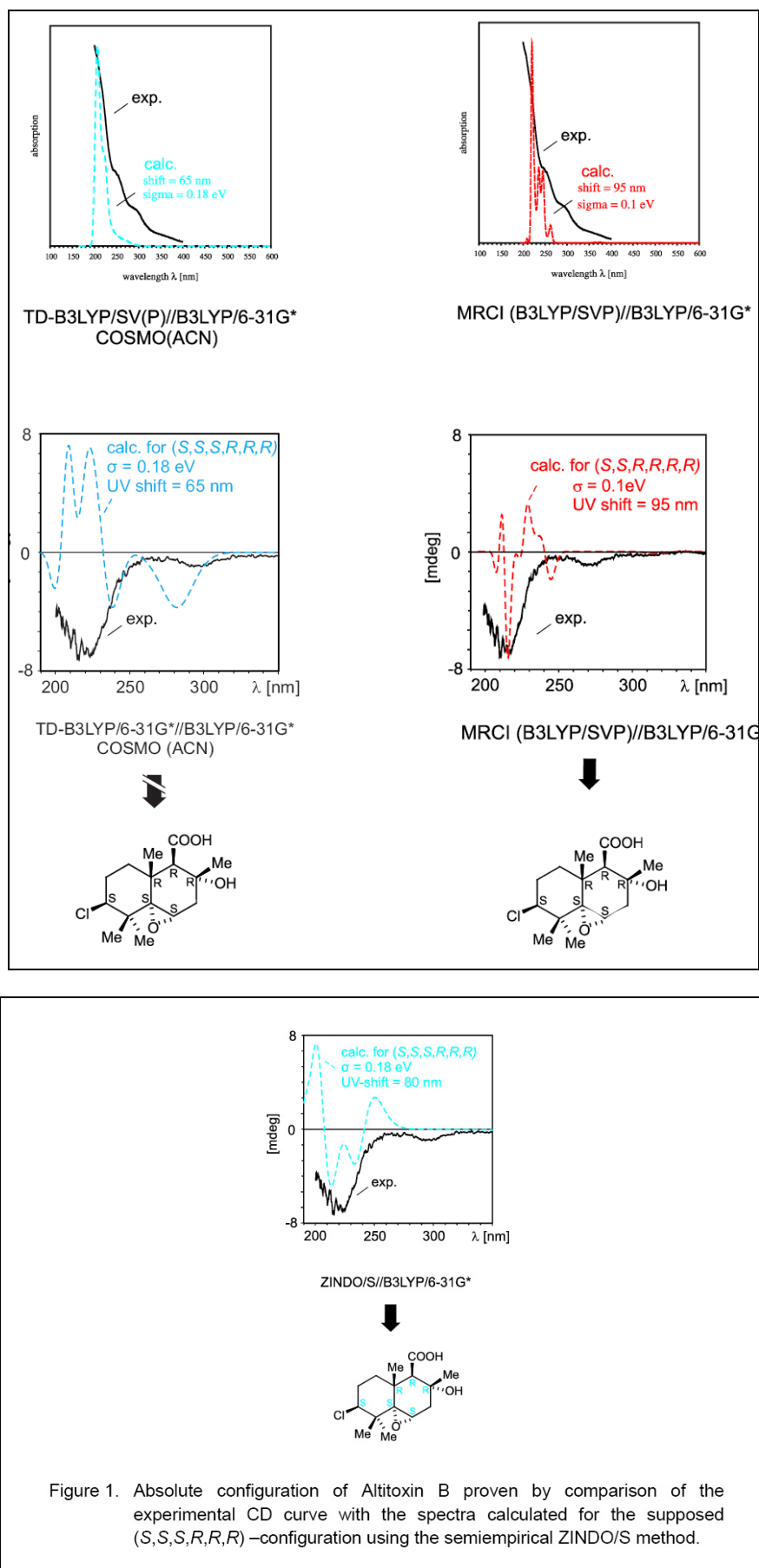
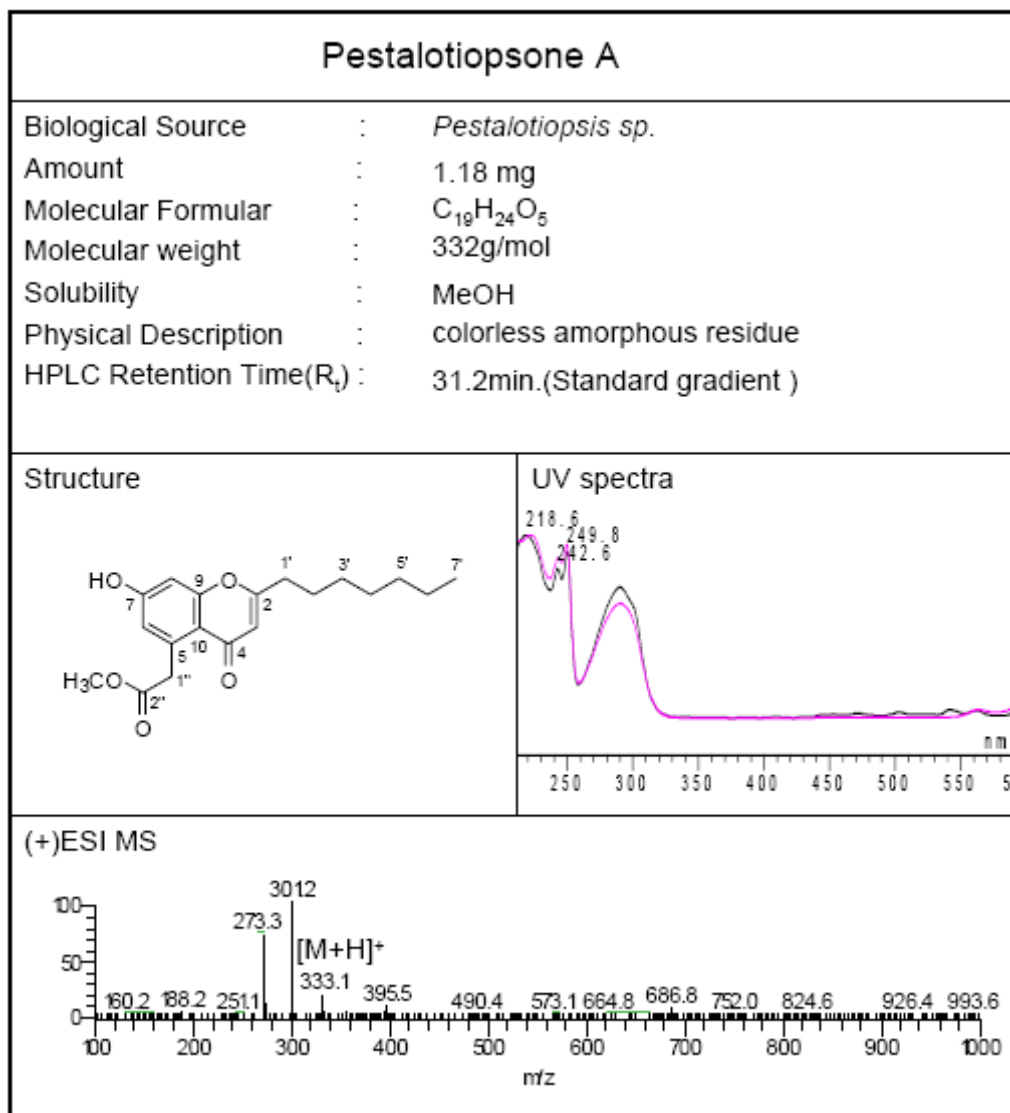


Figure 3.1.3.3 Quantum chemical CD calculation for compound 3

3.2 Chromone Derivatives

3.2.1 Pestalotiopsone A (4, new compound)



Pestalotiopsone A (**4**), a colorless amorphous solid, has the molecular formula C₁₉H₂₄O₅ established by HR-ESIMS (m/z 333.1697, calcd for [M+H]⁺ 333.1702). Consequently, **4** had eight degrees of unsaturation.

The ¹H and ¹³C NMR data of **4** (Tables 3.2.1.1) indicated that six of the eight units of unsaturation come from four carbon–carbon double bonds and two

carbonyls. Therefore, the other two units of unsaturation come from two rings. The UV absorption maxima at 219, 243, 250 nm indicated that **4** should be a chromone derivative. DEPT experiments showed that the compound had two methyl groups, including a methoxy and a terminal alkyl methyl, seven methylenes, three olefinic methines and seven quaternary carbons, including two carbonyls. The ^1H and ^{13}C NMR data of **4** (Tables 3.2.1.1) and its ^1H - ^1H COSY and HSQC spectra showed the presence of a methoxy substituent (δ_{H} 3.60, s, δ_{C} 52.6, q), an olefinic methine (δ_{H} 5.92, s, δ_{C} 111.9, CH-3), a methylene connecting a phenyl ring and a carboxyl group (δ_{H} 4.12, s, δ_{C} 41.9, t, CH₂-1''), two *meta*-coupled aromatic methines [δ_{H} 6.75 (d, $J = 2.2$ Hz), δ_{C} 119.6, d, CH-6; δ_{H} 6.81 (d, $J = 2.2$ Hz), δ_{C} 103.8, d, CH-8], and a seven-membered alkyl chain (CH₂-1' to CH₃-7').

Comparison of the ^1H and ^{13}C NMR data of **4** with those of 2-methyl-5-carboxymethyl-7-hydroxy-chromone (Kashiwada *et al.* 1984) revealed that both had the same chromone core. The strong HMBC correlation (Figure 3.2.1.1) from H-1' (δ 2.59) to C-2 (δ 169.3) revealed that the seven-membered alkyl side chain was attached to C-2 of the chromone core. Moreover, HMBC correlations (Figure 3.2.1.1) from the protons of the methyl ester group (δ 3.60, s) and H₂-1'' (δ 4.12, s) to C-2'' (δ 172.8), combined with that from H₂-1'' (δ 4.12, s) to C-5 (δ 139.8) disclosed the presence of the CH₂COOCH₃ group at C-5. This finding was further supported by the fragments m/z 301 and 273 observed in the positive ESI-MS (Figure 3.2.1.2) that originate from the subsequent loss of methanol and of carbon monoxide. In addition, shift of C-7 (162.8) in the ^{13}C NMR spectrum revealed that this carbon was oxygenated. The attachment of a hydroxyl group to C-7 was deduced from the molecular formula of compound **4**.

On the basis of the above results, the structure of pestalotiopsone A (4) was identified as 5-carbomethoxymethyl-2-heptyl-7-hydroxychromone.

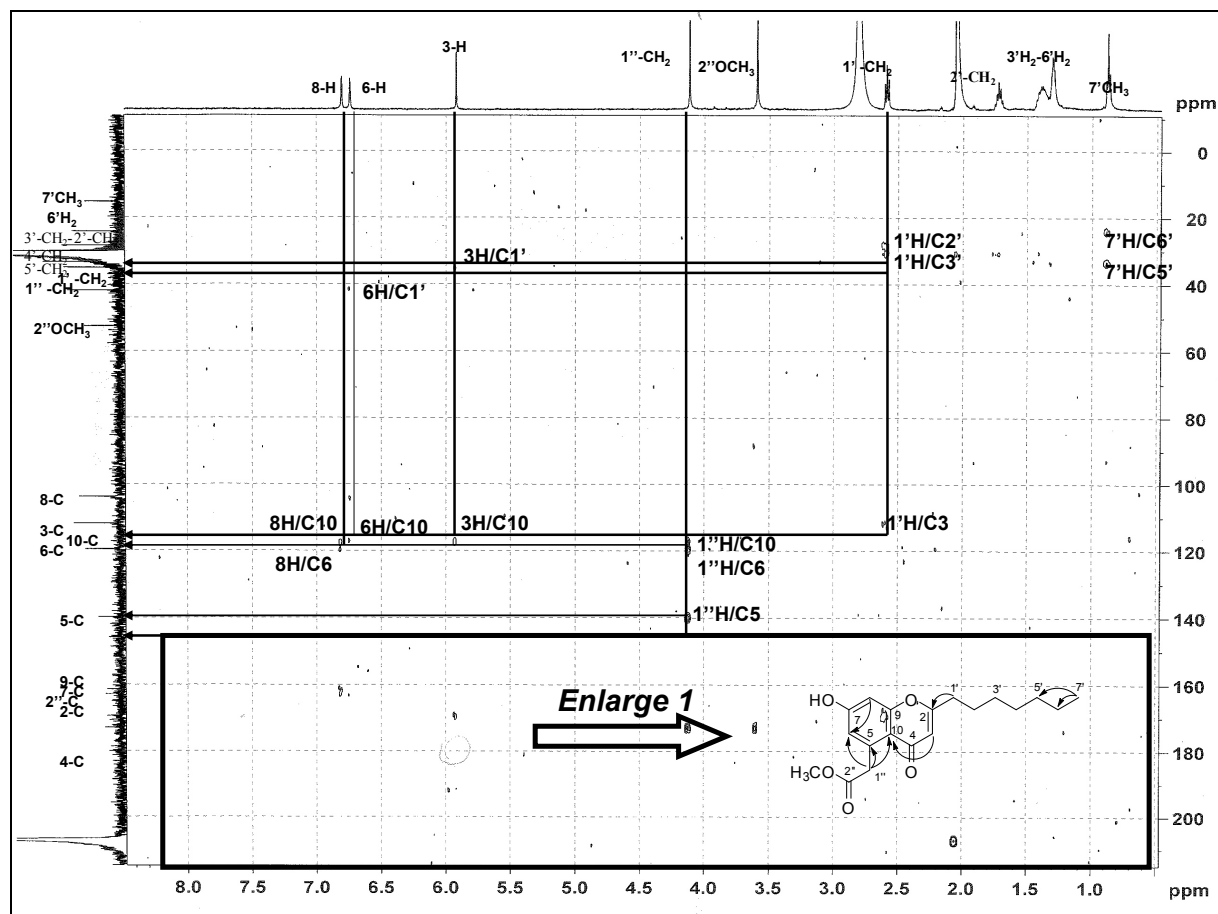


Figure 3.2.1.1a HMBC correlations for compound 4

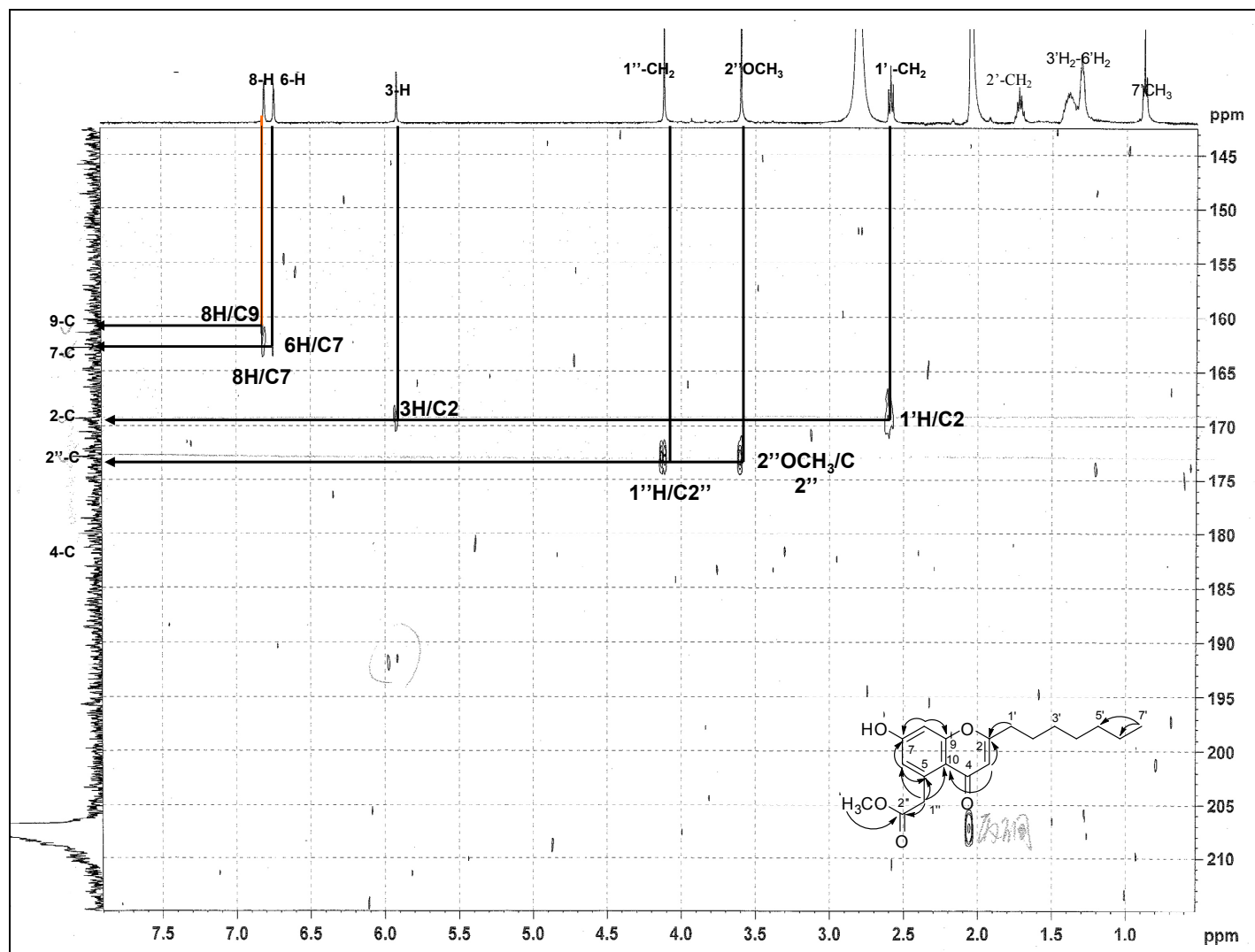
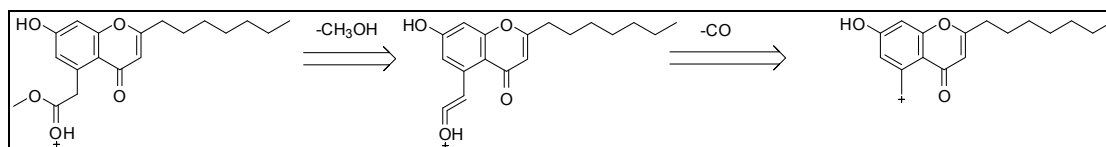
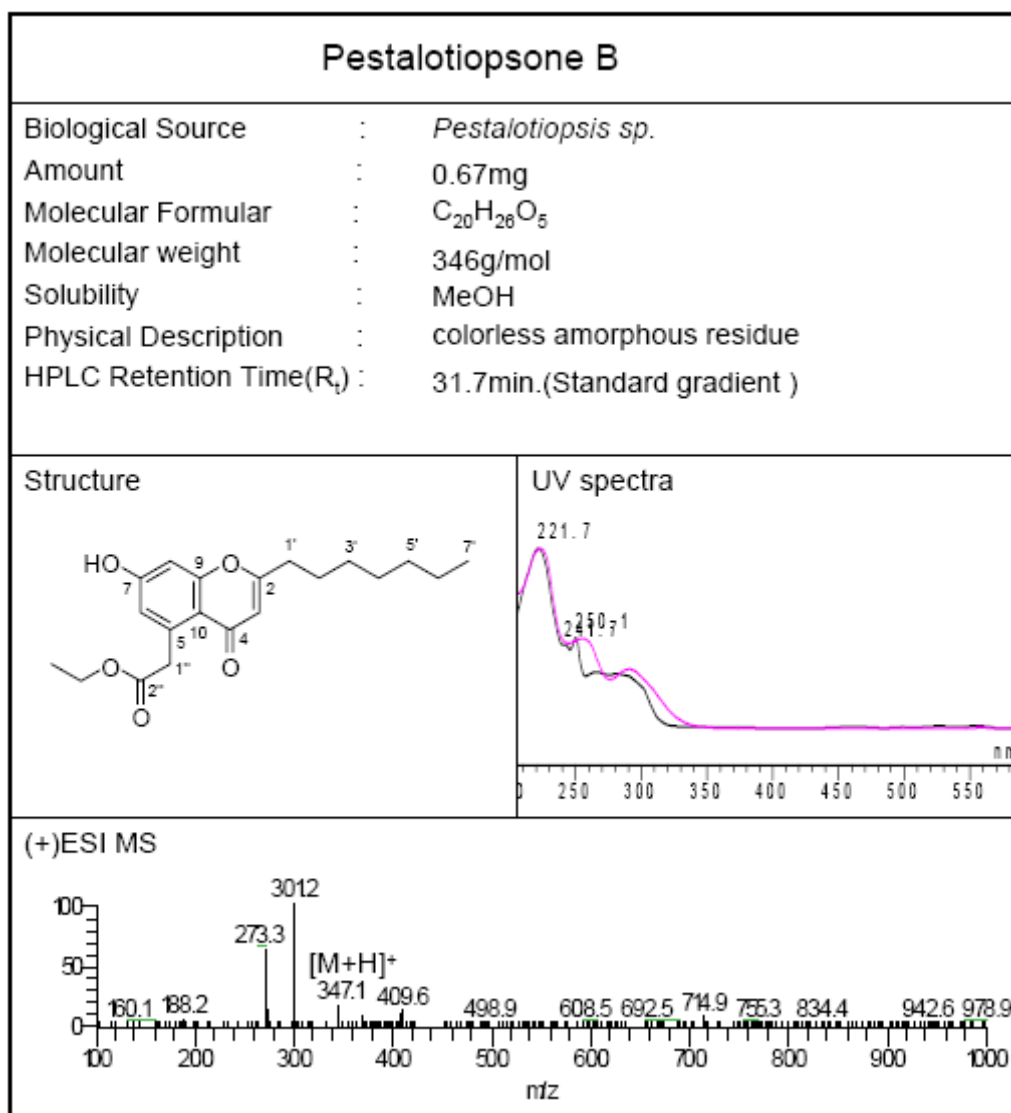


Figure 3.2.1.1b HMBC correlations for compound 4

**Figure 3.2.1.2** ESI-MS fragments for compounds **4****Table 3.2.1.1** ¹H NMR (500 MHz) and ¹³C NMR (125 MHz) spectroscopic data for pestalotiopsones A (**4**)

Atom no.	4 (in acetone- <i>d</i> ₆)		HMBC (H to C)	2-methyl-5-carboxymethyl-7-hydroxy-chromone from Reference (in DMSO- <i>d</i> ₆)	
	δ _H [ppm]	δ _C [ppm]		δ _H [ppm]	δ _C [ppm]
2		169.3, s			164.1, s
3	5.92, s	111.9, d	2, 4, 10, 1'	5.98, s	117.8, d
4		181.0, s			177.7, s
5		139.8, s			137.8, s
6	6.75, d, 2.2	119.6, d	5, 7	6.65, d, 2	110.3, d
7		162.8, s			160.8, s
8	6.81, d, 2.2	103.8, d	6, 7, 9, 10	6.72, d, 2	101.3, d
9		161.4, s			158.8, s
10		117.2, s			114.2, s
1'	2.59, t, 7.5	35.1, t	2, 3, 2', 3'	2.29, s	19.3, q
2'	1.73, m	28.5, t	2, 1', 3', 4'		
3'	1.35-1.45, 2H, overlapped	30.5, t	1', 2', 4', 5'		
4'	1.35-1.45, 2H, overlapped	30.5, t	2', 3', 5', '6		
5'	1.31, m	33.0, t	3', 4', '6		
6'	1.31, m	24.3, t	4', '5, 7'		
7'	0.88, t, 6.5	15.3, q	'5, 6'		
1''	4.12, s	41.9, t	5, 6, 10, 2''	4.00, s	40.2, t
2''		172.8, s			172.0, s
2''-OCH ₃	3.60, s	52.6, q	2''		

3.2.2 Pestalotiopsone B (5, new compound)



Pestalotiopsone B (**5**) was found to have the molecular formula $C_{20}H_{26}O_5$ (i.e. differing from that of **4** by an additional CH_2 group), which was established by HR-ESI-MS (m/z 347.1860, calcd for $[M+H]^+$ 347.1859).

The 1H NMR data (Table 3.2.2.1) of **5** were similar to those of **4**. This suggests that **5** might have the same basic molecular framework as **4**. However, the signal of the methyl ester group of **4** was absent in the 1H NMR spectrum of **5**. Instead, signals of an ethoxy group (δ 1.24, t, $J = 7.1$ Hz; 4.10, q, $J = 7.1$ Hz) appeared, indicating that an

ethoxy group had replaced the methoxy substituent of **4**. Confirming evidence was obtained from the ^1H - ^1H COSY (Figure 3.2.2.1) correlation and from characteristic ESI-MS fragments. Presence of the ethoxy group was corroborated by the ^1H - ^1H COSY correlation from the protons of the methyl group (1.24, t, $J = 7.1$ Hz) to the oxygenated methylene (4.10, q, $J = 7.1$ Hz). Connection to the carbonyl C-2'' was established by fragments m/z 301 and 273 in the positive ESI-MS of **5** (Figure 3.2.2.2) that originate from a sequential loss of one molecule of ethanol and of carbon monoxide.

Therefore, the structure of pestalotiopsone B was characterized as 5-carboethoxymethyl-2-heptyl-7-hydroxychromone.

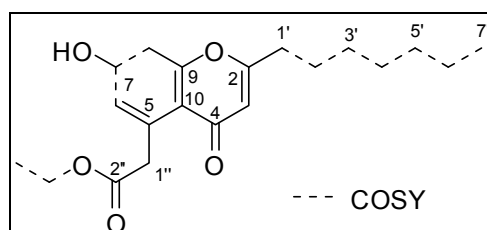


Figure 3.2.2.1 ^1H - ^1H COSY correlations for compound **5**

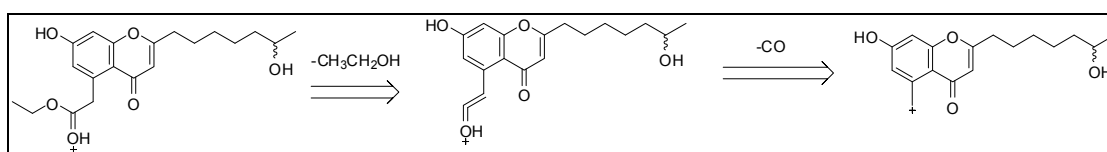
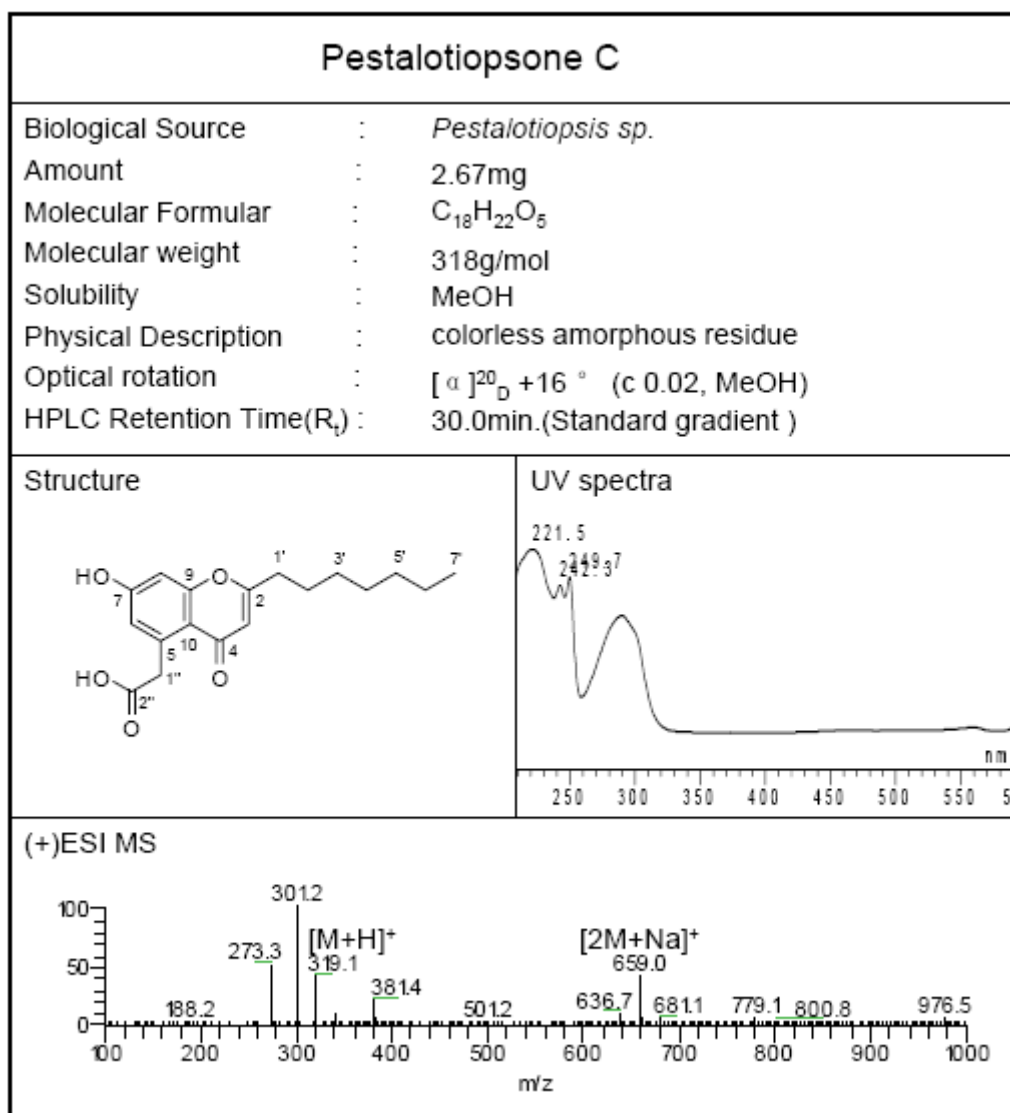


Figure 3.2.2.2 ESI-MS fragments of compound **5**

Table 3.2.2.1 ^1H NMR (500 MHz) spectroscopic data for pestalotiopsone B (**5**) in acetone- d_6

Atom no.	5	Comparison Compound 4	
	δ_{H} [ppm]	δ_{H} [ppm]	δ_{C} [ppm]
2			169.3, s
3	5.93, s	5.92, s	111.9, d
4			181.0, s
5			139.8, s
6	6.78, d, 2.2	6.75, d, 2.2	119.6, d
7			162.8, s
8	6.84, d, 2.5	6.81, d, 2.2	103.8, d
9			161.4, s
10			117.2, s
1'	2.62, t, 7.6	2.59, t, 7.5	35.1, t
2'	1.74, m	1.73, m	28.5, t
3'	1.22-1.43, 2H, overlapped	1.35-1.45, 2H, overlapped	30.5, t
4'	1.22-1.43, 2H, overlapped	1.35-1.45, 2H, overlapped	30.5, t
5'	1.33, m	1.31, m	33.0, t
6'	1.33, m	1.31, m	24.3, t
7'	0.90, t, 7.0	0.88, t, 6.5	15.3, q
1''	4.14, s	4.12, s	41.9, t
2''			172.8, s
2''-OCH ₂ CH ₃	4.10, q, 7.25	3.60, s	52.6, q
2''-OCH ₂ CH ₃	1.24, t, 7.1		

3.2.3 Pestalotiopsone C (6, new compound)



The molecular formula of pestalotiopsone C (**6**) was determined as $C_{18}H_{22}O_5$ by HR-ESI-MS (m/z 319.1540, calcd for $[M+H]^+$ 319.1545).

The 1H and ^{13}C NMR data (Tables 3.2.3.1) of **5** were similar to those of **4** except for the signals of the OCH_3 substituent within **4** which were absent in **6**. Instead, compound **6** featured a free carboxyl group (Figure 3.2.3.1) as established by the ESI-MS fragments m/z 301 and 273 (Figure 3.2.3.2), which originated from the subsequent loss of one molecule water and of carbon monoxide.

Thus, pestalotiopsone C was identified as 5-carboxymethyl-2-heptyl-7-hydroxychromone.

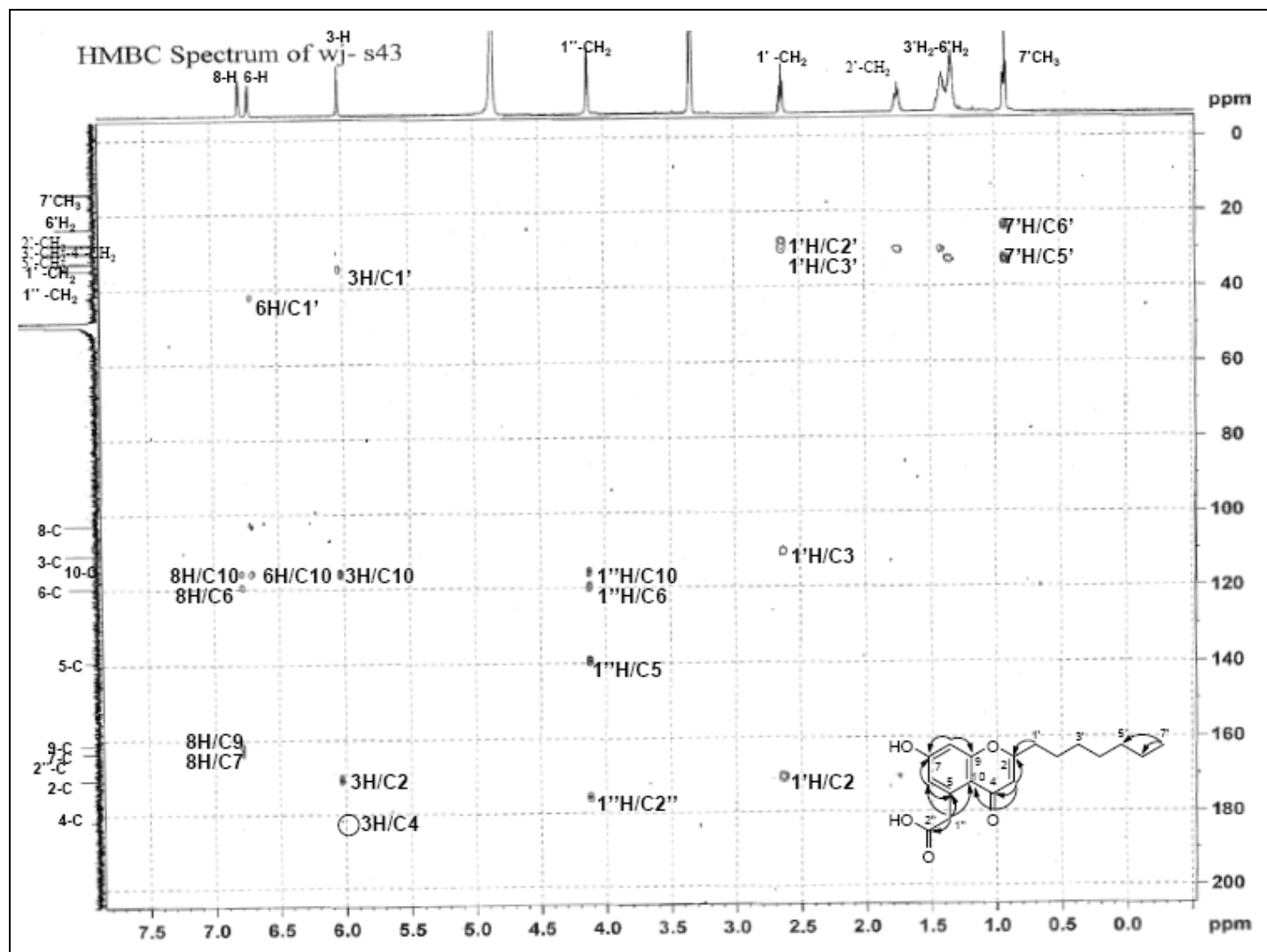
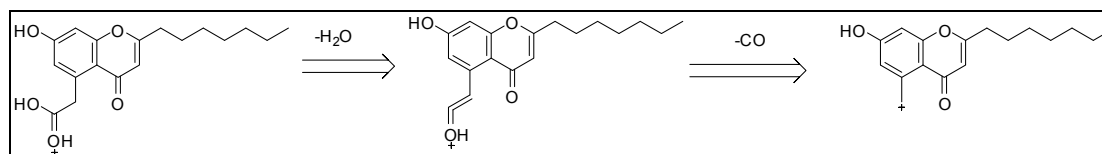
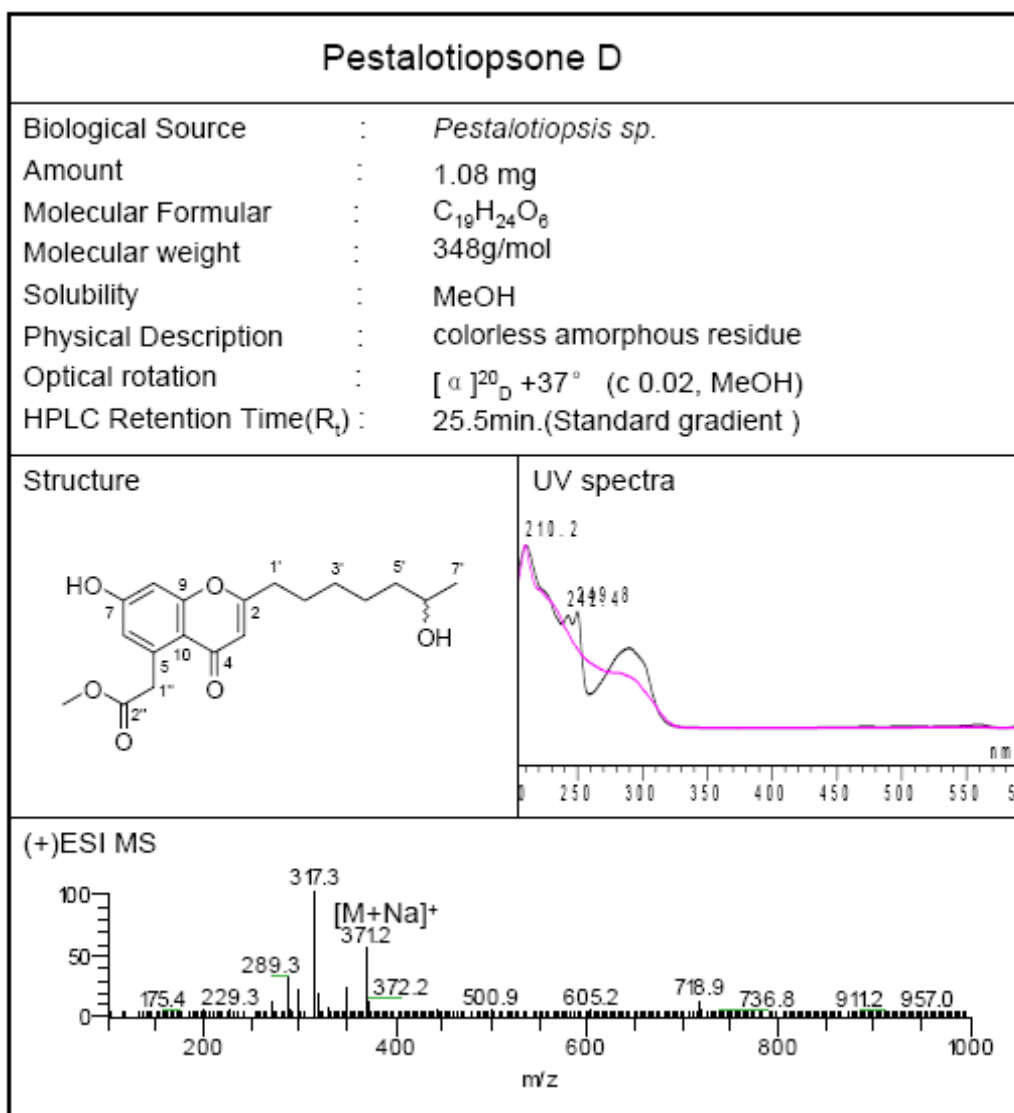


Figure 3.2.3.1 HMBC correlations for compound 6

**Figure 3.2.3.2** ESI-MS fragments of compounds **6****Table 3.2.3.1** ¹H NMR (500 MHz) and ¹³C NMR (125 MHz) spectroscopic data for pestalotiopsones C (**6**)

Atom no.	6 (in methanol- <i>d</i> ₄)		HMBC (H to C)	Comparison Compound 4 (in acetone- <i>d</i> ₆)	
	δ _H [ppm]	δ _C [ppm]		δ _H [ppm]	δ _C [ppm]
2		170.5, s			169.3, s
3	6.03, s	110.6, d	2, 4, 10, 1'	5.92, s	111.9, d
4		181.6, s			181.0, s
5		139.3, s			139.8, s
6	6.71, br s	119.5, d	5, 7	6.75, d, 2.2	119.6, d
7		163.3, s			162.8, s
8	6.78, br s	102.9, d	6, 7, 9, 10	6.81, d, 2.2	103.8, d
9		161.4, s			161.4, s
10		115.8, s			117.2, s
1'	2.63, t, 7.5	34.6, t	2, 3, 2', 3'	2.59, t, 7.5	35.1, t
2'	1.74, m	27.9, t	2, 1', 3', 4'	1.73, m	28.5, t
3'	1.35-1.45, 2H, overlapped	30.1, t	1', 2', 4', 5'	1.35-1.45, 2H, overlapped	30.5, t
4'	1.35-1.45, 2H, overlapped	30.1, t	2', 3', 5', '6	1.35-1.45, 2H, overlapped	30.5, t
5'	1.32, m	32.9, t	3', 4', '6	1.31, m	33.0, t
6'	1.32, m	23.7, t	4', '5, 7'	1.31, m	24.3, t
7'	0.96, t, 6.5	14.4, q	'5, 6'	0.88, t, 6.5	15.3, q
1''	4.12, s	42.1, t	5, 6, 10, 2''	4.12, s	41.9, t
2''		176.2, s			172.8, s
2''-OCH ₃				3.60, s	52.6, q

3.2.4 Pestalotiopsone D (7, new compound)



The molecular weight of pestalotiopsone D (7) was determined as $C_{19}H_{24}O_6$ by HR-ESI-MS m/z 349.1646 (calcd for $C_{19}H_{25}O_6$, 349.1651), which was 16 mass units larger than that of 4, suggesting the presence of an additional hydroxyl group.

The 1H and ^{13}C NMR data of 7 (Tables 3.2.4.1) clearly indicated that this hydroxyl group was attached at C-6'. Supporting evidence (Figure 3.2.4.1) for this assignment was obtained from the downfield chemical shifts of H-6' (δ 3.70, m) and C-6' (δ 68.0,

d) in **7** (δ_{H} 1.32, m for H-6' and δ_{C} 24.3, t for C-6' in **4**, respectively). Moreover, the presence of a hydroxyl group at C-6' was corroborated by the observed ^1H - ^1H COSY correlation from the doublet H₃-7' to H-6'. The ESI-MS fragments m/z 317 and 289 (Figure 3.2.4.2), which originated from the subsequent loss of one molecule water and of carbon monoxide.

Therefore, the structure of pestalotiopsone D was characterized as 5-carbomethoxymethyl-7-hydroxy-2-(6-hydroxyheptyl)chromone.

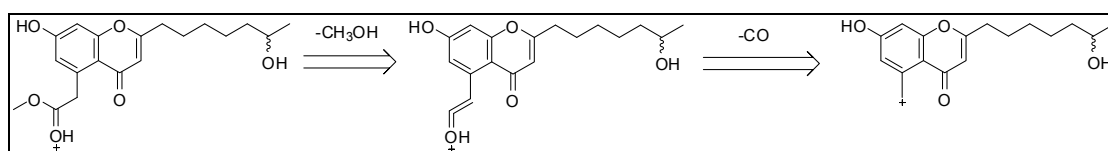


Figure 3.2.4.2 ESI-MS fragments of compounds **7**

Table 3.2.4.1 ^1H NMR (500 MHz) and ^{13}C NMR (125 MHz) spectroscopic data for pestalotiopsone D (**7**)

Atom no.	7 (in methanol- d_4)		HMBC (H to C)	Comparison Compound 4 (in acetone- d_6)	
	δ_{H} [ppm]	δ_{C} [ppm]		δ_{H} [ppm]	δ_{C} [ppm]
2		170.0, s			169.3, s
3	5.92, s	112.0, d	2, 4, 10, 1'	5.92, s	111.9, d
4		181.0, s			181.0, s
5		140.0, s			139.8, s
6	6.74, d, 2.2	120.0, d	5, 7	6.75, d, 2.2	119.6, d
7		162.8, s			162.8, s
8	6.82, d, 2.2	104.0, d	6, 7, 9, 10	6.81, d, 2.2	103.8, d
9		161.0, s			161.4, s
10		117.0, s			117.2, s
1'	2.59, dt, 7.5, 2.5	35.0, t	2, 3, 2', 3'	2.59, t, 7.5	35.1, t
2'	1.73, m	29.0, t	2, 1', 3', 4'	1.73, m	28.5, t
3'	1.36-1.47, 2H, overlapped	30.5, t	1', 2', 4', 5'	1.35-1.45, 2H, overlapped	30.5, t
4'	1.36-1.47, 2H, overlapped	30.5, t	2', 3', 5', '6	1.35-1.45, 2H, overlapped	30.5, t
5'	1.36-1.47, 2H, overlapped	41.0, t	3', 4', '6	1.31, m	33.0, t
6'	3.70, m	68.0, d	4', '5, 7'	1.31, m	24.3, t
7'	1.11, d, 6.1	23.5, q	'5, 6'	0.88, t, 6.5	15.3, q
1''	4.12, s	42.0, t	5, 6, 10, 2''	4.12, s	41.9, t
2''		172.5, s			172.8, s
2''-OCH ₃	3.60, s	52.6, q	2''	3.60, s	52.6, q

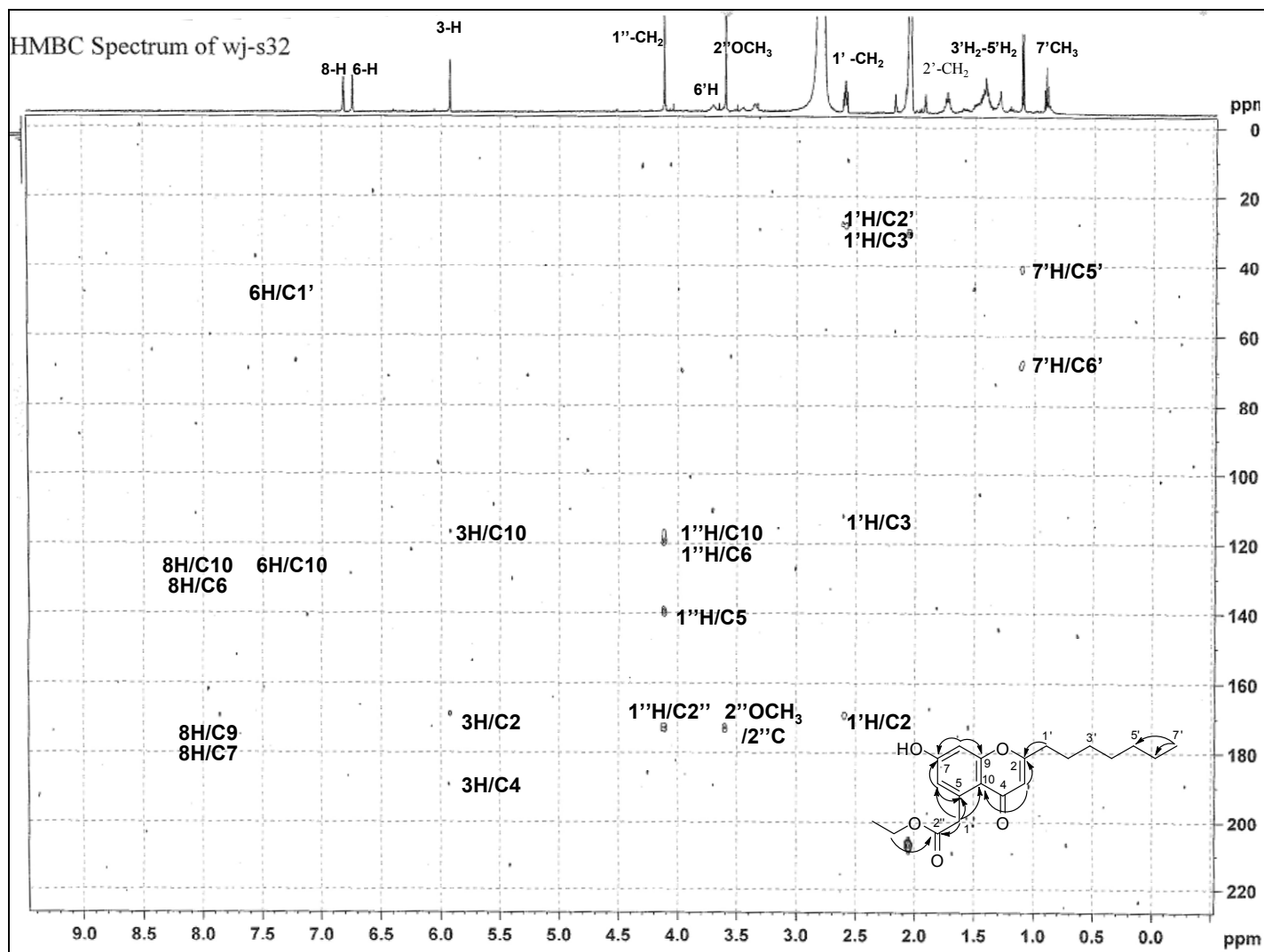
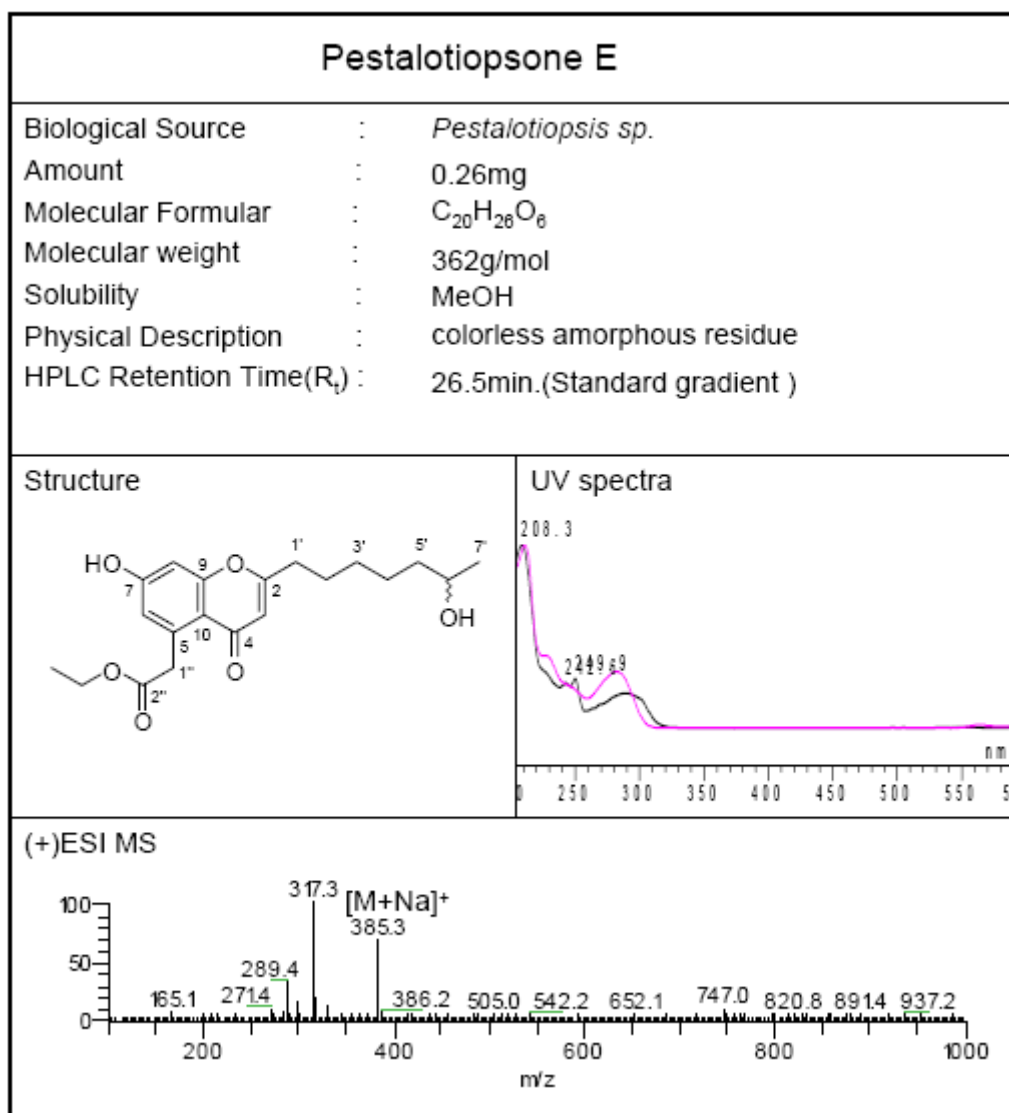


Figure 3.2.4.1 HMBC correlations for compound 7

3.2.5 Pestalotiopsone E (**8**, new compound)

The molecular weight of pestalotiopsone E (**8**) was determined as $C_{20}H_{26}O_6$ by HR-ESI-MS m/z 363.1802 (calcd for $C_{20}H_{27}O_6$, 363.1808), which was 14 mass units larger than that of **7**, indicating the presence of an additional CH_2 group in **8**.

The 1H and ^{13}C NMR data (Tables 3.2.5.1) of **8** were similar to those of **7**. However, the proton and carbon signals of the methoxy group in **7** were absent in **8**. Instead, the signals of an ethoxy group [δ_H 1.20 (t, $J = 7.1$ Hz), 4.07 (q, $J = 7.1$ Hz); δ_C 61.0, t, 14.5, q] appeared, indicating that an ethyl substituent had replaced the methyl group of **7**.

The presence of the ethoxy group was further corroborated by the ^1H - ^1H COSY correlations from the protons of the methyl group (1.20, t, $J = 7.1$ Hz) to the oxygenated methylene (4.07, q, $J = 7.1$ Hz). The connection of the latter to the carbonyl carbon C-2'' was established by the HMBC correlations (Figure 3.2.5.1) from the CH_2 group to C-2''. The existence of the ethoxy group was further supported by the ESI-MS fragments (Figure 3.2.5.2).

On the basis of these findings, the structure of pestalotiopson E was identified as 5-carboethoxymethyl-7-hydroxy-2-(6-hydroxyheptyl)chromone.

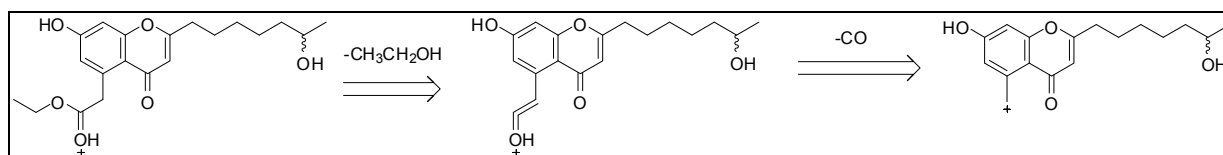


Figure 3.2.5.2 ESI-MS fragments of compounds 8

Table 3.2.5.1 ^1H NMR (500 MHz) and ^{13}C NMR (125 MHz) spectroscopic data for pestalotiopsones E (8)

Atom no.	8 (in acetone- d_6)		HMBC (H to C)	Comparison Compound 7 (in methanol- d_4)	
	δ_{H} [ppm]	δ_{C} [ppm]		δ_{H} [ppm]	δ_{C} [ppm]
2		170.0, s			170.0, s
3	5.92, s	112.0, d	2, 4, 10, 1'	5.92, s	112.0, d
4		181.0, s			181.0, s
5		140.0, s			140.0, s
6	6.74, d, 2.2	120.0, d	5, 7	6.74, d, 2.2	120.0, d
7		162.8, s			162.8, s
8	6.82, d, 2.2	104.0, d	6, 7, 9, 10	6.82, d, 2.2	104.0, d
9		161.0, s			161.0, s
10		117.0, s			117.0, s
1'	2.59, dt, 7.5, 2.5	35.0, t	2, 3, 2', 3'	2.59, dt, 7.5, 2.5	35.0, t
2'	1.73, m	29.0, t	2, 1', 3', 4'	1.73, m	29.0, t
3'	1.36-1.47, 2H, overlapped	30.5, t	1', 2', 4', 5'	1.36-1.47, 2H, overlapped	30.5, t
4'	1.36-1.47, 2H, overlapped	30.5, t	2', 3', 5', '6	1.36-1.47, 2H, overlapped	30.5, t
5'	1.36-1.47, 2H, overlapped	41.0, t	3', 4', '6	1.36-1.47, 2H, overlapped	41.0, t
6'	3.70, m	68.0, d	4', '5, 7'	3.70, m	68.0, d
7'	1.11, d, 6.1	23.5, q	'5, 6'	1.11, d, 6.1	23.5, q
1''	4.10, s	42.0, t	5, 6, 10, 2''	4.12, s	42.0, t
2''		172.5, s			172.5, s
2''-OCH ₂ CH ₃	4.07, q, 7.1	61.0, t	2'', 2''-OCH ₂ CH ₃	3.60, s	52.6, q
2''-OCH ₂ CH ₃	1.20, t, 7.1	14.5, q	2'', 2''-OCH ₂ CH ₃		

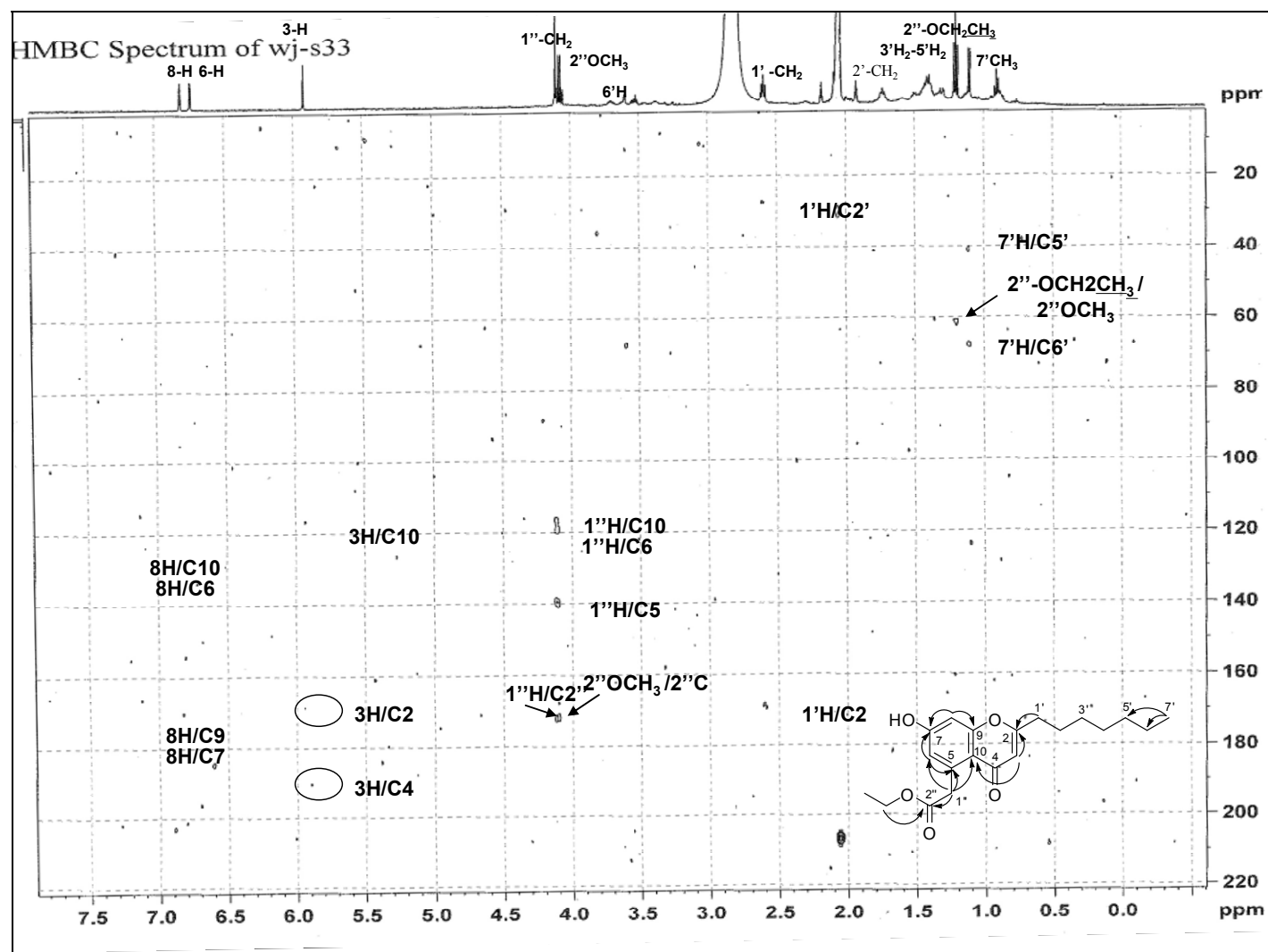
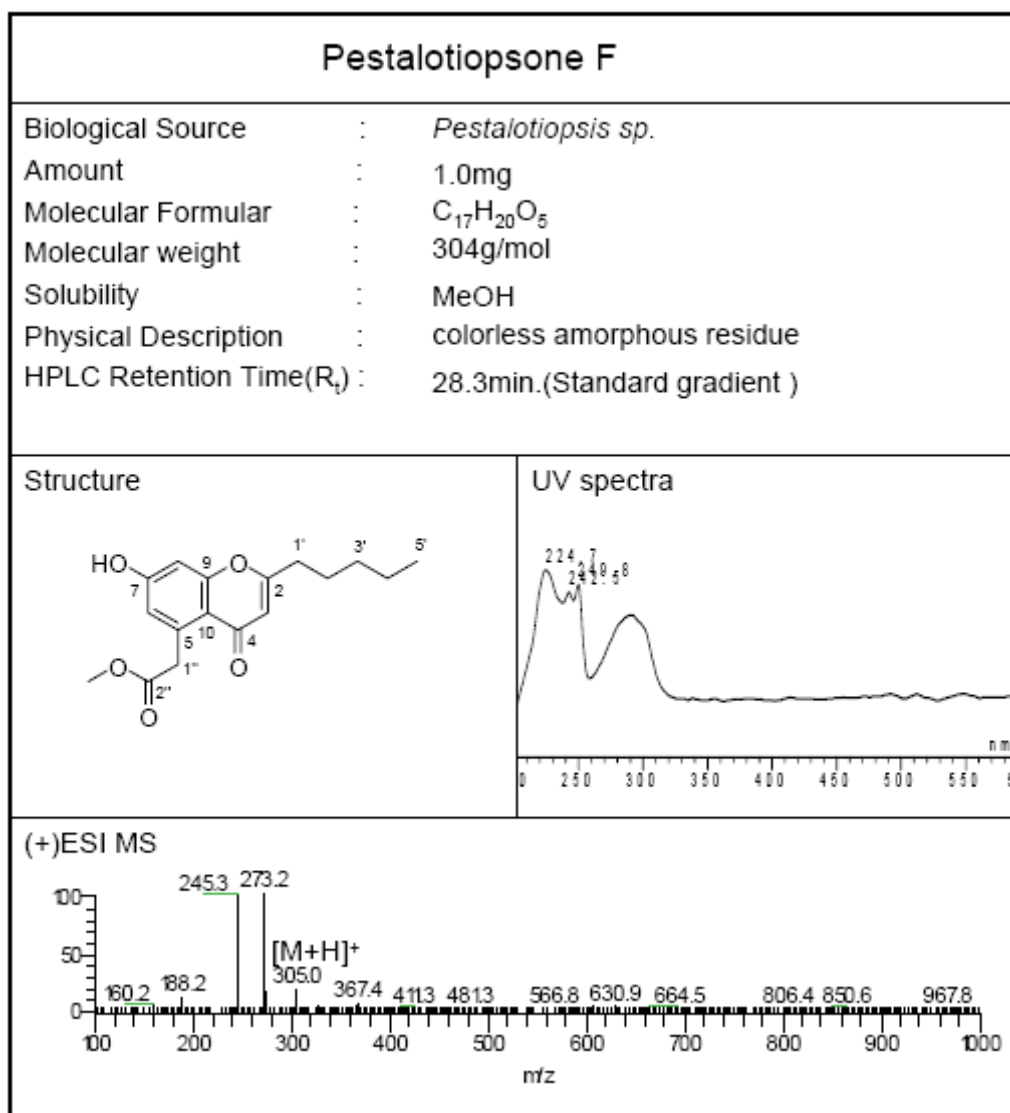


Figure 3.2.5.1 Selected HMBC correlations for compound 8

3.2.6 Pestalotiopsone F (9, new compound)



Pestalotiopsone F (**9**) was found to have the molecular formula $C_{17}H_{20}O_5$ (differing from that of **4** by the loss of a C_2H_4 unit), which was established by HR-ESI-MS (m/z 305.1384, calcd for $C_{17}H_{21}O_5$, 305.1389).

Comparison of its 1H NMR data (Table 3.2.6.1) to those of **4** revealed that the substituents at C-5 for both compounds were the same. Therefore, the alkyl side chain at C-2 in **9** differed from that of **4** by loss of a C_2H_4 unit. Therefore, the structure of pestalotiopsone F was characterized as

5-carbomethoxymethyl-7-hydroxy-2-pentylchromone . The ^1H - ^1H COSY correlations and ESI-MS fragments can be found in [Figure 3.2.6.1](#) and [Figure 3.2.6.2](#) respectively.

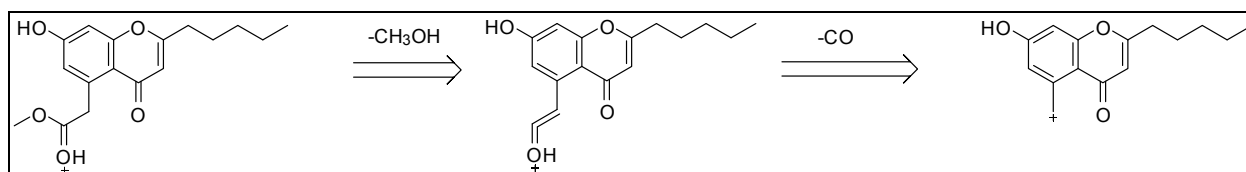


Figure 3.2.6.2 ESI-MS fragments of compounds **9**

Table 3.2.6.1 ^1H NMR (500 MHz) spectroscopic data for pestalotiopsone F (**9**)

Atom no.	9 (in methanol- d_4) δ_{H} [ppm]	Comparison Compound 4 (in acetone- d_6)	
		δ_{H} [ppm]	δ_{C} [ppm]
2			169.3, s
3	5.92, s	5.92, s	111.9, d
4			181.0, s
5			139.8, s
6	6.73, br s	6.75, d, 2.2	119.6, d
7			162.8, s
8	6.80, br s	6.81, d, 2.2	103.8, d
9			161.4, s
10			117.2, s
1'	2.58, t, 7.3	2.59, t, 7.5	35.1, t
2'	1.72, m	1.73, m	28.5, t
3'	1.28-1.49, m, overlapped	1.35-1.45, 2H, overlapped	30.5, t
4'	1.28-1.49, m, overlapped	1.35-1.45, 2H, overlapped	30.5, t
5'	0.9, brs	1.31, m	33.0, t
6'		1.31, m	24.3, t
7'		0.88, t, 6.5	15.3, q
1''	4.10, s	4.12, s	41.9, t
2''			172.8, s
2''-OCH ₃	3.59, s	3.60, s	52.6, q

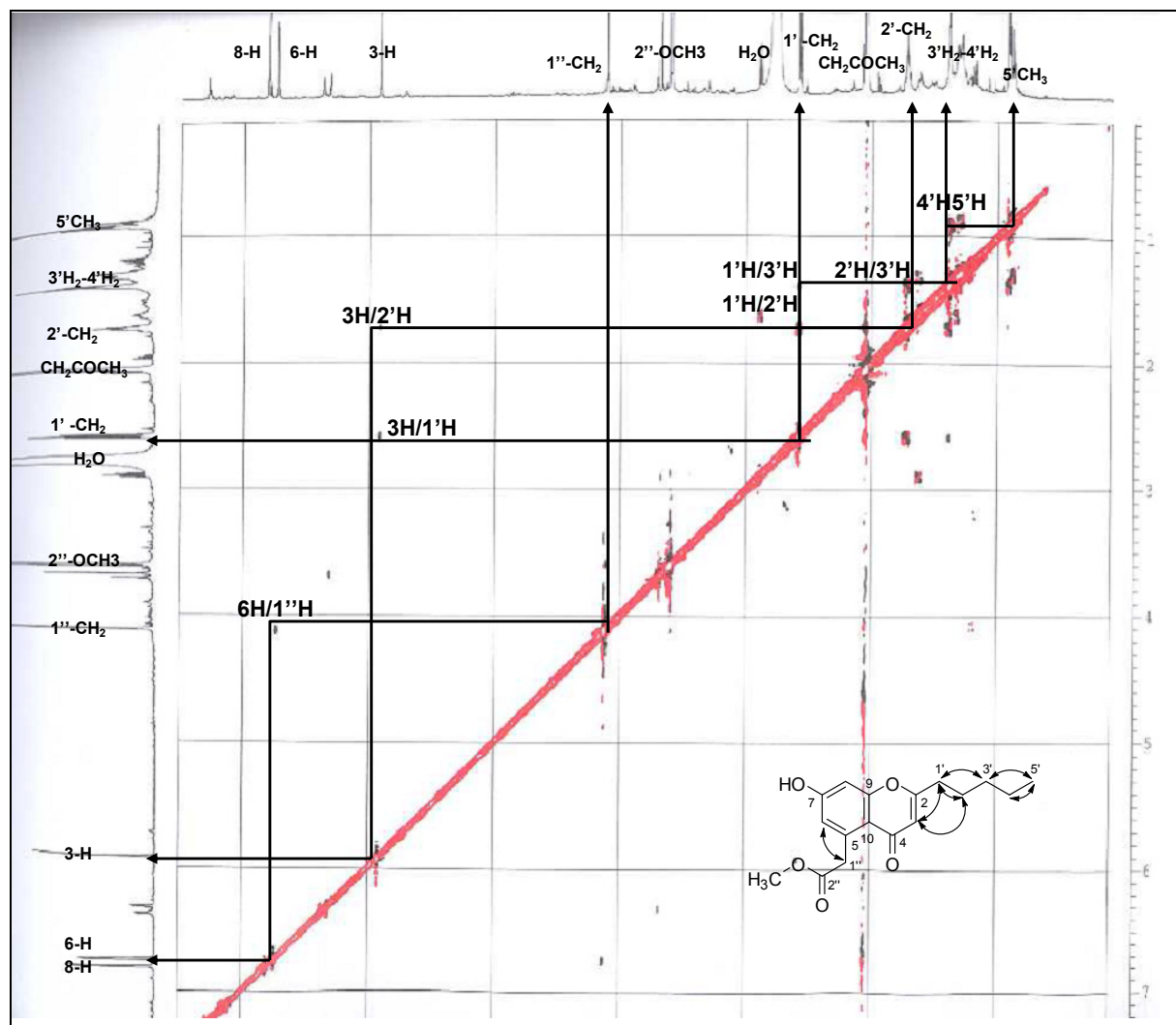
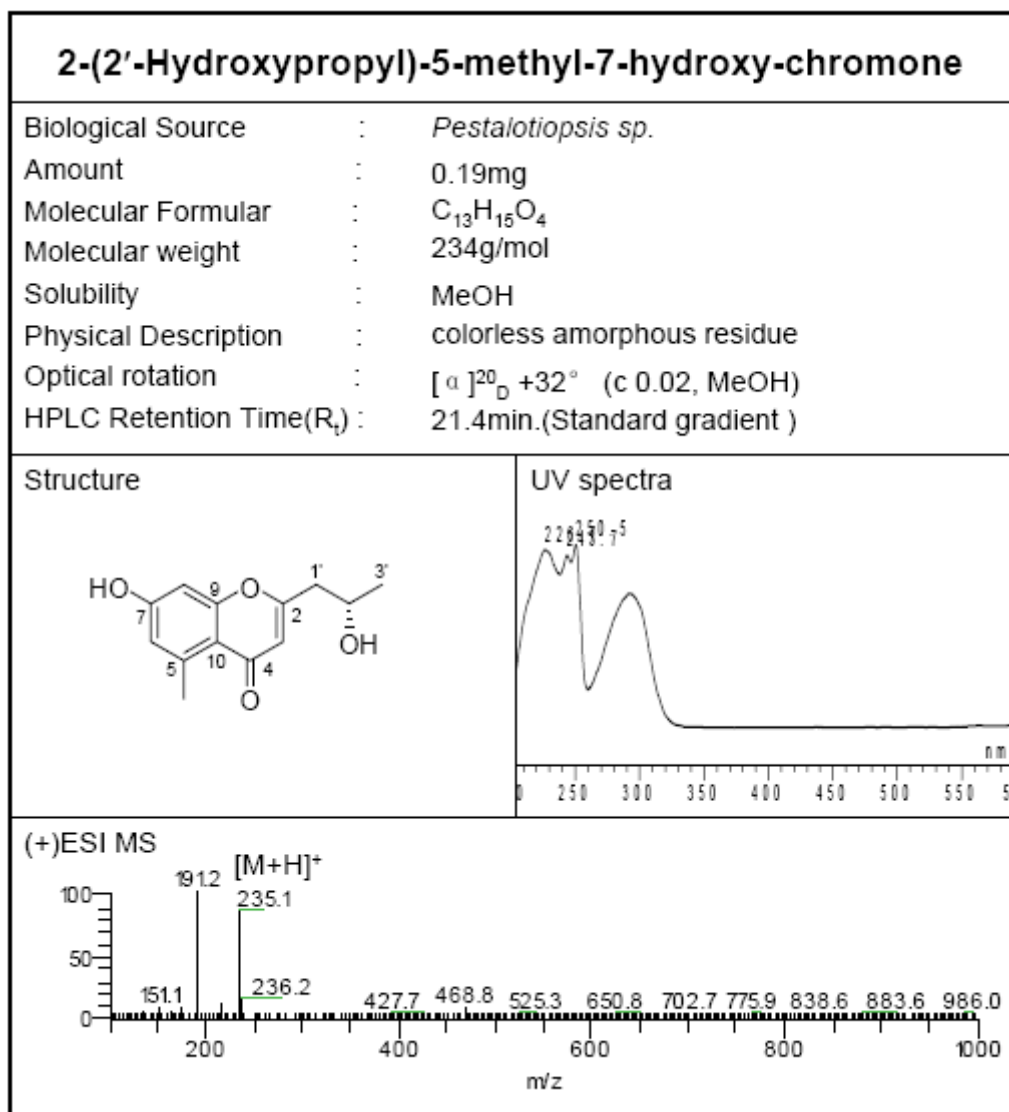


Figure 3.2.6.1 ^1H - ^1H COSY correlations for compound 9

3.2.7 2-(2'-Hydroxypropyl)-5-methyl-7-hydroxy-chromone (10, known compound)



2-(2'-Hydroxypropyl)-5-methyl-7-hydroxy-chromone (**10**) was isolated as a white amorphous powder in CH₃OH (0.19 mg). This compound exhibited a pseudomolecular ion at 235.1 [M + H]⁺ in the positive mode of EIS-MS. The molecular formula C₁₃H₁₅O₄ was established by the HRESI-MS (*m/z* 235.0965, calcd for [M+H]⁺ 235.0970), which indicated that seven degrees of unsaturation. The UV absorption maxima at 227, 244, 251 nm indicated that **10** should be a chromone

derivative.

The ^1H NMR data of **10** (Table 3.2.7.1) and its ^1H - ^1H COSY spectra (Figure 3.2.7.1) showed the presence of two methyl groups [δ_{H} 1.25 (d, $J = 6.3$ Hz, 3'-CH₃); δ_{H} 1.25 (d, $J = 6.3$ Hz, 1''-CH₃)], one methylene group (δ_{H} 2.65, m, 1'-CH₂), one oxygenated methine group (δ_{H} 4.17, m, 2'-CH) and three olefinic methines (δ_{H} 5.97, s, 3-CH; δ_{H} 6.47, s, 6-CH; δ_{H} 6.50, s, 8-CH).

Comparison of the UV and ^1H NMR data of **7** (Table 3.2.7.1) with those of 2-methyl-5-carboxymethyl-7-hydroxy-chromone, together with the positive ESI-MS (Figure 3.2.7.2) and the value of $[\alpha]_{\text{D}} +32$ (literature data $[\alpha]_{\text{D}} +38.4$) (Kashiwada *et al.* 1984) revealed that they are the same compound.

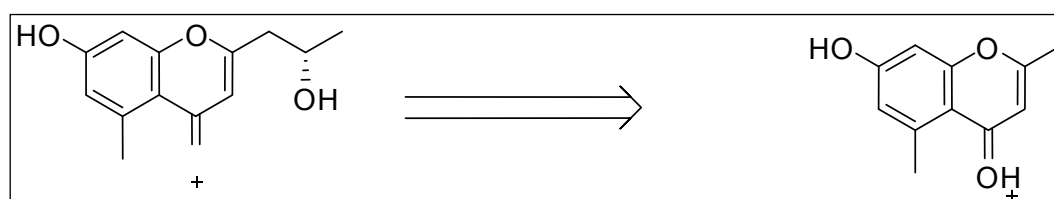


Figure 3.2.7.2 ESI-MS fragments of compounds **10**

Table 3.2.6.1 ^1H NMR (500 MHz) spectroscopic data for 2-methyl-5-carboxymethyl-7-hydroxy-chromone (**10**)

Atom no.	10 (in acetone- d_6) δ_{H} [ppm]	5-Carbomethoxymethyl-2-heptyl-7-hydroxychromone from Reference (in DMSO- d_6)	
		δ_{H} [ppm]	δ_{C} [ppm]
2			164.9, s
3	5.97, s	5.97, s	116.4, d
4			178.9, s
5			141.5, s
6	6.47, br s	6.61, s	111.4, d
7			160.6, s
8	6.50, br s	6.61, s	100.4, d
9			159.1, s
10			114.4, s
1'	2.65, 2H, overlapped	2.58, d, 7	42.7, t
2'	4.17, m	4.02, m	64.0, d
3'	1.25, d, 6.3	1.15, d, 7	23.2, q
1''	2.66, s	2.66, s	22.3, t

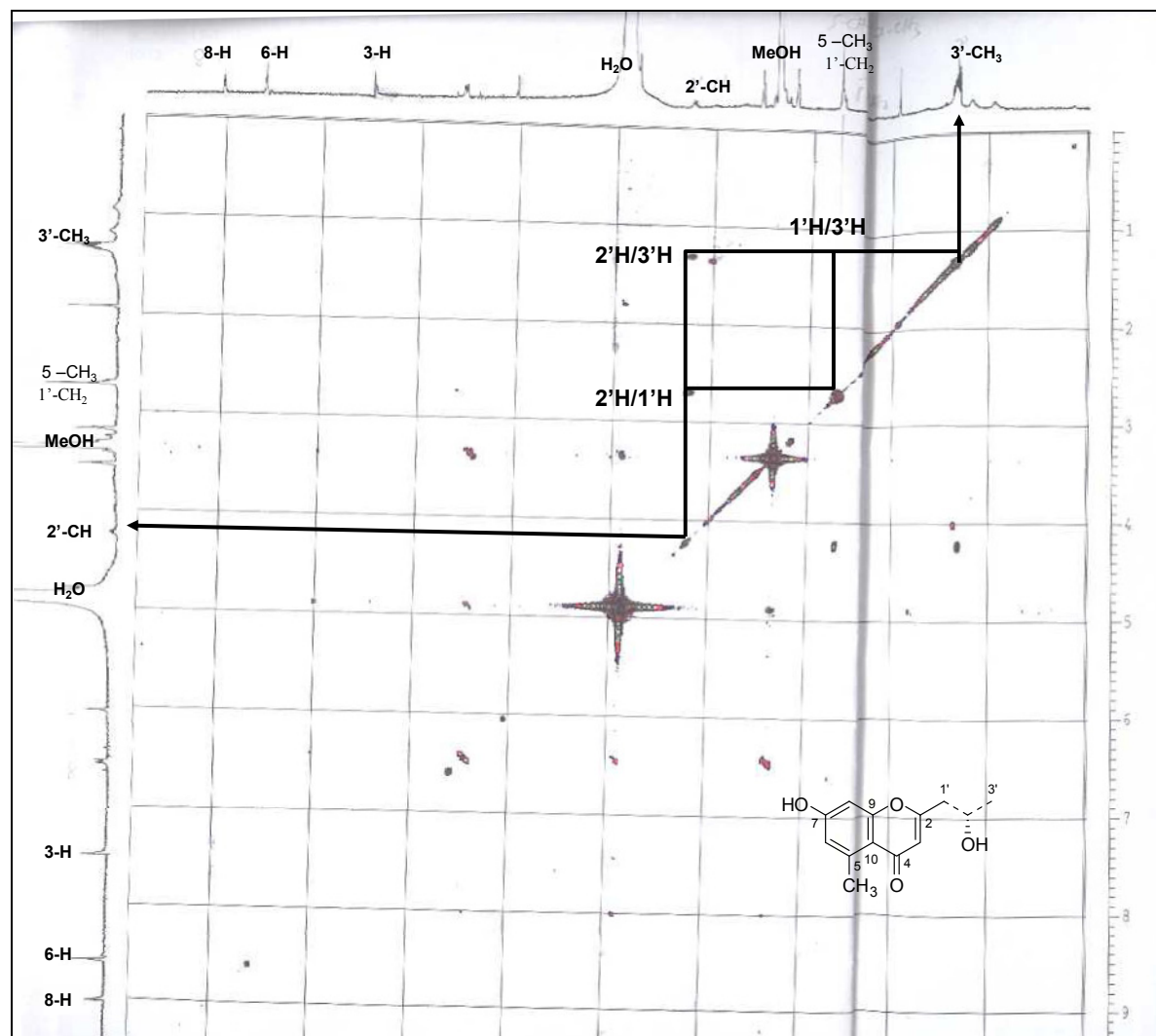
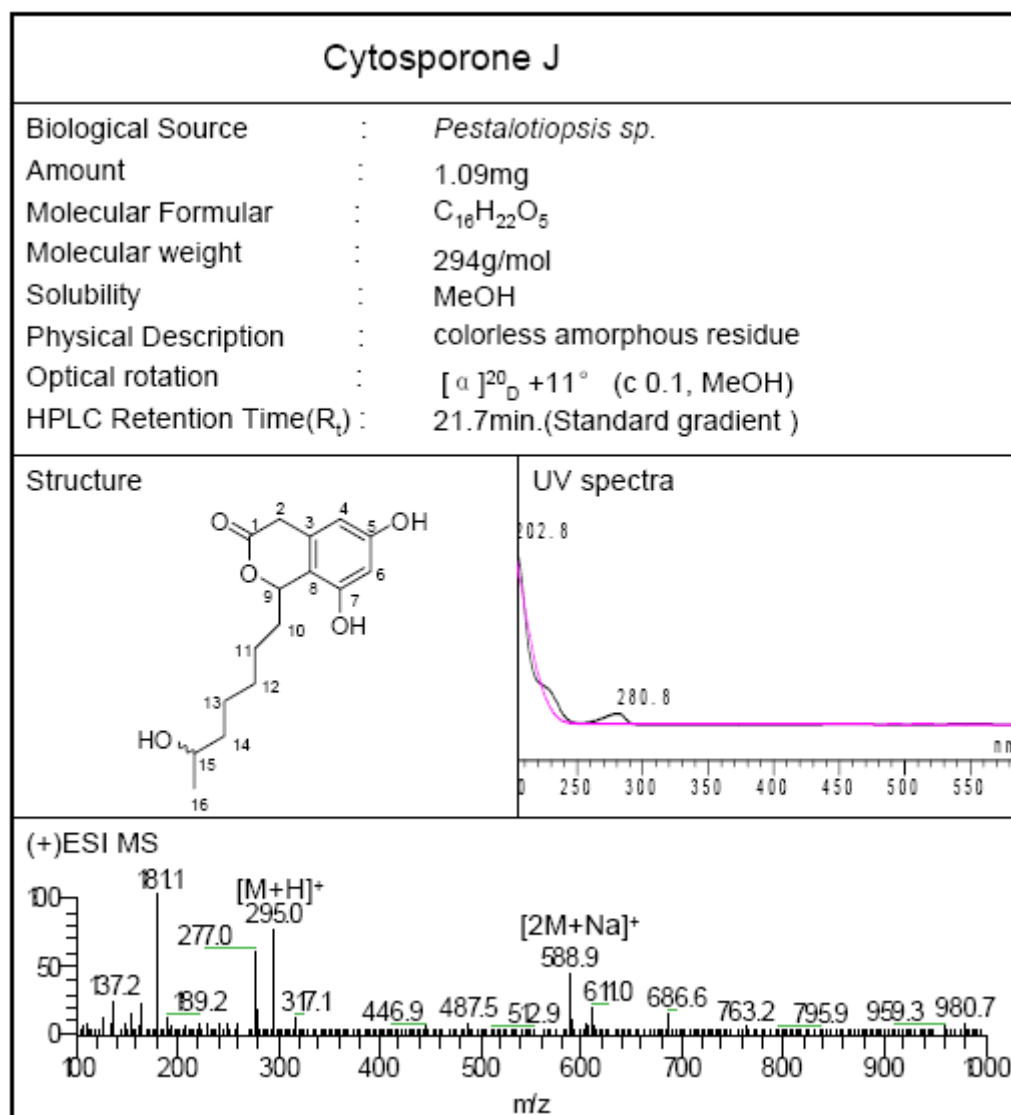


Figure 3.2.7.1 ^1H - ^1H COSY correlations for compound 10

3.3 Cytosporone Derivatives

3.3.1 Cytosporone J (11, new compound)



Cytosporone J (**11**), a colorless amorphous solid, has the molecular formula $C_{16}H_{22}O_5$, established by HR-ESIMS (m/z 295.1538, calcd for $[M+H]^+$ 295.1540), implying six degrees of unsaturation.

The 1H NMR data of **11** (Table 3.3.1.1) and its 1H - 1H COSY spectrum (Figure 3.3.1.1) exhibited an oxygenated methine signal at δ_H 3.68 (m, CH-15), two *meta*-coupled aromatic protons at δ_H 6.23 (br s, H-4) and 6.34 (d, J = 1.5 Hz, H-6),

two geminal protons at δ_{H} 3.45 (d, $J = 19.6$, H-2a) and 3.79 (d, $J = 19.6$ Hz, H-2b) situated between a phenyl ring and the carbonyl group of a six-membered lactone ring, an oxygenated methine at δ_{H} 5.56 (dd, $J = 8.7, 5.1$ Hz, H-9), and the signals of a seven-membered alkyl chain from CH₂-10 to CH₃-16.

These ¹H NMR data were very similar to those reported for cytosporone C (**14**) previously isolated from the endophytic fungus *Cytospora* sp. CR200 (Brady *et al.* 2000), suggesting that both compounds shared the same basic skeleton, except for the presence of an additional oxymethine proton (δ_{H} 3.68, m, H-15) in the side chain of **11**. The COSY correlation of the terminal methyl protons (δ_{H} 1.08, d, $J = 6.3$, H₃-16) to the neighbouring oxymethine proton revealed the extra hydroxyl group is bound to C-15.

Thus, **11** was 15-hydroxycytosporone C.

Table 3.3.1.1 ¹H NMR (500 MHz) data (J in Hz) for cytosporone J (**11**) in acetone-*d*₆.

Atom no.	11 δ_{H} [ppm]	Cytosporone C from Reference	
		δ_{H} [ppm]	δ_{C} [ppm]
1		170.5	
2	3.79, d, 19.55 3.45, d, 19.55	35.4	3.79, d, 24 3.45, d, 24
3		133.5	
4	6.23, s	101.8	6.23, s
5		159.0	
5-OH	8.74 br s		8.73 br s
6	6.34, d, 1.5	106.3	6.34, s
7		154.5	
7-OH	8.37 br s		8.36 br s
8		114.0	
9	5.56, dd, 8.7, 5.1	78.3	5.55, dd, 11.5, 3.0
10	1.86, m 1.79, m	36.4	1.86, m 1.78, m
11	1.55, m 1.34-1.47, m	26.4	1.42, m 1.55, m
12	1.34-1.47, m	29.9	1.27-1.30, 2H, overlapped
13	1.34-1.47, m	29.9	1.27-1.30, 2H, overlapped
14	1.34-1.47, m	32.5	1.27-1.30, 2H, overlapped
15	3.68, br s	23.3	1.27-1.30, 2H, overlapped
16	1.08, d, 6.3	14.3	0.86, t, 8.5

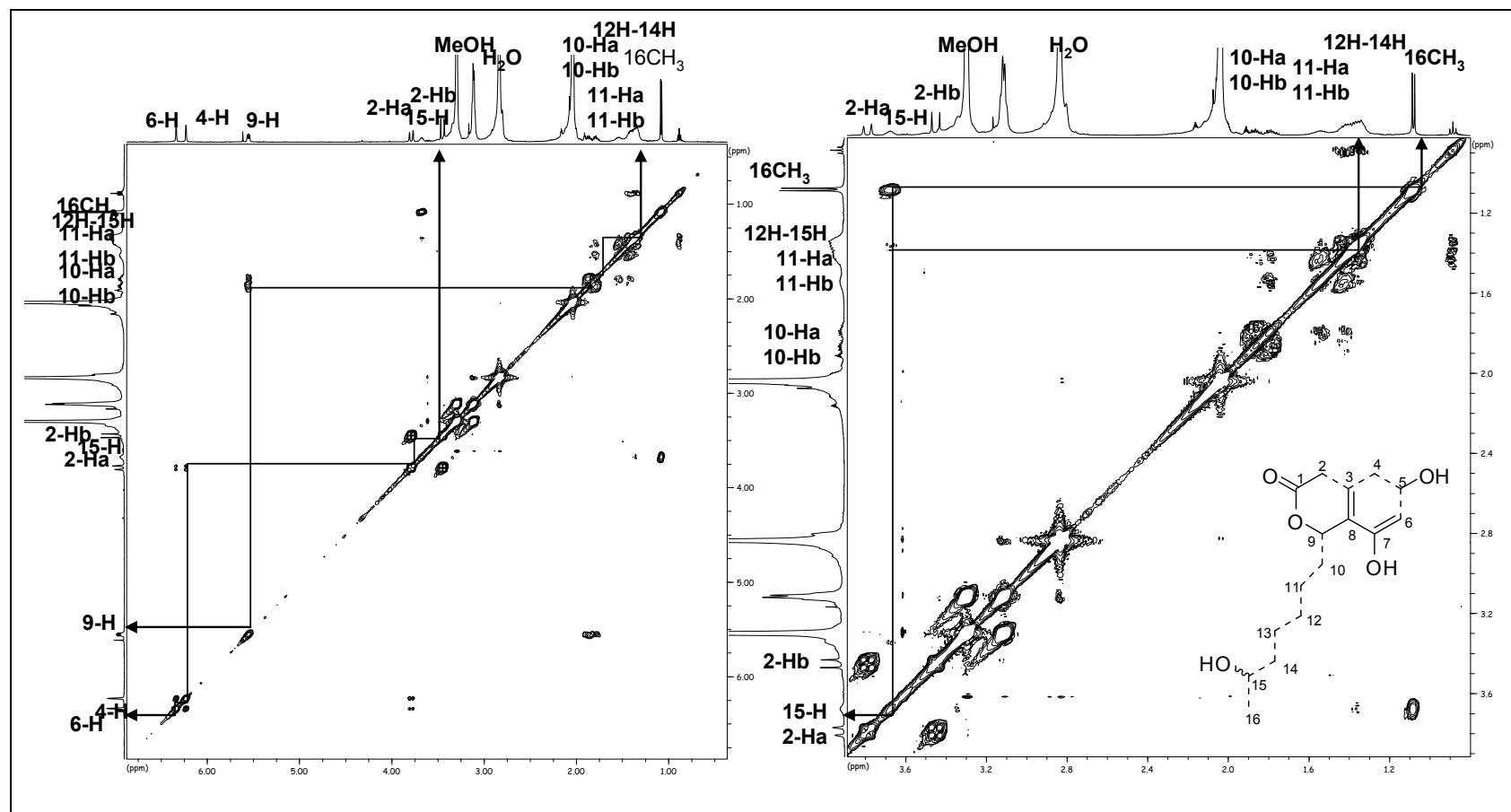
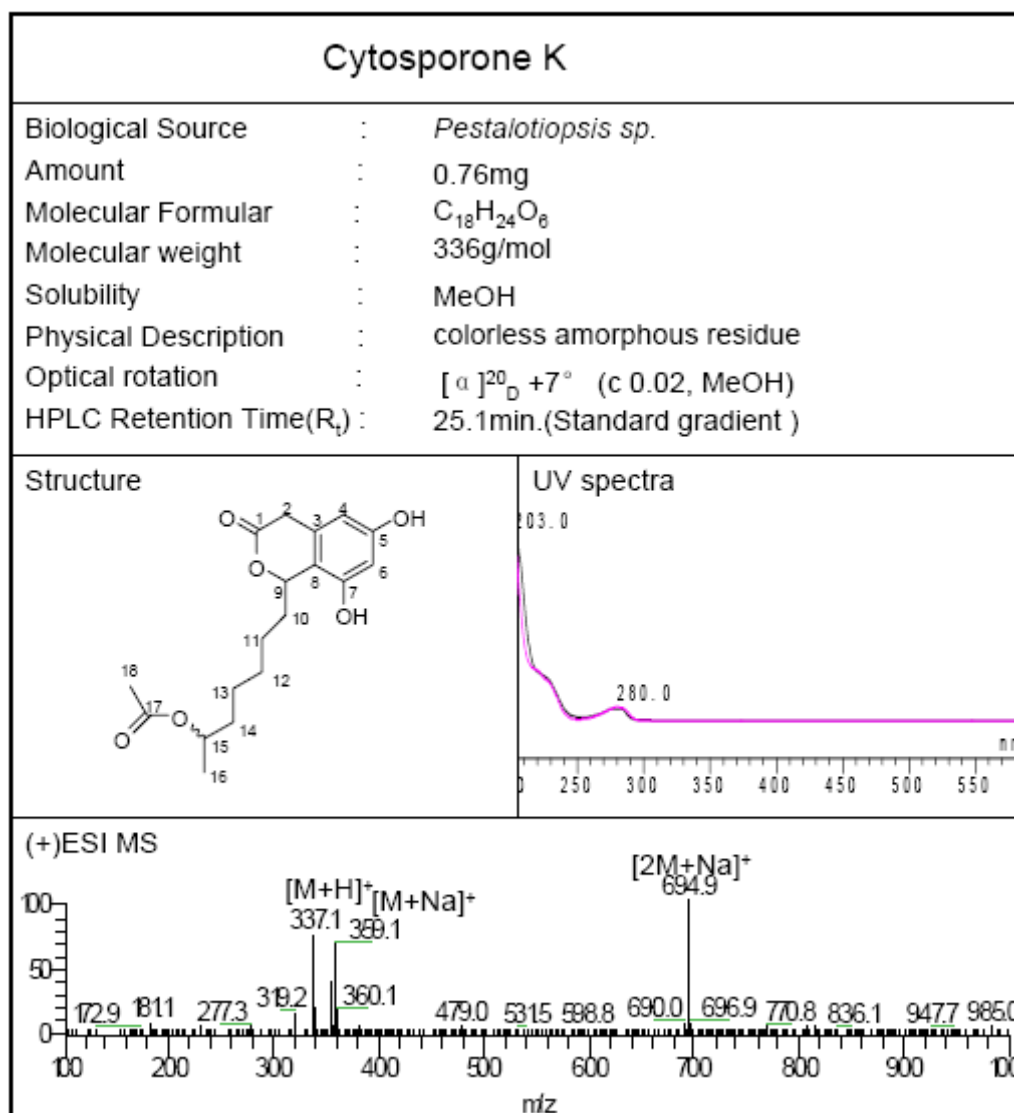


Figure 3.3.1.1 ^1H - ^1H COSY correlations for compound 11

3.3.2 Cytosporone K (12, new compound)



Cytosporone K (**12**) was found to have the molecular formula $C_{18}H_{24}O_6$, established by HR-ESIMS (m/z 337.1646, calcd for $[M+H]^+$ 337.1651), which is 43 amu larger than that of **11** and suggested the presence of an acetyl group from the observation of the fragment at m/z 277 in the ESI-MS spectrum (Figure 3.3.2.2), derived from loss of CH_3COOH .

The ^1H NMR data of **12** (Table 3.3.2.1) were similar to those of **11**, except for the significant downfield shift of H-15 (δ_{H} 4.82, m) and presence of a methyl signal at δ_{H} 2.2 (s, H₃-18) indicative of acetylation of the hydroxyl substituent at C-15.

Hence **12** was 15-acetoxycytosporone C.

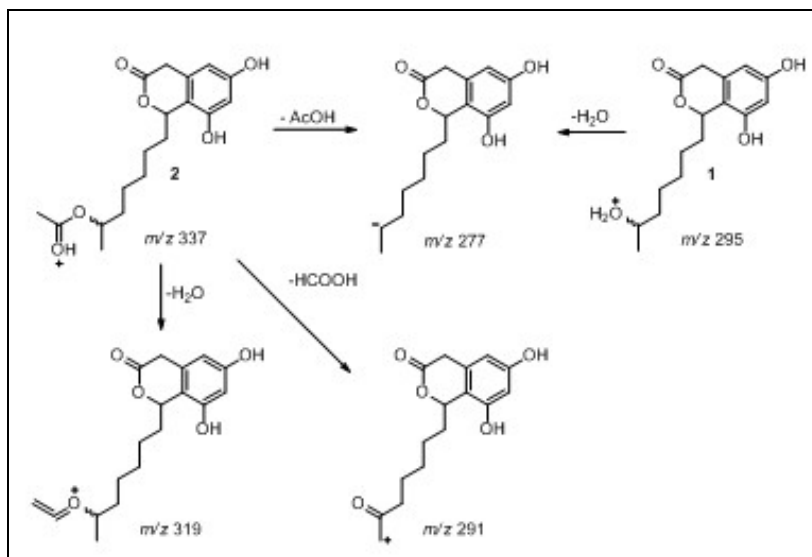


Figure 3.3.2.2 ESI-MS fragments of compounds **11-12**

Table 3.3.2.1 ^1H NMR (500 MHz) data (J in Hz) for cytosporone K (**12**) in acetone- d_6 .

Atom no.	12 δ_{H} [ppm]	Comparison Compound 11 δ_{H} [ppm]
1		
2	3.79, d, 18.9	3.79, d, 19.55
	3.45, d, 19.25	3.45, d, 19.55
4	6.24, s	6.23, s
5-OH		8.74 br s
6	6.35, d, 1.55	6.34, d, 1.5
7-OH		8.37 br s
9	5.56, dd, 9.0, 4.9	5.56, dd, 8.7, 5.1
10	1.92, m	1.86, m
	1.80, m	1.79, m
11	1.55, m	1.55, m
	1.28-1.40, m	1.34-1.47, m
12	1.28-1.40, m	1.34-1.47, m
13	1.28-1.40, m	1.34-1.47, m
14	1.28-1.40, m	1.34-1.47, m
15	4.82, m	3.68, br s
16	1.16, d, 6.3	1.08, d, 6.3
18	2.20, s	

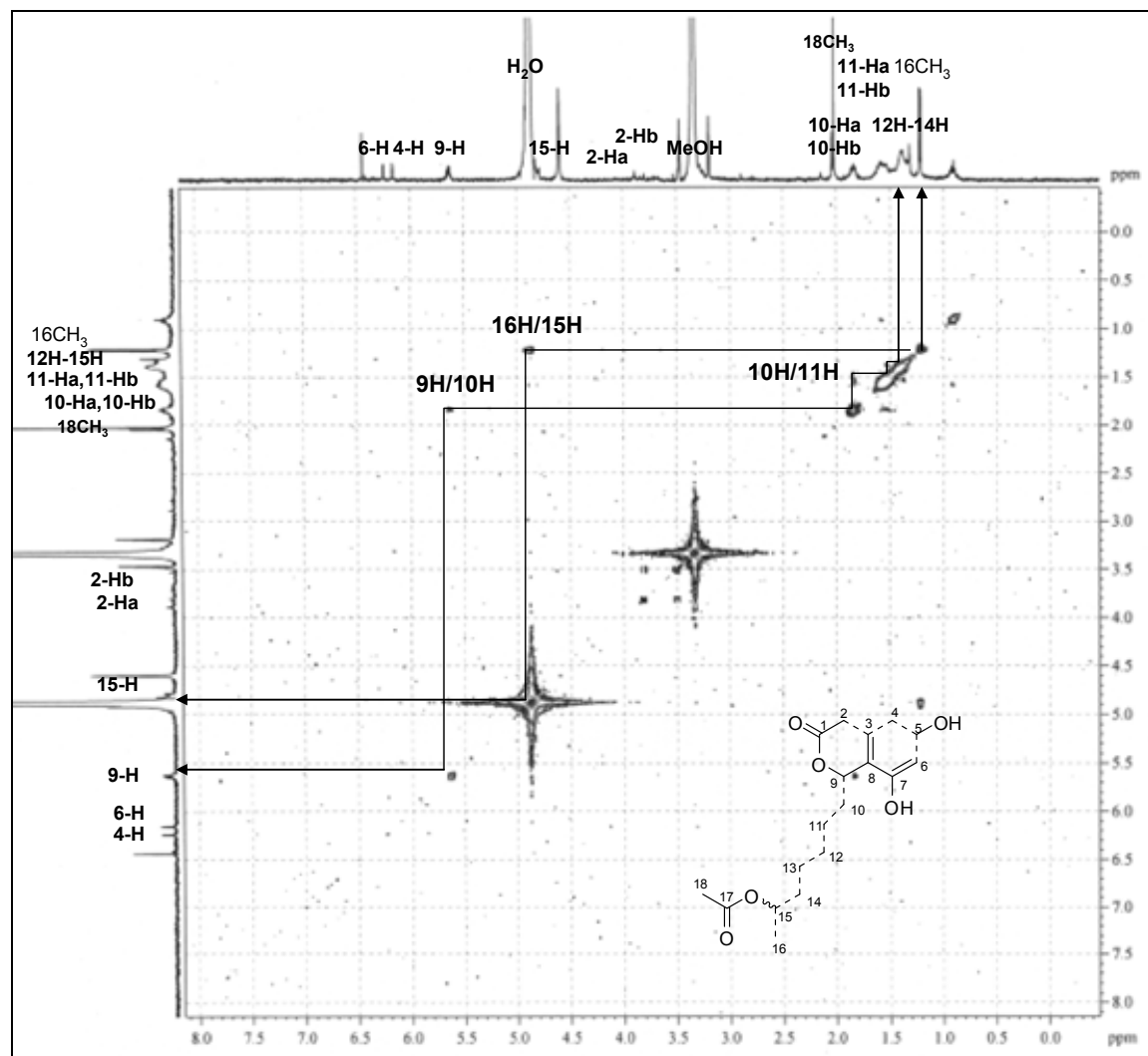
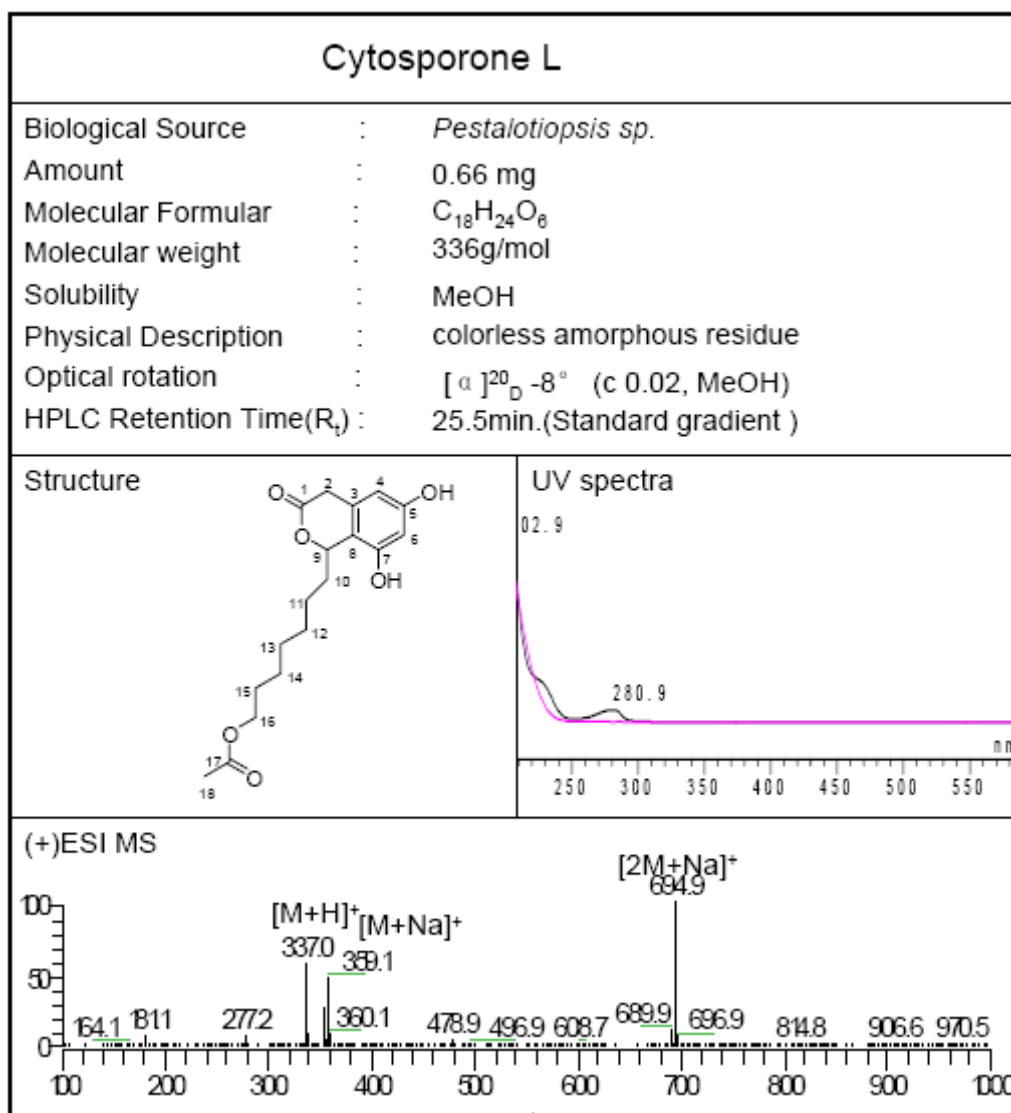


Figure 3.3.2.1 ^1H - ^1H COSY correlations for compound 12

3.3.3 Cytosporone L (13, new compound)



Cytosporone L (**13**) had the same molecular formula as **12** and the ESI-MS (Figure 3.3.3.2) fragment at m/z 277 again suggested the loss of CH₃COOH, indicating that **13** is an isomer of **12**.

The ¹H NMR data (Table 3.3.3.1) were similar to those of the known cytosporone C (**14**) (Brady *et al.* 2000), except for the methyl signal of an acetyl group at δ_H 2.2 (3H, s) and the signal of an oxymethylene group (δ_H 3.98, t, J = 6.6, H₂-16) that replaces the terminal methyl group of **14**. This clearly established the position of the acetoxy group at C-16 rather than at C-15 as observed in **12**.

Hence **13** was 16-acetoxycytosporone C.

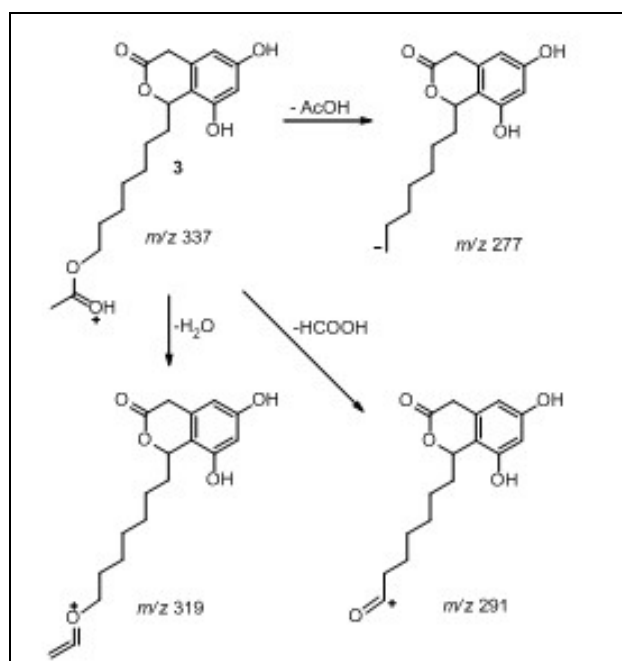


Figure 3.3.3.2 ESI-MS fragments of compound **13**

Table 3.3.3.1 ^1H NMR (500 MHz) data (J in Hz) for cytosporone L (**13**)

Atom no.	13 (in methanol- d_4) δ_{H} [ppm]	Comparison Compound 11 (in acetone- d_6) δ_{H} [ppm]	Cytosporone C from Reference (in acetone- d_6) δ_{H} [ppm] δ_{C} [ppm]	
1			170.5	
2	3.77, d, 19.2	3.79, d, 18.9	35.4	3.79, d, 24
	3.44, d, 19.55	3.45, d, 19.25		3.45, d, 24
3			133.5	
4	6.22, s	6.24, s	101.8	6.23, s
5			159.0	
5-OH				8.73 br s
6	6.33, d, 1.85	6.35, d, 1.55	106.3	6.34, s
7			154.5	
7-OH				8.36 br s
8			114.0	
9	5.53, dd, 9.0, 5.3	5.56, dd, 9.0, 4.9	78.3	5.55, dd, 11.5, 3.0
10	1.92, m	1.92, m	36.4	1.86, m
	1.80, m	1.80, m		1.78, m
11	1.25-1.47, m	1.55, m	26.4	1.42, m
		1.28-1.40, m		1.55, m
12	1.25-1.47, m	1.28-1.40, m	29.9	1.27-1.30, 2H, overlapped
13	1.25-1.47, m	1.28-1.40, m	29.9	1.27-1.30, 2H, overlapped
14	1.25-1.47, m	1.28-1.40, m	32.5	1.27-1.30, 2H, overlapped
15	1.25-1.47, m	4.82, m	23.3	1.27-1.30, 2H, overlapped
16	3.98, t, 6.6	1.16, d, 6.3	14.3	0.86, t, 8.5
18	2.20, s	2.20, s		

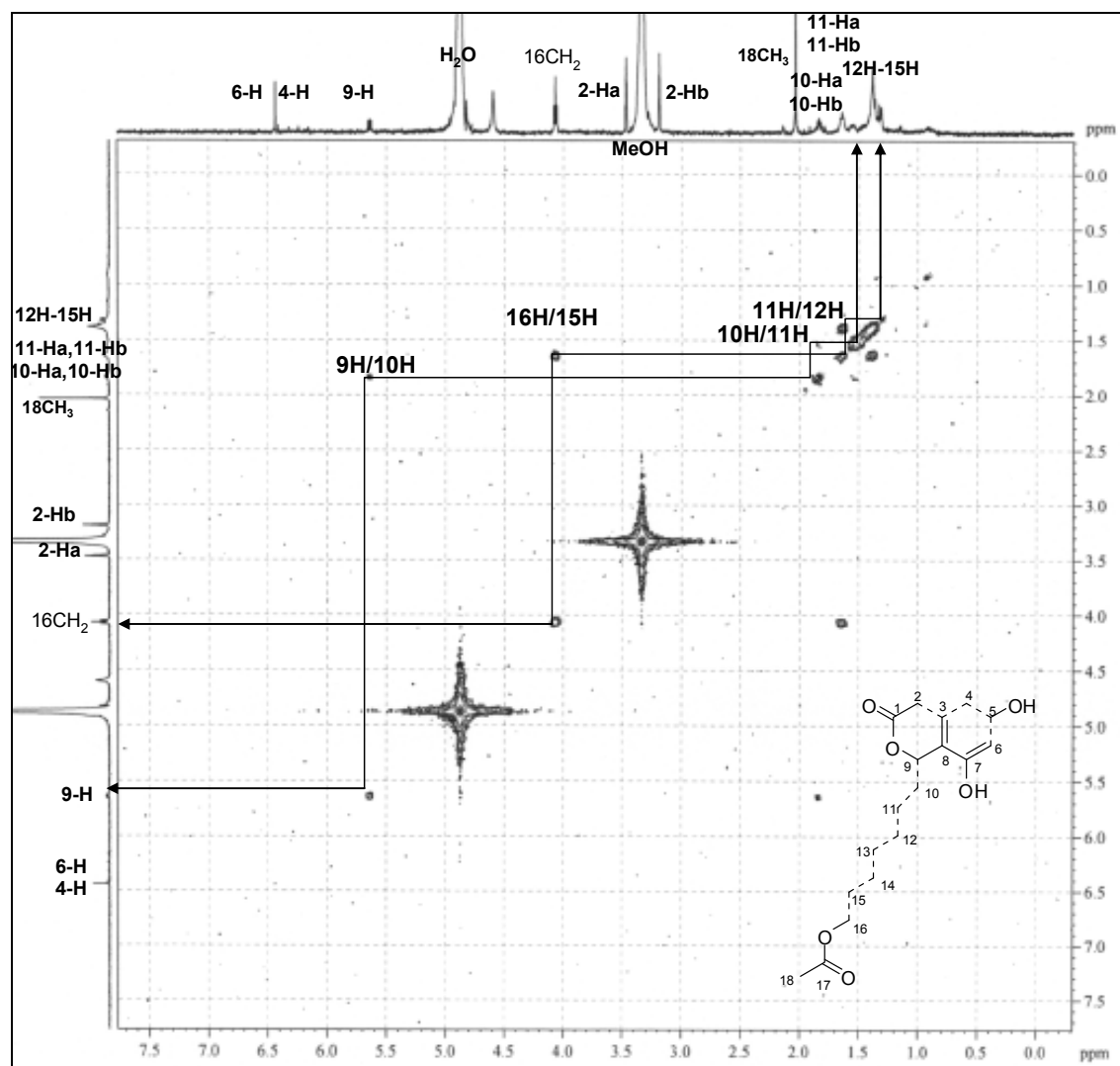
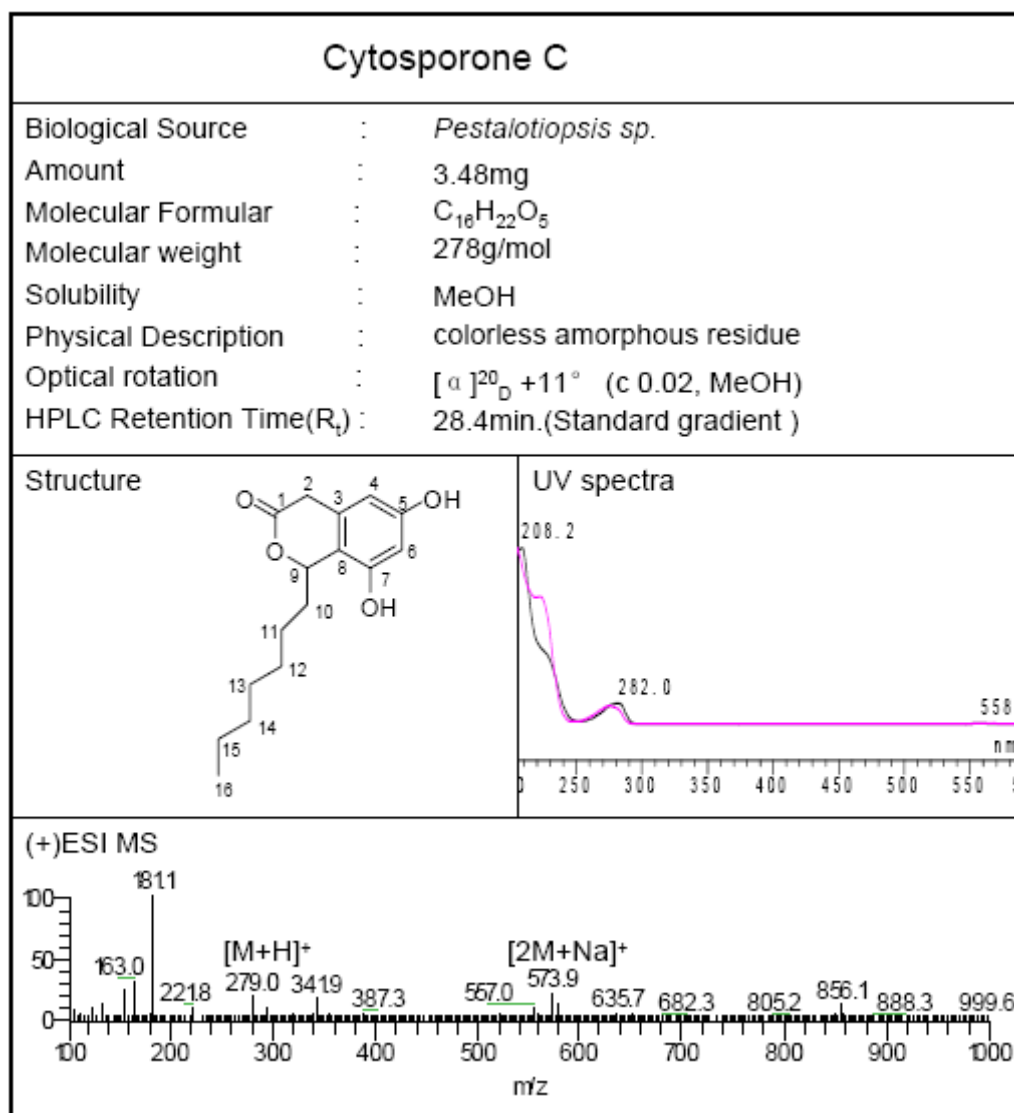


Figure 3.3.3.1 ^1H - ^1H COSY correlations for compound 13

3.3.4 Cytosporone C (**14**, known compound)

Cytosporone C (**14**) was isolated as a white amorphous powder (3.48 mg, CH_3OH). This compound exhibited a pseudomolecular ion at 279.0 $[M+H]^+$ in the positive mode of ESI-MS. The UV absorption maxima at 208, 282 nm indicated that **14** should have the same nucleus as that of cytosporone J (**11**). The NMR data of **14** (Table 3.3.4.1) and the information from its 2D NMR studies (1H - 1H COSY, HSQC, HMBC) indicated the molecular formula $C_{16}H_{22}O_4$ and thus six degrees of unsaturation for **14**.

The ^1H and ^{13}C NMR data of **14** (Table 3.3.4.1) and its ^1H - ^1H COSY spectra showed the presence of two *meta*-coupled aromatic protons of two methines [δ_{H} 6.23 (d, $J = 0.6$ Hz), δ_{C} 101.0, s, CH-4; δ_{H} 6.34 (d, $J = 0.6$ Hz), δ_{C} 106.3, s, CH-6], two geminal protons of a methylene [δ_{H} 3.79 (d, $J = 19.2$ Hz, H-2), 3.45 (d, $J = 19.2$ Hz, H-2); δ_{C} 35.4, t, CH₂-2] situated between a phenyl ring and the carbonyl group of a six-membered lactone ring, an oxygenated methine [δ_{H} 5.55 (dd, $J = 8.8$ Hz, $J = 5.0$ Hz), δ_{C} 78.3, d, CH-9], two hydroxyl signals [δ_{H} 8.73 (br s, 5-OH), 8.36 (br s, 7-OH)] and the signals of a seven-membered alkyl chain from CH₂-10 to CH₃-16.

Comparison of the UV, ^1H and ^{13}C NMR data of **14** (Table 3.3.4.1) with those of Cytosporone C (Brady *et al.* 2000), revealed that they are identical with each other, except for two *meta*-coupled aromatic protons observed in **14** at [δ_{H} 6.23 (d, $J = 0.6$ Hz), δ_{C} 101.0, s, CH-4; 6.34 (d, $J = 0.6$ Hz), δ_{C} 106.3, s, CH-6]. This was confirmed by ^1H - ^1H COSY correlations (Figure 3.3.4.1) between H-6/H-4 and H-2/H-4. The strong HMBC correlations (Figure 3.3.4.2) between H-4/C-2, H-4/C-3, H-4/C-6, H₂-2/C-4, and H-6/C-4, further corroborate the above chemical shifts for two aromatic protons.

Hence compound **14** was assigned as cytosporone C with revision of the NMR datas.

Table 3.3.4.1 ^1H , ^{13}C NMR data for compound cytosporone C (**14**) (500 and 125 MHz, acetone- d_6)

Atom no.	14 (in acetone- d_6)		Cytosporone C from Reference (in acetone- d_6)	
	δ_{H} [ppm]	δ_{C} [ppm]	δ_{H} [ppm]	δ_{C} [ppm]
1	170.5		170.5	
2	35.4	3.79, d, 19.2 3.45, d, 19.2	35.4	3.79, d, 24 3.45, d, 24
3	133		133.5	
4	106	6.23, d, 0.6	101.8	6.23, s
5	159.0		159.0	
5-OH		8.73 br s		8.73 br s
6	101	6.34, d, 0.6	106.3	6.34, s
7	155		154.5	
7-OH		8.36 br s		8.36 br s
8	114		114.0	
9	78	5.55, dd, 8.8, 5.0	78.3	5.55, dd, 11.5, 3.0
10	36.4	1.86, m 1.79, m	36.4	1.86, m 1.78, m
11	26.3	1.42, m 1.55, m	26.4	1.42, m 1.55, m
12	29.5	1.27-1.40, 2H, overlapped	29.9	1.27-1.30, 2H, overlapped
13	29.9	1.27-1.40, 2H, overlapped	29.9	1.27-1.30, 2H, overlapped
14	32.5	1.27-1.40, 2H, overlapped	32.5	1.27-1.30, 2H, overlapped
15	23.0	1.27-1.40, 2H, overlapped	23.3	1.27-1.30, 2H, overlapped
16	14.2	0.87, t, 6.93	14.3	0.86, t, 8.5

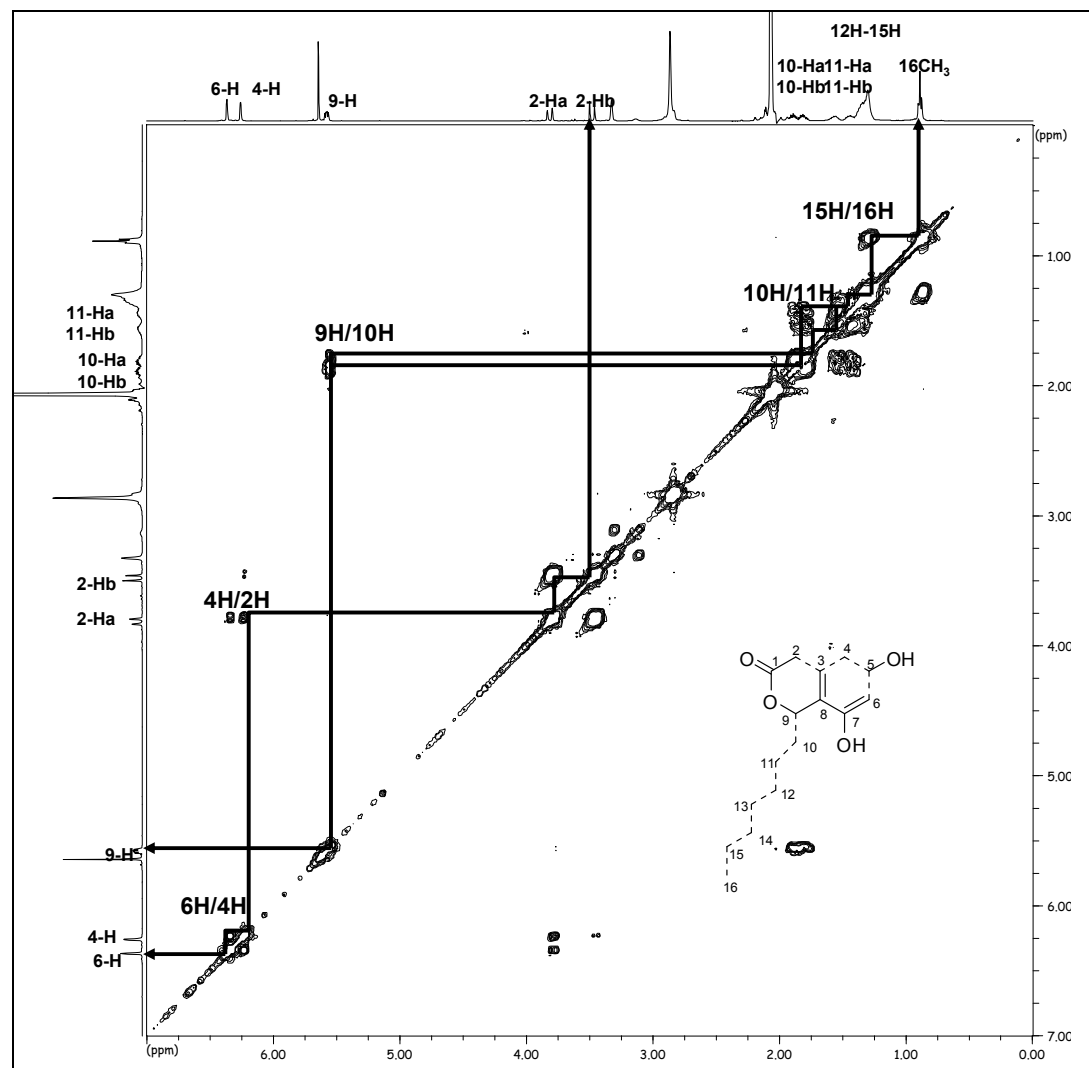


Figure 3.3.4.1 ^1H - ^1H COSY correlations for compound 14

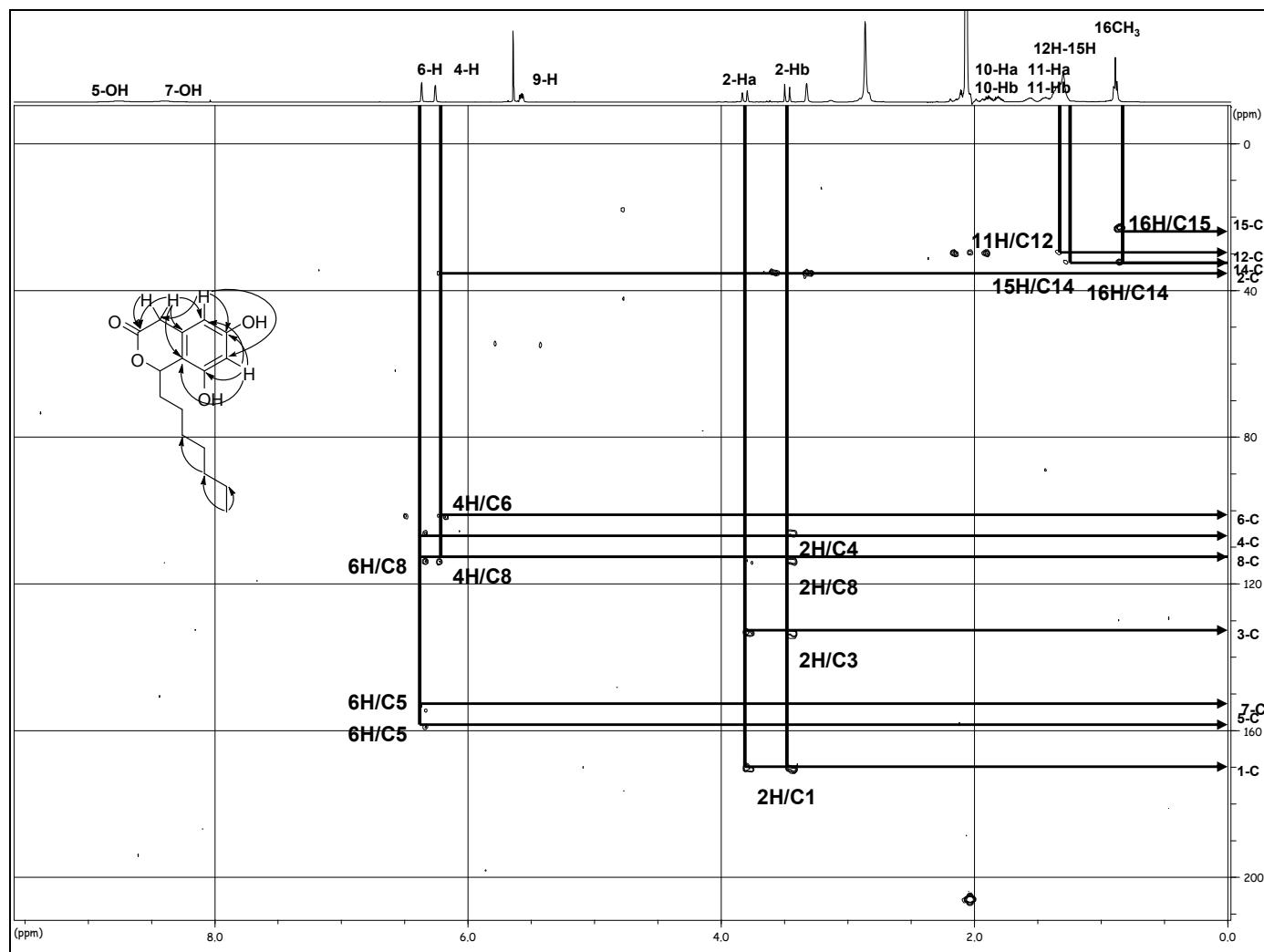
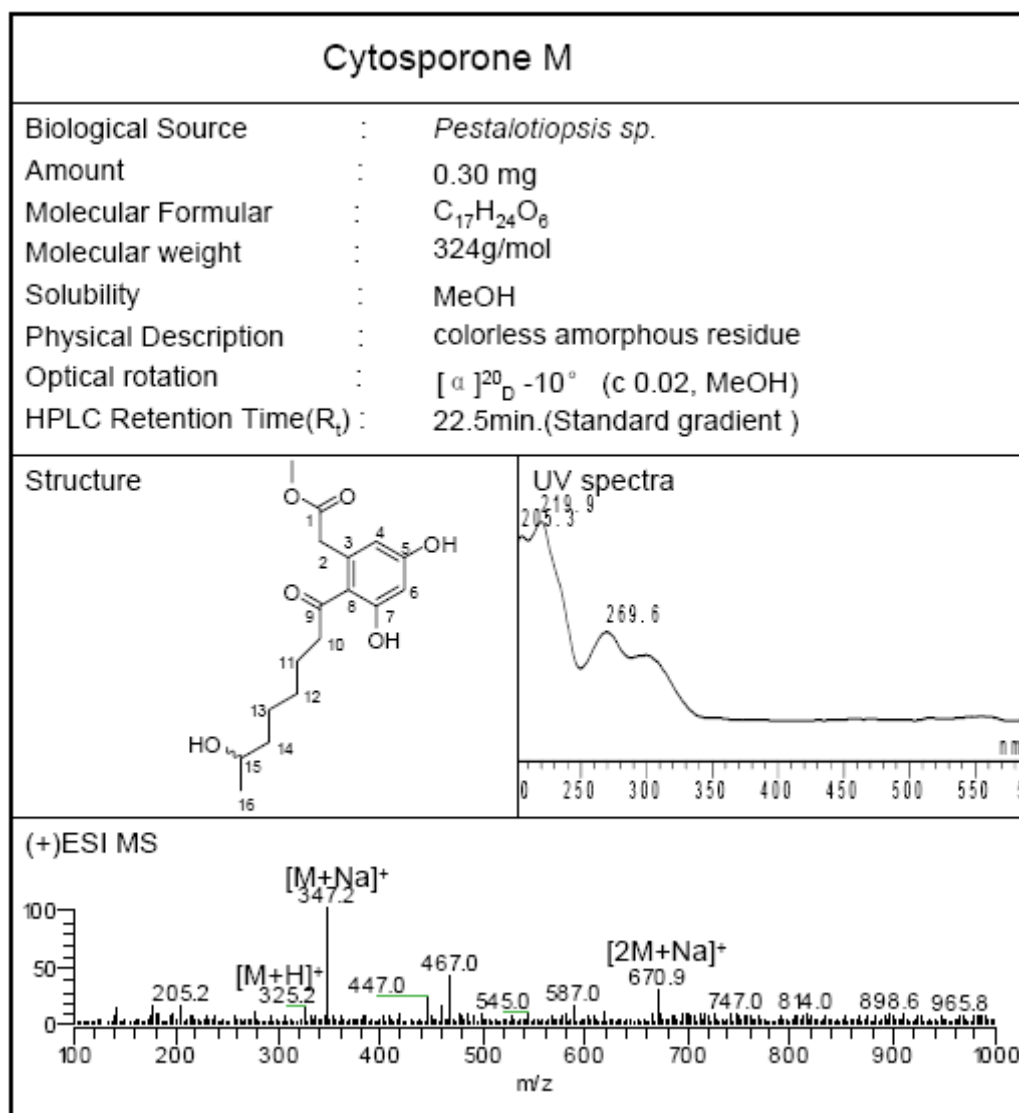


Figure 3.3.4.2 Selected HMBC correlations for compound 14

3.3.5 Cytosporone M (15, new compound)



Cytosporone M (**15**) has the molecular formula C₁₇H₂₄O₆, established by HR-ESIMS (m/z 325.1654, calcd for [M+H]⁺ 325.1646), indicating five degrees of unsaturation.

The ¹H NMR data of **15** (Table 3.3.5.1) and its ¹H-¹H COSY spectrum (Figure 3.3.5.1) displayed a methoxy singlet at δ_H 3.61 (s, H₃-17), a methylene at δ_H 3.67 (s, H₂-2) situated between a phenyl ring and a carboxyl group, an oxygenated methine at δ_H 3.68 (m, H-15), two *meta*-coupled aromatic protons at δ_H 6.30 (d, J = 2.3 Hz, H-4);

δ_{H} 6.37 (d, $J = 2.3$ Hz, H-6), and the resonances for a seven-membered alkyl chain (CH₂-10 to CH₃-16). The ¹H NMR data of **15** were very similar to those of dothiorelone B (**17**), previously isolated from the endophytic fungus *Dothiorella* sp. HTF3 (Xu *et al.* 2004). The only difference between the two compounds was the replacement of the ethyl group of **17** by a methyl group in **15**.

Hence **15** was 1-methoxy-1-desethoxy-dothiorelone B.

Table 3.3.5.1 ¹H NMR (500 MHz) data (J in Hz) for cytosporone M (**15**) in acetone- d_6 .

Atom no.	15 δ_{H} [ppm]	Dothiorelone A from Reference δ_{H} [ppm]	δ_{C} [ppm]
1		1710.9	
2	3.67, s	38.0	3.67, s
3		135.2	
4	6.30, d, 2.25	110.3	6.11, d, 2.2
5		159.5	
5-OH			9.74
6	6.37, d, 2.25	101.6	6.25, d, 2.2
7		157.5	
7-OH			9.96
8		120.0	
9		205.7	
10	2.92, t, 7.25	43.6	2.77, t, 6
11	1.62, m	24.0	1.47
12	1.27-1.47, m	29.0	1.20
13	1.27-1.47, m	25.4	1.24
14	1.27-1.47, m	38.9	1.24
15	3.68, m	65.8	3.55, m
16	1.09, d, 6.3	23.7	1.01, d, 5.3
17	3.61, s	60.0	3.99, q, 7
18		14.1	1.14, t, 7

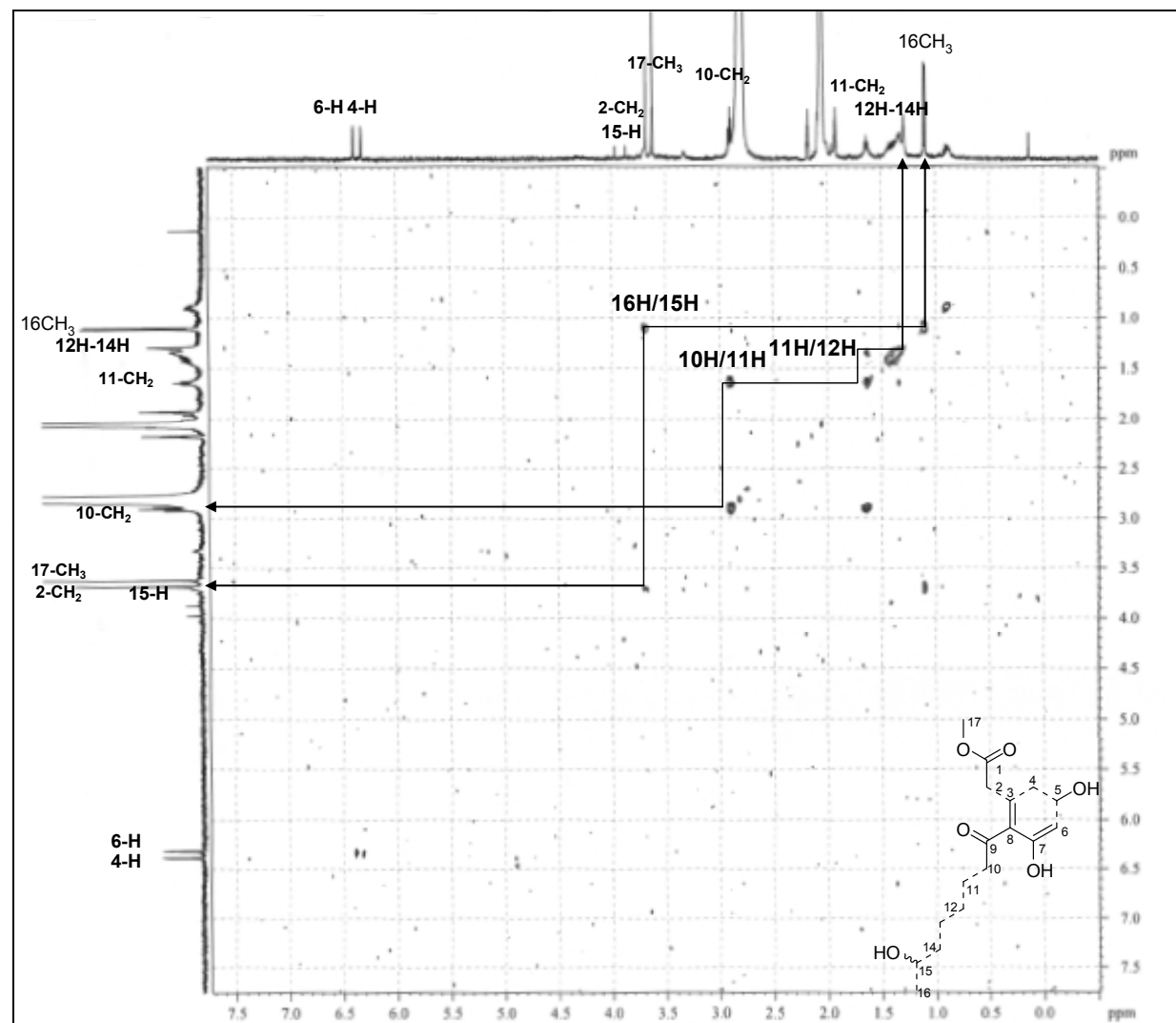
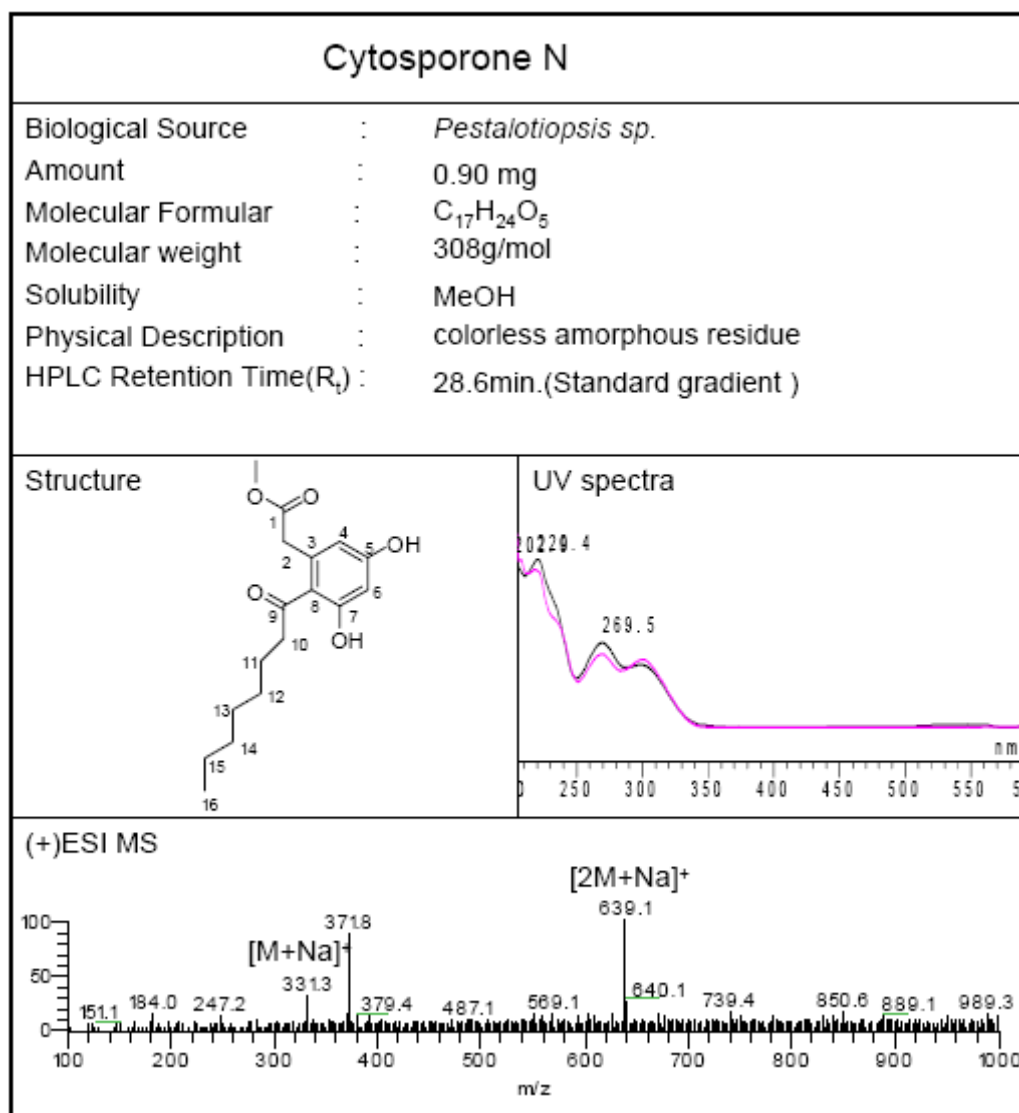


Figure 3.3.5.1 ^1H - ^1H COSY correlations for compound 15

3.3.6 Cytosporone N (16, new compound)



HRESIMS data of cytosporone N (**16**) differed from that of **15** by 16 amu, suggesting the loss of a hydroxyl group.

The ^1H NMR data (Table 3.3.6.1) and COSY spectrum of **16** indicated that the compound featured the same core structure as **15** and possessed an unsubstituted heptyl side chain as found in cytosporone A (Brady *et al.* 2000). This was confirmed from the triplet signal of the terminal methyl group at δ_{H} 0.88 (t, J = 5.8 Hz, H_3 -16).

Hence cytosporone N was 15-dehydroxy cytosporone M.

Table 3.3.6.1 ^1H NMR (500 MHz) data (J in Hz) for cytosporone N (**16**) in acetone- d_6 .

Atom no.	16 δ_{H} [ppm]	Comparison Compound 15 δ_{H} [ppm]
1		
2	3.67, s	3.67, s
3		
4	6.31, d, 1.8	6.30, d, 2.25
5		
5-OH		
6	6.37, d, 1.8	6.37, d, 2.25
7		
7-OH		
8		
9		
10	2.89, t, 6.2	2.92, t, 7.25
11	1.62, m	1.62, m
12	1.29-1.32, m	1.27-1.47, m
13	1.29-1.32, m	1.27-1.47, m
14	1.29-1.32, m	1.27-1.47, m
15	1.29-1.32, m	3.68, m
16	0.88, t, 5.8	1.09, d, 6.3
17	3.62, s	3.61, s

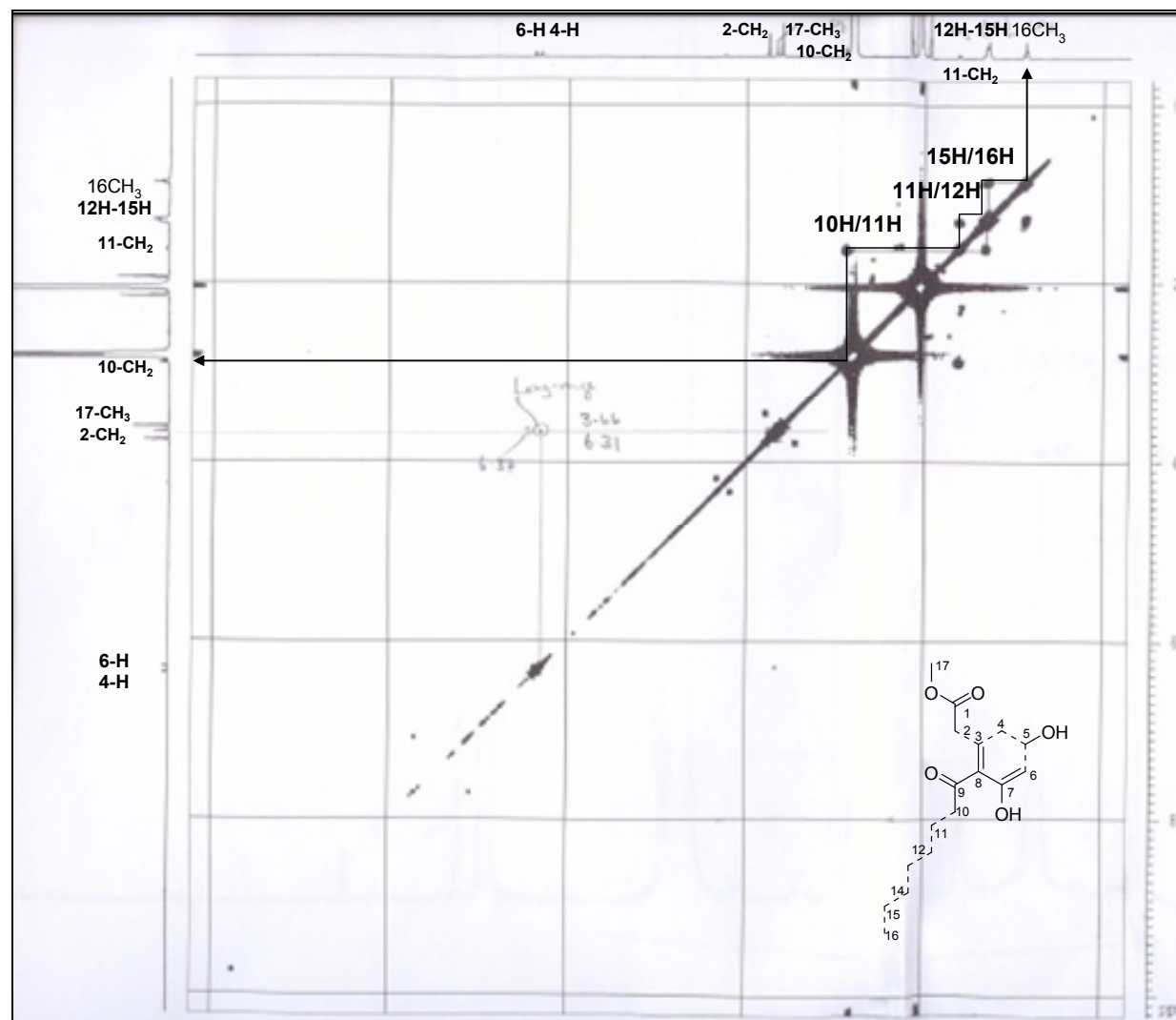
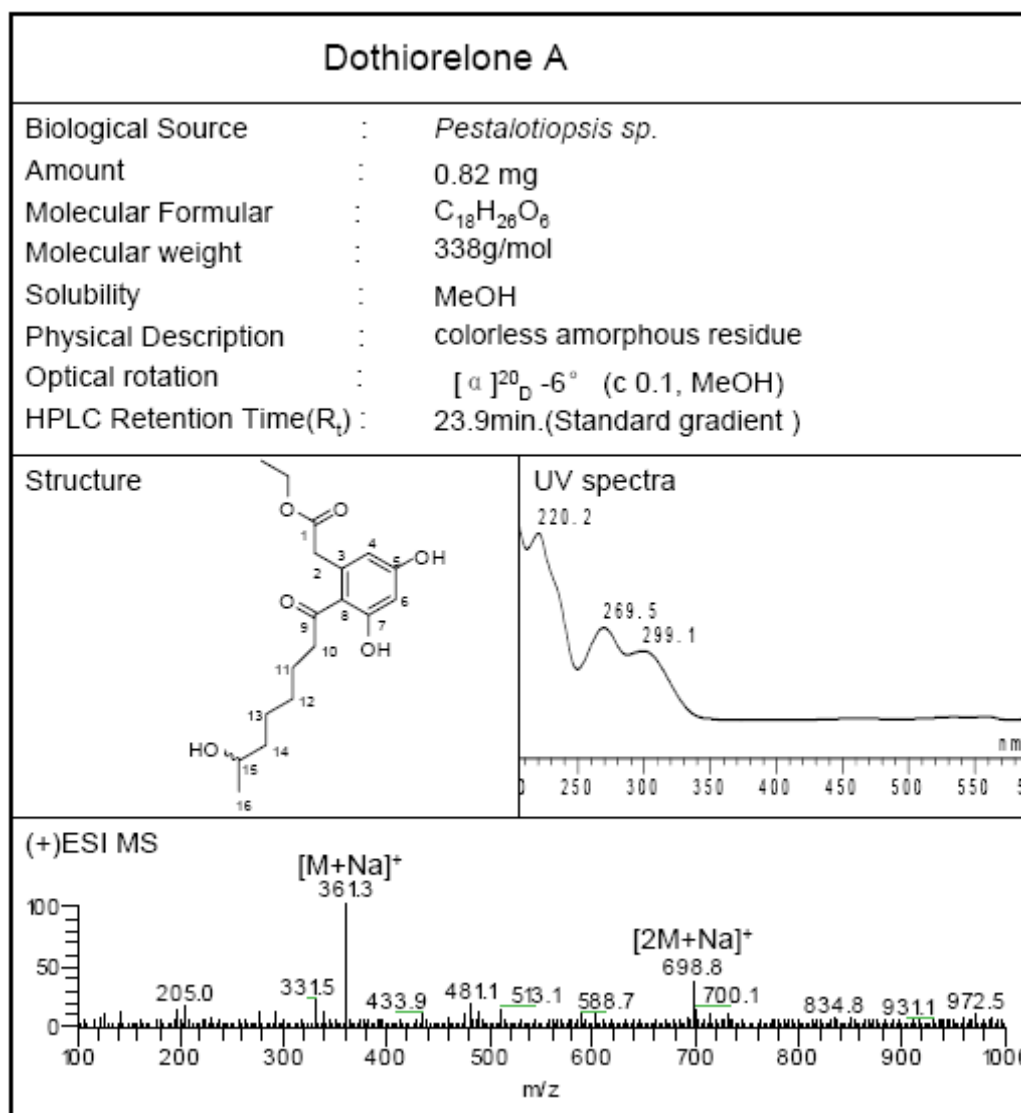


Figure 3.3.6.1 ^1H - ^1H COSY correlations for compound 16

3.3.7 Dothiorelone A (17, known compound)



Dothiorelone A (**17**) was obtained as a white amorphous powder (0.82 mg, CH_3OH). Its molecular formula $C_{18}H_{26}O_6$ was established by HR-ESIMS at m/z 339.1802 $[M + H]^+$ (calcd for $C_{18}H_{27}O_6$, 339.1807), indicating five degrees of unsaturation.

The 1H NMR data of **17** (Table 3.3.7.1) and its 1H - 1H COSY spectra (Figure 3.3.7.1) indicated the presence of a terminal ethoxy group (δ_H 4.07 (2H, q, $J = 7.25$ Hz, H_{2-17}); 1.20 (3H, t, $J = 7.25$ Hz, H_{3-18}), a methylene group (δ_H 3.67, s, H_{2-2})

situated between a phenyl ring and the carbonyl group, an oxymethine (δ_{H} 3.68, m, CH-15), two *meta*-coupled aromatic protons [δ_{H} 6.30 (d, J = 2.2 Hz, H-4), 6.36 (d, J = 2.2 Hz, H-6)], and the resonances for a seven-membered alkyl chain (CH₂-10 to CH₃-16).

The ¹H NMR data of **17** were very similar to those of dothiorelone B, previously isolated from the endophytic fungus *Dothiorella* sp. HTF3 (Xu *et al.* 2004). Detailed comparison of their NMR data and analysis of ¹H-¹H COSY spectra of **17** revealed that they are identical.

Table 3.3.7.1 ¹H, ¹³C NMR data for compound dothiorelone A (500 and 125 MHz, acetone-*d*₆)

Atom no.	17 δ_{H} [ppm]	Dothiorelone A from Reference	
		δ_{H} [ppm]	δ_{C} [ppm]
1		1710.9	
2	3.67, s	38.0	3.67, s
3		135.2	
4	6.30, d, 2.2	110.3	6.11, d, 2.2
5		159.5	
5-OH			9.74
6	6.36, d, 2.2	101.6	6.25, d, 2.2
7		157.5	
7-OH			9.96
8		120.0	
9		205.7	
10	2.92, t, 7.25	43.6	2.77, t, 6
11	1.62, p	24.0	1.47
12	1.34-1.47, 2H, overlapped	29.0	1.20
13	1.34-1.47, 2H, overlapped	25.4	1.24
14	1.34-1.47, 2H, overlapped	38.9	1.24
15	3.68, m	65.8	3.55, m
16	1.08, d, 6.3	23.7	1.01, d, 5.3
17	4.07, q, 7.25	60.0	3.99, q, 7
18	1.20, t, 7.25	14.1	1.14, t, 7

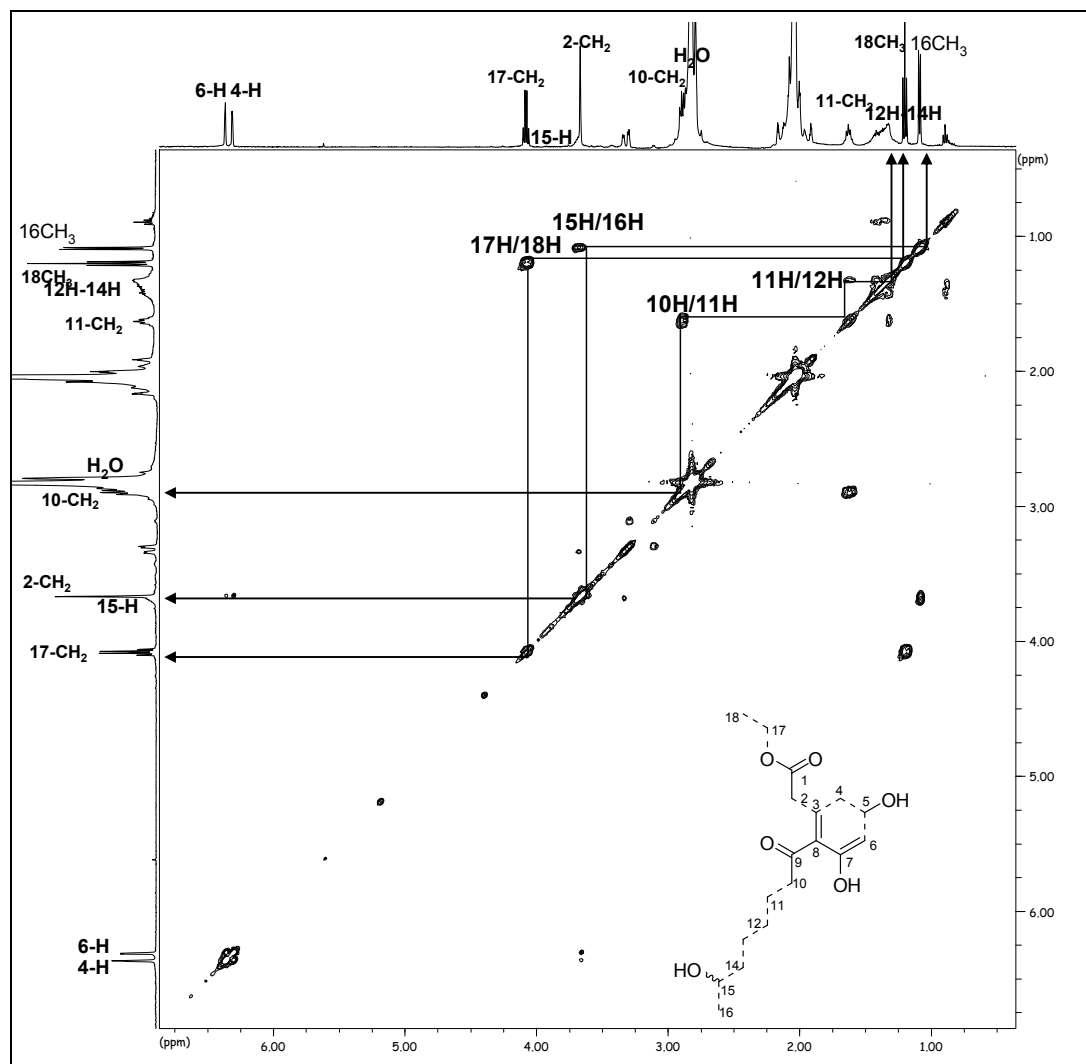
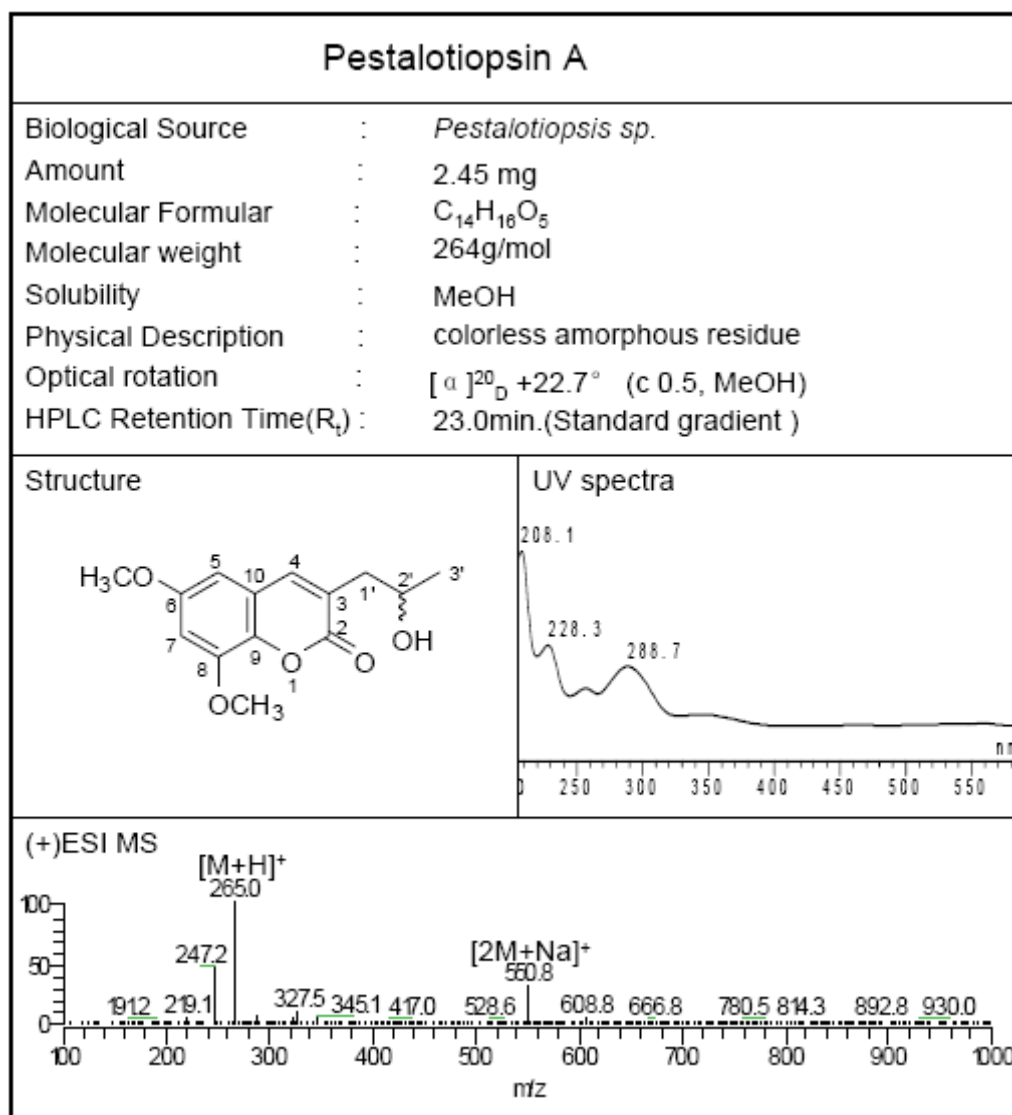


Figure 3.3.7.1. ^1H - ^1H COSY correlations for compound 17

3.4 Coumarin Derivatives

3.4.1 Pestalotiopsin A (18, new compound)



Pestalsin A (**18**), a colorless amorphous solid, has the molecular formula $C_{19}H_{24}O_5$, established by HR-ESIMS (m/z 265.1074, calcd for $[M+H]^+$ 265.1071), suggesting seven degrees of unsaturation.

The 1H and ^{13}C NMR data of **18** (Table 3.4.1.1) indicated that six of the seven units of unsaturation could be due to an aromatic ring, a double bond, and one

carbonyl group. Thus, the remaining unit of unsaturation was attributed to a ring formation. The UV absorption maxima at 208, 228, and 289 nm suggested that **18** is a coumarin derivative.

The ^1H and ^{13}C NMR data of **18** and its ^1H - ^1H COSY spectrum exhibited two methoxy groups (δ_{H} 3.82, s, δ_{C} 55.8, q, 6-OCH₃; δ_{H} 3.92, s, δ_{C} 56.3, q, 8-OCH₃), two *meta*-coupled aromatic protons [δ_{H} 6.43 (d, $J = 2.6$ Hz), δ_{C} 99.8, d, CH-5; δ_{H} 6.64 (d, $J = 2.6$ Hz), δ_{C} 102.6, d, CH-7], an olefinic singlet (δ_{H} 7.52, s, δ_{C} 141.3, d, CH-4), and a 2-hydroxypropyl group (CH₂-1' to CH₃-3'). Comparison of the NMR data of **8** with those of 6,8-dimethoxy-3-(2'-oxo-propyl)-coumarin (Teles *et al.* 2006), previously isolated from the endophytic fungus *Periconia atropurpurea* associated with *Xylopia aromatica*, revealed that both compounds differed only with regard to the nature of the side chain at C-3, where the 2'-oxo-propyl group of the latter was replaced by the 2'-hydroxypropyl group of **18**. This was confirmed from COSY correlations and HMBC correlations (Figure 3.4.1.1) from H-1' (δ_{H} 2.55, 2.71) to C-2 (δ_{C} 162.2), C-3 (δ_{C} 127.3), and C-4 (δ_{C} 141.3). The HMBC and ROESY correlations (Figure 3.4.1.1 and 3.4.1.2) supported the assignments of the methoxy groups 6-OCH₃ (δ_{H} 3.82, s) to C-6 (δ_{C} 156.4), and 8-OCH₃ (δ_{H} 3.92, s) to C-8 (δ_{C} 148.0).

Accordingly, the structure of pestalasin A (**18**) was 6,8-dimethoxy-3-(2'-hydroxy-propyl)-coumarin.

Table 3.4.1.1 ^1H NMR (500 MHz) data (J in Hz) for pestalotiopsin A (**18**)

Atom no.	18			HMBC (H to C)	NOESY (H to C)	6,8-Dimethoxy-3-(2'-oxo-propyl) -coumarin from Reference	
	(in acetone- <i>d</i> ₆)	(in CDCl ₃)				(in DMSO- <i>d</i> ₆)	
	δ _H [ppm]	δ _H [ppm]	δ _C [ppm]			δ _H [ppm]	δ _C [ppm]
2			162.2, s				161.0
3			127.3, s				125.0
4	7.73, s	7.52, s	141.3, d	2, 3, 5, 9, 10, 1'	5, 1'	7.80, s	142.1
5	6.71, d, 2.2	6.43, d, 2.6	99.8, d	4, 6, 10	4, 6-OCH ₃	6.76, d, 2.5	100.0
6			156.4, s				156.0
7	6.80, d, 2.2	6.64, d, 2.6	102.6, d	6, 8	6-OCH ₃ , 8-OCH ₃	6.87, d, 2.5	102.9
8			148.0, s				147.0
9			119.9, s				139.0
10			138.1, s				119.6
1'	2.55, dd, 8.2, 13.55 2.71, dd, 3.9, 13.55	2.55,dd,8.0, 14.0 2.71,dd,3.3, 14.0	40.9,t	2, 3, 4, 2', 3'	4, 2', 3'	3.68, s	44.2
2'	4.11, brs	4.15, m	66.7, d	1', 3'	1', 3'		205.0
3'	1.22, d, 6.3	1.27, d, 6.2	23.6, q	1', 2'	1', 2'	2.19, s	29.6
6-OCH ₃	3.86, s	3.82, s	55.8, q	6	5, 7	3.80, s	55.7
8-OCH ₃	3.95, s	3.92, s	56.3, q	8	7	3.80, s	56.5
2'-OH	3.82, br s						

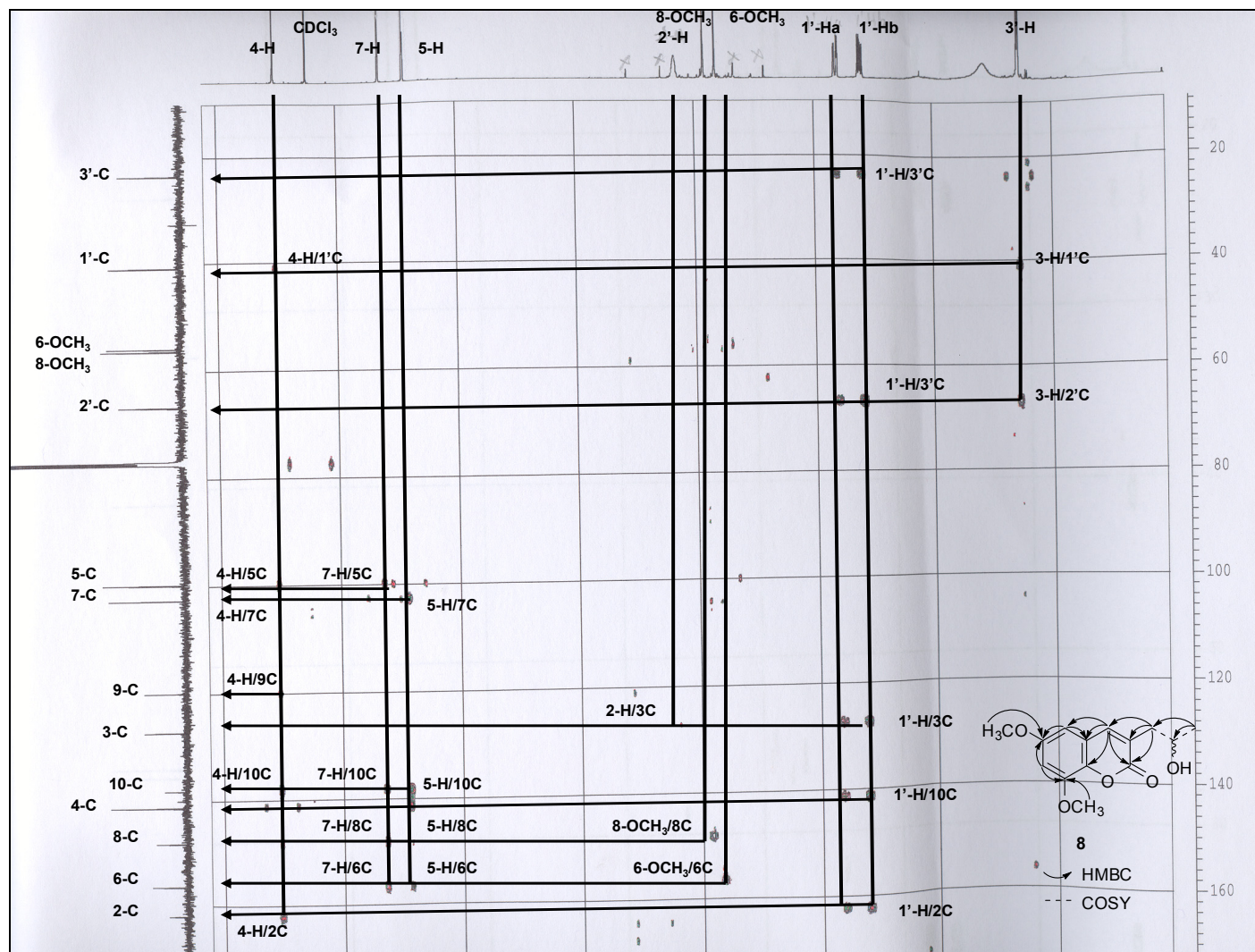


Figure 3.4.1.1 Selected HMBC and ^1H - ^1H COSY correlations for compound **18**

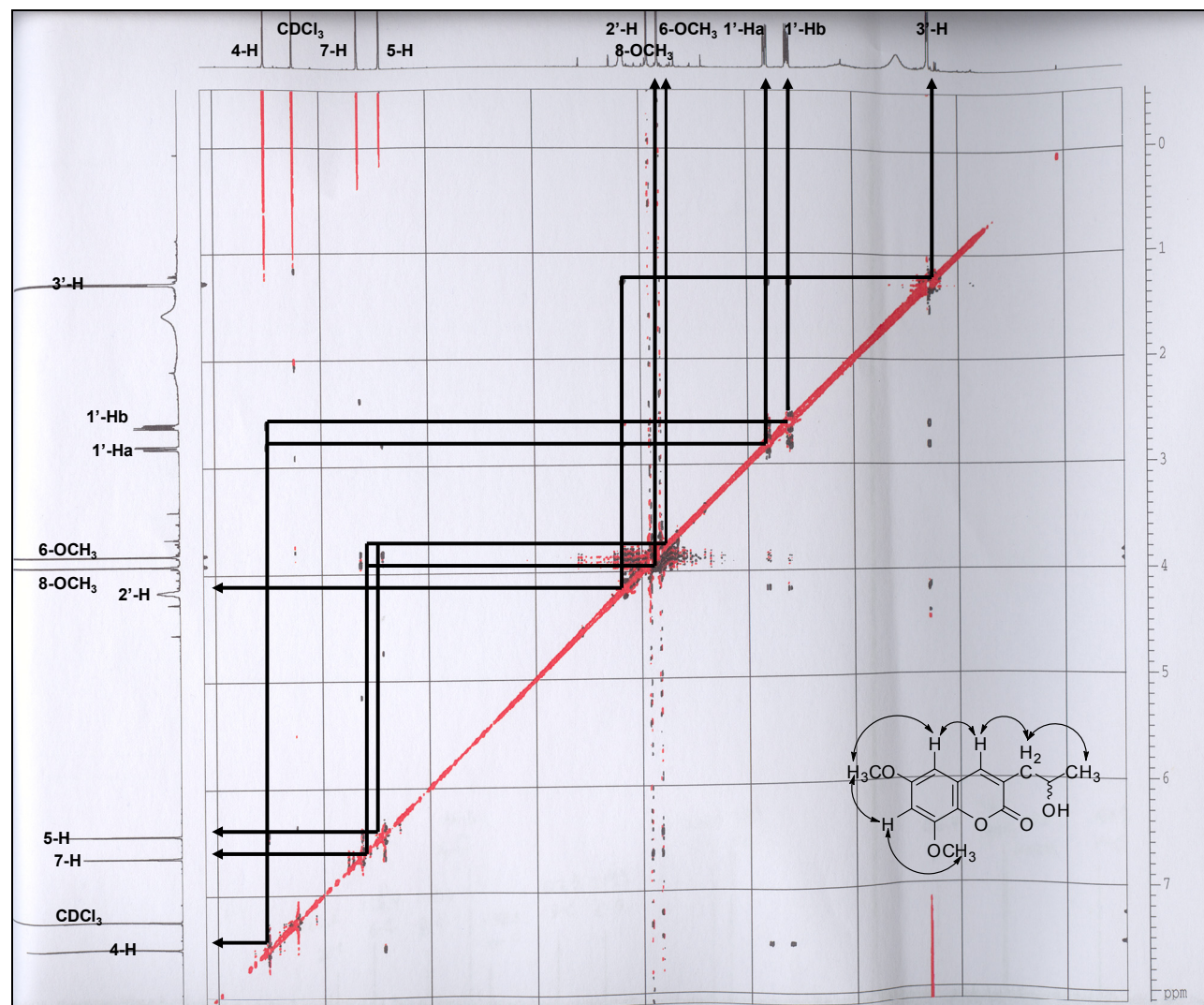
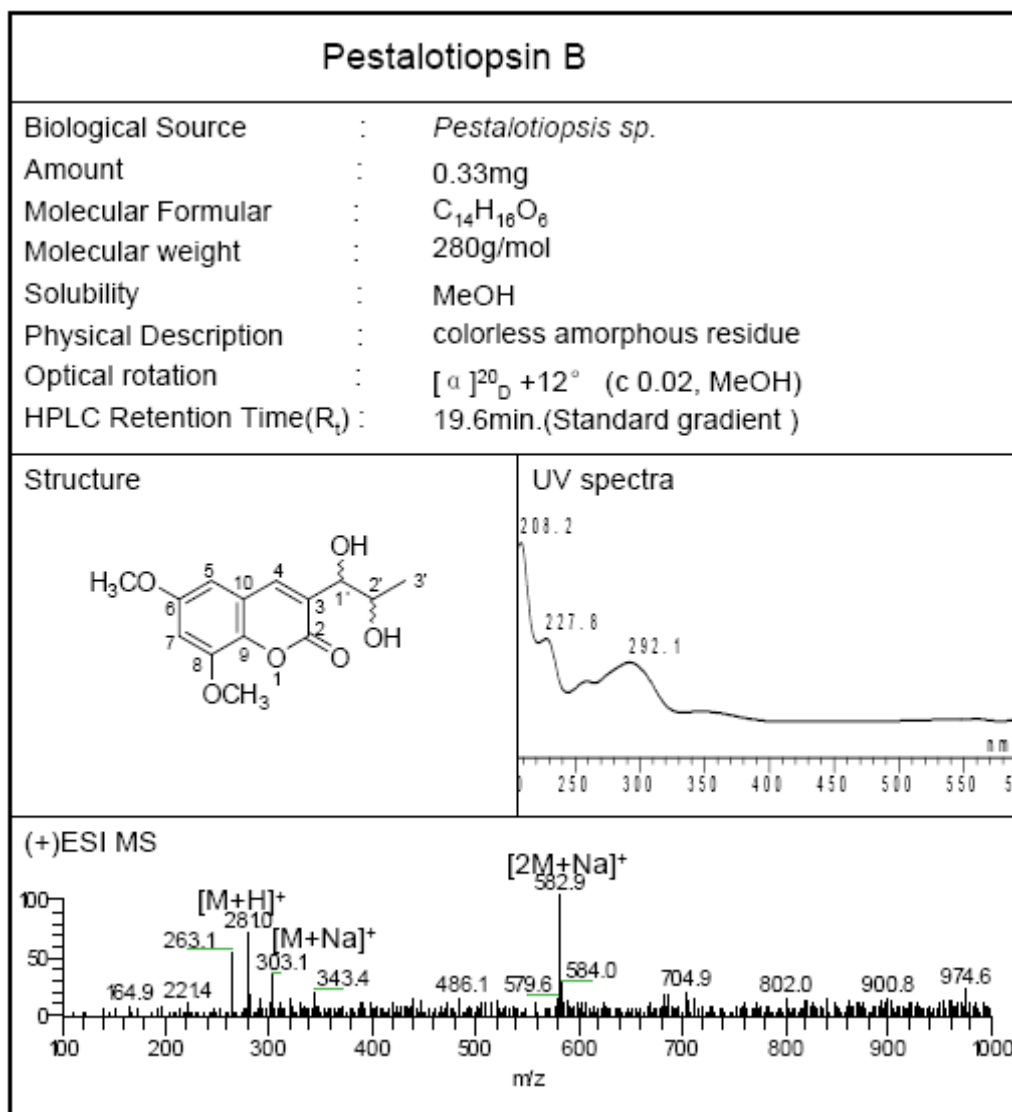


Figure 3.4.1.2 Selected ROSEY correlations for compound 18

3.4.2 Pestalotiopsin B (19, new compound)



Pestalsin B (**19**) had the molecular formula $C_{14}H_{16}O_6$, established by HR-ESIMS (m/z 281.1029, calcd for $[M+H]^+$ 281.1025), which is 16 amu larger than that of **18**. The 1H NMR data of **19** (Table 3.4.2.1) closely resembled those of **18**, suggesting that both compounds have the same basic molecular framework. The proton signals of the side chain methylene group [δ_H 2.55 (dd, $J = 8.0$ Hz, $J = 14.0$ Hz), δ_H 2.71 (dd, $J = 3.3$ Hz, $J = 14.0$ Hz), 1'-CH₂] in **18** were absent in **19** and one

additional hydroxymethine signal (δ_{H} 4.59, d, $J = 7.0$ Hz) indicated the presence of a second hydroxyl group at C-1' in **19**.

The COSY correlations (Figure 3.4.2.1) from H-2' to H-1' and H-3' revealed the presence of a 1',2'-dihydroxypropyl group. Fragments at m/z 263 and 245 in the positive ESIMS (Figure 3.4.2.2) originated from the sequential loss of two molecules of water, further supporting the side chain assignment.

Hence pestalasin B was 6,8-dimethoxy-3-(1',2'-dihydroxypropyl)-coumarin.

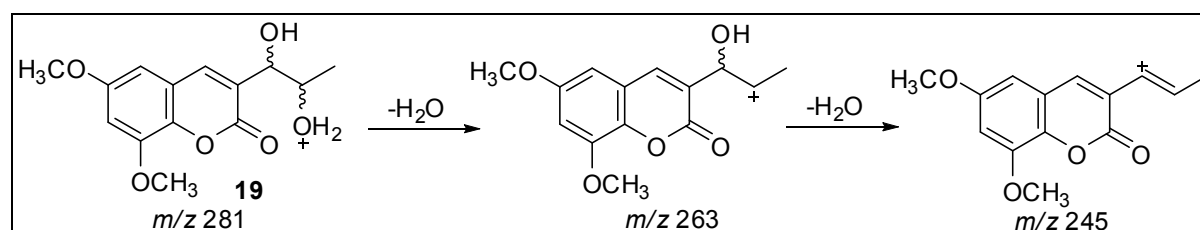


Figure 3.4.2.2 ESI-MS fragments of compound **19**

Table 3.4.2.1 ^1H NMR (500 MHz) data (J in Hz) for pestalotiopsin B (**19**)

Atom no.	19		Comparison Compound 18		
	(in Acetone- d_6)	(in CDCl_3)	(in Acetone- d_6)	(in CDCl_3)	
	δ_{H} [ppm]	δ_{H} [ppm]	δ_{H} [ppm]	δ_{H} [ppm]	δ_{C} [ppm]
2					162.2, s
3					127.3, s
4	7.94, s	7.70, s	7.73, s	7.52, s	141.3, d
5	6.69, d, 2.6	6.72, d, 2.55	6.71, d, 2.2	6.43, d, 2.6	99.8, d
6					156.4, s
7	6.83, d, 2.6	6.80, d, 2.55	6.80, d, 2.2	6.64, d, 2.6	102.6, d
8					148.0, s
9					119.9, s
10					138.1, s
1'	4.59, d, 7.0	2.54, dd, 8.55, 13.9 2.80, 1H, overlapped	2.55, dd, 8.2, 13.55 2.71, dd, 3.9, 13.55	2.55, dd, 8.0, 14.0 2.71, dd, 3.3, 14.0	40.9, t
2'	4.1, m	3.98, m	4.11, brs	4.15, m	66.7, d
3'	1.25, d, 6.3	3.55, d, 5.0 3.54, d, 5.0	1.22, d, 6.3	1.27, d, 6.2	23.6, q
6-OCH ₃	3.88, s	3.86, s	3.86, s	3.82, s	55.8, q
8-OCH ₃	3.96, s	3.96, s	3.95, s	3.92, s	56.3, q
2'-OH					

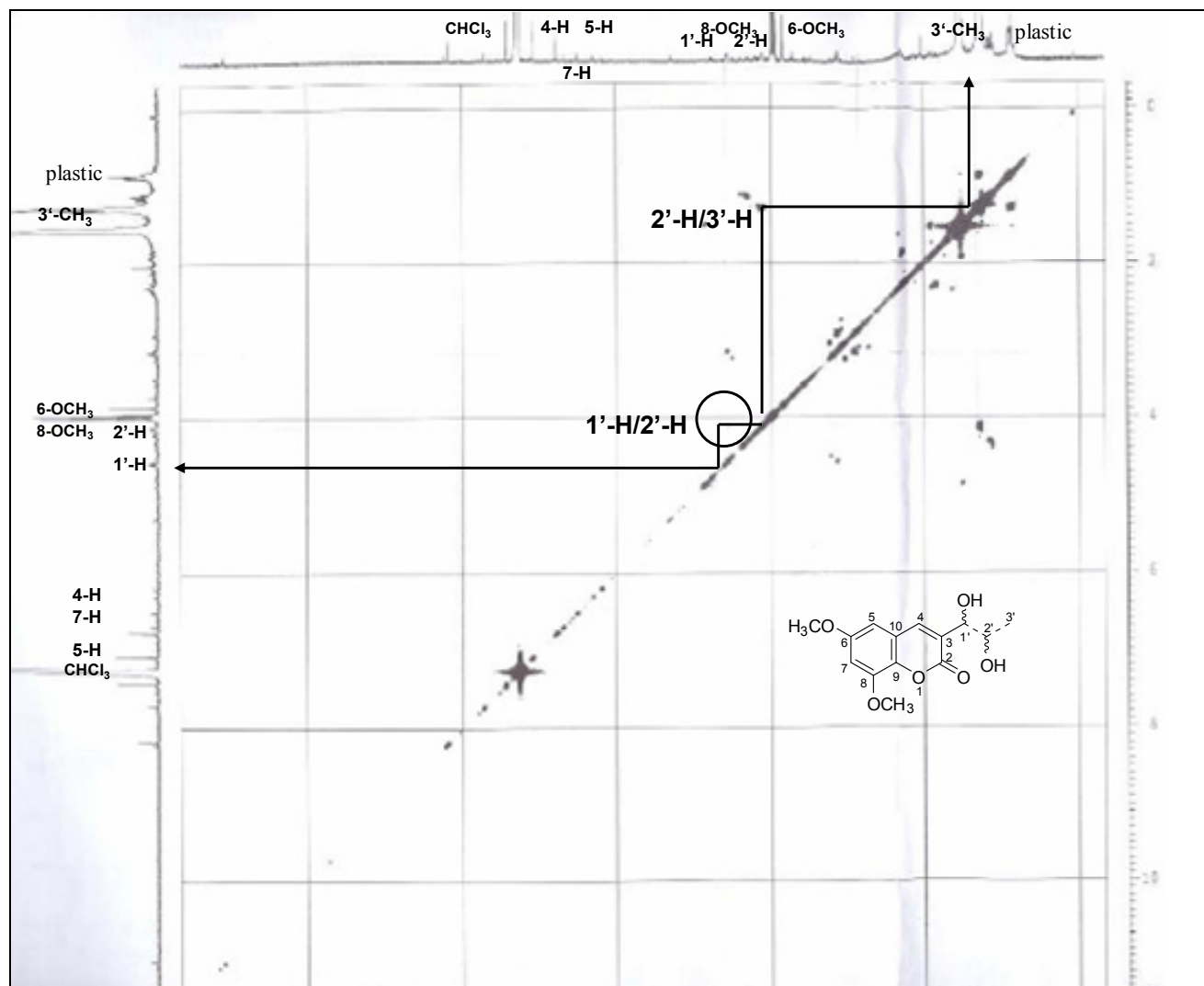
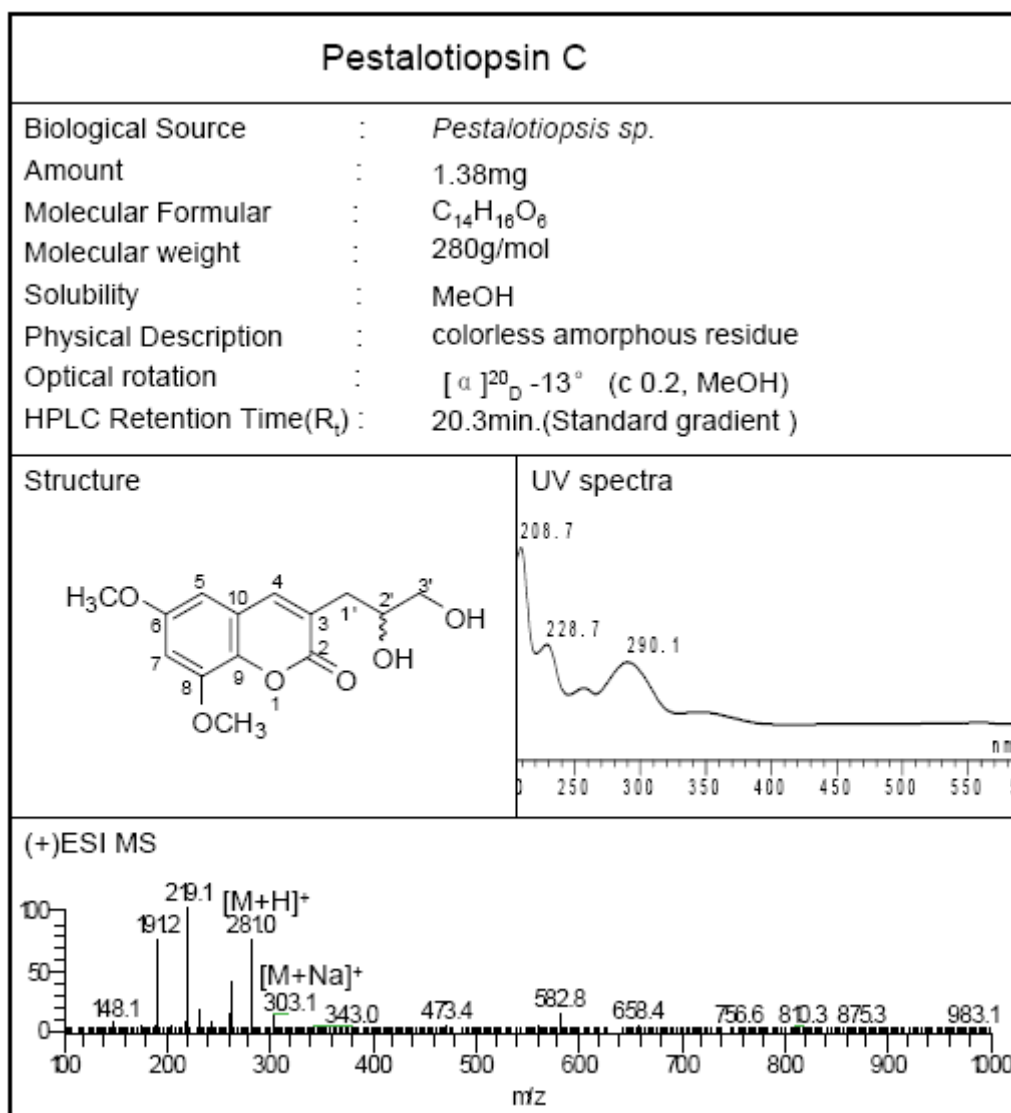


Figure 3.4.2.1 ^1H - ^1H COSY correlations for compound 19

3.4.3 Pestalotiopsin C (**20**, new compound)

Pestalsin C (**20**) has the same molecular formula as **19**, suggesting **20** is an isomer of **19**. The ¹H and ¹³C NMR data of **20** (Table 3.4.3.1) were similar to those of **18** except for replacement of the 3'-CH₃ group in **18** by a CH₂OH group [δ_{H} 3.38, (dd, J = 6.2 Hz, J = 11.4 Hz), δ_{H} 3.48 (dd, J = 4.0 Hz, J = 11.4 Hz); δ_{C} 65.8, t, 3'-CH₂]. The ¹H-¹H COSY and HMBC correlations further supported the presence a 2',3'-dihydroxypropyl group at C-3.

Hence pestalsin C (**20**) was 6,8-dimethoxy-3-(2',3'-dihydroxy-propyl)-coumarin.

Table 3.4.3.1 ^1H NMR (500 MHz) data (J in Hz) for pestalotiopsin C (**20**)

Atom no.	20		Comparison Compound 18		
	in CDCl_3 +10% methanol- d_4		(in Acetone- d_6)	(in CDCl_3)	
	δ_{H} [ppm]	δ_{C} [ppm]	δ_{H} [ppm]	δ_{H} [ppm]	δ_{C} [ppm]
2		162.2, s			162.2, s
3		126.2, s			127.3, s
4	7.53, s	142.0, d	7.73, s	7.52, s	141.3, d
5	6.37, d, 2.6	99.8, d	6.71, d, 2.2	6.43, d, 2.6	99.8, d
6		156.4, s			156.4, s
7	6.54, d, 2.6	102.2, d	6.80, d, 2.2	6.64, d, 2.6	102.6, d
8		148.0, s			148.0, s
9		119.8, s			119.9, s
10		138.0, s			138.1, s
1'	2.48,dd,8.2,14.2 2.67,dd,4.2,14.2	34.2, t	2.55, dd, 8.2, 13.55 2.71, dd, 3.9, 13.55	2.55,dd,8.0, 14.0 2.71,dd,3.3, 14.0	40.9,t
2'	3.83, m	70.0, d	4.11, brs	4.15, m	66.7, d
3'	3.38,dd,6.2,11.4 3.48,dd,4.0,11.4	65.8, t	1.22, d, 6.3	1.27, d, 6.2	23.6, q
6-OCH ₃	3.71, s	55.8, q	3.86, s	3.82, s	55.8, q
8-OCH ₃	3.79, s	56.3, q	3.95, s	3.92, s	56.3, q
2'-OH					

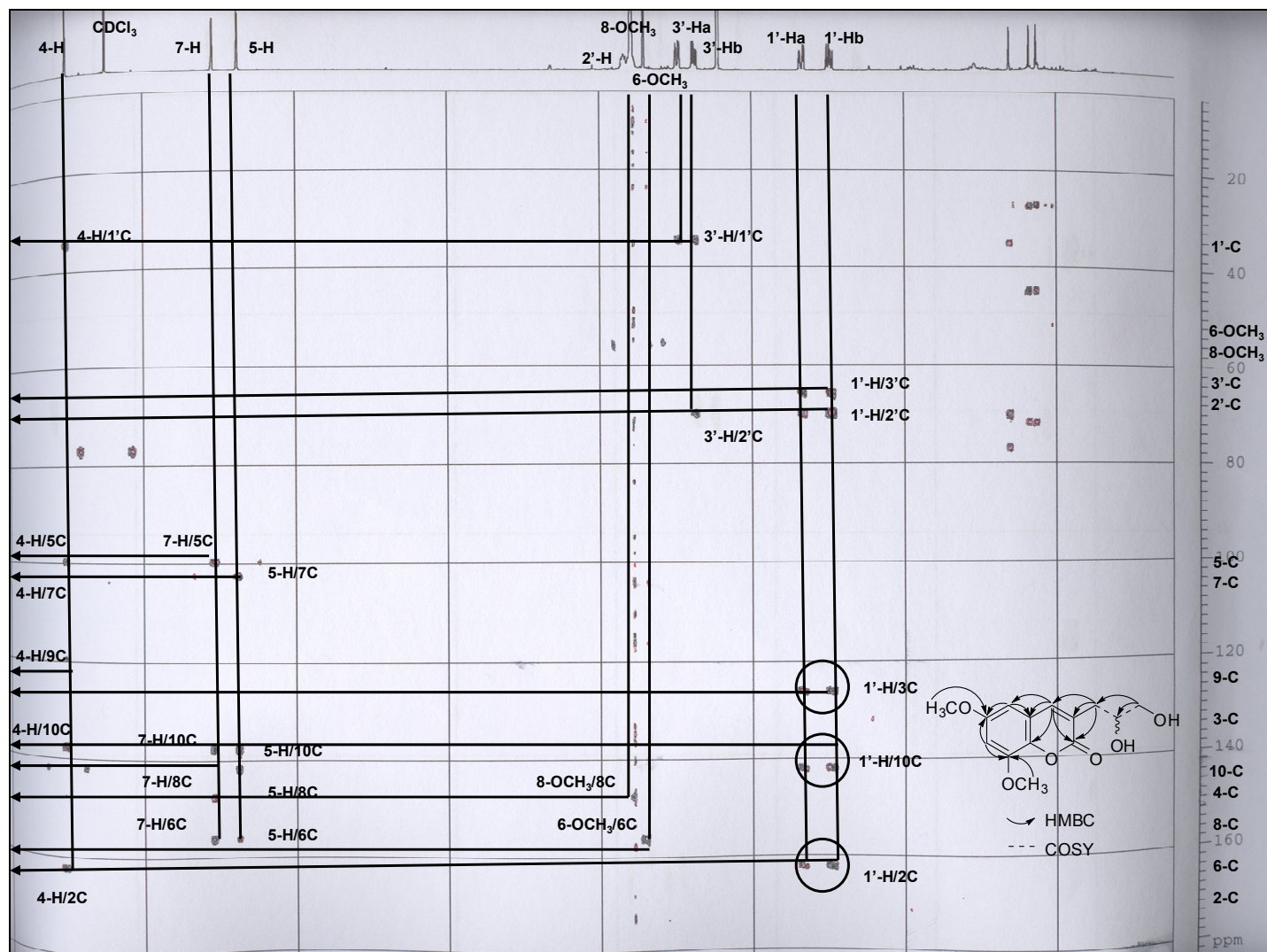
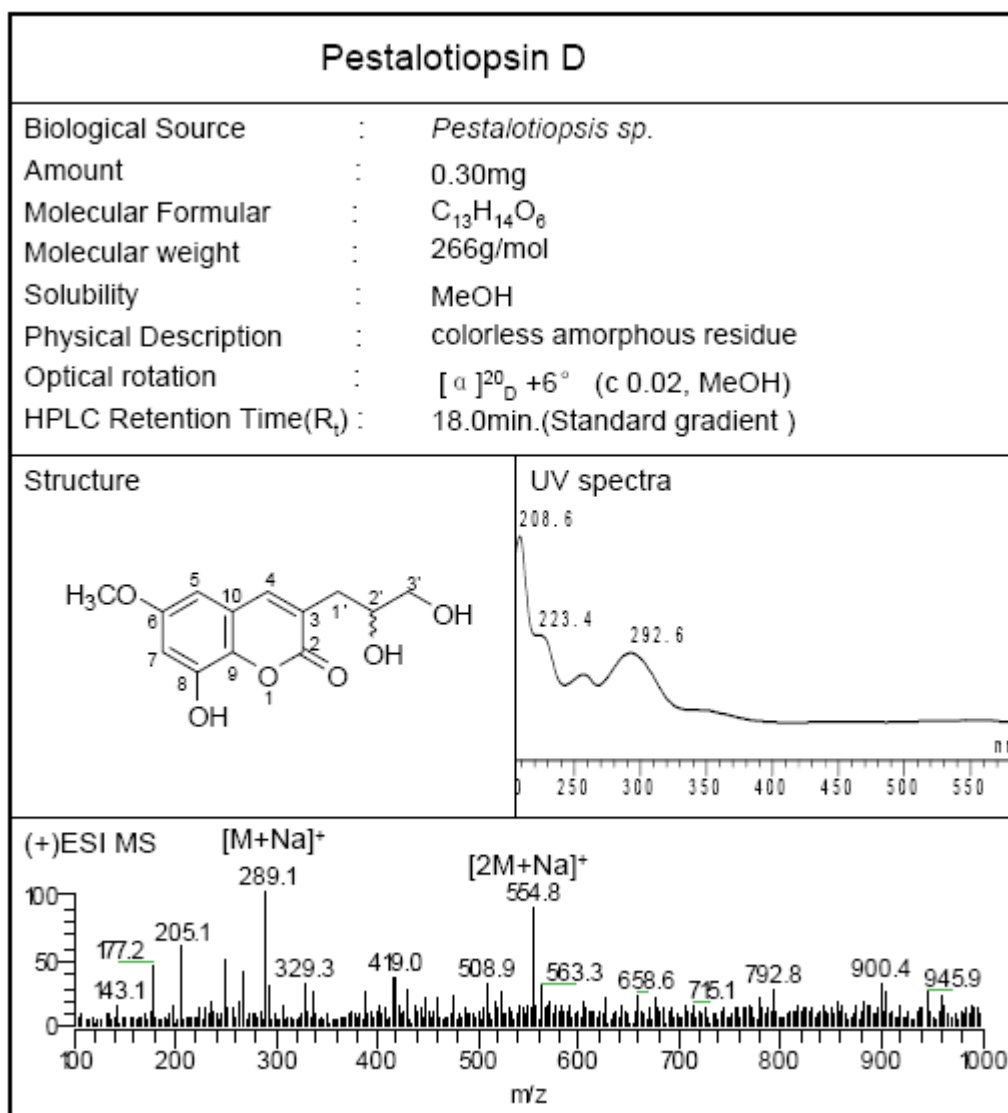


Figure 3.4.3.1 Selected HMBC and ^1H - ^1H COSY correlations for compound **20**

3.4.4 Pestalotiopsin D (**21**, new compound)

The ^1H NMR data of pestalasin D (**21**) (Table 3.4.4.1) were similar to those of **20**, except for the loss of one of the two methoxy groups present in **20**. HRESI-MS data of **21** (m/z 267.0863 $[\text{M} + \text{H}]^+$) established the molecular formula of $C_{14}H_{16}O_6$, indicating replacement of one of the two methoxy groups of **20** by a hydroxyl group. Comparison with the chemical shifts of the methoxy substituents of **18**, unequivocally assigned by HMBC and ROESY spectra, allowed the assignment of the methoxy group (δ_{H} 3.80, s) of **21** to C-6.

Hence pestalasin D was 8-hydroxy-6-methoxy-3-(2',3'-dihydroxy-propyl)-coumarin.

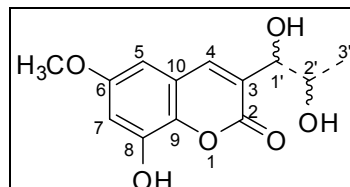
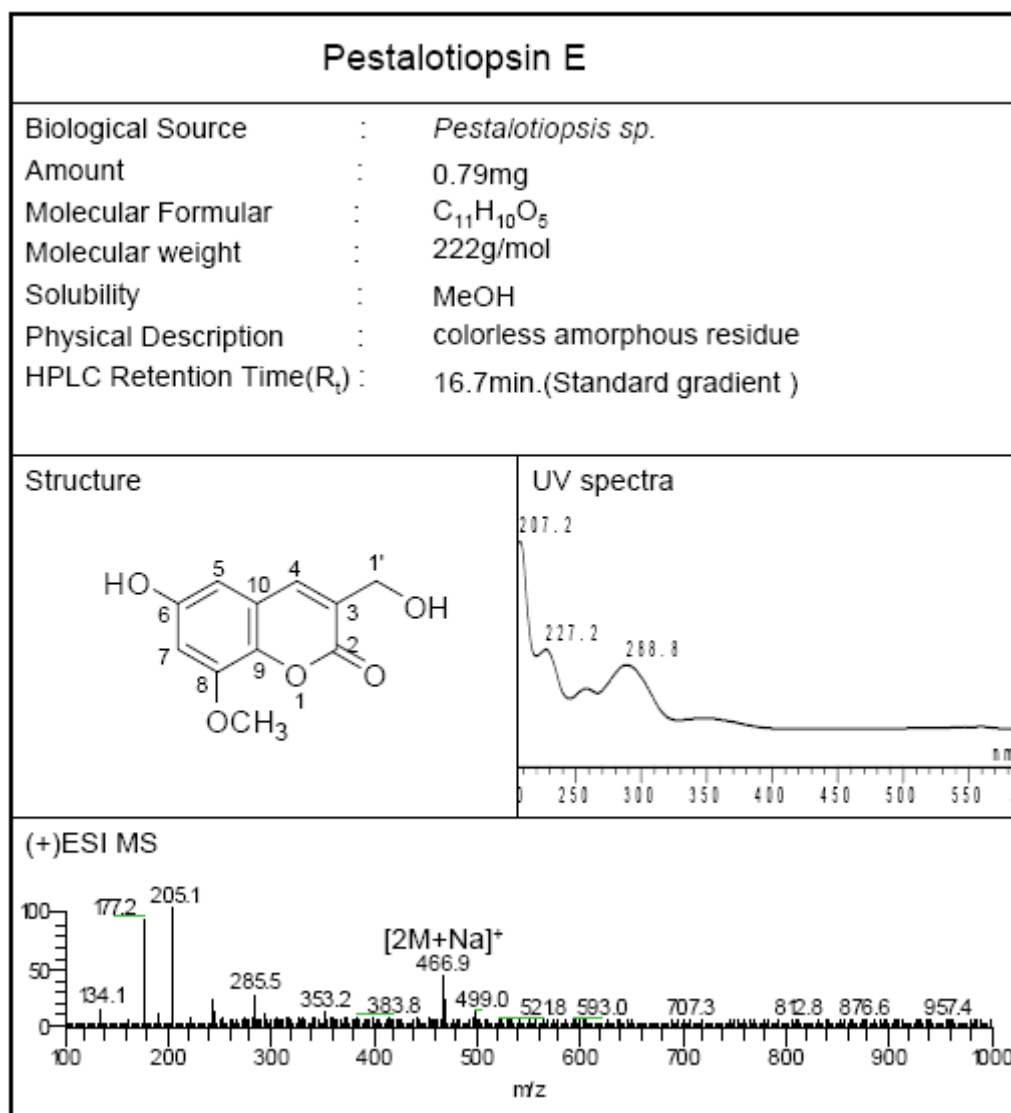


Figure 3.4.4.1 ^1H - ^1H COSY correlations for compound **21**

Table 3.4.4.1 ^1H NMR (500 MHz) data (J in Hz) for pestalotiopsin D (**21**)

Atom no.	21 (in acetone- d_6) δ_{H} [ppm]	Comparison Compound 20 in CDCl_3 +10% methanol- d_4	
		δ_{H} [ppm]	δ_{C} [ppm]
2			162.2, s
3			126.2, s
4	7.72, s	7.53, s	142.0, d
5	6.64, d, 2.85	6.37, d, 2.6	99.8, d
6			156.4, s
7	6.68, d, 2.85	6.54, d, 2.6	102.2, d
8			148.0, s
9			119.8, s
10			138.0, s
1'	2.51, dd, 9.0, 13.55 2.80, 1H, overlaped	2.48,dd,8.2,14.2 2.67,dd,4.2,14.2	34.2, t
2'	3.91, m	3.83, m	70.0, d
3'	3.52, d, 6.3 3.50, d, 5.05	3.38,dd,6.2,11.4 3.48,dd,4.0,11.4	65.8, t
6-OCH ₃	3.80, s	3.71, s	55.8, q
8-OCH ₃		3.79, s	56.3, q
2'-OH			

3.4.5 Pestalotiopsin E (22, new compound)



The molecular formula $C_{11}H_{10}O_5$ of pestalasin E (**22**) was established by HR-ESIMS (m/z 223.0606, calcd for $[M+H]^+$ 223.0601). Its 1H NMR data (Table 3.4.5.1) were closely related to those of the known analogue 3-hydroxymethyl-6,8-dimethoxycoumarin (**23**), previously isolated from *Talaromyces flavus* (Teles *et al.* 2006), except for the fact that only one methoxy group was present at δ_H 3.91 (s) that was assigned by comparison to C-8 rather than to C-6.

Hence pestalasin E was 6-hydroxy-8-methoxy-3-propyl-coumarin.

Table 3.4.5.1 ^1H NMR (500 MHz) data (J in Hz) for pestalotiopsin E (**22**)

Atom no.	22 (in acetone- d_6) δ_{H} [ppm]	Comparison Compound 23	
		in CDCl_3 +10% methanol- d_4	
		δ_{H} [ppm]	δ_{C} [ppm]
2			160.9
3			128.6
4	7.79, s	7.67, br s	138.7
5	6.64, d, 2.5	6.48, d, 2.5	100.2
6			156.6
7	6.75, d, 2.5	6.65, d, 2.5	103.0
8			148.1
9			138.0
10			119.6
1'	4.49, s	4.62, d, 1.3	61.3
6-OCH ₃		3.84, s	
8-OCH ₃	3.91, s	3.94, s	55.8

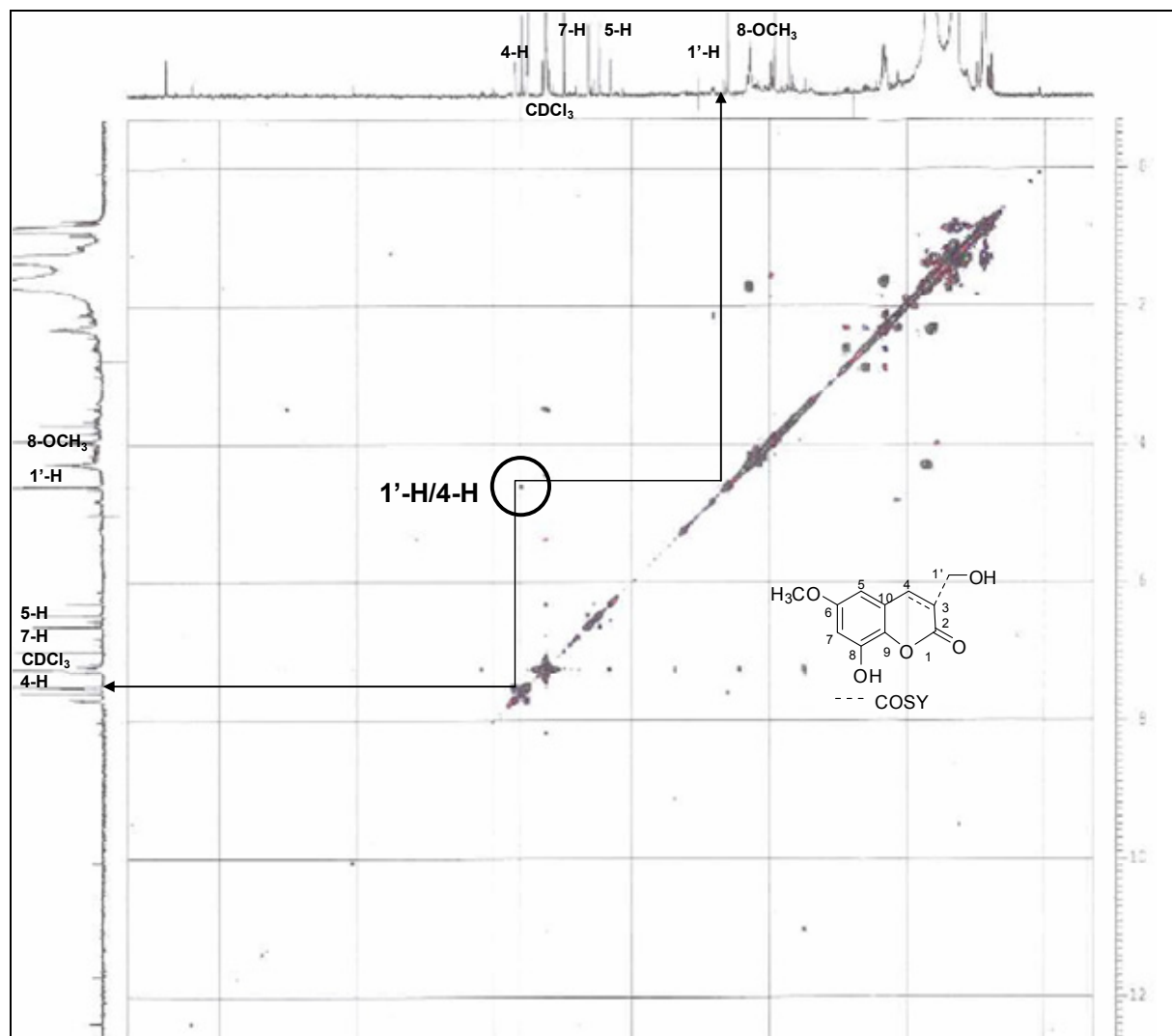
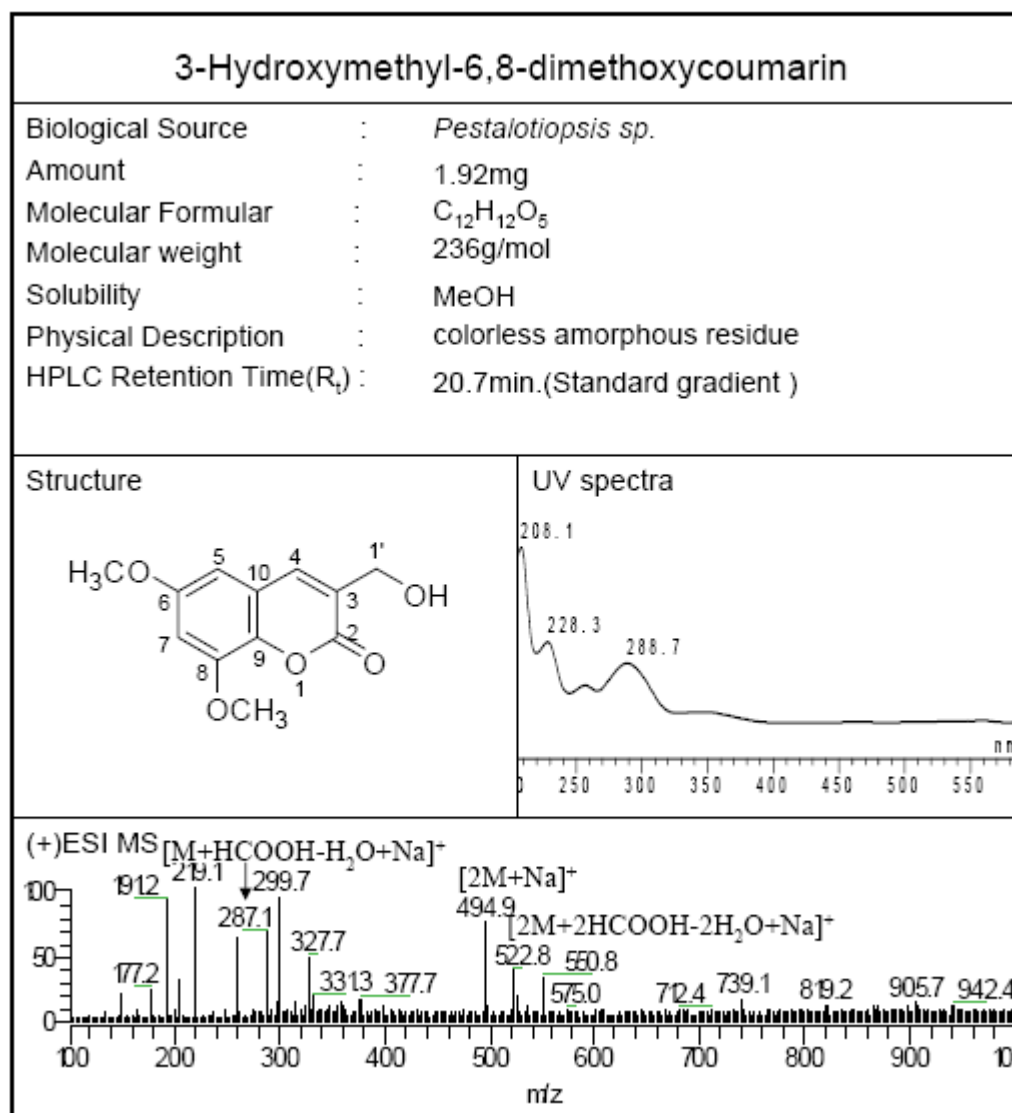


Figure 3.4.5.1 ^1H - ^1H COSY correlations for compound 22

3.4.6 3-Hydroxymethyl-6,8-dimethoxycoumarin (**23**, known compound)

3-Hydroxymethyl-6,8-dimethoxycoumarin (**23**), a white amorphous powder (1.92 mg), has the molecular formula C₁₂H₁₂O₅ as established by the positive ion peak at m/z 287.1 [M + HCOOH - H₂O + Na]⁺ in ESI-MS. Consequently, **23** had seven degrees of unsaturation.

The analysis of the ¹H and ¹³C NMR data of **23** (Table 3.4.6.1), its ¹H-¹H COSY and HSQC spectra showed the presence of two methoxy substituents (δ_H 3.94, s, 8-OCH₃, 3.84, s, 6-OCH₃; δ_C 56.3, 8-OCH₃, 55.8, 6-OCH₃), two *meta*-coupled aromatic methines [δ_H 6.48 (d, J = 2.5 Hz, H-5), 6.65 (d, J = 2.5 Hz, H-7); δ_C 100.2,

C-5, 103.0, C-7], an olefinic methine (δ_{H} 7.67, s, H-4; δ_{C} 138.7, C-4), and an oxygenated methylene group (δ_{H} 4.62, s, H₂-1'; δ_{C} 61.3, C-1').

Comparison of the ^1H and ^{13}C NMR data of **23** with those of 3-hydroxymethyl-6,8-dimethoxycoumarin (Teles *et al.* 2006) revealed that they are the same compound.

The strong HMBC correlation (Figure 3.4.6.1) from the olefinic methine H-4 (δ_{H} 7.67, s), two *meta*-coupled aromatic methines H-5 (δ_{H} 6.48, d, $J = 2.5\text{Hz}$) and H-7 (δ_{H} 6.65, d, $J = 2.5\text{Hz}$) to C-9 (δ_{C} 138.0), from H-4 (δ_{H} 7.67, s) to C-10 (δ_{C} 119.6) disclosed the chemical shifts for C-9 and C-10. HMBC correlations further supported the assignments of the methoxy groups, 6-OCH₃ (δ_{H} 3.84, s) to C-6 (δ_{C} 156.6), and 8-OCH₃ (δ_{H} 3.94, s) to C-8 (δ_{C} 148.1).

Hence, the ^{13}C NMR data of four carbons in 3-hydroxymethyl-6,8-dimethoxycoumarin were rectified as C-6 (δ_{C} 156.6), C-8 (δ_{C} 148.1), C-9 (δ_{C} 138.0), and C-10 (δ_{C} 119.6).

Table 3.4.6.1 ^1H , ^{13}C NMR data for compounds 3-Hydroxymethyl-6,8-dimethoxycoumarin (**24**) (500 and 125 MHz, CDCl₃)

No.	24		3-Hydroxymethyl-6,8-dimethoxycoumarin from Reference	
	δ_{H} [ppm]	δ_{C} [ppm]	δ_{H} [ppm]	δ_{C} [ppm]
2	160.9			
3	128.6			
4	138.7	7.67, br s	138.7	7.70, d, 1.4
5	100.2	6.48, d, 2.5	101.2	6.48, d, 2.6
6	156.6			
7	103.0	6.65, d, 2.5	103.0	6.65, d, 2.6
8	148.1			
9	138.0		128.6	
10	119.6		148.1	
1'	61.3	4.62, d, 1.3	61.3	4.55, d, 1.4
6-OCH ₃				
8-OCH ₃	55.8	3.84, s	55.8	3.81, s

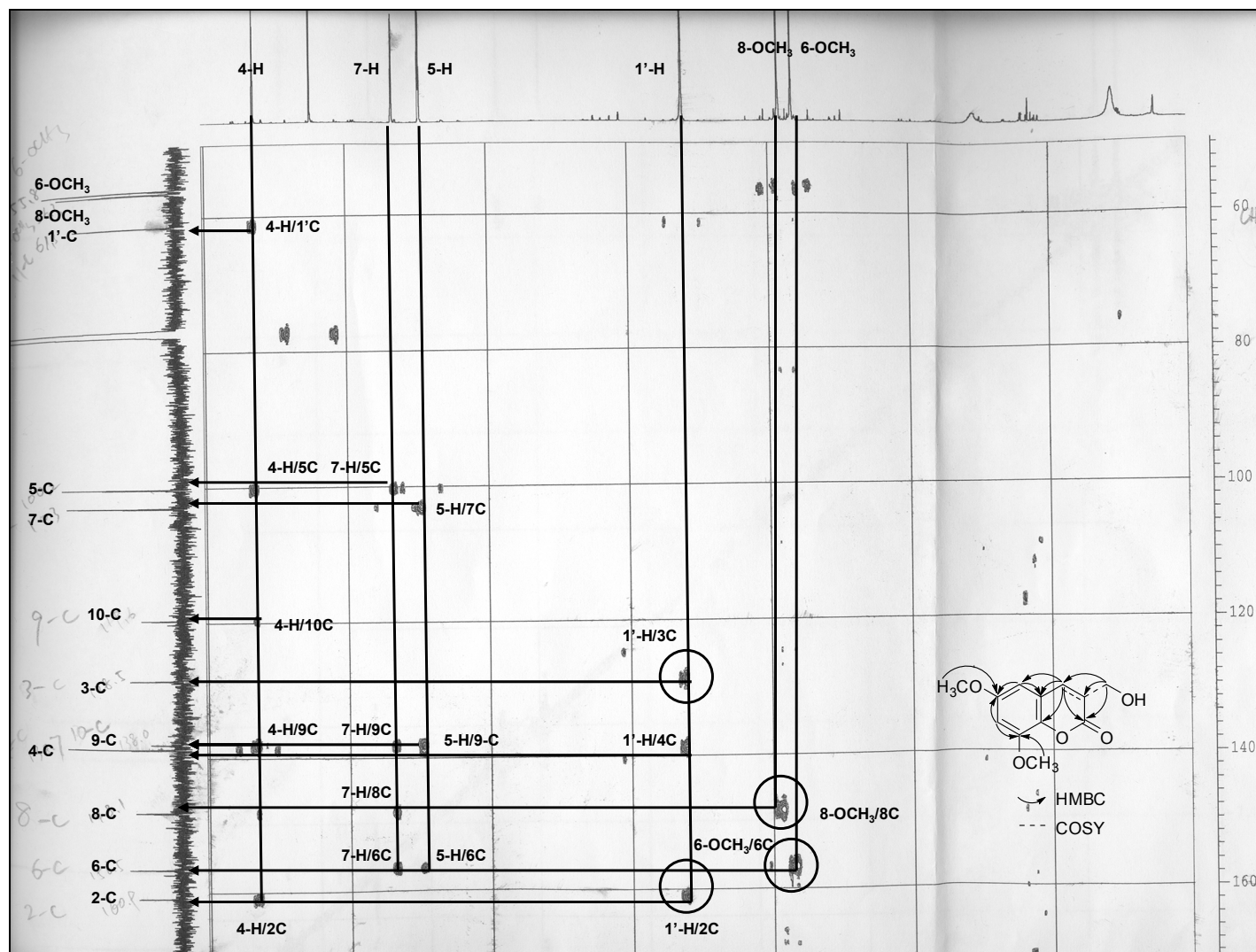
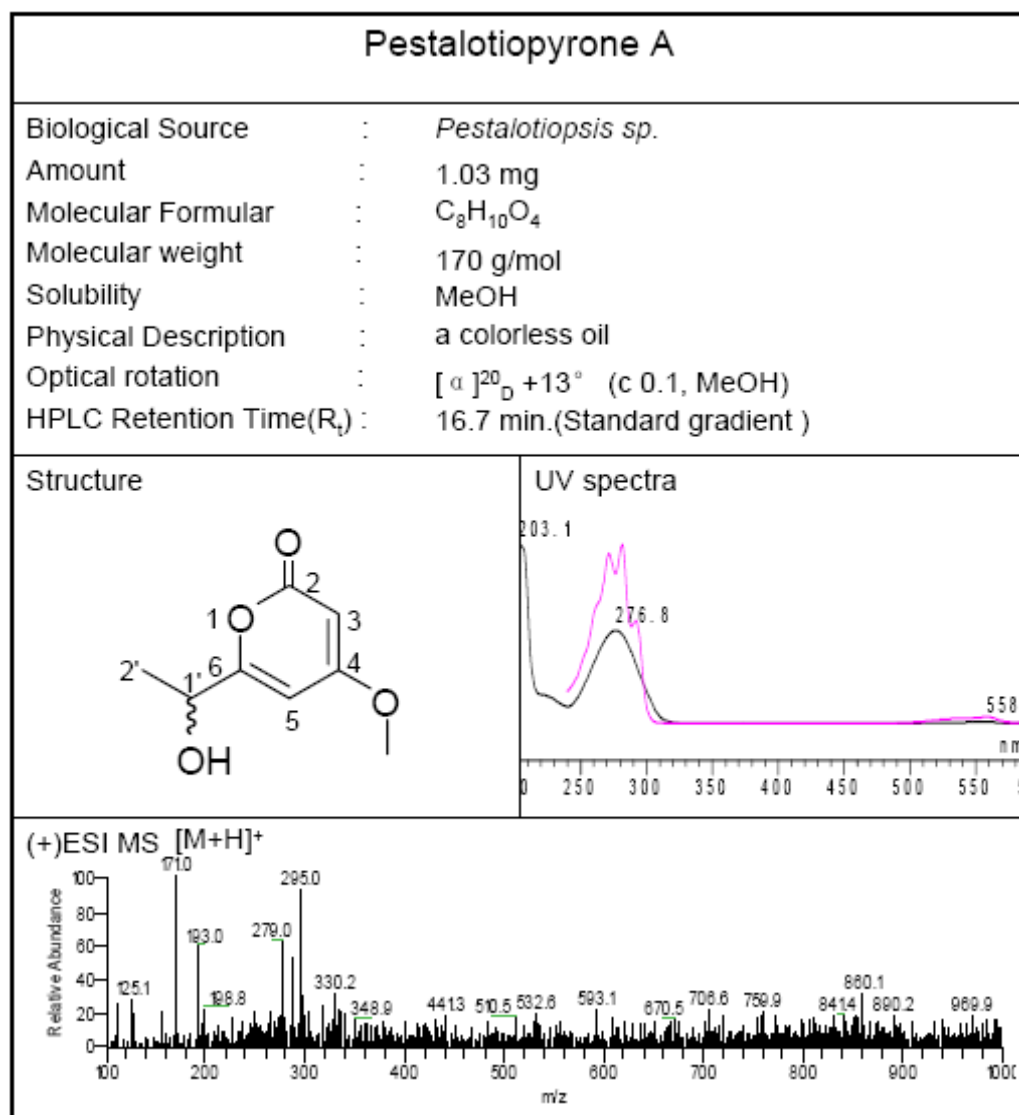


Figure 3.4.6.1 Selected HMBC correlations for compound 23

3.5 Pyrones

3.5.1 Pestalotiopyrone A (24, new compound)



Pestalotiopyrone A (**24**) was isolated as a colorless oil. Its molecular formula of C₈H₁₀O₄, suggested four degrees of unsaturation, as established by HR-ESIMS (m/z 171.0645, calcd for [M+H]⁺ 171.0657).

The ¹H and ¹³C NMR data of **24** (Tables 3.5.1.1) and the information from its ¹H-¹H COSY spectrum revealed the presence of one methoxy group (δ_H 3.86, s, δ_C 58.6, q, 4-OCH₃), two *meta*-coupled olefinic protons (δ_H 5.55 brs, δ_C 88.2, d, CH-3; δ_H 6.19 brs, δ_C 99.0, d, CH-5), and a 1-hydroxyethyl group (CH-1' to CH₃-2'). The

above observation disclosed that the nucleus of **24** was an α -pyrone. Comparison of the NMR data of **24** with those of verrucosapyrone B (Rahbaek *et al.* 2003), previously isolated from the endophytic fungus *Penicillium nordicum* (IBT 6573), revealed that both compounds differed only in the side chain substituted at C-6, where the 1'-hydroxypropyl group of verrucosapyrone B was replaced by the 1'-hydroxyethyl group of **24**. This replacement was further confirmed by the ^1H - ^1H COSY correlations between H-1'/H₃-2', and HMBC correlations (Figure 3.5.1.1) between H-1'/C-5, H-1'/C-6, and H-2'/C-6. The attachment of the methoxy group at C-4 was corroborated by the HMBC correlation from its protons (δ_{H} 3.86, s) to C-4 (δ_{C} 174.0) and ROESY correlations between H-3/4-OCH₃ and H-5/4-OCH₃.

The above structure was identical with that proposed for nigrosporapyrone (Trisuwan *et al.* 2008). However, previously published NMR data of nigrosporapyrone could not support its proposed structure. Therefore, the structure of pestalotiopyrone A (**24**) was unambiguously identified as 6-(1-hydroxyethyl)-4-methoxy-2H-pyran-2-one.

Table 3.5.1.1 ^1H NMR (500 MHz) and ^{13}C NMR (125 MHz) spectroscopic data for pestalotiopyrone A (**24**) in CD₃OD

Atom no.	24		HMBC (H to C)	Verrucosapyrone B from Reference	
	δ_{H} [ppm]	δ_{C} [ppm]		δ_{H} [ppm]	δ_{C} [ppm]
2		167.0, s			169.1, s
3	5.55, s	88.2, d	2, 4	5.46, s	90.6, d
4		174.0, s			175.7, s
5	6.19, s	99.0, d	4, 6	6.05, d, 2.4	102.0, d
6		169.8, s			170.7, s
1'	4.47, q, 6.6	67.5, d	5, 6, 2'	4.17, dd, 7.8, 4.8	74.3, d
2'	1.41, d, 6.6	21.5, q	6, 1'	1.75, m; 1.58, m	31.0, t
3'				0.87, t, 7.5	11.7, q
4-OCH ₃	3.86, s	58.6, q	4	3.77, s	59.0, q

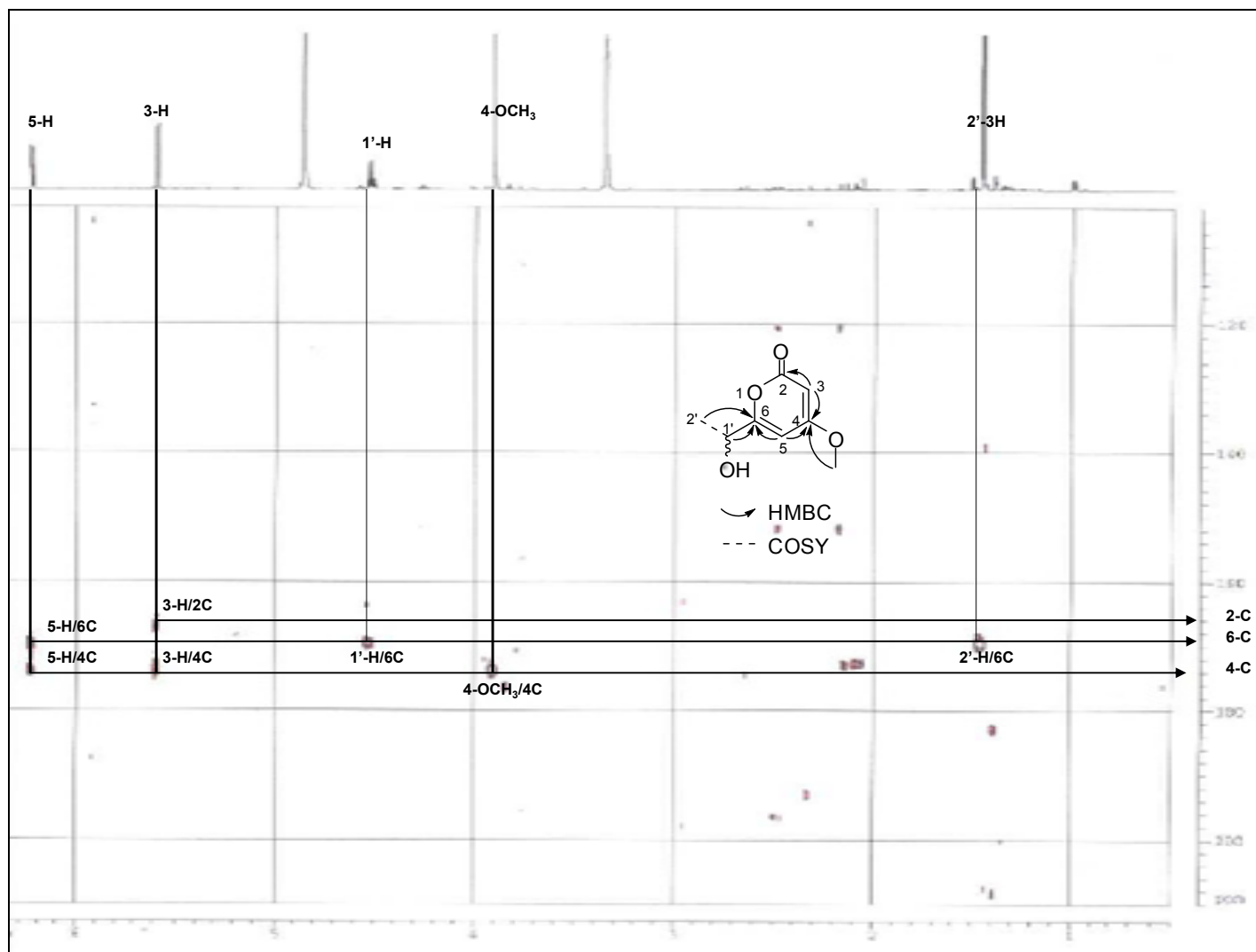


Figure 3.5.1.1a Selected HMBC correlations for compound **24**

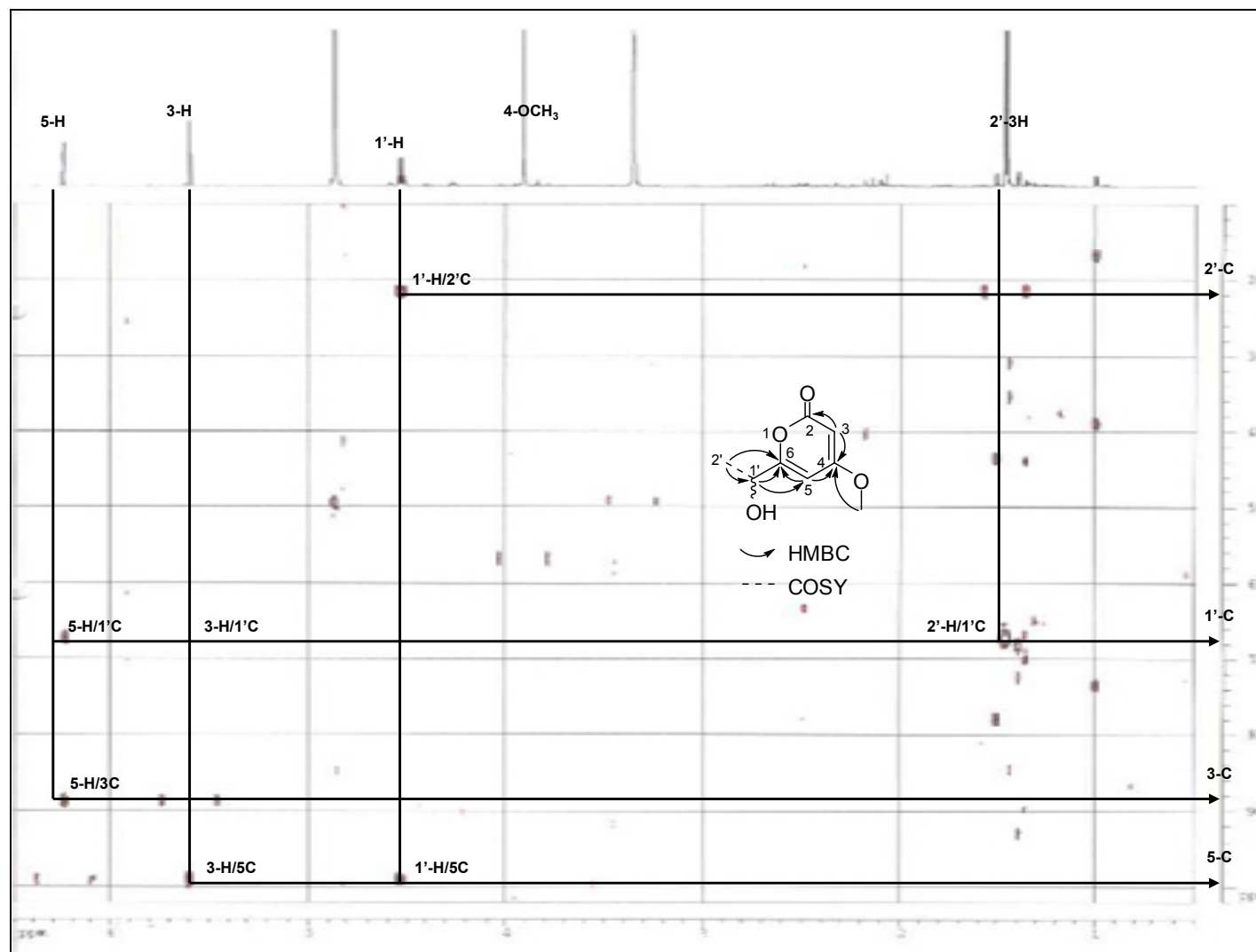
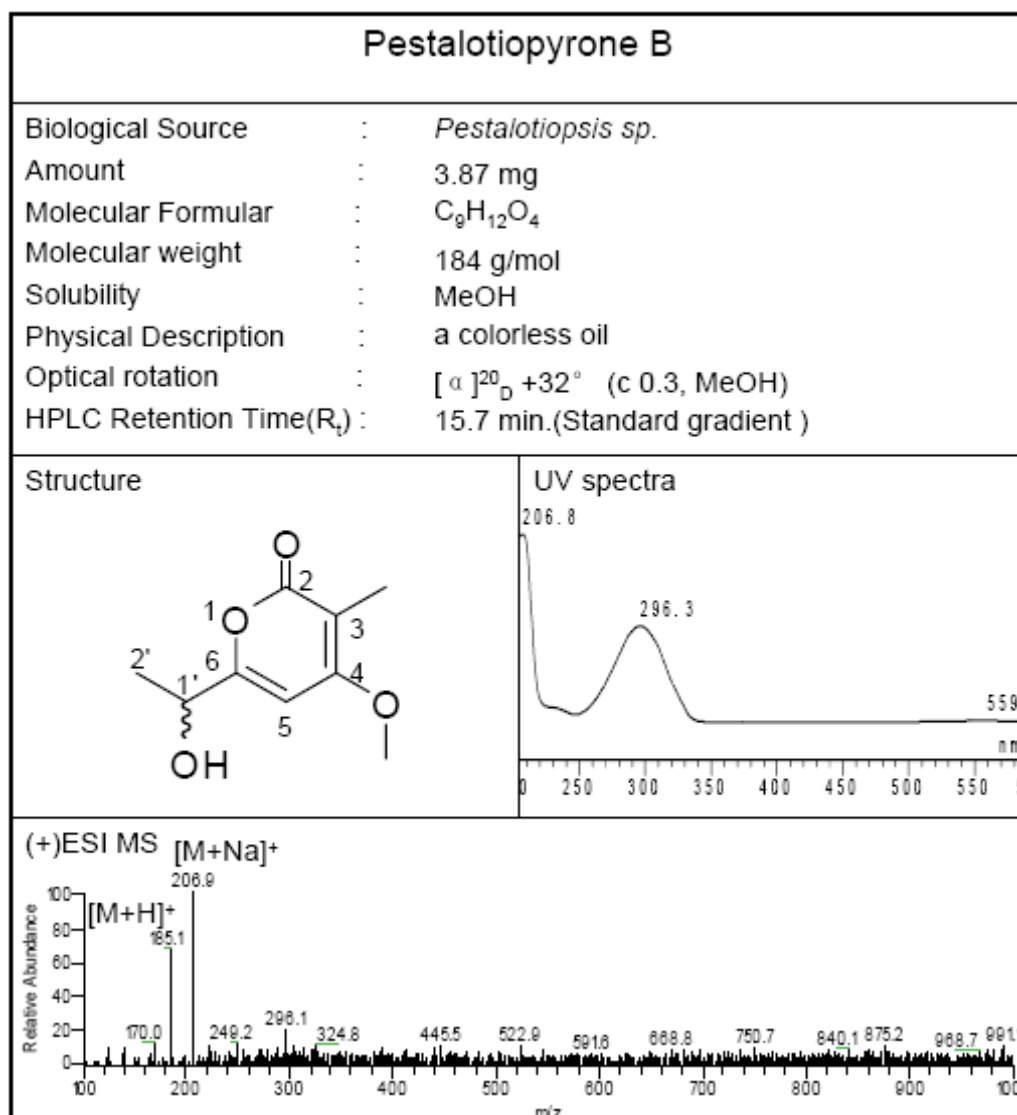


Figure 3.5.1.1b Selected HMBC correlations for compound **24**

3.5.2 Pestalotiopyrone B (25, new compound)



Pestalotiopyrone B (**25**) was found to have the molecular formula C₉H₁₂O₄ as established by HR-ESIMS (m/z 185.0802, calcd for [M+H]⁺ 185.0814). It is 14 amu larger than that of **24** suggesting the presence of an additional methyl group. The ¹H and ¹³C NMR data of **25** (Tables 3.5.2.1) were similar to those of **1** except for the presence of one additional methyl group [δ_H 1.89, s; δ_C 8.45, q, 3-CH₃]. The HMBC correlation (Figure 3.5.2.1) from protons of this methyl to C-3 disclosed its location at C-3.

Accordingly, pestalotiopyrone B (**25**) was concluded to be 6-(1-hydroxyethyl)-4-methoxy-3-methyl-2H-pyran-2-one.

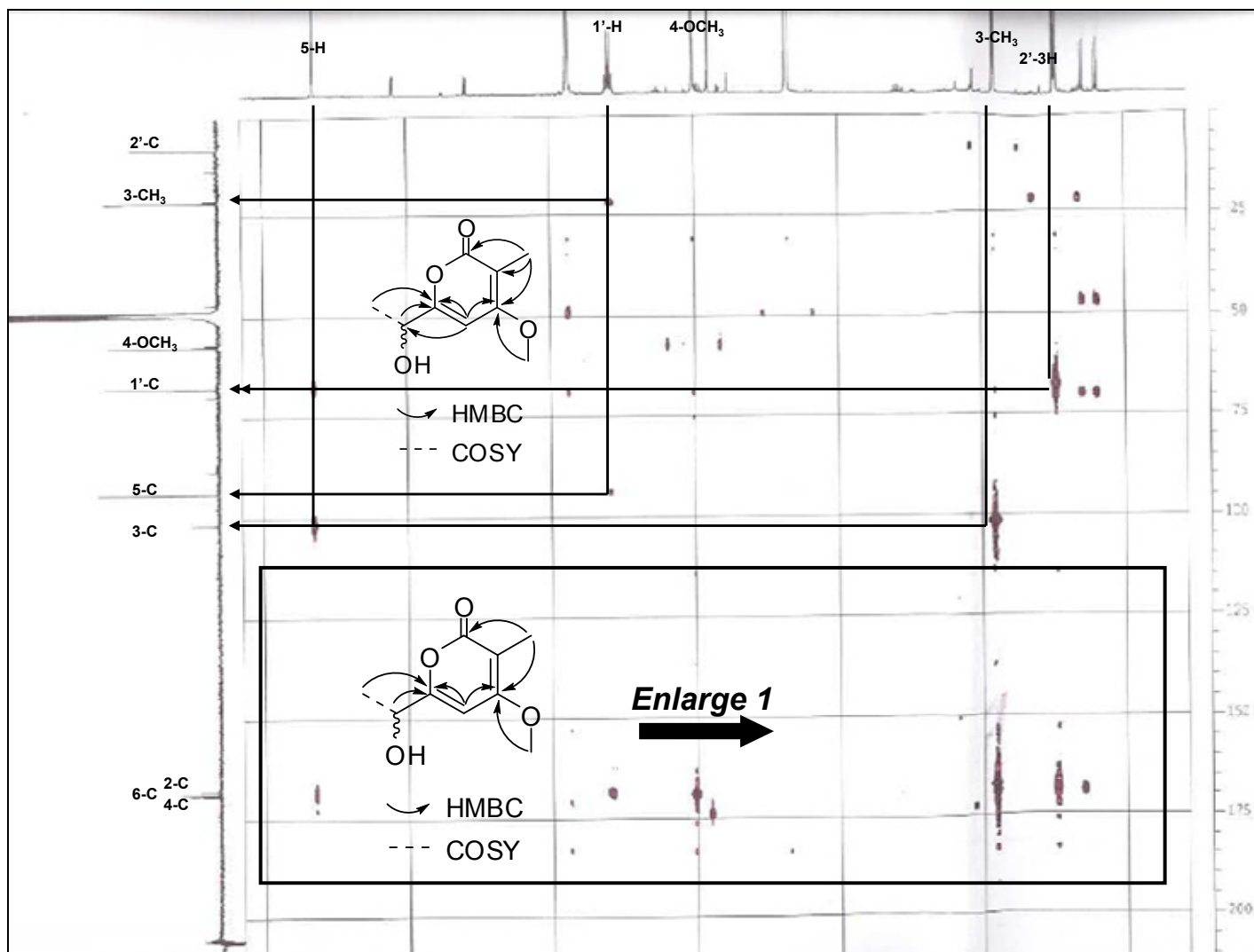


Figure 3.5.2.1a Selected HMBC correlations for compound 25

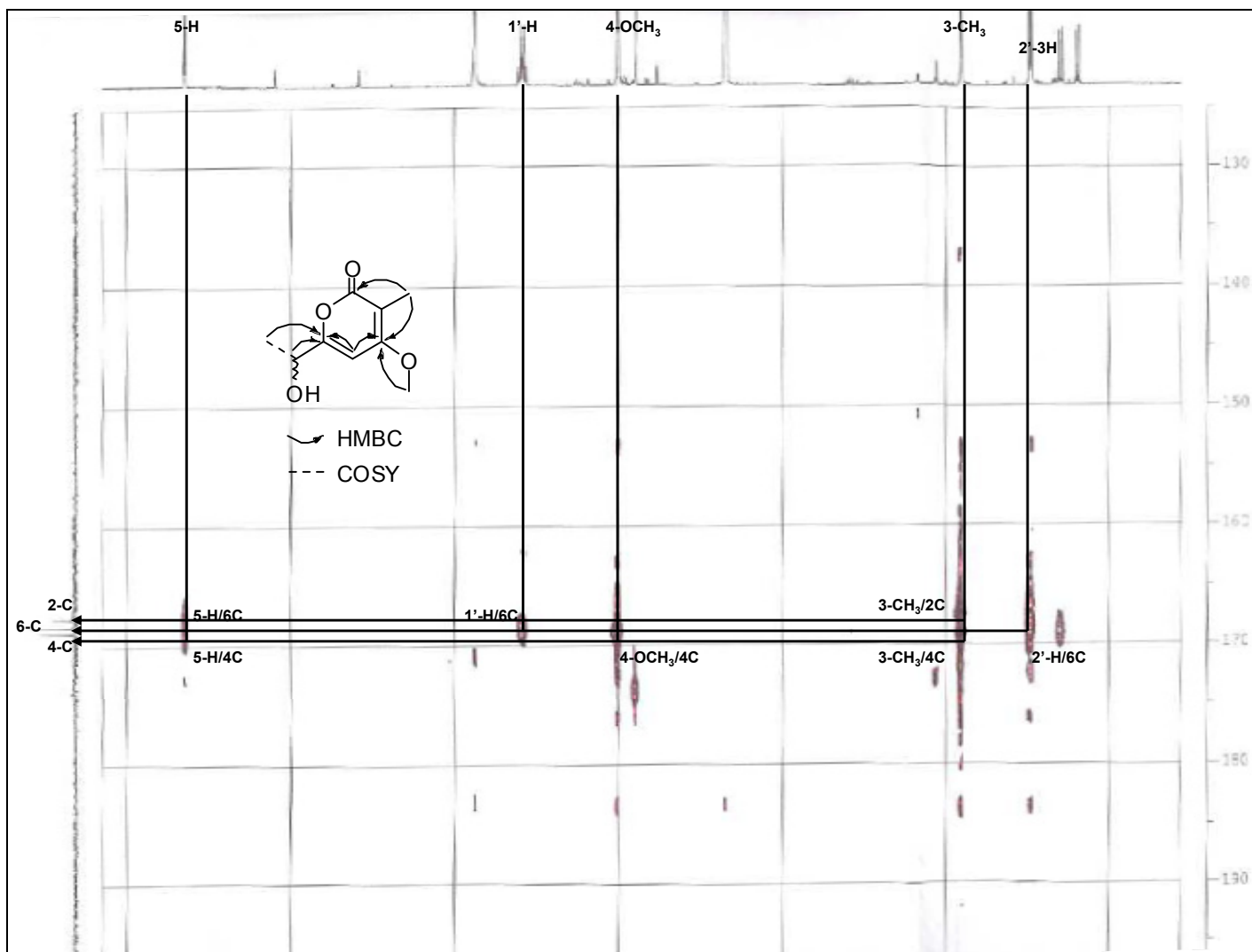
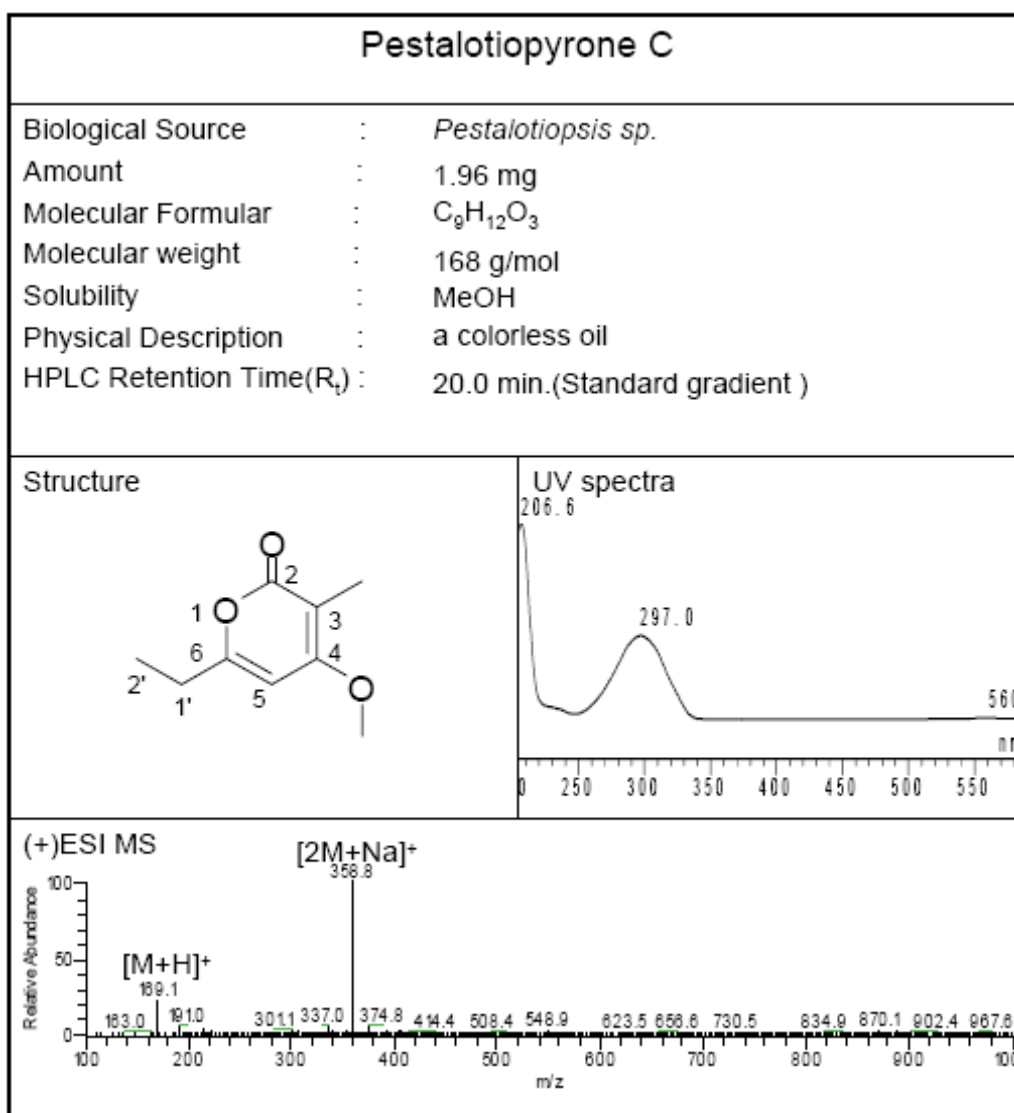


Figure 3.5.2.1b Selected HMBC correlations for compound **25**

Table 3.5.2.1 ^1H NMR (500 MHz) and ^{13}C NMR (125 MHz) spectroscopic data for pestalotiopyrone B (**25**) in CD_3OD

Atom no.	25		HMBC (H to C)	Comparison Compound 24	
	δ_{H} [ppm]	δ_{C} [ppm]		δ_{H} [ppm]	δ_{C} [ppm]
2		167.7, s			167.0, s
3		101.7, d		5.55, s	88.2, d
3-CH ₃	1.89, s	8.45, q	2, 3, 4		
4		168.9, s			174.0, s
5	6.63, s	93.9, d	4, 6	6.19, s	99.0, d
6		168.4, s			169.8, s
1'	4.57, q (6.6)	67.5, d	5, 6, 2'	4.47, q, 6.6	67.5, d
2'	1.46, d (6.6)	21.7, q	6, 1'	1.41, d, 6.6	21.5, q
4-OCH ₃	3.99, s	57.3, q	4	3.86, s	58.6, q

3.5.3 Pestalotiopyrone C (26, new compound)

Pestalotiopyrone C (**26**), a colorless oil, had the molecular formula of $C_9H_{12}O_3$, established by HR-ESIMS (m/z 169.0858, calcd for $[M+H]^+$ 169.0865). Its unsaturation degrees are the same as those of **25**. The 1H and ^{13}C NMR data of **26** (Tables 3.5.3.1) also closely resembled those of **25**. The difference between them was attributed to the side chain attached at C-6, where the 1'-hydroxyethyl group in **25** was replaced by the ethyl group in **26** [δ_H 2.57 (q, $J = 7.55$ Hz), δ_C 28.0, d, CH_2 -1'; δ_H 1.23 (d, $J = 7.55$ Hz), δ_C 12.0, d, CH_3 -2']. This finding was further supported by 1H - 1H COSY correlations (Figure 3.5.3.1) between H_2 -1'/ H_3 -2' and HMBC cross-peak between H_2 -1'/C-6.

Thus, pestalotiopyrone C (**26**) was identified as 6-ethyl-4-methoxy-3-methyl-2H-pyran-2-one.

Table 3.5.3.1 1H NMR (500 MHz) and ^{13}C NMR (125 MHz) spectroscopic data for pestalotiopyrone C (**26**) in CD_3OD

Atom no.	26		HMBC (H to C)	Comparision Compound 25	
	δ_H [ppm]	δ_C [ppm]		δ_H [ppm]	δ_C [ppm]
2		167.0, s			167.7, s
3		101.2, s			101.7, d
3- CH_3	1.84, s	8.2, q	2, 3, 4	1.89, s	8.45, q
4		170.1, s			168.9, s
5	6.31, s	96.3, d	4, 6	6.63, s	93.9, d
6		167.2, s			168.4, s
1'	2.57, q, 7.55	28.0, t	5, 6, 2'	4.57, q (6.6)	67.5, d
2'	1.23, t, 7.55	12.3, q	6, 1'	1.46, d (6.6)	21.7, q
4- OCH_3	3.93, s	?	4	3.99, s	57.3, q

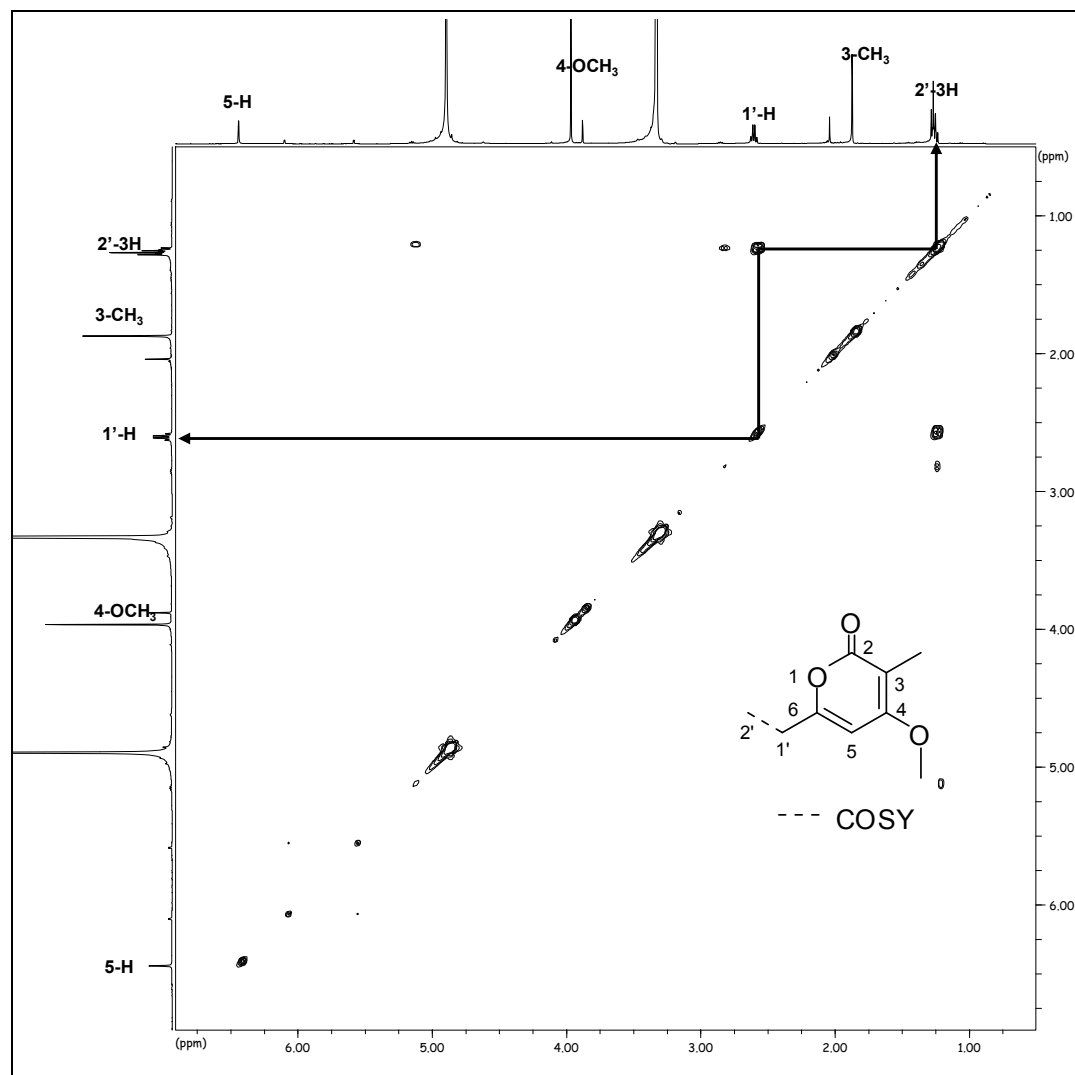
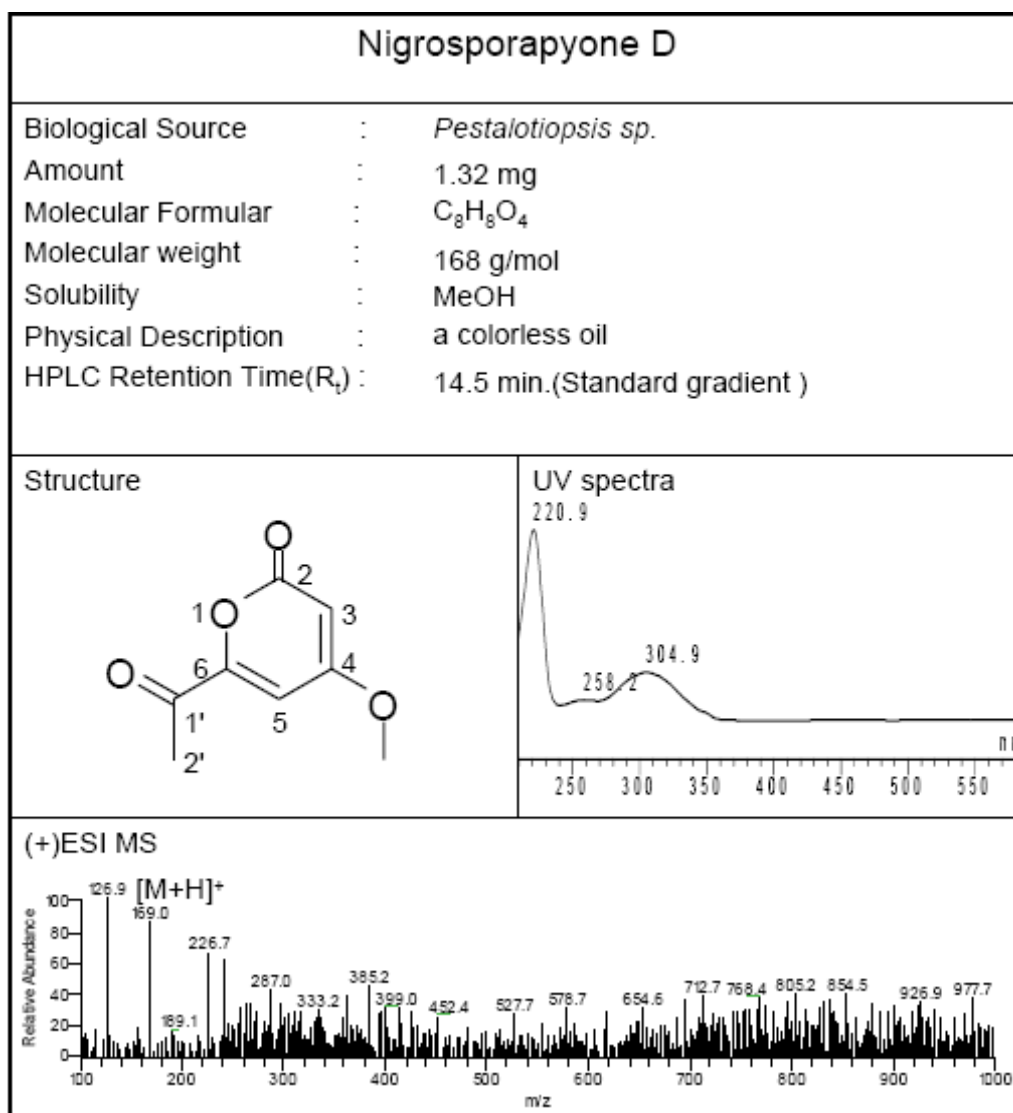


Figure 3.5.3.1 ^1H - ^1H COSY correlations for compound **26**

3.5.4 Nigrosporapyrone D (27, known compound)



Compound **27** was determined to have the molecular formula of C₈H₈O₄ by HR-ESIMS (m/z 172.0681, calcd for [C₈H₅O₄D₃+H]⁺ 172.0689). The ¹H and ¹³C NMR data (Tables 3.5.4.1) of **27** were similar to those of **24**. However, the signals of the 1'-hydroxymethine of the C-6 side chain in **24** were absent in the NMR spectra of **27**. Instead, signals of a carbonyl group (δ_C 192.0, C-1') appeared. It was indicated that the 1-hydroxyethyl group in **24** was replaced by an acetyl group. Confirming

evidence was obtained from HMBC correlations (Figure 3.5.4.1) between H-5/C-1', H-5/C-6, H-2'/C-1', and H-2'/C-6.

Comparison of the NMR data of **27** with those of nigrosporapyrone D (Trisuwana *et al.* 2009), previously isolated from *Nigrospora* sp. PSU-F18, revealed that compound **27** was identical to nigrosporapyrone D.

Table 3.5.4.1 ^1H NMR (500 MHz) and ^{13}C NMR (125 MHz) spectroscopic data for nigrosporapyrone D (**27**) in CD_3OD

Atom no.	27		HMBC (H to C)	Comparison Compound 24	
	δ_{H} [ppm]	δ_{C} [ppm]		δ_{H} [ppm]	δ_{C} [ppm]
2		163.8, s			167.0, s
3	5.88, d, 2.2	93.2, d	2, 4	5.55, s	88.2, d
4		171.0, s			174.0, s
5	6.85, d, 2.2	104.7, d	4, 6	6.19, s	99.0, d
6		152.9, s			169.8, s
1'		192.0, s		4.47, q, 6.6	67.5, d
2'	2.46, s	?	6, 1'	1.41, d, 6.6	21.5, q
4-OCH ₃	3.90, s	56.5, q	4	3.86, s	58.6, q

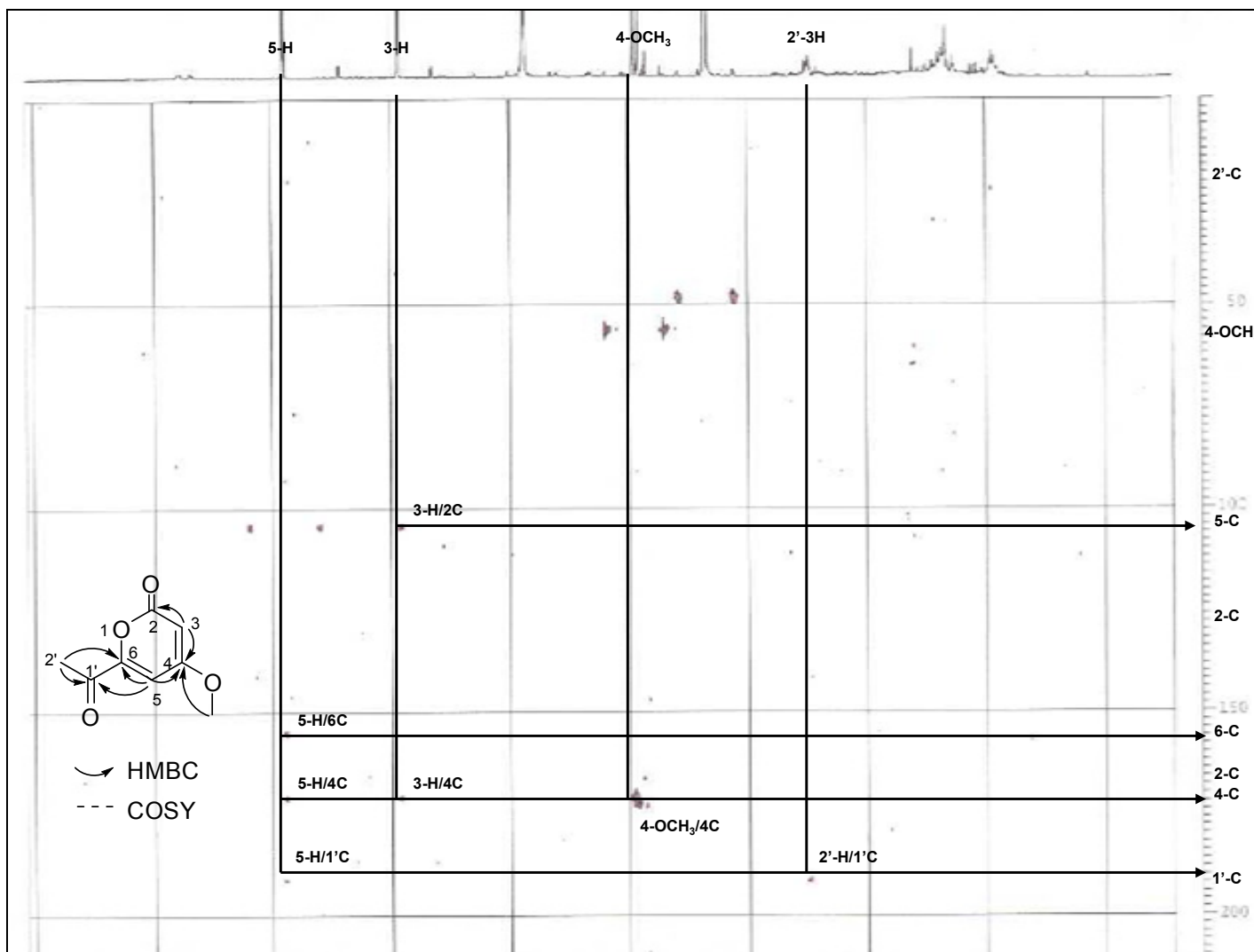
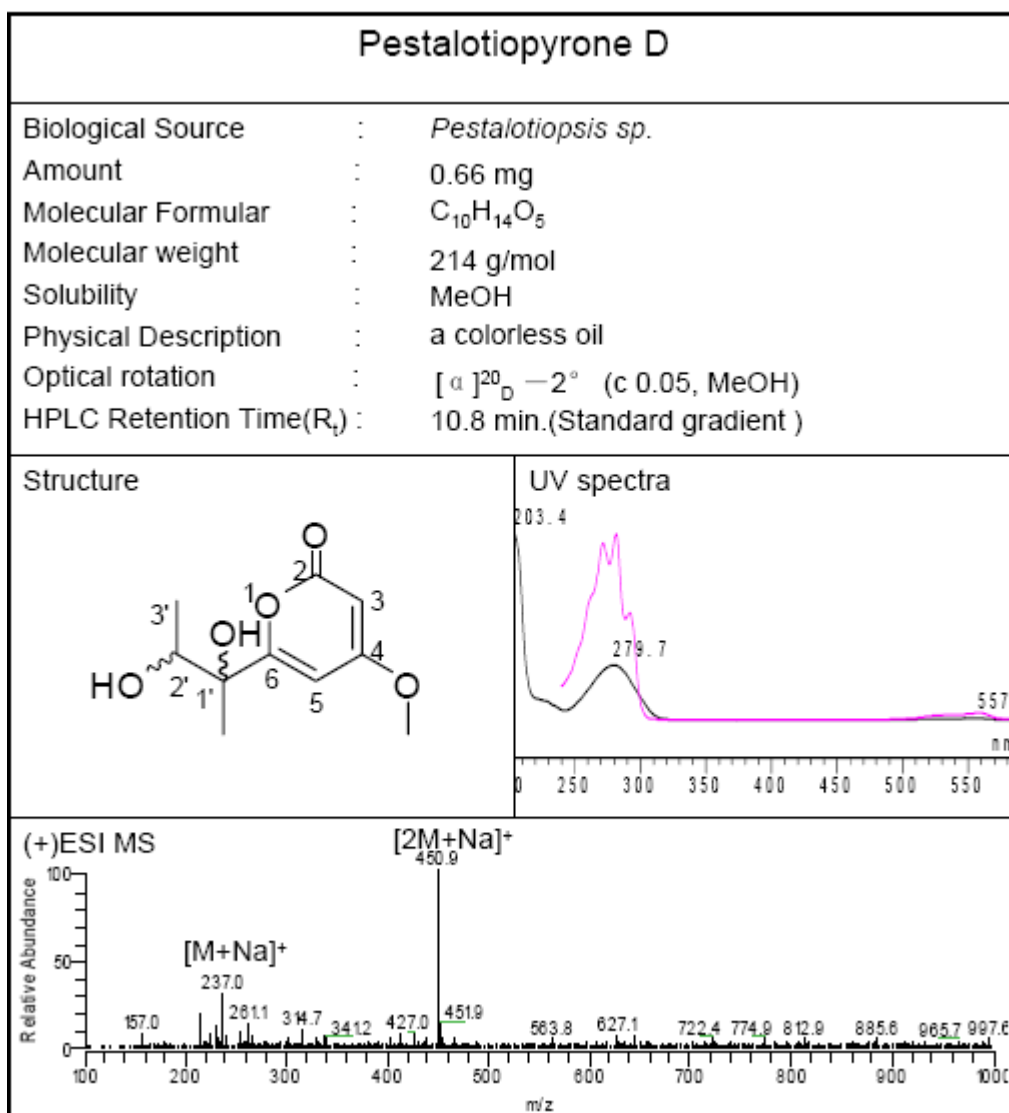


Figure 3.5.4.1 Selected HMBC correlations for compound **27**

3.5.5 Pestalotiopyrone D (**28**, new compound)

The molecular formula of pestalotiopyrone D (**28**) was established as C₁₀H₁₄O₅ by HR-ESIMS (m/z 215.0915, calcd for [M+H]⁺ 215.0919). Its ¹H NMR data (Table 3.5.5.1) were closely related to those of **24**, except for the absence of the 1'-hydroxymethine group [δ_H 4.47 (q, J = 6.6 Hz), δ_C 67.5, d, 1'-CH] in **24** and presence of one additional 1',2'-dihydroxypropyl group in **28**. This finding was confirmed by ¹H-¹H COSY correlations (Figure 3.5.5.1). One additional hydroxyethyl signal [δ_H 3.90, (d, J = 6.6 Hz), 2'-CH; δ_H 1.07, (d, J = 6.6 Hz), 3'-CH₃] indicated the

presence of a propyl-2,3-diol group substituted at C-6 in **28**. This change was also confirmed by the ^1H - ^1H COSY correlation of H-2' to H-3'.

The structure of pestalotiopyrone D (**28**) was thus assigned as 6-ethyl-4-methoxy-3-methyl-2H-pyran-2-one.

Table 3.5.5.1 ^1H NMR (500 MHz) spectroscopic data for pestalotiopyrone D (**28**) in CD_3OD

Atom no.	28 δ_{H} [ppm]	Comparison δ_{H} [ppm]	Compound 24 δ_{C} [ppm]
2			167.0, s
3	5.53, d, 2.2	5.55, s	88.2, d
4			174.0, s
5	6.31, d, 2.2	6.19, s	99.0, d
6			169.8, s
1'		4.47, q, 6.6	67.5, d
1'-CH ₃	1.45, s		
2'	3.90, q, 6.6	1.41, d, 6.6	21.5, q
3'	1.07, d, 6.6		
4-OCH ₃	3.85, s	3.86, s	58.6, q

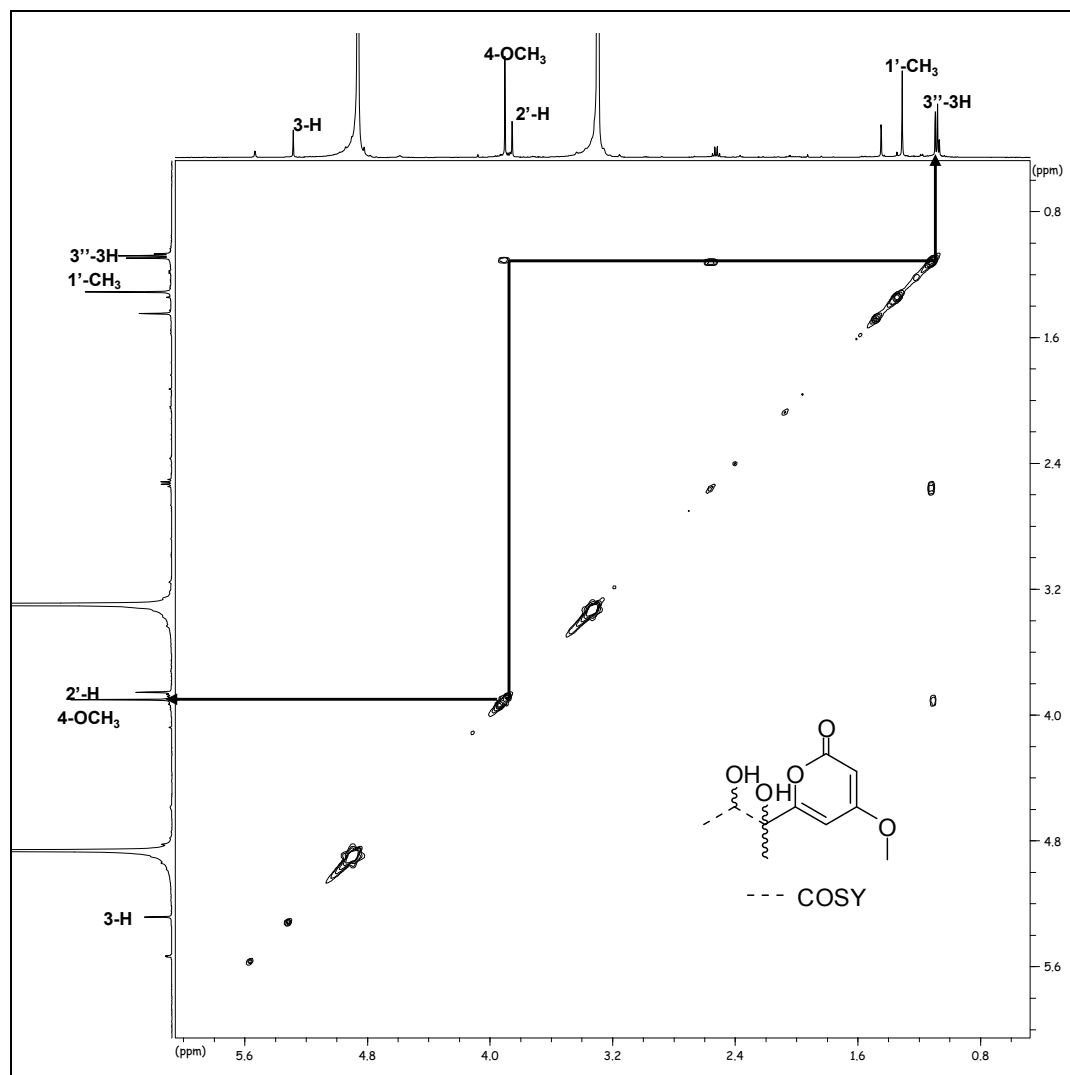
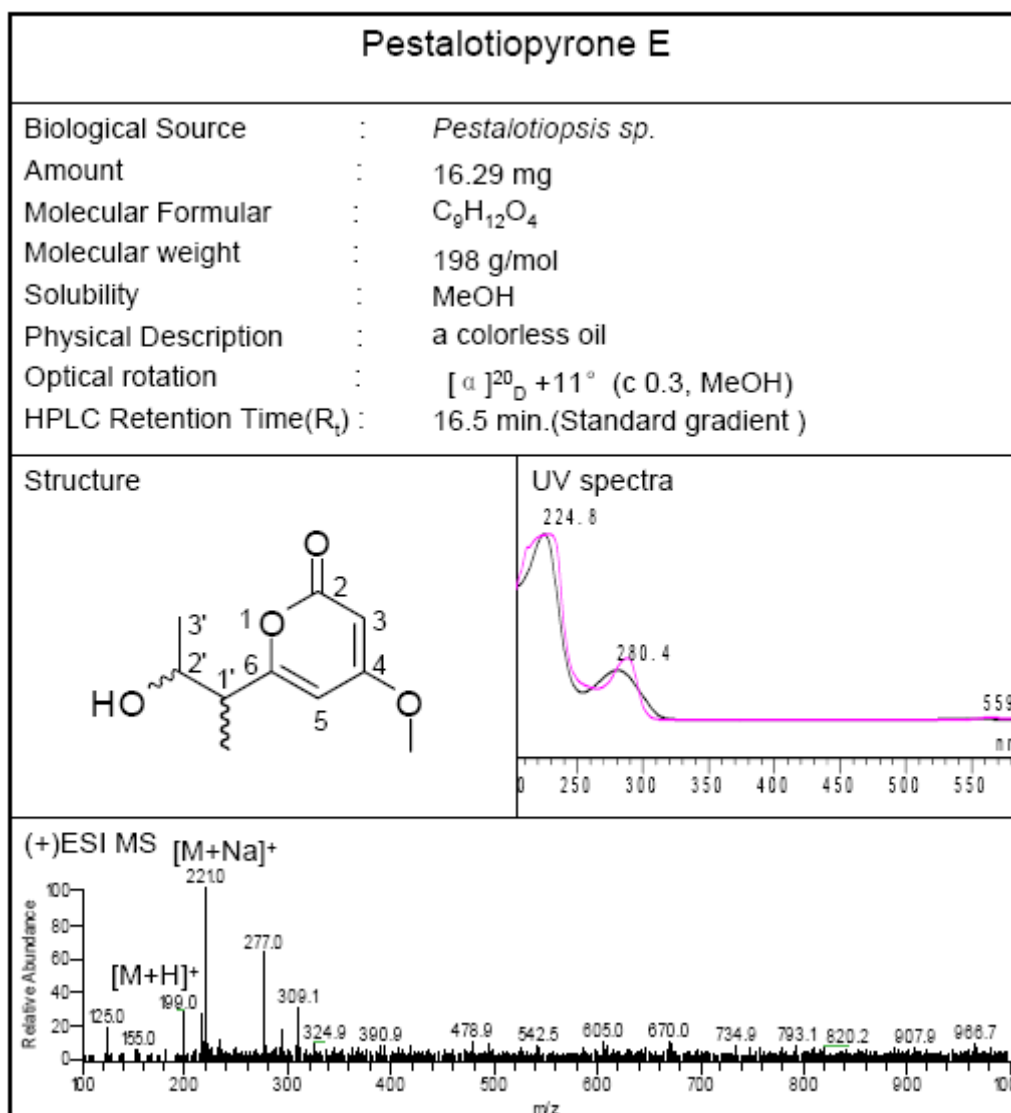


Figure 3.5.5.1 ^1H - ^1H COSY correlations for compound 29

3.5.6 Pestalotiopyrone E (**29**, new compound)

Pestalotiopyrone E (**29**) had the molecular formula of $C_{10}H_{14}O_4$, as established by HR-ESIMS (m/z 199.0959, calcd for $[M+H]^+$ 199.0970). The 1H and ^{13}C NMR data of **29** (Tables 3.5.6.1) were similar to those of **24**. However, the side chain at C-6 in **26** was replaced by a 1-methyl-2-hydroxy-propyl group [δ_H 2.57, m, δ_C 47.4, d, 1'-CH; δ_H 1.27, (d, $J = 6.85$ Hz), δ_C 14.0, q, 1'-CH₃; δ_H 3.95, m, δ_C 70.3, d, 2'-CH; δ_H 1.18, (d, $J = 6$. Hz), q, 3'-CH₃]. This assignment was further confirmed by 1H - 1H COSY

correlations (Figure 3.5.6.1) between 1'-CH₃/H-1', H-1'/H-2', H-2'/H₃-3' and HMBC cross peaks between H₃-3'/C-1', H-1'/C-6, and 1'-CH₃/C-6.

Thus, the structure of pestalotiopyrone E (**29**) was established as 6-(3-hydroxybutan-2-yl)-4-methoxy-2H-pyran-2-one.

Table 3.5.6.1 ¹H NMR (500 MHz) and ¹³C NMR (125 MHz) spectroscopic data for pestalotiopyrone E (**29**) in CD₃OD

Atom no.	29		HMBC (H to C)	Comparision Compound 24	
	δ_H [ppm]	δ_C [ppm]		δ_H [ppm]	δ_C [ppm]
2		168.0, s			167.0, s
3	5.57, d, 2.2	88.8, d	2, 4	5.55, s	88.2, d
4		174.1, s			174.0, s
5	6.07, d, 2.2	102.3, d	4, 6, 1'	6.19, s	99.0, d
6		173.1, s			169.8, s
1'	2.57, m	47.4, d	5, 6, 2', 3', 1'-CH ₃	4.47, q, 6.6	67.5, d
1'-CH ₃	1.27, d, 6.85	14.0, q	6, 1', 2'		
2'	3.95, m	70.3, d	6, 1', 3', 1'-CH ₃	1.41, d, 6.6	21.5, q
3'	1.18, d, 6.3	21.7, q	1', 2'		
4-OCH ₃	3.88, s	57.3, q	4	3.86, s	58.6, q

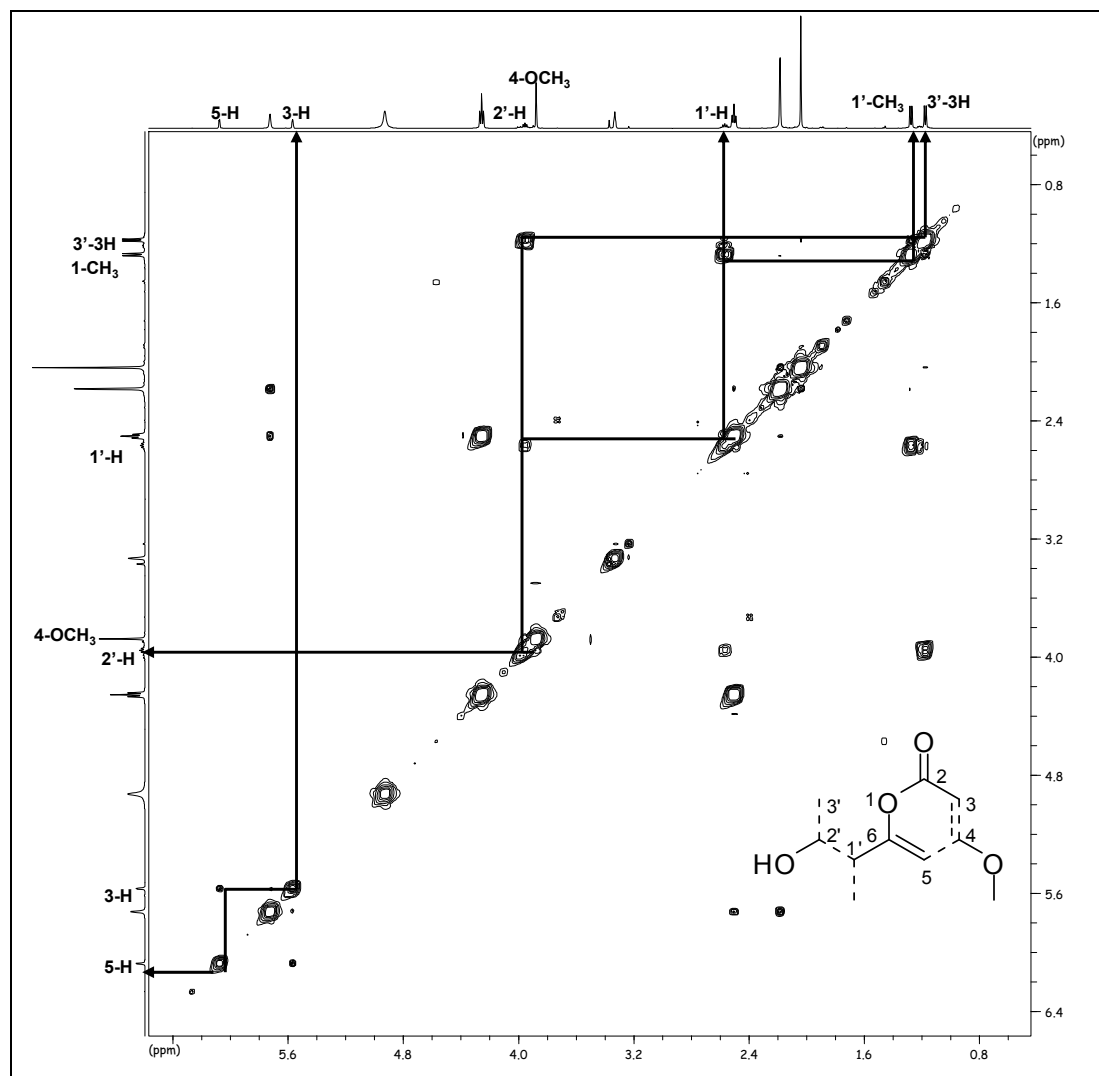
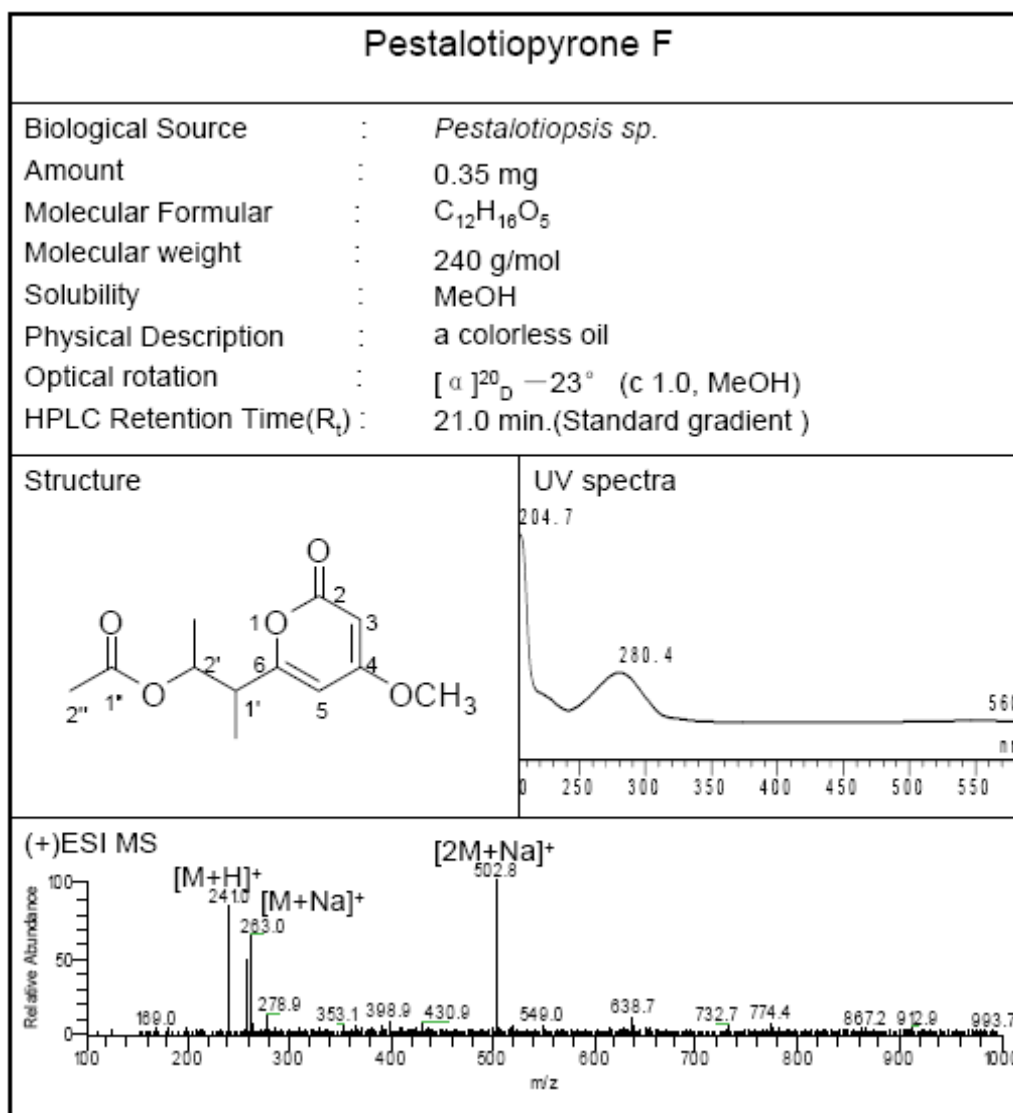


Figure 3.5.6.1 ^1H - ^1H COSY correlations for compound 29

3.5.7 Pestalotiopyrone F (30, new compound)



The molecular formula of pestalotiopyrone F (**30**) was established as C₁₂H₁₆O₅ by HR-ESIMS (m/z 241.1070, calcd for [M+H]⁺ 241.1076), which is 43 amu larger than that of **29**. The presence of one additional acetyl group in **30** was suggested by the detection of a mass fragment at m/z 199 in its ESI-MS spectrum, which was derived from loss of CH₃COOH. The ¹H NMR data of **30** (Table 3.5.7.1) were similar to those of **29**, except for the significant downfield shift of H-2' (δ_H 5.12, m) and presence of one more methyl signal at δ_H 2.02 (s, H₃-2''), indicating the acetylation of the hydroxyl at C-2' in **29**.

Hence, **30** was conclude to be 3-(4-methoxy-2-oxo-2H-pyran-6-yl)butan-2-yl acetate.

Table 3.5.7.1 ^1H NMR (500 MHz) and ^{13}C NMR (125 MHz) spectroscopic data for pestalotiopyrone F (**30**) in CD_3OD

Atom no.	30 δ_{H} [ppm]	Comparison Compound 29 δ_{H} [ppm]	δ_{C} [ppm]
2			168.0, s
3	5.56, d, 2.2	5.57, d, 2.2	88.8, d
4			174.1, s
5	6.07, d, 2.2	6.07, d, 2.2	102.3, d
6			173.1, s
1'	2.83, m	2.57, m	47.4, d
1'-CH ₃	1.24, d, 7.25	1.27, d, 6.85	14.0, q
2'	5.12, m	3.95, m	70.3, d
2'-CH ₃	1.22, d, 6.6		
3'		1.18, d, 6.3	21.7, q
2''	2.02, s		
4-OCH ₃	3.86, s	3.88, s	57.3, q

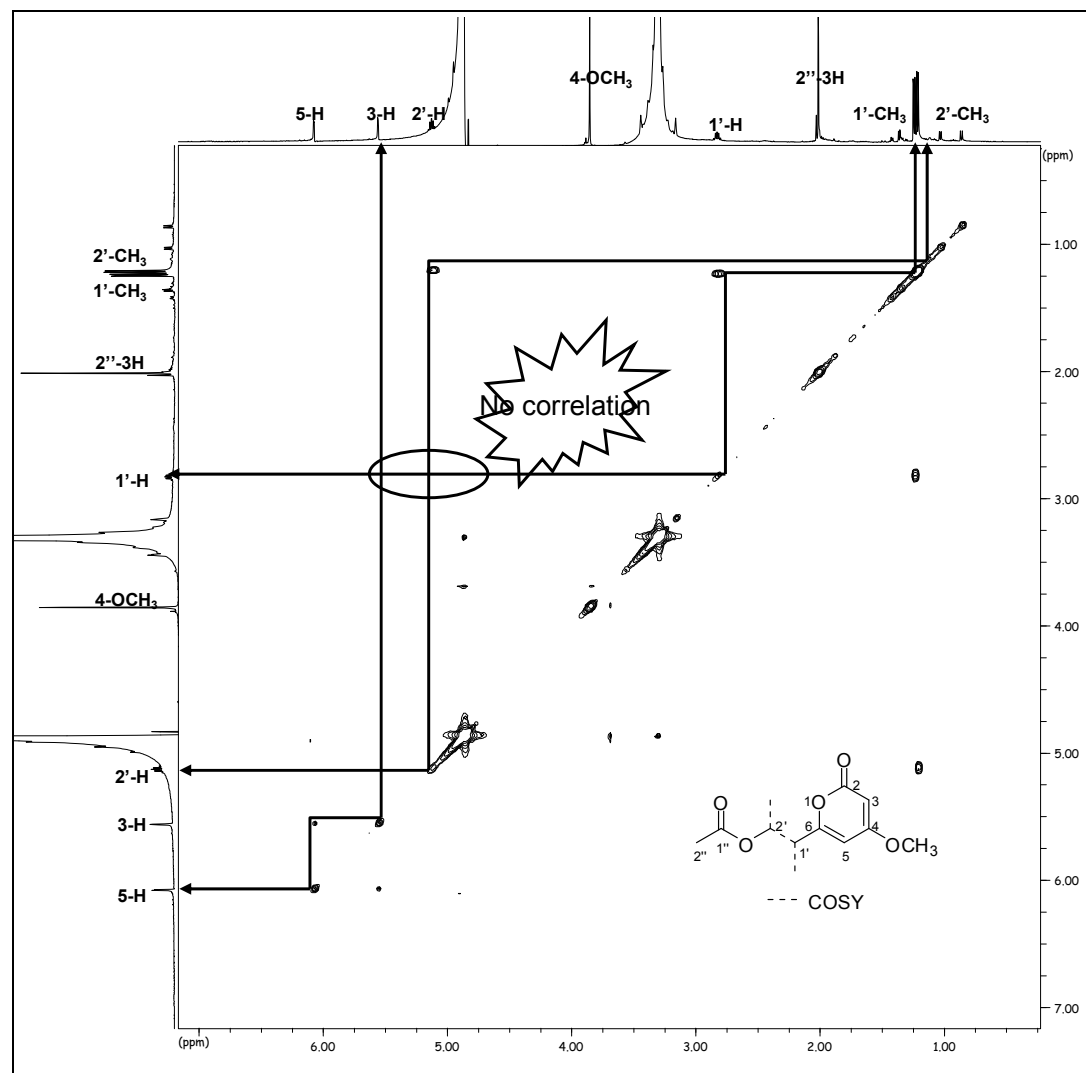
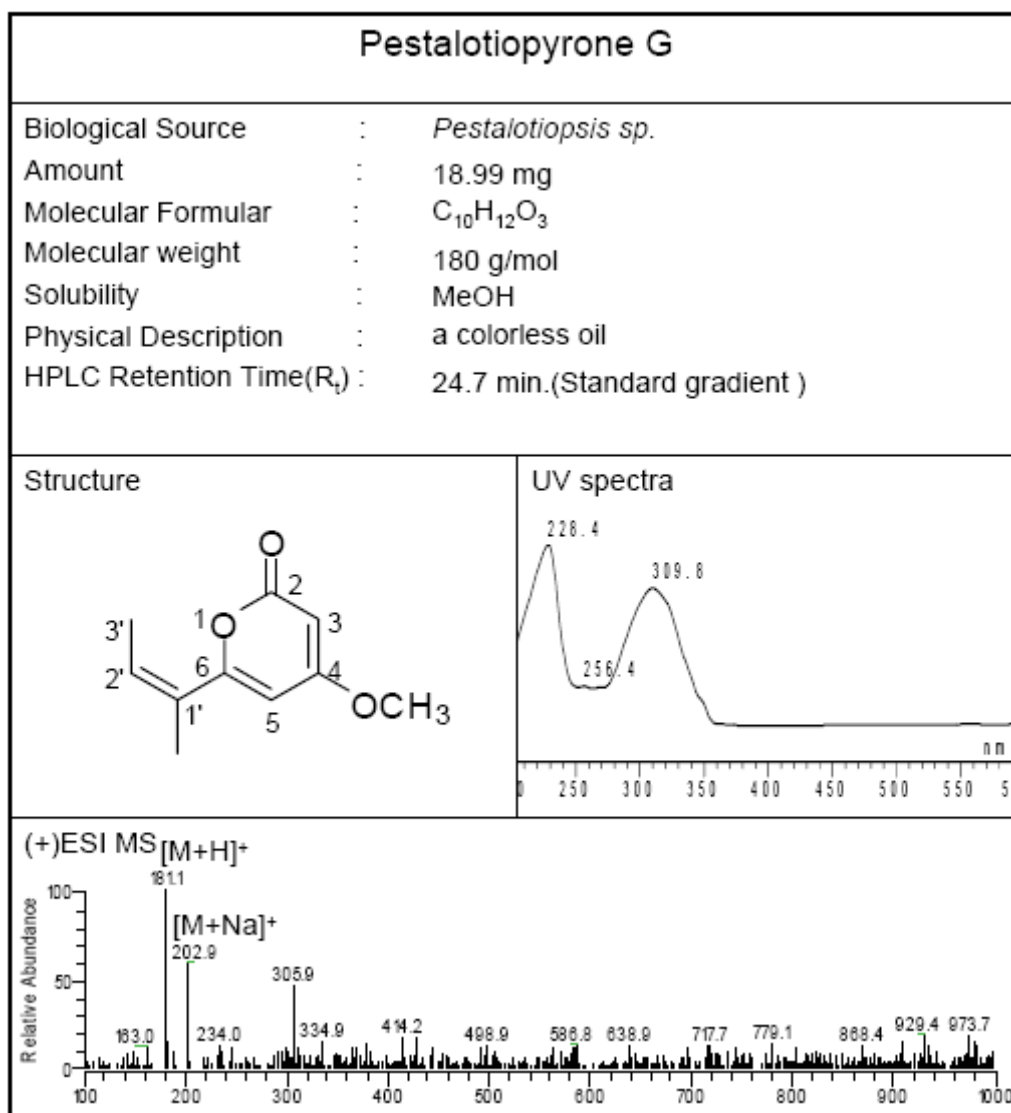


Figure 3.5.7.1 ^1H - ^1H COSY correlations for compound 30

3.5.8 Pestalotiopyrone G (31, new compound)



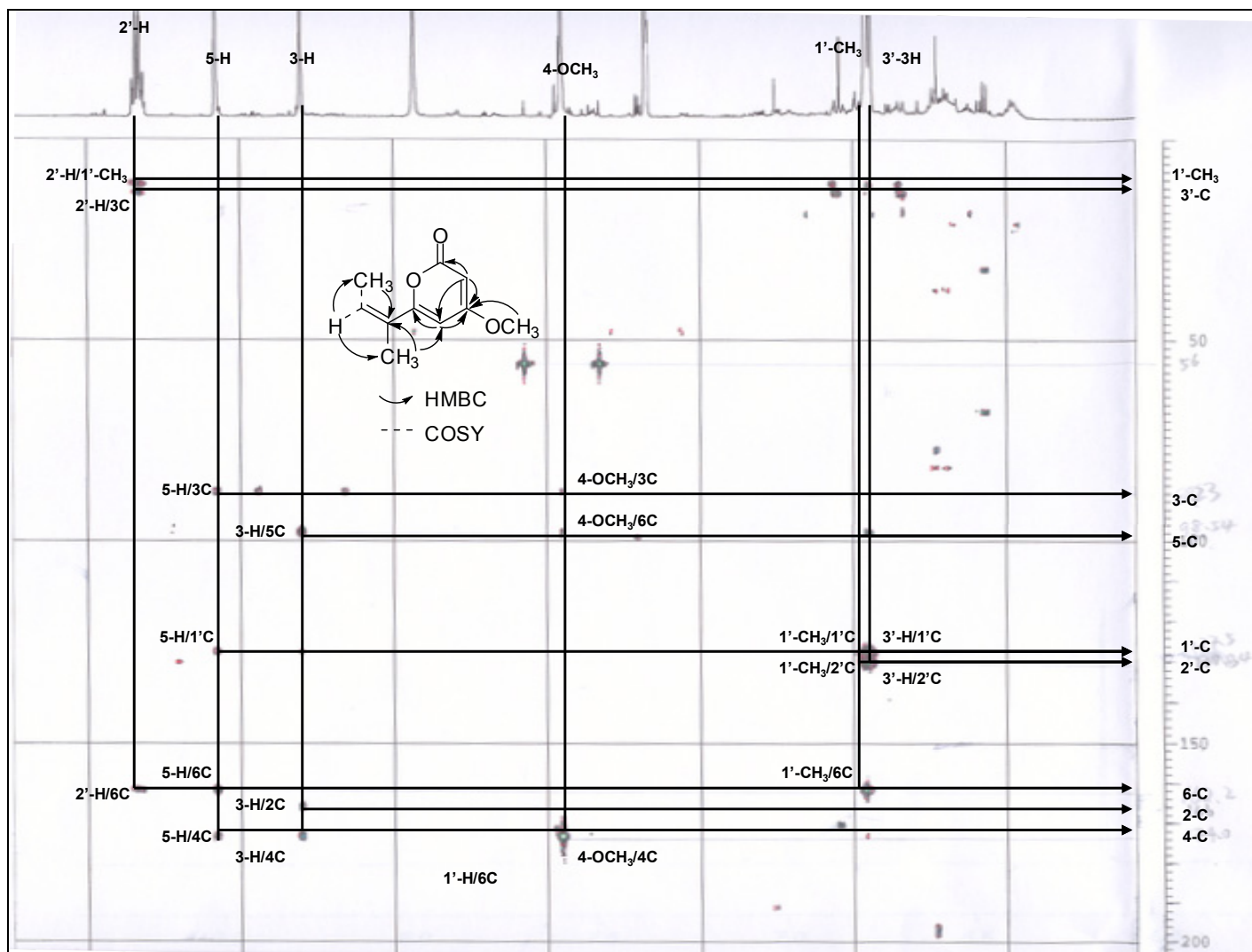
The molecular formula of $C_{10}H_{12}O_3$, indicating five degrees of unsaturation, was suggested for pestalotiopyrone G (**31**) by HR-ESIMS (m/z 181.0859, calcd for $[M+H]^+$ 181.0854). The 1H NMR data of **31** (Tables 3.5.8.1) were very compatible with those of pestalopyrone, previously isolated from the pathogenic fungus *Pestalotiopsis oenotherae* (Venkatasubbaiah *et al.* 1991), suggesting that both compounds shared the same skeleton. HMBC correlations from H-5 (δ_H 6.11, s), H-2' (δ_H 6.62, d), H-3' (δ_H 1.85, d), and CH_3 -1' (δ_H 1.87, s) to C-1' (δ_C 128.3), and those

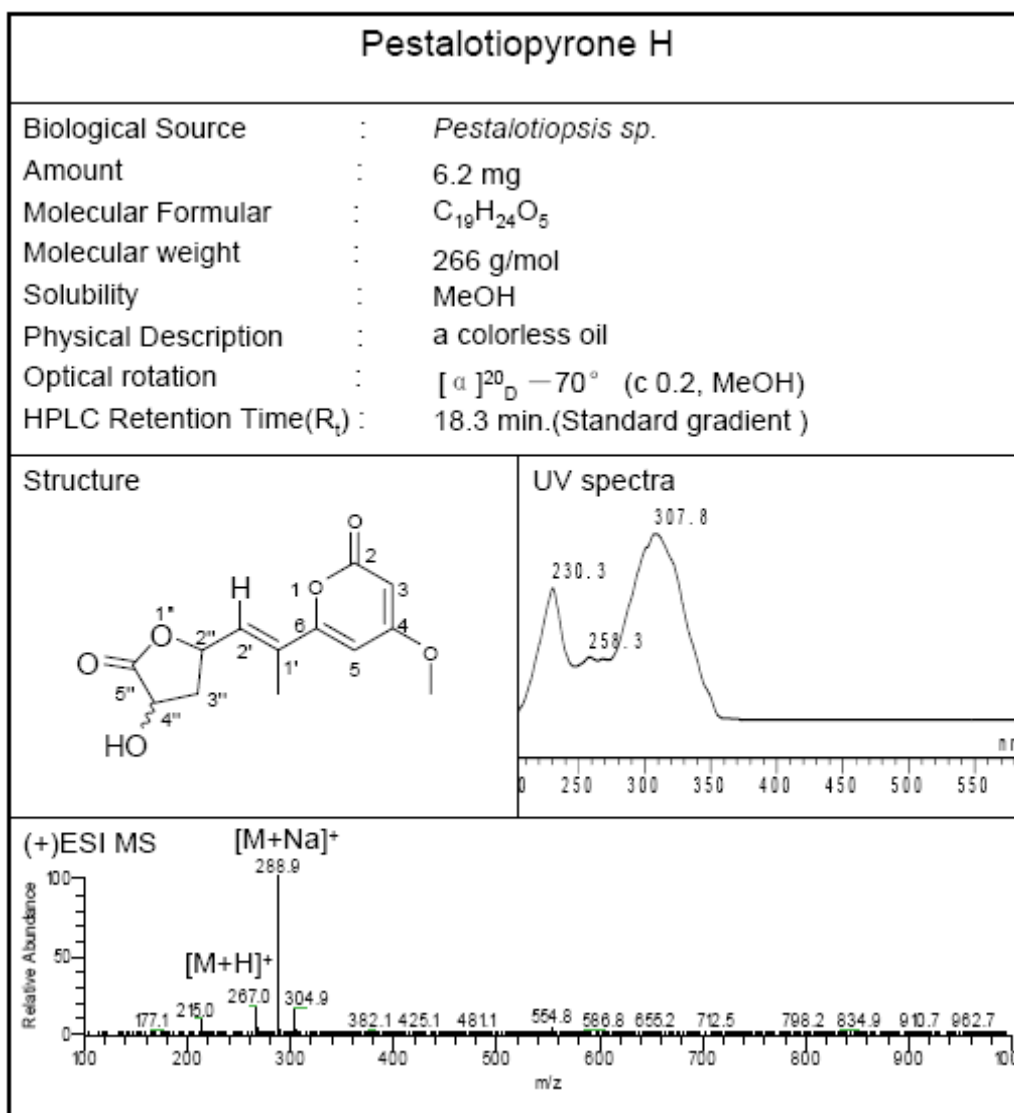
from H-2' and CH₃-1' to C-6 (δ_C 162.7) revealed that the planar structure of **31** is identical to that of pestalopyrone. The NOE correlation between 1'-CH₃ (δ_H 1.87, s) and H₃-3' disclosed the Z-geometry of the double bond in the side chain at C-6.

Therefore, **31** was identified as (Z)-6-(but-2-en-2-yl)-4-methoxy-2H-pyran-2-one.

Table 3.5.8.1 ¹H NMR (500 MHz) and ¹³C NMR (125 MHz) spectroscopic data for pestalotiopyrone G (**31**) in CD₃OD

Atom no.	31		HMBC (H to C)	Pestalopyrone from Reference δ_H [ppm]
2		166.9, s		
3	5.56, s	88.6, d	2, 4, 5	5.45, d, 1
4		174.1, s		
5	6.11, s	98.8, d	4, 6, 1'	5.90, d, 1
6		162.7, s		
1'		128.3, d	5, 6, 2', 3', 1'-CH ₃	
1'-CH ₃	1.87, s	12.1, q	6, 1', 2'	1.86, s
2'	6.62, q (6.9)	131.0, d	6, 1', 3'	6.69, q, 7
3'	1.85, d (7.25)	14.3, q	1', 2'	1.84, d, 7
4-OCH ₃	3.86, s	57.3, q	4	3.81, s

**Figure 3.5.8.1** Selected HMBC correlations for compound **31**

3.5.9 Pestalotiopyrone H (**32**, new compound)

Pestalotiopyrone H (**32**), a colorless oil, was determined to have the molecular formula of $C_{19}H_{24}O_5$ by HR-ESIMS (m/z 267.0867, calcd for $[M + H]^+$ 267.0869). Obviously, it had seven degrees of unsaturation. Comparison of the NMR data of **32** with those of pestalotiopyrone G (**31**) disclosed that both compounds differed only in the side chain at C-6. The terminal methyl group of this side chain in **31** was replaced by a 3-hydroxydihydrofuran-2(3H)-one group in **32**. This replacement was further confirmed by 1H - 1H COSY correlations between H-2'/H-2'', H-2''/H-3'', H-3''/H-4'' and HMBC cross-peaks between H-2''/C-1', H-2''/C-2', H-2''/C-3'', H-2''/C-4'',

4''-OH/C-3'', 4''-OH/C-4'', 4''-OH/C-5'' (Figure 3.5.9.1). Moreover, the relative configuration of **32** was established by the observed NOE interactions between H-5/1'-CH₃, H-2''/H-2', and H-2''/H-4''.

Accordingly, the structure of pestalasin A (**32**) was characterized as (*E*)-6-(1-(4-hydroxy-5-oxotetrahydrofuran-2-yl)prop-1-en-2-yl)-4-methoxy-2H-pyran-2-one.

Table 3.5.9.1 ¹H NMR (500 MHz) and ¹³C NMR (125 MHz) spectroscopic data for pestalotiopyrone H (**32**) in CD₃OD

Atom no.	32 δ_H [ppm]	δ_C [ppm]	HMBC (H to C)	Comparison Compound 31 δ_H [ppm]	δ_C [ppm]
2		162.3, s			166.9, s
3	5.69, d, 1.9	89.2, d	2, 4	5.56, s	88.6, d
4		170.7, s			174.1, s
5	6.36, d, 1.9	99.7, d	4, 6, 1'	6.11, s	98.8, d
6		159.0, s			162.7, s
1'		130.3, s	5, 6, 2', 3', 1'-CH ₃		128.3, d
1'-CH ₃	1.92, s	12.6, q	6, 1', 2'	1.87, s	12.1, q
2'	6.30, d, 8.5	130.1, d	6, 1', 3', 1'-CH ₃	6.62, q (6.9)	131.0, d
3'			1', 2'	1.85, d (7.25)	14.3, q
2''	5.32, m	71.9, d			
3''	1.85, q, 10.7	37.3, t			
	2.67, m				
4''	4.48, m	67.2, d			
4''-OH	6.0, d, 6.6	176.7, s			
4-OCH ₃	3.83, s	57.3, q	4	3.86, s	57.3, q

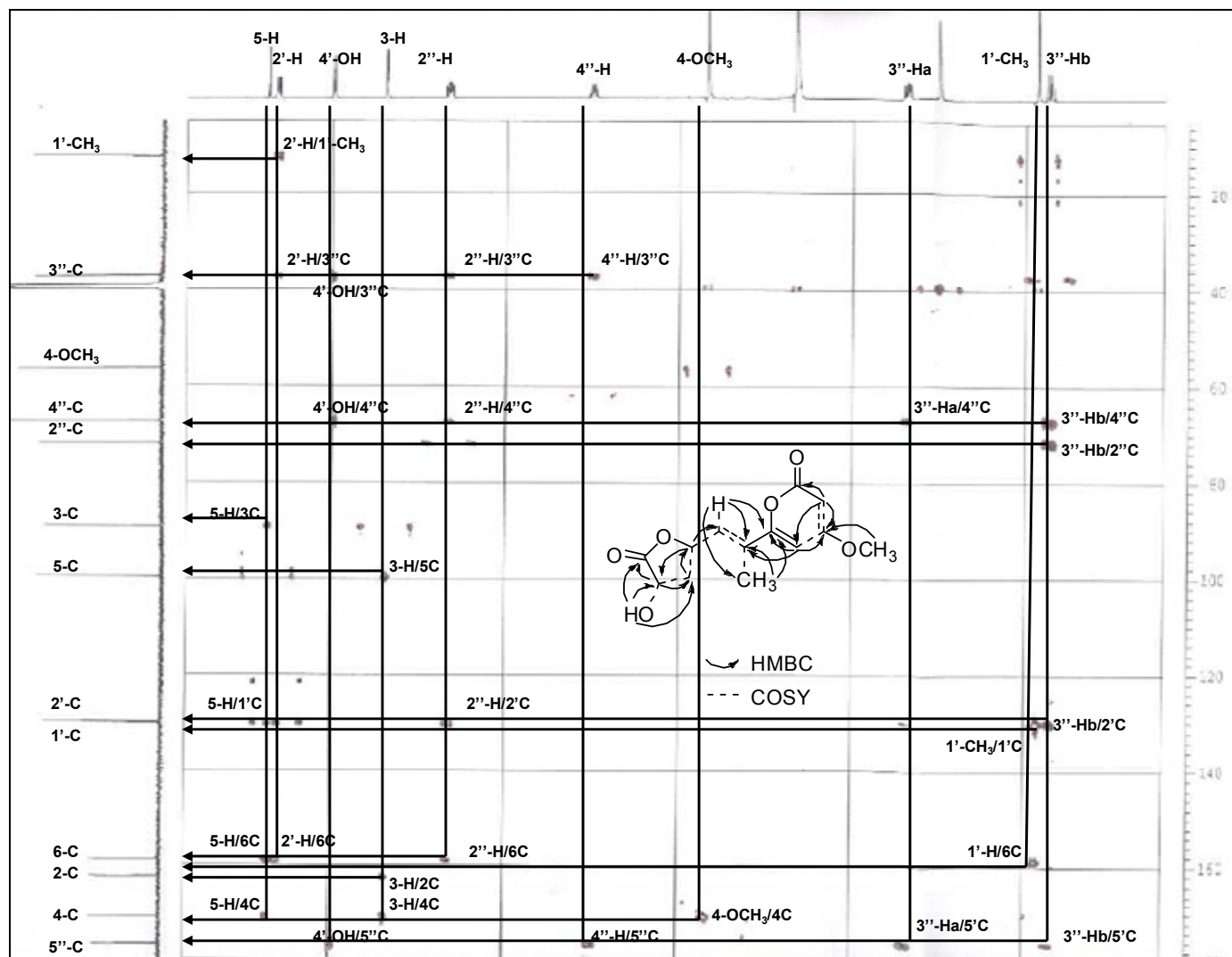
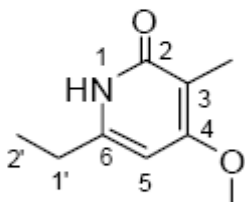
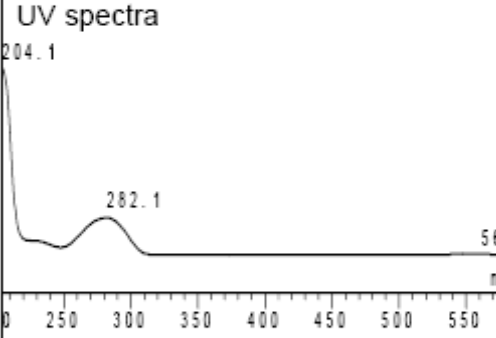


Figure 3.5.9.1 Selected HMBC correlations for compound 32

3.6 Alkaloids

3.6.1 Pestalotiopyridine (**33**, new compound)

Pestalotiopyridine	
Biological Source	: <i>Pestalotiopsis</i> sp.
Amount	: 0.74 mg
Molecular Formula	: C ₉ H ₁₃ NO ₂
Molecular weight	: 147 g/mol
Solubility	: MeOH
Physical Description	: a colorless oil
HPLC Retention Time(R _t)	: 12.0 min.(Standard gradient)
Structure	UV spectra
	
(+)-ESI MS	

Pestalotiopyridine (**33**), a colorless oil, had the molecular formula of C₉H₁₃NO₂, established by HR-ESIMS (m/z calcd for [M+H]⁺ 148.1025). Its ¹H and ¹³C NMR data were similar to those of **25**, except for the upshifted resonances of C-6 at δ 149.8 and H-5 at δ 5.89 in **33**. It was indicated that the δ -lactone group of the pyrone nucleus in **25** was replaced by a δ -lactam group in **33**. However, the C-6 side chain was the same as that of **25**. This conclusion was further confirmed by HMBC

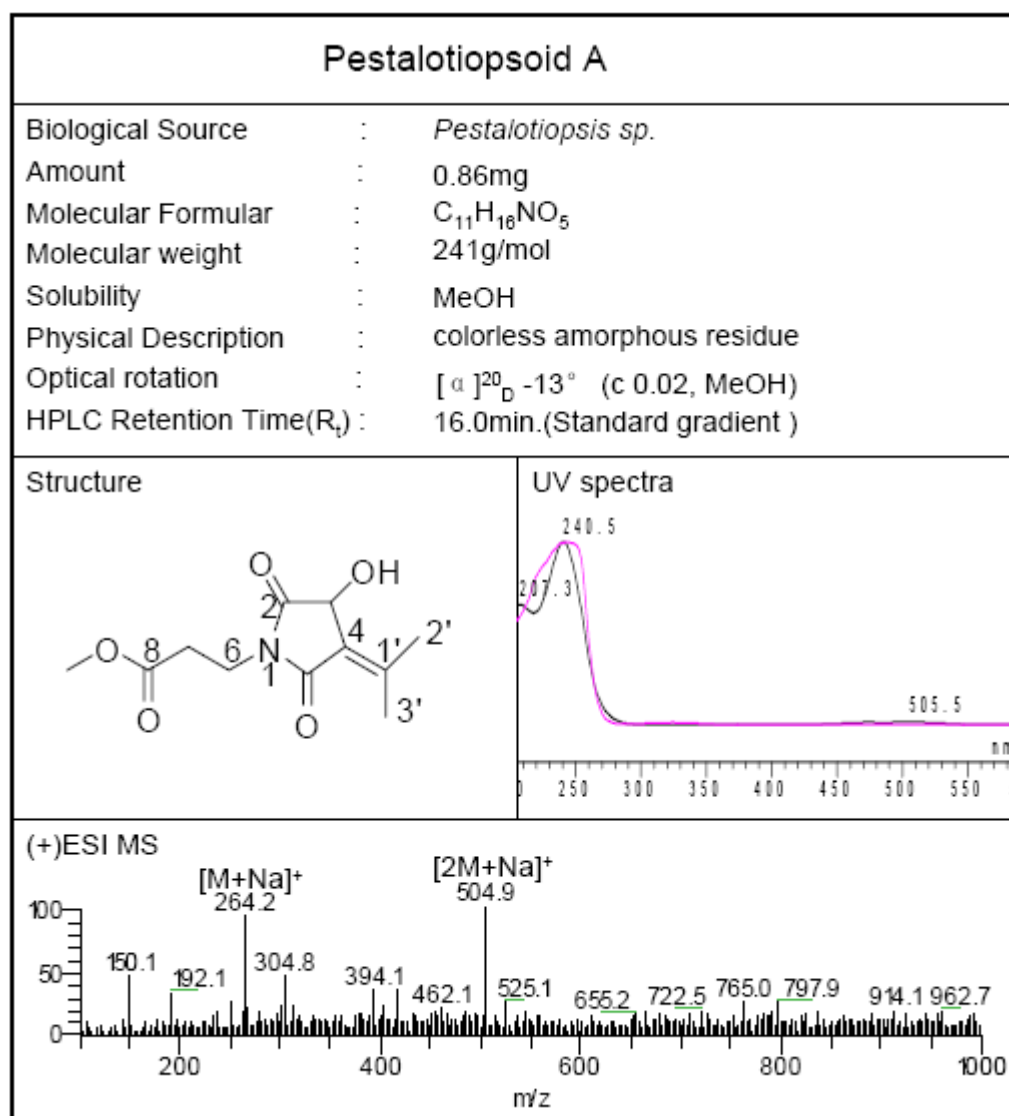
interactions from H-5 (δ_{H} 5.89, s), H-1' (δ_{H} 2.48, q) and H-2' (δ_{H} 1.20, d) to C-6 (δ_{C} 149.8).

Thus, the structure of pestalotiopyridine (**33**) was elucidated as 6-(1-hydroxyethyl)-4-methoxy-3-methylpyridin-2(1H)-one.

Table 3.6.1.1 ^1H NMR (500 MHz) and ^{13}C NMR (125 MHz) spectroscopic data for pestalotiopyridine (**33**) in CD_3OD

Atom no.	33		HMBC (H to C)	Comparison Compound 24	
	δ_{H} [ppm]	δ_{C} [ppm]		δ_{H} [ppm]	δ_{C} [ppm]
2		167.7, s			167.7, s
3		101.7, d			101.7, d
3- CH_3	1.89, s	8.45, q	2, 3, 4	1.89, s	8.45, q
4		168.9, s			168.9, s
5	6.63, s	93.9, d	4, 6	6.63, s	93.9, d
6		168.4, s			168.4, s
1'	4.57, q, 6.6	67.5, d	5, 6, 2'	4.57, q (6.6)	67.5, d
2'	1.46, d, 6.6	21.7, q	6, 1'	1.46, d (6.6)	21.7, q
4- OCH_3	3.99, s	57.3, q	4	3.99, s	57.3, q

3.6.2 Pestalotiopsoid A (34, new compound)



Pestalotiopsoid A (**34**) was obtained as a colorless oil. Its molecular formula $C_{11}H_{15}NO_5$ was established by HR-ESIMS m/z 242.1020 $[M+H]^+$ (calcd for $C_{11}H_{16}NO_5$, 242.1023), indicating five degrees of unsaturation.

The 1H and ^{13}C NMR data (Table 3.6.2.1) of **34** revealed that four of the five units of unsaturation were attributed to three carbonyls and to one double bond. Thus, the remaining unit of unsaturation comes from a ring. The 1H and ^{13}C NMR data of **34** in

association with its ^1H - ^1H COSY and HMQC spectra indicated a methoxy group (δ_{H} 3.65, s, δ_{C} 51.2, q, 8-OCH₃), two methyl groups [δ_{H} 2.1, s, δ_{C} 23.4, q, 3'-CH₃; δ_{H} 2.39, (d, J = 1.25 Hz), δ_{C} 21.0, q, 2'-CH₃] which showed homoallylic coupling to an oxymethine (δ_{H} 4.85, s, δ_{C} 67.5, d, H-3), and a 1,2-disubstituted ethyl group [δ_{H} 2.65 (t, J = 7.25 Hz), δ_{C} 31.7, 7-CH₂; δ_{H} 3.85 (t, J = 7.25 Hz), δ_{C} 33.9, 6-CH₂]. HMBC correlations (Figure 3.6.2.1) from H-3 to both amidocarbonyl carbons at δ_{C} 174.6 (s, C-2) and δ_{C} 167.4 (s, C-5), together with C-4 (δ_{C} 121.1) and C-1' (δ_{C} 157.3), combined with that from 2'-CH₃ and 3'-CH₃ to C-5, C-4 and C-1', established the 3-hydroxy-2,5-pyrrolidinedione nucleus and the connection of two methyl groups to C-1'. Moreover, a methyl propanoate group was assigned through HMBC correlations from the methoxy protons and the protons of 1,2-disubstituted ethyl group to C-8 (δ_{C} 170.7). This moiety was linked to the nitrogen atom of the 2,5-pyrrolidinedione unit based on the observed HMBC correlations from 6-H₂ to both amidocarbonyl carbons C-2 and C-5.

Thus, pestalotiopsoid A was methyl-3-(3-hydroxy-2,5-dioxo-4-(propan-2-ylidene)pyrrolidin-1-yl)propanoate. Due to the low amounts of the compound isolated, it was not possible to assign the configuration of the chiral center at C-3.

Table 3.6.2.1 ^1H , ^{13}C NMR (500 MHz) data (J in Hz) for pestalotiopsoid A in CDCl₃

position	δ_{H}	δ_{C}
2		167.4, s
3	4.85, s	67.5, d
4		121.1, s
5		174.6, s
6	3.85, t, 7.25	33.9, t
7	2.65, t, 7.25	31.5, t
8		179.7, s
8-OCH ₃	3.65, s	51.2, q
1'		157.3, s
2'	2.1, s	23.4, q
3'	2.39, d, 1.25	21.0, q

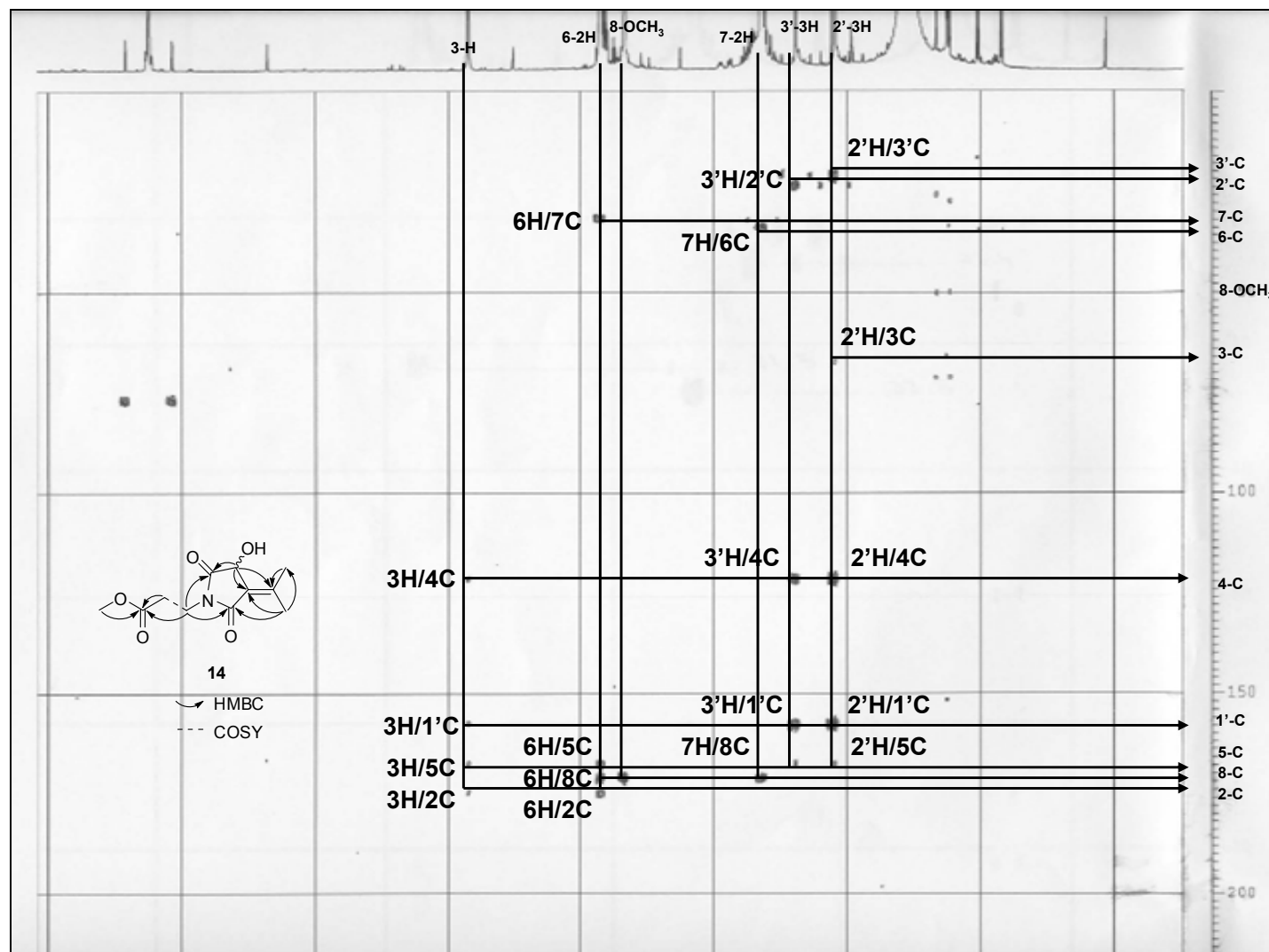
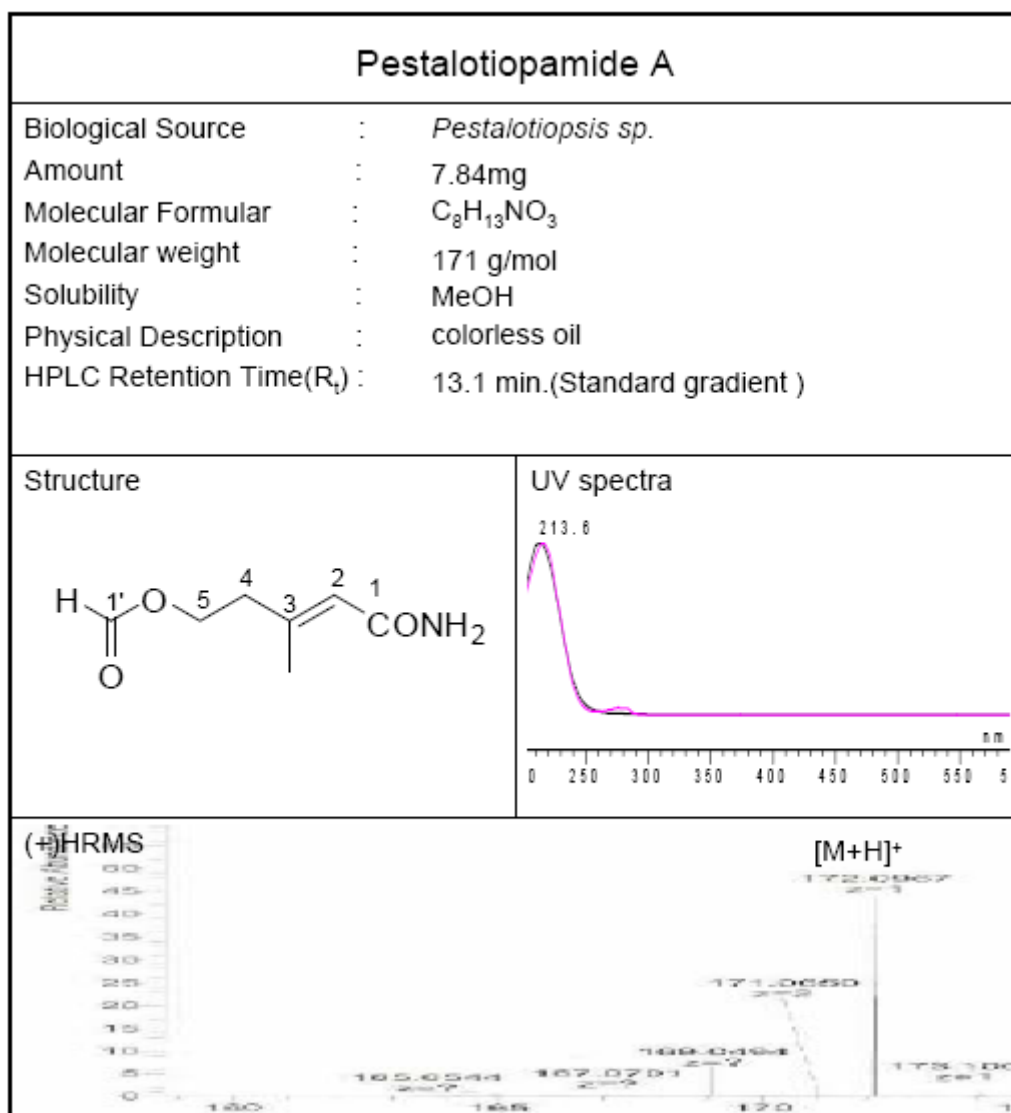


Figure 3.6.2.1 Selected HMBC correlations for compound **34**

3.6.3 Pestalotiopamide A (**35**, new compound)

The NMR spectroscopic data of pestalotiopamide A (**35**) (Tables 3.6.3.1) were very similar to those of **43**. The HR-ESIMS of **35** (m/z 172.0967, calcd for $[M+H]^+$ 172.0974; m/z 194.0786, calcd for $[M+Na]^+$ 194.0793) gave its molecular formula $C_8H_{13}NO_3$, suggesting the replacement of the terminal carboxyl group in **43** by an amide group. Similar NOE interactions observed in **35** as those in **43** allowed the assignment of the *E* geometry for the double bond in **35**.

Hence pestalotiopamide A (**35**) was concluded to be (*E*)-5-amino-3-methyl-5-oxopent-3-enyl acetate.

Table 3.6.3.1 ^1H NMR (500 MHz) and ^{13}C NMR (125 MHz) spectroscopic data for pestalotiopamide A (**35**) in CD_3OD

Atom no.	δ_{H} [ppm]	35 δ_{C} [ppm]	HMBC (H to C)	Comparision Compound 43 δ_{H} [ppm]	δ_{C} [ppm]
1		171.8, s			172.7, s
2	5.75, brs	120.6, d	1, 3, 4	5.75, brs	120.6, d
3		151.8, s			151.8, s
4	2.43, t, 6.3	40.4, t	2, 4, 3-CH ₃	2.43, t, 6.3	40.4, t
5	4.22, t, 6.3	63.1, t	3, 4, 1'	4.22, t, 6.3	63.1, t
1'		172.8, s	2'		171.7, s
2'	2.01, s	20.7, q	1'	2.01, s	20.7, q
3-CH ₃	2.12, s	18.3, q	2, 3, 4	2.12, s	18.3, q

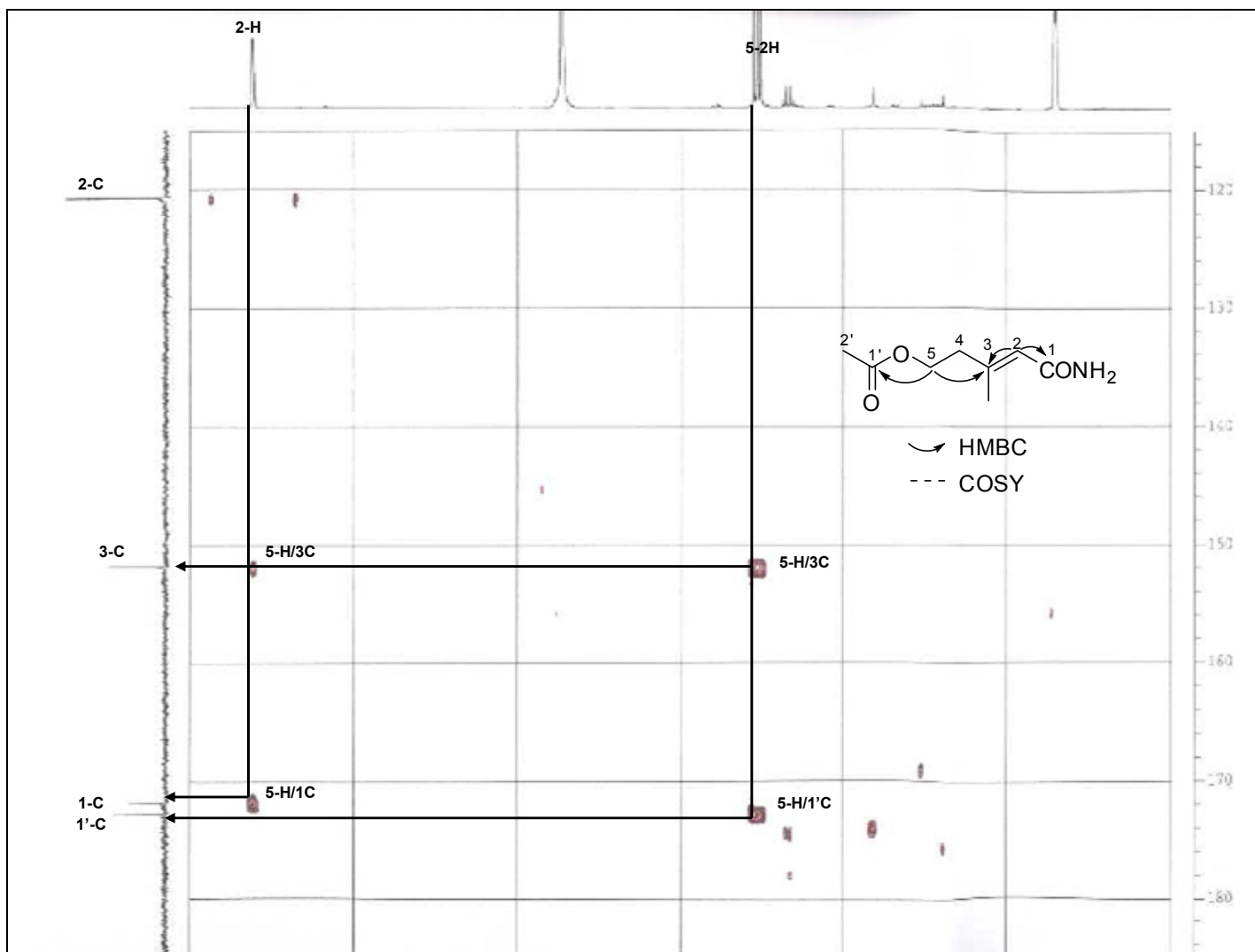


Figure 3.6.3.1a Selected HMBC correlations for compound **35**

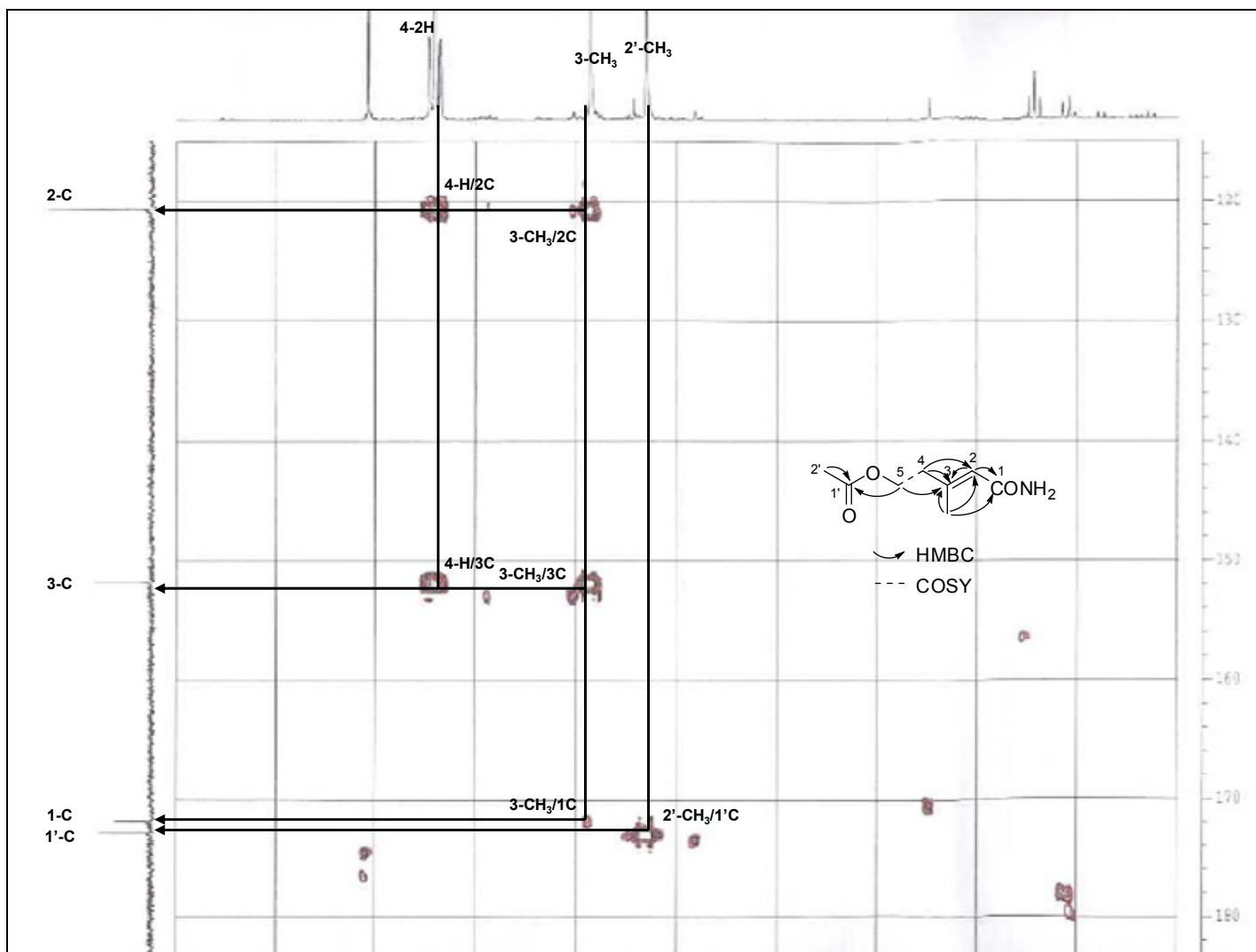


Figure 3.6.3.1b Selected HMBC correlations for compound **35**

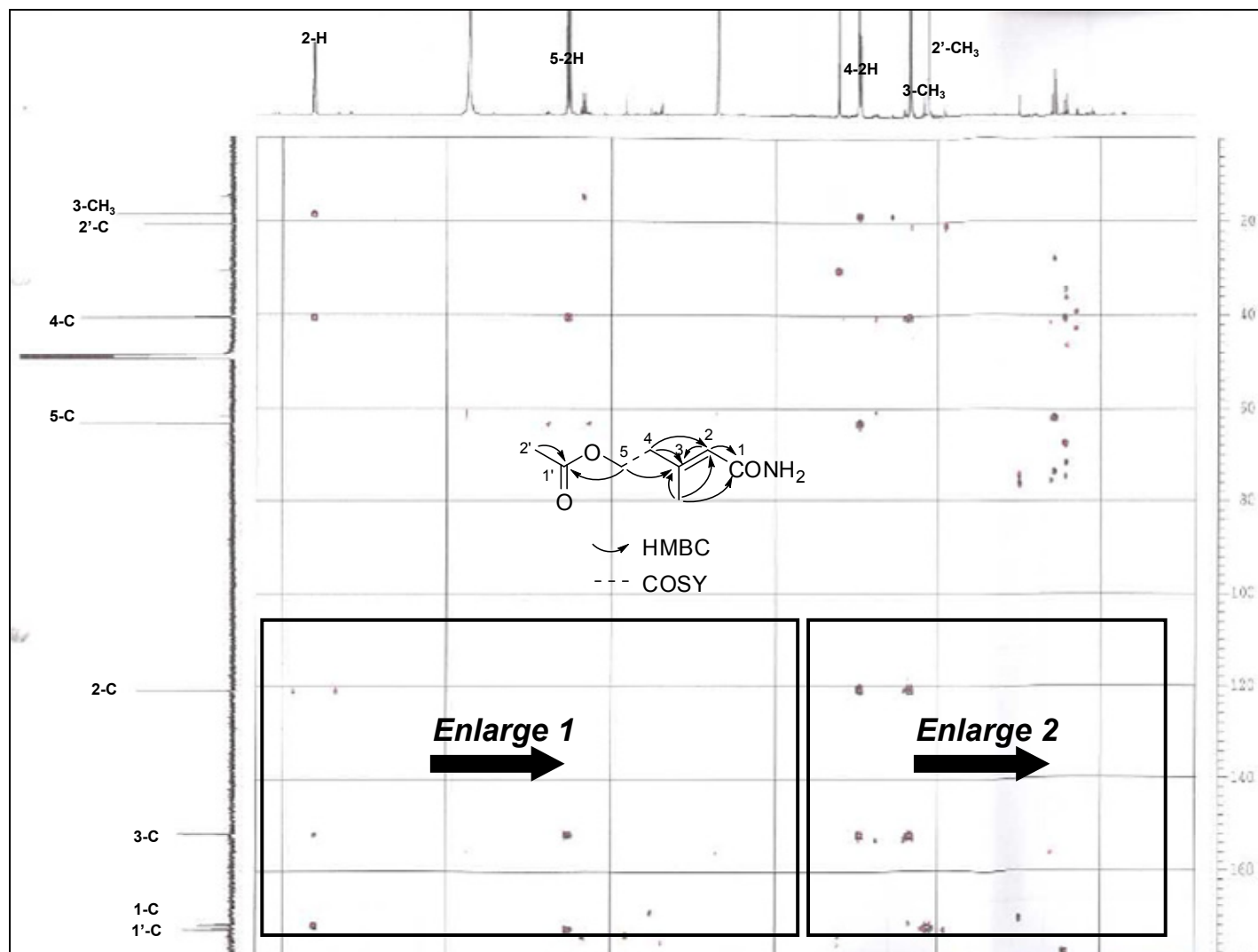
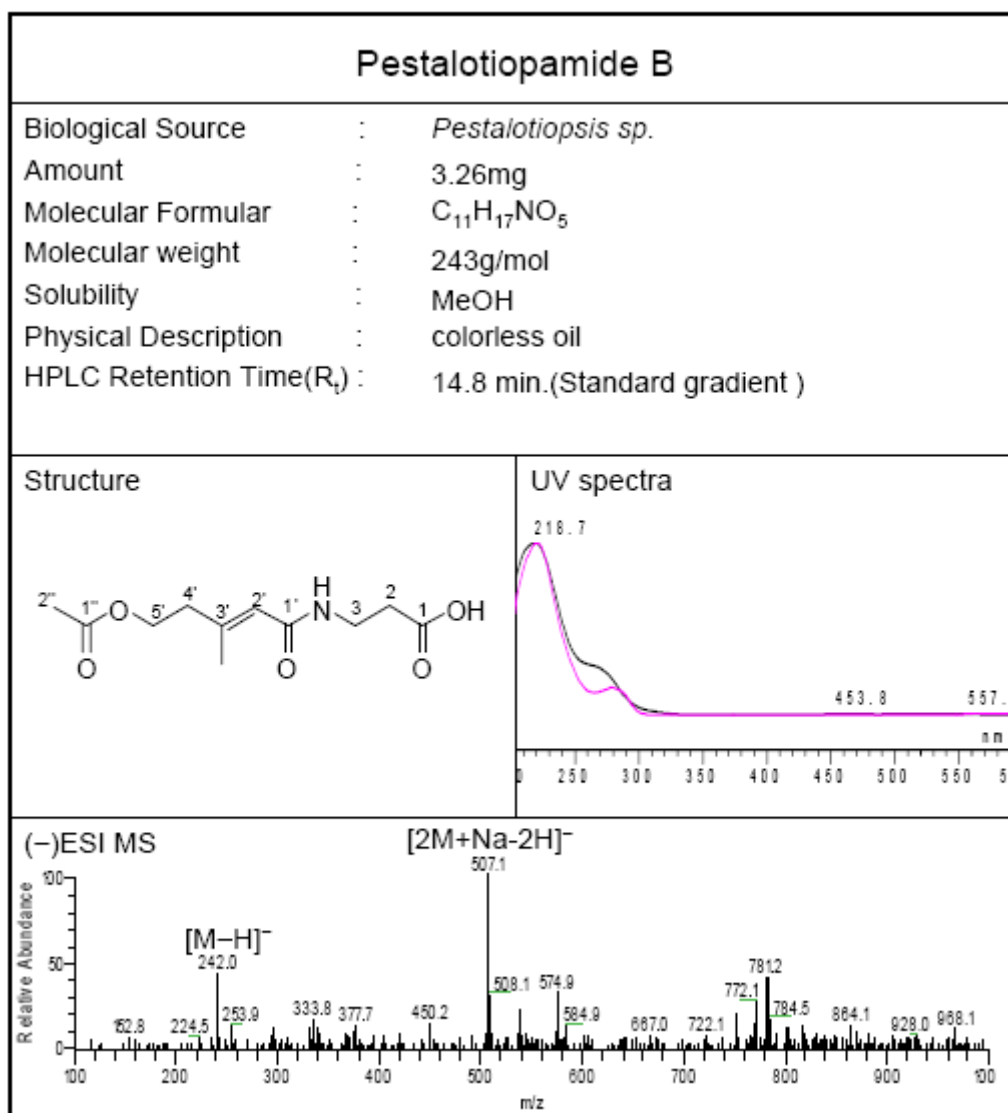


Figure 3.6.3.1c Selected HMBC correlations for compound 35

3.6.4 Pestalotiopamide B (36, new compound)



Pestalotiopamide B (**36**) was obtained as a colorless oil. Its molecular formula of $C_{11}H_{17}NO_5$ was established by HR-ESIMS (m/z 243.2572, calcd for $[M+H]^+$ 243.2575). The 1H and ^{13}C NMR data of **36** (Tables 3.6.4.1) indicated that four unsaturation degrees of the molecule are due to a double bond and three carbonyl groups. Comparison of the NMR data of **36** with those of the literature (Jursic *et al.* 2001) revealed that the amine part of the molecule consisted of 3-aminopropanoic acid. HMBC correlations between H-3''/C-1, H-5/C-1' (Figure 3.6.4.1) connected three parts of **36** together. The *E*-geometry of the double bond (Figure 3.6.4.2) in **36** was characterized by NOE interactions as those in **35**.

Based on the above results, the structure of pestalotiopamide B (**36**) was identified as (*E*)-3-(5-acetoxy-3-methylpent-2-enamido)propanoic acid.

Table 3.6.4.1 ^1H NMR (500 MHz) and ^{13}C NMR (125 MHz) spectroscopic data for pestalotiopamide B (**36**) in CD_3OD

Atom no.	36 δ_{H} [ppm]	δ_{C} [ppm]	HMBC (H to C)	Comparison Compound 35 δ_{H} [ppm]	δ_{C} [ppm]
1		169.3, s			171.8, s
2	5.69, d, 1.25	121.1, d	1, 3, 4	5.75, brs	120.6, d
3		150.8, s			151.8, s
4	2.41, t, 6.6	40.4, t	2, 4, 3-CH ₃	2.43, t, 6.3	40.4, t
5	4.20, t, 6.6	63.2, t	3, 4, 1'	4.22, t, 6.3	63.1, t
1'		172.8, s	2'		172.8, s
2'	2.0, s	20.7, q	1'	2.01, s	20.7, q
1''		176.2, s			
2''	2.50, t, 6.8	35.1, t	1'', 3''		
3''	3.43, t, 6.8	36.3, t	1, 1'', 2''		
3-CH ₃	2.11, d, 1.25	18.4, q	2, 3, 4	2.12, s	18.3, q

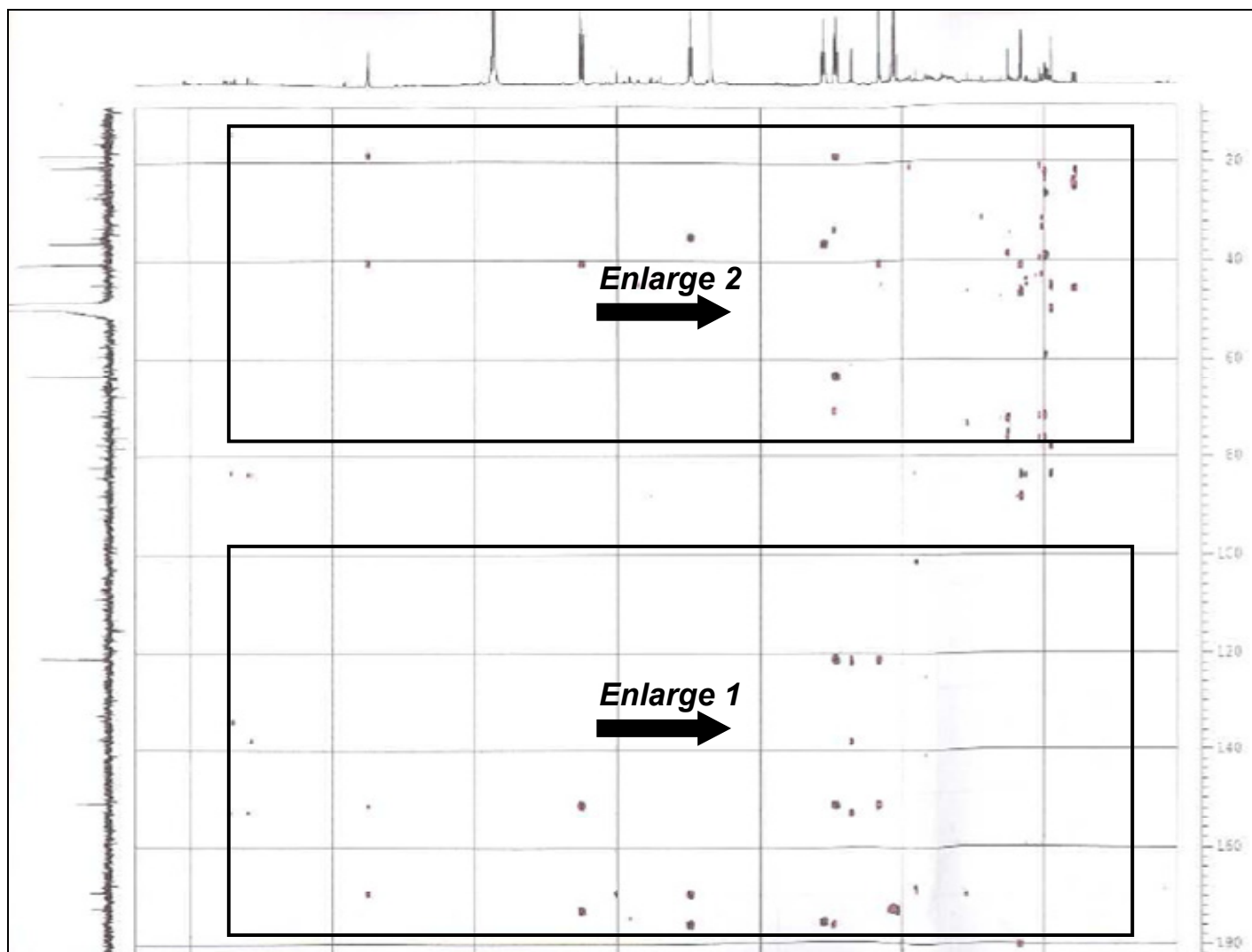


Figure 3.6.4.1a Selected HMBC correlations of compound 36

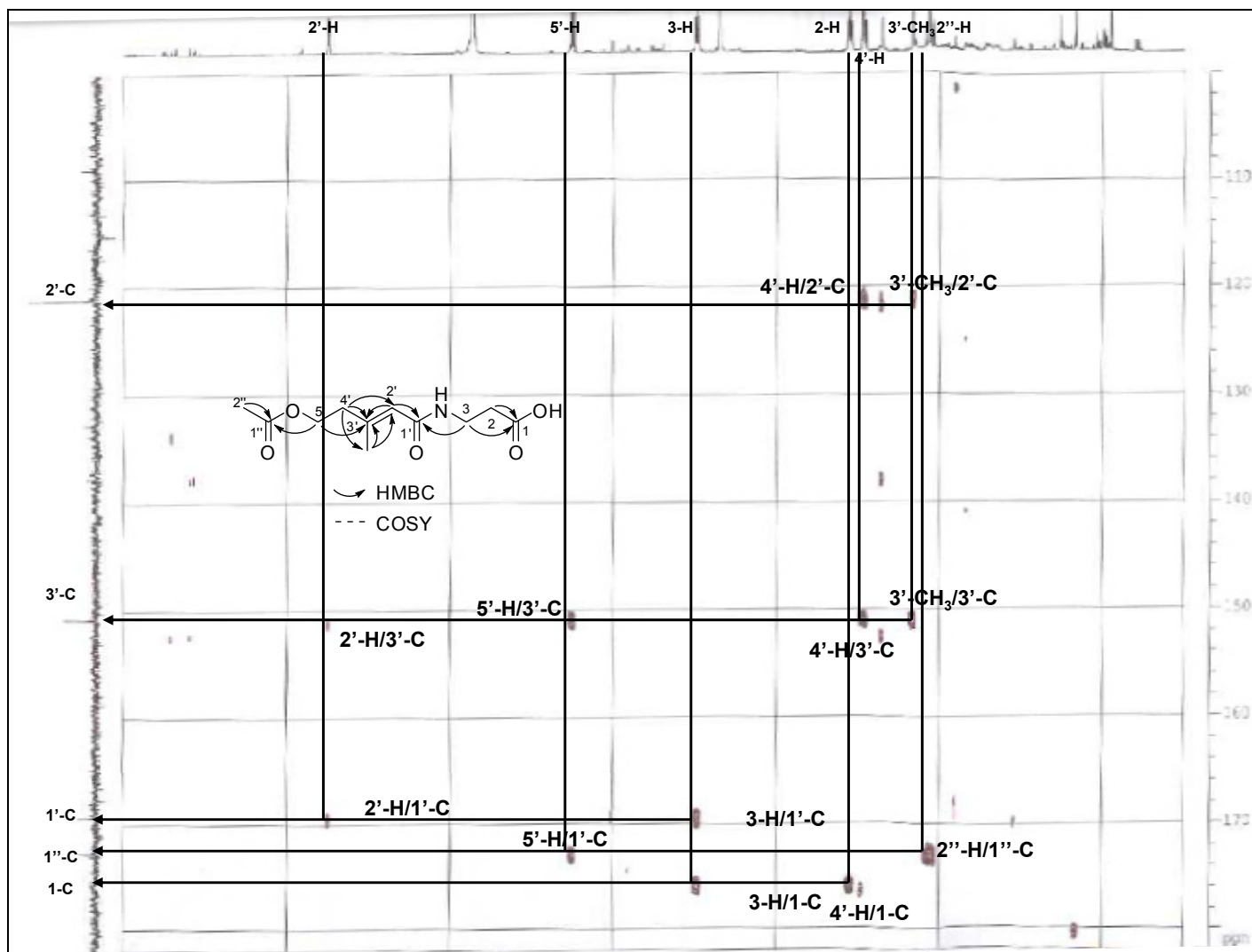


Figure 3.6.4.1b Selected HMBC correlations of compound 36

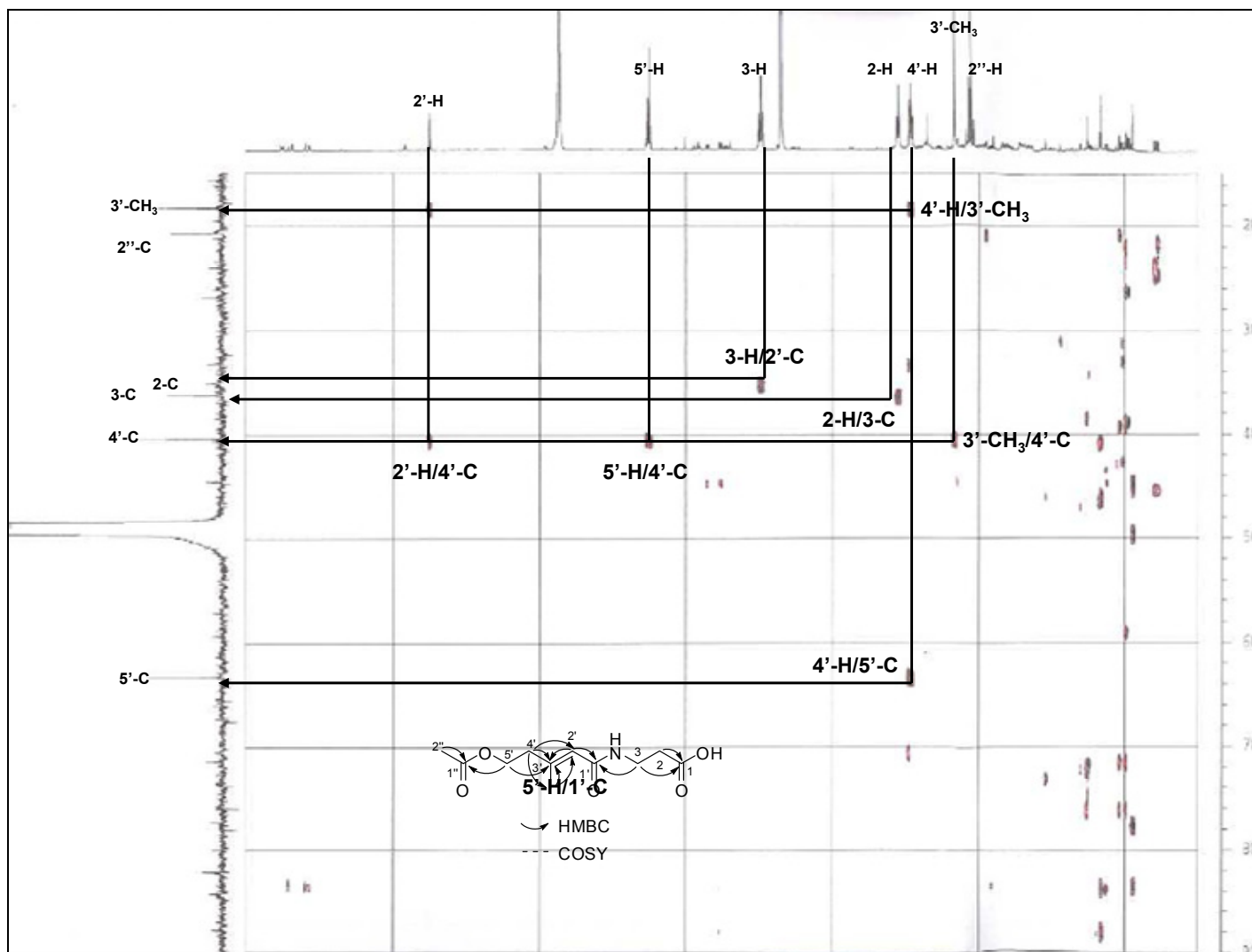


Figure 3.6.4.1c Selected HMBC correlations of compound 36

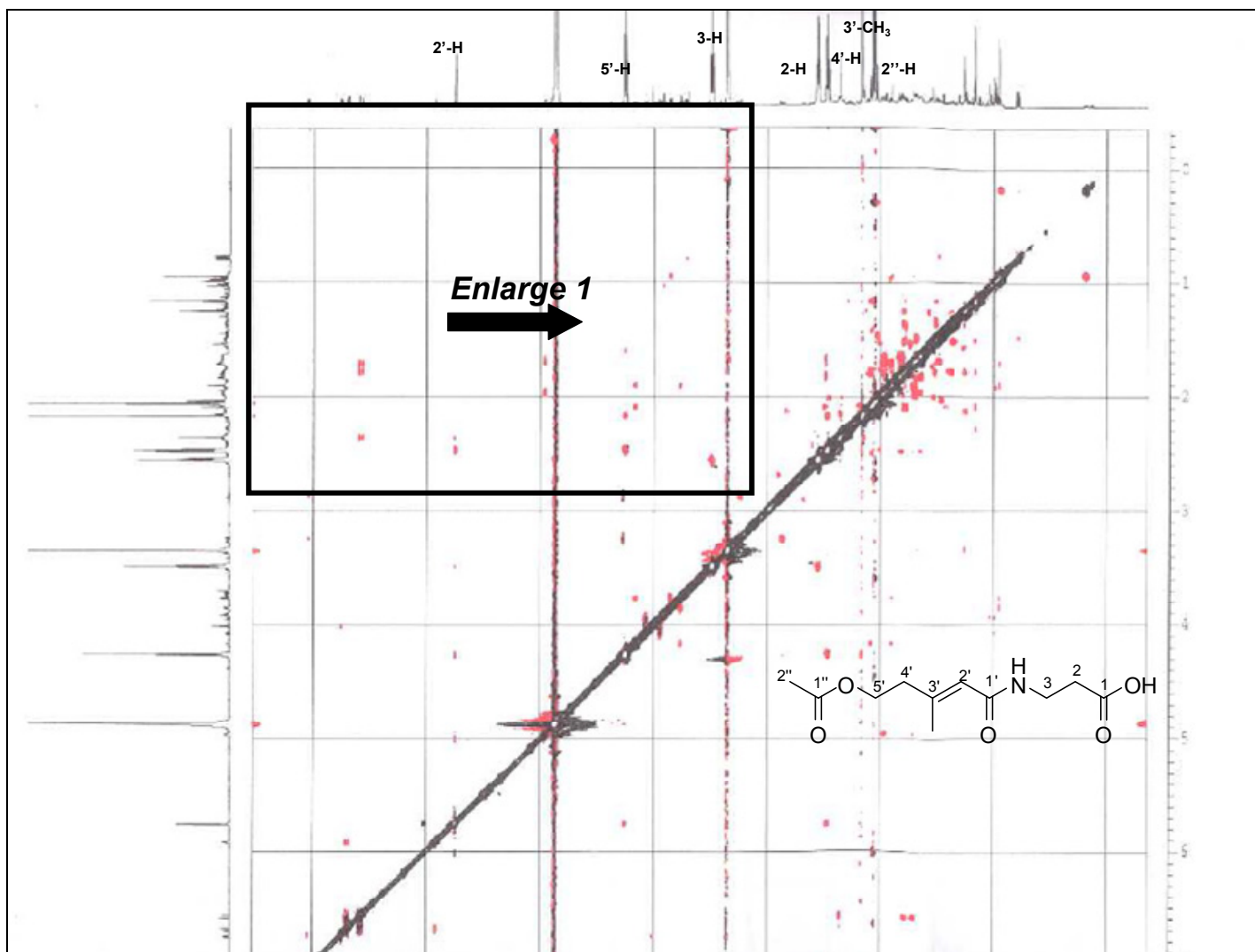


Figure 3.6.4.2a Selected NOESY correlations of compound **36**

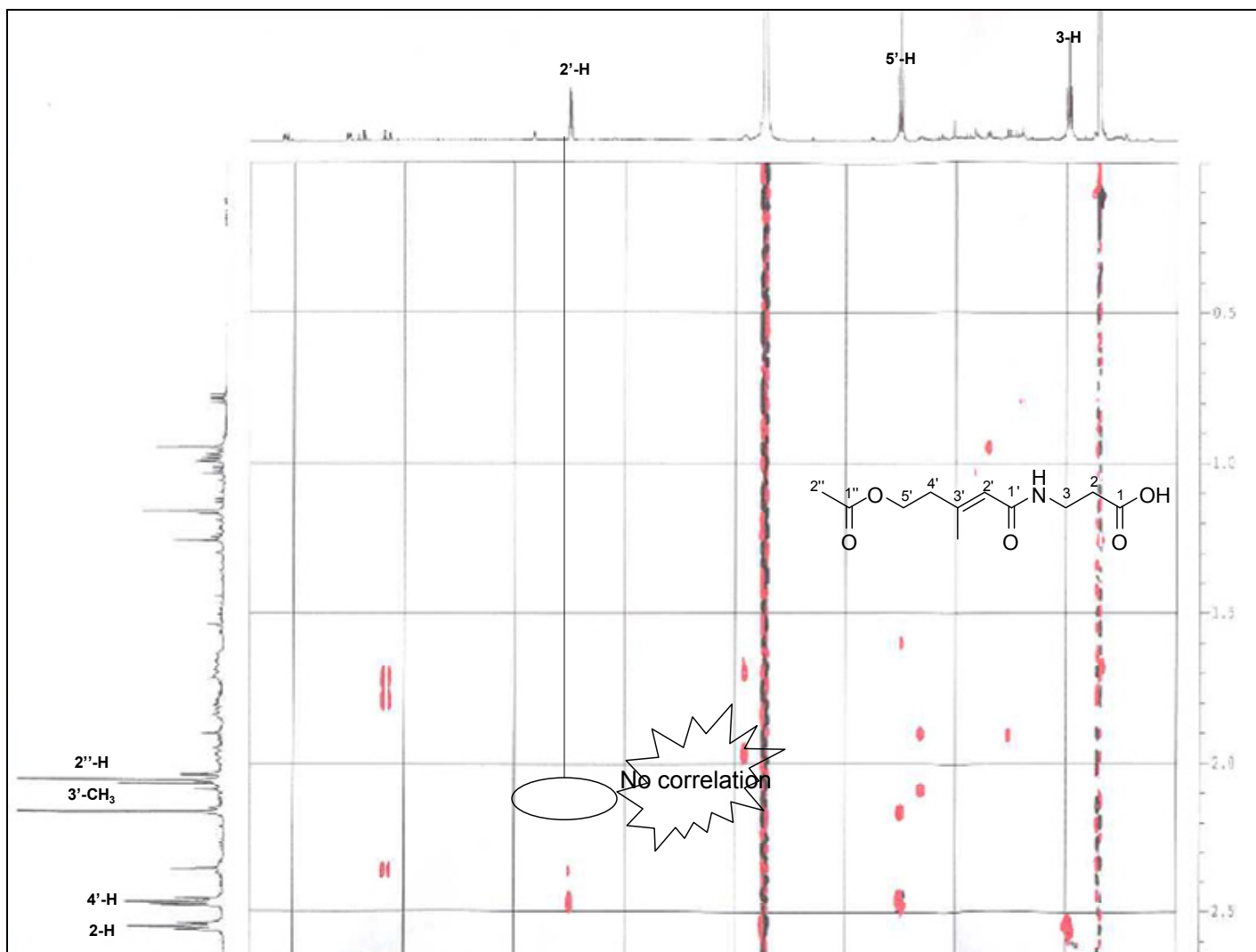
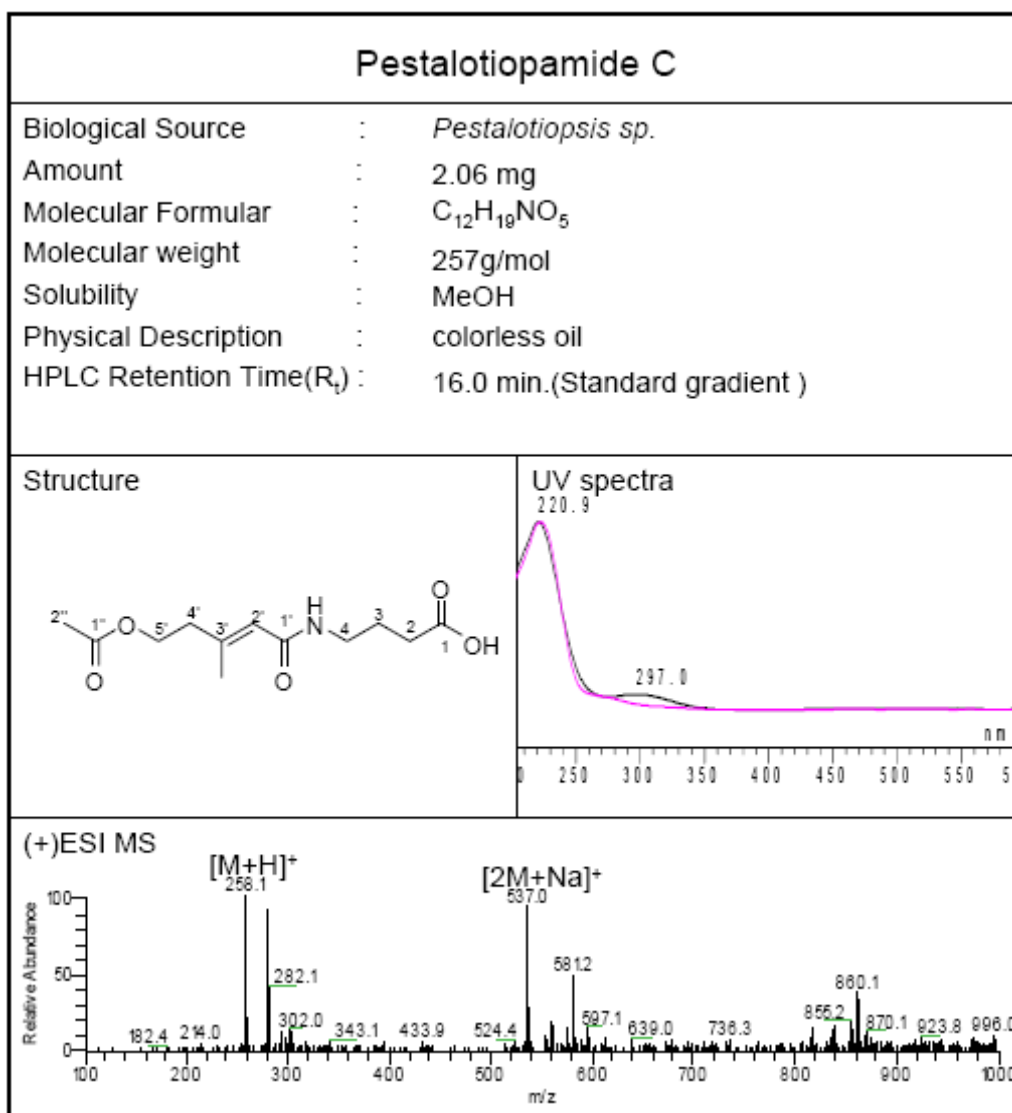


Figure 3.6.4.2b Selected NOESY correlations of compound 36

3.6.5 Pestalotiopamide C (**37**, new compound)

Pestalotiopamide C (**37**) was found to have the molecular formula of $C_{12}H_{19}NO_5$, established by HR-ESIMS (m/z 258.1335, calcd for $[M+H]^+$ 258.1342), which was larger than that of **36** by an additional CH_2 group.

The 1H and ^{13}C NMR data of **37** (Tables 3.6.5.1) were similar to those of **36**, except for the replacement of the propanoic acid group in **36** by a butyric acid group in **37** [δ_C 176.5, s, C'' -1; δ_H 2.32 (t, J = 7.25 Hz), δ_C 32.6, $2''$ - CH_2 ; δ_H 1.89, m, δ_C 26.2, $3''$ - CH_2 ; δ_H 3.23 (t, J = 6.9 Hz), δ_C 39.5, $4''$ - CH_2]. This assignment was further

confirmed by ^1H - ^1H COSY, HMQC and HMBC analysis. The *E*-geometry of the double bond in **37** was evidenced by NOE interactions as those in **35**.

Hence the structure of pestalotiopamide C (**37**) was characterized as (*E*)-4-(5-acetoxy-3-methylpent-2-enamido)butanoic acid.

Table 3.6.5.1 ^1H NMR (500 MHz) and ^{13}C NMR (125 MHz) spectroscopic data for pestalotiopamide C (**37**) in CD_3OD

Atom no.	δ_{H} [ppm]	37 δ_{C} [ppm]	HMBC (H to C)	Comparision Compound 36 δ_{H} [ppm]	δ_{C} [ppm]
1		170.2, s			169.3, s
2	5.70, d, 0.95	121.1, d	1, 3, 4	5.69, d, 1.25	121.1, d
3		150.5, s			150.8, s
4	2.42, t, 6.66	40.4, t	2, 4, 3- CH_3	2.41, t, 6.6	40.4, t
5	4.21, t, 6.66	63.2, t	3, 4, 1'	4.20, t, 6.6	63.2, t
1'		172.8, s	2'		172.8, s
2'	2.01, s	20.7, q	1'	2.0, s	20.7, q
1''		176.5, s			176.2, s
2''	2.32, t, 7.25	32.6, t	1'', 3''	2.50, t, 6.8	35.1, t
3''	1.89, m	26.2, t	1'', 2'', 4''	3.43, t, 6.8	36.3, t
4''	3.23, t, 6.9	39.5, t	1, 2'', 3''		
3- CH_3	2.12, d, 0.95	18.4, q	2, 3, 4	2.11, d, 1.25	18.4, q

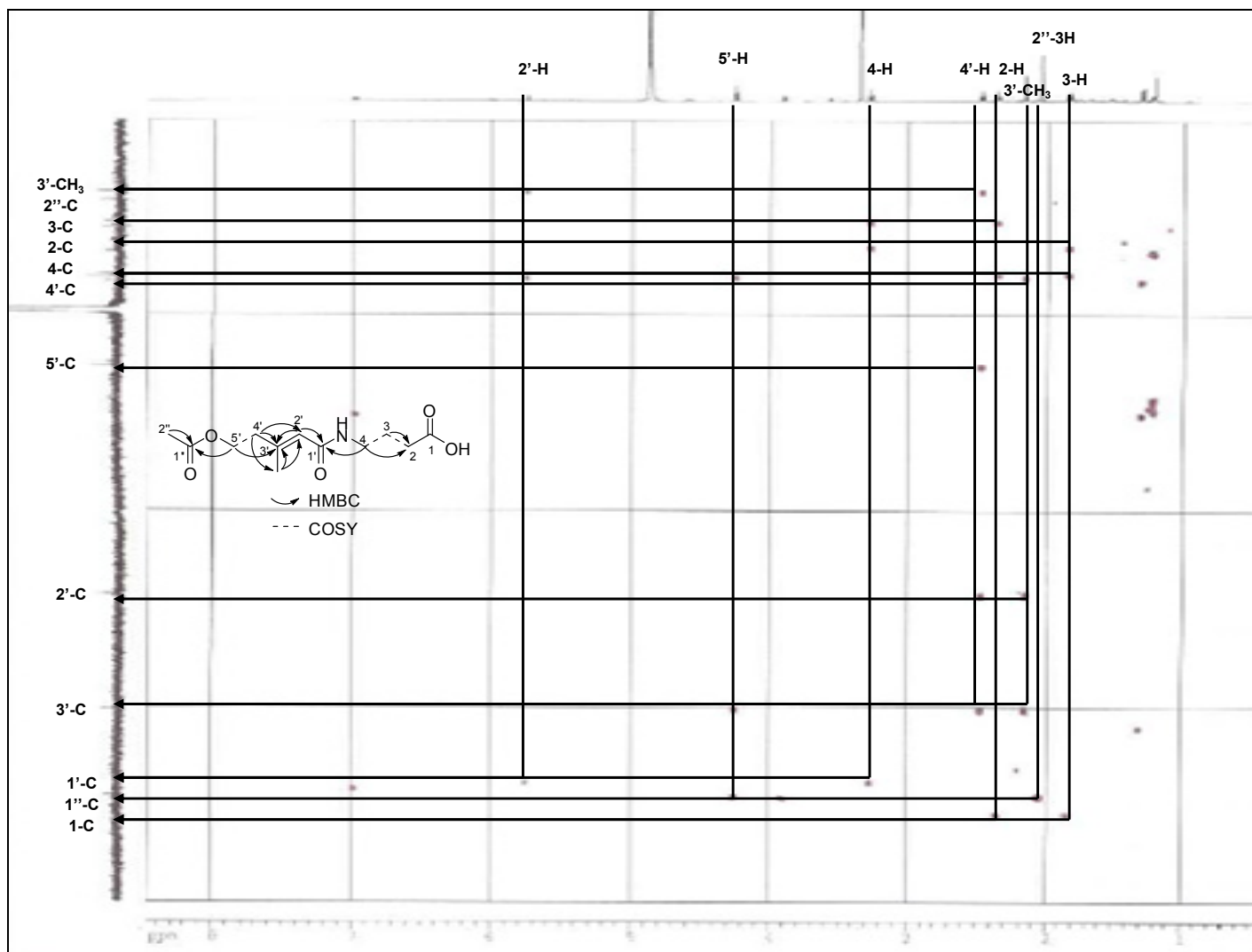
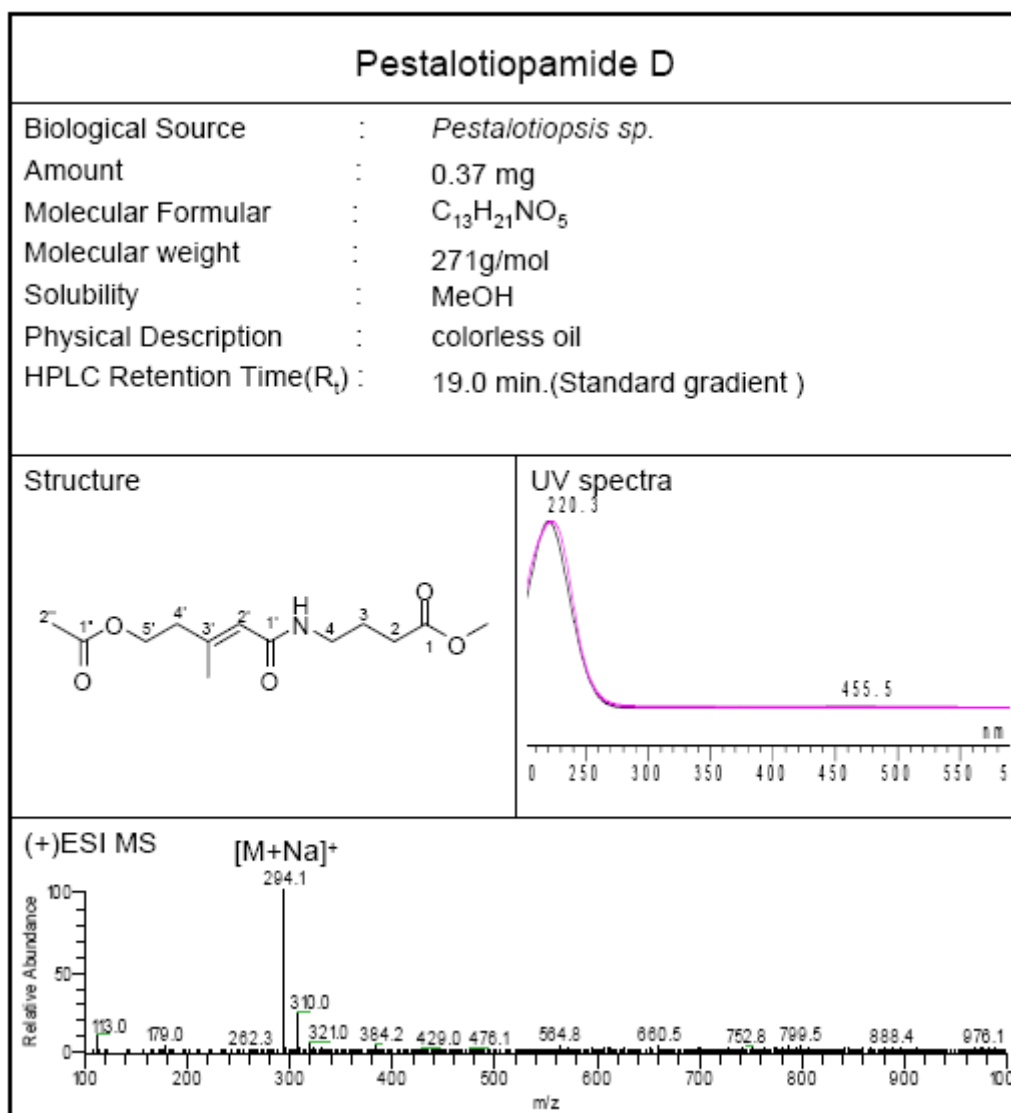


Figure 3.6.5.1 Selected HMBC correlations of compound 37

3.6.6 Pestalotiopamide D (**38**, new compound)

The molecular formula of pestalotiopamide D (**38**) was established as $C_{13}H_{21}NO_5$ by HR-ESIMS (m/z 272.1484). The 1H and ^{13}C NMR data of **38** (Table 3.6.6.1) were similar to those of **37**, except for the replacement of the terminal carboxyl group in **37** by a methoxycarbonyl group (δ_H 3.64, s; δ_C 52.0, q, 1''-OCH₃, 176.0, s, C-1''). HMBC correlations (Figure 3.6.6.1) from protons of 1''-OCH₃ to C-1'' (δ_C 176.0) further confirmed its location at C-1''. The stereochemistry of **38** (Figure 3.6.6.2) was the same as **37** as indicated by the similar NOESY data observed.

Thus the structure of pestalotiopamide D (**38**) was elucidated as (*E*)-methyl 4-(5-acetoxy-3-methylpent-2-enamido)butanoate.

Table 3.6.6.1 ^1H NMR (500 MHz) and ^{13}C NMR (125 MHz) spectroscopic data for pestalotiopamide D (**38**) in CD_3OD

Atom no.	δ_{H} [ppm]	38 δ_{C} [ppm]	HMBC (H to C)	Comparision Compound 37 δ_{H} [ppm]	δ_{C} [ppm]
1		170.0, s			170.2, s
2	5.69, br s	121.1, d	1, 3, 4	5.70, d, 0.95	121.1, d
3		151.0, s			150.5, s
4	2.42, t, 6.6	42.0, t	2, 4, 3- CH_3	2.42, t, 6.66	40.4, t
5	4.20, t, 6.6	63.8, t	3, 4, 1'	4.21, t, 6.66	63.2, t
1'		173.0, s	2'		172.8, s
2'	2.01, s	21.0, q	1'	2.01, s	20.7, q
1''		176.0, s			176.5, s
2''	2.50, t, 6.8	35.1, t	1'', 3''	2.32, t, 7.25	32.6, t
3''	1.79, m	28.5, t	1'', 2'', 4''	1.89, m	26.2, t
4''	3.43, t, 6.9	36.3, t	1, 2'', 3''	3.23, t, 6.9	39.5, t
1''- OCH_3	3.64, s	52.0, q	1''		
3- CH_3	2.12, br s	18.4, q	2, 3, 4	2.12, d, 0.95	18.4, q

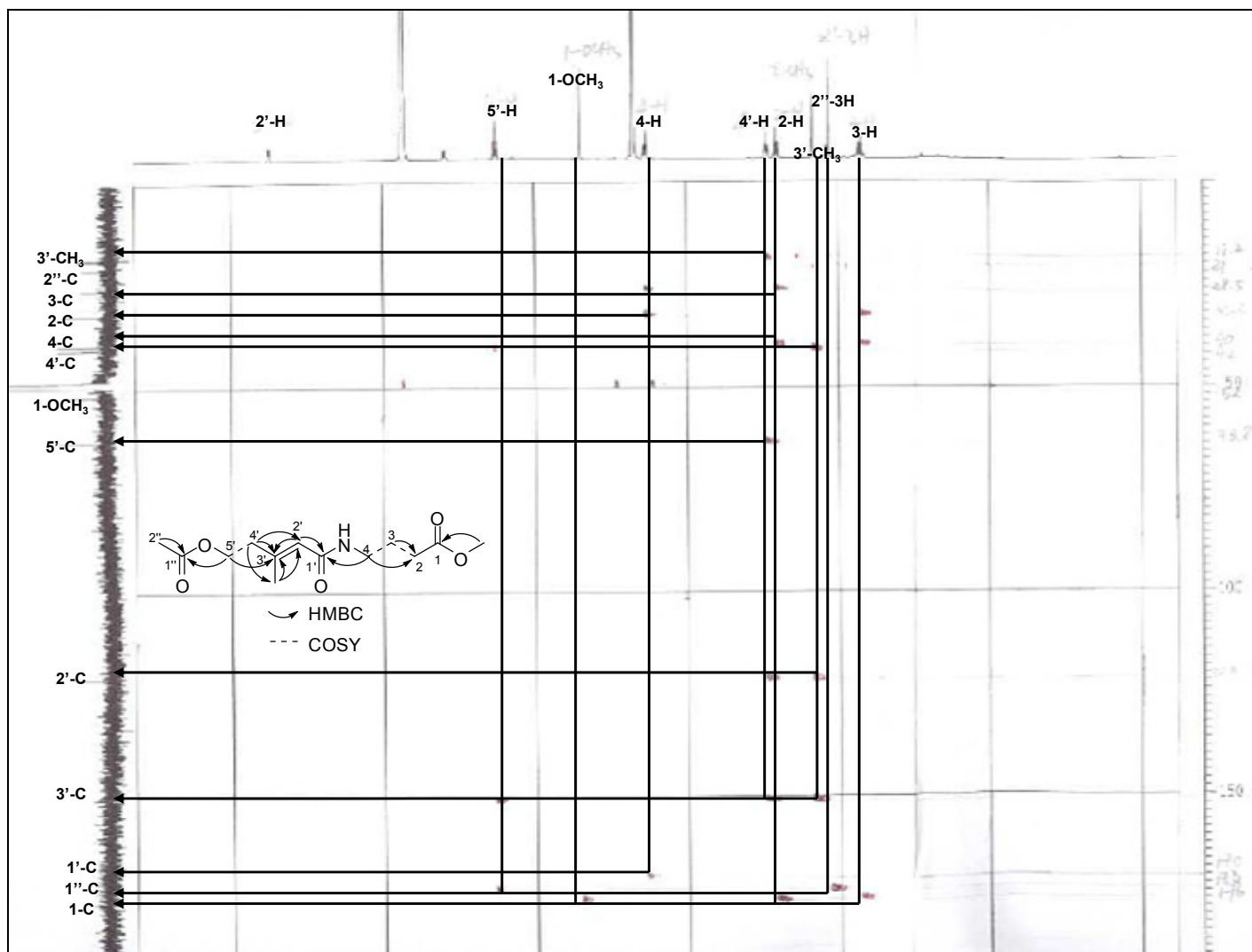


Figure 3.6.6.1 Selected HMBC correlations for compound 38

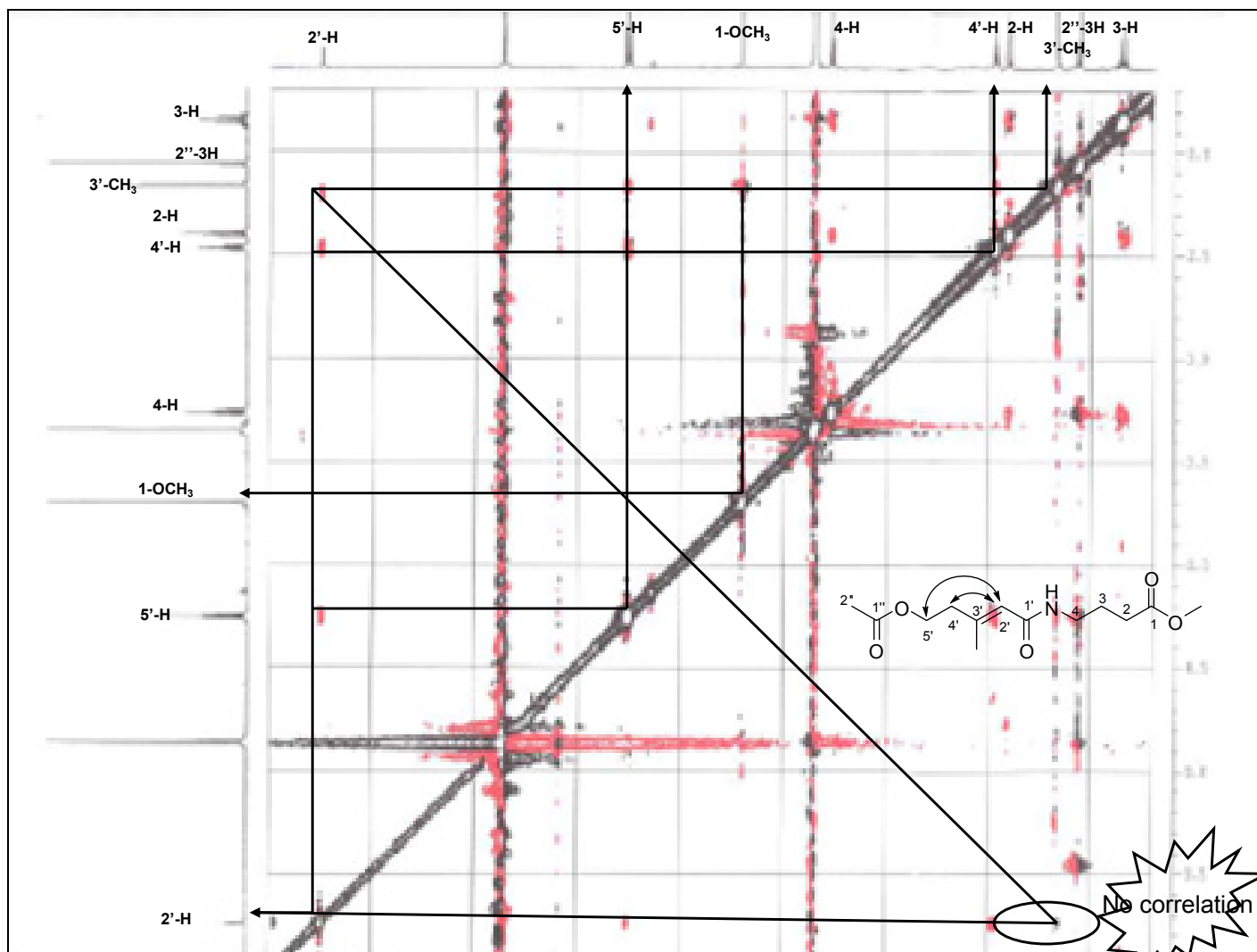
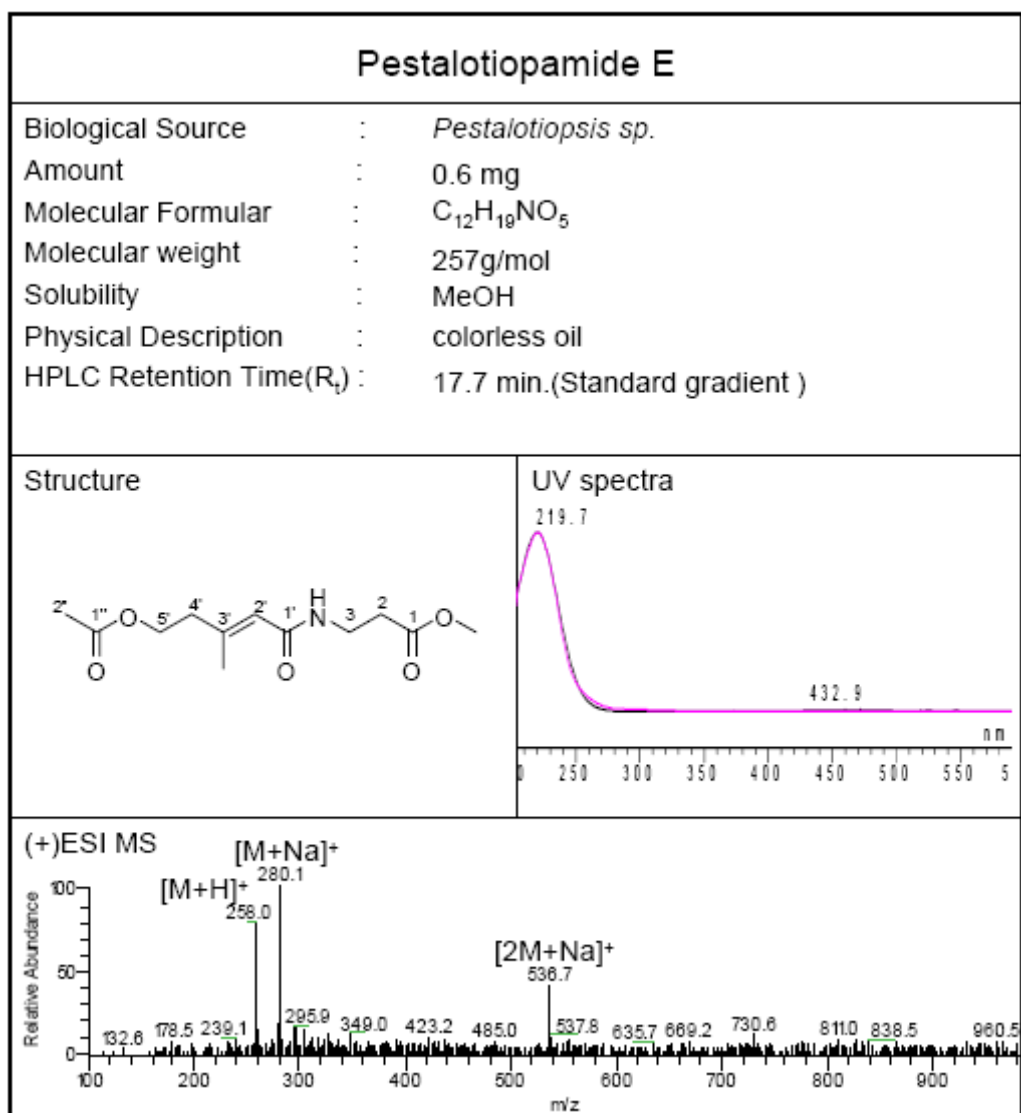


Figure 3.6.6.2 Selected NOESY correlations for compound **38**

3.6.7 Pestalotiopamide E (**39**, new compound)

The molecular formula of pestalotiopamide E (**39**), established by HR-ESIMS (m/z 258.1339), was the same as that of **37**. It was suggested that **39** should be an isomer of **37**. The 1H and ^{13}C NMR data of **39** (Table 3.6.7.1) were similar to those of **36**, except for the replacement of the hydroxy group in the terminal carboxyl group in **36** by a methoxy group (δ_H 3.67, s). Comparison with the chemical shifts of the methoxy substituent in **38**, unequivocally assigned by HMBC and NOESY spectra, allowed the

assignment of the methoxy group (δ_{H} 3.67, s) of **39** to C-1. The geometry of the double bond was identical to **37** based on the similar of NOE interaction.

Therefore, the structure of pestalotiopamide E (**39**) was characterized as (*E*)-methyl 3-(5-acetoxy-3-methylpent-2-enamido)propanoate.

Table 3.6.7.1 ^1H NMR (500 MHz) and ^{13}C NMR (125 MHz) spectroscopic data for pestalotiopamide E (**39**) in CD_3OD

Atom no.	39 δ_{H} [ppm]	Comparison Compound 38 δ_{H} [ppm]	δ_{C} [ppm]
1			170.0, s
2	5.69, d, 1.25	5.69, br s	121.1, d
3			151.0, s
4	2.41, t, 6.6	2.42, t, 6.6	42.0, t
5	4.20, t, 6.6	4.20, t, 6.6	63.8, t
1'			173.0, s
2'	2.0, s	2.01, s	21.0, q
1''			176.0, s
2''	2.53, t, 6.6	2.50, t, 6.8	35.1, t
3''	3.43, t, 6.6	1.79, m	28.5, t
4''		3.43, t, 6.9	36.3, t
1''-OCH ₃	3.67, s	3.64, s	52.0, q
3-CH ₃	2.11, d, 1.25	2.12, br s	18.4, q

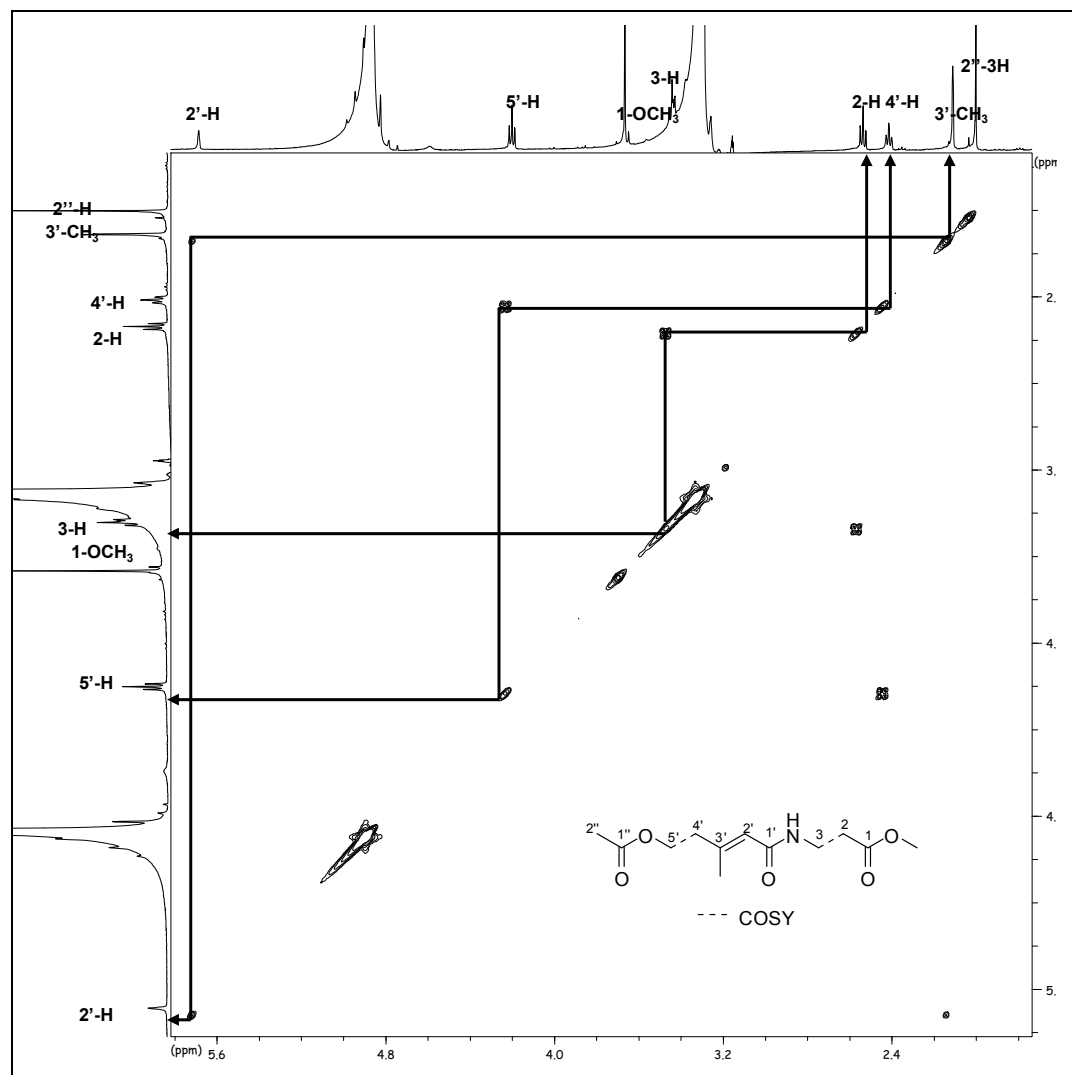
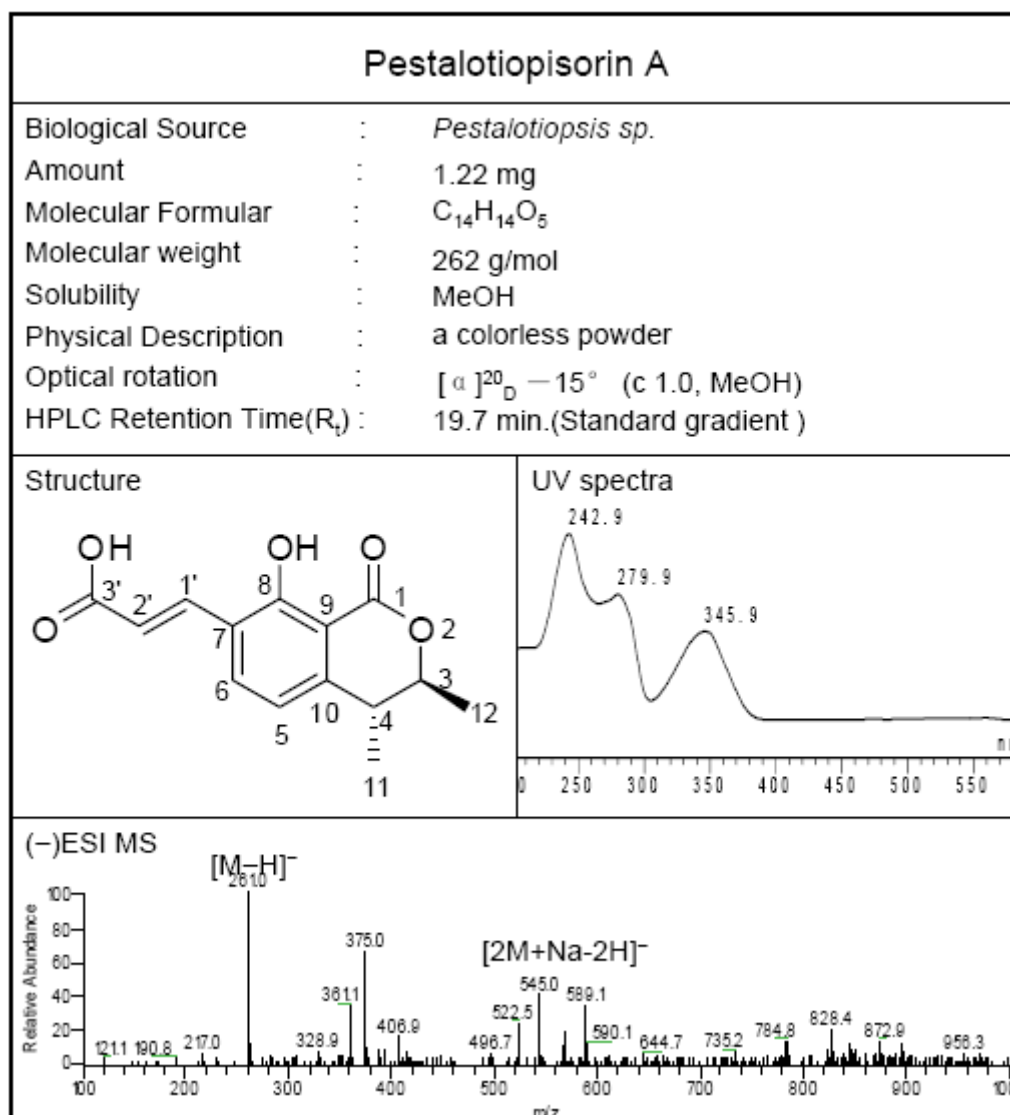


Figure 3.6.7.1 ^1H - ^1H COSY correlations for compound **39**

3.7 Miscellaneous metabolites

3.7.1 Pestalotiopisorin A (40, new compound)



Pestalotiopisorin A (**40**), a colorless amorphous solid, had the molecular formula of C₁₄H₁₄O₅, established by HR-ESIMS data (m/z 263.0910, calcd for [M+H]⁺ 263.0919). Consequently, **40** had eight degrees of unsaturation. The ¹H and ¹³C NMR data (Table 3.7.1.1) of **40** disclosed that seven of eight unsaturation degrees come from a benzene ring, a double bond, and two carbonyl groups. Thus, the last unsaturation degree was attributed to an additional ring. The ¹H and ¹³C NMR data of **40** and the information from its ¹H-¹H COSY and HSQC spectra revealed the

presence of two methyl groups [δ_{H} 1.36 (d, $J = 6.95$ Hz), δ_{C} 19.8, q, 11-CH₃; δ_{H} 1.44 (d, $J = 6.95$ Hz), δ_{C} 17.8, q, 12-CH₃], being connected with two methine groups [δ_{H} 3.97, m, δ_{C} 38.5, d, CH-4; δ_{H} 4.59, m, δ_{C} 82.8, d, CH-3], respectively. Two *ortho*-coupled aromatic protons of two methines [δ_{H} 6.95 (d, $J = 8.9$ Hz), δ_{C} 119.0, d, CH-5; δ_{H} 7.84 (d, $J = 8.9$ Hz), δ_{C} 136.5, d, CH-6], and two *E*-geometry olefinic methines [δ_{H} 6.62 (d, $J = 16.4$ Hz), δ_{C} 120.8, d, CH-2'; δ_{H} 7.91 (d, $J = 16.4$ Hz), δ_{C} 139.0, d, CH-1'] were also observed. Comparison of the NMR data of **40** with those of gamahorin (Koshino *et al.* 1992), previously isolated from the phytopathogenic fungus *Epichloe typhina*, revealed that both compounds only differed in the side chain substituted at C-7. The hydroxymethylene group in gamahorin was replaced by an acrylic acid group in **40**. This was further corroborated by HMBC correlations (Figure 3.7.1.1) between H-1'/C-6, H-1'/C-8, H-1'/C-2', H-1'/C-3', H-2'/C-7, and H-2'/C-3'. The *E*-geometry of the $\Delta^{2',3'}$ double bond was evidenced by the proton-proton coupling constant of $J = 16.4$ Hz and NOE correlation (Figure 3.7.1.2) from H-2' (δ_{H} 6.62) to H-6 (δ_{H} 7.84). H-3 (δ_{H} 4.59, m) and H-4 (δ_{H} 3.97, m) were suggested on the different orientation of the δ -lactone ring based on the absence of NOE interactions between 11-CH₃ and 12-CH₃.

Therefore, the structure of pestalotiopisorin A (**40**) was identified as (*E*)-3-((3*R**,4*S**)-8-hydroxy-3,4-dimethyl-1-oxoisochroman-7-yl)acrylic acid.

Table 3.7.1.1 ^1H NMR (500 MHz) and ^{13}C NMR (125 MHz) spectroscopic data for pestalotiopisorin A (**40**)

Atom no.	40 (in methanol- d_4)		HMBC (H to C)	Gamahorin from Reference (in CDCl_3)	
	δ_{H} [ppm]	δ_{C} [ppm]		δ_{H} [ppm]	δ_{C} [ppm]
1		170.7, s			169.1, s
3	4.59, m	82.8, d	1, 4, 10, 12	4.50, dq, 6.6, 6.5	81.1, d
4	3.97, m	38.5, d	3, 9, 10, 11	2.88, dq, 6.6, 7.1	37.3, d
5	6.95, d, 8.9	119.0, d	6, 7, 9, 10	6.78, d, 7.6	116.4, d
6	7.84, d, 8.9	136.5, d	5, 7, 8, 10	7.50, d, 7.6	135.3, d
7		122.6, s			127.7, s
8		162.0, s			160.1, s
8-OH				11.55, s	
9		109.7, s			107.2, s
10		148.0, s			143.3, s
11	1.36, d, 6.95	19.8, q	3, 4, 10	1.36, d, 7.1	17.4, q
12	1.44, d, 6.6	17.8, q	3, 4,	1.48, d, 6.5	19.7, q
1'	7.91, d, 16.4	139.0, d	6, 7, 8, 2', 3'	4.73, d, 6.0	61.1, t
1'-OH				2.35, t, 6.0	
2'	6.62, d, 16.4 Hz	120.8, d	7, 1', 3'		
3'		170.2, s	1', 2'		

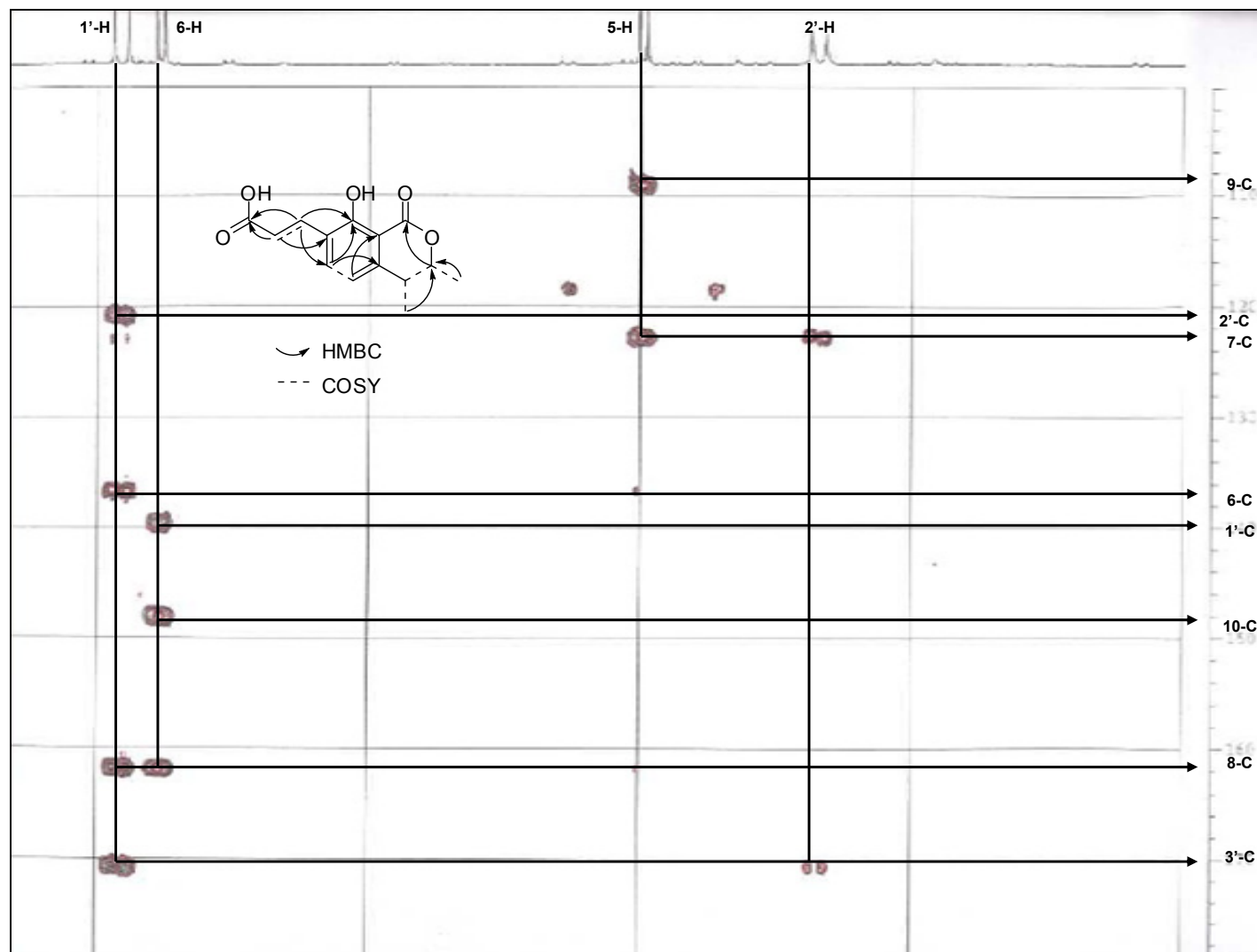


Figure 3.7.1.1a Selected HMBC correlations for compound 40

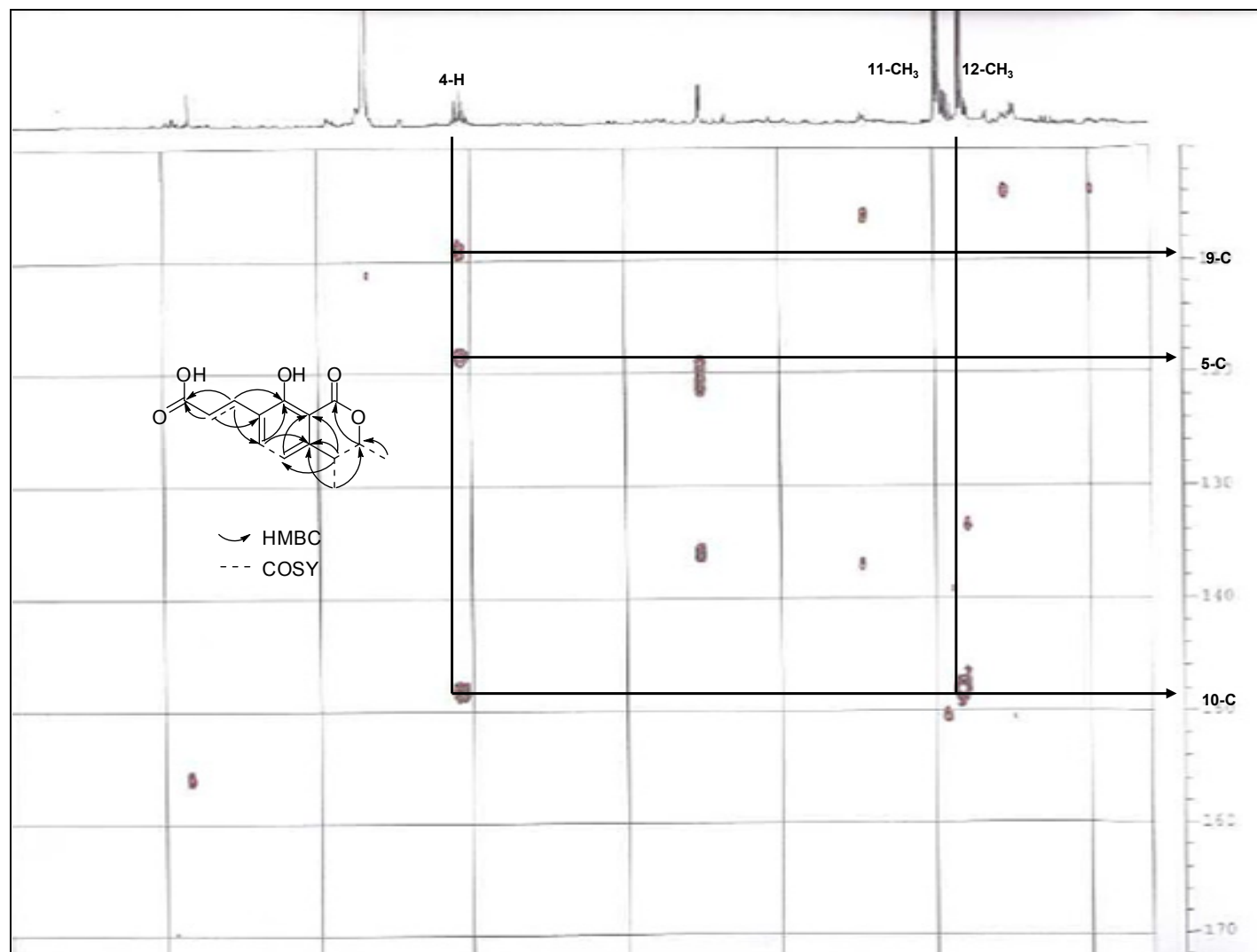


Figure 3.7.1.1b Selected HMBC correlations for compound **40**

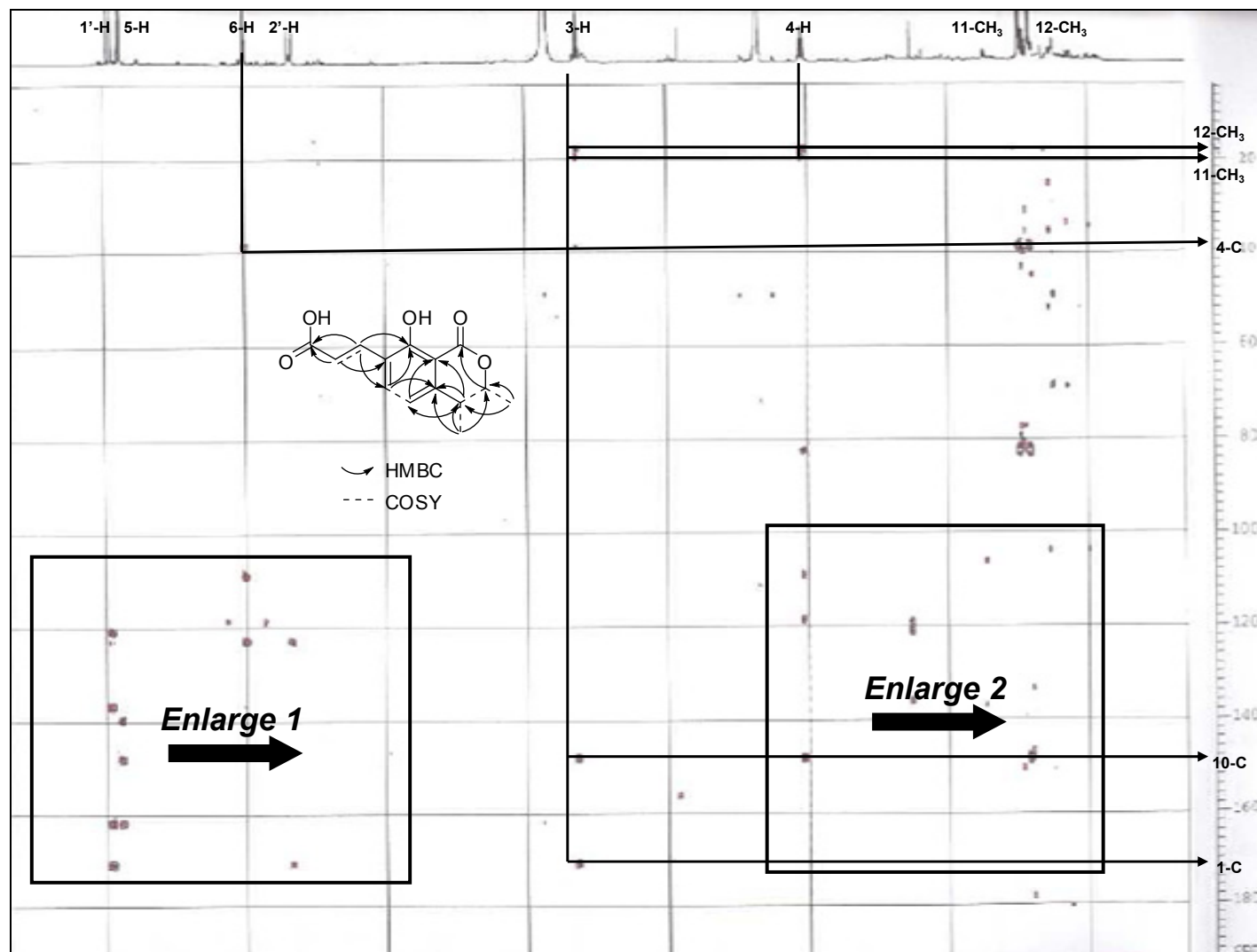


Figure 3.7.1.1c Selected HMBC correlations for compound 40

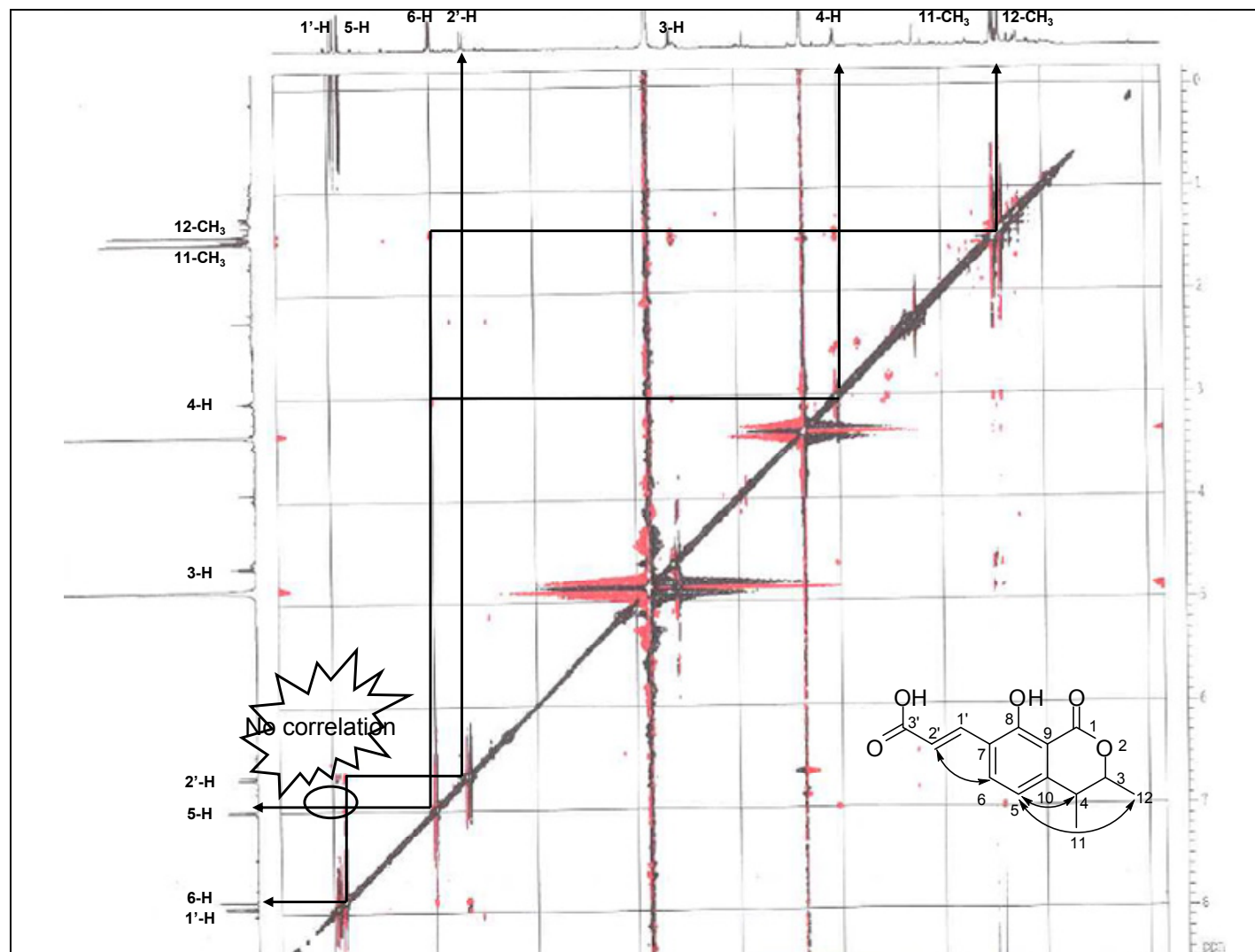
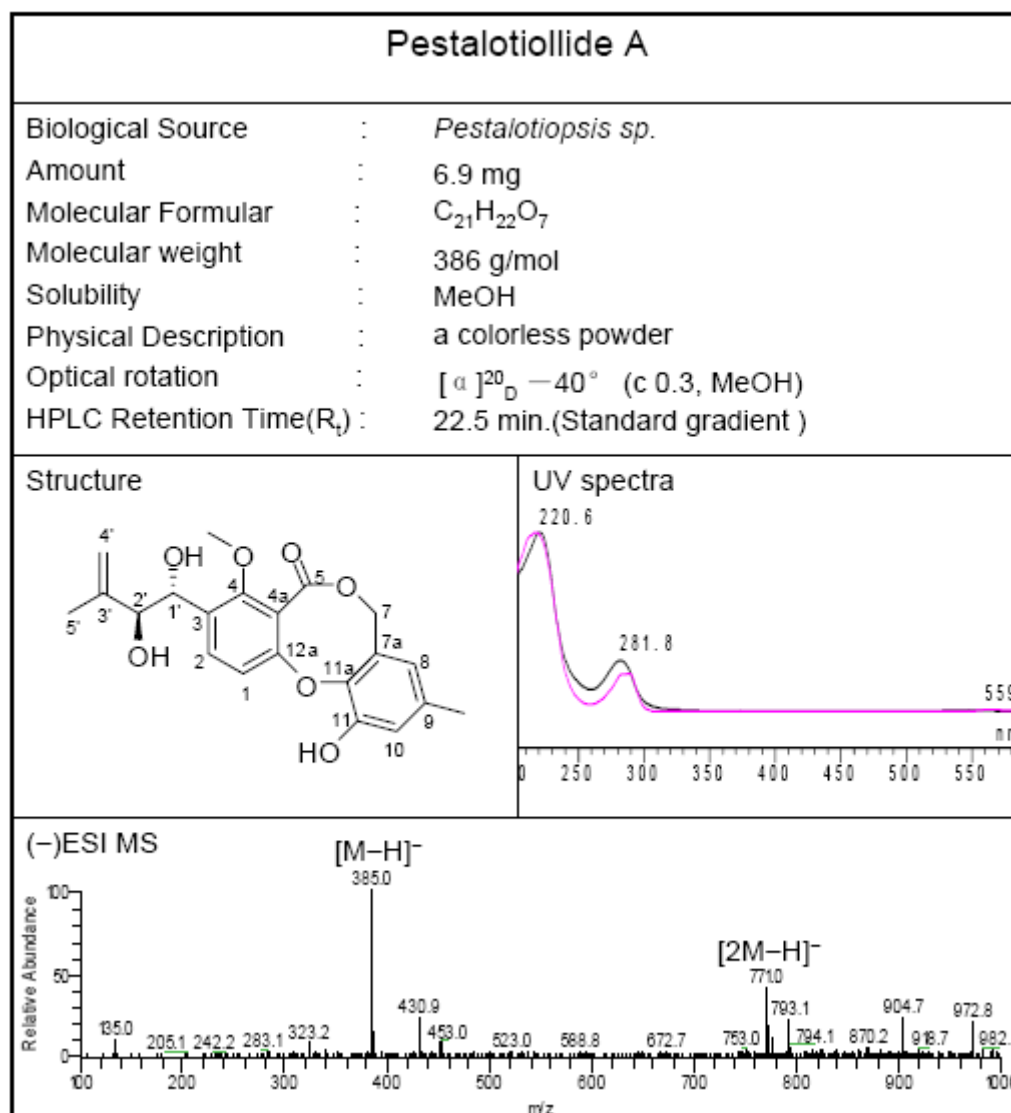


Figure 3.7.1.2 Selected NOESY correlations for compound 40

3.7.2 Pestalotiollide A (**41**, new compound)

The molecular formula of pestalotiollide A (**41**) was established as $C_{21}H_{22}O_7$ by HR-ESIMS (m/z 409.1249, calcd for $[M+Na]^+$ 409.1263). The 1H and ^{13}C NMR data of **41** (Table 3.7.2.1) indicated that ten of eleven unsaturation degrees come from a double bond, a carbonyl group, and two benzene rings. Thus, the last remaining unsaturation degree was attributed to an additional ring. The 1H and ^{13}C NMR data of **41** and the information from its 1H - 1H COSY spectrum uncovered a methoxy group (δ_H 3.92, s, δ_C 62.9, q, 4-OCH₃), a terminal double bond [δ_H 4.72 br s, δ_C 113.1, t, CH₂-4'; δ_C 146.3, s, C-3'], an oxygenated methylene [δ_H 5.07 br s, δ_C 70.4, t, CH₂-7],

two methyls (δ_{H} 1.76, s, δ_{C} 18.8, q, 5'-CH₃; δ_{H} 2.20, s, δ_{C} 20.8, q, 9-CH₃), two *ortho*-coupled aromatic methines [δ_{H} 6.97 (d, J = 8.5 Hz), δ_{C} 118.6, d, CH-1; δ_{H} 7.69 (d, J = 8.5 Hz), δ_{C} 134.0, d, CH-2], two *meta*-coupled aromatic methines [δ_{H} 6.40, br s, δ_{C} 121.2, d, CH-8; δ_{H} 6.77 (d, J = 1.6 Hz), δ_{C} 119.3, d, CH-10], and two oxygenated methines [δ_{H} 4.12 (d, J = 6.0 Hz), δ_{C} 80.2, d, CH-2'; δ_{H} 5.01 (d, J = 6.0 Hz), δ_{C} 70.1, d, CH-1']. Comparison of the NMR data of **41** with those of 2'-hydroxy-3',4'-didehydropenicillide (Kawamura *et al.* 2000), previously isolated from the endophytic fungus *Penicillium* sp., revealed that both compounds shared the same planar structure. This was confirmed from ¹H-¹H COSY correlations and HMBC cross peaks as shown in (Figure 3.7.2.1). The NOE interactions observed from H-2' (δ_{H} 4.25) to H-2 (δ_{H} 7.73), but not H-1' (δ_{H} 5.05) and H-2, deduced the different orientation of H-1'.

Hence pestalotiollide A (**41**) was proposed as 3-((1R*,2S*)-1,2-dihydroxy-3-methylbut-3-enyl)-11-hydroxy-4-methoxy-9-methyldi benzo[b,g][1,5]dioxocin-5(7H)-one.

Table 3.7.2.1 ^1H , ^{13}C NMR NMR (500 MHz) data (J in Hz) of pestalotiollide A (**41**) in CD_3OD

Atom no.	41 δ_{H}	δ_{C}	HMBC (H to C)	NOESY (H to C)	2'-Hydroxy-3',4'-didehydropenicilli from Reference	
					δ_{H}	δ_{C}
1	6.97, d, 8.5	118.6, d	1, 3, 4a, 12a	2	6.99, d, 8.8	118.8, d
2	7.69, d, 8.5	134.0, d	1, 3, 4, 12a	1, 2'	7.72, d, 8.8	133.9, d
3		135.2, s				135.2, s
4		156.1, s				156.8, s
4-OCH ₃	3.92, s	62.9, q		1'	3.93, s	634, q
4a		120.7, s				120.9, s
5		169.9, s				169.9, s
7	5.07, br s	70.4, t	6, 7a, 8, 11a	8	5.05, br d, 14.6; 5.13, br d, 14.6	70.3, t
7a		128.2, s				128.2, s
8	6.40, br s	121.2, d	7a, 9, 10, 11a	7, 9-CH ₃	6.40, d, 2.0	121.1, d
9		136.1, s				135.9, s
9-CH ₃	2.20, s	20.8, q	8, 9, 10	8, 10	2.20, s	20.8, q
10	6.77, d, 1.6	119.3, d	9, 11, 11a, 9-CH ₃	9-CH ₃	6.77, d, 2.0	119.2, d
11		149.7, s				149.7, s
11a		143.4, s				143.3, s
12a		153.6, s				153.4, s
1'	5.01, d, 5.65	70.1, d	2, 3, 4, 2', 3'	2'	5.04, d, 7.3	69.2, d
2'	4.12, d, 6.0	80.2, d	3, 1', 3', 4', 5'	1', 2	4.24, d, 7.3	79.5, d
3'		146.3, s				146.5, s
4'	4.72, br s	113.1, t	2', 3', 5'	2', 5'	4.86, br s	114.1, t
5'	1.76, s	18.8, q	2', 3', 4'	2', 4'	1.80, s	18.4, q

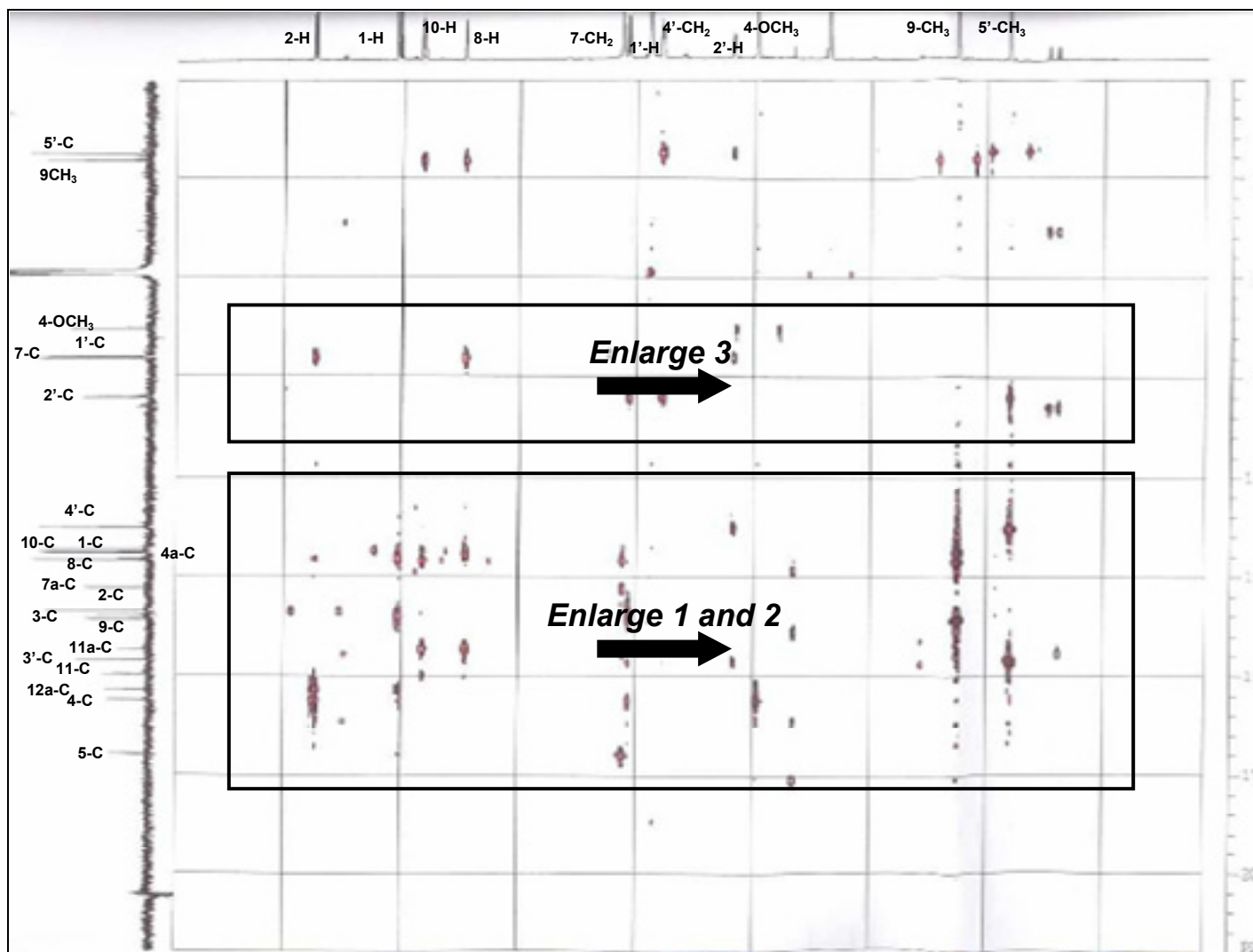


Figure 3.7.2.1a Selected HMBC correlations for compound **41**

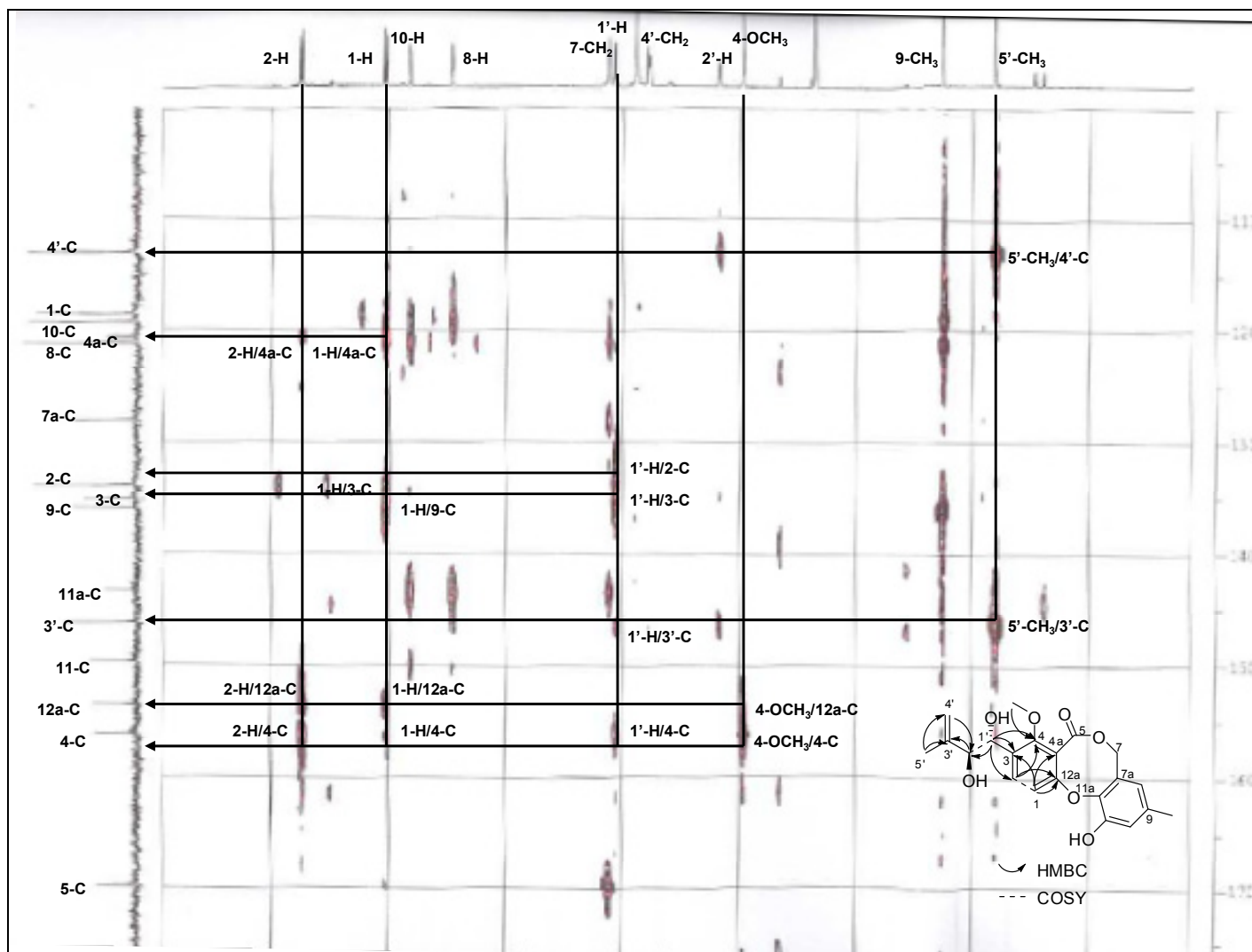


Figure 3.7.2.1b Selected HMBC correlations for compound **41**

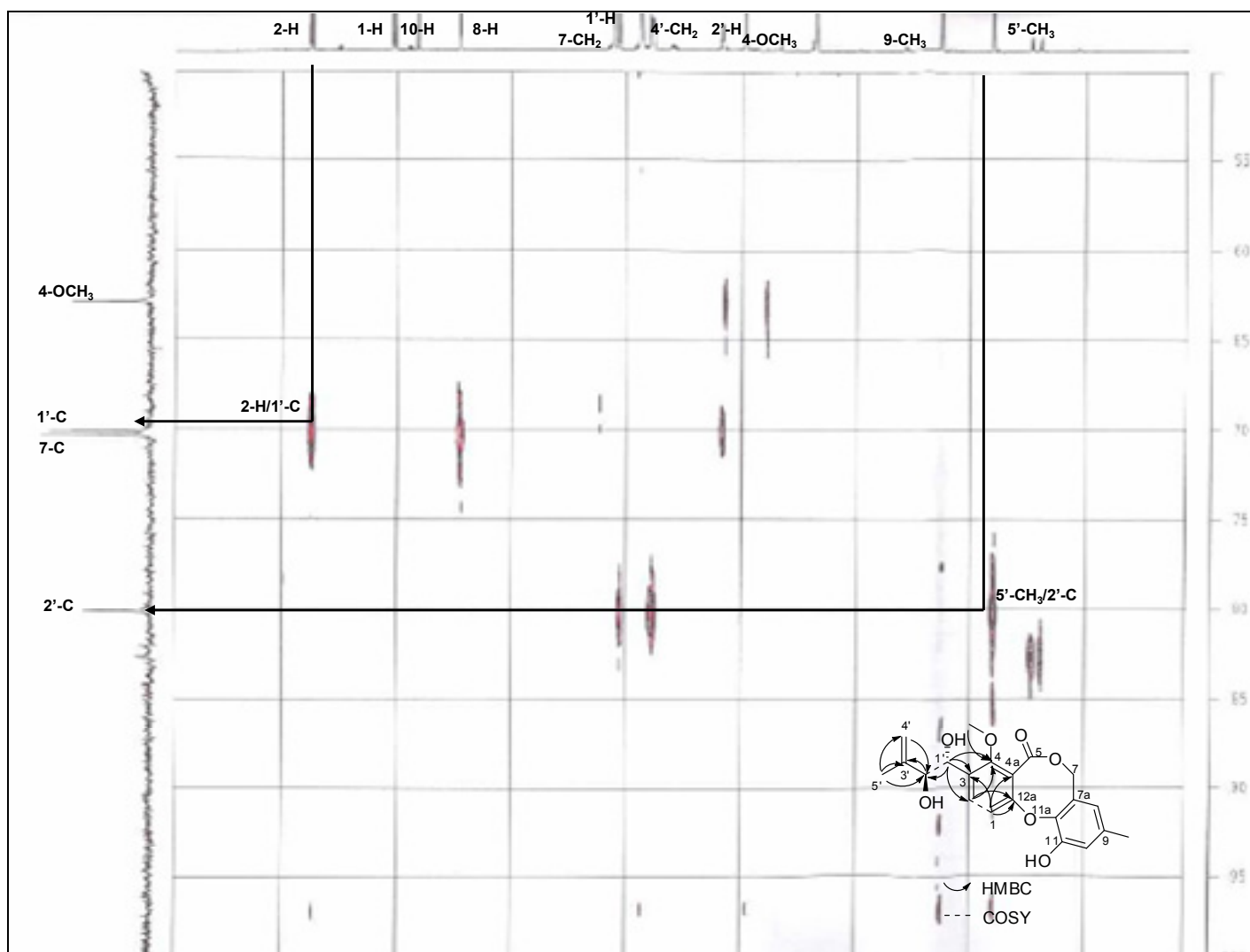


Figure 3.7.2.1d Selected HMBC correlations for compound **41**

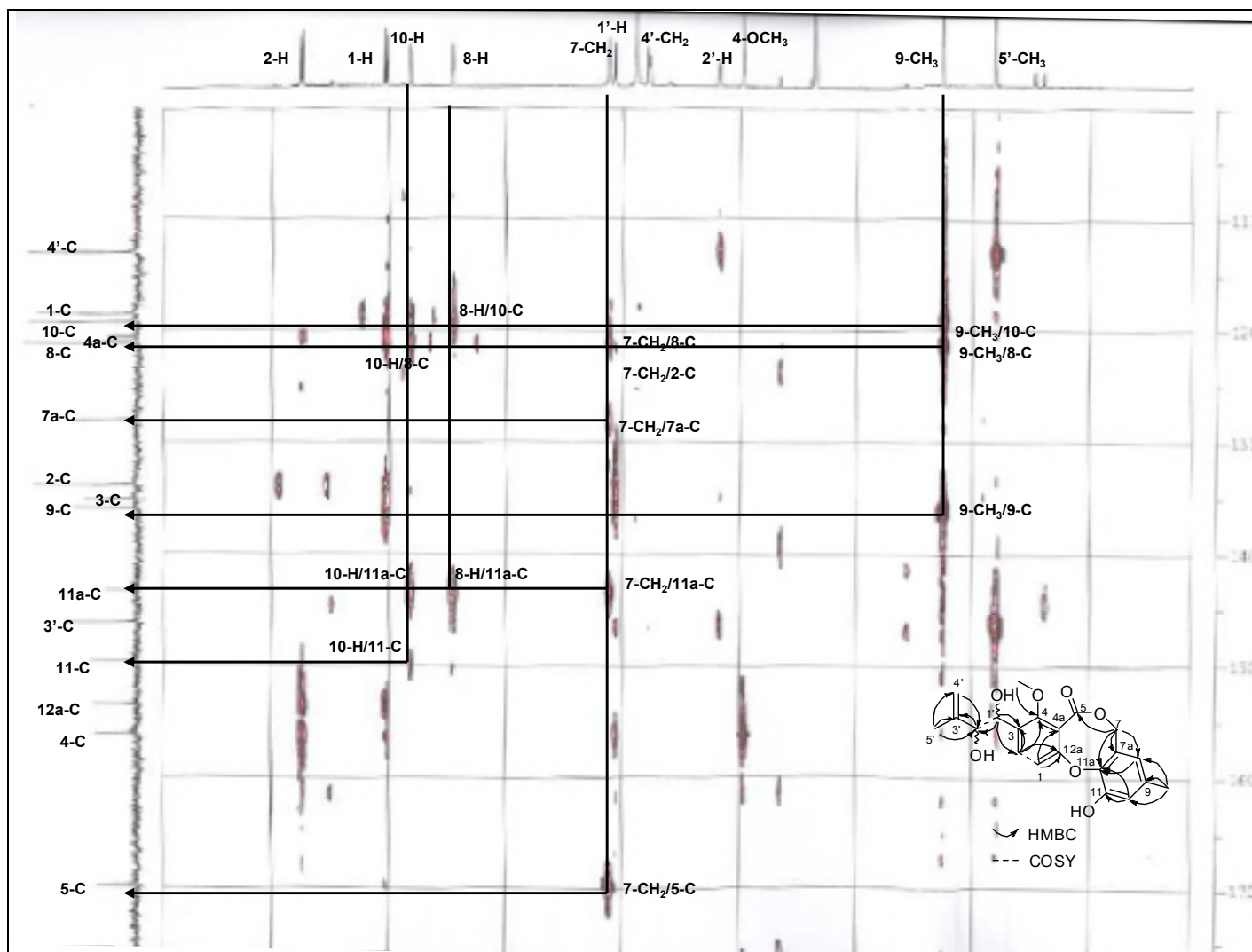
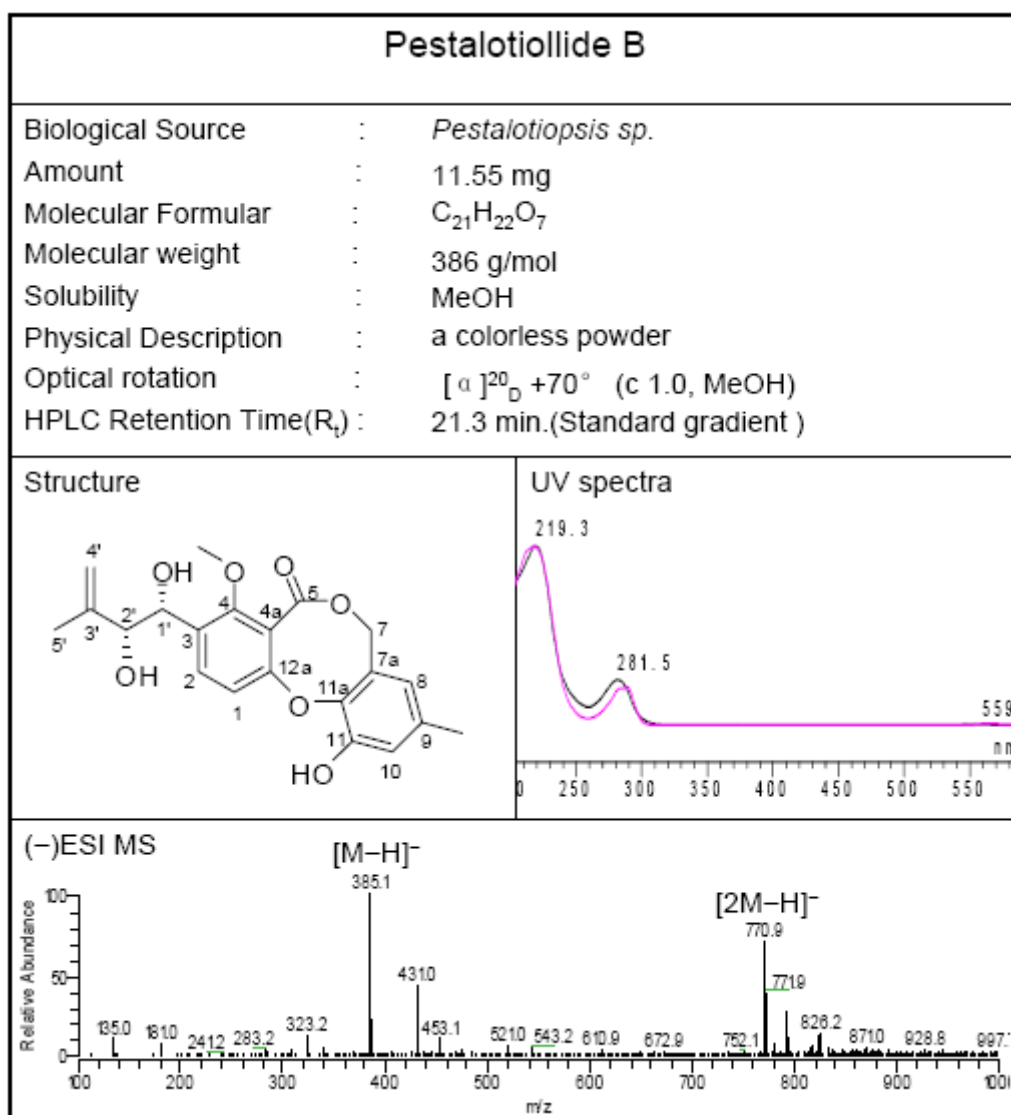


Figure 3.7.2.1d Selected HMBC correlations for compound 41

3.7.3 Pestalotiollide B (**42**, new compound)

Pestalotiollide B (**42**) shared the same molecular formula of C₂₁H₂₂O₇ with **41**, determined by the HR-ESIMS data (m/z 409.1247, calcd for [M+Na]⁺ 409.1263). Its NMR data, ¹H-¹H COSY and HMBC spectra of **42** (Table 3.7.3.1) were very similar to those of **41**. The difference was attributed to the NOESY correlations (Figure 3.7.3.1) of H-2 (δ_H 7.69) to both of H-1' (δ_H 5.01) and H-2' (δ_H 4.12), assigned the same orientation of the protons H-1' and H-2'.

Pestalotiollide B (42) was thus identified as 3-((1R*,2R*)-1,2-dihydroxy-3-methylbut-3-enyl)-11-hydroxy-4-methoxy-9-methyl-10H-benzo[*b,g*][1,5]dioxocin-5(7H)-one.

Table 3.7.3.1 ^1H , ^{13}C NMR (500 MHz) data (*J* in Hz) of pestalotiollide B (42) in CD_3OD

Atom no.	42 δ_{H}	δ_{C}	HMBC (H to C)	NOESY (H to C)	Comparison Compound 41 δ_{H}	δ_{C}
1	7.0, d, 8.55	119.0, d	1, 3, 4a, 12a	2	6.97, d, 8.5	118.6, d
2	7.73, d, 8.55	134.1, d	1, 3, 4, 12a	1, 2'	7.69, d, 8.5	134.0, d
3		135.5, s				135.2, s
4		157.1, s				156.1, s
4-OCH ₃	3.95, s	63.6, q		1'	3.92, s	62.9, q
4a		121.1, s				120.7, s
5		170.1, s				169.9, s
7	5.07, m; 5.16, m	70.5, t	6, 7a, 8, 11a	8	5.07, br s	70.4, t
7a		128.4, s				128.2, s
8	6.41, d, 1.25	121.4, d	7a, 9, 10, 11a	7, 9-CH ₃	6.40, br s	121.2, d
9		136.2, s				136.1, s
9-CH ₃	2.2s, s	21.0, q	8, 9, 10	8, 10	2.20, s	20.8, q
10	6.78, d, 1.9	119.4, d	9, 11, 11a, 9-CH ₃	9-CH ₃	6.77, d, 1.6	119.3, d
11		149.9, s				149.7, s
11a		143.5, s				143.4, s
12a		153.6, s				153.6, s
1'	5.05, d, 7.25	69.4, d	2, 3, 4, 2', 3'	2, 2'	5.01, d, 5.65	70.1, d
2'	4.25, d, 7.25	79.8, d	3, 1', 3', 4', 5'	1', 2	4.12, d, 6.0	80.2, d
3'		146.7, s				146.3, s
4'	4.85, br s	114.3, t	2', 3', 5'	2', 5'	4.72, br s	113.1, t
5'	1.81, s	18.6, q	2', 3', 4'	2', 4'	1.76, s	18.8, q

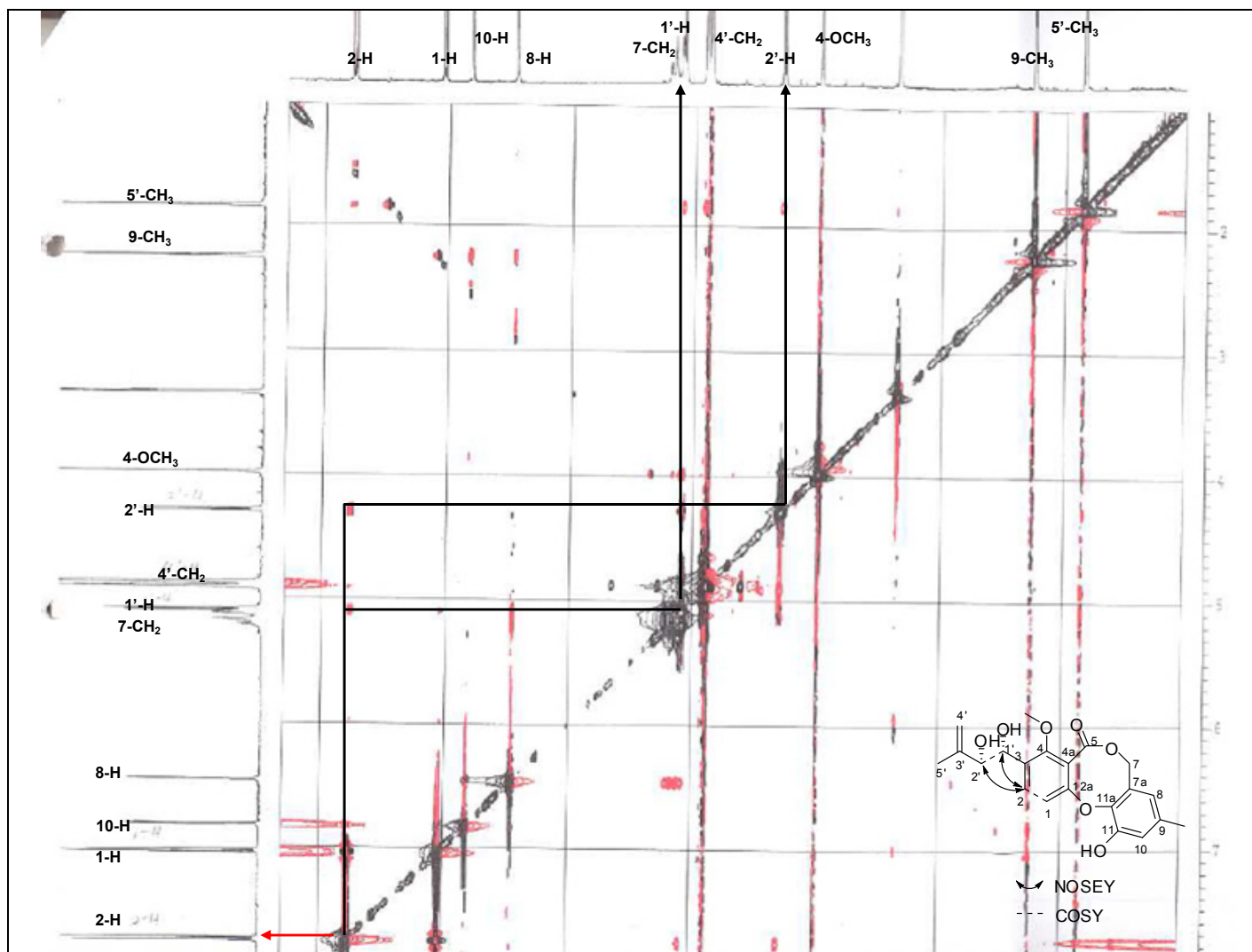


Figure 3.7.3.1a Selected NOSEY correlations for compound 42

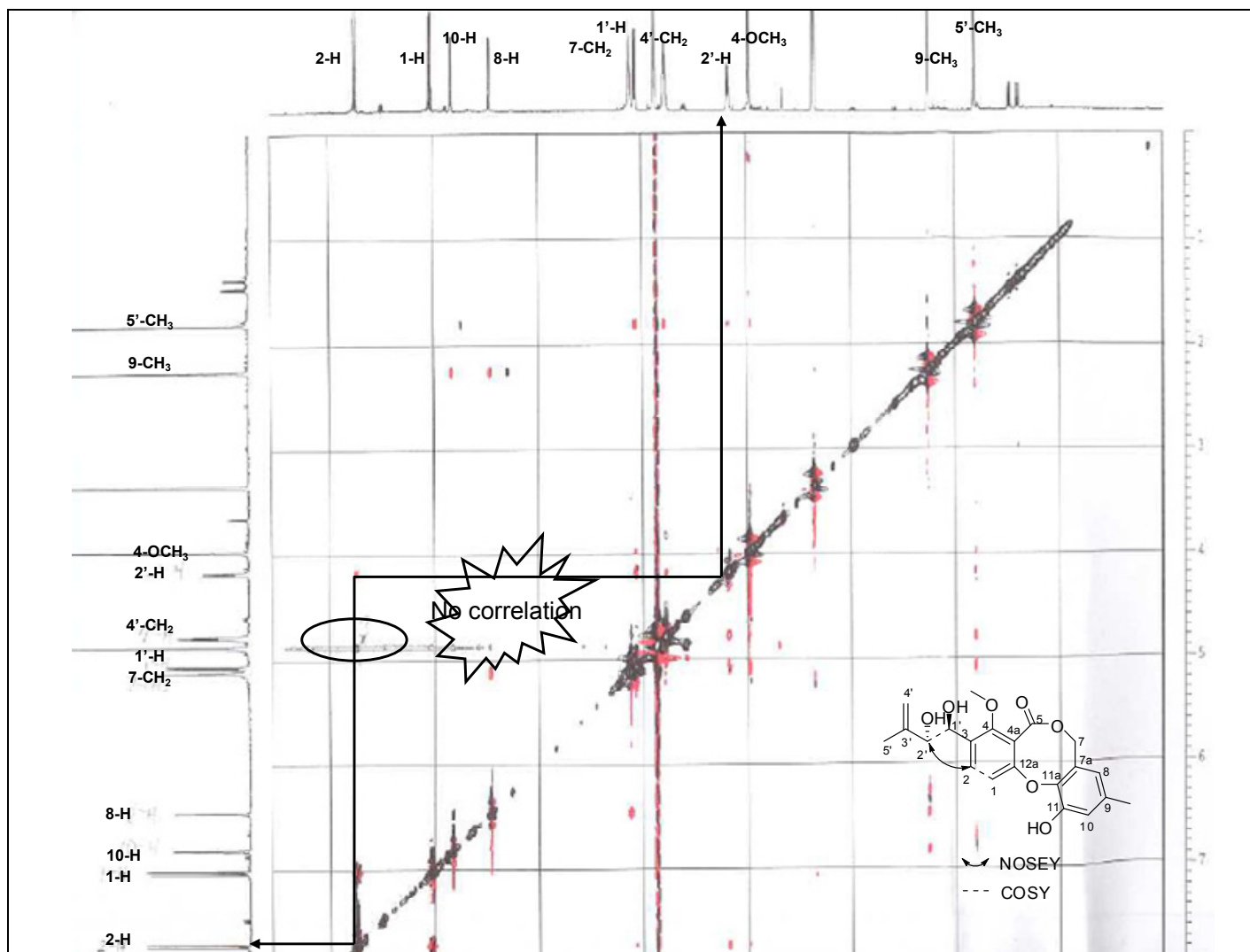
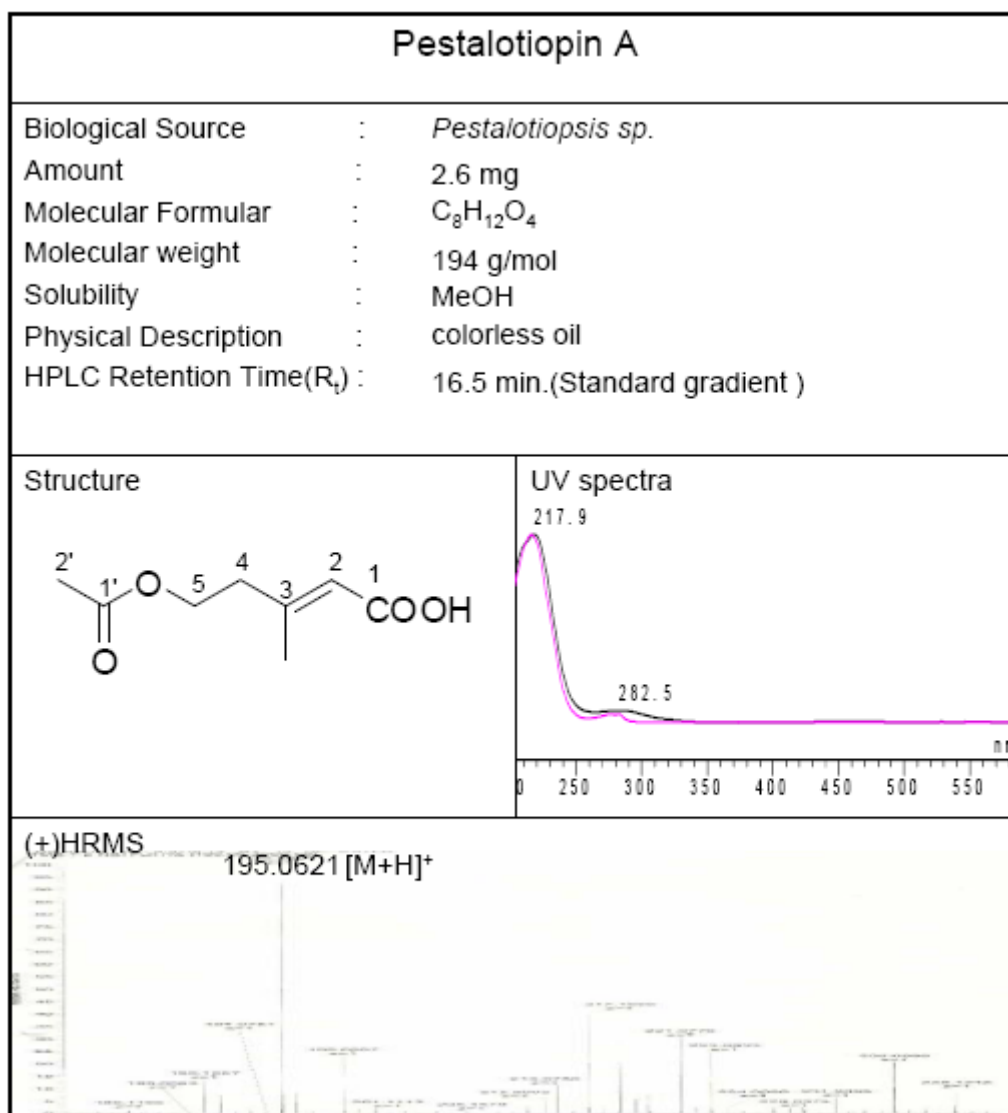


Figure 3.7.3.1b Selected NOSEY correlations for compound **41**

3.7.4 Pestalotiopin A (43, new compound)



Pestalotiopin A (**43**) had the molecular formula of $C_8H_{12}O_4$, established by HR-ESIMS (m/z 195.0621, calcd for $[M+Na]^+$ 195.0633). The 1H and ^{13}C NMR data of **43** revealed that three unsaturation degrees of this molecule were attributed to one double bond and two carbonyls. The NMR data (Tables 3.7.4.1) of **43** and the information from its 1H - 1H COSY and HMQC spectra indicated the presence of an olefinic methine (δ_H 5.75, brs; δ_C 121.1, d, CH-2), a 1,2-disubstituted ethoxy group [δ_H 2.43 (t, J = 6.3 Hz), δ_C 40.4, 4- CH_2 ; δ_H 4.22 (t, J = 6.3 Hz), δ_C 63.1, 5- CH_2], and

two methyls (δ_{H} 2.01, s, δ_{C} 20.7, q, 2'-CH₃; δ_{H} 2.12, s, δ_{C} 18.3, q, 3-CH₃). These NMR data were similar to those reported for (*E*)-5-hydroxy-3-methylpent-2-enoic acid (Dieckmann *et al.* 1968; Xiang *et al.* 2004), previously isolated from the endophytic fungus *Fusarium* sp.. It was suggested that both compounds shared the same basic skeleton except for the different substituents at C-5, where 5-OH in (*E*)-5-hydroxy-3-methylpent-2-enoic acid was replaced by an acetoxy group in **43**. This was further confirmed by the HMBC correlation (Figure 3.7.4.1) from H-5 to C-1' (δ_{C} 171.7). The NOE interactions between H-2/H-4, H₃-3/H-5 helped to establish the *E* geometry for the double bond.

Accordingly, the structure of pestalotiopin A (**43**) was assigned as (*E*)-5-acetoxy-3-methylpent-2-enoic acid.

Table 3.7.4.1 ¹H NMR (500 MHz) and ¹³C NMR (125 MHz) spectroscopic data for pestalotiopin A (**43**) in CD₃OD

Atom no.	⁴³ δ_{H} [ppm]	δ_{C} [ppm]	HMBC (H to C)
1		172.7, s	
2	5.75, brs	120.6, d	1, 3, 4
3		151.8, s	
4	2.43, t, 6.3	40.4, t	2, 4, 3-CH ₃
5	4.22, t, 6.3	63.1, t	3, 4, 1'
1'		171.7, s	2'
2'	2.01, s	20.7, q	1'
3-CH ₃	2.12, s	18.3, q	2, 3, 4

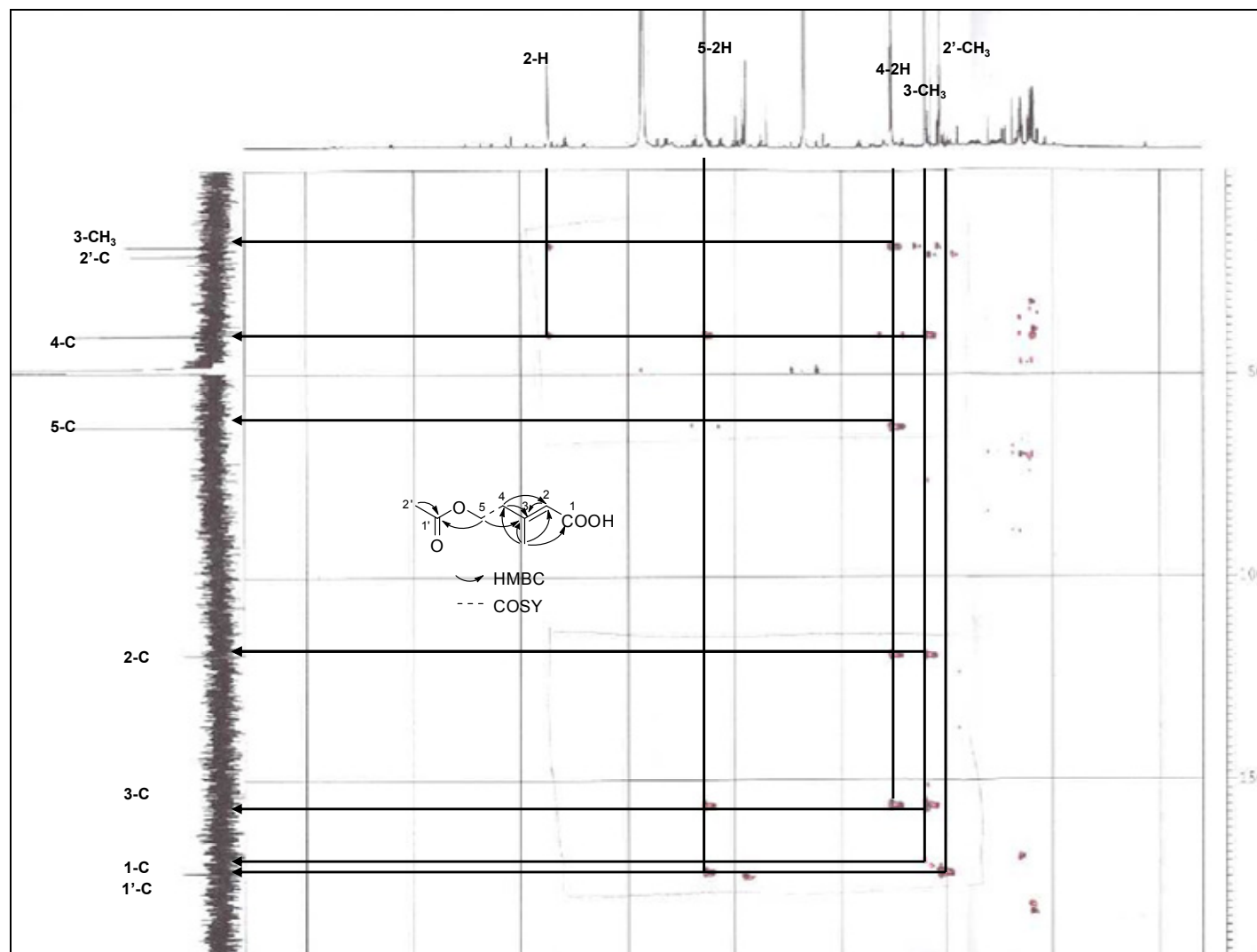
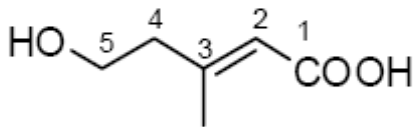
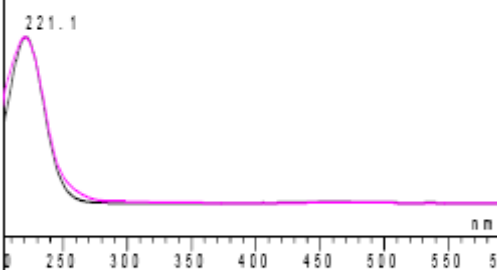


Figure 3.7.4.1 Selected HMBC correlations for compound **43**

3.7.5 2-Anhydromevalonic acid (**44**, known compound)

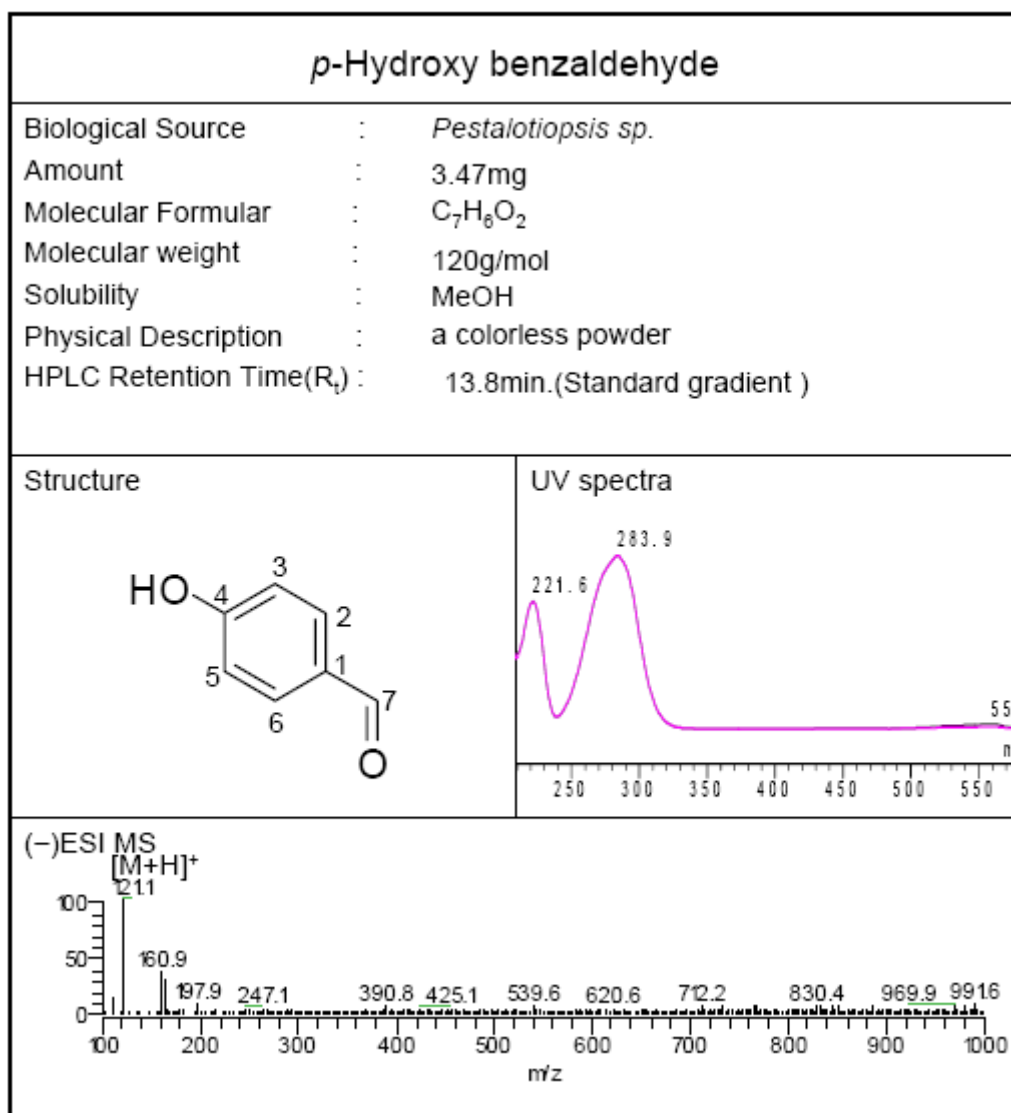
2-anhydromevalonic acid	
Biological Source	: <i>Pestalotiopsis</i> sp.
Amount	: 0.99mg
Molecular Formular	: C ₆ H ₁₀ O ₃
Molecular weight	: 130g/mol
Solubility	: MeOH
Physical Description	: colorless oil
HPLC Retention Time(R _t)	: 6.6min.(Standard gradient)
Structure	UV spectra
	
(+ESI MS	

2-Anhydromevalonic acid (**44**) was isolated as a colorless oil (0.99 mg, CH₃OH). This compound exhibited a pseudomolecular ion at m/z 131 [M+H]⁺ (calcd for C₆H₁₀O₃, 131.0708) in the positive mode EIS-MS. Obviously, It had two degrees of unsaturation. The NMR data (Tables 3.7.5.2) of **44** and the information from its ¹H-¹H COSY and HMQC spectra indicated the presence of an olefinic methine (δ_H 5.71, br s; δ_C 120.0, d, CH-2), a 1,2-disubstituted ethoxy group [δ_H 2.36 (t, J = 6.3 Hz), δ_C 44.0, 4-CH₂; δ_H 3.69 (t, J = 6.3 Hz), δ_C 60.2, 5-CH₂], and one methyl (δ_H 2.15, s, δ_C 18.3, q, 3-CH₃).

The ^1H NMR data of **44** were the same as those of (*E*)-5-hydroxy-3-methylpent-2-enoic acid, previously isolated from the endophytic fungus *Fusarium* and other fungi (Dieckmann *et al.* 1968), disclosing that they are identical.

Table 3.7.5.1 ^1H NMR (500 MHz) and ^{13}C NMR (125 MHz) spectroscopic data for 2-Anhydromevalonic acid (**44**) in CD_3OD

44		
Atom no.	δ_{H} [ppm]	δ_{C} [ppm]
1		172.7, s
2	5.71, brs	120.6, d
3		151.8, s
4	2.36, t, 6.3	40.4, t
5	3.69, t, 6.3	63.1, t
1'		171.7, s
2'		20.7, q
3-CH ₃	2.15, s	18.3, q

3.7.6 *p*-Hydroxy benzaldehyde (**45**, new compound)

p-Hydroxy benzaldehyde (**45**) was obtained as a white amorphous crystal (3.47 mg, CH₃OH). Its molecular formula C₇H₆O₂, indicating five degrees of unsaturation, was established by ESI-MS at m/z 121.1 [$M - H$]⁻ (calcd for C₇H₆O₂, 121.0290).

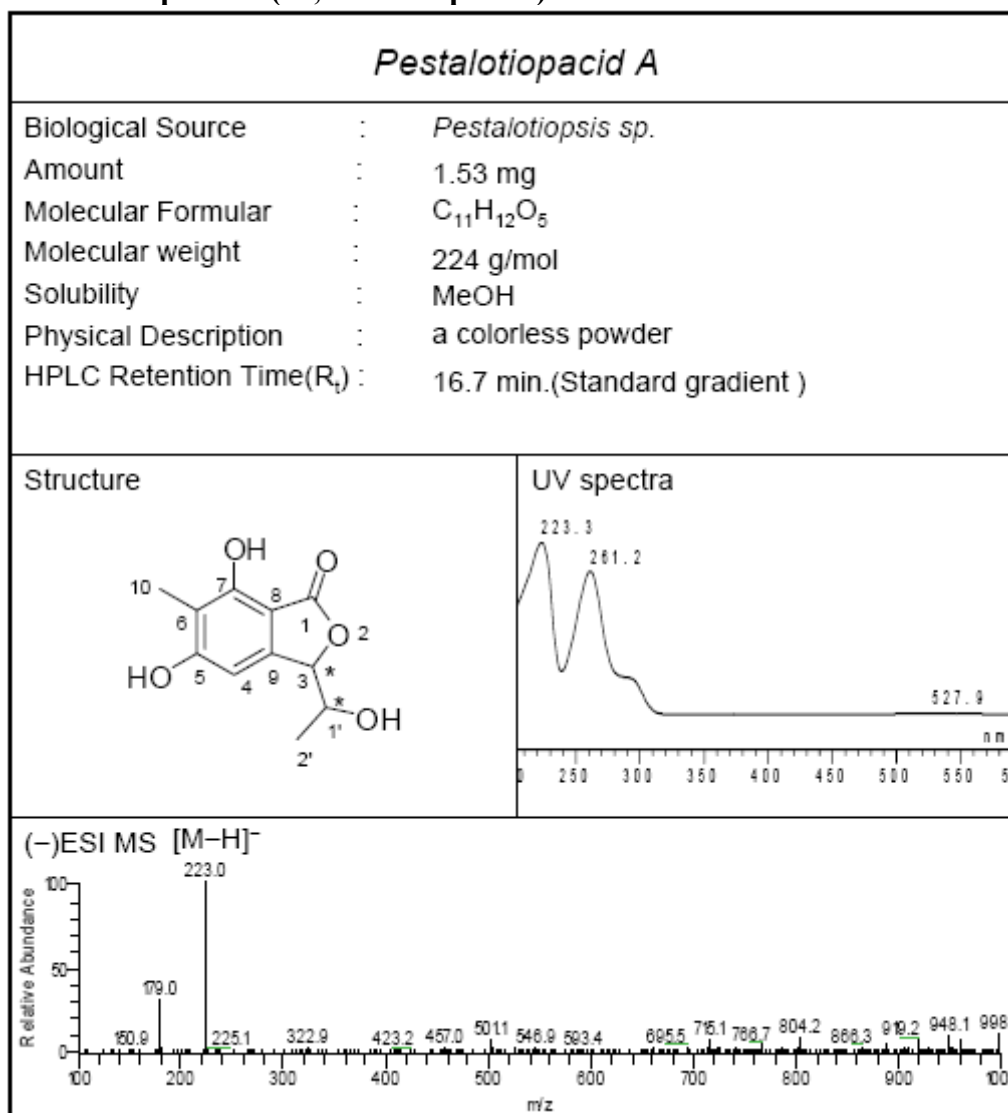
The ¹H NMR data of **45** and its ¹H-¹H COSY spectra indicated an aldehyde group (δ_H 9.76, s, δ_C 192.8, 7-CHO), two pairs of symmetrical *ortho*-coupled aromatic protons of four methines [δ_H 7.76 (2H, d, J = 8.85 Hz), δ_C 133.4, CH-2, CH-6); 6.90 (2H, d, J = 8.85 Hz), δ_C 116.9, CH-3, CH-5)].

Comparison of the ^1H and ^{13}C NMR data of **45** with those of *p*-hydroxy benzaldehyde (Wang *et al.* 2000; Beistel *et al.* 1976) revealed that they are the same compound.

Table 3.7.6.1 ^1H NMR (500 MHz) and ^{13}C NMR (125 MHz) spectroscopic data for *p*-hydroxy benzaldehyde (**45**) in CD_3OD

Atom no.	δ_{H} [ppm]	45 δ_{C} [ppm]	HMBC (H to C)	<i>p</i> -Hydroxy benzaldehyde from Reference δ_{H} [ppm]	δ_{C} [ppm]
1		130.3, s			129.9
2	7.76, d, 8.85	133.4, d	1, 3	7.82, d, 9.2	132.3, d
3	6.90, d, 8.85	116.9, d	2, 4	6.98, d, 9.2	115.8, d
4		165.2, s	3, 5		161.3, s
5	6.90, d, 8.85	116.9, d	4, 6	6.98, d, 9.2	115.8, d
6	7.76, d, 8.85	133.4, d		7.82, d, 9.2	132.3, d
7	9.76, s	192.8, d	1	9.86, s	190.8, d

3.7.7 Pestalotilopacid A (**46**, new compound)



Pestalotilopacid A (**46**), a colorless amorphous solid, had the molecular formula $C_{11}H_{12}O_5$, established by HR-ESIMS (m/z 247.0572, calcd for $[M+Na]^+$ 247.0582), implying six degrees of unsaturation.

The 1H NMR data of **46** (Table 3.7.7.1) and its 1H - 1H COSY spectrum exhibited an oxygenated methine [δ_H 5.26 (d, J = 3.5 Hz), δ_C 86.0, d, CH-3], an aromatic proton (δ_H 6.51, s, δ_C 102.6, d, CH-4), a methyl group (δ_H 2.15, s, δ_C 8.5, q, 10-CH₃), and a 1'-hydroxyethyl group (CH-1' to CH₃-2'). Comparison of the NMR data of **46** with those of 5,7-dihydroxy-6-methyl-l(3H)-isobenzofuranon, previously isolated from the fungus *Aspergillus duricaulis* (Achenbach *et al.* 1985), revealed that both compounds shared the same basic skeleton, except for the presence of an additional 1'-hydroxyethyl group at C-3 in **46**. This was confirmed by 1H - 1H COSY correlations and HMBC correlations (Figure 3.7.7.1) from H-1' (δ_H 4.13, m) to C-9 (δ_C 148.2), H-3 (δ_H 5.26) to C-1 (δ_C 174.3), C-8 (δ_C 105.0), and C-9. The NOE correlations (Figure 3.7.7.2) further supported the assignments of 1'-hydroxyethyl group at C-3 (δ_C 156.4).

Accordingly, the structure of pestalotilopacid A (**46**) was 5,7-dihydroxy-3-(1-hydroxyethyl)-6-methylisobenzofuran-1(3H)-one. The stereochemistry was not assigned so far.

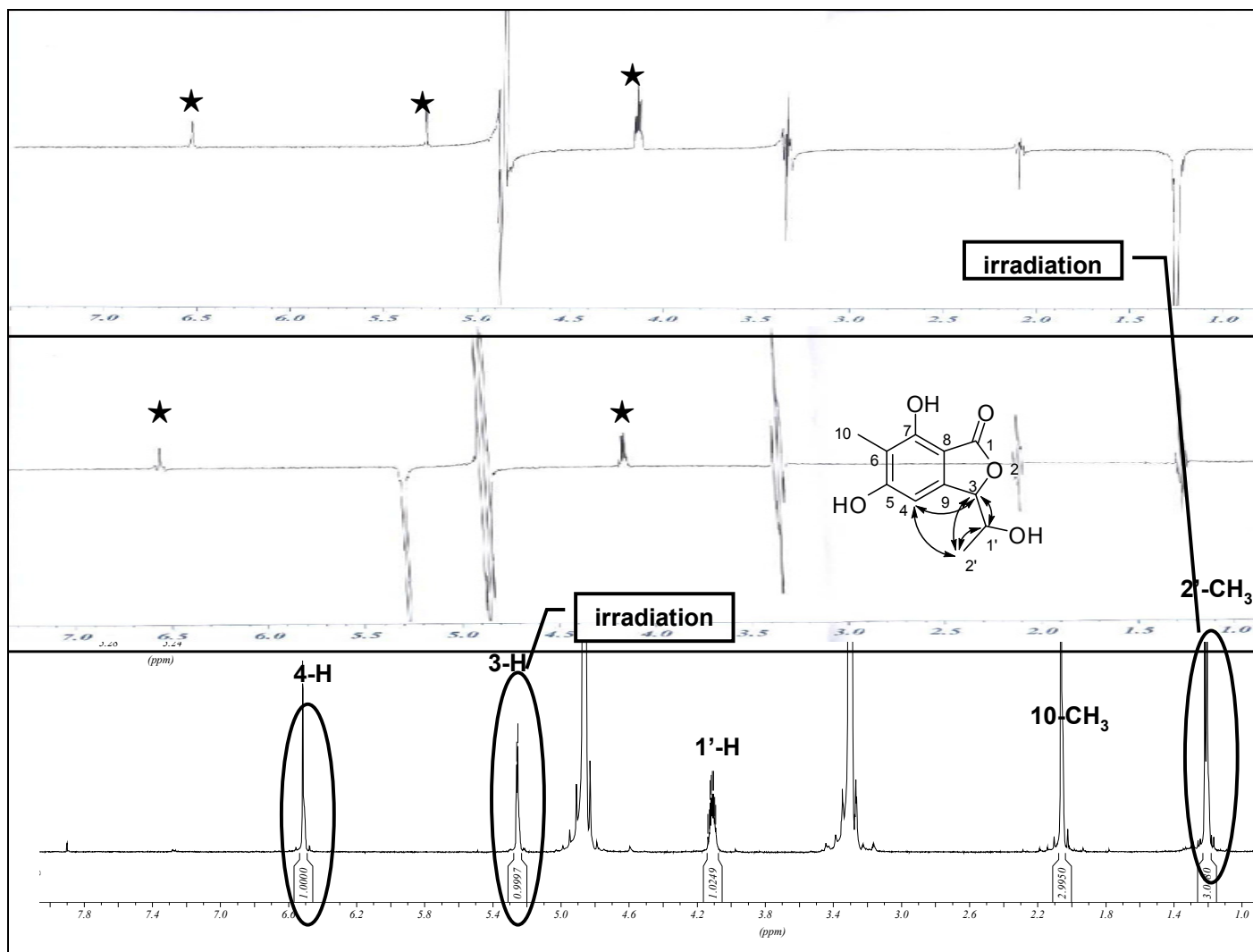
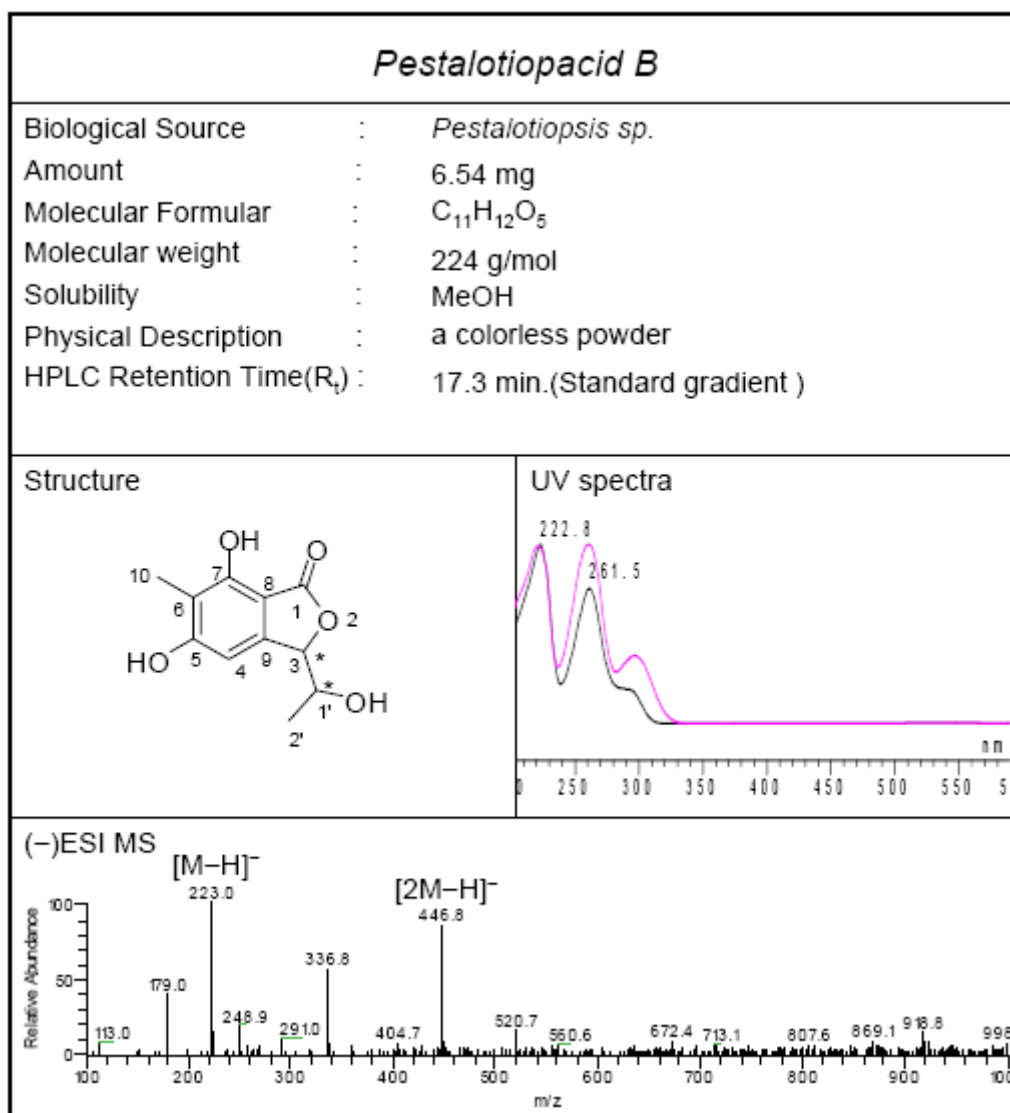


Figure 3.7.7.2 NOE correlations for compound 46

Table 3.7.7.1 ^1H NMR (500 MHz) and ^{13}C NMR (125 MHz) spectroscopic data for pestalotiopacid A (**46**) in CD_3OD

Atom no.	δ_{H} [ppm]	46 δ_{C} [ppm]	HMBC (H to C)
1		174.3, s	
3	5.26, d, 3.5	86.0, d	1, 8, 9
4	6.51, s	102.6, d	3, 5, 6, 8, 9
5		163.7, s	
6		114.2, s	
7		156.3, s	
8		105.0, s	
9		148.2, s	
10	2.15, s	8.5, q	5, 6, 7
1'	4.13, m	68.9, d	3, 2'
2'	1.20, d, 6.35	19.1, q	3, 1'

3.7.8**B (47, new compound)****Pestalotilopacid**



The molecular formula of pestalotilopacid B (**47**), being the same as that of **46**, was established by HR-ESIMS (m/z 247.0571).

It was suggested that **47** should be an isomer of **46**. Its ^1H and ^{13}C NMR data of **47** (Table 3.7.8.1) were closely related to those of **46** with the exception of the minor upfield shift of H-1' (δ_{H} 3.96, m), indicating a different configuration of the 1'-hydroxyethyl substituent at C-1'. However, the configuration (Figure 3.7.8.1) was not assigned so far.

Table 3.7.8.1 ^1H NMR (500 MHz) and ^{13}C NMR (125 MHz) spectroscopic data for pestalotilopacid B (**47**) in CD_3OD

Atom no.	47		HMBC (H to C)	Comparison Compound 46	
	δ_{H} [ppm]	δ_{C} [ppm]		δ_{H} [ppm]	δ_{C} [ppm]
1		173.6, s			174.3, s
3	5.26, d, 3.5	86.0, d	1, 8, 9	5.26, d, 3.5	86.0, d
4	6.51, s	102.1, d	3, 5, 6, 8, 9	6.51, s	102.6, d
5		164.8, s			163.7, s
6		112.8, s			114.2, s
7		156.7, s			156.3, s
8		105.0, s			105.0, s
9		148.4, s			148.2, s
10	2.15, s	7.9, q	5, 6, 7	2.15, s	8.5, q
1'	4.13, m	69.8, d	3, 2'	4.13, m	68.9, d
2'	1.20, d, 6.35	18.1, q	3, 1'	1.20, d, 6.35	19.1, q

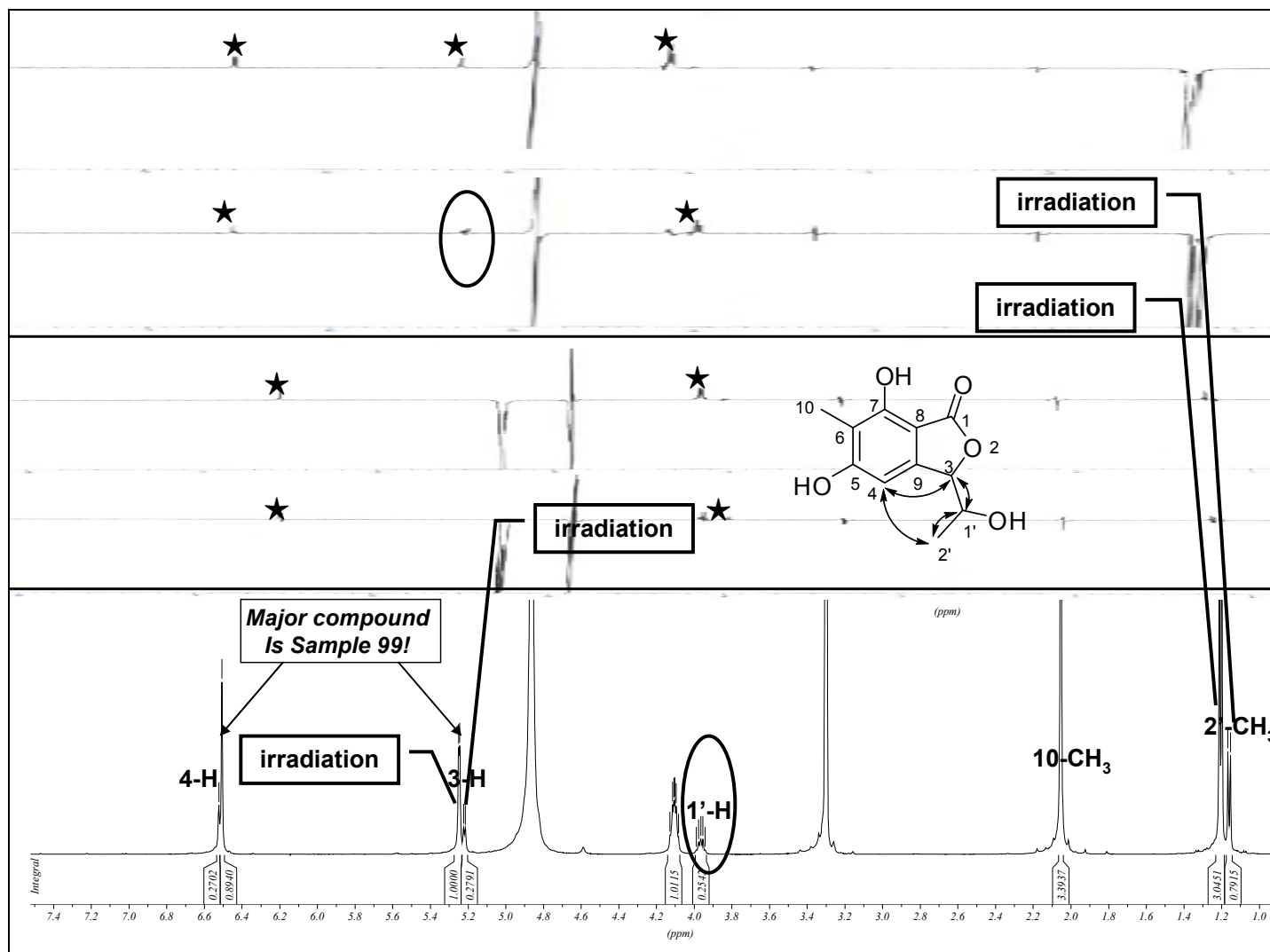
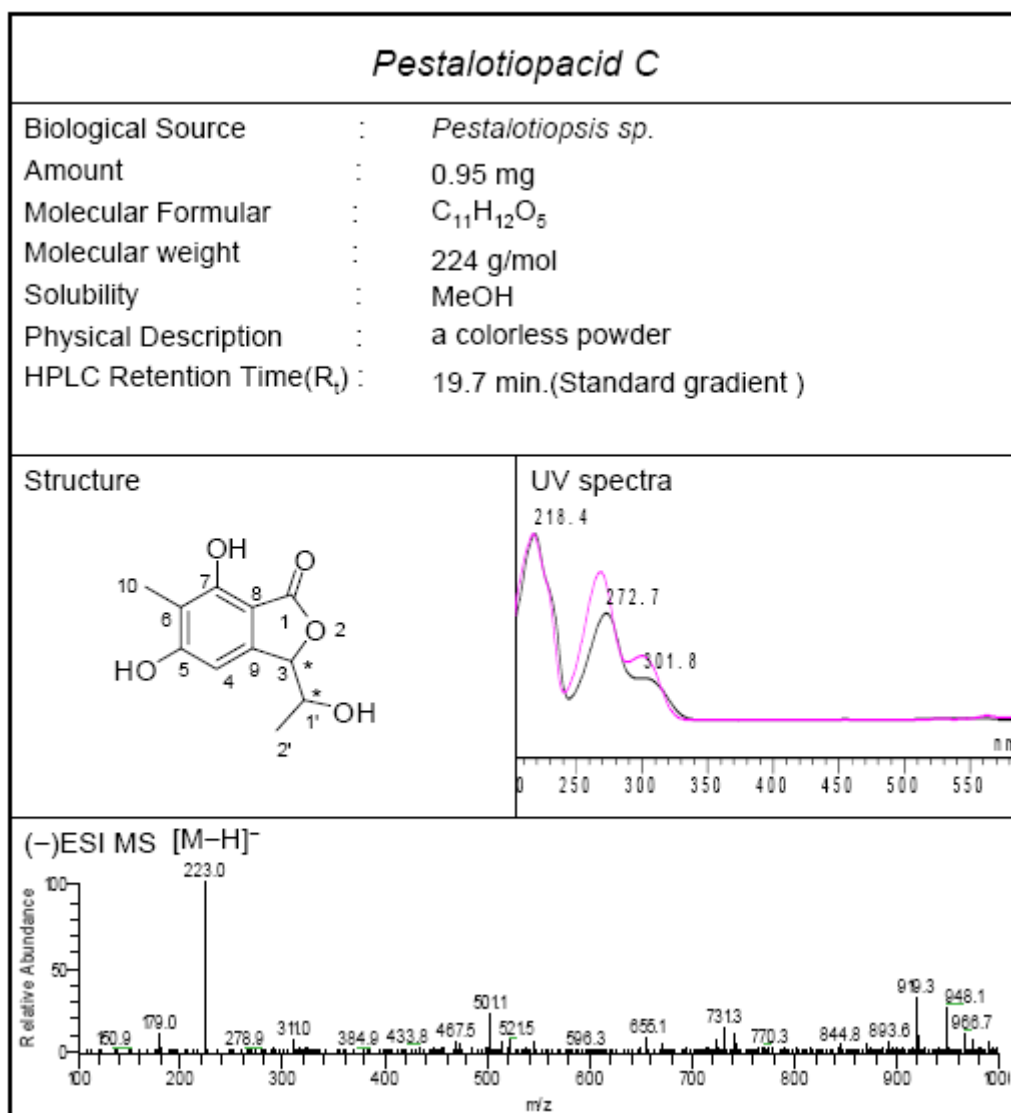


Figure 3.7.8.1 NOE correlations for compound 47

3.7.9 Pestalotilopacid C (48, new compound)



Pestalotilopacid C (**48**) shared the same molecular formula as those of **46** and **47**, as determined by the HR-ESIMS and NMR data. The ^1H and ^{13}C NMR data, and the ^1H - ^1H COSY and HMBC spectra of **48** (Table 3.7.9.1) indicated that this compound featured the same planar structure as that of **46**. The difference was attributed to the significant upfield shift of H-3 [δ_{H} 4.33, (d, $J = 2.25$ Hz), δ_{C} 79.5, d, H-3] and minor downfield shift of H-1' [δ_{H} 4.54, m, δ_{C} 67.9, d, CH-1'] and H-2' [δ_{H} 1.44, (d, $J = 6.35$ Hz), δ_{C} 16.0, d, 2'-CH₃], due to the different configuration of C-3 and C-1'. However, those configurations were not determined so far.

Table 3.7.9.1 ^1H NMR (500 MHz) and ^{13}C NMR (125 MHz) spectroscopic data for pestalotiopacid C (**48**) in CD_3OD

Atom no.	48		HMBC (H to C)	Comparison Compound 46	
	δ_{H} [ppm]	δ_{C} [ppm]		δ_{H} [ppm]	δ_{C} [ppm]
1		?			174.3, s
3	4.33, d, 2.25	79.5, d	1, 8, 9	5.26, d, 3.5	86.0, d
4	6.32, s	108.0, d	3, 5, 6, 8, 9	6.51, s	102.6, d
5		163.8, s			163.7, s
6		112.8, s			114.2, s
7		?			156.3, s
8		101.0, s			105.0, s
9		?			148.2, s
10	2.15, s	8.0, q	5, 6, 7	2.15, s	8.5, q
1'	4.54, m	67.9, d	3, 2'	4.13, m	68.9, d
2'	1.44, d, 6.35	16.0, q	3, 1'	1.20, d, 6.35	19.1, q

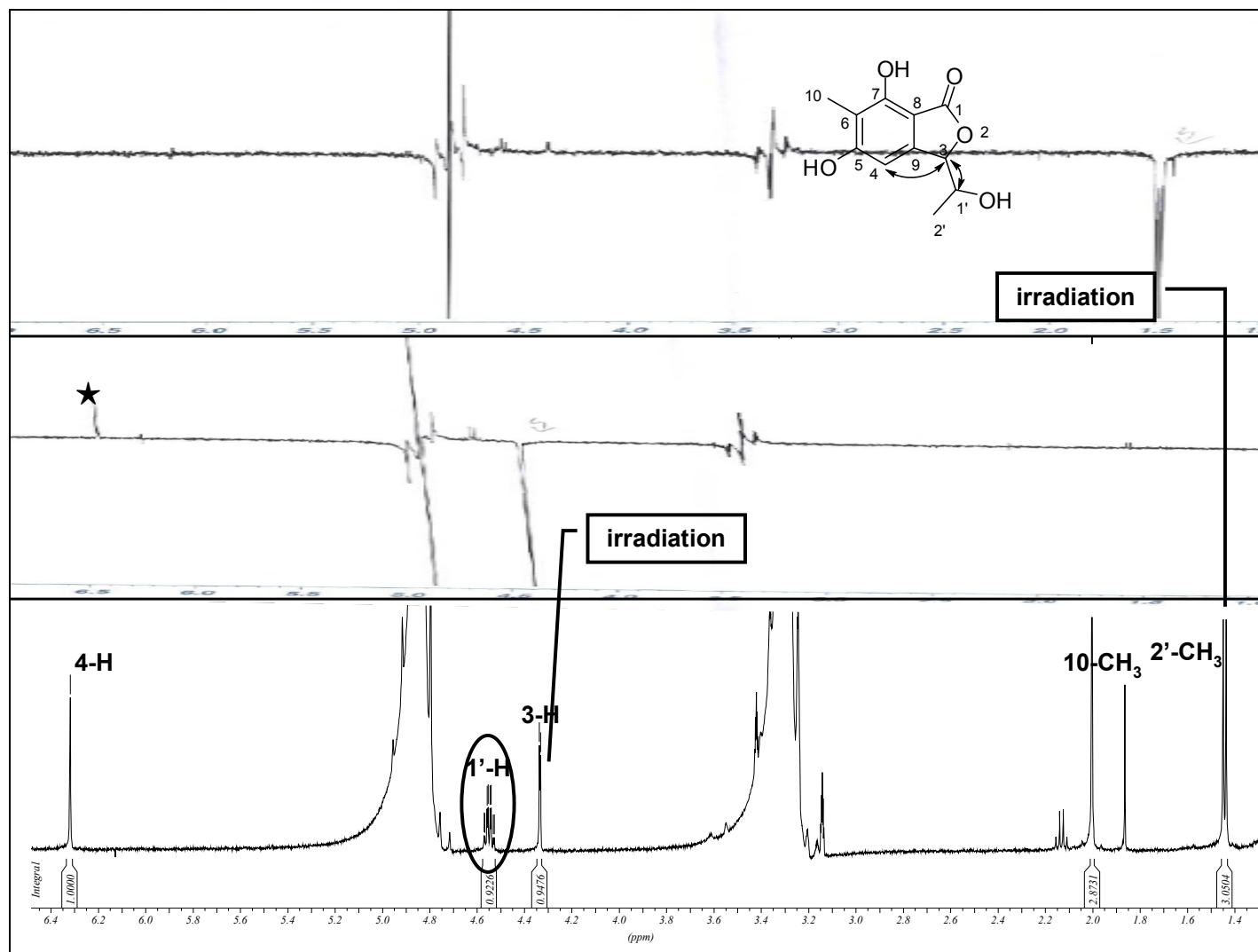


Figure 3.7.9.1 NOE correlations for compound 48

3.8 Biological Activities

The isolated secondary metabolites of *Pestalotiopsis* sp. were subjected to the several bioassays, such as cytotoxicity, antimicrobial and antifungal assays.

3.8.1 Cytotoxicity

Compounds **4-10** were evaluated for their cytotoxicity against the murine cancer cell line L5178 Y, and compounds **1-3, 11-23** were evaluated for their cytotoxicity against the murine cancer cell line L5178Y, and against the humane cell lines Hela and PC12 (Aly, A. H. *et al* 2008). However, in contrast to the previous report on its analogues (Xu, Q. *et al* 2004), only **23** showed a weak activity. The remaining compounds having not been previously investigated did not show any significant activity when tested at an initial concentration of 10 $\mu\text{g} / \text{mL}$. Pestalotiopsone F (**9**) exhibited moderate cytotoxicity with an EC_{50} value of 8.93 $\mu\text{g} / \text{mL}$. The results are shown in [Table 3.8.1.1](#).

Table 3.8.1.1 Cytotoxicity Assay results for **1-23***

Compound Code	Cell growth(%) of test cell lines at the respective concentration of substances			EC_{50} ($\mu\text{g} / \text{mL}$)
	L 5178Y	HeLa	PC12	
1	n.a	n.t	n.t	n.a
2	n.a	n.t	n.t	n.a
3	n.a	n.t	n.t	n.a
4	n.a	n.t	n.t	n.a
5	n.a	n.t	n.t	n.a
6	n.a	n.t	n.t	n.a
7	n.a	n.t	n.t	n.a
8	n.a	n.t	n.t	n.a
9	43.2%	n.t	n.t	8.93
10	n.a	n.a	n.a	n.a
11	n.a	n.a	n.a	n.a
12	n.a	n.a	n.a	n.a
13	n.a	n.a	n.a	n.a

14	n.a	n.a	n.a	n.a
15	n.a	n.a	n.a	n.a
16	n.a	n.a	n.a	n.a
17	n.a	n.a	n.a	n.a
18	n.a	n.a	n.a	n.a
19	n.a	n.a	n.a	n.a
20	n.a	n.a	n.a	n.a
21	n.a	n.a	n.a	n.a
22	n.a	n.a	n.a	n.a
23	n.a	n.a	n.a	n.a

* The assays were conducted by Prof. W. E. G. Müller at the Institute of Physiological Chemistry, University of Mainz

n.a = not active n.t = not tested

3.9 Tracing fungal metabolites in the host plant *Rhizophora mucronata* extract

In order to investigate the relationship between the endophytic *Pestalotiopsis* sp. and its host plant, the Chinese Mangrove *Rhizophora mucronata*, the crude 90% MeOH extract of the host plant *Pestalotiopsis* sp. was fractionated over Diaion HP20 and the obtained fractions were analyzed by LC/MS to detect the presence of the above identified fungal metabolites. Starting with the pure metabolites, the plant fractions were analyzed to presence of fungal metabolites and the obtained spectra were evaluated for matching of retention times, the presence of the molecular ions of the target compounds and patterns of MS and MS/MS.

The gradient of the fractionation of the crude extract of *R. mucronata* over Diaion HP-20 was as follows:

- 100% H₂O
- 80% H₂O: 20% MeOH
- 60% H₂O: 40% MeOH
- 40% H₂O: 60% MeOH

- 20% H₂O: 80% MeOH
- 100% MeOH
- 50% Acetone: 50% MeOH

All of the compounds isolated from *Pestalotiopsis* sp. were detected in the crude extract of this fungus. Most remarkably, pestalotiopene A and cytosporone M were also traced in subfractions of the extract of *Rhizophora mucronata* (see Table 3.8.1 and Figures 3.8.1-3.8.4), which is the host plant for the fungal strain.

Table 3.8.1 Compounds detected in the fractions of the *Rhizophora mucronata* extract

Compound	Subfraction
Pestalotiopene A	Twig 100%MeOH
Cytosporone M	Leaf40%MeOH, Leaf80%MeOH, Twig 40%MeOH, Twig 50%Acetone:50%MeOH

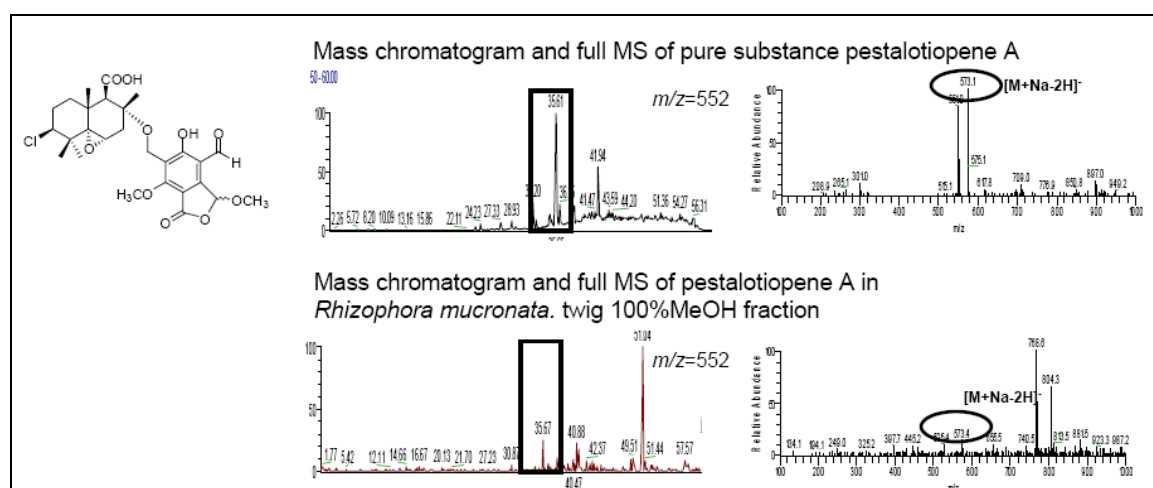


Figure 3.8.1 MS detection of pestalotiopene A

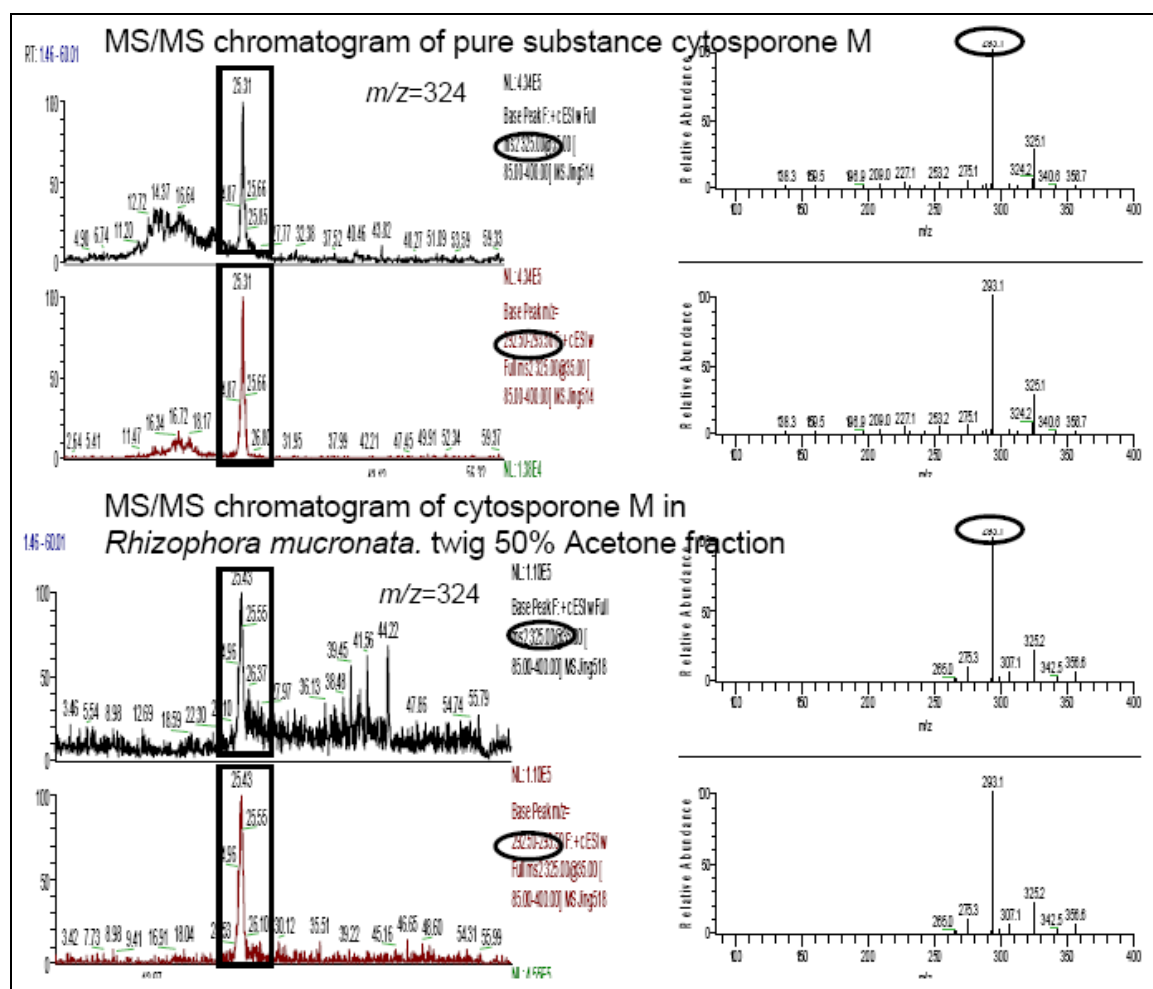


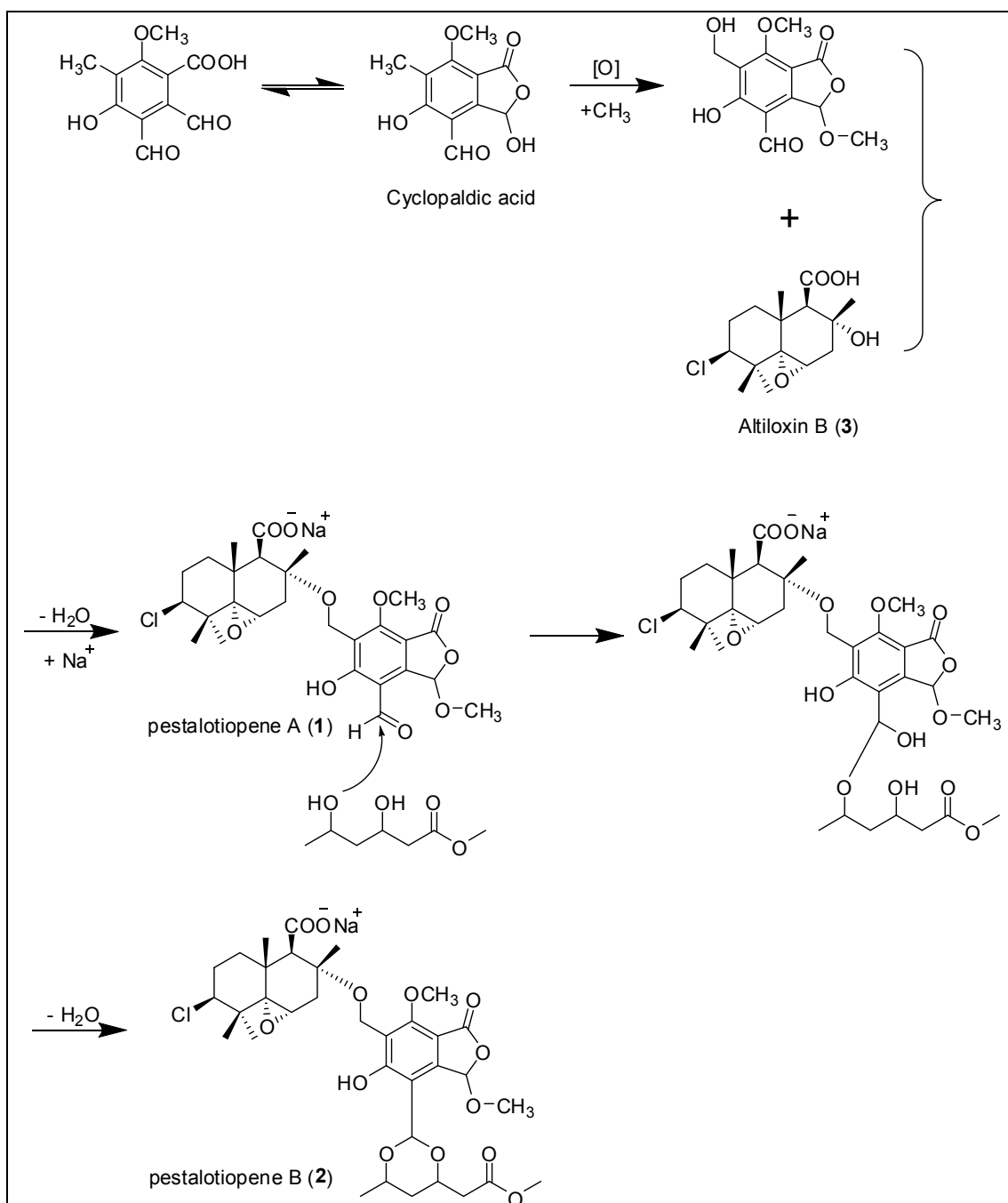
Figure 3.8.4 MS/MS detection of cytosporone M

4 DISCUSSION—Secondary Metabolites from *Pestalotiopsis* sp.

4.1 Possible joint biosynthetic origin of new sesquiterpene derivatives

(Pestalotiopenes A and B)

Pestalotiopenes A and B (**1** and **2**) constituted a novel type of natural products with an unprecedented hybrid carbon skeleton derived from a drimane-type sesquiterpene acid and a polyketide. Considering the moiety of the core structure of cyclopaldic acid in these compounds, the concurrence of cyclopaldic acid in the same endophytic fungal strain of *Pestalotiopsis* sp. intrigued us to think rationally about the intrinsic correlations between these two new compounds and the known altiloxin B (**3**). From the viewpoint of biosynthesis, it is suggested that altiloxin B (**3**), should occur before pestalotiopenes A and B, because the core skeleton of altiloxin B is still preserved in their structures. Scheme 1 shows the suggested mechanism, which is started with the oxidation of the methyl group of cyclopaldic acid on the position of C-11 to afford a hydroxylated cyclopaldic acid. Attack on the OH group at C-8 of altiloxin B followed by dehydration afforded pestalotiopene A. Finally, nucleophilic addition of two hydroxyl groups of methyl 3,5-dihydroxyhexanoate to the aldehyde group at C-10' of pestalotiopene A generates the most complicated compound, pestalotiopene B.



Scheme 4.1.1 Plausible biogenetic pathway for pestalitiopene A and B

4.2 Possible biosynthetic origin of chromones

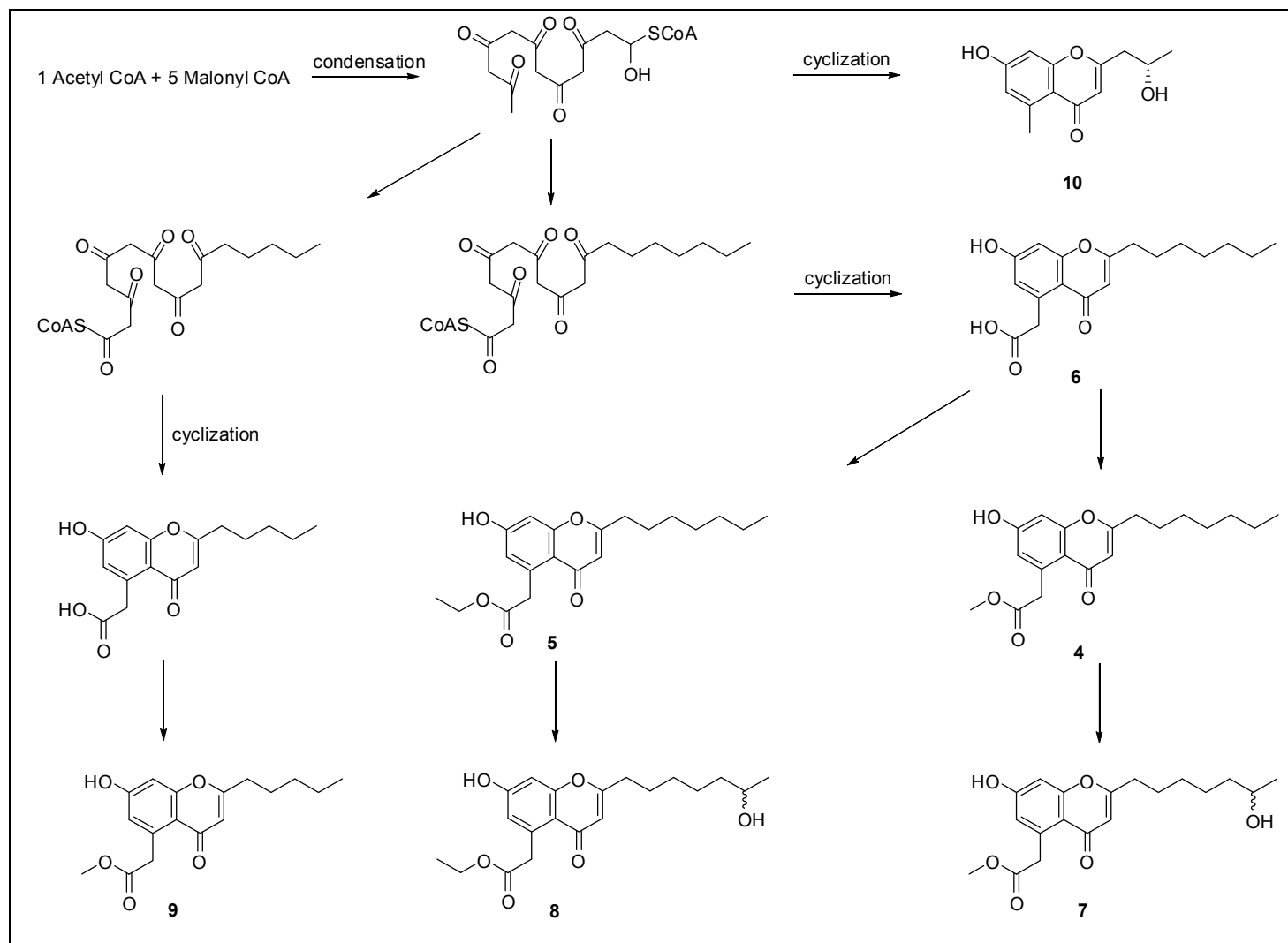
(Pestalotiopsones A-F, 5-carbomethoxymethyl-2-heptyl-7-hydroxychromone, **4-10**)

Pestalotiopsones A-F are new chromones featuring both an alkyl side chain substituted at C-2 and a free or esterified carboxyl group at C-5.

To our knowledge, these compounds belong to a rare subtype of chromones found in nature. Previously reported examples include 5-acetonyl-7-hydroxy-2-methylchromone and 5-carboxymethyl-7-hydroxy-2-methylchromone from medicinal rhubarb *Rhei Rhizoma* (*Rheum officinale*) (Kashiwada *et al.* 1984), and phaeochromycins D and E isolated from the soil actinomycete *Streptomyces phaeochromogenes* (Graziani *et al.* 2005).

Our chromones are proposed to be biosynthesized from C12 polyketide precursors. One molecule of acetyl-CoA condenses with five molecules of malonyl-CoA to give a polyhexanone, following by cyclization, thus yielding different chromone intermediates bearing an acetonyl at C-5 and alkyl side chain substituted at C-2.

The putative biogenetic pathway is proposed in [Scheme 4.2.1](#).

**Scheme 4.2.1** Putative biogenetic pathway for **4-10**

4.3 Possible biosynthetic origin of cytosporones

(Cytosporone J-N, Cytosporone C, Dothiorelone B)

Compounds with their carbon skeletons based on dihydroisocoumarin (McInerney *et al.* 1995) and dihydrocoumarin (Hoult *et al.* 1996) are commonly isolated natural products. However, very few compounds with their carbon skeletons based on isochroman-3-one derived from benzeneacetic acid (Murray *et al.* 1982) have been reported to date. (Figure 4.3.1)

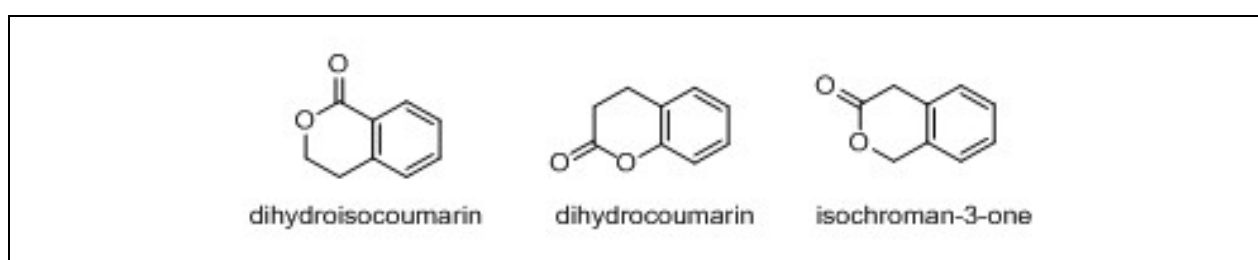


Figure 4.3.1 Basic biogenetic nucleus

Professor Clardy's group reported that the cytosporones (Brady *et al.* 2000) could be biosynthetically related to the popular fungal metabolites, curvularins (Birch *et al.* 1962) and macrolactone dihydroxybenzenes. Both curvularins and cytosporones are polyketides based on the skeleton of benzeneacetic acid. However, the former are produced by the closure at C-15 to give a 12-membered macrolactone ring and the latter at C-9 to give a six-membered lactone instead as seen in the structures of cytosporones C and D (Figure 4.3.2).

Chemical examination of the endophytic fungus, *Pestalotiopsis* sp., isolated from the leaves of the Chinese mangrove *Rhizophora mucronata*, yielded five new cytosporones, including cytosporones J-N (**11-13**, **15-16**), along with the known cytosporone C (**14**) and, dothiorelone B (**17**). Clearly, the acyclic derivatives **15** to **17** are closely related to the cyclized cytosporones **11** to **14**, and their probable biogenetic relationship is depicted and summarized in Scheme 4.3.1.

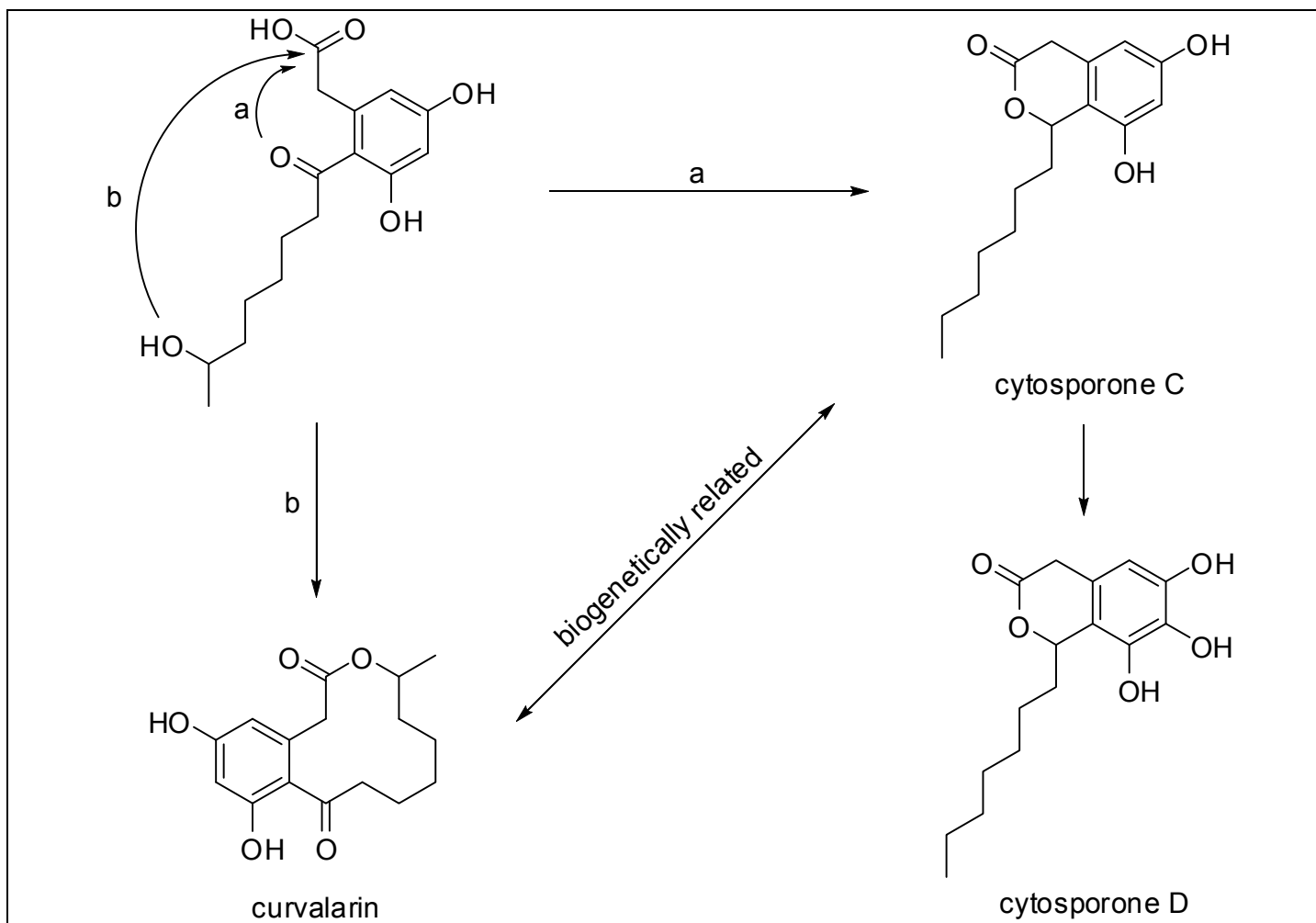
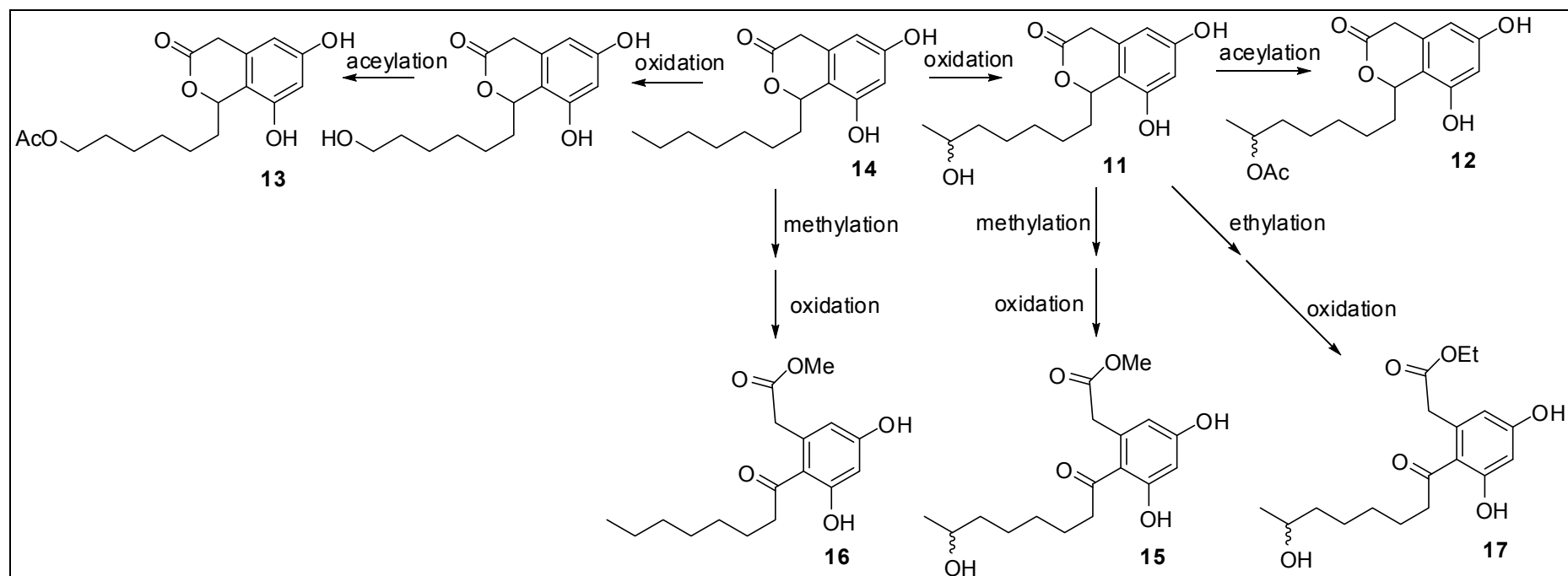
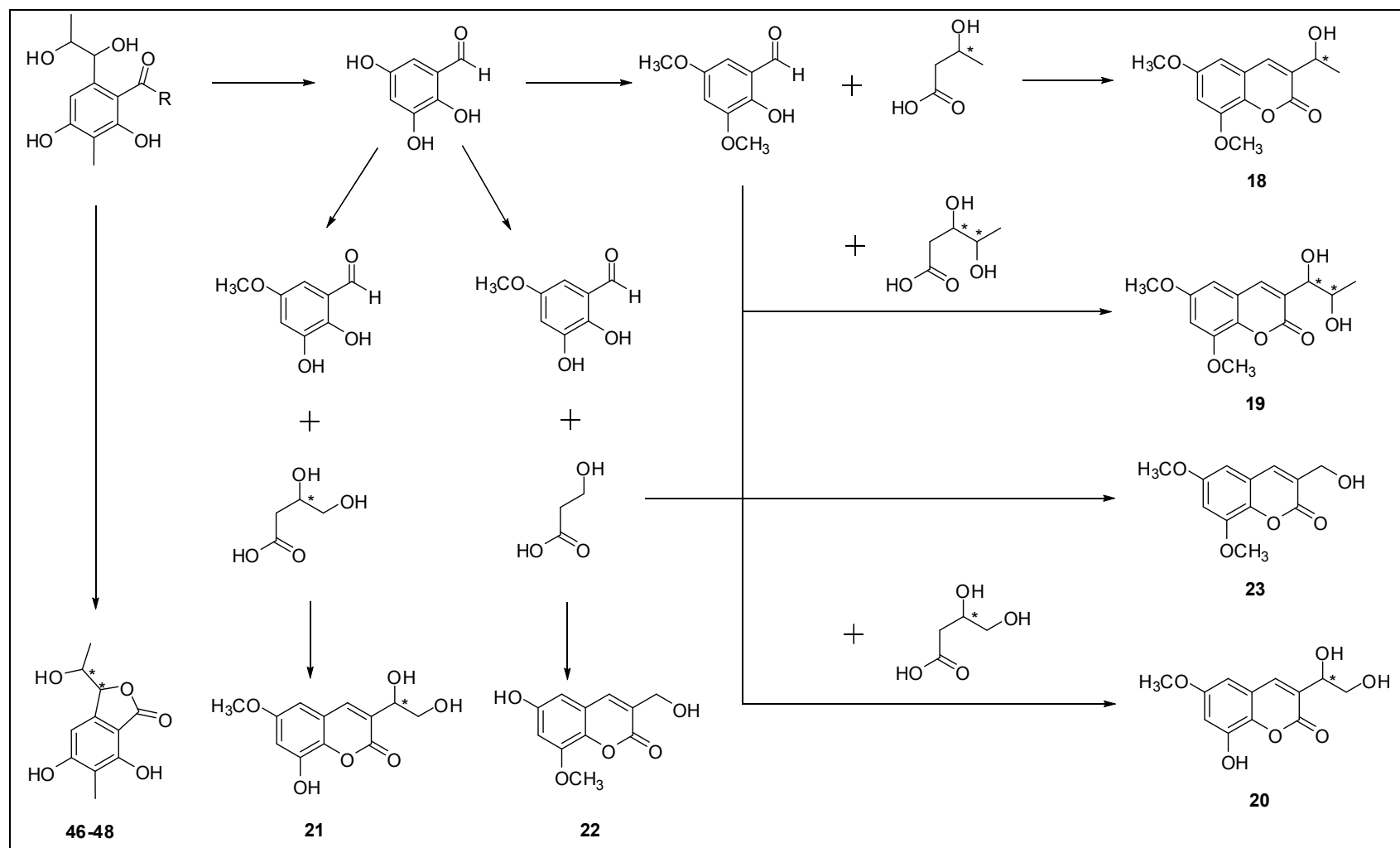


Figure 4.3.2 The carbon skeletons of cytosporones and curvularins are biosynthetically linked by a hypothetical intermediate similar to cytosporone A

Scheme 4.3.1 Proposed biogenetic relationship for cytosporones **11-17**

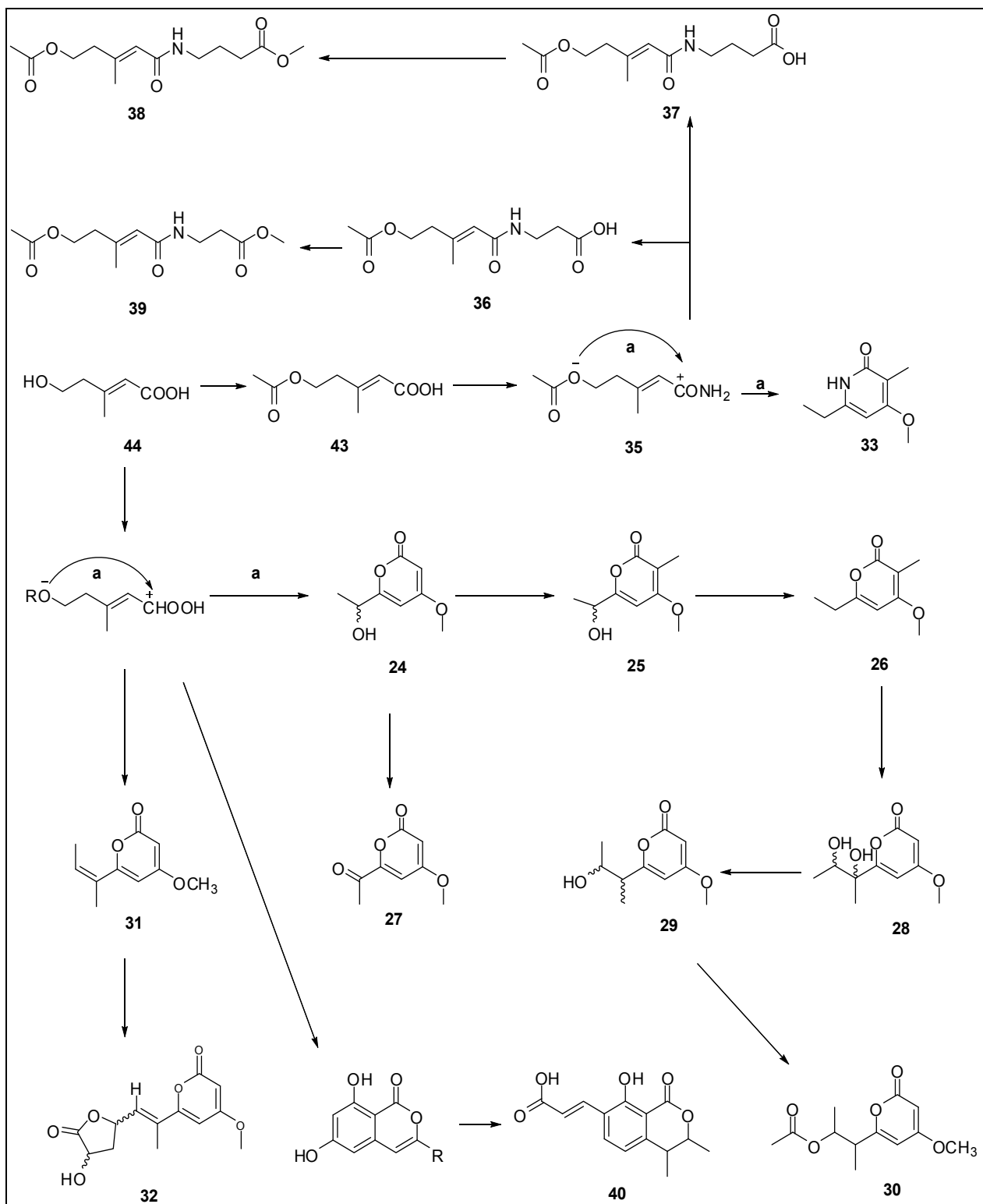
4.4 Possible biosynthetic origin of coumarins and cyclopaldic acid derivatives (Pestalotiopsins A-E, 3-Hydroxymethyl-6,8-dimethoxycoumarin, Pestalotiopacid A-C)

Isocoumarins are quite popular secondary metabolites from endophytic fungi. However, coumarin derivatives are rarely reported from endophytic fungi. Their biosynthetic pathways are shown in [Scheme 4.4.1](#).

Scheme 4.4.1 Proposed biogenetic relationship between coumarins and the derivatives of cyclopaldic acid

4.5 Possible biosynthetic origin of alkaloids, pyrones and isocoumarins (Pestalotiopamide A-E, Pestalotiopin A, 2-anhydromevalonic acid, Pestalotiopyrones A-H and Nigrosporapyrone D)

According to the biogenetic viewpoint from literature, β -polyketone carboxylic acids are supposed to be converted into the corresponding pyrones and isocoumarins under enzymatic cyclization (Lai *et al.*, 1991). From the ethyl acetate extract of the endophytic fungus, *Pestalotiopsis* sp., five new amides pestalotiopamides A-E (**35-39**), one new pyridine alkaloid pestalotiopyridine (**33**), one new and one known aliphatic chain ester pestalotiopin A (**43**), 2-anhydromevalonic acid (**44**), eight new pyrone derivatives pestalotiopyrones A-H (**24-26**, **28-32**), one new dihydroisocoumarin pestalotiopisorin A (**40**) and the known nigrosporapyrone D (**27**) were identified. Their biosynthetic pathways are proposed as shown in [Scheme 4.5.1](#).



Scheme 4.5.1 Proposed biogenetic relationship among alkaloids, pyrones and isocoumarins

4.6 Hypothesis about the relationship between the endophytic fungus *Pestalotiopsis* sp. and its host plant *Rhizophora mucronata*

Relationships between endophytes and their host plants are proposed to range from latent phytopathogenesis to mutualistic symbiosis (Strobel *et al.* 1998).

However, very few experiments have been done to evaluate the hypotheses about the relationship between the endophyte and its host plant. Some hypotheses about the relationship between the endophytic fungus *Pestalotiopsis* sp. and its host plant, *Rhizophora mucronata*, are established based on the pure compounds, pestalotiopene A and cytosporone M, which were obtained from the fungus *Pestalotiopsis* sp. and could also be detected in the extract of the host plant *Rhizophora mucronata* and its subfractions.

·Pestalotiopene A: a metabolite is produced by collaboration of the endophyte and its host ?

During the long co-evolution of the phytopathogen and its host plant, an endophytic mutant may result from the balanced antagonism and/or gene mutation. Further investigation led to the development of a hypothesis that the endophyte–host interaction could be a balanced pathogen–host antagonism (Tan *et al.* 2001).

Pestalotiopene A was proposed to be biosynthesized from two precursors with the origin of phytotoxic fungus, altiloxin B and cyclopaldic acid, which were previously isolated from culture of filtrate of *Phoma asparagi* Sacc and *Seiridium*

cupressi. The former is the causal fungus of stem blight disease on asparagus and the latter is the pathogen of a canker disease of cypress. To reach pathogen–host balance, the host plant *Rhizophora mucronata* may antagonize the pathogenic endophytic fungus, *Pestalotiopsis* sp., by facilitating the biosynthesis of pestalotiopene A, which was derived from two phytotoxins, altiloxin B and cyclopaldic acid.

·Pestalotiopene A is a metabolite only produced by the endophyte. But it could be accumulated and utilized by the host ?

Presumably, the host plant provides the essential nutrition to the endophyte and in turn the endophyte produces bioactive substances to enhance the growth, self-defense and/or competitiveness of its host plant. *Rhizophora mucronata* is generally found along the coastline of tropical and subtropical regions. Five basic requirements for the development of mangrove plants are:

- (1) tropical temperature;
- (2) fine grained alluvium soil;
- (3) low wave and tidal action;
- (4) salt water;
- (5) large tidal range.

To our knowledge, most land plants are killed by salt. But mangroves are able to filter it out. It was hypothesized that endophytes inside mangroves could produce related secondary metabolites to improve the resistance of the host plants

against the environmental stress, such as high salinity . Pestalotiopene A, a chlorinated metabolite obtained from the endophytic fungus, *Pestalotiopsis* sp., may be a pivotal compound for *Rhizophora mucronata* to remove the sodium chloride from the salt water in order to complete its life cycle and enhance the host's ecological adaptability.

5 SUMMARY

Mangrove endophytic fungi, a special kind of poorly-studied microorganisms, are known as a new reservoir for the production of bioactive metabolites today. Some endophytes yield small molecules with unique structures and notable bioactivities, and these findings will continue to drive the research of chemical characterization and biological evaluation in this field

The aim of this work is to obtain and identify the secondary metabolites from the interesting fungus, *Pestalotiopsis* sp., being an endophyte within the leaves of the Chinese Mangrove plant, *Rhizophora mucronata*., and to examine their pharmacological potential, and utilize them to disclose the host–microbe relationship. The fungus was continuously grown on solid rice medium at room temperature under static conditions for 39 days and its ethyl acetate extract was then subjected to various separation methods to obtain its secondary metabolites.

The structure elucidation was mainly performed using mass spectrometry (MS) and nuclear magnetic resonance (NMR) experiments. The former was used to determine the molecular weight of the obtained metabolites and the latter is applied to identify their structures. Moreover, quantum chemical CD calculations were employed for the determination of the absolute configuration of selected chiral compounds. Most of the isolated compounds were subjected to various bioassays, such as cytotoxic, antimicrobial and antifungal assays.

Pestalotiopenes A and B (**1-2**), two unprecedented compounds with new carbon skeleton, were obtained from the endophytic fungus, *Pestalotiopsis* sp., together with

the known phytotoxin, altiloxin B (**3**). The structures of the above mentioned three metabolites were unambiguously identified by spectroscopic methods and quantum chemical CD calculations.

Six new chromones named pestalotiopsones A-F (**4-9**), having both an alkyl side chain substituted at C-2 and a free or substituted carboxyl group at C-5, were successfully characterized from this fungus, together with the known derivative, 7-hydroxy-2-(2-hydroxypropyl)-5-methylchromone (**10**). Compound **9** exhibited moderate cytotoxicity against the murine cancer cell line L5178Y with an EC₅₀ value of 8.93 μg / mL.

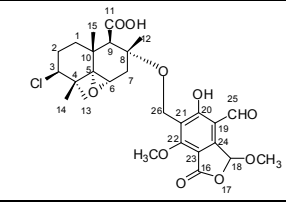
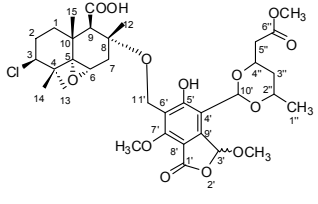
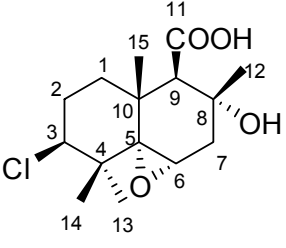
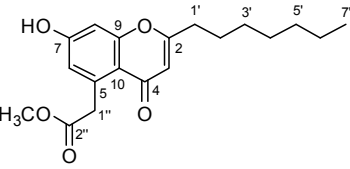
Continued chemical investigation of the minor components from the extract of the fermentation of the fungus on solid rice medium afforded a series of compounds, including five new cytosporones, cytosporones J-N (**11-13**, **15-16**), five new coumarins, pestalasins A-E (**18-22**), and a new alkaloid named pestalotiopsoid A (**34**), along with the known compounds, cytosporone C (**14**), dothiorelone B (**17**), and 3-hydroxymethyl-6,8-dimethoxycoumarin (**23**).

Further analysis of the minor metabolites from the cultivation of the fungus on solid rice medium further yielded twenty-five metabolites, which included twenty-three new natural products and highlighted the biosynthetic potential of this endophyte. The new metabolites are mainly polyketides, including pyrone derivatives (**24 – 31**), depsidones (**41**, **42**), long chain aliphatic amide compounds (**35 – 39**), and three cyclopaldic acid derivatives, pestalotilopacid A-C (**46-48**). The bioassays

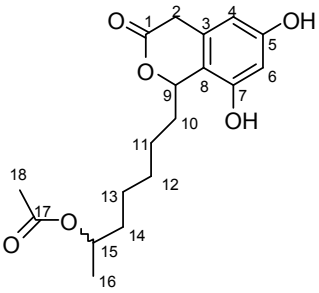
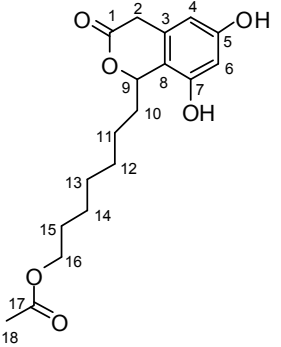
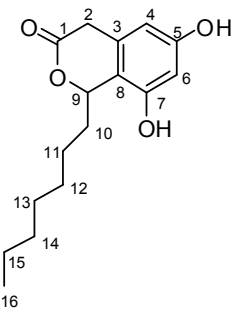
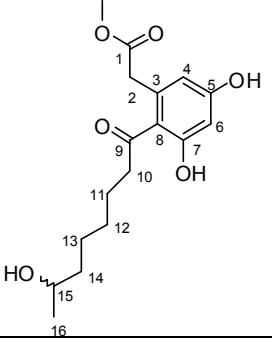
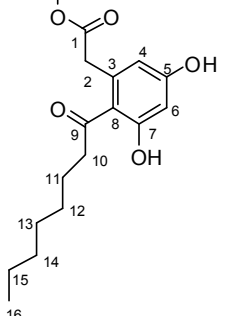
indicated that compound **1** exhibited moderate antimicrobial activity and compound **9** exhibited weak cytotoxicity.

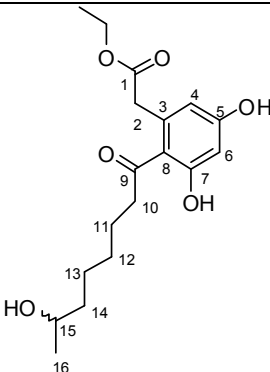
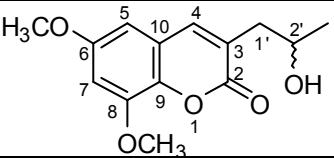
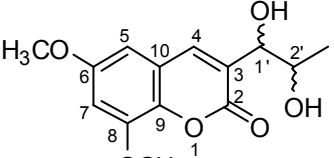
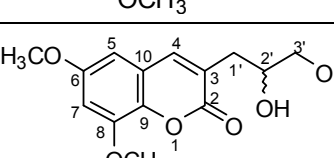
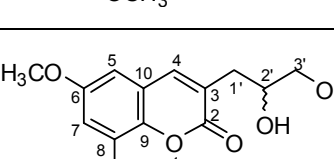
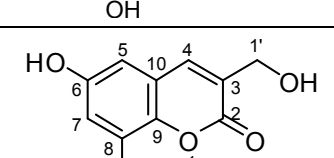
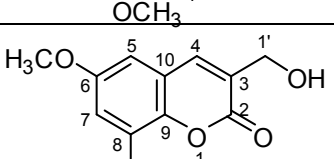
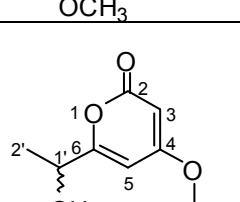
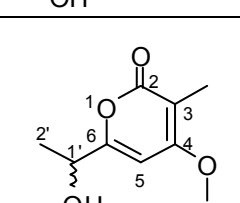
In summary, forty-eight compounds were successfully identified from the endophyte in this study. To the best of our knowledge, forty was new compounds, including two compounds with new carbon skeletons ([Table 5.1](#)). In this thesis, the discussion was mainly focused on the proposed biosynthetic pathways for different types of structures. In addition, the relationship between the endophytic fungus, *Pestalotiopsis* sp., and the host plant *Rhizophora mucronata*, was also hypothesized.

Table 5.1 Summary of the Identified Secondary Metabolites

Compound Code	Structure	Name	Weight mg	Origin	Comment
1		Pestalotiopene A	3.4 mg	<i>Pestalotiopsis</i> sp.	Novel
2		Pestalotiopenes B	3.0 mg	<i>Pestalotiopsis</i> sp.	Novel
3		Altioxin B	4.94 mg	<i>Pestalotiopsis</i> sp.	Known
4		Pestalotiopsone A	1.18 mg	<i>Pestalotiopsis</i> sp.	New

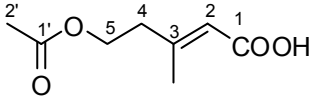
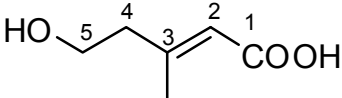
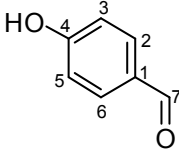
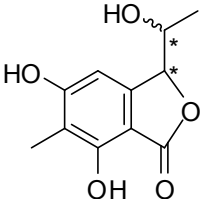
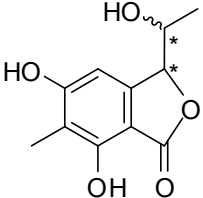
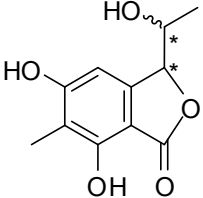
5		Pestalotiopsone B	0.67 mg	<i>Pestalotio psis sp.</i>	New
6		Pestalotiopsone C	2.67 mg	<i>Pestalotio psis sp.</i>	New
7		Pestalotiopsone D	1.08 mg	<i>Pestalotio psis sp.</i>	New
8		Pestalotiopsone E	0.26 mg	<i>Pestalotio psis sp.</i>	New
9		Pestalotiopsone F	1.0 mg	<i>Pestalotio psis sp.</i>	New
10		2-(2'-hydroxypropyl)-5-methyl-7-hydroxy-chromone	0.19 mg	<i>Pestalotio psis sp.</i>	Known
11		Cytosporone J	1.09 mg	<i>Pestalotio psis sp.</i>	New

12		Cytosporone K	0.76 mg	<i>Pestalotia psis sp.</i>	New
13		Cytosporone L	0.66 mg	<i>Pestalotia psis sp.</i>	New
14		Cytosporone C	3.48 mg	<i>Pestalotia psis sp.</i>	Known
15		Cytosporone M	0.30 mg	<i>Pestalotia psis sp.</i>	New
16		Cytosporone N	0.90 mg	<i>Pestalotia psis sp.</i>	New

17		Dothiorelone A	0.82 mg	<i>Pestalotia psis sp.</i>	Known
18		Pestalotiopsin A	2.45 mg	<i>Pestalotia psis sp.</i>	New
19		Pestalotiopsin B	0.33 mg	<i>Pestalotia psis sp.</i>	New
20		Pestalotiopsin C	1.38 mg	<i>Pestalotia psis sp.</i>	New
21		Pestalotiopsin D	0.30 mg	<i>Pestalotia psis sp.</i>	New
22		Pestalotiopsin E	0.79 mg	<i>Pestalotia psis sp.</i>	New
23		3-hydroxymethyl-6,8-dimethoxycoumarin	1.92 mg	<i>Pestalotia psis sp.</i>	Known
24		Pestalotiopyrone A	1.03 mg	<i>Pestalotia psis sp.</i>	New
25		Pestalotiopyrone B	3.87 mg	<i>Pestalotia psis sp.</i>	New

26		Pestalotiopyrone C	1.96 mg	<i>Pestalotio psis sp.</i>	New
27		Nigrosporapyone D	1.32 mg	<i>Pestalotio psis sp.</i>	Known
28		Pestalotiopyrone D	0.66 mg	<i>Pestalotio psis sp.</i>	New
29		Pestalotiopyrone E	16.29 mg	<i>Pestalotio psis sp.</i>	New
30		Pestalotiopyrone F	0.35 mg	<i>Pestalotio psis sp.</i>	New
31		Pestalotiopyrone G	18.99 mg	<i>Pestalotio psis sp.</i>	New
32		Pestalotiopyrone H	6.2 mg	<i>Pestalotio psis sp.</i>	New
33		Pestalotiopyridine	0.74 mg	<i>Pestalotio psis sp.</i>	New
34		Pestalotiopsoid A	0.86 mg	<i>Pestalotio psis sp.</i>	New

35		Pestalotiopamide A	7.84 mg	<i>Pestalotio psis sp.</i>	New
36		Pestalotiopamide B	3.26 mg	<i>Pestalotio psis sp.</i>	New
37		Pestalotiopamide C	2.06 mg	<i>Pestalotio psis sp.</i>	New
38		Pestalotiopamide D	0.37 mg	<i>Pestalotio psis sp.</i>	New
39		Pestalotiopamide E	0.6 mg	<i>Pestalotio psis sp.</i>	New
40		Pestalotiopisorin A	1.22 mg	<i>Pestalotio psis sp.</i>	New
41		pestalotiollide A	6.99 mg	<i>Pestalotio psis sp.</i>	New
42		pestalotiollide B	11.55 mg	<i>Pestalotio psis sp.</i>	New

43		Pestalotiopin A	2.6 mg	<i>Pestalotio psis sp.</i>	New
44		2-anhydromevalonic acid	0.99 mg	<i>Pestalotio psis sp.</i>	New
45		p-hydroxy benzaldehyde	3.47 mg	<i>Pestalotio psis sp.</i>	Known
46		Pestalotiopacid A	1.53 mg	<i>Pestalotio psis sp.</i>	New
47		Pestalotiopacid B	6.54 mg	<i>Pestalotio psis sp.</i>	New
48		Pestalotiopacid C	0.95 mg	<i>Pestalotio psis sp.</i>	New

6 REFERENCE

- Achenbach, H., Mühlenfeld, A., Brillinger, G. U. *Liebigs Ann. Chem.* **1985**, 1596-1628.
- Agarwal, A.K., Chauhan, S. *Indian Phytopathology*. **1988**, *41*, 625-627.
- Aly, A. H.; Edrada-Ebel RA; Indriani, I. D.; Wray, V.; Mueller, W. E. G.; Totzke, F., Zirrgebel, U; Schaechtele, C; Kubbutat, M/ H. G.; Lin W. H.; Proksch, P.; Ebel R.. *J. Nat. Prod.*, **2008**, *71*, 972-980.
- Bayman, P., Angulo-Sandoval, P., Baez-Ortiz, Z. and Lodge, D.J. *Mycological Research*. **1998**, *102*, 944-948.
- Beistel D. W., Edwards W. D. *J. Phys. Chem.* **1976**, *80*, 2023- 2027.
- Birch, A. J.; Moore, B.; Rickards, R. W. *J. Chem. Soc.* **1962**, 220-222.
- Brady, S. F.; Wagenaar, M. M.; Singh, M. P.; Janso, J.E.; Clardy, J. *Org. Lett.* **2000**, *2*, 4043-4046.
- Cannon P. F.; Simmons C. M. *Mycologia*, **2002**, *94*, 210-220.
- Caruso, M., Colombo, A. L., Fedeli, L., Pavesi, A., Quaroni, S., Saracchi, M., Ventrella, G. *Ann. Microbiol.*, **2000**, *50*, 3.
- Crawley, G. *J. Chem Soc., Perkin Trans. I* **1981**, *59*, 221-223.
- Deyrup, S. T., Swenson, D. C., Gloer, J. B., Wicklow, D. T.. *J. Nat. Prod.* **2006**, *69*, 608- 611.
- Ding,G., Jiang, L. H., Guo, L. D., Chen, X. L., Zhang, H., Che, Y. S. *J. Nat. Prod.* **2008**,
- Ding, G., Liu, S. C., Guo, L. D., Zhou, Y. G., Che, Y. S. *J. Nat. Prod.* **2008**, *71*, 615-618.
- Ding, G., Li, Y., Fu, S., Liu, S. C., Wei, J. C., Che, Y. S. *J. Nat. Prod.*, **2009**, *72*, 182-186.

- Ding, G., Zheng, Z. H., Liu, S. C., Zhang, H., Guo, L. D., Che, Y. S. *J. Nat. Prod.*, **2009**, dio 10.1021/np900084d.
- Duke, J.A. and Wain, K.K. 1981. Medicinal plants of the world. Computer index with more than 85,000 entries. 3 vols.
- Foster, C. A., Dreyfuss, M., Mandak, B., Merngassner, J. G., Naegeli, H. U., Nussbaumer, A., Oberer, L., Schell, G., Swoboda, E. M. *J. Dermatol.* **1994**, *21*, 847-854.
- Gangadevi, V., Murugan, M., Muthumary, J. *Chin J. of Biotech.*, **2008**, *24*, 1433-1438.
- Graniti, A., Sparapano, L. *Plant Pathology*, **1992**, *41*, 563- 568.
- Graziani, E. I.; Ritacco, F. V.; Bernan, V. S.; Telliez, J.-B. *J. Nat. Prod.*, **2005**, *68*, 1262-1265.
- Harper, J. K., Arif, A. M., Ford, E. J., Strobel, G. A., Porco, J. A., Tomer, J. D. P., Oneill, K. L., Herder, EL M., Grant, D. M. *Tetrahedron*, **2003**, *59*, 2471- 2476.
- Holmes, F. A., Kudelka, A. P., Kavanagh, J. J., Huber, M. H., Ajani, J. A., Valero, V. *ACS Symposium Series 583, American Chemical Society, Washington, DC*, **1995**, 31.
- Hommel, U., Weber, H. P., Oberer, L., Naegeli, H. U., Oberhauser, B., Foster, C. A. *FEBS Letters*, **1996**, *379*, 69-73.
- Hopkins, K. E., McQuilken, M. P. *Eur. J. Plant Pathol.* **2000**, *106*, 77-85.
- Hoult, J. R. S.; Paya, M. *Gen. Pharmacol.* **1996**, *27*, 713-722.
- Ichihara, A., Sawamura, S., Sakamura, S. *Tetrahedron Letters*, **1984**, *24* (30), 3209-3212.
- Ichihara, A., Sakamura, S., Kawakami Y. *Tetrahedron Letters*, **1986**, *27* (1), 61-64.
- Japan. Pat.*, **1995**, 95109299, *CA*, 123,110270d.

- Jeewon R., Liew E. C. Y., Simpson J. A., Hodgkiss, I. J., Hyde K. D. *Molecular Phylogenetics and Evolution*, **2003**, 27, 372- 383.
- Kang, J.C., Kong, R.Y.C., Hyde, K.D. *Fung. Divers.* **1998**, 1, 147–157.
- Kashiwada, Y.; Nonaka G.-I.; Nishioka I. *Chem. Pharm. Bull.*, **1984**, 32, 3493-3500.
- Kang, J.C., Hyde, K.D., Kong, R.Y.C. *Mycol. Res.* **1999**, 103, 53–64.
- Keith, L. M., Velasquez, M. E., Zee, F. T.. *Plant Dis.* **2006**, 90, 16- 23.
- Kimura, Y., Kouge, A., Nakamura, K., Koshino, H., Uzawa, J., Fujikoka, S., Kawano, T. *Biosci. Biotechnol. Biochem.*, **1998**, 62(8), 1624- 1626.
- Kohlmeyer, J., Volkmann-Kohlmeyer, B. *Botanica Marina*. **2001**, 44, 147-156.
- Lai, S., Shizuri, Y., Yamamura, S., Kawai, K., and Furukawa, H. *Heterocycles*, **1991**, 32(2), 297-305.
- Lee, J. C., Yang, X. S., Schwartz, M., Strobel, G., Clardy, J. *Chem. Biol.*, **1995**, 2(11), 721- 727.
- Lee, J. C., Strobel, G. A., Lobkovsky, E., Clardy, J. *J. Org. Chem.* **1996**, 61, 3232-3233.
- Li, E. W., Jiang, L. H., Guo, L. D., Zhang, H., Che, Y. S.. *Bioorg. Med. Chem.* **2008**, 16, 7894- 7899.
- Li, E. W., Tian, R., Liu, S. C., Chen, X. L., Guo, L. D., Che, Y. S. *J. Nat. Prod.* **2008**, 71, 664- 668.
- Li, J. Y., Harper, J. K., Grant, D. M., Tombe, B. O., Bashyal, B., Hess, W. M., Strobel, G. A. *Phytochemistry*, **2001**, 56, 463- 468.
- Li, J. Y., Strobel, G.A., Sidhu, R., Hess, W. M., Ford, F. J. *Microbiology*, **1996**, 142, 2223-2226.
- Li, J. Y., Strobel, G. A. *Phytochemistry*, **2001**, 57, 261- 265.

- Liu, L., Liu, S. C., Jiang, L. H., Chen, X. L., Guo, L. D., Che, Y. S. *Organic Letters*, **2008**, *10*(7), 1397- 1400.
- Liu, L., Tian, R. R., Liu, S. C., Chen, X. L., Guo, L. D., Che, Y. S.. *Bioorg. Med. Chem.* **2008**, *16*, 6021- 6026.
- Liu, L., Li, Y., Liu, S. C., Zheng, Z. H., Chen, X. L., Zhang, H., Guo, L. D., Che, Y. S. *Organic Letters*, **2009**, *11*(13), 2836- 2839.
- Liu, L., Tian, R. R., Liu, S. C., Chen, X. L., Guo, L. D., Che, Y. S. *Bioorg. Med. Chem.* **2009**.
- Liu A. R., Wu, X. P., Xu T. *Chin. J. Appl. Ecol.* **2007**, *18*, 912- 918.
- Magnani, R. F., Rodrigues-Fo, E., Daolio, C., Ferreira, A. G., Souza, A. Q. L. Z. *Naturforsch*, **2003**, *58c*, 319-324.
- McInerney, B. V.; Taylor, W. C. *Stud. Nat. Prod. Chem.* **1995**, *15*, 381-422.
- Murray, R. D. H.; Mendez, J.; Brown, S. A. *The natural coumarins: occurrence, chemistry, and biochemistry*; Wiley: London, **1982**.
- Nagata, T., Ando Y. *Agric. Biol. Chem.*, **1989**, *53*(10), 2811.
- Nagata, T., Ando, Y., Hirota, A. *Biosci. Biotech. Biochem.*, **1992**, *56*(5), 810- 811.
- Nicolaou, K. C., Yang, Z., Liu, J. J., Ueno, H., Nantermet, P. G., Guy, P. K., Claiborne, C. F., Renaud, J., Couladouros, E. A., Paulvannan, K., Sorensen, E. J. *Nature*, **1994**, *367*, 630.
- Ogawa, T., Ando, K., Aotani, Y., Shinoda, K., Tanaka, T., Tsukuda, E., Yoshida, M., Matsuda Y. *The Journal of Antibiotics*, **1995**, *48*(12), 1401-1406.
- Okane, I., Nagagiri, A. and Ito, T. *Canadian Journal of Botany*. **1998**, *76*, 657-663.
- Osono, T., Takeda, H. *European Journal of Soil Biology*. **1999**, *35*, 51-56.
- Perry, L.M. 1980. Medicinal plants of east and southeast Asia. MIT Press, Cambridge.

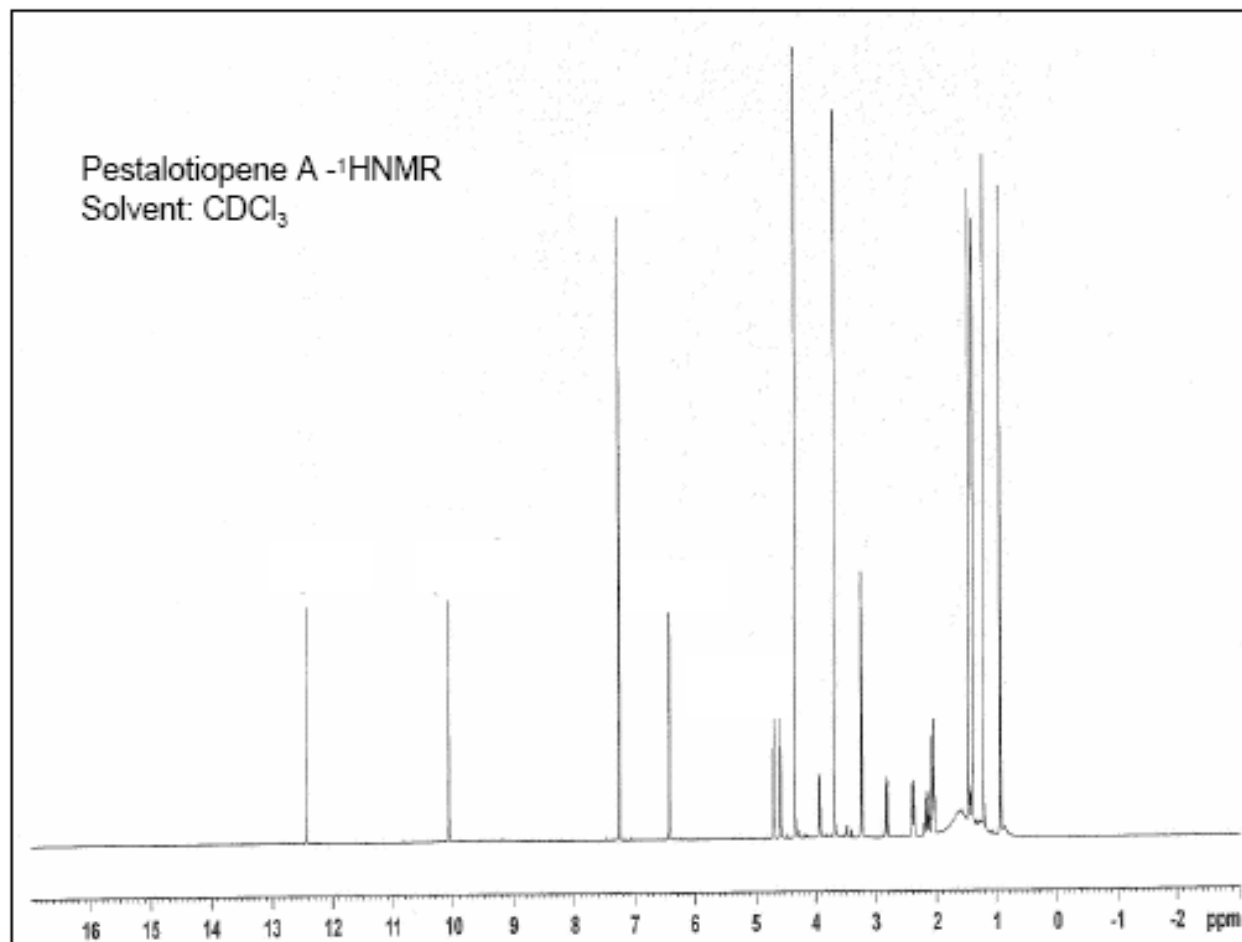
- Pulici, M., Sugawara, F., Koshino, H., Uzawa, J., Yoshida, S. *Phytochemistry*, **1997**, 46(2), 313- 319.
- Pulici, M., Sugawara, F., Koshino, H., Uzawa, J., Yoshida, S., Lobkovsky, E., Clardy, J. *J. Org. Chem.* **1996**, 61, 2122- 2124.
- Pulici, M., Sugawara, F., Koshino, H., Uzawa, J., Yoshida, S., Lobkovsky, E., Clardy, J. *J. Nat. Prod.* **1996**, 59, 47- 48.
- Qiu, D. Y., Huang, M. J., X. H. Fang, C. Zhu and Z. Q. Zhu, *Acta Mycol. Sinica.* **1994**, 13, 314.
- Shimada, A., Takahashi, I., Kawano, T., Kimura, Y. *Z. Naturforsch*, **2001**, 56b, 797- 803.
- Schulz, B.; Boyle, C.; Draeger, S.; Rommert, A. K.; Krohn, K. *Mycol. Res.* **2002**, 106, 996-1004.
- Steyaert, R.L. *Bull. Jard. Bot. EEtat Bruxelles.* **1949**, 19, 285–354.
- Steyaert, R.L. *Nuovo Gior. Bot. Ital.* **1953**, 60, 943–947.
- Stierle, A., Strobel G., Stierle D. *Science*, **1993**, 260, 214-216.
- Stierle, A., Strobel, G., Stierle, D., Grothaus, P., Bignami, G. *J. Nat. Prod.*, **1995**, 58, 1315.
- Strobel, G. A. *Can. J. Plant Pathol*, **2002**, 24,14-20.
- Strobel G.; Daisy B.; Castillo U., Harper J. *J. Nat. Prod.* **2004**, 67: 257-268.
- Strobel, G. A., Ford, E., Worapong, J., Harper, J. K., Arif, A. M., Grant, D. M., Fung, P. C. W., Chau, R. M. W. *Phytochemistry*, **2002**, 60, 179- 183.
- Strobel, G. A., Hess, W. M., Ford, E. J., Siduhu, R. S., Yang, X. *J. Ind. Microbiology*, **1996a**, 17, 417- 423.
- Strobel, G., Hess, W. M., Li, J.Y., Ford, E., Sidhu, R.S. and Summerell, B. *Australian Journal of Botany.* **1997**, 45, 1073-1082.

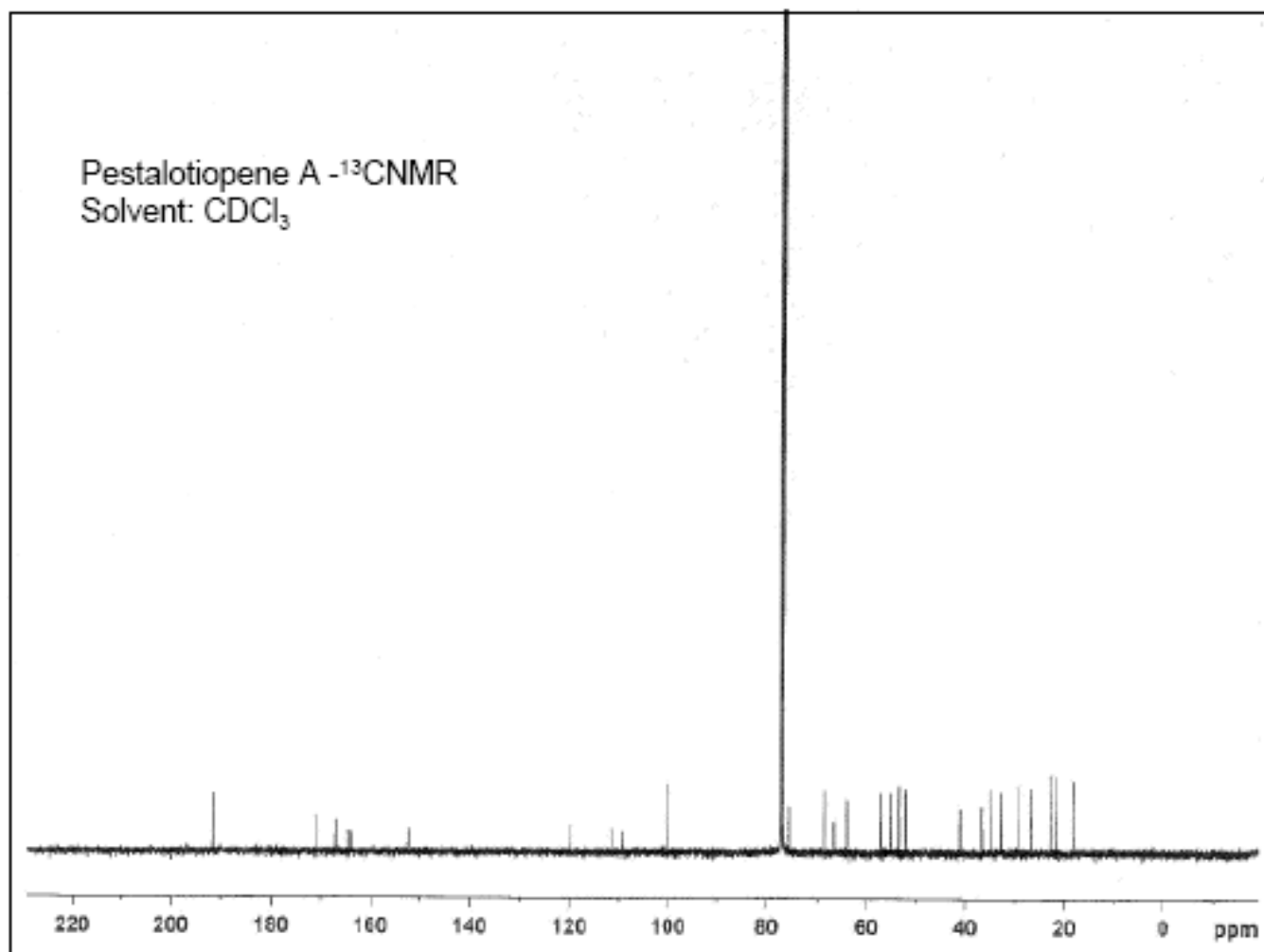
- Strobel, G., Li, J.Y., Ford, E., Worapong, J., Gary, I.B. and Hess, W.M. *Mycotaxon*. **2000**, 76, 257-266.
- Strobel G. A., Long D. M. *ASM News*, **1998**, 64, 263.
- Strobel, G., Yang, X.S., Sears, J., Kramer, R., Sidhu, R.S. and Hess, W.M. *Microbiology*. **1996**, 142, 435-440.
- Suryanarayanan, T. S.; Senthilarasu, G.; Muruganandam, V. *Fungal Divers*, **2000**, 4, 117-123.
- Tang, A., Hyde, K.D., Corlett, R.T.C. *Fungal Diversity*. **2003**, 14, 165-185.
- Tan R. X., Zou W. X. *Nat. Prod. Rep.*, **2001**, 18, 448-459.
- Taylor, J.E., Crous, P.W., Palm, M.E. *Mycotaxon*. **2001**, 78, 449-490.
- Tokumasu, S. and Aoiki, T. *Fungal Diversity*. **2002**, 10, 167-183.
- Toofanee, S. B.; Dulymamode, R. *Fungal Divers*, **2002**, 11, 169-175.
- Turner, W. B., Aldridge, D. C. *Polyketides In The Fungal Metabolites*. II. Academic Press, New York. **1983**, 68.
- Venkatasubbaiah, P., Wan Dyke, C. G., Chilton, W. S. *Phytochemistry*, **1991**, 30(5), 1471- 1474.
- Wang, J., Li, G., Lu, H., Zhang, Z., Huang, Y., Su, W. *FEMS Microbiol. Lett.*, **2000**, 193, 249.
- Wang S. J., Pei Y. H. *J. Shenyang Pharm. Uni.* **2000**, 17, 256- 257.
- Wang, Y.; Guo, L.D.; Hyde, K.D. *Fungal Diversity*, **2005**, 20: 235-260.
- Wang, Z. M., Shen, M. *Tetrahedron*, **1997**, 8(20), 3393- 3396.
- Wani, M. C., Taylor, H. L., Wall, M. E., Coggon, P., Mcphail, A. T. *J. Am. Chem. Soc.*, **1971**, 93, 2325-2327.

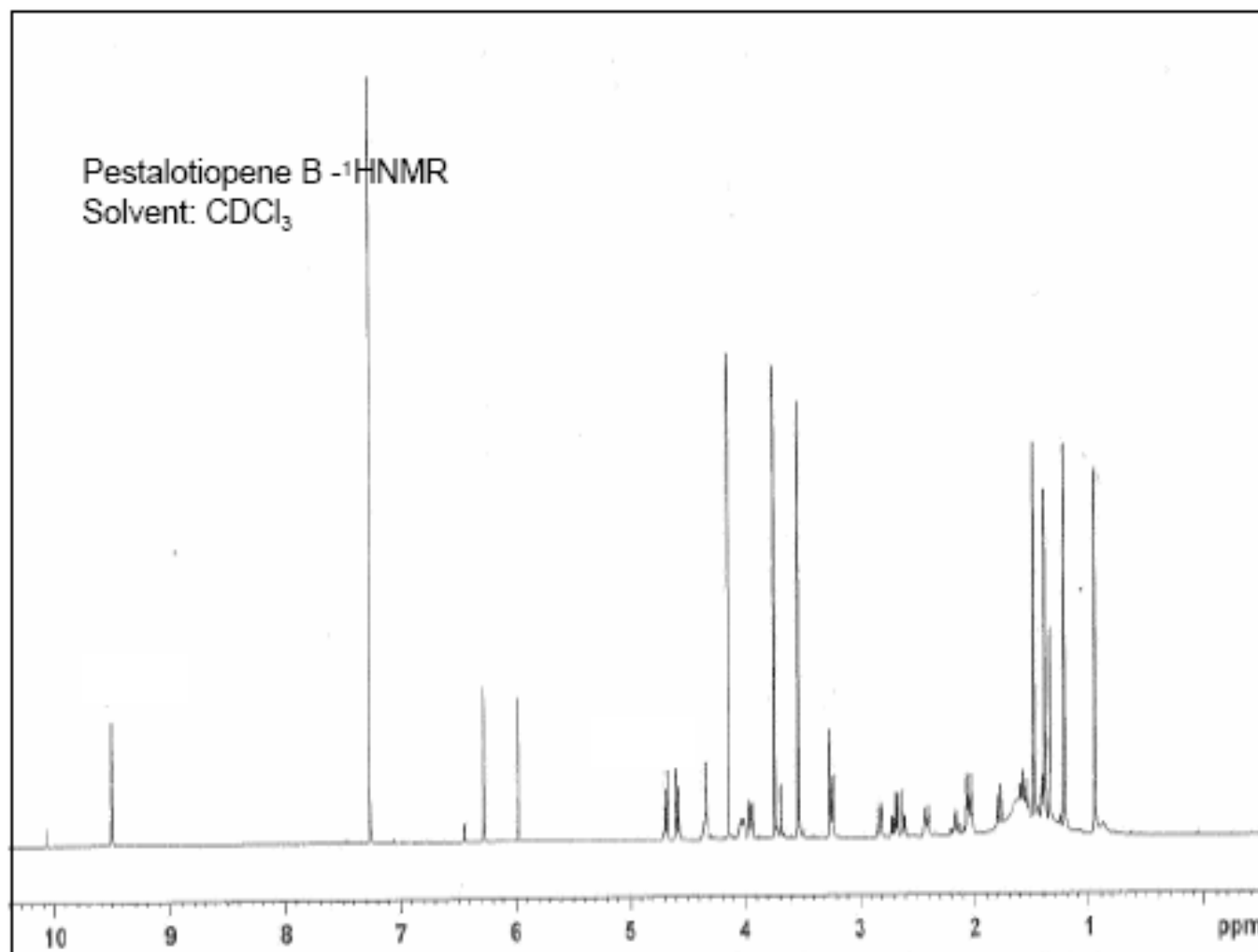
- Watt, J.M., Breyer-Brandwijk, M.G. 1962. The medicinal and poisonous plants of southern and eastern Africa. 2nd ed. E.&S. Livingstone, Ltd., Edinburgh and London.
- Wei, J. G., Xu T., Guo. L. D., Liu. A. R., Zhang, Y., Pan, X. H. *Fungal Diversity*. **2007**, 24, 55-74.
- Wu, C.G., Tseng, H.Y., Chen, Z.C. *Taiwania*, **1982**, 27, 35–38.
- Xu, Q.; Wang, J.; Huang, Y.; Zheng, Z.; Song, S.; Zhang, Y.; Su, W. *Acta Oecarnolog. Sin.* **2004**, 23, 541-47.
- Zhang, Y. L., Ge, H. M., Li, F., Song, Y. C., Tan, R. X. *Chemistry & Biodiversity*, **2008**, 5, 2402- 2407.
- Zhu, P. L., Ge, Q. X. and Xu, T. *Mycotaxon*. **1991**, 40, 129-140.

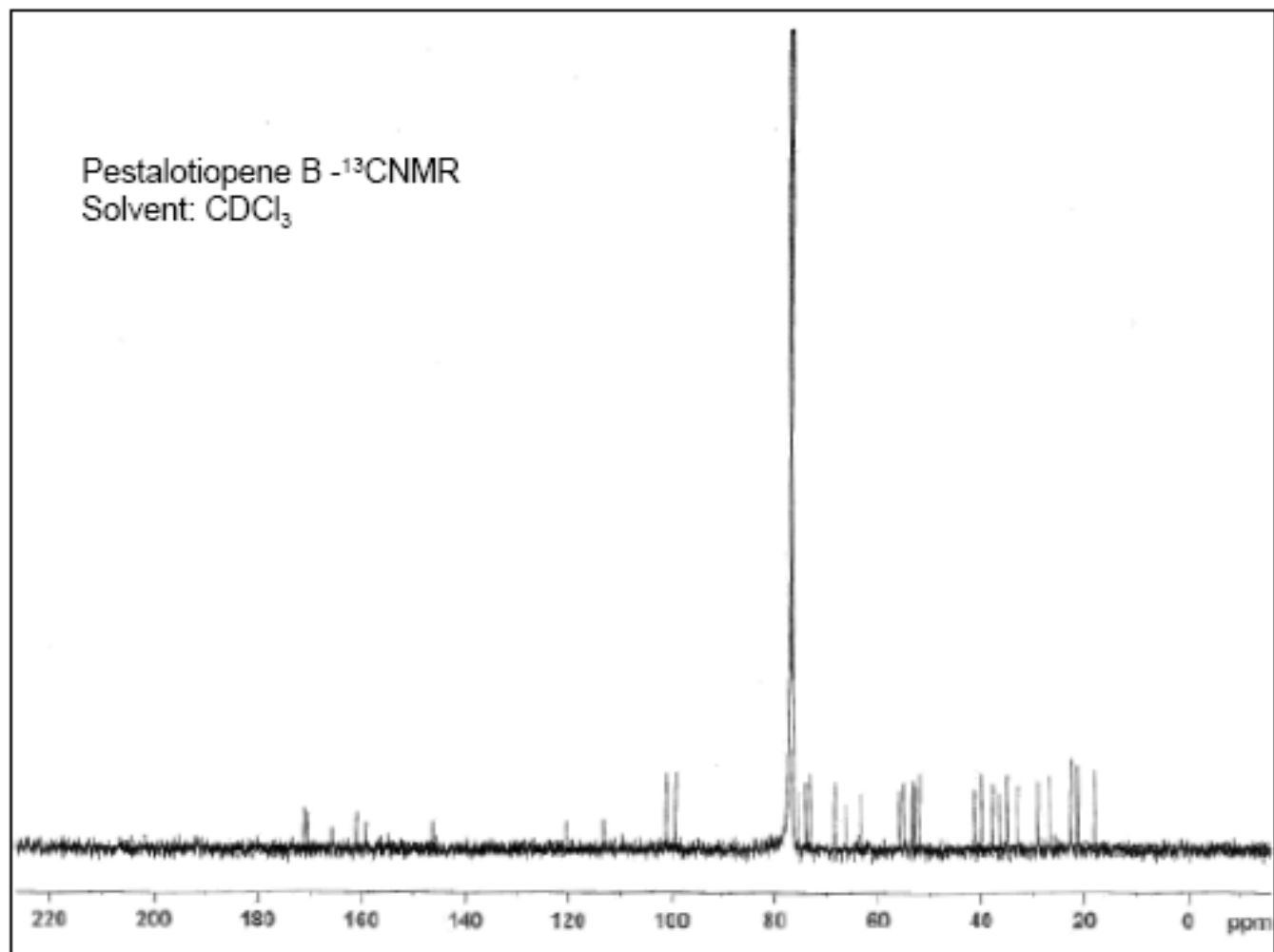
7 ATTACHMENTS

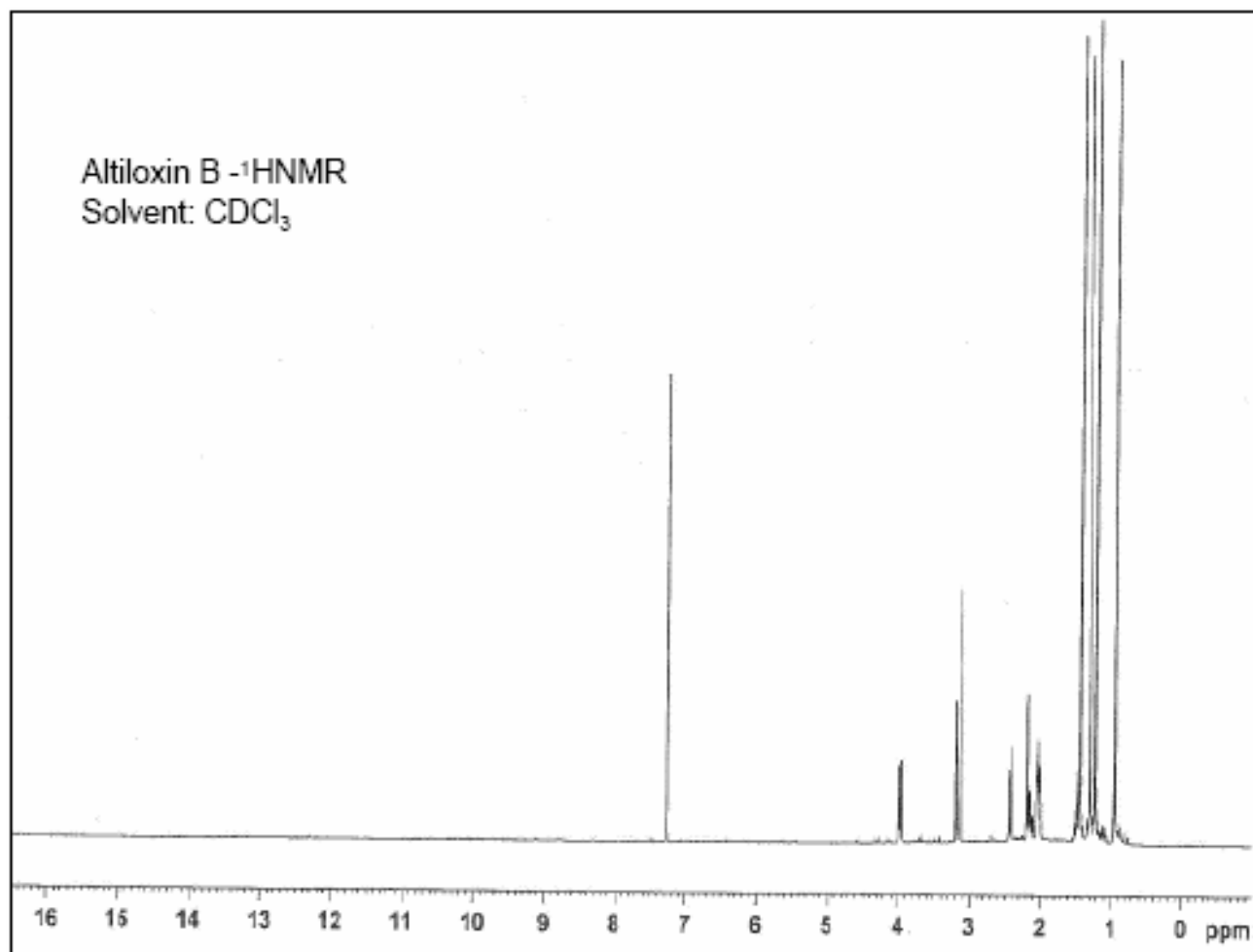
Attachment 1. The ^1H NMR Spectrum of Pestalotiopene A (**1**)

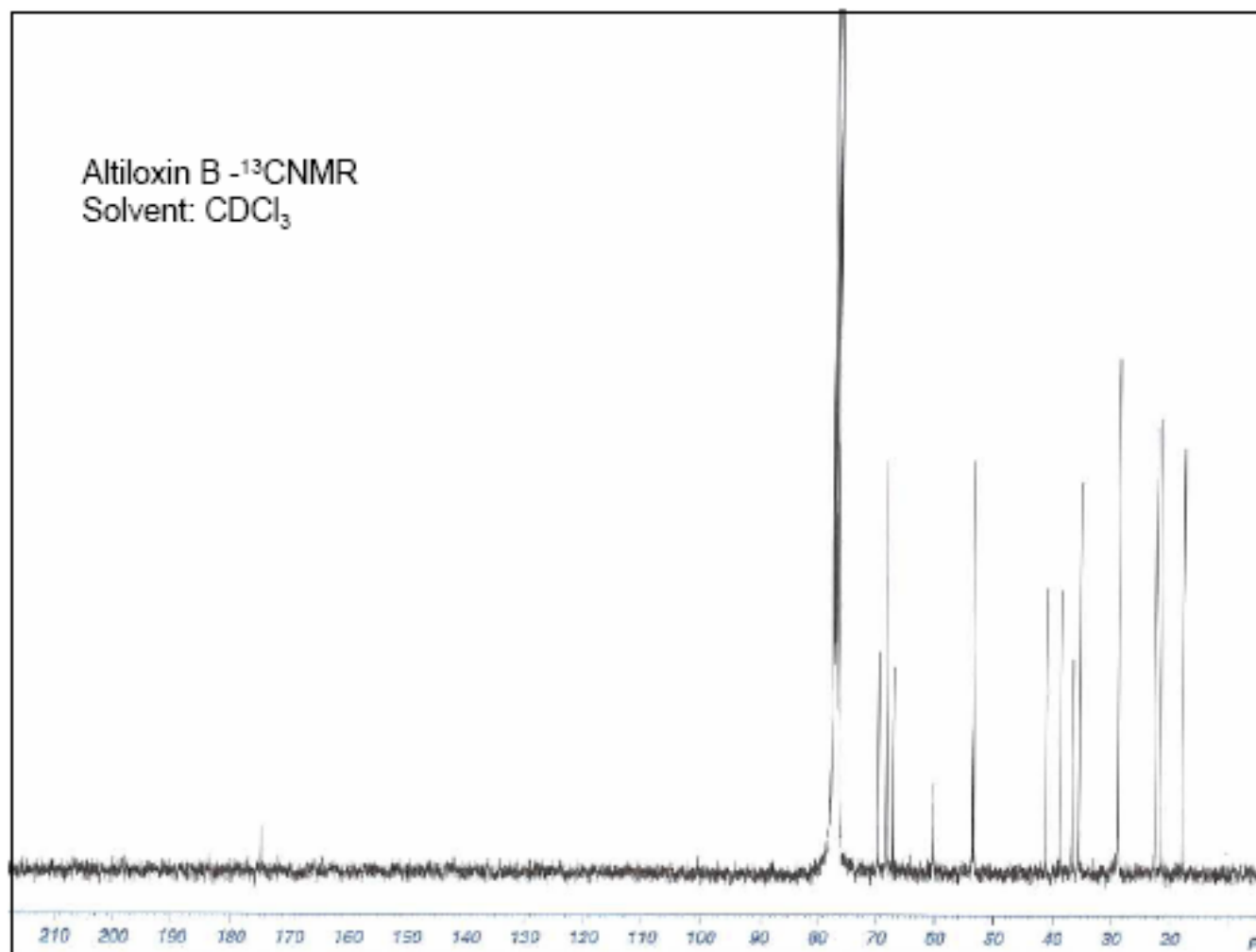


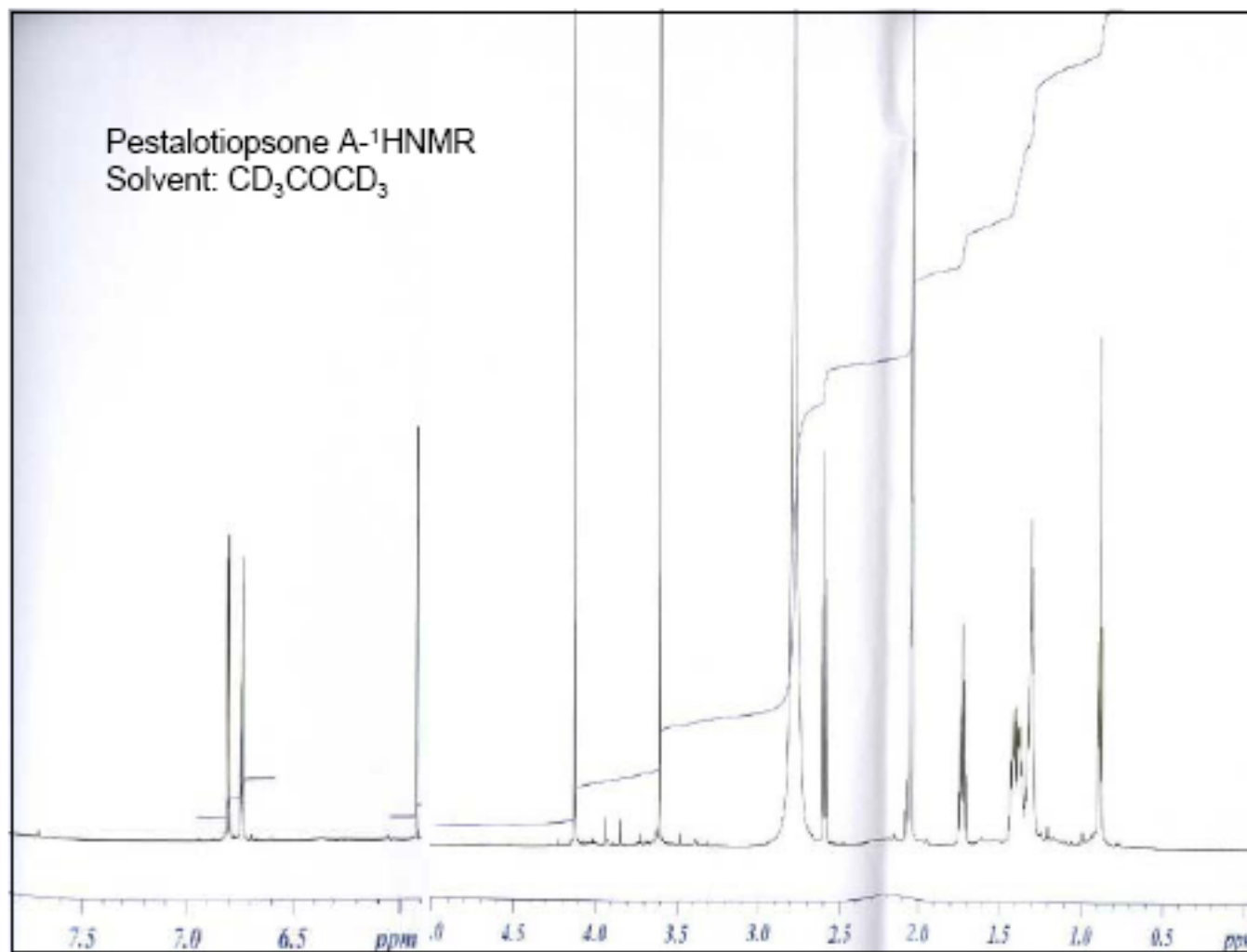
Attachment 2. The ^{13}C NMR Spectrum of Pestalotiopene A (**1**)

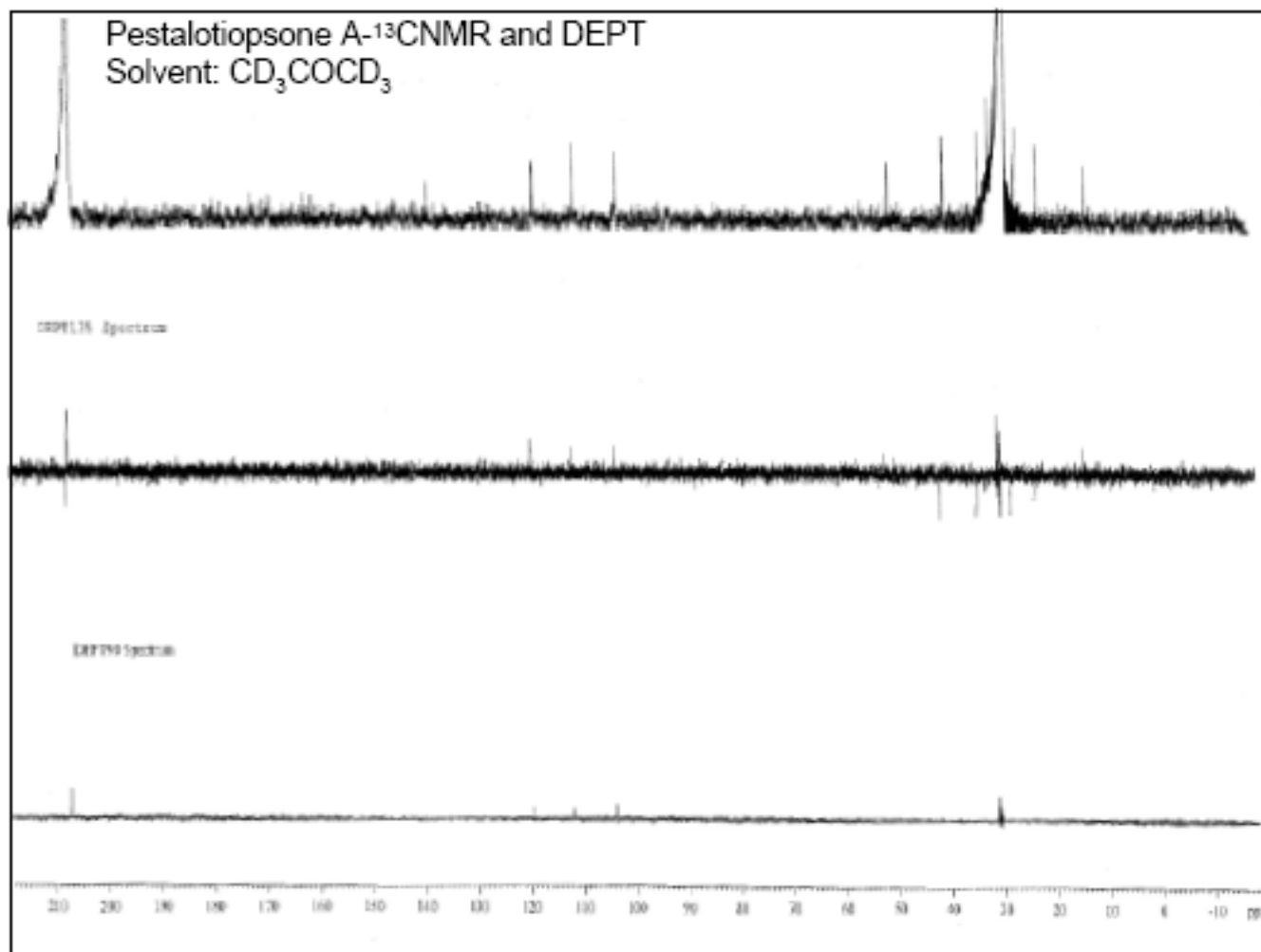
Attachment 3. The ^1H NMR Spectrum of Pestalotiopene B (**2**)

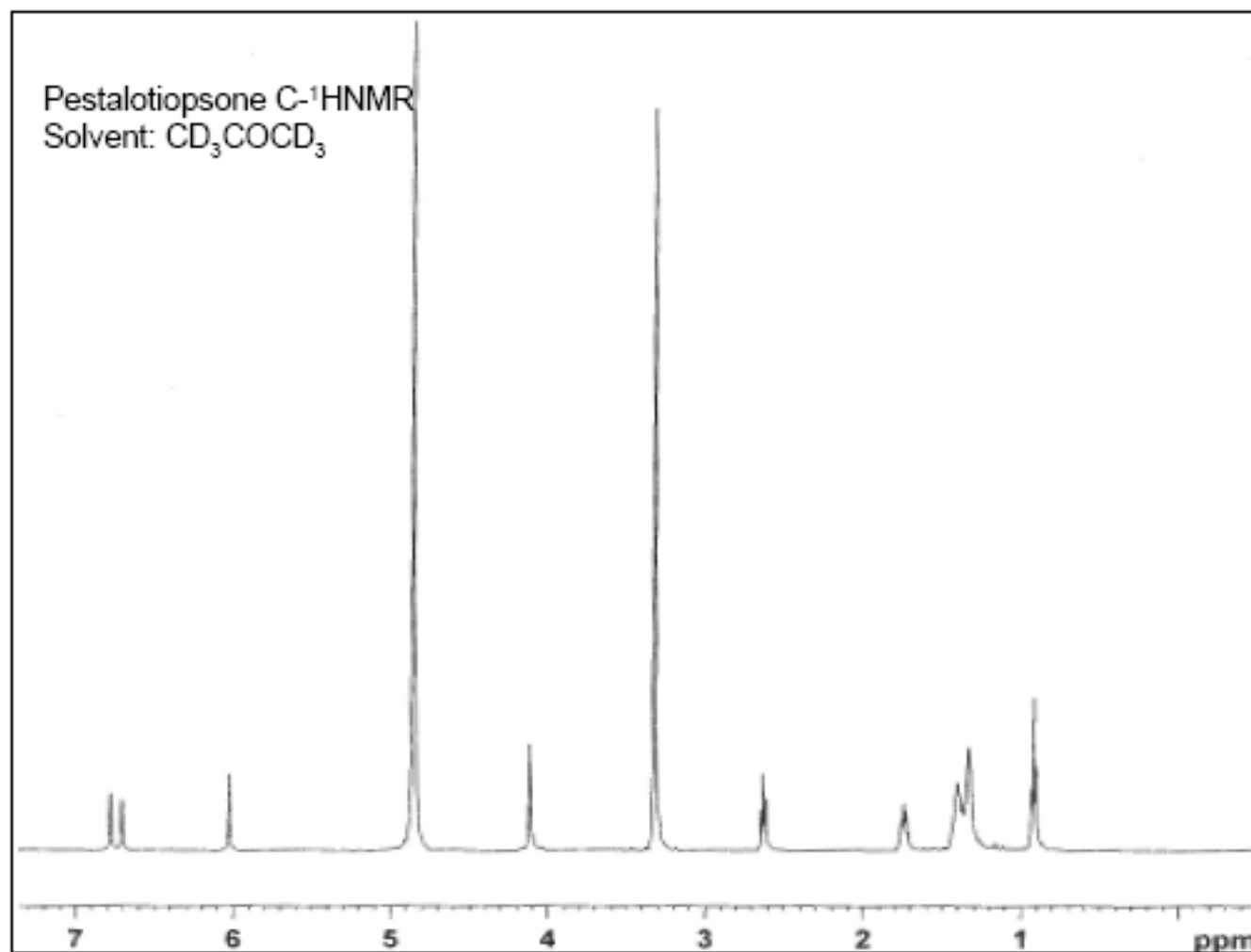
Attachment 4. The ^{13}C NMR Spectrum of Pestalotiopene B (2)

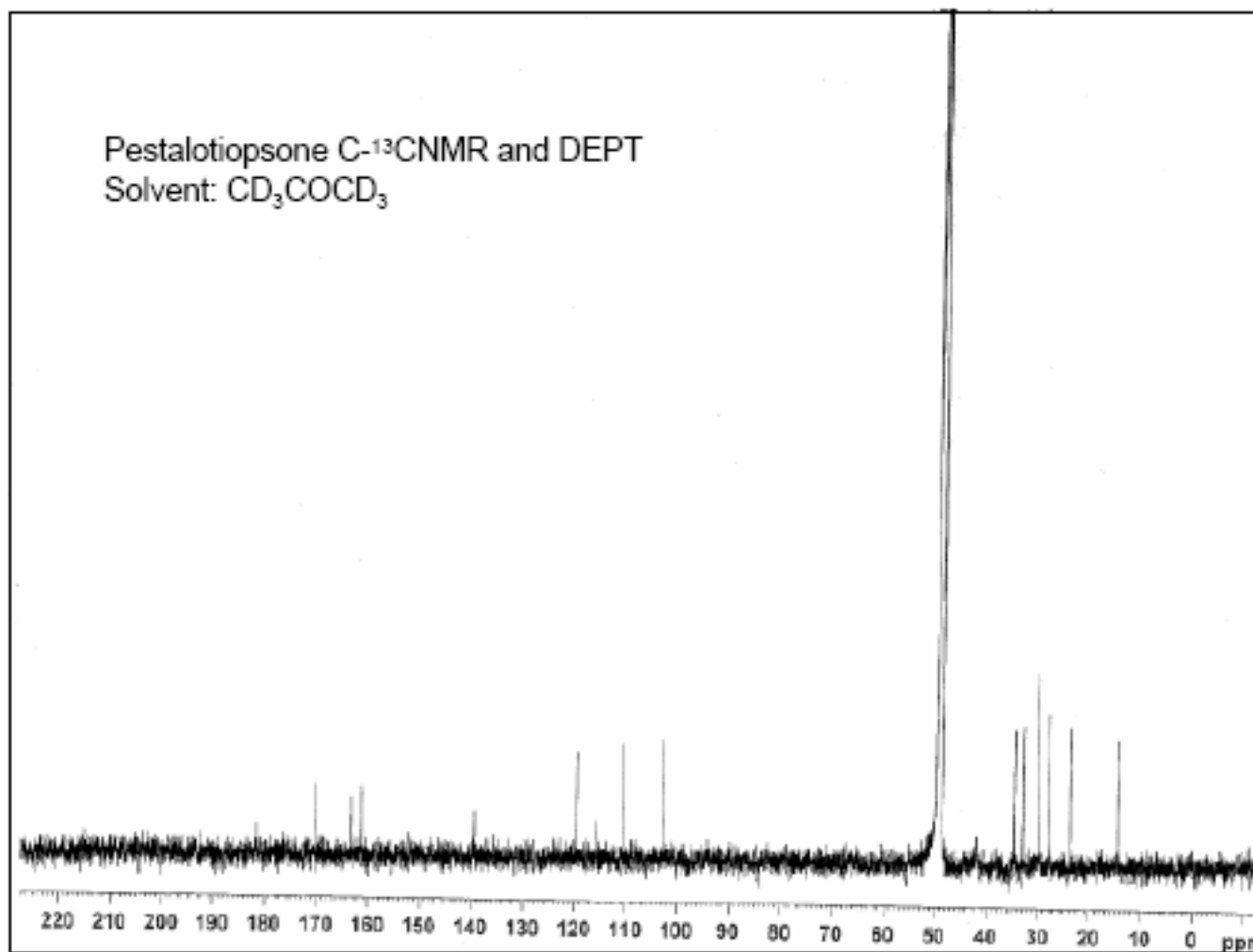
Attachment 5. The ^1H NMR Spectrum of Altiloxin B (**3**)

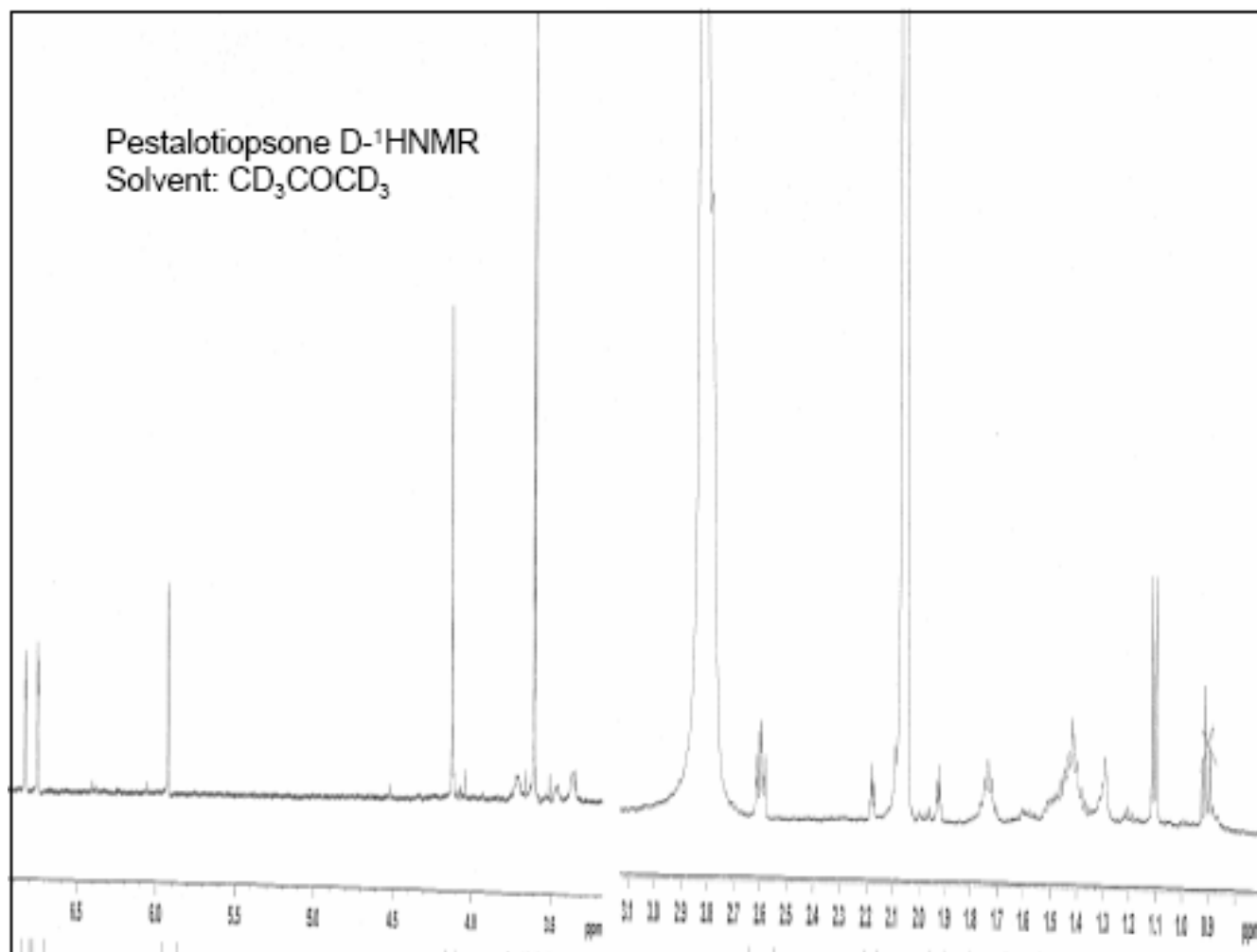
Attachment 6. The ^{13}C NMR Spectrum of Altiloxin B (**3**)

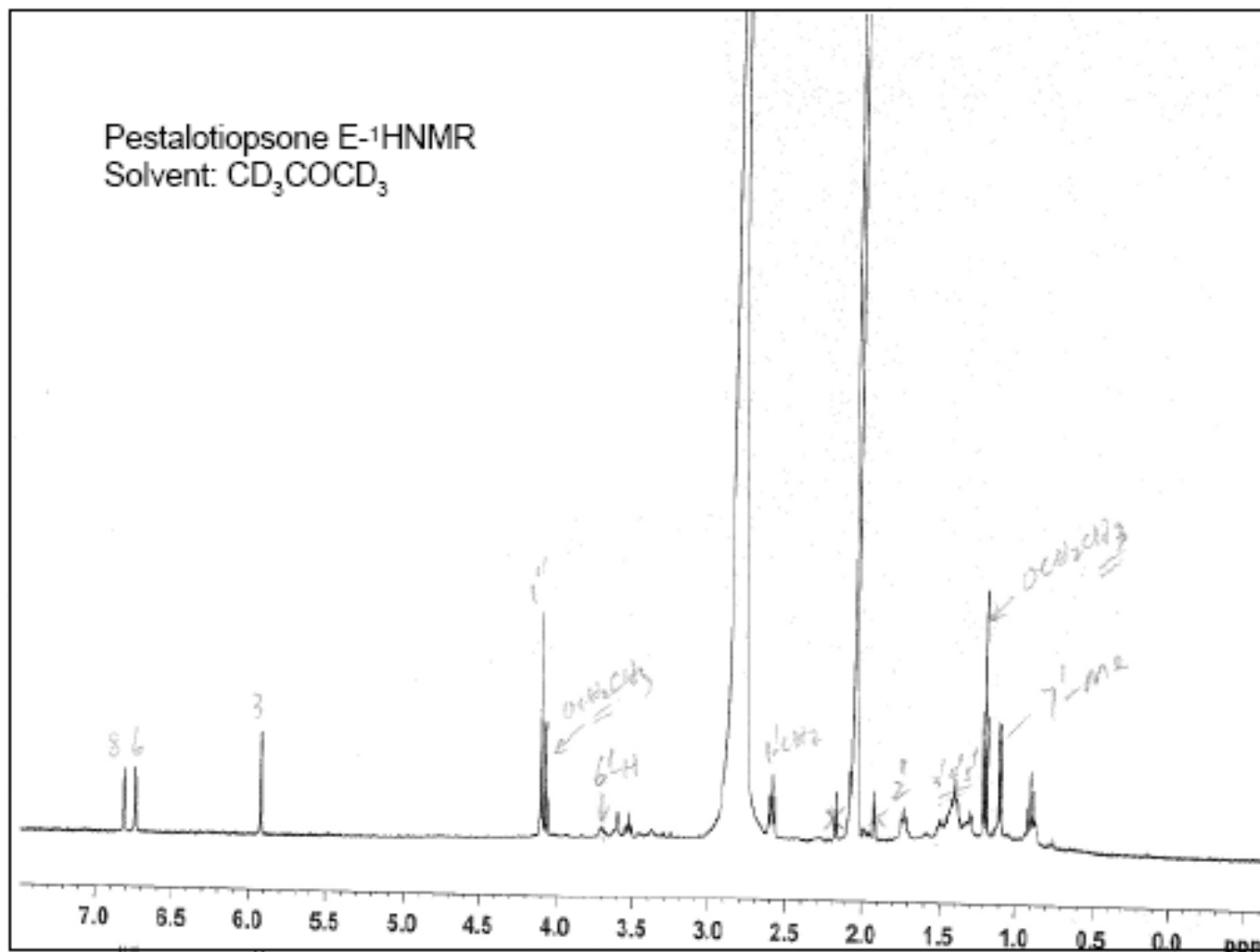
Attachment 7. The ^1H NMR Spectrum of Pestalotiopsone A (**4**)

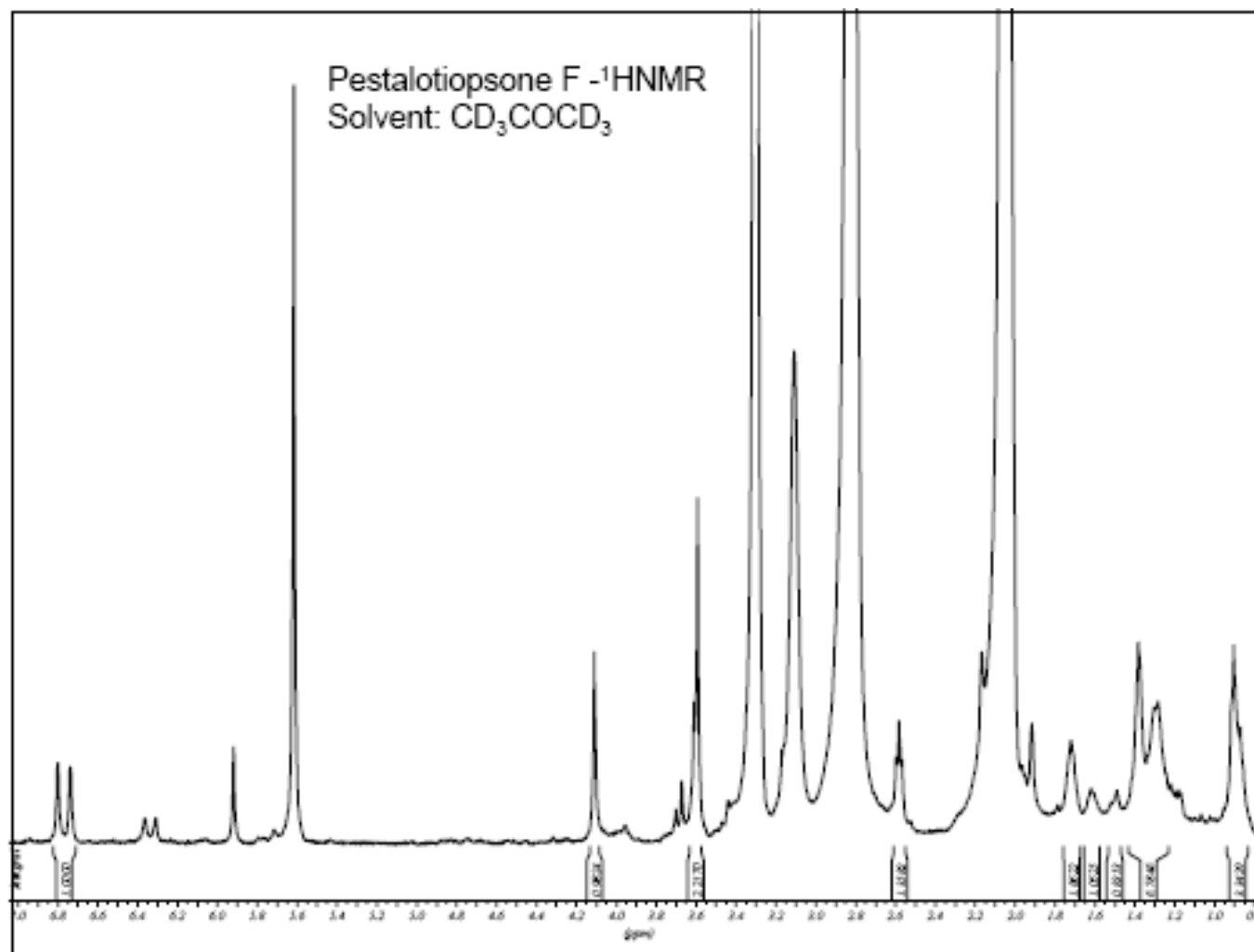
Attachment 8. The ^{13}C NMR and DEPT Spectrum of Pestalotiopsone A (4)

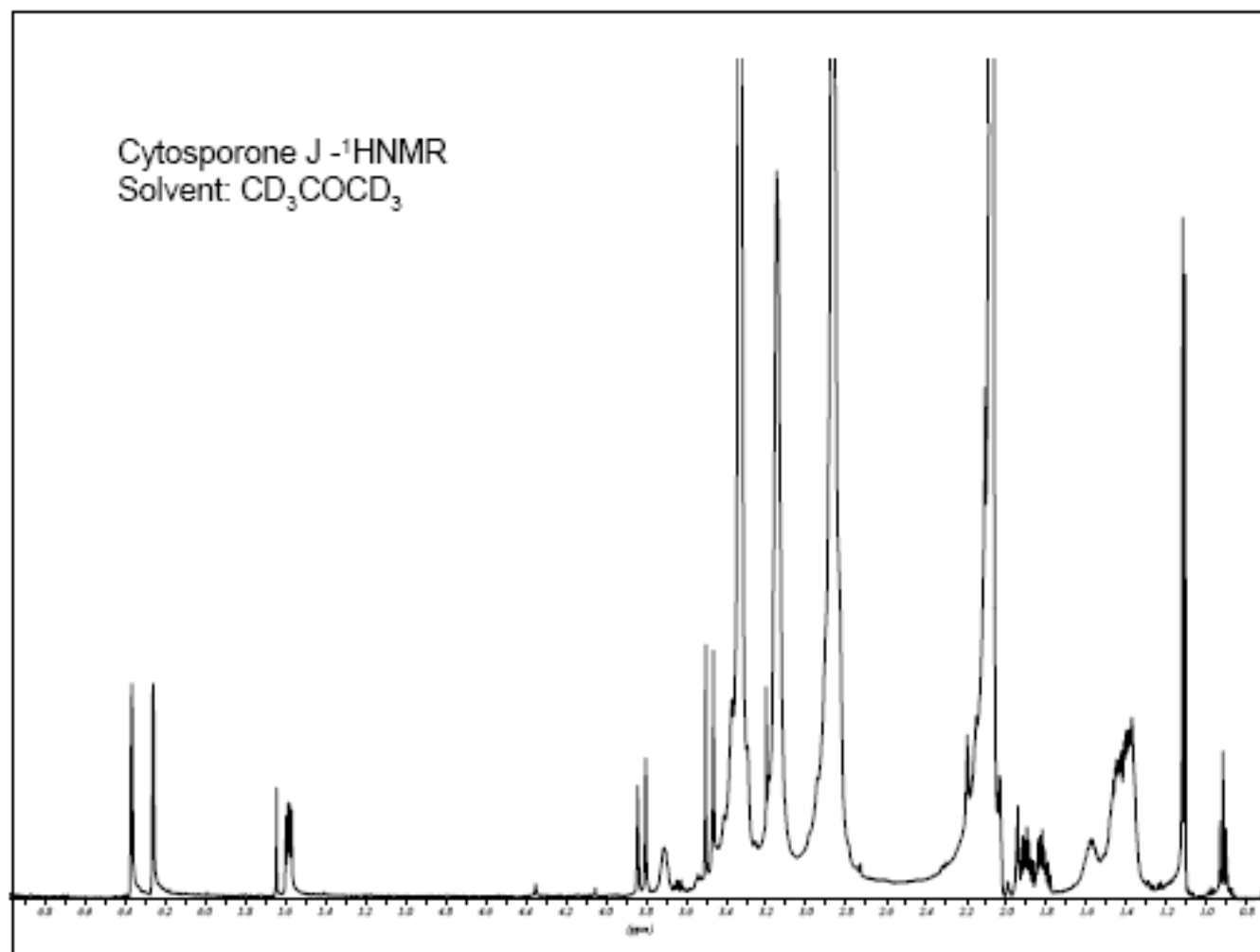
Attachment 9. The ^1H NMR Spectrum of Pestalotiopsone C(6)

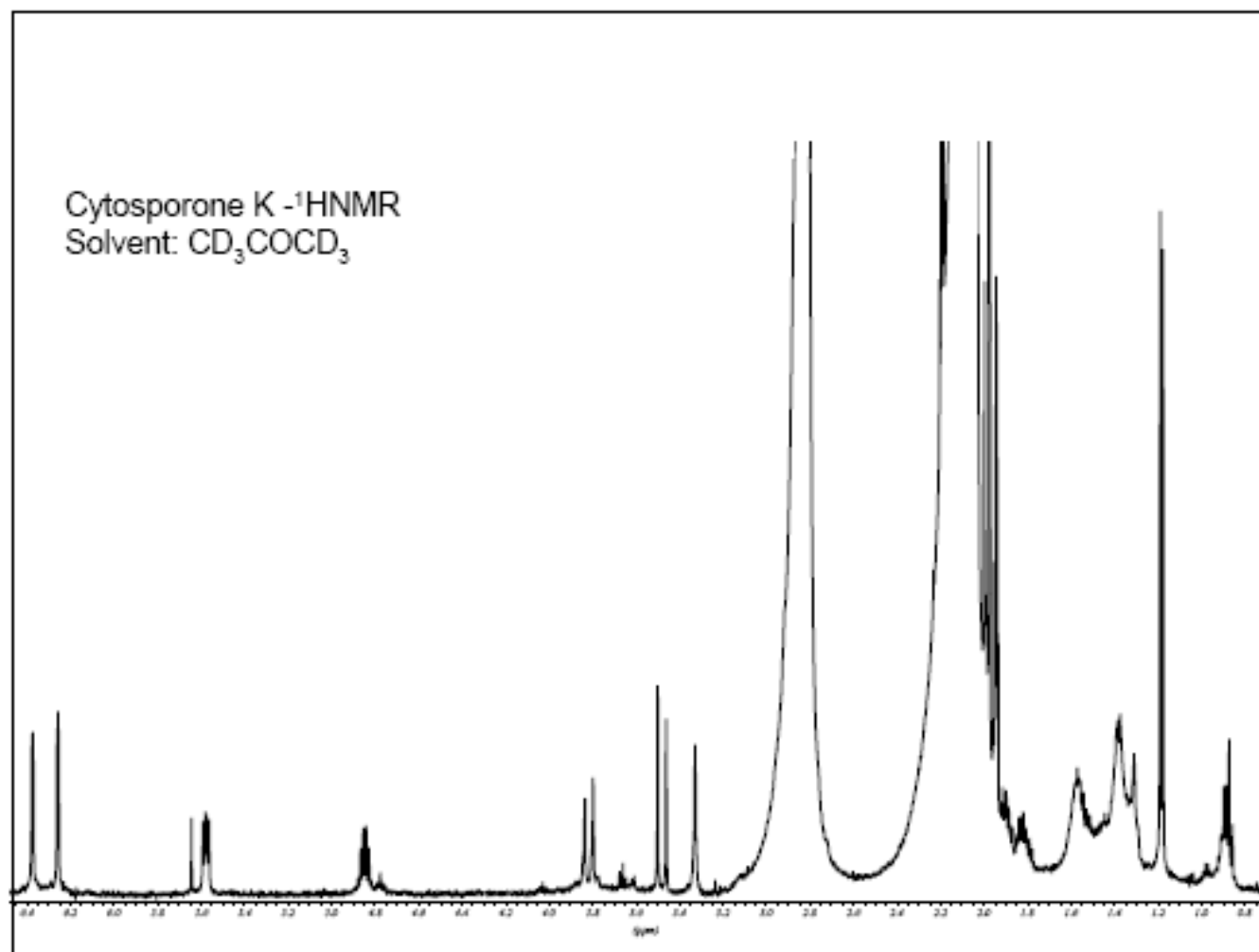
Attachment 10. The ^{13}C NMR Spectrum of Pestalotiopsone C (**6**)

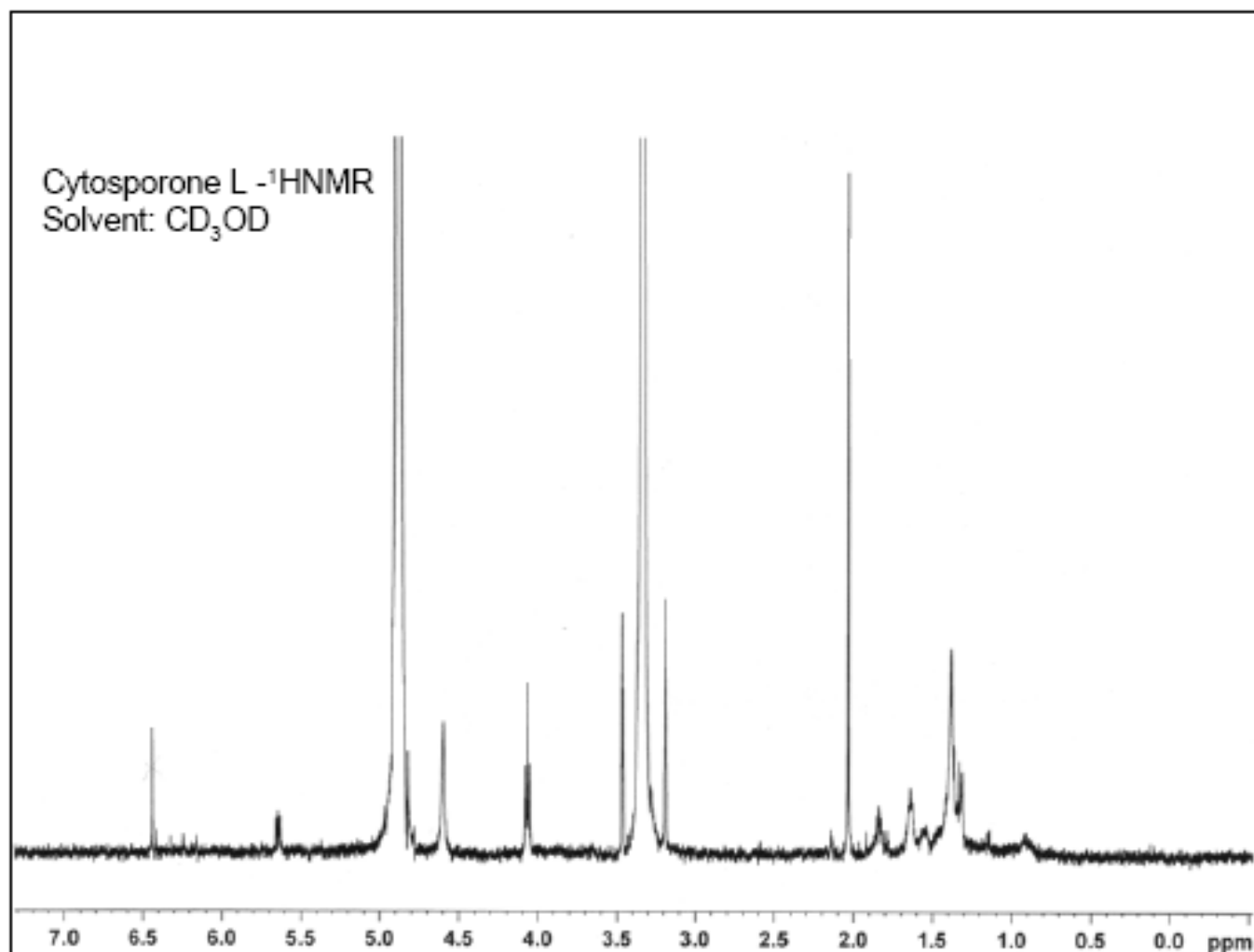
Attachment 11. The ^1H NMR Spectrum of Pestalotiopsone D (7)

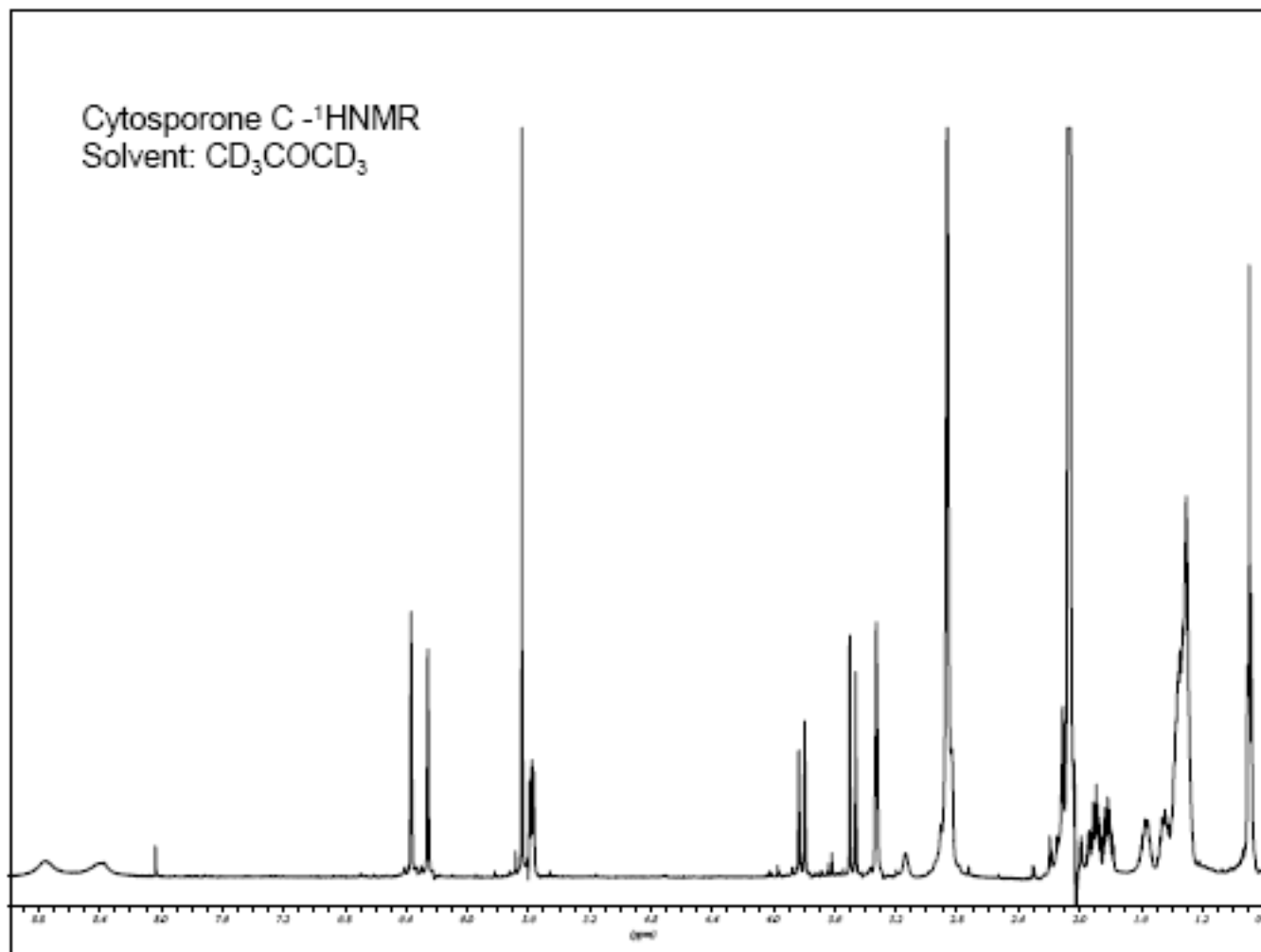
Attachment 12. The ^1H NMR Spectrum of Pestalotiopsone E (8)

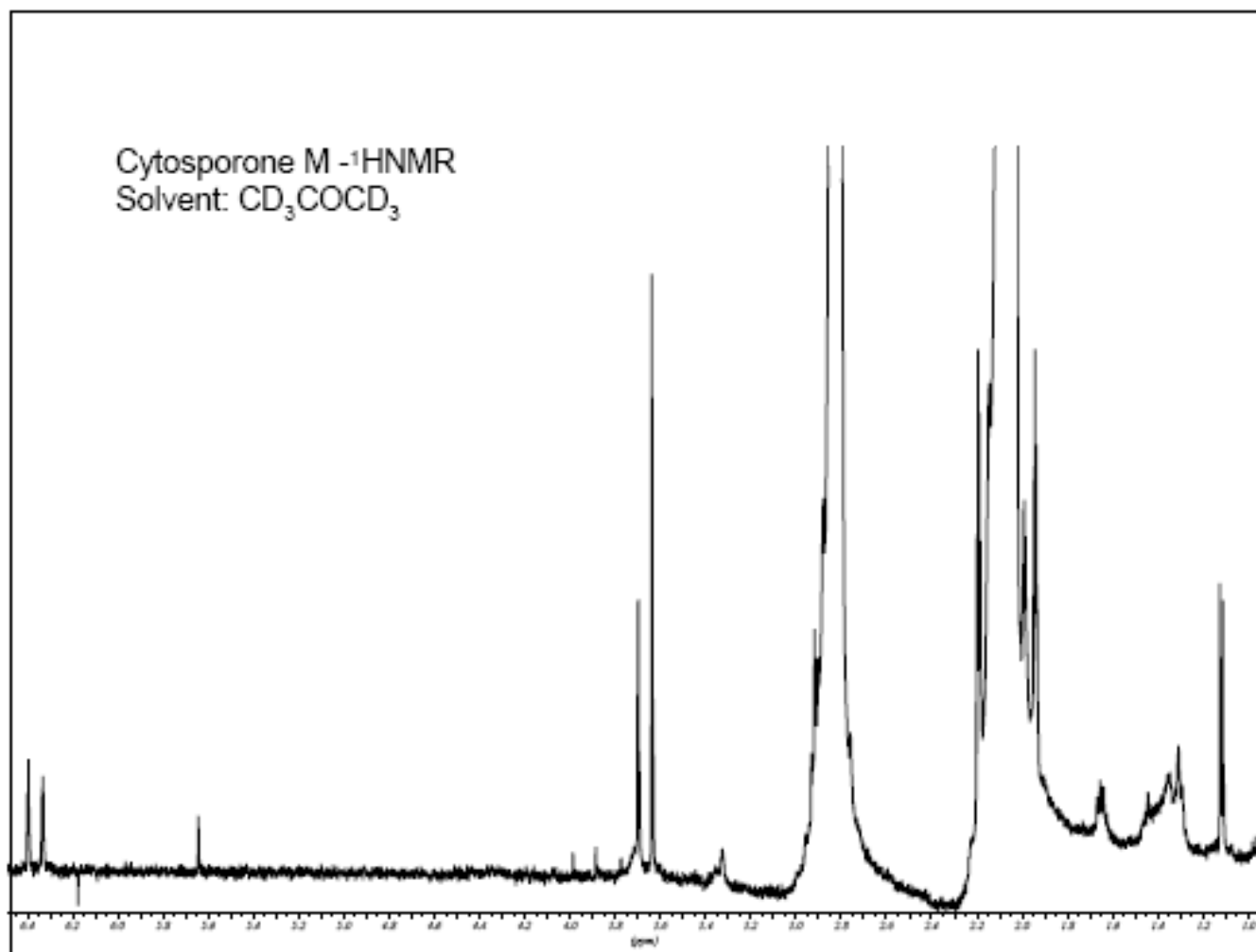
Attachment 13. The ^1H NMR Spectrum of Pestalotiopsone F (9)

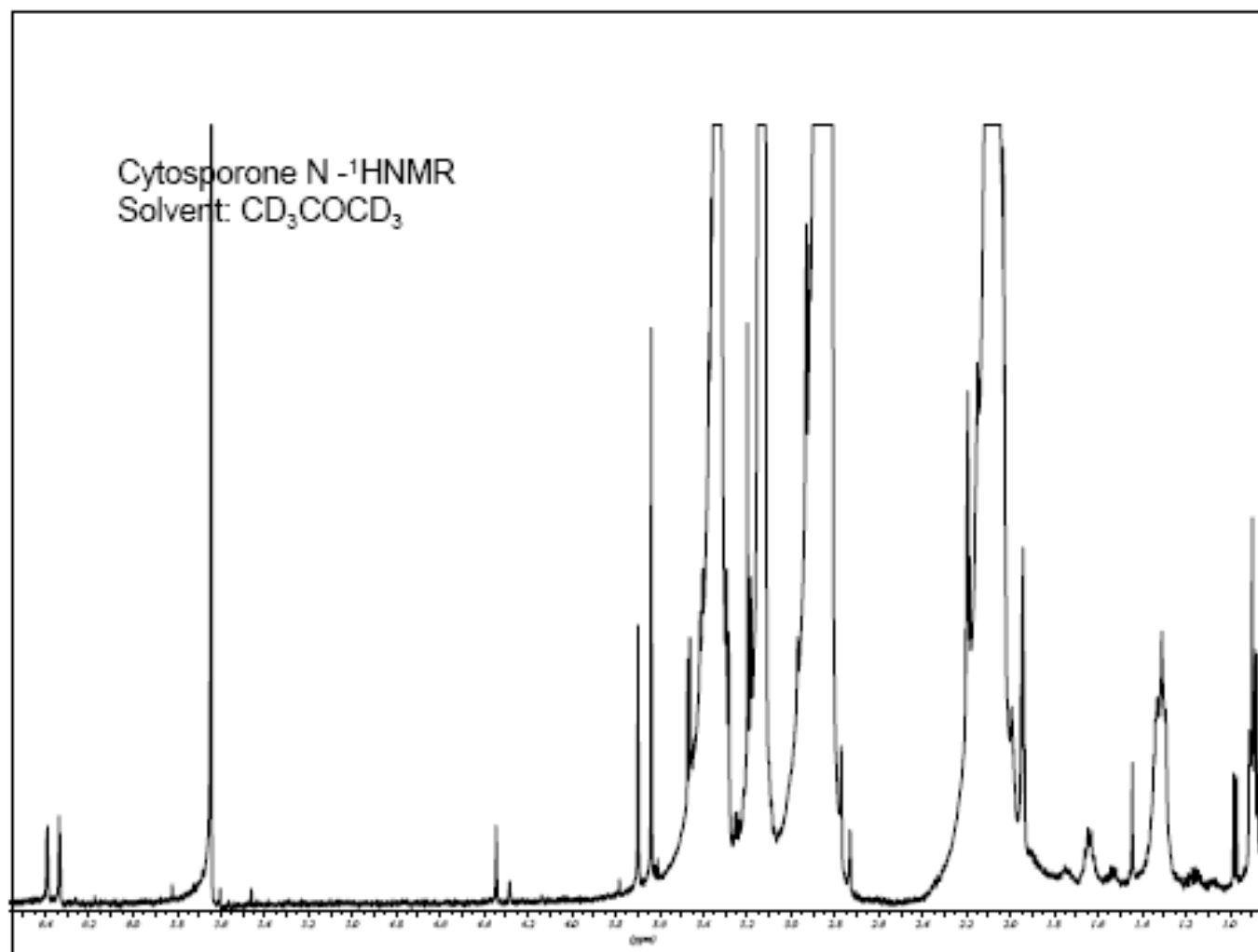
Attachment 14. The ^1H NMR Spectrum of Cytosporone J (**11**)

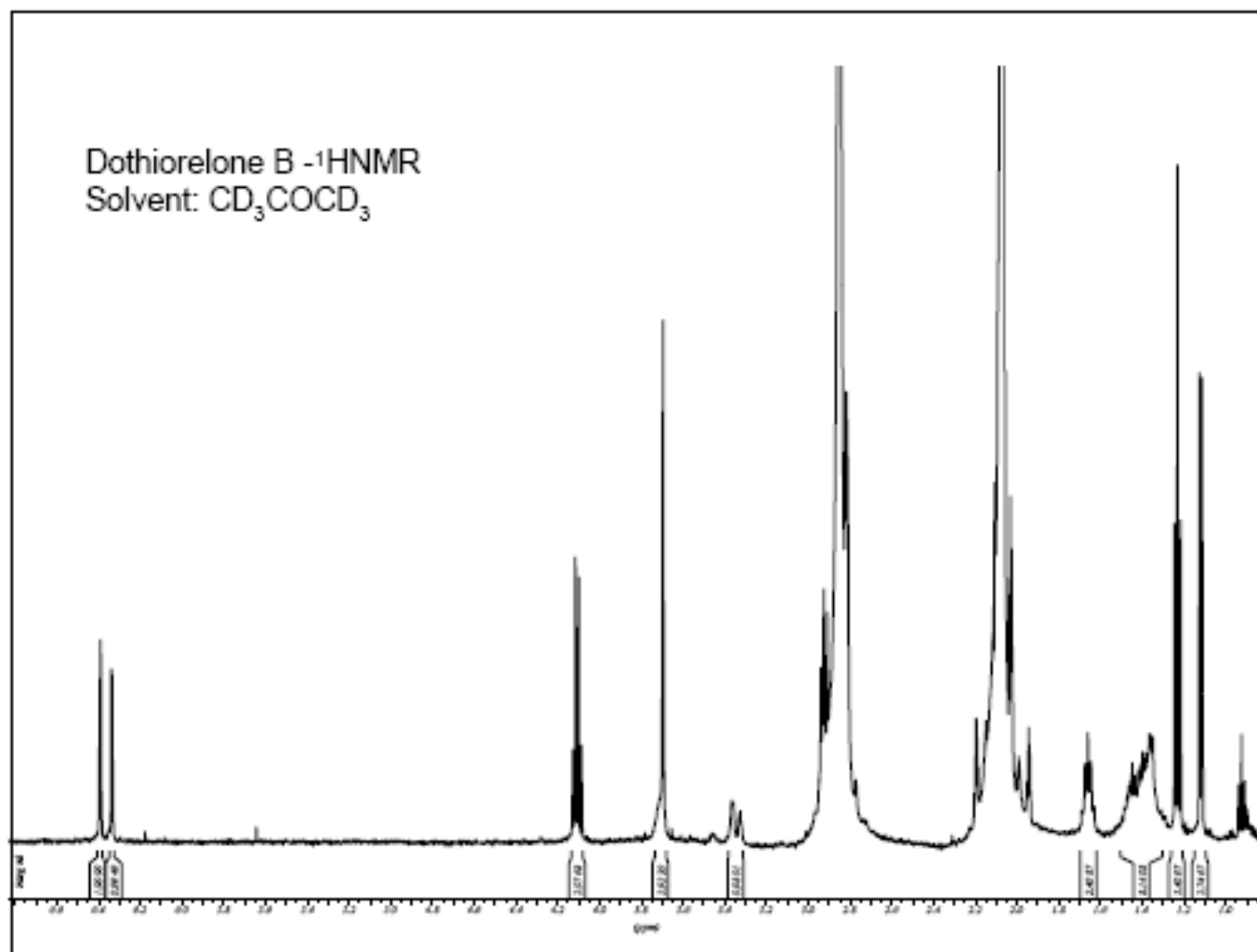
Attachment 15. The ^1H NMR Spectrum of Cytosporone K (**12**)

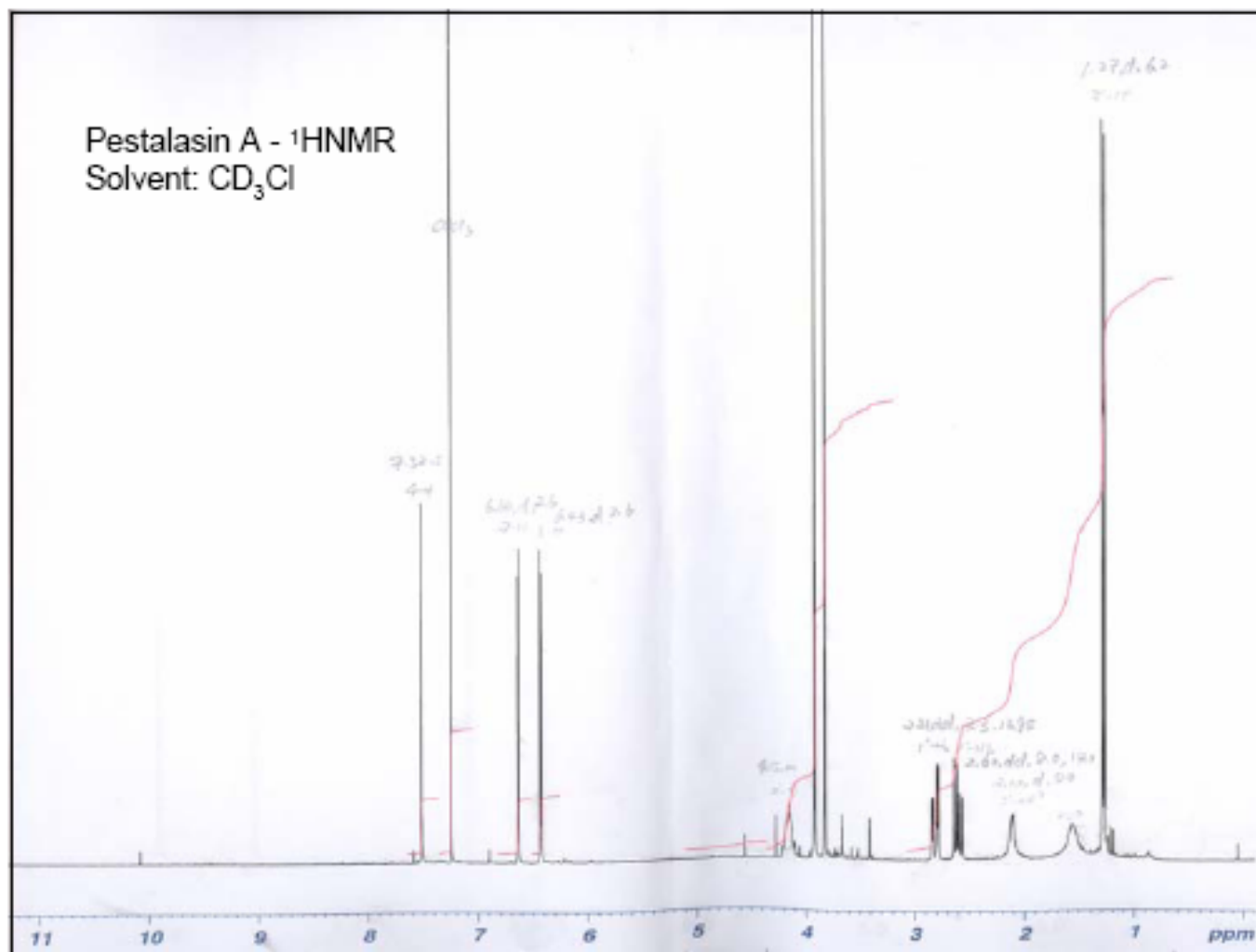
Attachment 16. The ^1H NMR Spectrum of Cytosporone L (**13**)

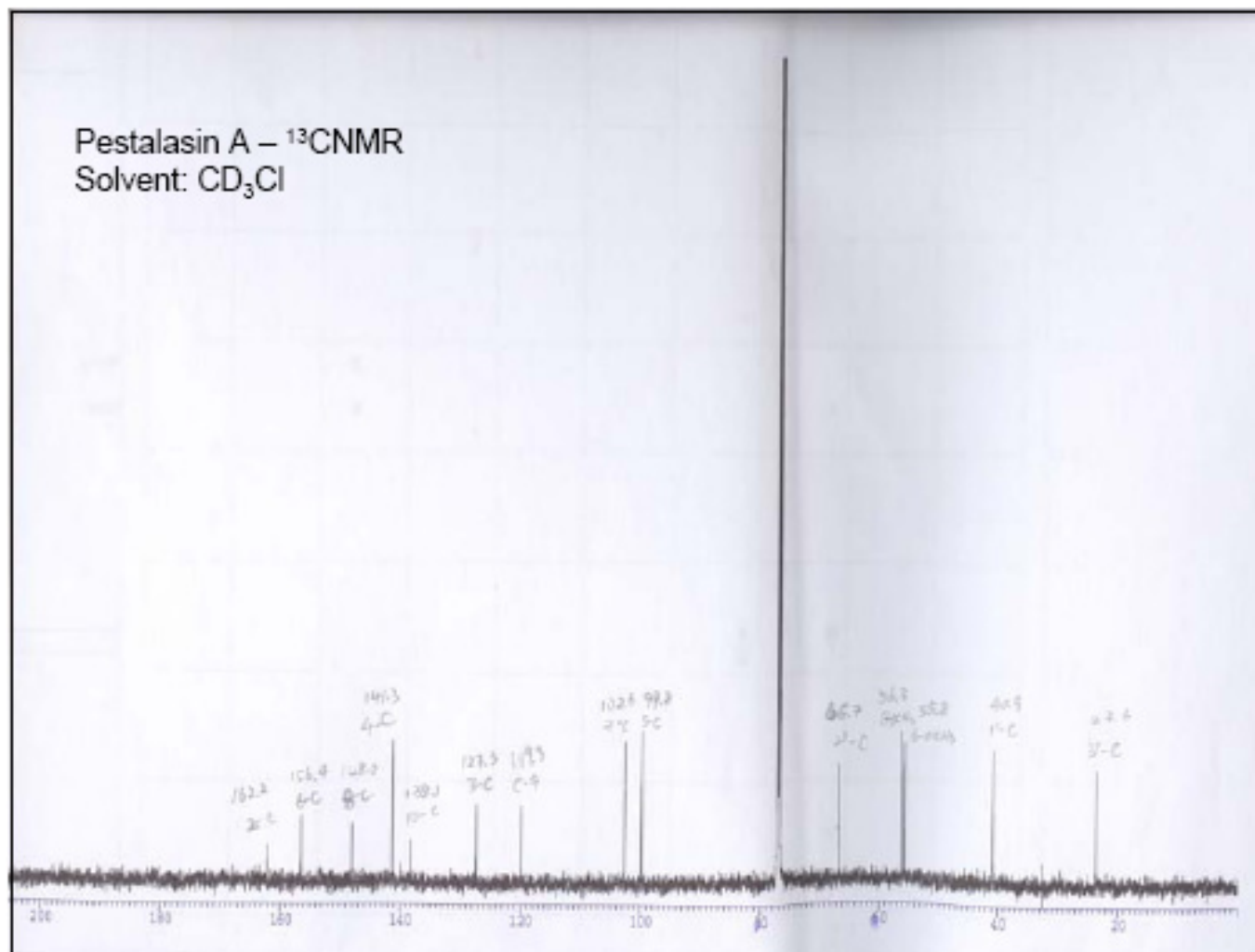
Attachment 17. The ^1H NMR Spectrum of Cytosporone C (**14**)

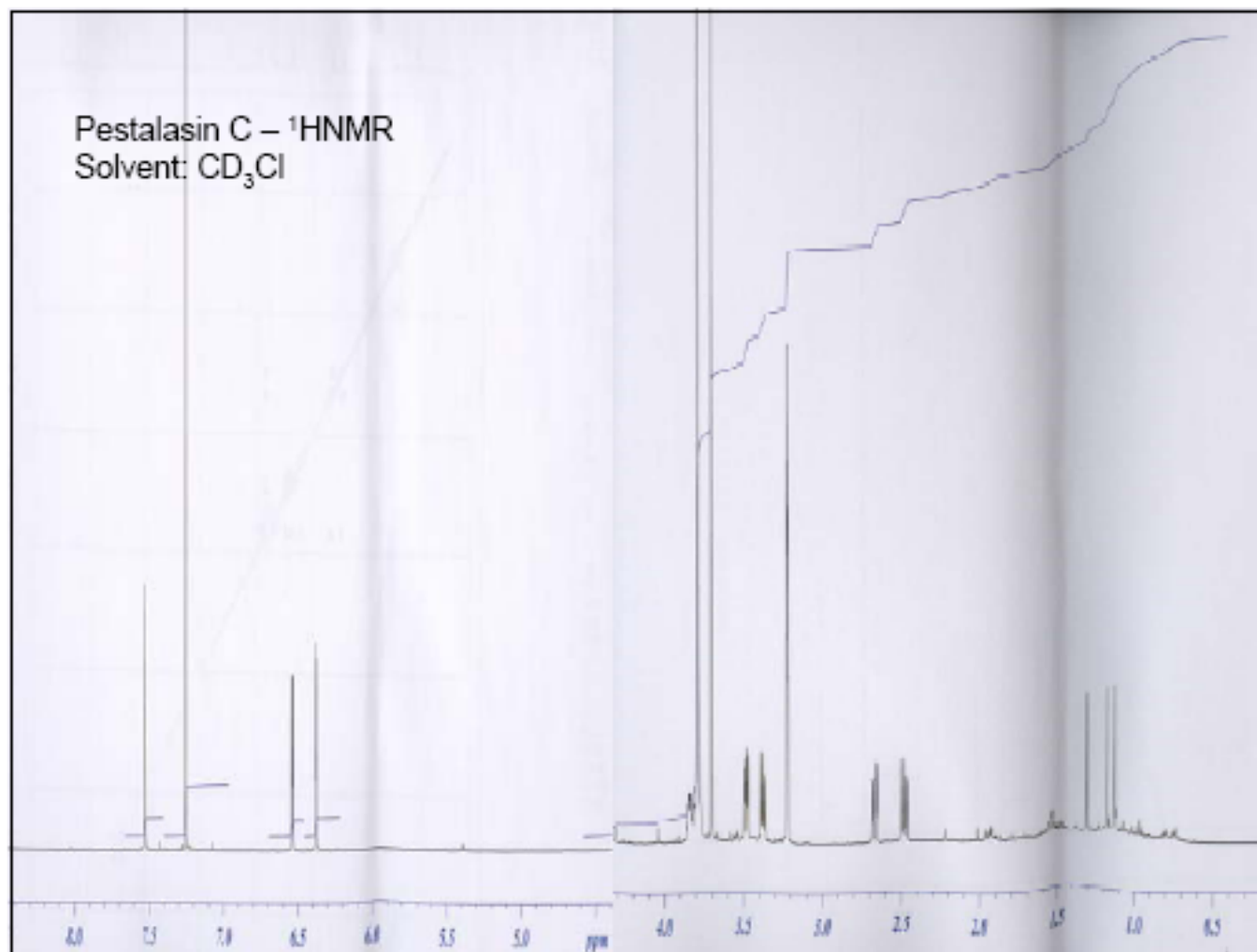
Attachment 18. The ^1H NMR Spectrum of Cytosporone M (**15**)

Attachment 19. The ^1H NMR Spectrum of Cytosporone N (**16**)

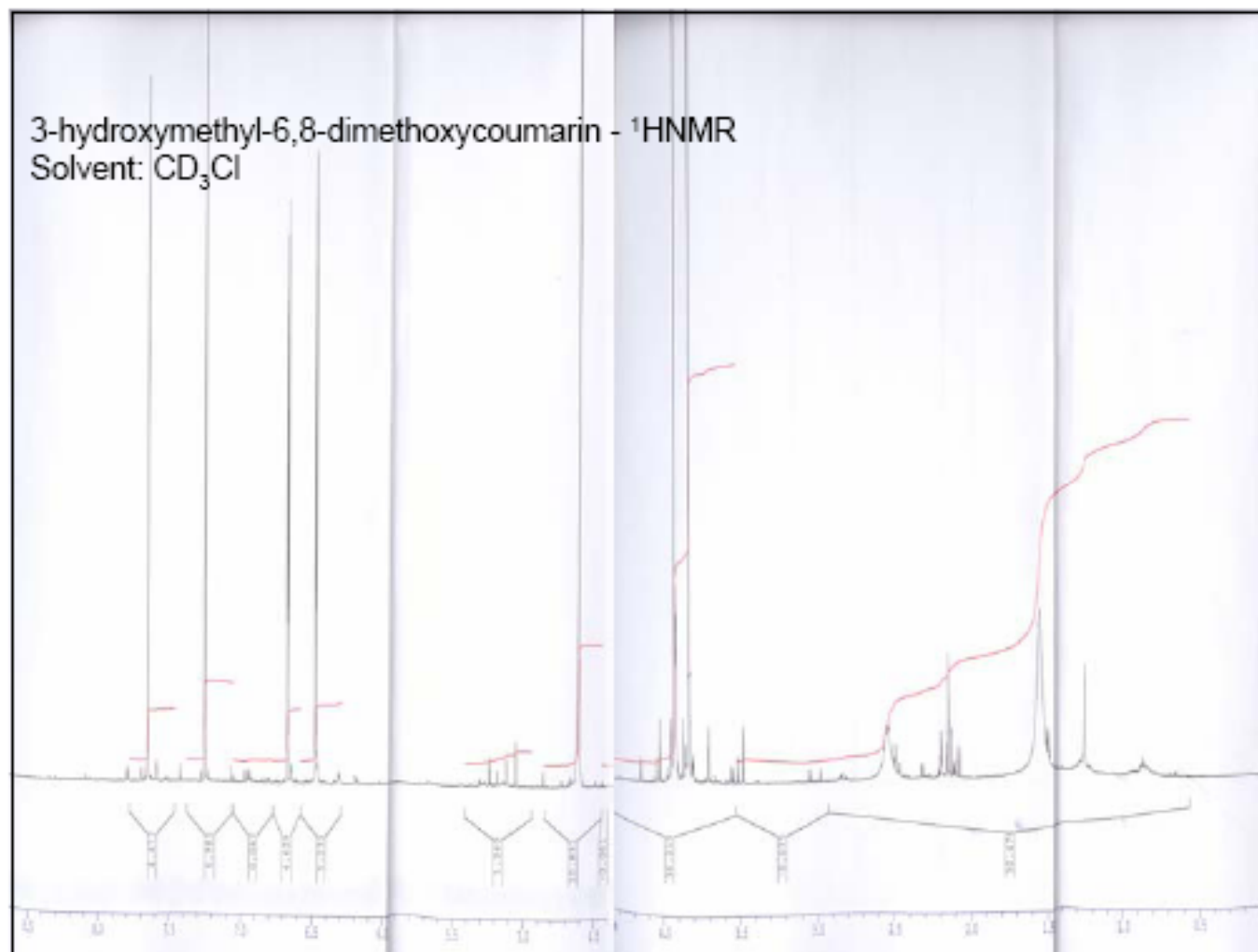
Attachment 20. The ^1H NMR Spectrum of Dothiorelone B (**17**)

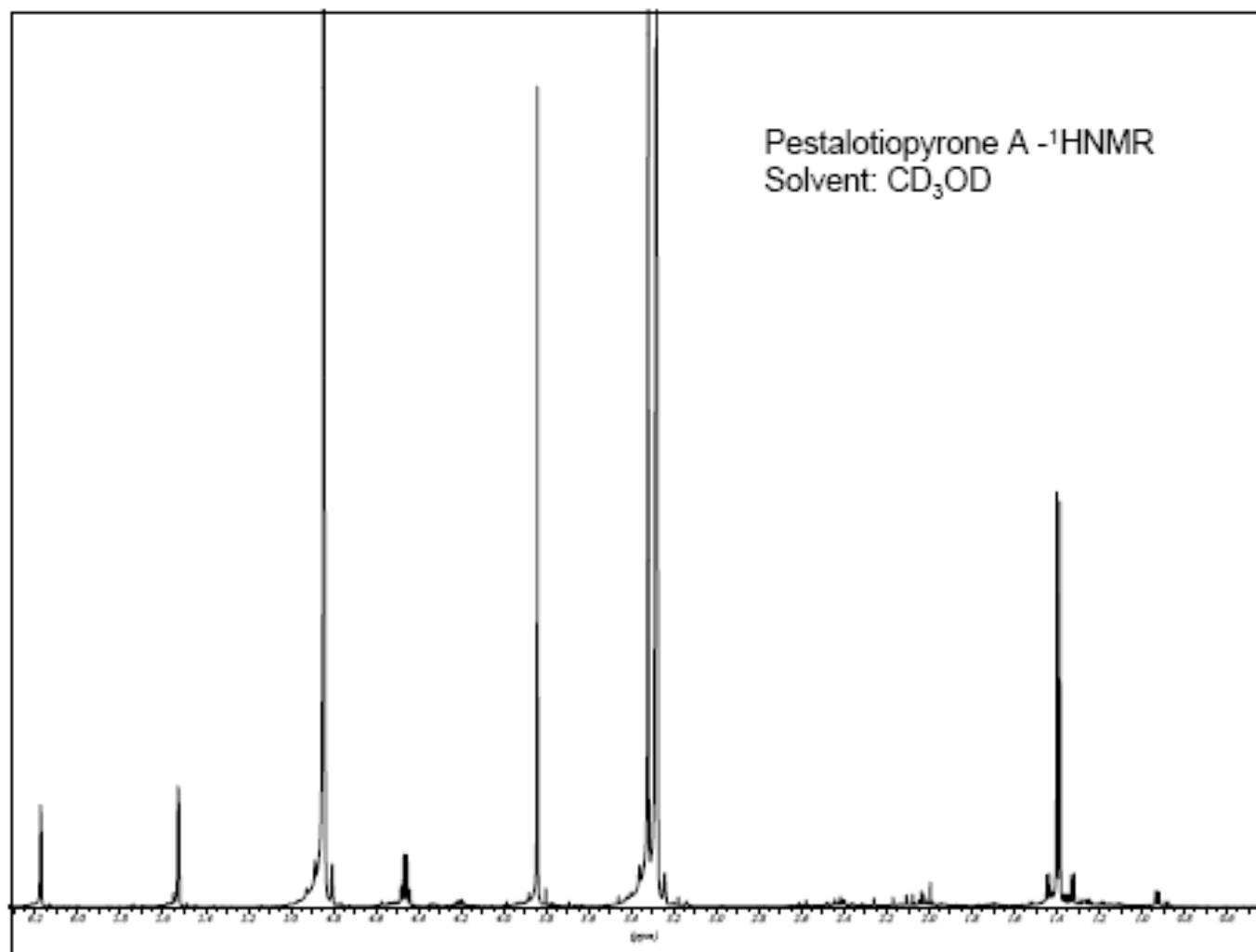
Attachment 21. The ^1H NMR Spectrum of Pestalasin A (18)

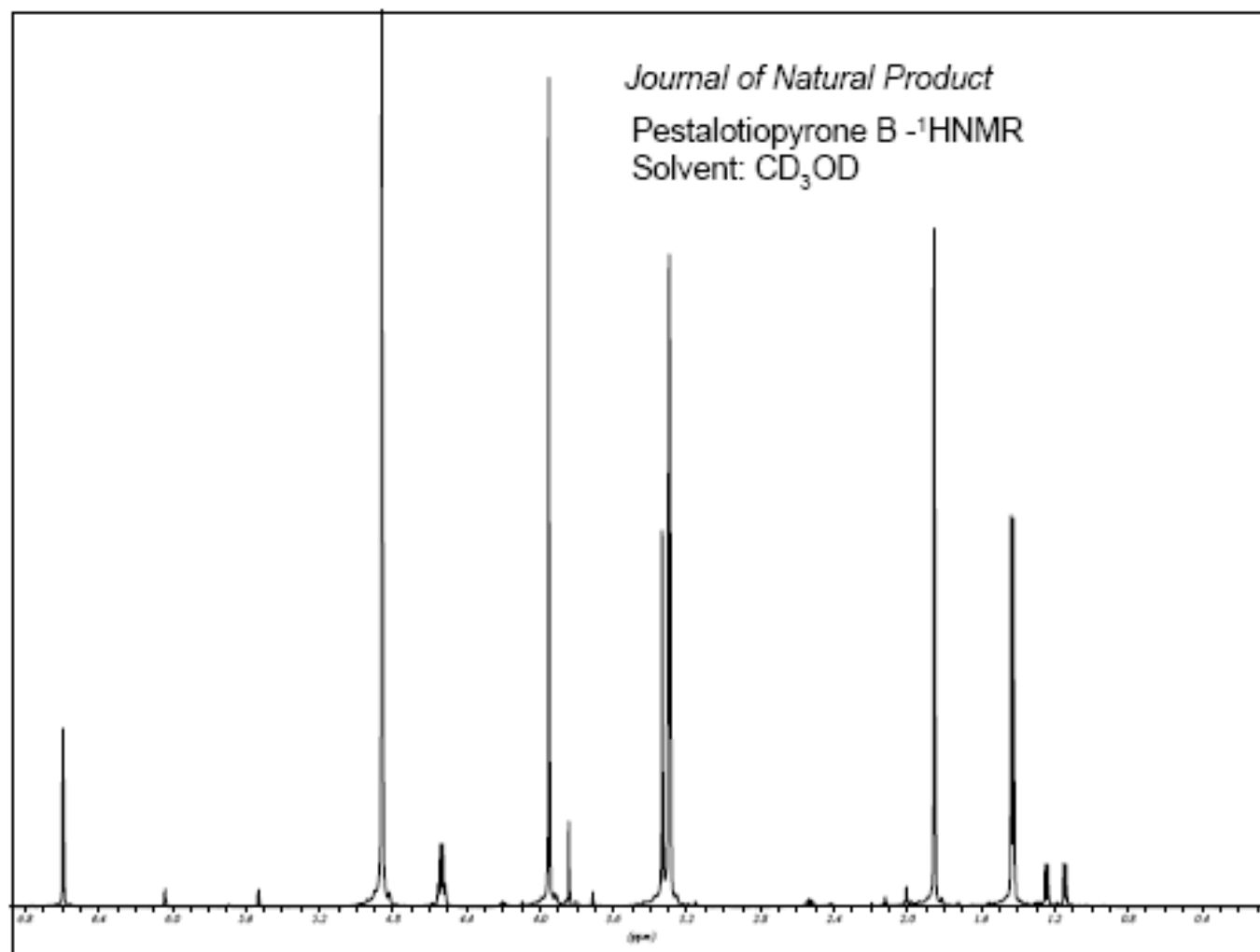
Attachment 22. The ^{13}C NMR Spectrum of Pestalasin A (**18**)

Attachment 23. The ^1H NMR Spectrum of Pestalasin C (**20**)

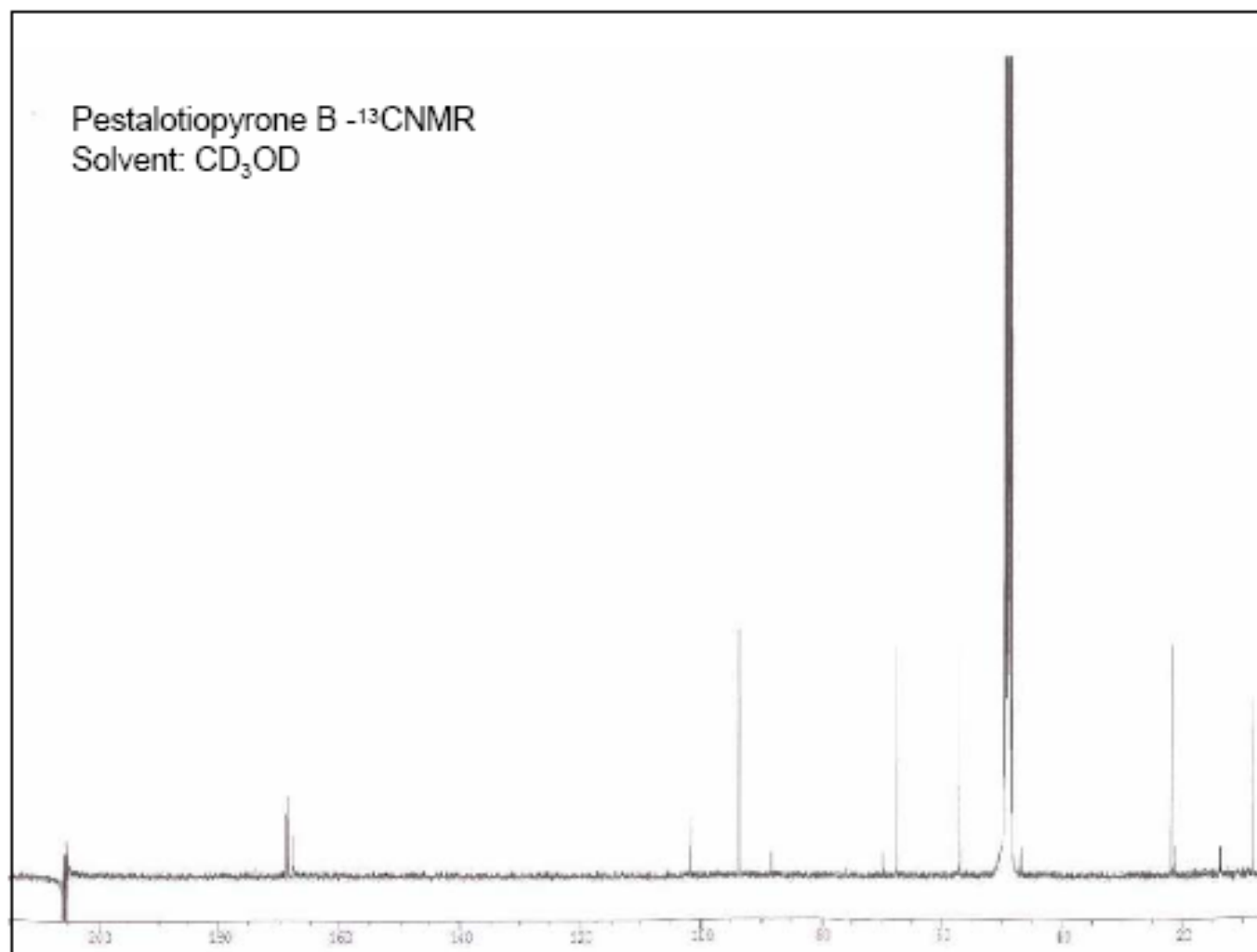
Attachment 24. The ^1H NMR Spectrum of 3-hydroxymethyl-6,8-dimethoxycoumarin (**23**)

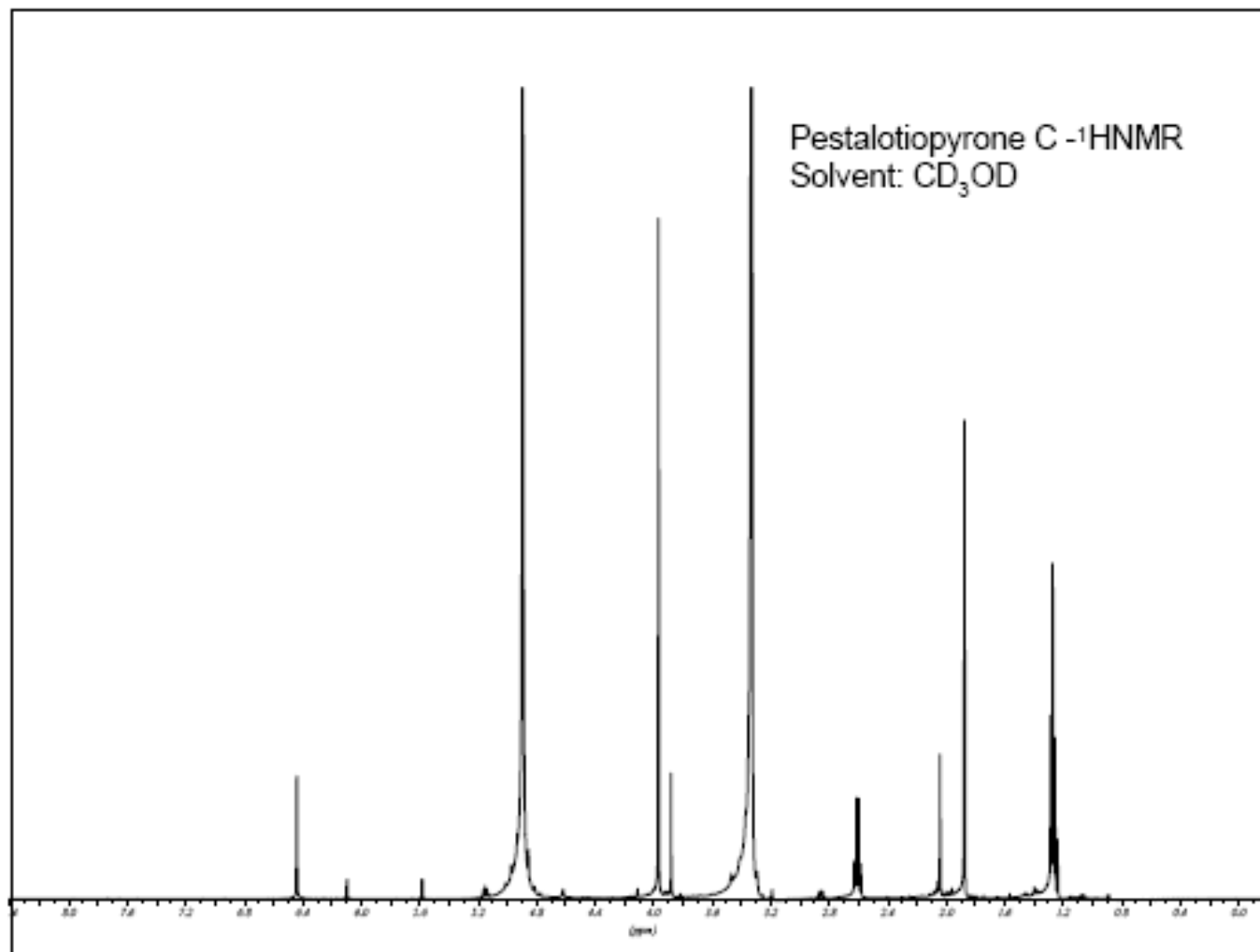


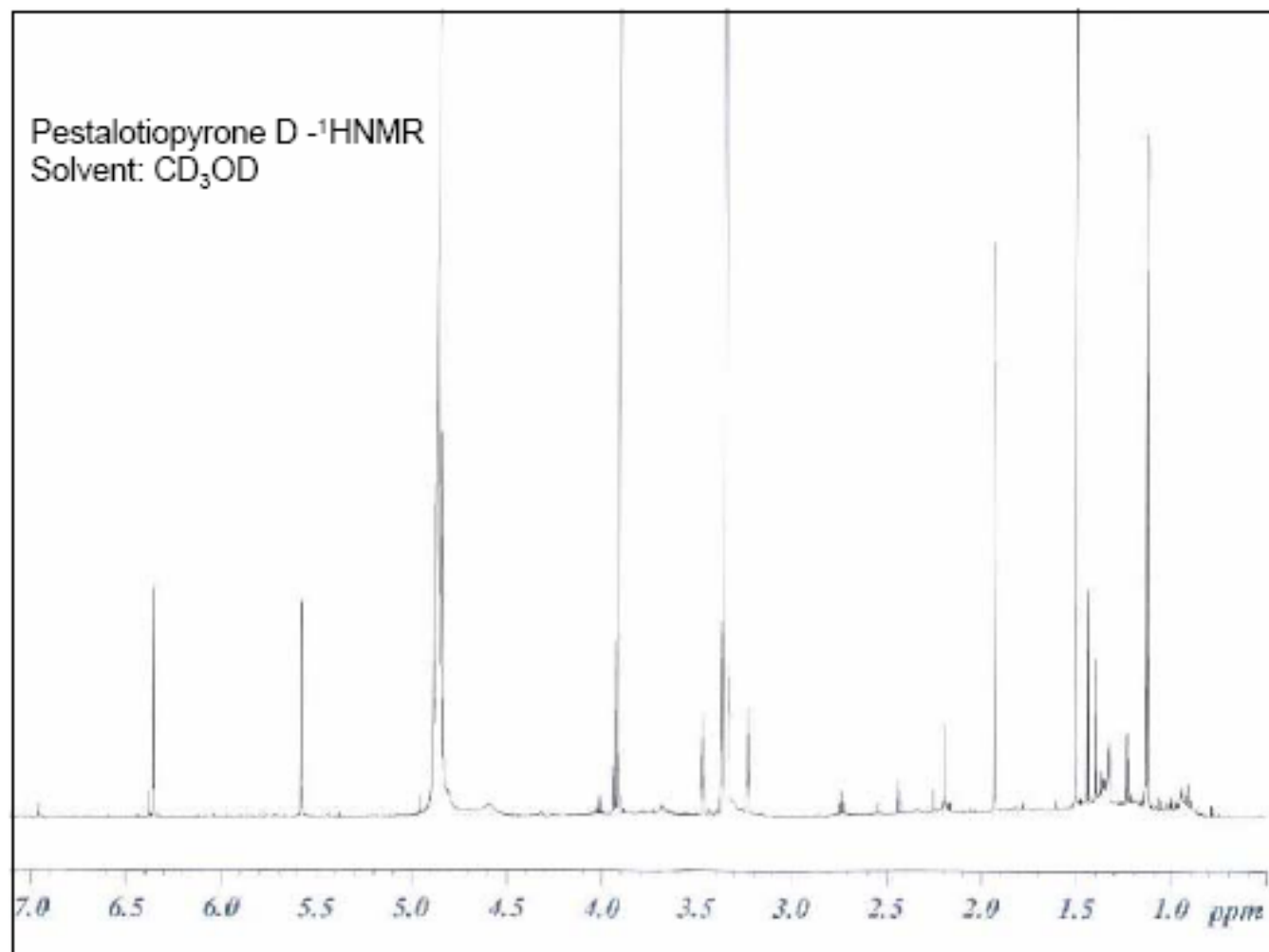
Attachment 25. The ^1H NMR Spectrum of Pestalotiopyrone A (**24**)

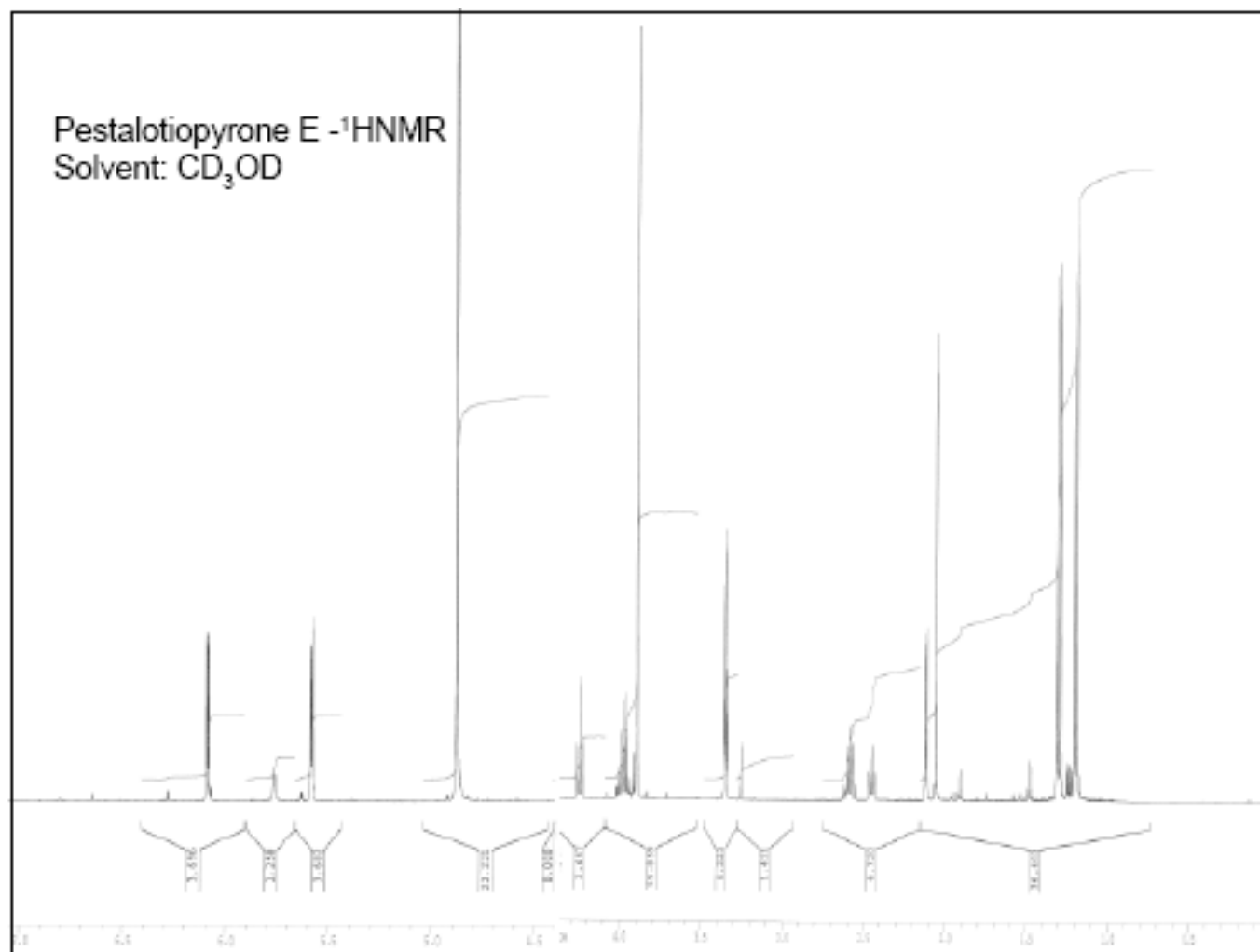
Attachment 26. The ^1H NMR Spectrum of Pestalotiopyrone B (**25**)

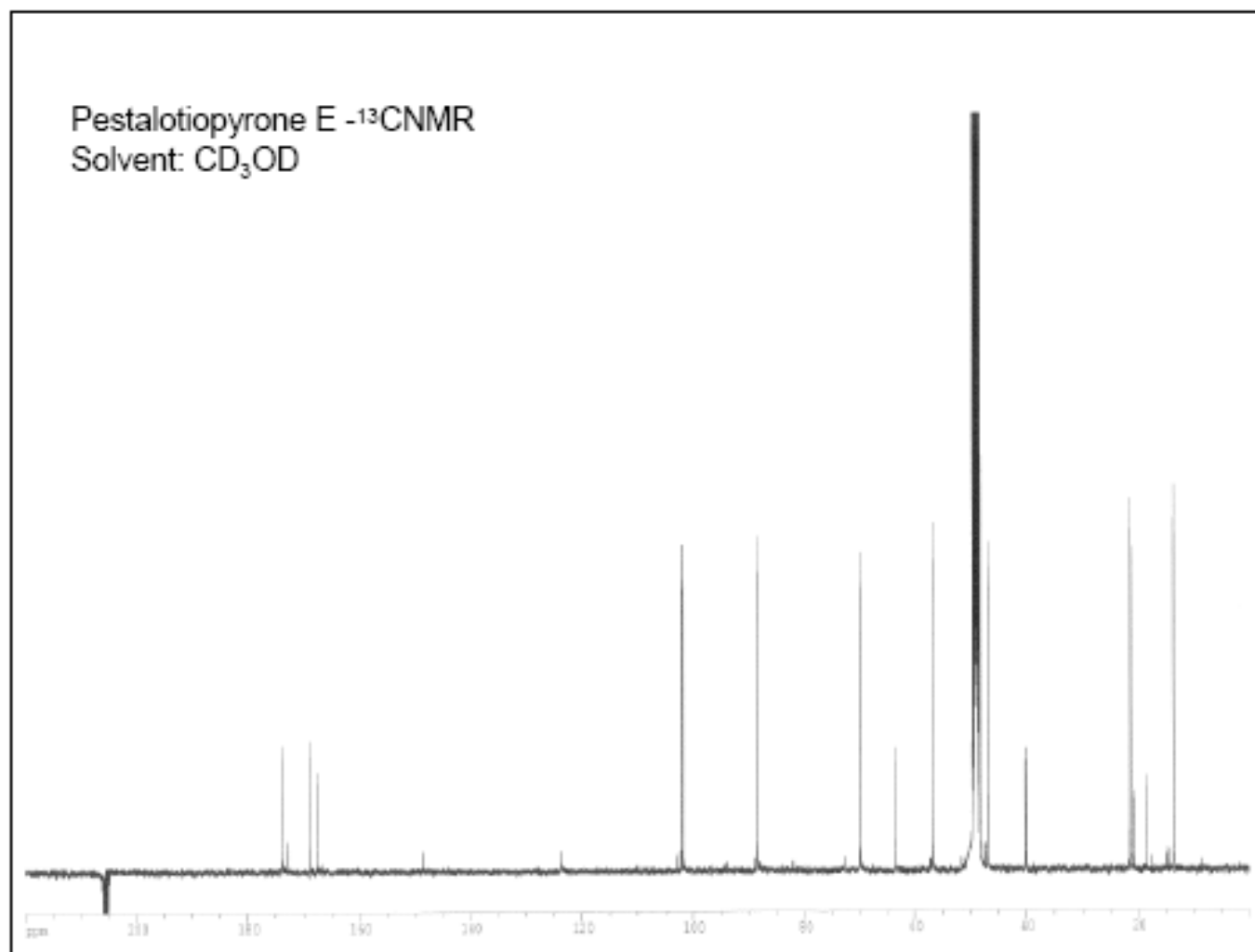
Attachment 27. The ^{13}C NMR Spectrum of Pestalotiopyrone B (**25**)

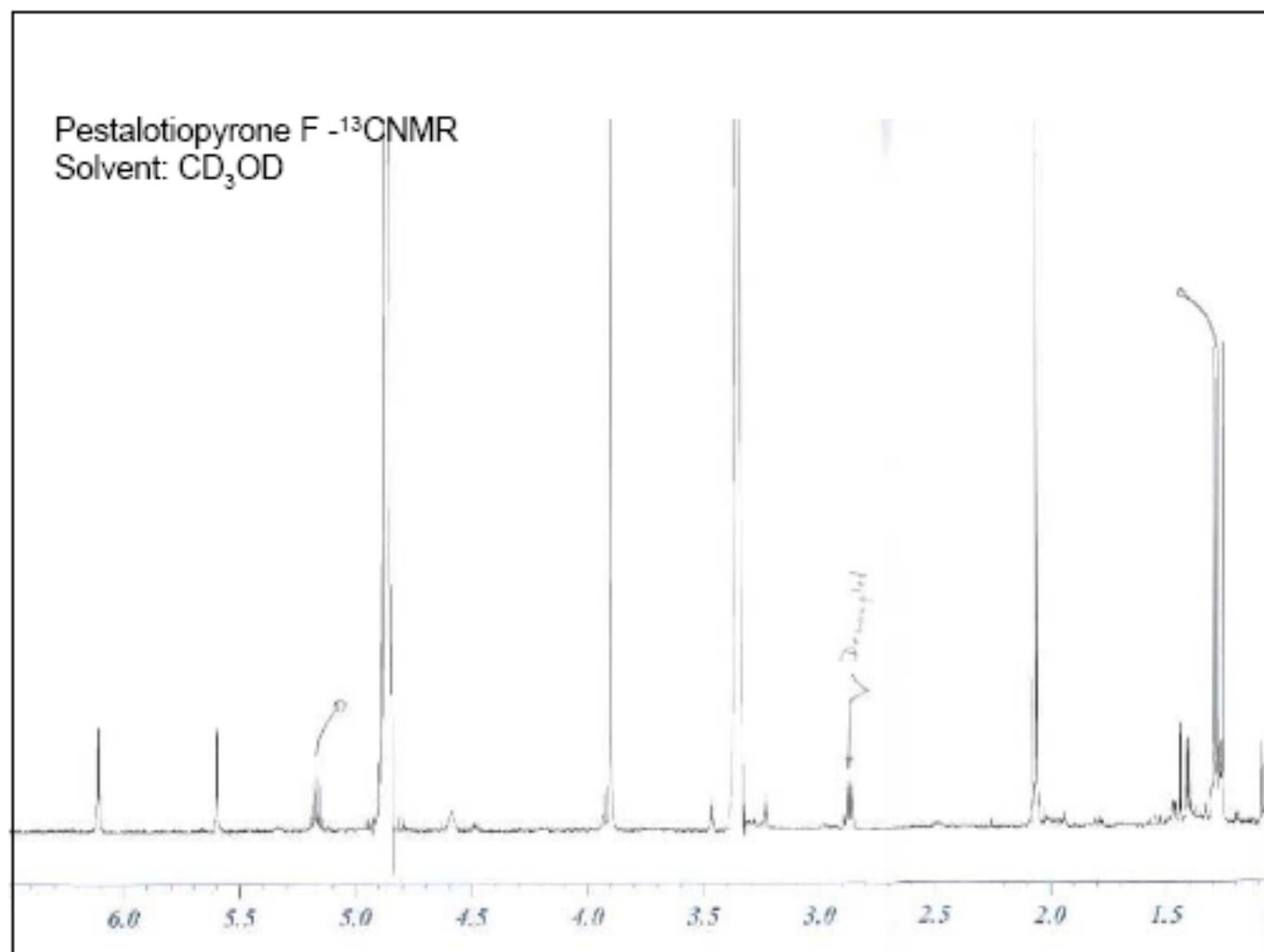


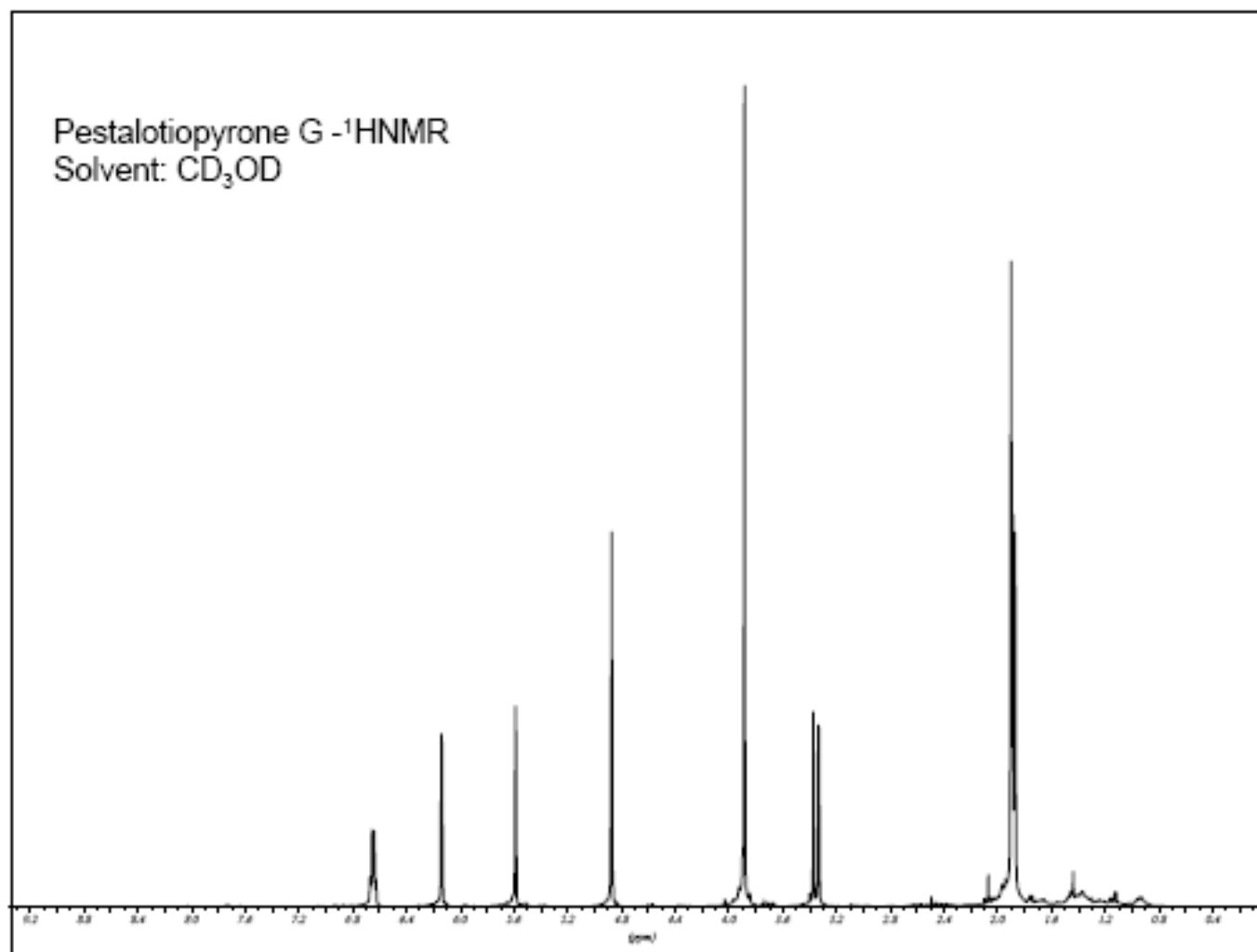
Attachment 28. The ^1H NMR Spectrum of Pestalotiopyrone C (**26**)

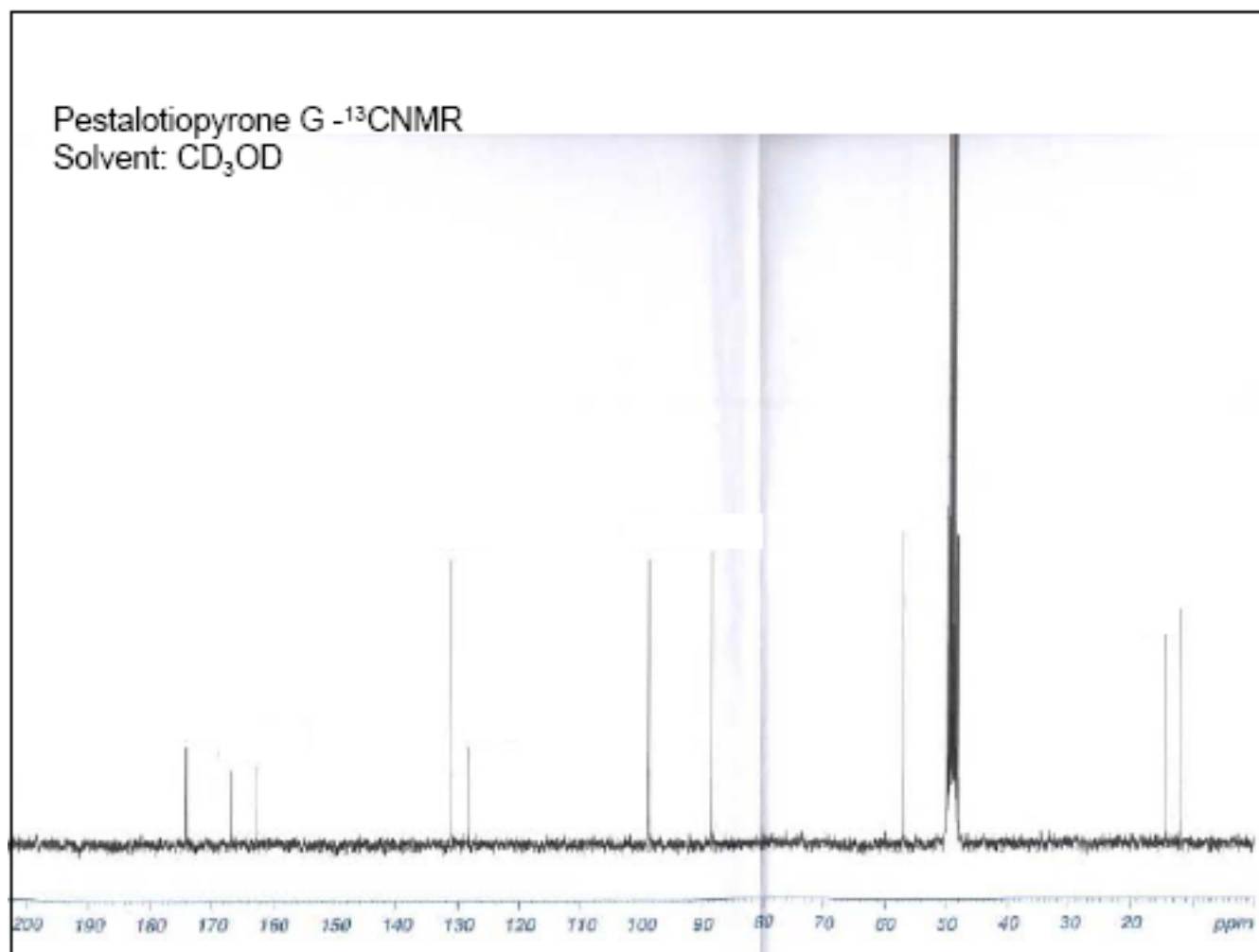
Attachment 29. The ^1H NMR Spectrum of Pestalotiopyrone D (**28**)

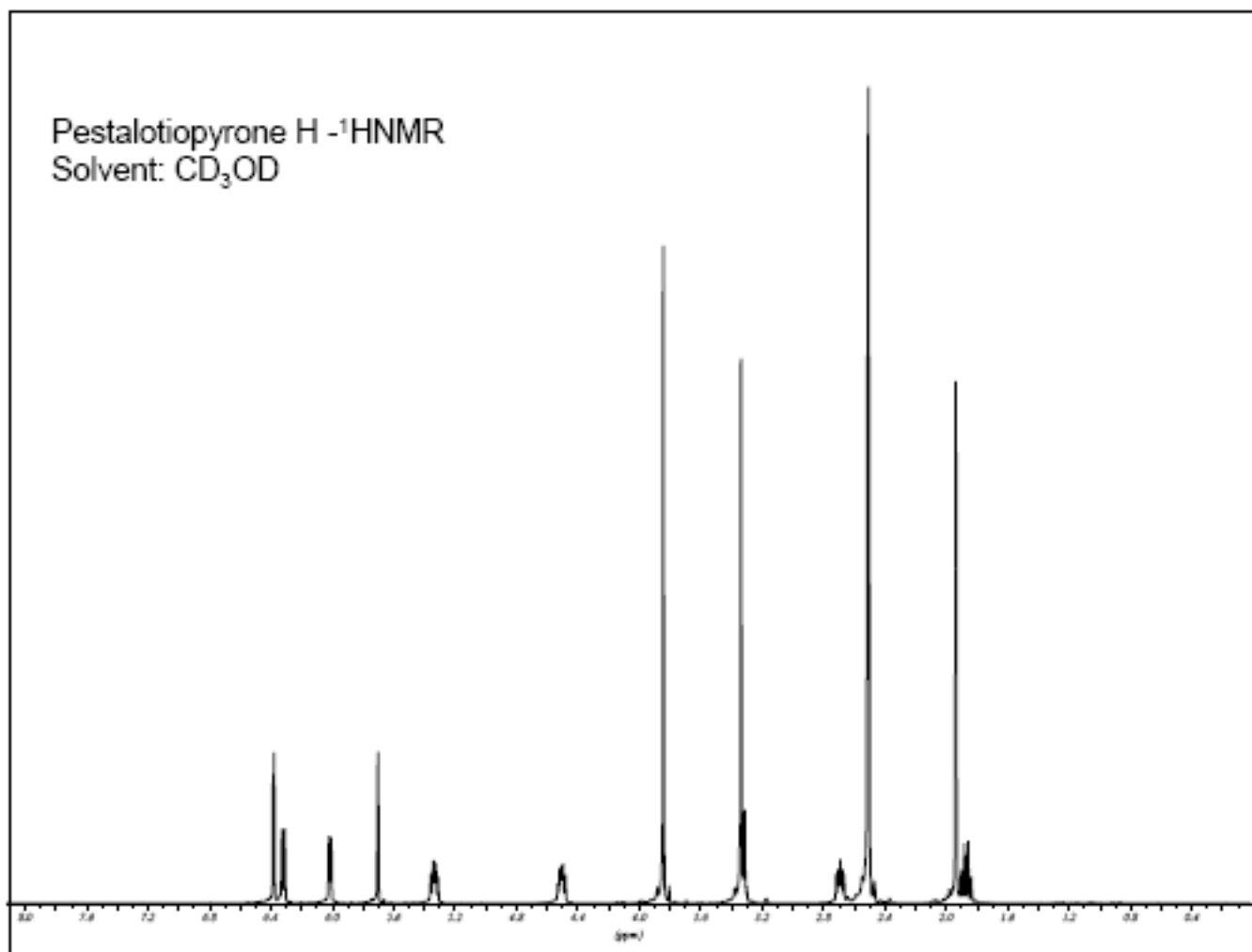
Attachment 30. The ^1H NMR Spectrum of Pestalotiopyrone E (**29**)

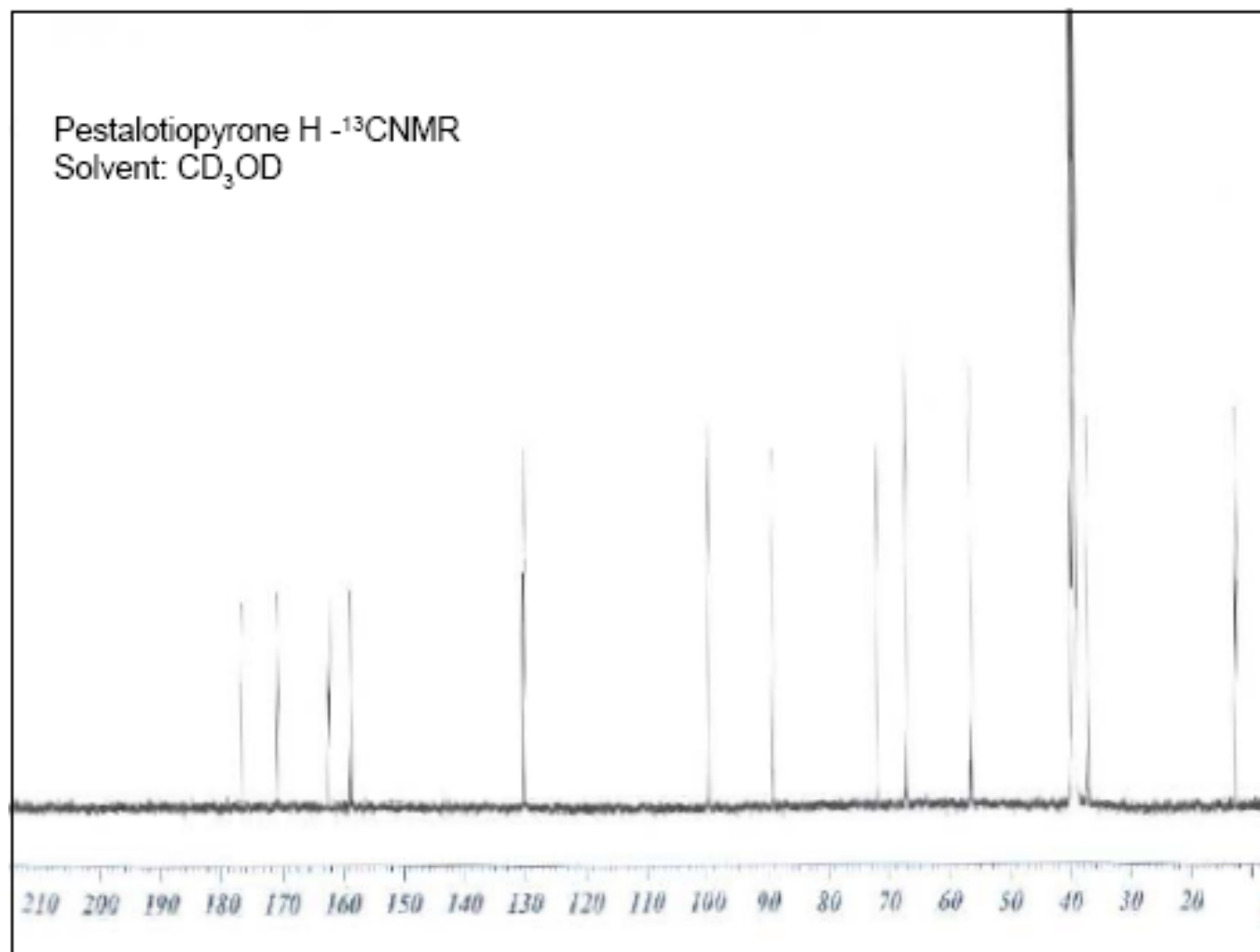
Attachment 31. The ^{13}C NMR Spectrum of Pestalotiopyrone E (**29**)

Attachment 32. The ^1H NMR Spectrum of Pestalotiopyrone F (**30**)

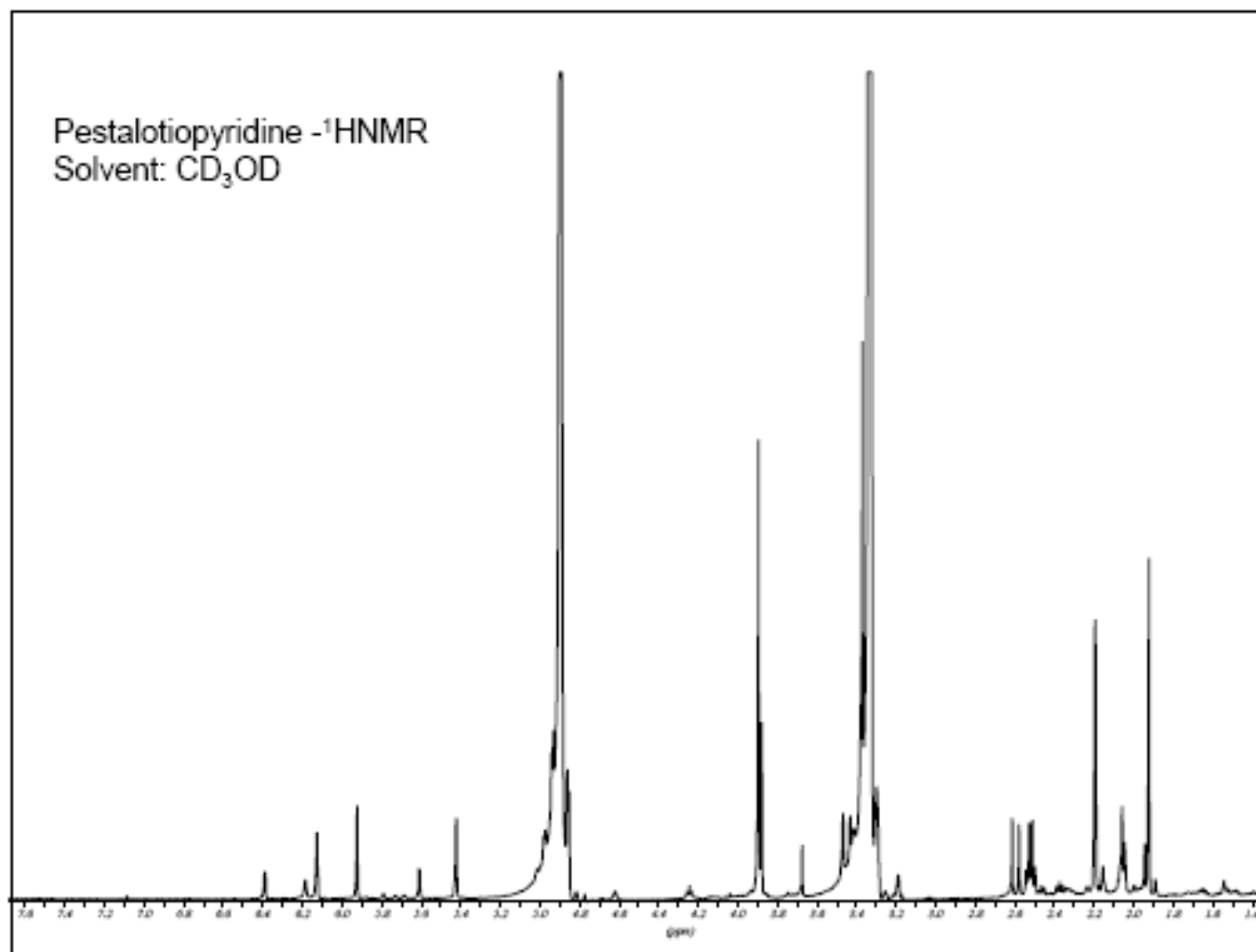
Attachment 33. The ^1H NMR Spectrum of Pestalotiopyrone G (**31**)

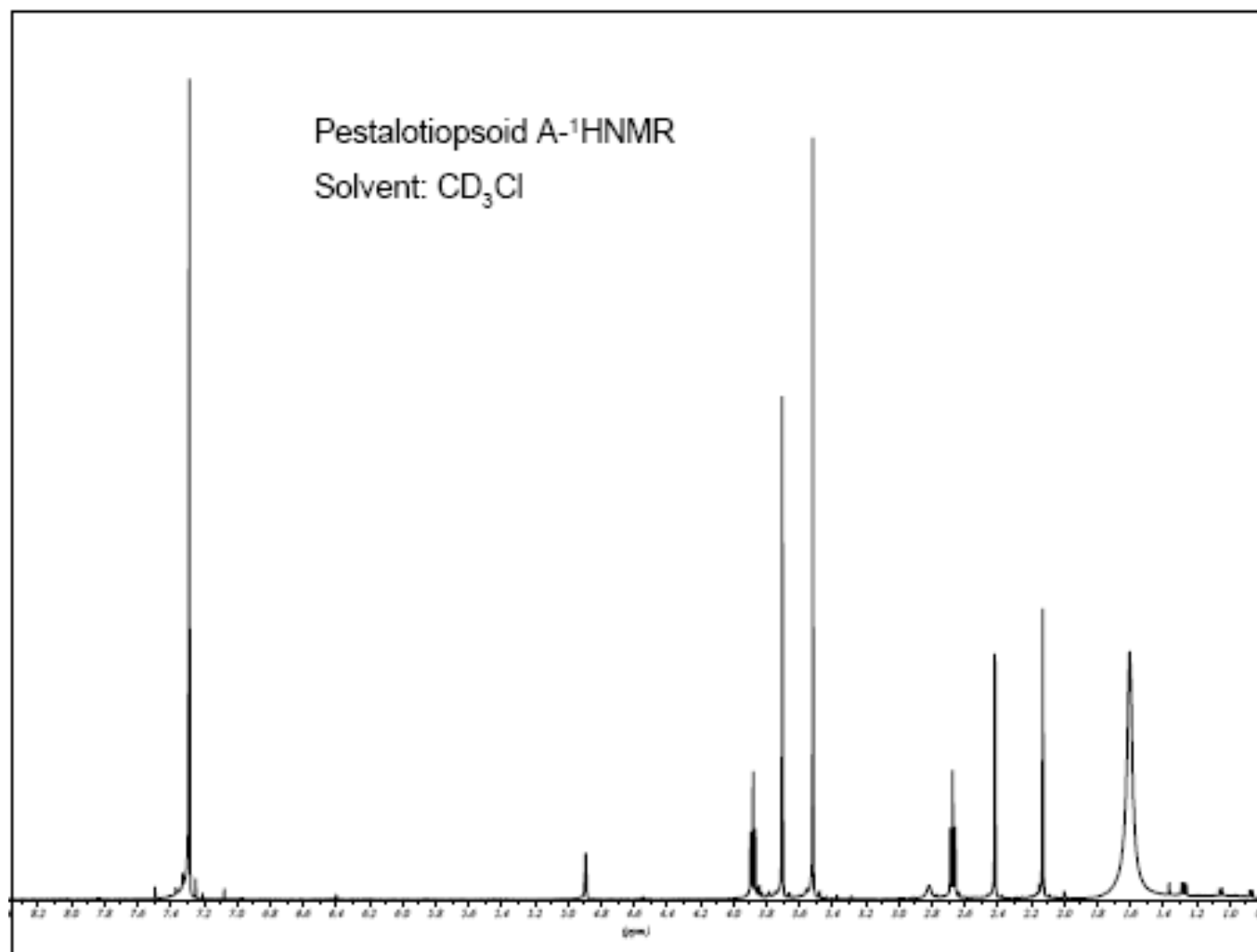
Attachment 34. The ^{13}C NMR Spectrum of Pestalotiopyrone G (**31**)

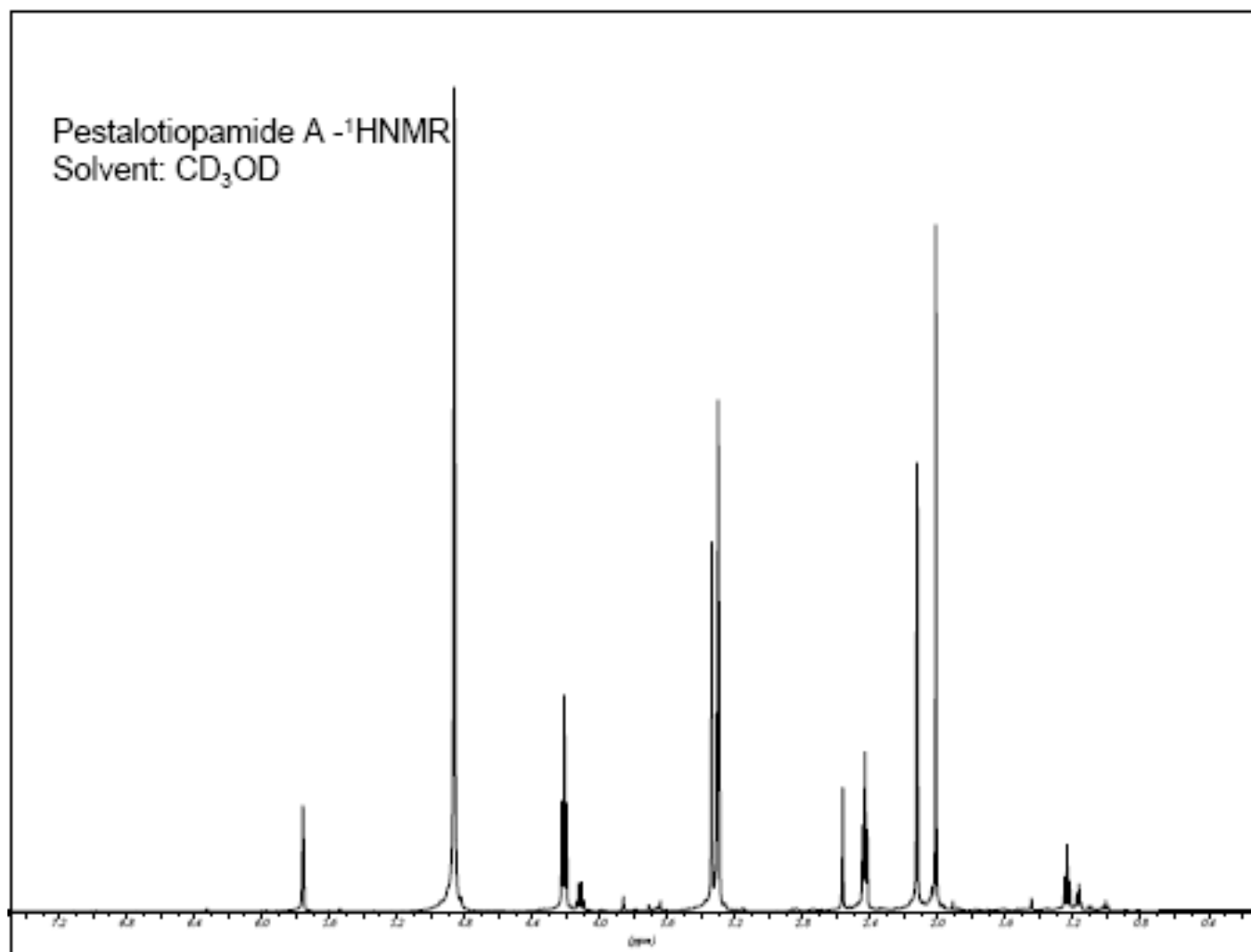
Attachment 35. The ^1H NMR Spectrum of Pestalotiopyrone H (**32**)

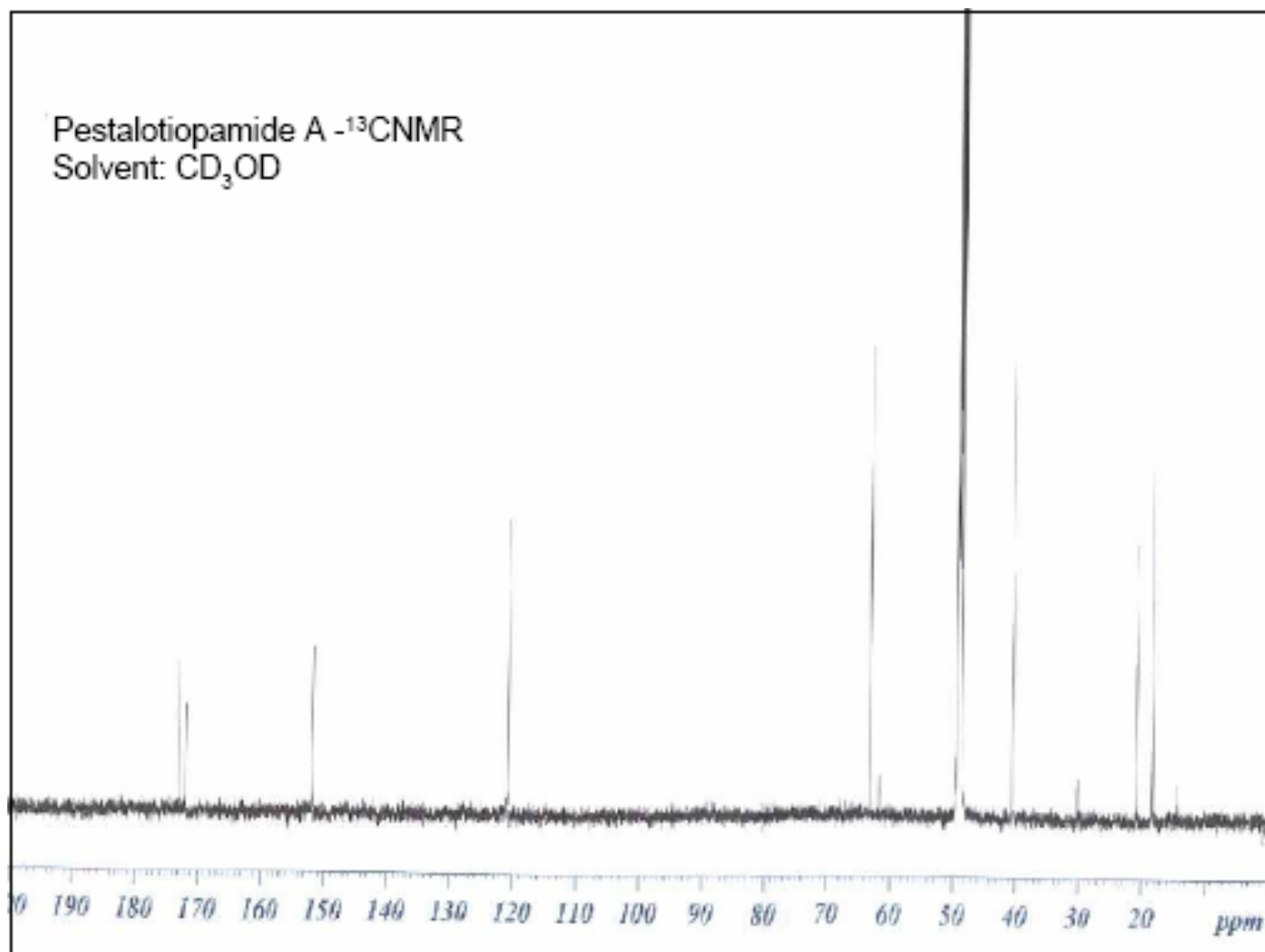
Attachment 36. The ^{13}C NMR Spectrum of Pestalotiopyrone H (**32**)

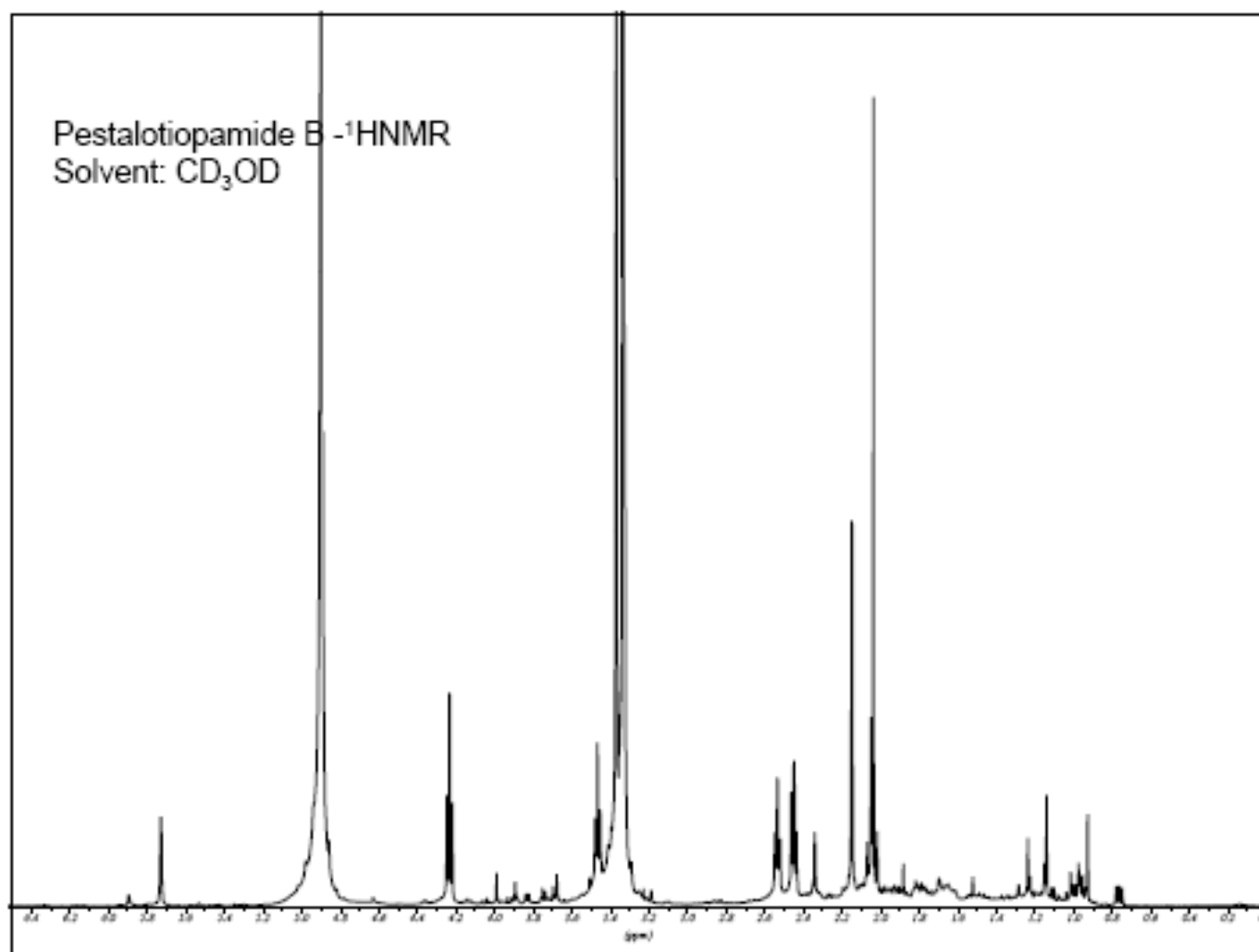
Attachment 37. The ^1H NMR Spectrum of Pestalotiopyridine (**33**)



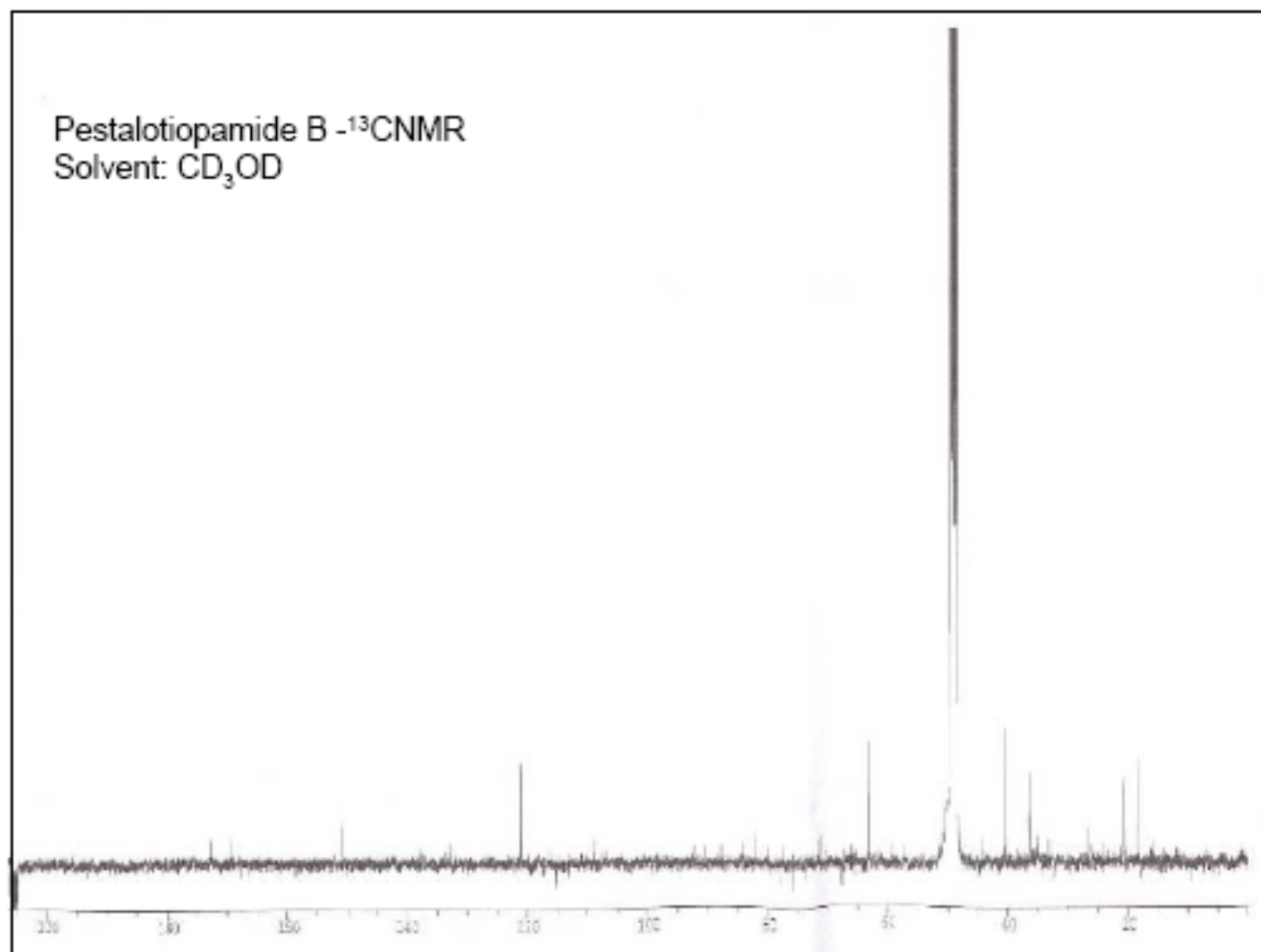
Attachment 38. The ^1H NMR Spectrum of Pestalotiopsoid A (**34**)

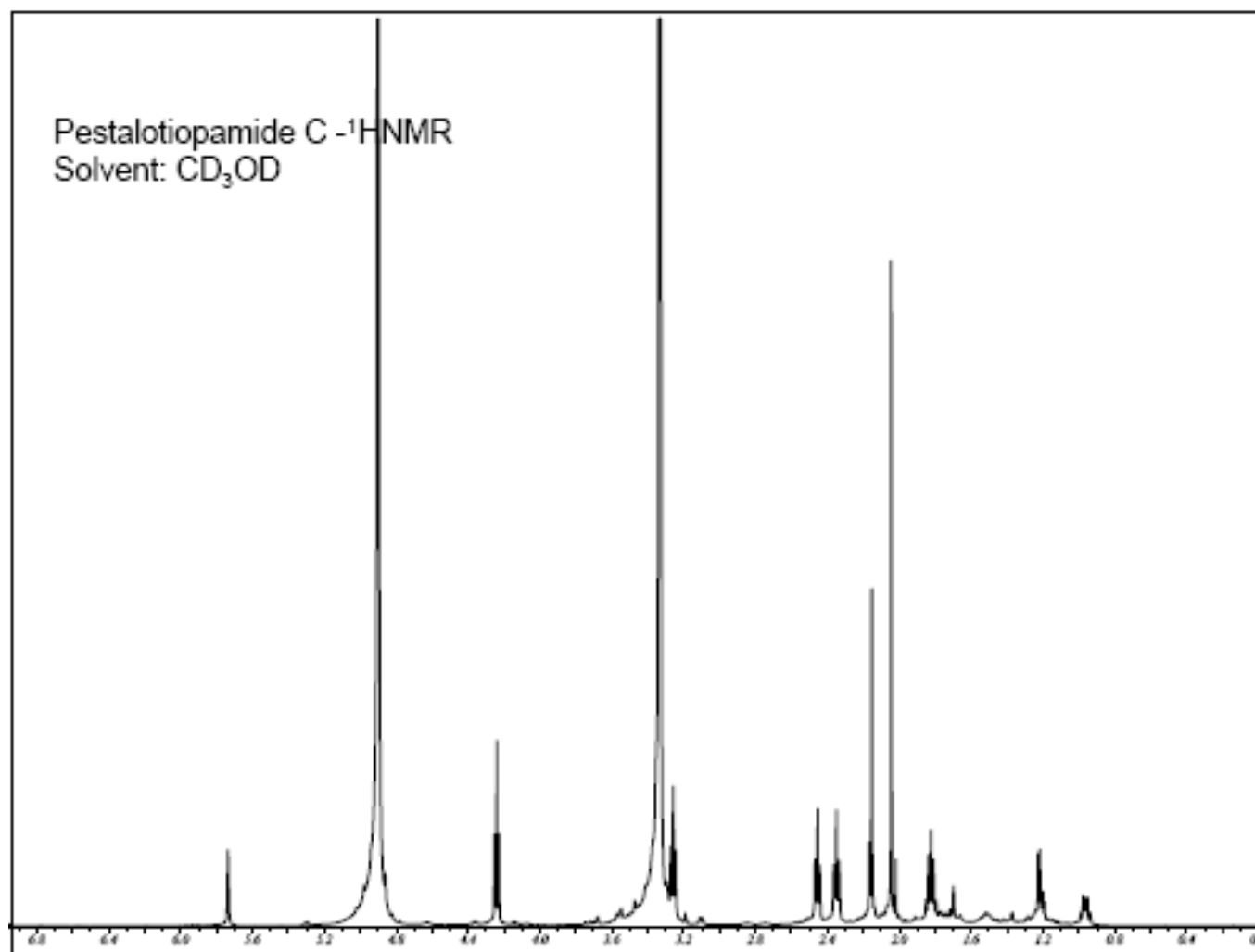
Attachment 39. The ^1H NMR Spectrum of Pestalotiopamide A (**35**)

Attachment 40. The ^{13}C NMR Spectrum of Pestalotiopamide A (**35**)

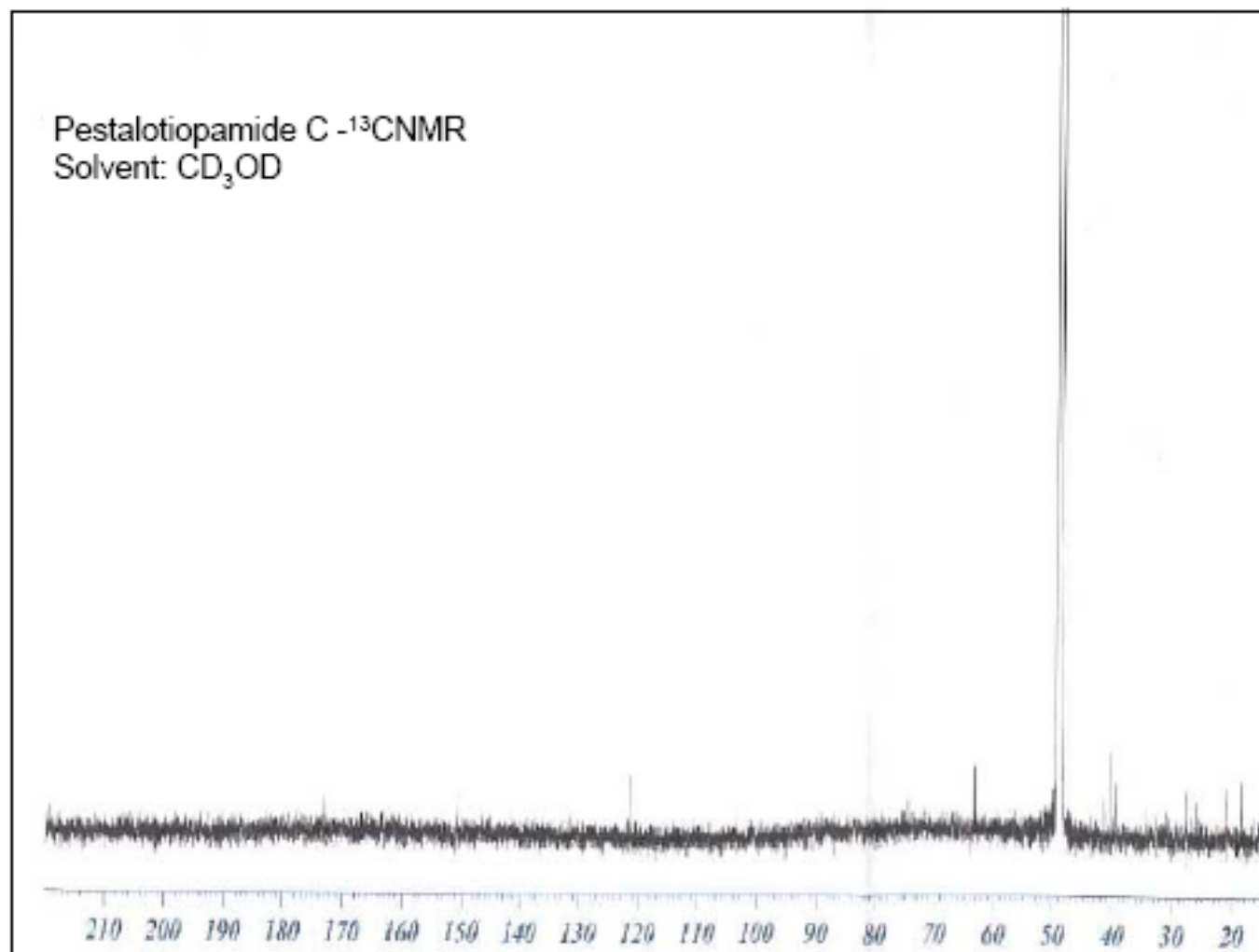
Attachment 41. The ^1H NMR Spectrum of Pestalotiopamide B (**36**)

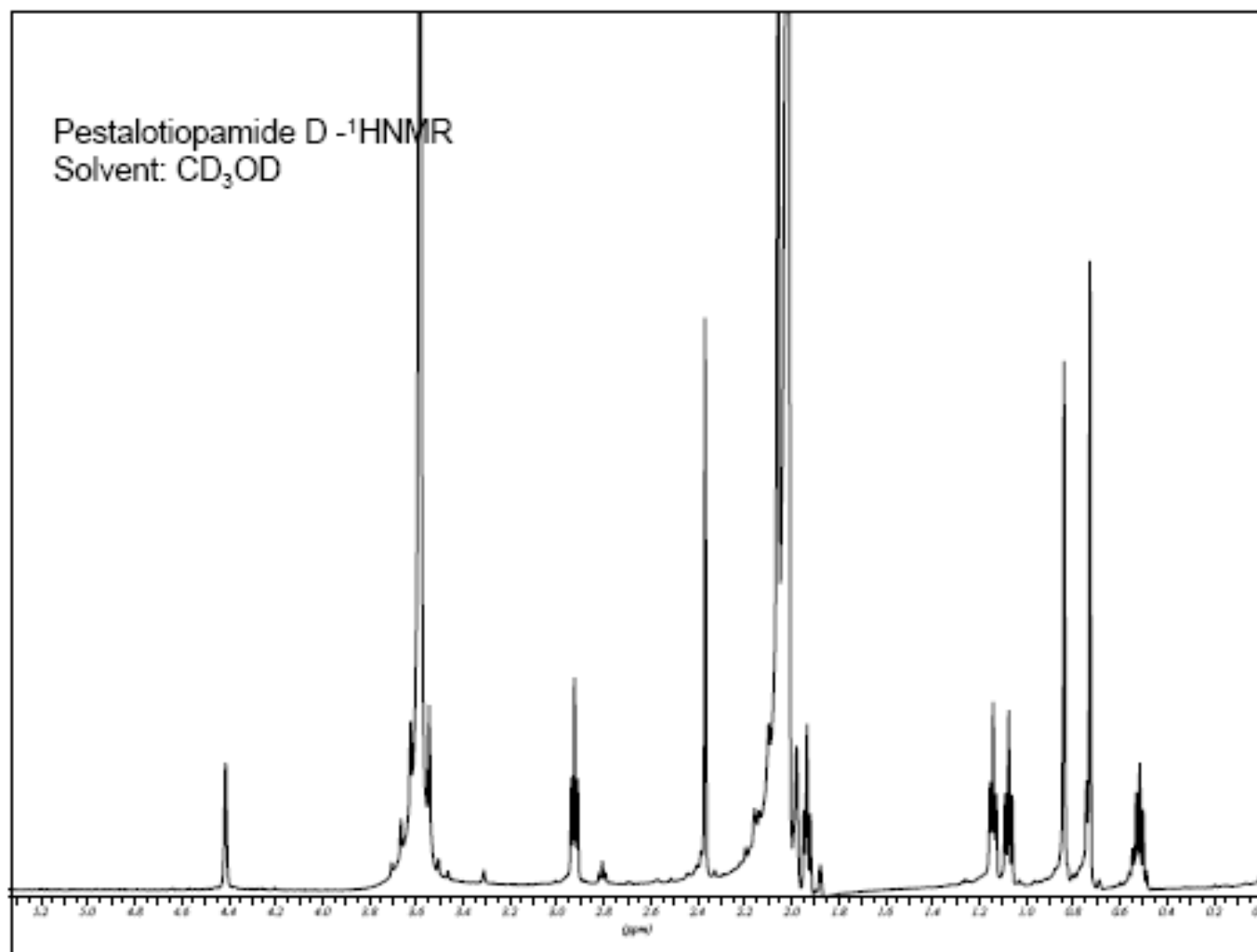
Attachment 42. The ^{13}C NMR Spectrum of Pestalotiopamide B (**36**)

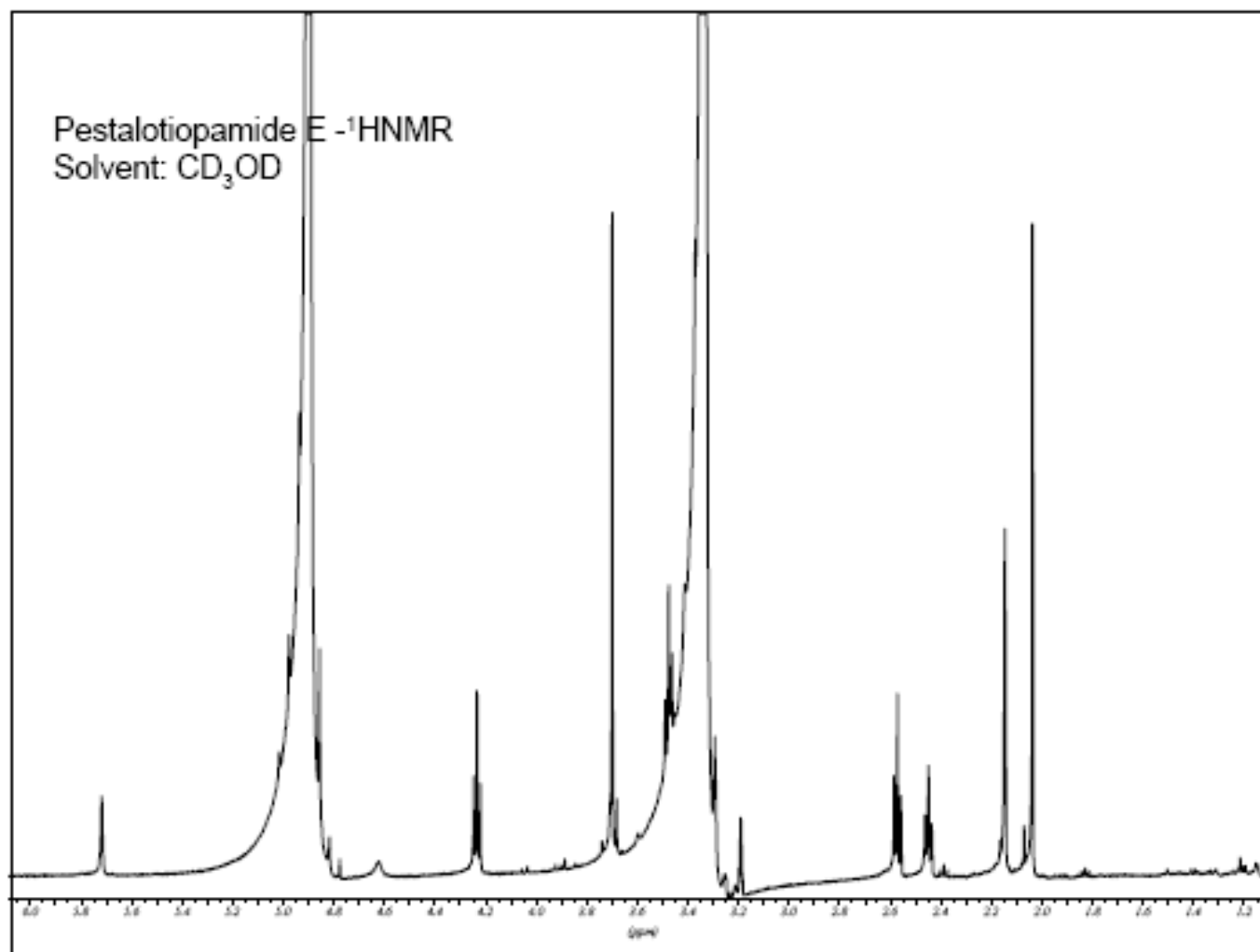


Attachment 43. The ^1H NMR Spectrum of Pestalotiopamide C (**37**)

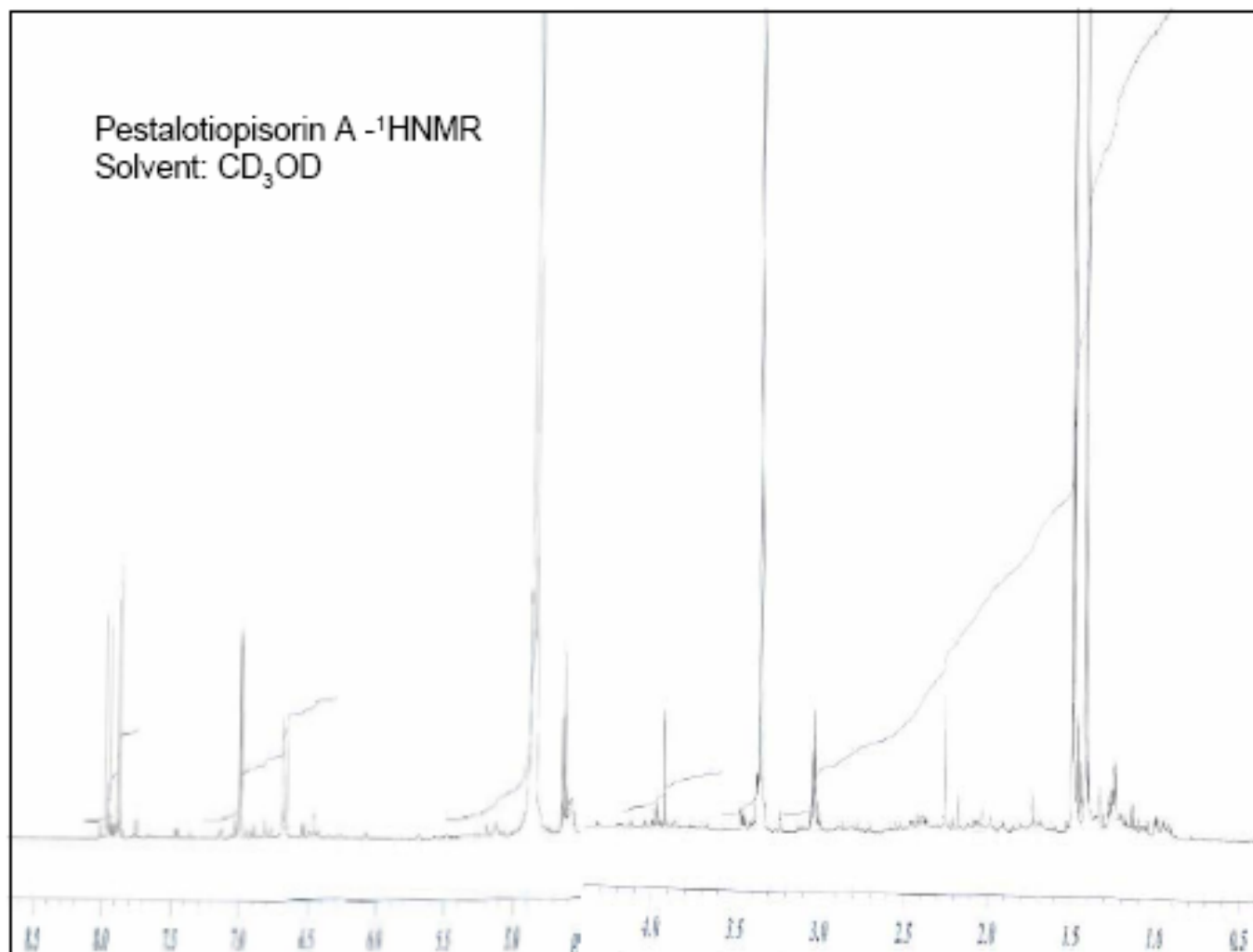
Attachment 44. The ^{13}C NMR Spectrum of Pestalotiopamide C (**37**)

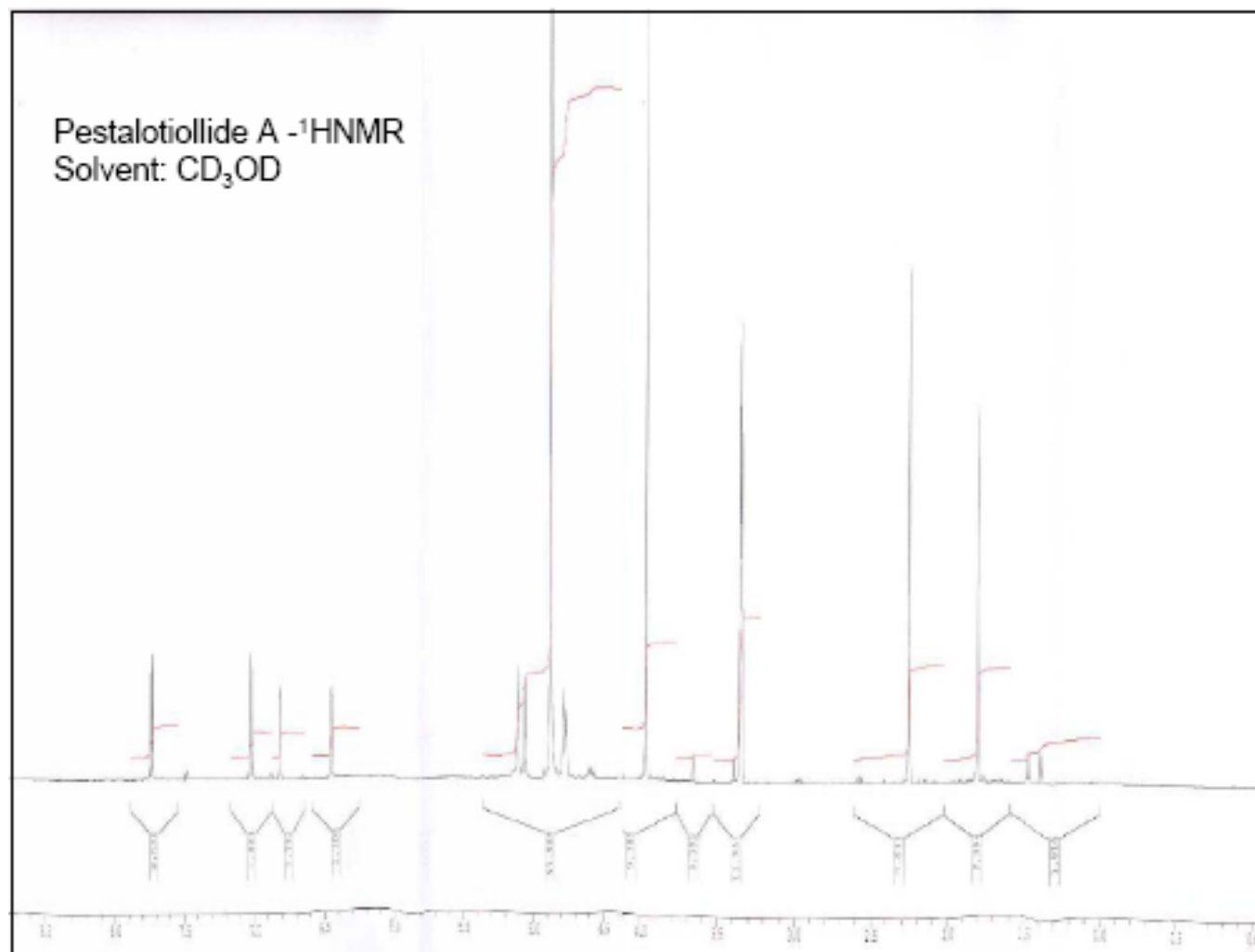


Attachment 45. The ^1H NMR Spectrum of Pestalotiopamide D (**38**)

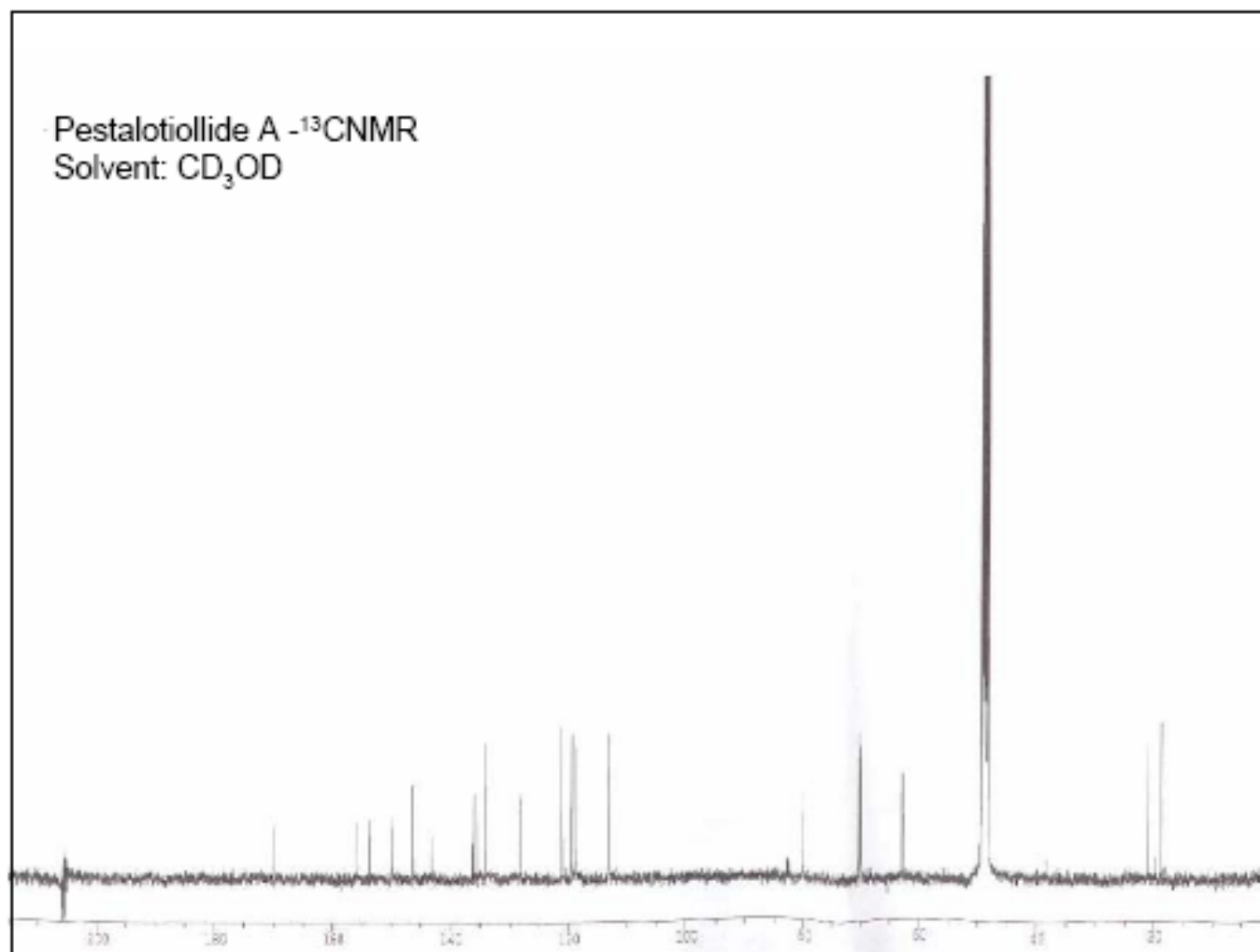
Attachment 46. The ^1H NMR Spectrum of Pestalotiopamide E (**39**)

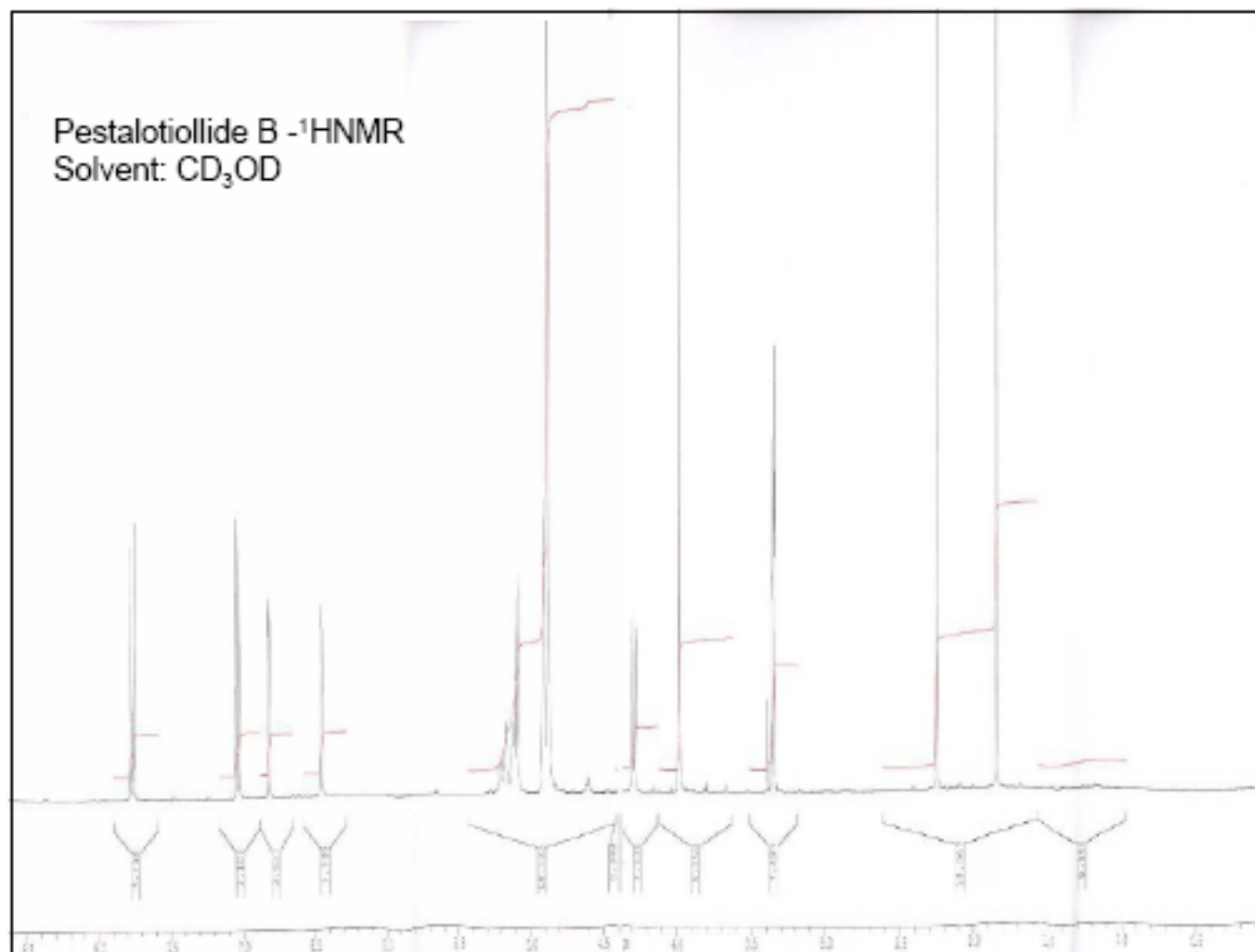
Attachment 47. The ^1H NMR Spectrum of Pestalotiopisorin A (**40**)

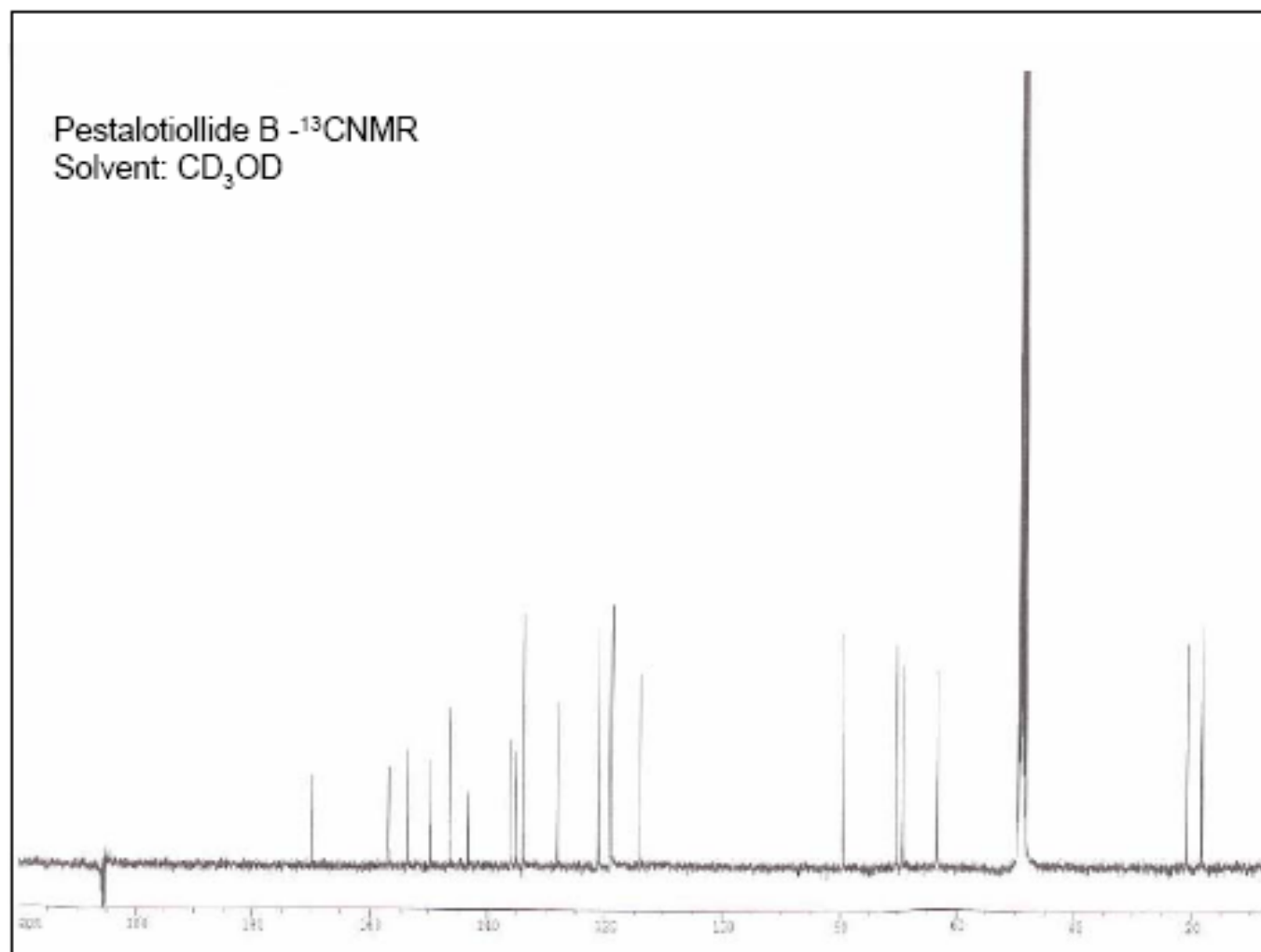


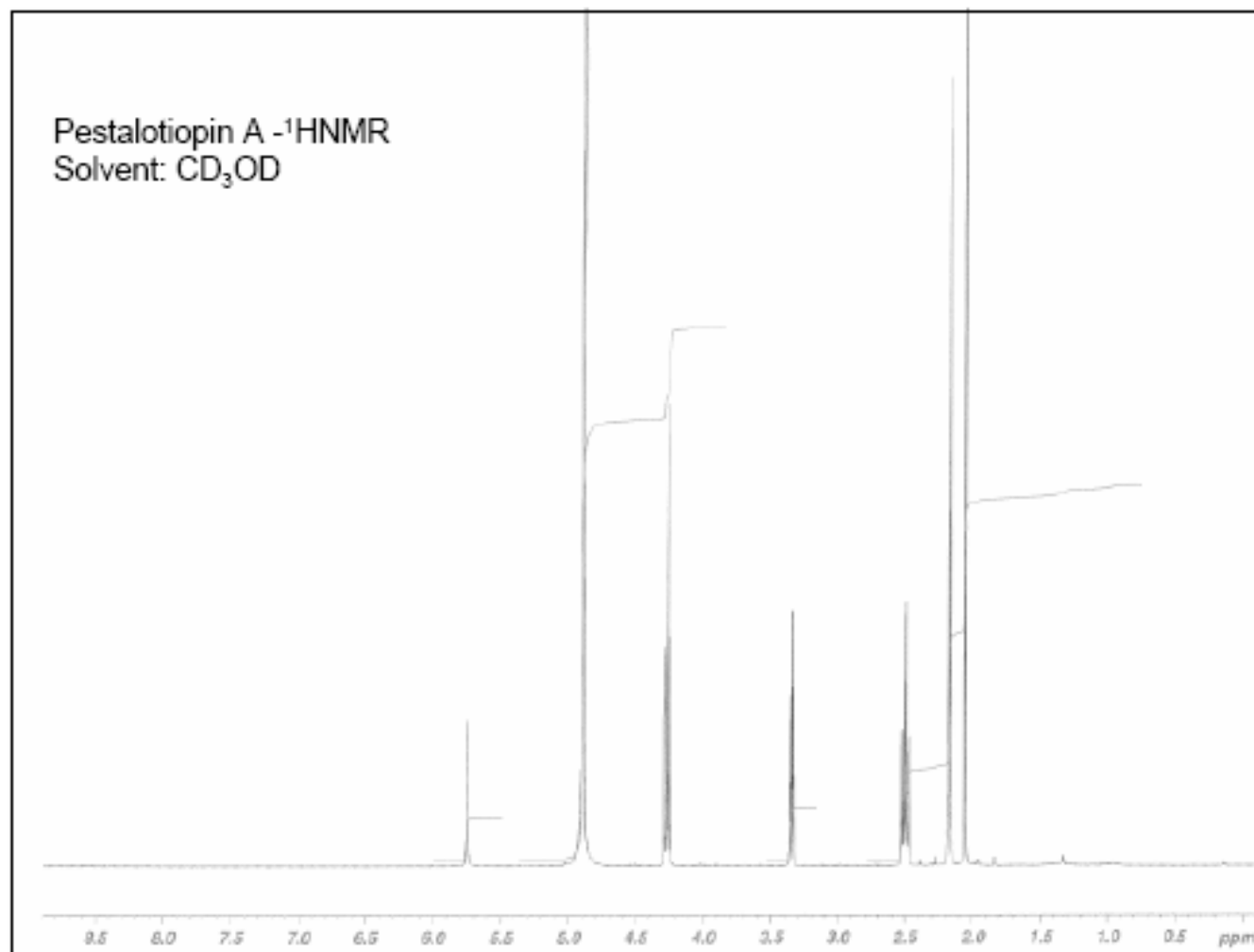
Attachment 48. The ^1H NMR Spectrum of Pestalotiollide A (**41**)

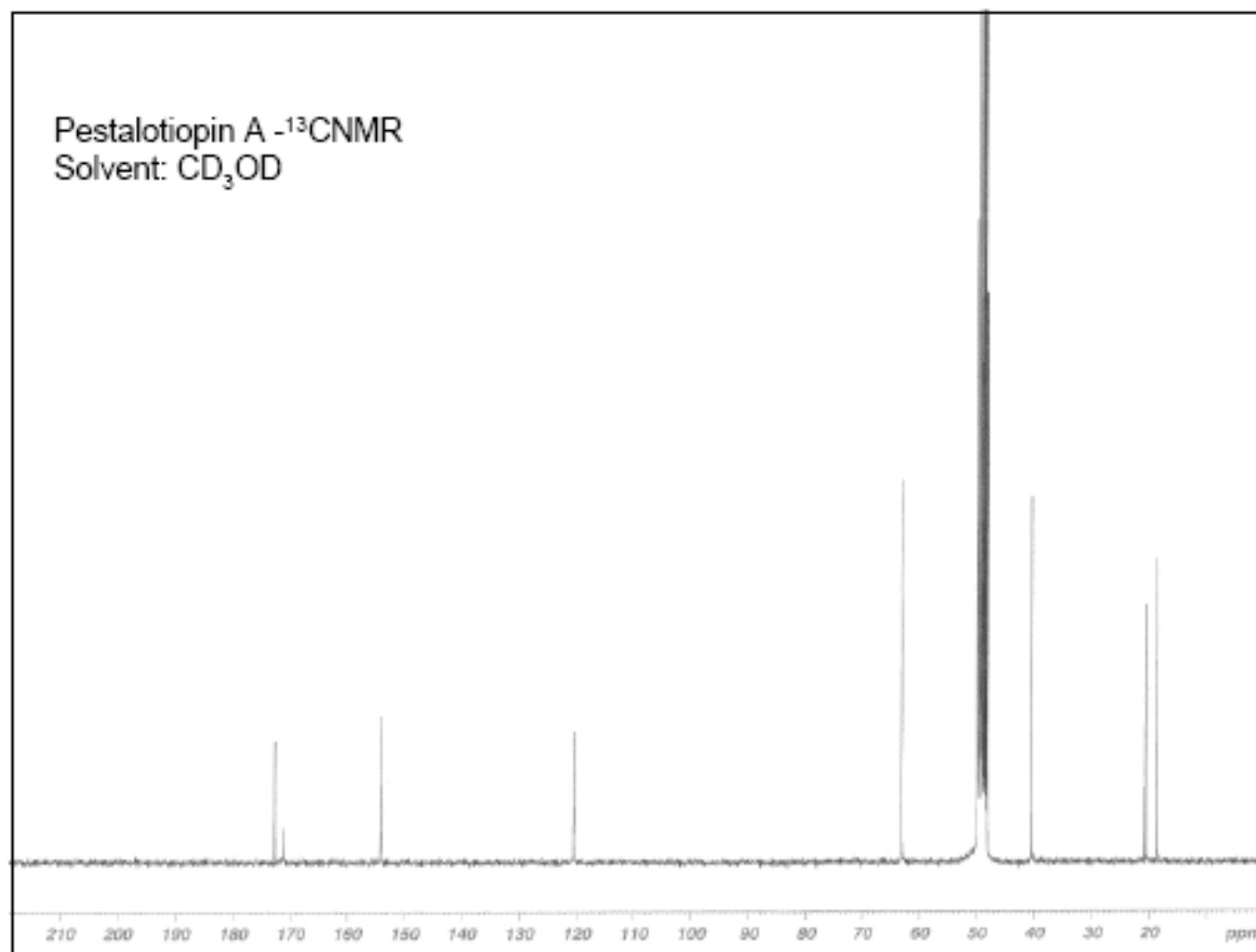
Attachment 49. The ^{13}C NMR Spectrum of Pestalotiollide A (**41**)

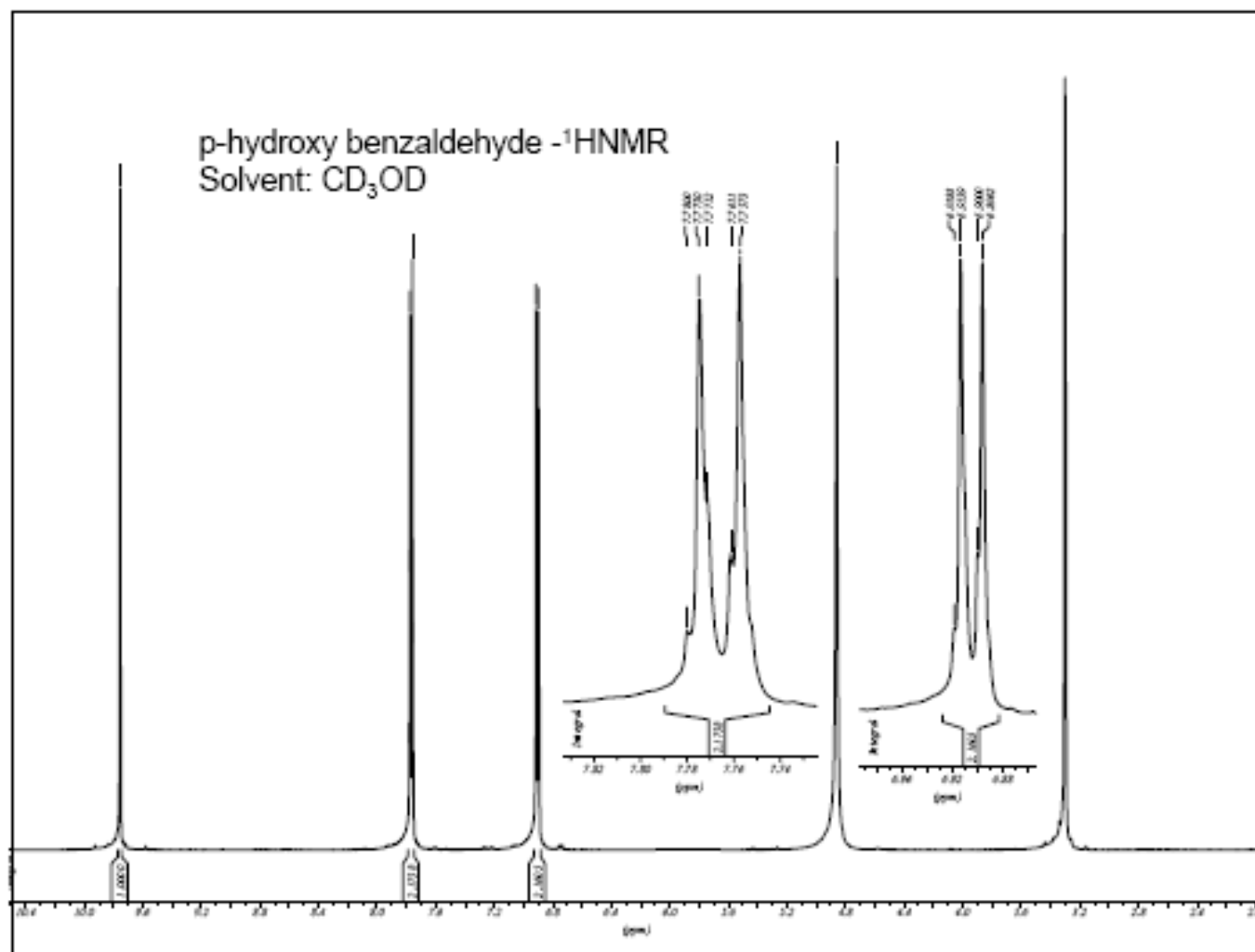


Attachment 50. The ^1H NMR Spectrum of Pestalotiollide B (**42**)

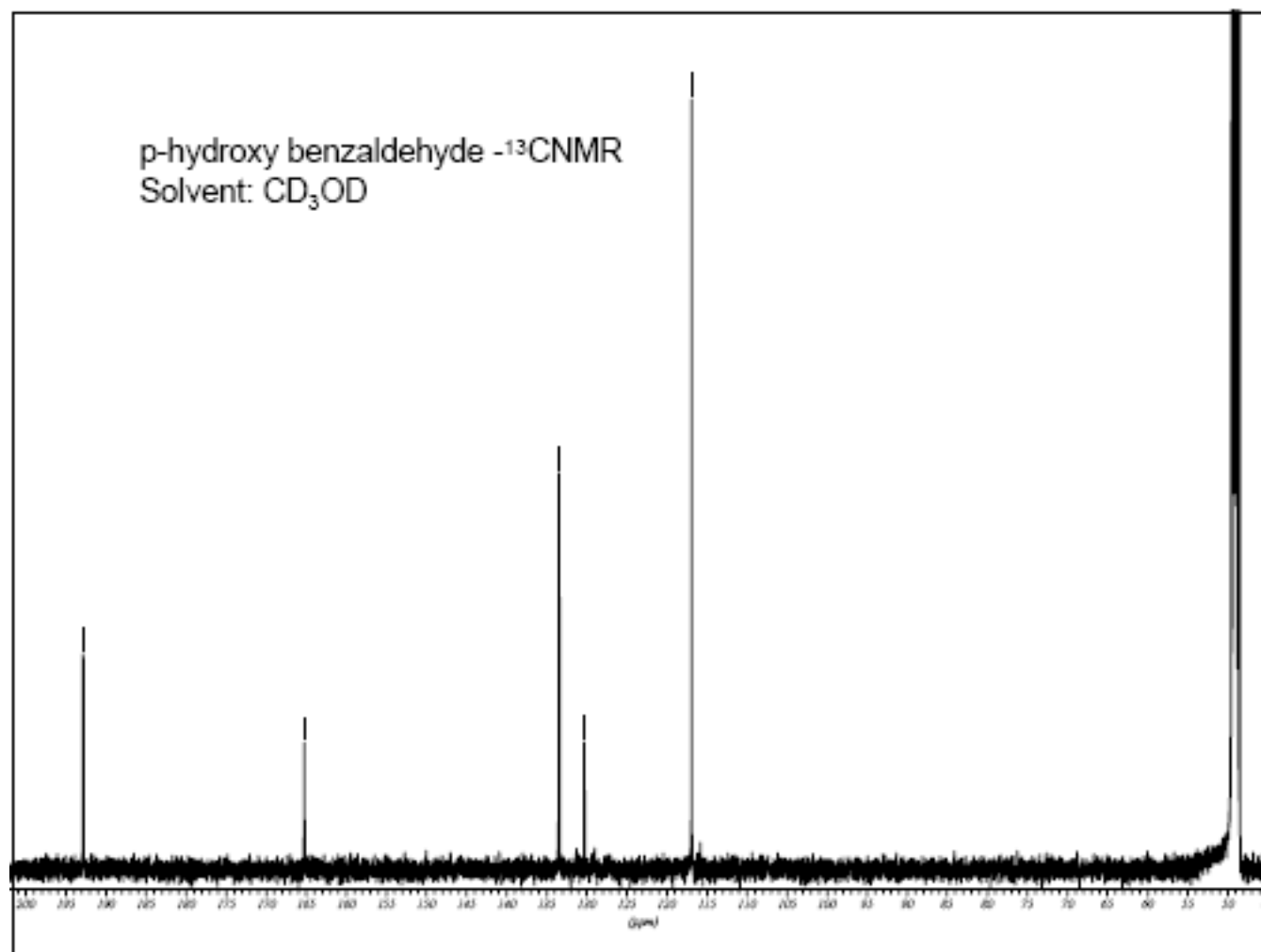
Attachment 51. The ^{13}C NMR Spectrum of Pestalotiollide B (**42**)

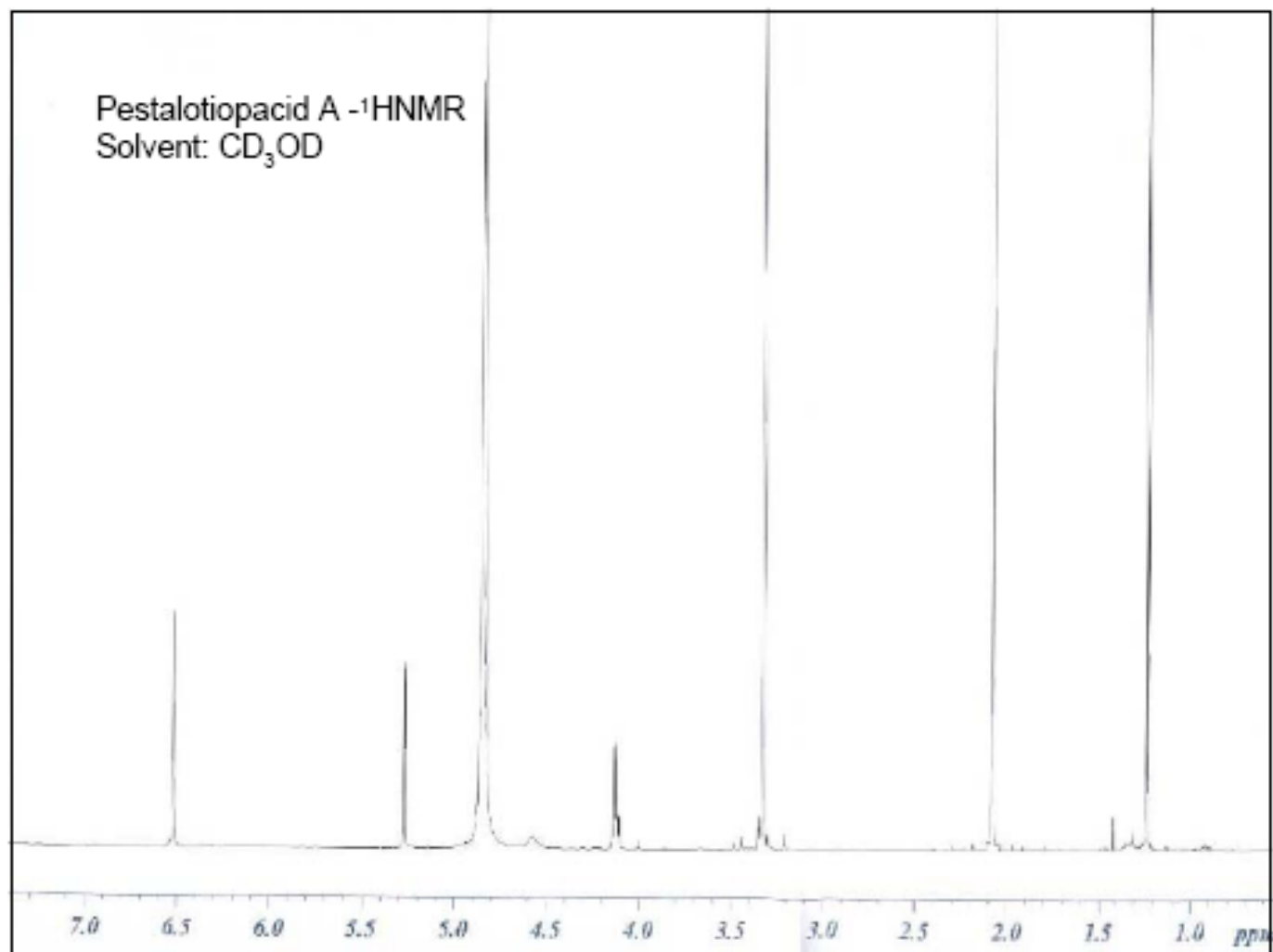
Attachment 52. The ^1H NMR Spectrum of Pestalotiopin A (**43**)

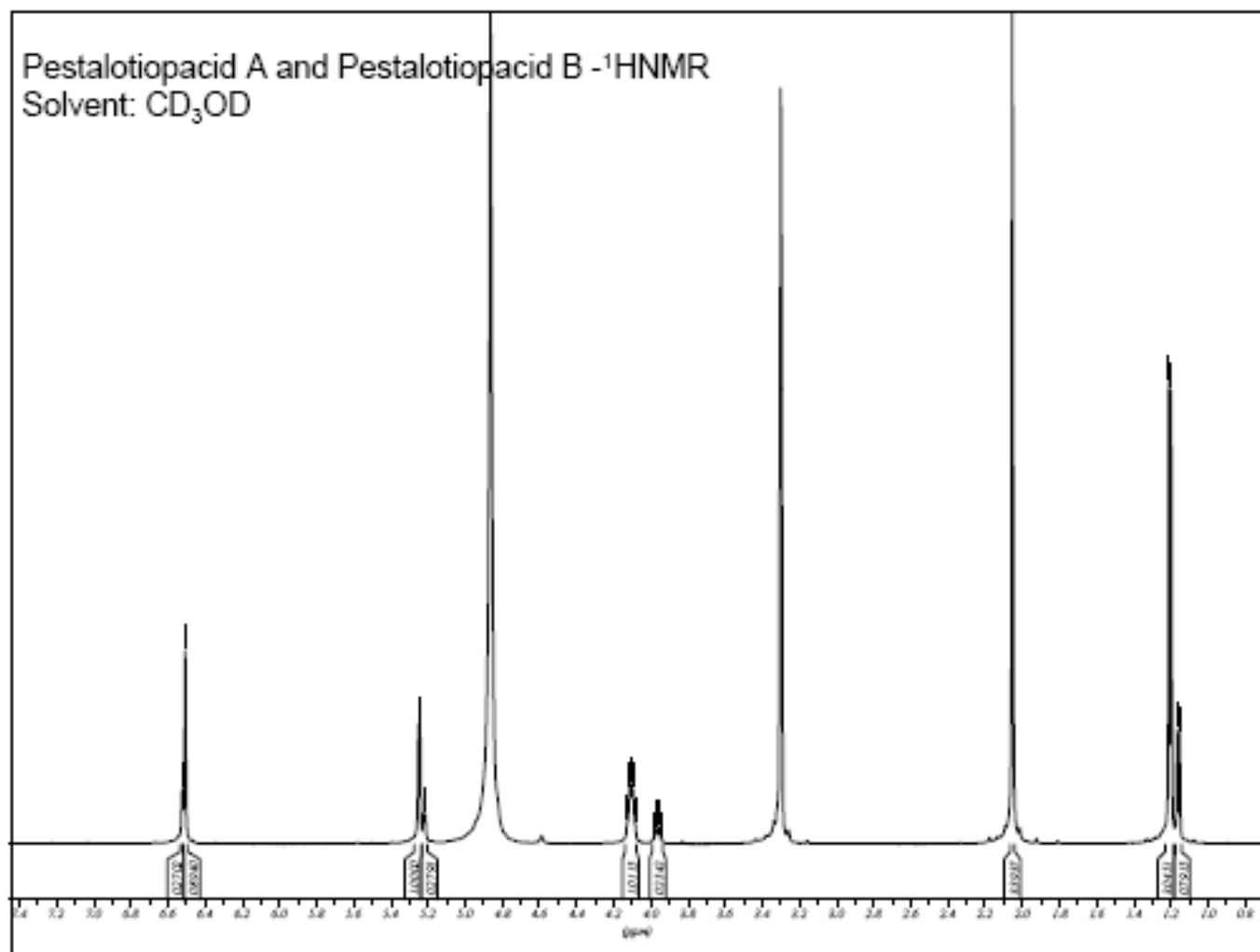
Attachment 53. The ^{13}C NMR Spectrum of Pestalotiopin A (**43**)

Attachment 54. The ^1H NMR Spectrum of *p*-hydroxy benzaldehyde (**45**)

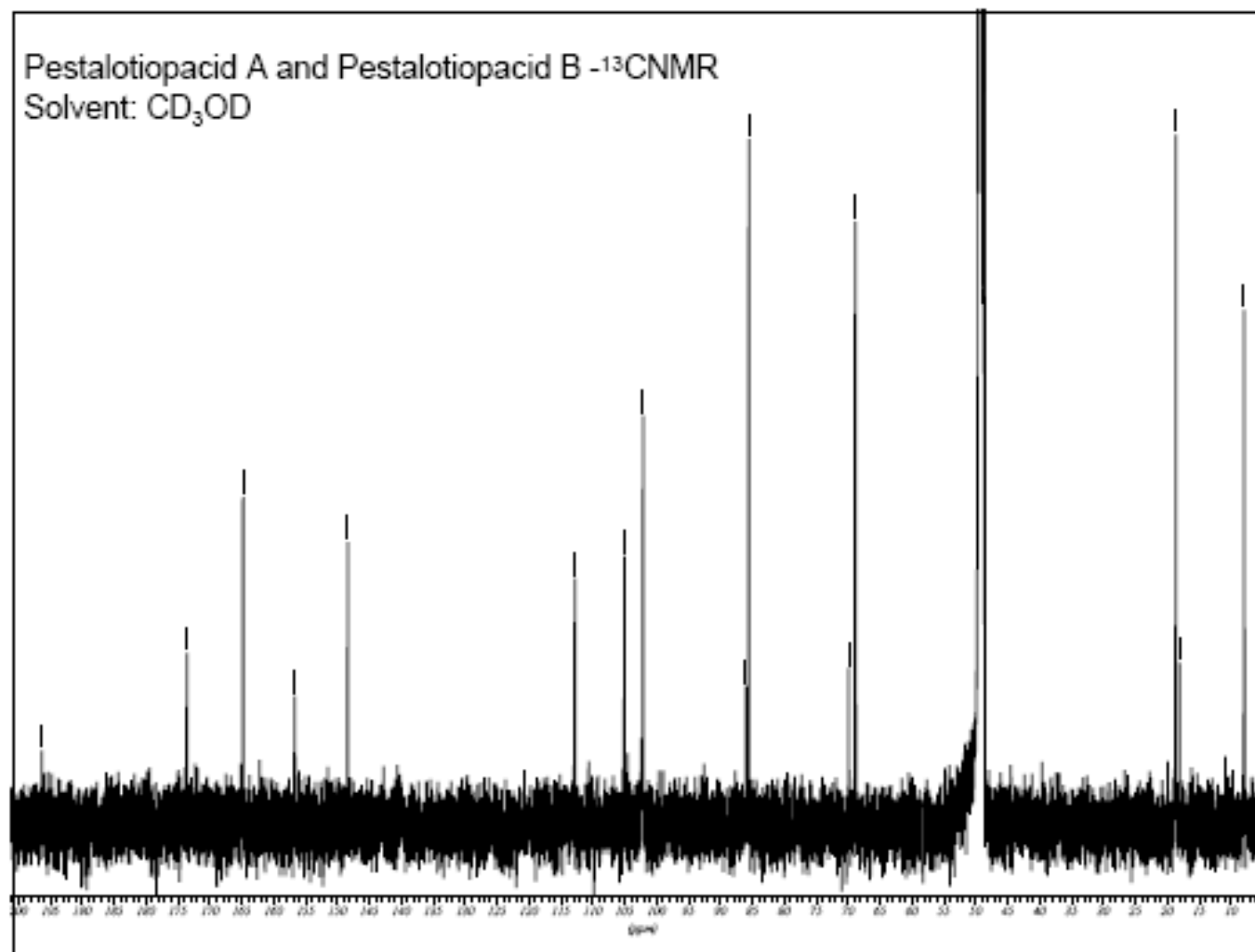
Attachment 55. The ^{13}C NMR Spectrum of *p*-hydroxy benzaldehyde (**45**)



Attachment 56. The ^1H NMR Spectrum of Pestalotiopacid A (**46**)

Attachment 57. The ^1H NMR Spectrum of Pestalotiopacid A (**46**) and Pestalotiopacid B (**47**)

Attachment 58. The ^{13}C NMR Spectrum of Pestalotiopacid A (**46**) and Pestalotiopacid B (**47**)



Curriculum Vitae

Self-Introduction:

Name Xu Jing **Sexual** F. **Height** 1.69m **health status** healthy
Birthday 01/04/1981 **Hometown** Qingdao City, Shandong Prov.
C.P. ++49 211 8114164 **Email** happyjing3@163.com

Educational Background:

School	Major	Degree	Starting and Ending Time
Hainan University	Chemistry Engineering	B.E.	01.09.1999- 01.07.2003
Hainan University	Applied Chemistry	M.S.	01.09.2003- 01.07.2006
Ocean U. of China	Pharmaceutical Chemistry	Phd student	01.09.2006- 01.09.2007
Heinrich-Heine-Universität Düsseldorf	Pharmaceutical Biology	Phd student	18.09.2007- now

Research Field:

Studied for my Doctor degree in Pharmaceutical Biology and Biotechnology Institute, Heinrich-Heine-Universität Düsseldorf from 2007-2009. The research direction is the Novel Secondary Metabolites from the Endophytic Fungus *Pestalotiopsis* sp. JCM2A4 and Microbe-Host Relationship with the Mangrove Plant *Rhizophora mucronata*. Totally 55 compounds were successfully isolated and over 40 of them were new. Three manuscripts had already been published with the first author on *J. Nat. Prod.*, *Bioorg. Med. Chem.* and *Planta Med.*, respectively. Another three would be submitted soon.

My M.S. degree in the applied chemistry Dpt., Hainan U. began at 2003 and started my research from 2004. Since then, I used to take part in the extraction and separation of the active ingredient in *Ficus microcarpa* L. f. and *Baccaurea ramiflora* Lour.. The chemical constituents of the Essential Oil in the fruit, leaf and root of *Baccaurea ramiflora* Lour. were analyzed and the extraction parameters of *Baccaurea* root were optimized. Meanwhile, 3 compounds were isolated and a new compound was named *epidihydrotutin*. Totally nine paper were published and seven of them with the first author in the MS period.

Publications:

1. J. Xu, J. Kjer, J. Sendker, V. Wray, H. S. Guan, R. A. Edrada, W. H. Lin, J. Wu, P. Proksch. *J. Nat. Prod.* **2009**, 72(4), 662- 665.
2. J. Xu, J. Kjer, J. Sendker, V. Wray, H. S. Guan, R. A. Edrada, W. E. G. Müller, M. Bayer, W. H. Lin, J. Wu, P. Proksch. *Bioor. Med. Chem.* **2009**, 17(20), 7362-7367.
3. J. Xu, J. Kjer, J. Sendker, V. Wray, H. S. Guan, W. H. Lin, J. Wu, P. Proksch. *Planta Med.* **2009**, 75, 1074.
4. J. Xu, J. Wu, W. H. Lin, J. Kjer, J. Sendker, V. Wray, H. S. Guan, P. Proksch. 10th Symposium on Marine Drugs, China. **2009**, Conference paper, 289-294.
5. J. Xu, J. Wu, V. Wray, H. S. Guan, W. H. Lin, P. Proksch. Chemistry and bioactivity of secondary metabolites from the fungal genus *Pestalotiopsis*. Under preparation.
6. J. Xu, A. E. H. A. Hassan, R.A. Edrada, J. Wu, W. H. Lin, H. S. Guan, V. Wray, P. Proksch. Polyketide Derivatives of Endophytic Fungus *Pestalotiopsis* sp. Isolated from the Chinese Mangrove Plant *Rhizophora mucronata*. Under preparation.
7. J. Xu, H. S. Guan, V. Wray, W. H. Lin, J. Wu, G. Bringmann, P. Proksch. Pestalotiopene A: Antibiotic with an Unprecedented Skeleton from Endophytic *Pestalotiopsis* sp. from the Chinese Mangrove Plant *Rhizophora mucronata*. Under preparation.
8. X. J. Fu, X. X. Song, J. Xu, et al.. The analysis of the distribution pattern of the constituent herbs in Classical Traditional Chinese Medicine prescriptions treating Respiratory disease by data mining methods. Submitted.
9. W. M. Hu, J. Xu, J. Sinkkonen, et al.. Polyketides from Marine Dinoflagellated of the Genus *Prorocentrum*, Biosynthetic Origin and Bioactivity of Their Okadaic Acid Analogues. *Mini-Reviews in Medicinal Chemistry*, **2010**, 10, accepted.
10. X. J. Fu, H. S. Guan, H. B. Liu, J. Xu, et al.. *Chinese Journal of Information on TCM.* **2009**, 16(10), 94-96.
11. J. Wu, Q. Xiao, J. Xu, et al.. Natural products from true mangrove flora: source, chemistry and bioactivities. *Natural Product Report*, **2008**, 25, 955-981.
12. Xu Jing, Xie Yonghui, Xie Rongzhang, etc.. Advance in the study of Pharmacological actions of Euphorbiaceae. *China Tropical Medicine*, **2007**, 7(1), 106 -107.

13. Xu Jing, Guan Hua-shi, Lin Qiang. A New Sesquiterpene Lactone from *Baccaurea ramiflora* Lour.. *Chinese Herbal Medicine*, **2007**, 38(10), 1450- 1452.
14. Xu Jing, Lin Qiang, Liang Zhenyi, etc.. Study on the chemical constituents of essential oil from fruit, leaf and root of *Baccaurea ramiflora* Lour.. *Food Science*, **2007**, 28(11), 439- 442.
15. Xu Jing, Gao Ling, Xie Yonghui, et al.. Advance in the pharmacological actions of Sesquiterpene lactone. *China Tropical Medicine*, **2007**, 7(4), 623- 624.
16. Xu Jing, Liang Zhenyi, Lin Qiang, etc.. Study on the Chemical Constituents of Essential Oil from the *Baccaurea ramiflora* Lour.. *Chemical Analysis and Meterage*, **2007**, 16(3), 42- 43.
17. Liang Zhenyi , Wang Yongqiang , Xu Jing. Determination of Residual Solvents in Lidocaine Hydrochloride by Head-space Capillary Gas Chromatography. *Natural Science Journal of Hainan University*, **2007**, 25(1), 43- 45.
18. Xu Jing, Xie Rongtao, Lin Qiang, etc.. The category and bioactivity of polysacchoride of marine organisms. *China Tropical Medicine*, **2006**, 6(7), 1277-1278.
19. Xu Jing, Liang Zhenyi, Lin Qiang, etc.. Advances and methods in the extraction of alkaloids from plants. *Natural Product Research and Development*, **2006**, 18, 390-394.
20. Su Xiufang, Lin Qiang, Xu Jing. Hydrolytic Reaction of Organic Compound and its Recent Research. *Journal of Nanning Teachers College*, **2006**, 23(2), 101-104.

Relevant information:

Have team spirit. Interested in social activity and was selected to join BOAO FORUM FOR ASIA 3 times from the first annual conference as the only student in Science. Used to take in charge of Ramos who is the former President of Philippines, ambassadors from the Asia, the arrangement of Press Conference and Government Dinner Party.

Had a good command of English as to pass the College English Test-4 when I was a freshman and the CET-6 on the second year. Passed the National Computer Rank-2 as a senior. Used to win the College English Competition and Debating Competition. Good at writing songs and sports, both won rank when I was an undergraduate. Used to be monitor, University Secretary-general of Chemistry Engineering Association, Representative of the University Congress, Organizing Commissioner of the Communist Party.